ICPIG 2017

XXXIII INTERNATIONAL CONFERENCE ON PHENOMENA IN IONIZED GASES

CONFERENCE PROCEEDINGS

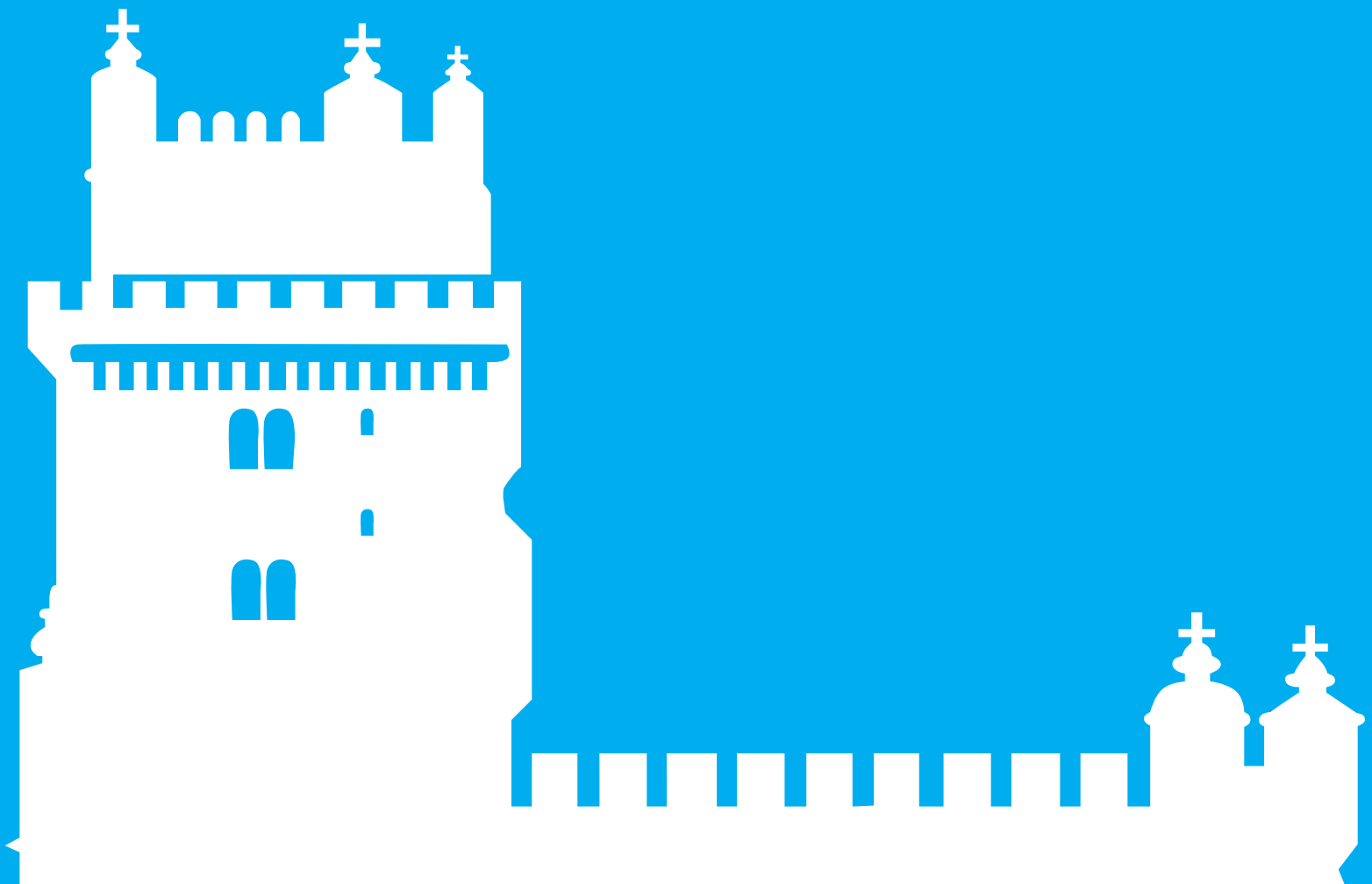

Proceedings of the

XXXIII International Conference on Phenomena in Ionized Gases

Estoril, Portugal. 9-14 July 2017

Editors:
Luís Lemos Alves
Antonio Tejero-del-Caz

FCT Fundação para a Ciência e a Tecnologia
MINISTÉRIO DA CIÊNCIA, TECNOLOGIA E ENSINO SUPERIOR

Published by:
Instituto de Plasmas e Fusão Nuclear
Instituto Superior Técnico
Universidade de Lisboa
http://icpig2017.tecnico.ulisboa.pt

Credits:
Editors: Luís Lemos Alves
Antonio Tejero-del-Caz
Cover design: Irene Lemos Alves

The XXXIIII ICPIG (International Conference on Phenomena in Ionized Gases) has been organized by Instituto de Plasmas e Fusão Nuclear from Instituto Superior Técnico, Universidade de Lisboa, Universidade do Porto and Universidade do Minho.

The XXXIII ICPIG was organized in accordance with IUPAP principles, regarding the free circulation of scientists for international collaborations and discussions, as stated in the declaration of the International Council of Science, adopted at the 26th General Assembly in 2008 and endorsed by the 27th General Assembly in 2011. In particular, no *bona fide* scientist is excluded from participation on grounds of origin, nationality or political considerations unrelated to science.

International Scientific Committee

Eugen **STAMATE**, President of ISC (chair) Technical University of Denmark, Denmark	Denmark, Finland, Norway and Sweden
Sudeep **BHATTACHARJEE**, Indian Institute of Technology, Kanpur, India	Australia, New Zealand, Indonesia, Polynesia, India and South Africa
Gilles **CARTRY**, Aix-Marseille University, France	France and North Africa
Olga **DE PASCALE**, CNR Institute of Nanotechnology_PLasMI Lab, Italy	Italy, Greece and Israel
Ute **EBERT**, Centre for Mathematics and Computer Science, The Netherlands	Belgium, The Netherlands and Luxembourg
Francisco J. **GORDILLO VÁZQUEZ**, Consejo Superior de Investigaciones Científicas, Granada, Spain	Spain, Portugal, Mexico and South and Central America
Holger **KERSTEN**, Kiel University, Germany	Germany, Austria, Lichtenstein and Switzerland
Mark J. **KUSHNER**, University of Michigan, USA	USA and Canada
Zdenko **MACHALA**, Comenius University, Bratislava, Slovakia	Poland, Hungary, Czech Republic and Slovakia
Marija **RADMILOVIC RADJENOVIC**, University of Belgrade, Serbia	Bulgaria, Romania, Serbia, Bosnia, Montenegro, Croatia and Slovenia
Masaharu **SHIRATANI**, Kyushu University, Japan	Japan
Eduard **SON**, Joint Institute for High temperature RAS, Russia	Russia and the area of the former SU
Miles **TURNER**, Dublin City University, Ireland	UK and Ireland

Local Organizing Committee

Instituto de Plasmas e Fusão Nuclear
Instituto Superior Técnico

Luís **LEMOS ALVES**, Chair

Vasco **GUERRA**, Co-Chair

Antonio **TEJERO-DEL-CAZ**

Ana **DIAS**

Susana **ESPINHO**

Marija **GROFULOVIC**

Júlio **HENRIQUES**

Mário **LINO DA SILVA**

Luís **MARQUES**

Polina **OGLOBLINA**

Nuno **PINHÃO**

Carlos Daniel **PINTASSILGO**

Secretary

Anabela **GONÇALVES**

Image & Website

Joana **CABRAL**

Irene **LEMOS ALVES**

Conference Sponsors

Instituto de Plasmas e Fusão Nuclear

The International Union of Pure and Applied Physics

Fundação para a Ciência e a Tecnologia

IOP: Institute of Physics

Sociedade Portuguesa de Física

Sairem. Microwave and radio-frequency professional solution

Foreword

The XXXIII edition of the International Conference on Phenomena in Ionized Gases (ICPIG 2017) celebrates 90 years since Irvin Langmuir used the word "plasma" to describe ionized gases. ICPIG was found three decades later, in 1953, and today is one of the oldest and most important international conferences on plasma physics. In its early editions ICPIG was mostly dedicated to fundamental science (focusing on topics such as elementary processes and fundamental data, plasma diagnostics, wave and instabilities and space physics), but the recent burst of interest in plasma-based applications has pushed the community to follow new research paths, contributing also to enlarge the scope of ICPIG, for example with the addition of topics on plasma processing of surfaces and particles, and medical, biological, environmental and aeronautical applications. Although this diversification led inherently to the foundation of more specialized plasma conferences and workshops, ICPIG kept the role of interconnecting the broad community of low-temperature plasma physics, holding a key position as a "forum for the discussion of nearly all fields of plasma science".

ICPIG 2017 is held in Estoril, Portugal, from 9 to 14 July. The Local Organizing Committee (LOC) is composed by members of the Instituto de Plasmas e Fusão Nuclear, Instituto Superior Técnico, belonging to the University of Lisbon, the University of Oporto and the University of Minho. Leveraging on the large diversity that characterizes ongoing research in plasma physics, and aiming also on broaden opportunities for the diffusion of scientific results by both young and senior researchers, the International Scientific Committee (ISC) of ICPIG has decided to change the conference format by reducing the number of general invited talks and by introducing, for the first time, oral and poster contributions. The scientific program of ICPIG 2017 is composed by 6 invited general lectures, including the von Engel & Franklin Prize Lecture, 29 invited topical lectures and 36 oral contributions, organized in two parallel sessions, in addition to 4 poster sessions and 1 special session. ICPIG 2017 received 416 submissions, corresponding to 357 registered participants from 40 countries.

ICPIG awards the 'von Engel and Franklin Prize', established in 1998. It is sponsored by the 'Hans von Engel and Gordon Francis Fund' and is administered by the Board of Physical Sciences, University of Oxford. The prize is named in honor of two distinguished colleagues who had a major role in ICPIG and its community since the first meeting in 1953. The prize, consisting of 1000€ and a certificate, is awarded every two years to an individual for work in the field of physics and technology of plasmas and ionized gases, as covered by ICPIG meetings. The selection is conducted by the ISC, based either on long-standing and important contributions to the field, or an outstanding achievement giving rise to a new field, or both.

The ISC have chosen Prof. Uwe Czarnetzki as the 2017 winner of ICPIG's von Engel & Franklin prize.

The members of the International Scientific Committee and the Local Organizing Committee thank all those who contributed to the success of ICPIG 2017, wishing to all participants a very fruitful conference in Estoril.

July 2017

Dr. Eugen Stamate
Chair of the ISC

Professor Luís Lemos Alves
Chair of the LOC

CONFERENCE CONTRIBUTIONS

General Invited Lectures

The Von Engel & Franklin Prize Lecture

Topical Invited Lectures

Special Session Lectures

Oral Contributions

Poster Contributions

General Invited Lectures

Topic number

MODELLING, SIMULATION AND DIAGNOSTICS, 5) & 6)
Invited General Lecture

VUV Radiation from Streamers

A. Neuber[1], A. Fierro[2], J. Stephens[3]

[1] *ECE Dept., Ctr. for Pulsed Power & Power Electronics, Texas Tech University, Lubbock, TX, USA*
[2] *Applied Optical and Plasma Sciences, Sandia National Laboratories, Albuquerque, NM, USA*
[3] *Plasma Science and Fusion Center, Massachusetts Institute of Technology, Cambridge, MA, USA*

The self-produced light emission from pulsed streamer discharges is challenging to characterize through experiment or modeling; on the one hand, the high absorption cross sections make VUV detection often impossible, on the other hand, the large number of radiating species clashes with computer memory limitations. Two principal methods of efficiently detecting VUV radiation from streamers in atmospheric gases, including air, are introduced. These methods cover the wavelength range from 80 to 180 nm. The experimental results are supplemented with modeling the increase in charge carrier density and VUV intensity through implementing a parallel computing Particle-in-Cell /Monte Carlo Collision model, which is capable of discretely tracking photons and their corresponding wavelengths. Radiative transitions from the $c'_4\Sigma^+_u$ (Carroll–Yoshino) singlet state of N_2 are found to be a dominant contributor for streamer propagation in air.

1. Background

It is generally accepted that photoionization, PI, and photoemission play a critical role during discharge inception. Their impact, however, has typically been lumped in the simplest case into a single feedback constant or more sophisticated into some actual spectral modeling. While the former is more of an empirical attempt that is unable to cover a large parameter space, the latter has suffered from the lack of fundamental transition data. This work addresses both: Verification of major transitions in the VUV in gases at atmospheric pressure, including air, and advanced photon modeling [1, 2] in a first principle based approach.

2. Experimental Approach

To reasonably extract VUV radiation from a developing streamer, the propagation distance through the surrounding gas (at ~ 1 atm pressure) has to be kept in the sub-mm range considering that the absorption depth is typically in the mm range. Thus, two methods were successfully explored, a) streamer breakdown across a VUV transmitting surface, which yielded experimental spectra down to 120 nm, and b) pulsed volume breakdown in a high-pressure gas puff, spectral range down to 80 nm.

3. Results

As an example, the theoretical spectra of N I and O I, calculated assuming a Boltzmann distribution of the excited states are compared with the experimentally recorded VUV emission of air breakdown in the streamer phase, see Fig. 1. Other experiments identify PI critical emission as the N_2 $c'_4\Sigma_u^+(0)$– $X^1\Sigma_g^+(1)$ band and O I and O II transitions. The experimentally verified transitions gave rise to the PI driven streamer modeling, see Fig. 2.

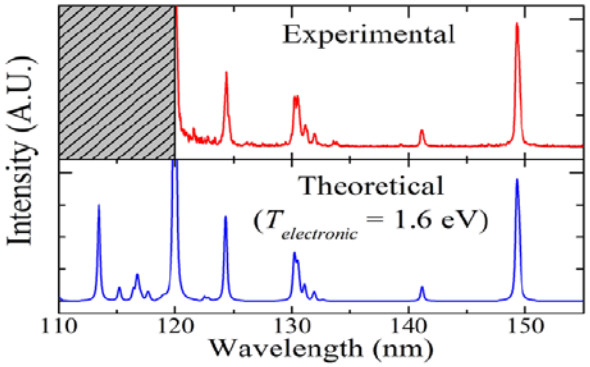

Fig. 1. (top) Experimental VUV spectra of the developing breakdown. (bottom) Theoretical spectra [3]

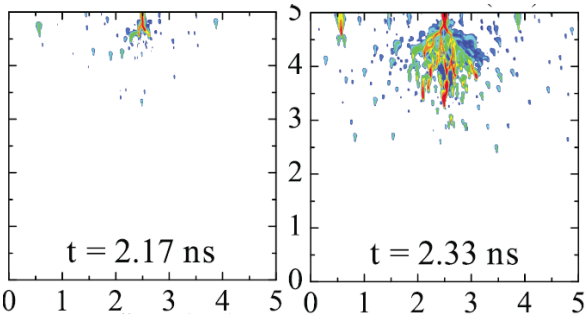

Fig. 2. 2D Streamer modeling with a 2 ns risetime, 60 kV voltage excitation applied to the top plane. Gaussian seed density near anode (top), no other background [2].

4. References

[1] A. Fierro, J. Stephens, S. Beeson, J. Dickens, and A. Neuber, Phys. Plasmas, **23** (2016) 013506.

[2] J. Stephens, A. Fierro, S. Beeson, G. Laity, D. Trienekens, R.P. Joshi, J. Dickens, A. Neuber, Plasma Sources Sci. Technol. **25** (2016) 025024.

[3] A. Fierro, G. Laity, A. Neuber, J. Phys. D: Appl. Phys. **45** (2012) 495202.

Topic number

Plasma-material Interactions: diagnostics and control

M. Hori[1]

[1] *Institute of Future Society for Innovation, Nagoya University, Japan*

In order to realize high performances of plasma material processes, various kinds of plasma diagnostics techniques have been developed. These processes were basically determined by the interaction of plasma with the surface of materials. Therefore, it is extremely important to diagnose and control the kinetics of the surface reactions with a high accuracy. The science and technologies on plasma-material interactions will be overviewed and the forward prospective is mentioned.

1. Introduction

Plasma etching and deposition processes have been core technologies to make the manufacturing innovation, such ultralarge integrated circuits (ULSIs) etc. In these processes, the quantitative measurement and the spatiotemporal control of ion, radical and light in the reactive plasma became key issues to obtain high processing performances as well as the establishment of the plasma process science. Here, the interaction of plasma with the material surfaces has been investigated by employing various kinds of diagnostics techniques not only in the gas phase but also in the surface. The advanced methods to control them have been introduced.

2. Experimental and results

The solar cell devices with a-Si and μc-Si thin films have been fabricated employing a plasma enhanced chemical vapor deposition (PECVD) with SiH_4/H_2 gases. In this processing, SiH_3 and H radicals which were reported to play important roles were measured at a relatively high pressure of 1 kPa in a capacitively coupled VHF of 60 MHz excited plasma by using the cavity ring down spectroscopy (CRDS) and the vacuum violet laser absorption spectroscopy (VUVLAS), respectively. Additionally, the behaviors of higher order species in the condition were evaluated by using the quadruple mass spectroscopy. The systematical measurement of behaviors of species in the gas phase enabled us to evaluate the sticking coefficiencies of these species on material surfaces. Considering the surface loss probability of 0.5 for SiH_3 radical and 1 for H radical, it was found that SiH_3 radical constituted 45% of the deposition precursors and the others will be higher order radicals [1]. On the basis of these diagnostics results, the control technology to synthesize films of high quality at a higher deposition rate was proposed.

The SiO_2 etching processes with a high aspect ratio in ULSIs have been investigated employing the fluorocarbon gas chemistry. In this processing, synergetic effects of fluorocarbon radicals with the ion bombardment with a high energy formed the intermediated layers between fluorocarbon films and the SiO_2 surfaces during the etching. Control of such a layer induced by the plasma is a key issue for the etching of SiO_2. It is so difficult, however, to identify the chemical composition of layers and design the structures for obtaining the high performances of etching. Then, the thin SiOF intermediate layer < 2 nm in thickness induced by the $C_4F_6/O_2/Ar$ etching plasma was precisely analysed by the ex situ time-of-flight secondary ion mass spectroscopy (TOF-SIMS) using a C_{60}^{2+} sputtering. The clearly observed signal of $SiOF^-$, SiO_2F^- and $Si_2O_4F^-$ between the top fluorocarbon film and the SiO_2 were found to be a key layer to be controlled for the etching [2].

Recently, the non-equilibrium atmospheric pressure plasma was applied to the cleaning and modification of the material surfaces. The O and N atoms together with UV were measured by the VUV absorption spectroscopy and optical emission spectroscopy (OES). The interaction of O radical and UV attributed to NO-γ with the organic contamination of glass decomposed organic monolayers for the surface cleaning [3].

3. References

[1] Y. Abe et al., Appl. Phys. Lett. **110** (2017) 043902.

[2] Y. Ohya et al. J. Vac. Sci. Technol. A34 (2016) 040602.

[3] M. Iwasaki et al. Jpn. J. Appl. Phys. 46 (23), 2007 L540.

Unified model of the streamer initiated gas breakdown

M. Černák[1], T. Hoder[1], Z. Bonaventura[1]

[1] *Department of Physical Electronics, Masaryk University, Brno, Czech Republic*

A common feature of the discharges at near-atmospheric pressures is that the most important physical processes leading to the formation of non-equilibrium plasmas occur on the time scales of 10^{-9}s in regions of characteristic size of 0.1 mm. The reasons for the unsatisfactory understanding of such phenomena are both experimental and computer simulation constraints. They are given by the ultra-fast changing basic plasma parameters on given extremely small areas. Based on experimental study and computer simulations of the cathode spot formation for a wide range of electrode geometries and materials, an integrated model describing a wide range of streamer micro-discharges and pre-breakdown phenomena will be presented.

1. Introduction

Since ”the development of atmospheric–pressure plasma sources to replace plasma processing in vacuum systems is a current trend in industrial plasma engineering” [1] in the last two decades the centre of both experimental and theoretical study of the gas discharge ionisation phenomena has been shifted from the low-pressure gas discharges to the discharges generated at near-atmospheric pressures [2].

A common feature of the discharges at near-atmospheric pressures is that the most important physical processes leading to the formation of non-equilibrium plasmas occur on the time scales of 10^{-9}s in regions of characteristic size of 0.1 mm. This is result of the fact that the discharge formation in such conditions is usually associated with the formation of fast and narrow ionization waves, termed ”primary streamers” and consequently, such discharges are now frequently referred to as micro-discharges.

The arrival of a primary streamer to the cathode forming an active cathode spot/region marks an important turning point in the development of micro-discharges and is a significant bottleneck in the understanding of the micro-discharge formation mechanism [3]. Similar phenomena occur also as streamer-like instabilities in the cathode region leading to the plasma filamentation and glow-to-arc transitions in various types of atmospheric-pressure glow discharges. The reasons for the unsatisfactory understanding of such phenomena are both experimental and computer simulation constraints: The main experimental difficulties are due to small size of the cathode spots, their random distribution on the cathode surface, and the nanosecond time scale of their formation. As a consequence, computer simulations are the essential tools that can be used to increase our understanding of the cathode spot formation. The simulations, however, are constrained by the fact that they typically fail as the streamer reaches the cathode due to instabilities introduced by numerical discretization.

Based on experimental study and computer simulations of the cathode spot formation for a wide range of electrode geometries and materials, an integrated theoretical model describing a wide range of streamer micro-discharges and pre-breakdown phenomena will be presented. Except for narrow-gap ($< 5.10^{-6}$m) and microwave breakdowns, the model is applicable to all high-pressure discharge types, serving as a necessary guide in the selection of cases for further study by experiment or computer simulation, as well as for the design of atmospheric-pressure sources of non-thermal plasmas.

2. Acknowledgements

This research was funded by the project LO1411 (NPU I) of Ministry of Education Youth and Sports of Czech Republic.

3. References

[1] J.R. Roth, Industrial Plasma Engineering., Vol.2: Appl. to Non-thermal Plasma Processing” IOP Publishing Ltd. 2001, ISBN 9780750305440

[2] K.H. Becker, U. Kogelschatz, K.H. Schoenbach, R.J. Barker (eds.), Non-Equilibrium Air Plasmas At Atmospheric pressure, IOP Publishing Ltd. 2004, ISBN 9780750309622

[3] T. Hoder, M. Černák, J. Paillol, D. Loffhagen, R. Brandenburg, Physical Review E **86** (2012) 05540190 (R)

Microwave Plasmas Applied for Synthesis of Free-Standing Carbon Nanostructures at Atmospheric Pressure Conditions

Elena Tatarova

Instituto de Plasmas e Fusão Nuclear, Instituto Superior Técnico, Universidade de Lisboa, Lisboa, Portugal

This lecture addresses selective, single step synthesis of advanced free-standing carbon nanostructures using microwave driven plasmas at atmospheric pressure conditions. Controllable bottom-up self-organization of graphene, N-graphene sheets and nanodiamonds achieved via tailoring of the plasma environment is discussed.

Recently a renewed interest to carbon materials has been generated as new advanced carbon nanostructures are being introduced bringing new prospects for applications. Multiple processes have been reported for free-standing carbon nanostructures synthesis, corresponding to either "top-down" or "bottom-up" approaches. It is to be noted that the main challenge of conventional, i.e., widely used chemical routes, is the very limited control, or lack of, over the synthesis process.

Our work extends the scope of previous efforts to fabricate free-standing carbon nanostructures using large-scale configurations of microwave plasmas driven by surface waves at atmospheric pressure conditions [1-5]. Here, we present a microwave plasma-enabled scalable route for a single step, continuous, synthesis of free-standing graphene sheets and nanodiamond particles. The method's crucial advantage relies on harnessing unique plasma mechanisms to control the material and energy fluxes of the main building units (C_2,C) at the atomic scale level. By tailoring the high energy density plasma environment a selective synthesis of high quality graphene sheets at high yield (2 mg/min) with prescribed structural qualities was attained. A high level of control over oxygen functionalities and sp^2/sp^3 carbon ratios has been achieved and with approximately 40% of the graphene being synthesized in the form of single atomic layers. The method is highly cost-efficient, fast and environmentally friendly, since it does not require the use of catalysts and noxious chemicals. It is also versatile, allowing the synthesis of different types of 2D nanostructures (e.g. N-graphene) in the same reactor. Furthermore, the high energy density of the generated plasma allows the use of gaseous, liquid or solid carbon precursors.

Here we intent to provide substantial evidence that microwave plasma based technologies are a highly competitive, green, cost-effective and disruptive alternative route to presently used cumbersome, toxics dependant, multistep conventional methods.

Acknowledgements

This work was funded by Portuguese FCT—Fundação para a Ciência e a Tecnologia, under Project UID/FIS/50010/2013, Project INCENTIVO/FIS/LA0010/2014, and grant SFRH/BD/52413/2013 (PD-F APPLAuSE)

References

[1] E. Tatarova, N. Bundaleska, J.Ph. Sarrette and C.M.Ferreira, Plasma Sources Sci. Technol. **23** (2014) 063002.

[2] E. Tatarova, J. Henriques, C.C. Luhrs, A. Dias, J. Phillips, M.V. Abrashev and C.M. Ferreira,. Appl. Phys. Lett. **103** (2013) 134101.

[3] E.Tatarova, A. Dias, J. Henriques, A.M. Botelho de Rego, A.M. Ferraria, M. Abrashev, C.C. Luhrs, J. Phillips, F.M. Dias, C.M. Ferreira, J. Phys. D: Appl. Phys. **47** (2014) 385501.

[4] A. Dias, N. Bundaleski, E. Tatarova, F.M. Dias, M. Abrashev, U. Cvelbar, O.M.N.D. Teodoro, J. Henriques J. Phys. D: Appl. Phys. **49** (2016) 055307.

[5] D. Tsyganov, N. Bundaleska, E. Tatarova, A.Dias, J. Henriques, A. Rego, A. Ferraria, M.V. Abrashev, F.M. Dias, C.C. Luhrs, J. Phillips, Plasma Sources Sci. Technol. **25** (2016) 015013.

Surface and volume kinetics of molecules in air depollution processes

Christelle Barakat[1], XianJie Wang, Loganathan Sivachandiran,[1-3], Zixian Jia[1], Olivier Guaitela[1], Frédéric Thevenet[2,3], Antoine Rousseau[1]

[1]*LPP, Ecole Polytechnique, UPMC, Université Paris Sud 11, CNRS, Palaiseau, France*
[2]*Université Lille Nord-de-France, F-59000 Lille, France*
[3]*Mines Douai, CE, F-59508 Douai, France*
Antoine.rousseau@lpp.polytechnique.fr

Plasma-catalyst coupling for air depollution has been extensively studied for more than two decades. Studies dealing with the plasma induced heterogeneous reactivity are analysed as well as the possible modifications of the catalyst surface under plasma exposure. Alternatively to the conventional and widely studied plasma catalyst-coupling, a sequential approach has been recently proposed, where pollutants are first adsorbed on the material, then oxidized by switching on the plasma. This allows direct monitoring of surface reactions decoupled from gas phase reactions.

1. Plasma-catalyst coupling for Volatile Organic Compounds oxidation

Plasma-catalyst coupling has proven to be very effective for the destruction of diluted pollutants and is therefore suitable for indoor air-treatment [1]. Now commercially available indoor air treatment units can be found on the market. Most of these devices combine dielectric barrier discharge (DBD) or corona discharges with an adsorbent, which may have a catalytic activity. The plasma generates highly oxidizing species at low energetic cost, which oxidize the pollutants. The respective importance of gas phase oxidation versus surface oxidation has long been discussed.

Historically, various high dielectric permittivity materials ($BaTiO_3$, TiO_2, …) were introduced inside the plasma region, partly to favours plasma ignition and energy transfer [2] as well as high mineralisation (complete oxidation to CO_2) [3]. The positive effect of a porous material inserted in a discharge was evidenced [4]. Because of the diffusion of the species inside the porous structure of alumina and silica, active species lifetime and Volatile Organic Compounds (VOC) residence time increase favouring higher mineralization.

2. Evidencing oxidation at the surface

More recently, a sequential approach has been recently proposed, where pollutants are first adsorbed on the material, then oxidized by switching on the plasma. Monitoring the gas phase composition AND the VOCs adsorbed onto the catalytic surface allows analysing oxidation mechanisms [5].

Different parameters are studied, such as the injected power, the relative humidity, the type of VOC and the type of catalytic materials. In-plasma and post-plasma configuration are studied [5-6]. The analysis of the chemical composition of the gas phase is performed using an FTIR cell and the in situ surface analysis of adsorbed species and intermediates is followed using a DRIFTS cell

In addition, we will present results obtained using Sorbent-TRACK, a new device , developed to monitor adsorption and surface oxidation of pollutants under direct plasma exposure [7-8]. It is based on direct transmitted Fourier Transformed Infrared (FTIR) spectroscopy. Performances and sensitivity of Sorbent-TRACK are reported Adsorption and oxidation of acetone leads to production of adsorbed isobutene and acetic acid, where oxidation of isopropanol gives mainly to adsorbed acetone, mesityl oxide and acetate.

References

[1] F. Thevenet, L. Sivachandiran, O. Guaitella, C. Barakat, A. Rousseau, J. Phys. D: Appl. Phys, 2014 J. Phys. D: Appl. Phys. 47 224011

[2] A. Ogata, K. Yamanouchi, K. Mizuno, S. Kushiyama, T. Yamamoto, Plasma Chem. Plasma Process. 19 (1999) 383-394

[3] H.H. Kim, A. Ogata, S. Futamura, J. Phys. D: Appl. Phys. 38 (2005) 1292–1300

[4] F. Holzer, U. Roland, F.D. Kopincke, Appl. Catal. B: Env. 38 (2002) 163-171

[5] C. Barakata, P. Gravejat, O. Guaitella, F. Thevenet, A. Rousseau, Applied Catalysis B: Environmental 147 (2014) 302– 313

[6] L. Sivachandiran , F. Thevenet, A. Rousseau, Plasma Chemistry & Plasma Processing, (2013)

[7] Z. Jia and A. Rousseau, Scientific Reports, 6, 31888; (2016).

[8] Z. Jia, X. Wang, F. Thevenet, A. Rousseau Plasma Process Polym. 2017;e1600114

This work has been supported by ANR, French DGA, LABEX PLAS@PAR and ALKOTHERM

The Von Engel & Franklin Prize Lecture

Distribution Functions in Non-Equilibrium Plasmas

Uwe Czarnetzki [1]

[1] *Institute for Plasma and Atomic Physics, Faculty for Physics and Astronomy, Ruhr-University Bochum, Germany*

The non-equilibrium character of low-temperature plasmas is exhibited by the form of the distribution functions of free electrons and ions as well as in the population of excited states of atoms and molecules. Strong interactions between particles from different ensembles as well as inhomogeneous and non-stationary electric fields are usually causing the complex forms of non-equilibrium distributions. The talk will show a number of experimental examples ranging from low to atmospheric pressures. The underlying physical mechanisms will be explained, the diagnostic techniques highlighted, and the consequences for application and diagnostics discussed.

1. Introduction

Low-temperature plasmas are characterized by non-equilibrium distribution functions. Generally, the various particle ensembles do not share the same distribution and typically also the particles within an ensemble, especially electrons and ions but also the population of bounded states in neutrals, do not follow thermal distributions, i.e. cannot be described by a Maxwell-Boltzmann equilibrium distribution. This deviation from thermal equilibrium is caused by weak interaction between particles within an ensemble but strong interaction with particles from other ensembles. Further, oscillating and inhomogeneous electric fields on a scale shorter than the charged particle mean free path can have a strong contribution. Consequently, the particular form of the non-equilibrium distributions and the processes causing their formation are at the heart of the physics in these systems. The distributions play a key role for all physical processes, in particular excitation and ionization but also transport properties can be very sensitive.

In this talk a selection of particular non-equilibrium conditions of interest in recent research and application is presented. The underlying physics is explained, the various aspects are illustrated by experimental examples, and the diagnostic techniques are introduced. Recent advances and current challenges are highlighted. Examples will be shown from three general categories.

2. Examples

2.1. Electron Distribution Function

In Radiofrequency discharges the oscillating and spatially inhomogeneous electric field can lead to ballistic electrons and correspondingly strong deviations from simple Maxwellian distribution functions. The related excitation patterns are the basis of spectroscopic access to the spatial-temporal dynamics. In ICP the evanescent electric field penetrating into the plasma can again be imaged by taking advantage of the temporal modulation of the EVDF. Further downstream at sufficiently low pressures, the EEDF becomes non-local which in principle allows determination in the entire volume from a single measurement in the centre. Arrays of smaller ICPs with a clear phase correlation provide an opportunity for a new plasma source based on non-collisional heating of electrons.

2.2. Ion Distribution Function

IVDF in non-equilibrium plasmas generally show show complex profiles which are additionally strongly depending on the particular location in the plasma. Recently it was discovered that in case of charge-exchange dominated transport at low pressures, measurements taken on the wall allow a full spatially resolved reconstruction of the distribution function and basically all plasma parameters, including also the electron density and temperature as well as the ambipolar electric field and potential. While at low pressures the IVDF is effectively one-dimensional, it exhibits a much wider angular distribution at higher pressures. This has consequences not only for the interaction with surfaces but requires also careful interpretation of measurements.

2.3. Bounded Electrons in Atoms and Molecules

The distribution of bounded electrons in non-equilibrium plasmas is usually governed by a balance between collisional excitation and radiative and collisional de-excitation. In the afterglow recombination of cold electrons can lead to an even stronger deviation from thermodynamic equilibrium by population of highly excited Rydberg states. Recently it was discovered that in the afterglow of atmospheric pressure discharges in Helium actually almost all free electrons are converted to Helium Rydberg molecules.

Topical Invited Lectures

Topic number 10

Pre-breakdown phenomena and discharges in gas-liquid system

Babaeva N.Yu., Naidis G.V., Panov V.A., Smirnov B.M.,
Son E.E. and Tereshonok D.V.

Joint Institute for High Temperatures of the Russian Academy of Sciences - 13, bldg. 2 Izhorskaya str., Moscow, 125412, Russia

Presented work consists of two parts: experimental and theoretical investigations of pre-breakdown and discharge in disperse systems. We theoretically investigated the development of discharge in two types of bubble clusters immersed in water and transformer oil: seven and fifteen equidistant bubbles with the prevalence of a horizontal orientation perpendicular to the applied electric field. The bubbles were filled with air. We present the principal difference in the streamer propagation from bubble-to-bubble due to mutual polarization of bubbles. Hydrodynamics simulation for the movement of the dielectric liquid under the electrostrictive stress was performed. We also investigated cavitation of a dielectric liquid under the ponderomotive forces. Results of the simulation are in good agreement with the experiment.

One of the main properties of a system consisting of a liquid with gaseous bubbles is the low electric field strength of electric breakdown in comparison with a pure liquid. Presented work consists of two parts: experimental and theoretical investigations of pre-breakdown and discharge in such disperse systems.

Experimental setup for the investigation of the electrical breakdown in fluid with a gas contains the microporous membrane which is made of anodized alumina with an average pore size (100 ± 50) nm. The distance between the pores is 300 nm, a thickness of the porous layer is 200 microns. Experiments with the penetration of the gas into the liquid through a porous medium are performed. Gas forms bubbles in the liquid which float.

Optical interference method and statistical analysis of interferometric images was used in order to obtain the distribution of the microbubbles. The most probable value obtained for the mixture of "air-water" (without the addition of surfactants) is about 70-80 microns. We experimentally studied the development of discharge in such multiphase system.

We theoretically investigated the development of discharge in two types of bubble clusters immersed in water and transformer oil: seven and fifteen equidistant bubbles with the prevalence of a horizontal orientation perpendicular to the applied electric field. The bubbles were filled with air. We show the principal difference in the streamer propagation from bubble-to-bubble due to mutual polarization of bubbles.

It's well known that the fluid stream flows in the direction towards the high electric field. Fluid behavior with a different permittivity is calculated on the basis of the hydrodynamics numerical simulation in the strong inhomogeneous pulsed electric field. The negative pressure under ponderomotive forces can lead to the cavitations near the needle electrode and can lead to the occurrence of the electrical breakdown in the fluid. Results of the simulation are compared with the experiment for the cavity extension.

The main results are presented in papers [1-8].

This work is supported by the Russian Science Foundation (Project Number **14-50-00124**).

[1] Babaeva N.Yu., Tereshonok D.V., Naidis G.V., J. Phys. D: Appl. Phys. **48** (2015) 355201.

[2] Naidis G.V., IEEE Transactions on Plasma Science. **43** (2015) No. 9 3138-3141.

[3] Natalia Yu. Babaeva, PSST **24** (2015) 034012.

[4] Babaeva N.Yu., Tereshonok D.V., Naidis G.V. and Smirnov B.M., J. Phys. D: Appl. Phys. **49** (2016) 025202

[5] Boris M. Smirnov and R. Stephen Berry, Chemistry Central Journal **9** (2015) 48 1-8.

[6] V. P. Krainov, B. M. Smirnov and D. V. Tereshonok, EPL **108** (2014) 34002-34002.

[7] Dmitry V Tereshonok, Natalia Yu Babaeva, George V Naidis and Boris M Smirnov, J. Phys. D: Appl. Phys. **49** (2016) 505501.

[8] Dmitry V Tereshonok, J. Phys. D: Appl. Phys. **50** (2017) 015603.

Atmospheric pressure plasmas for surface and medical applications

K. G. Kostov[1], V. Prisyazhnyi[1], A. H. R. Castro[1], T. M. C. Nishime[1], C. Y. Koga-Ito[2], T. S. M. Mui[1], L. L. G. da Silva[1], R. P. Mota[1], A. C. Borges[2], M. Machida[3]

[1]*Faculty of Engineering – FEG , São Paulo State University – UNESP, Guaratinguetá, SP, Brazil*
[2]*Institute of Science & Techology – ICT, São Paulo State University – UNESP, São José dos Campos, SP, Brazil*
[3]*Insitute of Physics – IFGW, University of Campinas – UNICAMP, Campinas, SP, Brazil*

Non-thermal plasma jets at atmospheric pressure have attracted much attention in recent years due to their simplicity and low cost combined with a great variety of applications ranging from material processing to medicine. This work will give a brief overview of recent works focusing on the research and development performed at FEG, UNESP.

1. Introduction

The cold atmospheric pressure plasma jets (APPJs) were first reported in nineteen-nineties and since then they have been subject of intense research and development. For instance, over the last decade the number of publications on plasma jets in the literature has grown exponentially [1]. Also, various high impact journals published special issues and review papers dedicated on APPJs. A distinguishable feature of cold plasma jets is that they can be operated in air and provide enhanced chemistry via production of reactive species (radicals, photons and charged particles) while the gas temperature is maintained sufficiently low for processing of organic and biological components. Nowadays, plasma jets are routinely used in material processing for surface cleaning and deposition, etching, surface activation of polymers, decontamination of surfaces etc. [1]. Recently, application of non-thermal plasma jets in living tissues has been extensively studied giving the origin of so-called plasma medicine [1, 2].

2. Experimental

2.1. Plasma jet geometry

An important issue for the operation of a plasma jet is its geometry, which together with dielectric properties of the substrate, strongly influences the shape and the extension of generated plasma plume. Therefore, depending on the intended application many different plasma jet configurations have been investigated. Here, we report the effect of a horn-like jet nozzle, which allows extending plasma over larger area of the sample. This jet configuration was used for adhesion improvement of Al alloys and also for treatment of seeds.

2.2. Plasma polymerization

A three-electrode plasma jet configuration (one powered electrode and two grounded) was especially developed for deposition of polymer films at atmospheric pressure. Argon was employed as working gas for plasma generation. Mixtures of air with acetylene or hexamethyldisiloxane (HMDSO) were used as polymerizing agents. The films were deposited on glass substrates placed on an auxiliary grounded electrode and can be used as biocompatible coating or for corrosion protection.

2.3. Plasma jet at the end of long plastic tube

A crucial question in plasma medicine is how to deliver active plasma species to tissues or organs inside human body. Most commercially available plasma sources are too big and rigid for this purpose. Here, we report a method that allows generation of cold plasma jet at the end of long (up to few meters), flexible, plastic tube. The tube can be held with hand without risk of electric shock and the plasma jet can be easily handled and directed to a target. Here, we will describe the method and present some results of surface modification of polymers. Also, *in-vitro* experiments for microbial inactivation using APPJs at the end of plastic tube will be presented. Special attention will be given to plasma treatment of biofilms that represent major infection risk for medical gear in hospitals.

2.4. Microbial inactivation *in-vivo*

Finally, we will report some results of *in-vivo* tests performed on the tongues of laboratory rats that were experimentally infected with *C. albicans.*

3. References

[1] J. Winter, R. Brandenburg, and K.-D. Weltmann, Plasma Sources Sci. Technol. **24** (2015) 064001.

[2] H. Tanaka and M. Hori, J. Clin. Biochem. Nutr. **60** (2017) 29.

Nanosecond pulsed discharges: generation, measurement and plasma processing

T. Huiskamp[1], F.J.C.M. Beckers[1], E.J.M. van Heesch[1], W.F.L.M. Hoeben[1] and A.J.M. Pemen[1]

[1] *Eindhoven University of Technology, Electrical Energy Systems Group, Department of Electrical Engineering, Eindhoven, The Netherlands (t.huiskamp@tue.nl)*

In this contribution we report on our recent progress in generating and measuring nanosecond pulsed discharges for plasma processing applications. The nanosecond pulses are generated by a single-line pulse topology which is able to output 0.5-10-ns, positive and negative 0-50-kV pulses with a rise time of less than 200 ps at a pulse repetition rate of 1 kHz. With D-dot and B-dot sensors and spatiotemporal resolved iCCD imaging we monitor voltage and current waveforms and the development of the streamer discharge. In addition, we perform several plasma processing experiments. The results show extremely high yields in ozone generation and NO removal. A general conclusions is that the shortest rise time pulses result in the highest plasma processing yields and the highest streamer velocities.

1. Introduction

It has been known for some time that pulsed discharges result in high plasma processing yields. In this project we developed (sub)nanosecond pulsed power technology to explore this further.

2. Technology

The nanosecond pulse technology consists of an adjustable, microsecond charged, pulse forming line, switched by a fast oil spark gap, that outputs 0.5-10 ns, ±0-50-kV pulses with an adjustable rise time with a minimum of less than 200 ps (example in Fig. 1) [1]. In addition, we developed high-frequency D-dot and B-dot sensors to measure the (sub)ns pulses [2].

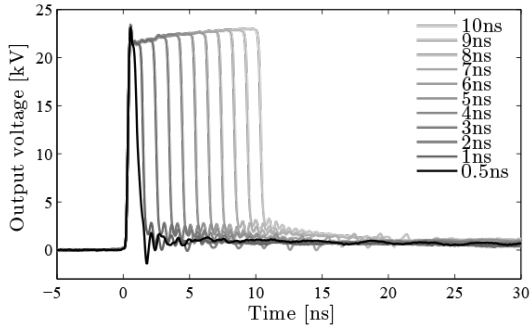

Fig. 1 Example waveforms of the ns pulse source.

3. Transient plasma interaction

In this topic we first studied the energy transfer from the pulse source to the highly dynamic plasma load with the result that we can achieve a very high energy transfer (over 90 %) [3]. Second, we studied the development of the streamer discharges in the plasma reactor with spatiotemporally resolved iCCD imaging [4]. The conclusion from the imaging results is that the development of the streamers is a complex interaction of the length of the plasma reactor and the local voltage in the reactor as a result of the propagation and attenuation of the very short nanosecond pulses.

4. Plasma processing

Finally, we studied ozone generation and NO removal with the nanosecond discharges and found that the shortest rise-time pulses result in the highest plasma processing yields (at the cost of high by-product formation). Figure 2 shows an example. The maximum obtained ozone yield was 190 g/kWh in air and the maximum NO removal yield was 2.5 mol/kWh.

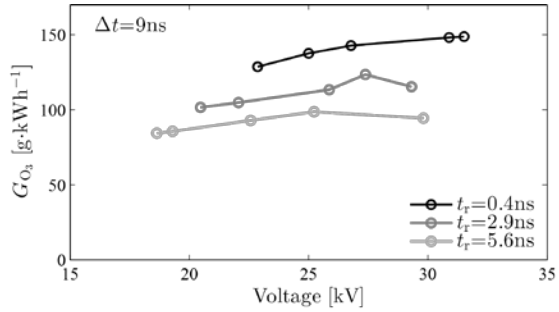

Fig. 2 O_3 yield for 9-ns pulses with different rise times.

5. References

[1] T. Huiskamp *et al.*, IEEE T. Plasma. Sci, **43** (2015) 444-451.

[2] T. Huiskamp *et al.*, IEEE Sens. J., **16** (2016) 3792-3801.

[3] T. Huiskamp *et al.*, Plasma Sources Sci. T., **25** (2016) 054006.

[4] T. Huiskamp *et al.*, Rev. Sci. Instrum., **87** (2016) 123509.

Topic number: 6

Characterization of electronic transport properties of semiconductor films during plasma processing

S. Nunomura, I. Sakata, K. Matsubara

Research center for photovoltaics, National institute of advanced industrial science and technology(AIST), Tsukuba, Ibaraki 305-8568, Japan

The electronic transport properties of hydrogenated amorphous silicon (a-Si:H) film during plasma enhanced chemical vapor deposition (PECVD) have been studied. We find that during PECVD, carrier transport is governed by plasma induced defects located near the surface (< 20nm). On the other hand, trapped carriers are distributed not only in the defect rich surface layer but also in the bulk layer. The origin for carrier trapping is recognized to be the band tail states, rather than the deep level defect states, associated Si dangling bonds.

Carrier transport is an key factor that determines the performances of semiconductor devices such as solar cells and transistors. Particularly, in those devices including amorphous materials of semiconductors, the transport is limited by carrier trapping, related to various defects and impurities. So far, the transport and trapping phenomena have been studied mainly for as-grown films or devices at room temperature. However, those have not been studied under plasma processing, even though the defects are usually created under plasma processing. Here, we study the electronic transport properties of a-Si:H film during PECVD [1].

We measured the photo and trap-induced currents in a-Si:H film growing on a glass substrate during PECVD [2]. These currents are measured under pump (532 nm, 0.4mW) and probe (1432 nm, 500mW) light. The pump generated photoexcited carriers and filled the traps, whereas the probe was used to emit trapped carriers to the conduction band. These carriers were then collected by the interdigitated contacts on the glass substrates.

The measured optoelectronic properties of a-Si:H films during PECVD are shown in Fig. 1. It is confirmed that the thickness, d, is nicely proportional to the growth time, t, while the optical constants stay nearly constant. The growth rate and optical constants are 0.17 nm/s, E_g = 1.61 eV, n = 4.6, and k = 0.45 at 532 nm. Figure 1 (c) shows the time evolution of photo and trap currents, I_p and I_t. Interestingly, both currents remain nearly zero at an initial stage of growth (t < 120 s, i.e., d < 20 nm) and then increase gradually with t. The photoconductivity, σ_p, is improved with t, as shown in Fig. 2(d). Such time evolutions suggest that a defect-rich surface layer is formed initially, and then the bulk layer is grown underneath it. This defect-rich surface layer is evaluated to be less than 20 nm. The time evolution of trapped carrier density, n_t/n_v, determined from I_t/I_p [3] is shown in Fig. 2(d). We find that n_t/n_v stays roughly constant as the film grows with t. The result indicates that the trapped carriers are distributed homogeneously along the direction of growth. The absolute density of trapped carriers is the order of 10^{17} cm^{-3} for the device grade intrinsic a-Si:H [2]. In the talk, the correlation between transport properties and device performances will be also presented.

[1] S. Nunomura, I. Sakata, M. Kondo, *Appl. Phys. Express*. **6** (2013) 126201.

[2] S. Nunomura and I. Sakata, *AIP Adv.* **4** (2014) 097110.

[3] S. Nunomura, X. Che, and S. R. Forrest, *Adv. Mater*. **26** (2014) 7555.

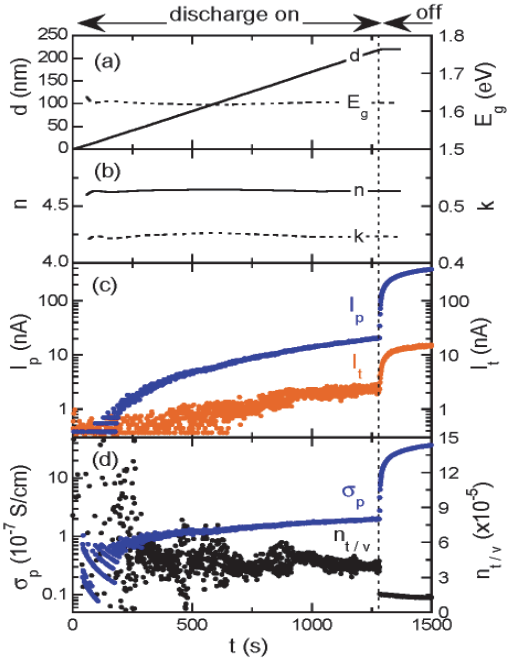

Fig. 1. Opt-electrical properties of a-Si:H film during PECVD. (a) Thickness, d, and optical bandgap, E_g. (b) refractive index, n, and extinction coefficient, k. (c) photo and trap currents, I_p and I_t. (d) photoconductivity, σ_p, and the normalized trapped carrier density, n_t/n_v,

Two-dimensional plasma crystals: waves and instabilities

L. Couëdel[1], V. Nosenko[2], S. Zhdanov[2], I. Laut[2], A. V. Ivlev[3], E. V. Yakovlev[4], A. Y. Kislov[4], S. O. Yurchenko[4], and A. M. Lipaev[5]

[1] *CNRS, Aix-Marseille-Université, Laboratoire PIIM, UMR 7345, Marseille, France.*
[2] *Institut für Materialphysik im Weltraum, Deutsches Zentrum für Luft- und Raumfahrt (DLR), Weßling, Germany.*
[3] *Max Planck Institute for extraterrestrial Physics, Garching b. München, Germany.*
[4] *Bauman Moscow State Technical University, Moscow, Russia.*
[5] *Joint Institute for High Temperatures, Russian Academy of Sciences, Moscow, Russia.*

Wake-mediated interactions result in the coupling between wave modes in 2D complex plasma crystals, which can trigger the mode-coupling instability and cause melting. Spectra of phonons with out-of-plane polarization were studied experimentally in 2D plasma crystals during dedicated experiments on the mode-coupling instability. The kinematics of dust particles during the early stage of mode-coupling induced melting is explored. It is found that the formation of the hybrid mode causes the particle vibrations to partially synchronize at the hybrid frequency. The spatial orientation of the synchronization pattern correlates well with the directions of the maximal increment of the shear-free hybrid mode.

Complex plasmas consist of particles immersed in a weakly ionised plasmas. Due to the absorption of ambient electrons and ions, microparticles acquire negative charges and can form coupled systems. Microparticles injected in capacitively-coupled radio-frequency discharges levitate in the sheath region near the bottom electrode, where the electric field can balance gravity. Under certain conditions the particles can form a monolayer and arrange themselves into ordered structures: 2D plasma crystals. In such crystals, two in-plane wave modes with an acoustic dispersion can be sustained (longitudinal and transverse modes). Since the strength of the vertical confinement is finite, there is a third fundamental wave mode associated with the out-of- plane oscillations that has a negative optical dispersion [1]. Due to the strong electric field in the sheath region, every particle is influenced by a strong ion flow. The ions tend to focus downstream of the particles making the system highly polarized (plasma wake). In 2D plasma crystals, wake-mediated interactions result in the coupling of the crystal in-plane and out-of-plane modes into a shear-free hybrid mode of the lattice layer and trigger the mode-coupling instability (MCI) [1, 2, 3] which can melt the crystal [4]. Localised "hot spots" in the lattice phonon spectra are a typical signature of this mode [1, 3]. MCI induced melting can only be triggered if (i) the modes intersect, and (ii) the neutral gas damping is sufficiently low.

In this paper, spectra of phonons with out-of-plane polarisation were studied experimentally in 2D plasma crystals. The dispersion relation was directly measured using a method of particle imaging that allowed us to resolve the particle motion in the 3 dimensions. We observed experimentally the coupling between the out-of-plane mode and the in-plane longitudinal mode which under certain conditions can form hybridised modes and trigger the MCI[5, 6]. The kinematics of dust particles during the early stage of MCI revealed that the formation of the hybrid mode induces the partial synchronisation of the particle oscillations at the hybrid frequency [7, 8]. Phase- and frequency-locked hybrid particle motion in both vertical and horizontal directions was evidenced. The spatial orientation of the synchronisation pattern correlates well with the directions of the maximal increment of the shear-free hybrid mode. Asymmetries observed in the current fluctuation spectra come from inhomogeneities of the horizontal confinement [8]. A theory of MCI in shear-deformed crystals explains the asymmetry of hot spots[9].

References

[1] S. K. Zhdanov, et al., Phys. Plasmas **16** (2009), 083706.
[2] A. V. Ivlev, G. Morfill, Phys. Rev. E **63** (2001), 016409.
[3] L. Couëdel, et al., Phys. Plasmas **18** (2011) 083707.
[4] J. D. Williams, et al., Phys. Rev. E **86** (2012), 046401.
[5] L. Couëdel, et al., Phys. Rev. Lett. **104** (2010), 195001.
[6] L. Couëdel, et al., EPL **115** (2016), 45002.
[7] L. Couëdel, et al., Phys. Rev. E **89** (2014), 053108.
[8] I. Laut, et al., EPL **110** (2015), 65001.
[9] A. V. Ivlev, et al., Phys. Rev. E **91** (2015), 063108.

Topic 1

Reactivity, relaxation and dissociation of molecules in plasma modeling

Fabrizio Esposito[1]

[1]*Consiglio Nazionale delle Ricerche, PlasmiLab@Nanotec, Bari, Italy*

Detailed information on the dynamics and kinetics of molecular collisions are of key importance in accurate modeling of aerothermodynamics, combustion, laser and plasma physics. A discussion of the relevant problems, solutions and achievements will be presented, taking into account the need of complete data in the plasma modeling community.

1. Vibrational kinetics: the input data

In the plasma community it is nowadays well recognized the key role of vibrational energy exchanges among molecular species in plasmas [1]. Non-equilibrium conditions including vibrational energy are commonly studied in this field, and this implies the use of state-to-state (sts) data for all the relevant species of interest. In the past, simple models of vibrational energy transfer and dissociation from excited vibrational states have been used for this aim, and often continue to be used. However, it is now possible to calculate sts data accurately, with reasonable amounts of computational resources and with accurate interaction potentials [2,3,4]. These data can also include reaction, with production of new species with vibrational distributions quite different from the purely inelastic data. The insights and possibilities offered by these accurate and detailed data will be shown, with particular emphasis on the differences with simple models. Different methods are available, with specific features that have to be wisely studied, exploited and merged in order to get the most accurate and complete results [1,5], without neglecting the computational efficiency, which is a strict requirement, due to the large mass of calculations involved. A discussion about the use of these methods for both vibrational energy exchange with and without reaction and dissociation will be presented.

2. References

[1] M.Capitelli, R.Celiberto, G.Colonna, F.Esposito, C.Gorse, K.Hassouni, A.Laricchiuta, S.Longo, Fundamental Aspects of Plasma Chemical Physics. Springer New York (2016). Available from: http://link.springer.com/10.1007/978-1-4419-8185-1

[2] R.Celiberto, I.Armenise, M.Cacciatore, M. Capitelli, F.Esposito, P.Gamallo, R.K.Janev, A.Laganà, V.Laporta, A.Laricchiuta, A.Lombardi, M.Rutigliano, R.Sayós, J.Tennyson and J.M Wadehra, Atomic and molecular data for spacecraft re-entry plasmas. Plasma Sources Science and Technology. **25** (2016) 033004.(doi: 10.1088/0963-0252/25/3/033004)

[3] G.D'Ammando, M.Capitelli, F.Esposito, A.Laricchiuta, L.D.Pietanza, G.Colonna. The role of radiative reabsorption on the electron energy distribution functions in H_2/He plasma expansion through a tapered nozzle. Physics of Plasmas. **21** (2014) 093508.(doi: 10.1063/1.4895481)

[4] M.Capitelli, D.Bruno, C.Catalfamo, R.Celiberto, G.Colonna, C.M.Coppola, G.D'Ammando, O.De Pascale, P.Diomede, F.Esposito, C.Gorse, A.Laricchiuta, S.Longo, and F.Taccogna, in *Atomic and Plasma–Material Interaction Data for Fusion* (International Atomic Energy Agency, Vienna, 2014), pp. 24–36 (http://www-pub.iaea.org/MTCD/publications/PDF/apid16_web.pdf)

[5] F.Esposito, C.M.Coppola, D.De Fazio. Complementarity between Quantum and Classical Mechanics in Chemical Modeling. The H + HeH^+ → H_2^+ + He Reaction: A Rigourous Test for Reaction Dynamics Methods. The Journal of Physical Chemistry A. **119** (2015) 12615−12626 (doi: 10.1021/acs.jpca.5b09660)

Plasma generation and processing of interstellar carbonaceous dust analogs

V. J. Herrero[1], I. Tanarro[1], B. Maté[1], R. J. Peláez[1], G. Molpeceres[1], V. Timón[1], R. Escribano[1], and M. Jiménez-Redondo[2]

[1] *Instituto de Estructura de la Materia (IEM-CSIC), Serrano 121-123, 28006, Madrid, Spain*
[2]*Centro de Física da Universidade do Minho, Universidade do Minho, 4710-057, Braga, Portugal*

Different samples of plasma deposited amorphous hydrogenated carbon (HAC or a-C:H) are used as analogs of carbonaceous dust in the diffuse interstellar (IS) medium. Comparison of measured and theoretically calculated spectra suggests that IS dust grains are likely made of small aromatic islands linked by aliphatic chains. Irradiation of the HAC deposits with 5 keV electrons shows that the effects of cosmic rays on the aliphatic dust component, characterized by an absorption band at 3.4 μm, are small and cannot explain the disappearance of this band in dense interstellar clouds.

1. Introduction

IR absorption spectra indicate that carbonaceous dust in the diffuse IS medium is largely made of some sort of amorphous hydrogenated carbon (HAC). Two alternative models for the structure of this dust can be found in the literature. One of them favors small aromatic islands linked by aliphatic chains [1], whereas the other one proposes large polyaromatic structures with small aliphatic substituents at the edges [2].

The most prominent spectroscopic feature of the aliphatic component of IS carbonaceous dust (the 3.4 μm absorption band) disappears inside dense molecular clouds. In this environment, shielded from the UV galactic field, cosmic rays (CR) could provide a destruction mechanism, but again discrepant CR destruction efficiencies are found in the literature [3, 4].

In this work, we use IS carbonaceous dust analogs produced in cold hydrocarbon plasmas in combination with theoretical calculations and irradiation with high energy electrons to help clarify these questions.

2. Experimental

Dust grains and thin films of HAC were generated by plasma deposition in RF discharges. Mixtures of hydrocarbons and He were used as plasma precursors. The deposition conditions were selected to obtain HAC films with a variable proportion of aliphatic and aromatic structures.

Optical spectroscopy, mass spectrometry and Langmuir probes were used for plasma diagnosis. HAC deposits were analyzed mainly with IR spectroscopy, but other techniques (SEM, AFM, ...) were also used.

The effects of cosmic rays on the carriers of the 3.4 μm feature were investigated by irradiating the HAC samples with 5 keV electrons.

3. Theoretical calculations

Models of HAC solids of variable density, based on the mentioned competing structures [1,2], were constructed using Montecarlo/Molecular Mechanics and their electronic energies and IR spectra were computed at Density Functional Theory (DFT) level.

4. Results and conclusion

The comparison of measured and calculated IR spectra [5] suggests that the structure of carbonaceous dust in the diffuse IS medium is intermediate between those of the two literature models [1,2] but closer to that with small aromatic units [1].

The estimated effects of cosmic rays are found to be small and are not enough to explain the disappearance of the 3.4 μm band inside dense clouds [6].

At present, we intend to relate the gas-phase characteristics of the plasma with the properties of the carbonaceous solids produced in the discharges. We expect thus to shed light on gas phase polymerization mechanisms that might be of relevance for the interstellar medium.

5. References

[1] E. Dartois et al. A&A **432** (2005) 895
[2] M. Steglich et al. ApJSS **208** (2013) 26
[3] V. E. Mennella et al. ApJ. **587** (2003) 727
[2] M. Godard et al., A&A, **529** (2011) A146
[5] G. Molpeceres et al. PCCP **19** (2017) 1352
[6] B. Maté et al. ApJ **831** (2016) 51

Modelling and interpretation of micrometric dust behaviour in tokamaks

E. Lazzaro[1], F. Ghezzi[1], A. Uccello[1], G. Gervasini[1], M. De Angeli[1]

[1] *Istituto di Fisica del Plasma – CNR, Milan, Italy*

As tokamak devices approach more closely and reliably the technical conditions required for confinement of a deuterium-tritium burning plasma, it becomes clear that optimization of the plasma performance requires better understanding of important physics processes occurring in the scrape-off layer which is actually a "composite" plasma, consisting of multiple ion species and heterogeneous dust with variable charge and mass. A number of questions are addressed by numerical models, concerning the mobilization of dust from the plasma facing components, its migration and redeposition in the tokamak configuration and eventually its destiny of ablation and plasmoid formation. A brief overview of selected problems is presented here, with an assessment of the most interesting results and open questions, especially focused on the tungsten and beryllium dust particles in the tokamak JET-ILW (ITER-like wall).

The performance of magnetic confinement nuclear fusion systems, like tokamaks, depends significantly on the "purity" of the reacting mixture (Z_{eff} not » 1). Realistic confinement implies some interaction of the thermonuclear plasma with the tokamak's wall thorough the plasma facing components (PFCs), mainly leading to PFCs sputtering and eventually to the production of mobilizable solid particulate or dust [1].

The expected number density of these particles is low, but they can be important sources of plasma contamination through input of high Z elements, causing strong radiative losses (observed often as transient impurity events, TIEs) and also gross magnetohydrodynamic instabilities eventually evolving in disruptions. Alternatively, their impact and interaction with the PFCs can cause the damage of their surface, instantaneous and cumulative. Moreover, these meso-sized dust particles can retain the radioactive tritium (T) and, moving almost freely within the vessel, could significant affect the T inventory of the tokamak.

Validated numerical modeling tools such as dust trajectory calculators [2-4], can provide qualitative and quantitative description of the mobilization and fate of selected bunches of dust grains. Key issues are addressed here in a first investigation of tungsten (W) and beryllium (Be) dust mobilization, redeposition and plasma pollution in the tokamak JET-ILW (i.e. ITER-like wall).

The results presented are produced by the dust trajectory code DUSTTRACK [2,3] of IFP-CNR, based on real and realistic background plasma configurations of JET-ILW. Figure 1 shows a pragmatic example of the output of the code relative to the motion of several tungsten dust particles mobilized from the JET-ILW's full-W divertor. On one hand, it is clear that several dust particles can reach the hot and confined plasma (the region inside the last closed magnetic surface, LCMS) significantly polluting it. On the other hand, one can see that the dust particles could be transported and finally deposited in places far away from their mobilization spot. In case of dust particles with a high fraction of T, this can be particularly relevant since their behaviour possibly affects the tokamak's inventory of tritium.

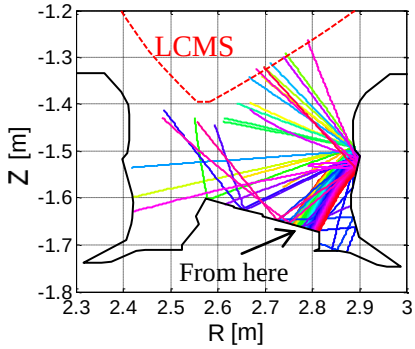

Fig.1: Poloidal trajectories of 101 W dust particles launched from the divertor of JET-ILW.

References

[1] J. Sharpe, et al., Fusion Eng. Des. **63-64** (2002) 153.

[2] A. Uccello, et al., Phys. Plasmas **23** (2016) 102506.

[3] G. Gervasini, et al., J. Fusion Energ. **36** (2017) 25-39.

[4] M. Bacharis, et al., Phys. Plasmas **17** (2010) 042505.

Non-conventional plasma and sheath diagnostics: force probes and calorimetric probes

Thomas Trottenberg and Holger Kersten

Institute of Experimental and Applied Physics, University of Kiel, D-24098 Kiel, Germany

The talk focusses on measurements of forces that low-temperature plasmas exert on a boundary. Two different discharge types are used: a microwave generated plasma and a parallel plate radio-frequency discharge. The force measuring probe uses a small test surface integrated into a grounded wall or a grounded electrode, respectively. It is found that the plasma exerts pressures in the order of magnitude of the electron pressure in front of the wall, where the plasma pressure can range from below the electron pressure to a few times the electron pressure. Moderate collisions in the plasma seem to enhance the pressure at the wall, whereas too many collisions reduce the pressure. A recently published model is discussed. Furthermore, another non-conventional diagnostic, the calorimetric probe, is shortly presented together with measurements.

Recently, we reported on simple experiments that allowed measurements of the forces exerted by low-temperature plasmas on boundaries [1,2]. The measured "plasma pressures" were in the order of magnitude of up to a few times the electron pressure close to the sheath edge, i.e. some 10 mPa.

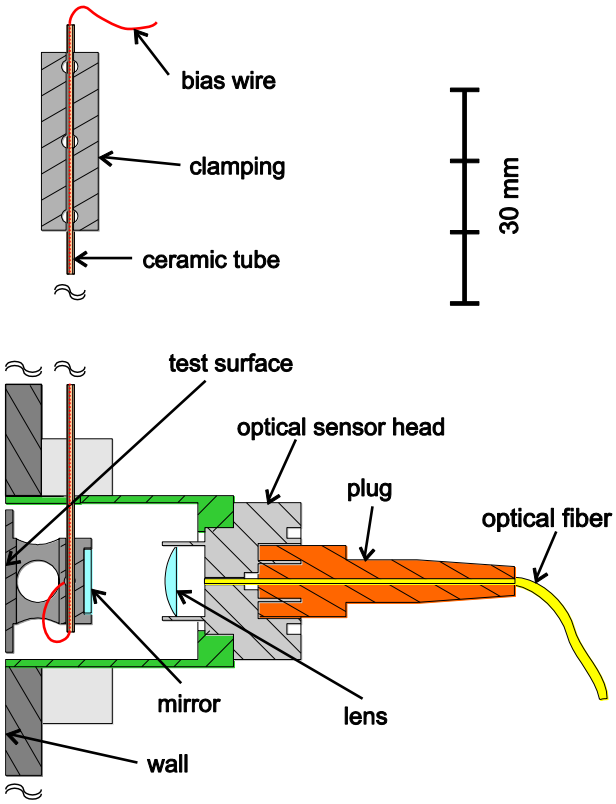

Fig. 1. Metal wall or electrode with integrated force probe. Only a small detail of the 170 mm disk is shown.

The forces were discussed on the basis of a simple model taking into account the momentum fluxes across the sheath edge. It was concluded that ion-neutral collisions in the presheath can enhance the force caused by electron pressure and ion flux by a larger accelerated mass consisting of ions and fast neutral atoms.

The force probe is based on a cantilever and a test surface attached to its free end. The displacement is measured interferometrically and translated into the causing force by calibration. Figure 1 shows the implementation of the wall with probe. The circular test surface is flush with front surface of the wall. Langmuir probes are used for the basic diagnostics of the plasma environments (microwave plasma and radio-frequency parallel plate discharge).

The measurements are discussed in the light of a model for plane geometry [3].

Currently, we are working on the application of additional diagnostics (retarding field analyzer and calorimetric probe), which are integrated in the wall similarly to the force probe.

References

[1] T. Trottenberg, T. Richter, and H. Kersten. Eur. Phys. J. D **69**, 91 (2015).

[2] T. Trottenberg and H. Kersten. Plasma Sources Sci. Technol., accepted for publication (2017).

[3] U. Czarnetzki and T. V. Tsankov, Eur. Phys. J. D **69**, 236 (2015).

Diagnostics of atmospheric pressure plasma jets

A. West, J. Bredin, S. Schröter, K. Niemi, T. Gans, J. Dedrick, D. O'Connell, E.Wagenaars

York Plasma Institute, Department of Physics, University of York, York, YO10 5DD, UK

Atmospheric-pressure plasma jets (APPJs) are widely studied for potential applications in industry and healthcare. Plasma diagnostics play a pivotal role in developing an understanding of the science underpinning APPJs. This is essential to guarantee effective and safe use of these devices in applications. We present a picosecond Two-photon Absorption Laser Induced Fluorescence technique that is capable of directly measuring the effects of collisional quenching on the fluorescence decay and therefore allows accurate, absolute measurements of densities of N and O radicals in the open-air effluent of an APPJ. Additional power measurements allow the study of energy efficiency of N and O generation in APPJs as a function of operating frequency.

1. Introduction

Atmospheric-pressure plasma jets (APPJs) are examples of plasmas that can operate in open air, remain at room temperature and still have a non-equilibrium chemistry. The unique combination of characteristics of these APPJ devices makes them ideal tools for novel applications in industry and healthcare, e.g. surface modification of plastics, plasma medicine and photoresist removal [1-3]. Although it is clear that reactive species play a pivotal role in the success of APPJs in many applications, the exact mechanisms through which APPJs affect target surfaces remain largely unknown. Moreover, control of the mixture of reactive species production as a function of operational parameters is often empirical. Diagnostics of APPJs play an important role in further developing our understanding of the plasma chemistry and will enable increases in treatment efficacy.

2. Picosecond Two-photon Absorption Laser Induced Fluorescence

Two-photon Absorption Laser Induced Fluorescence (TALIF) is a well-known technique in low-pressure plasmas for the measurement of absolute densities of atomic species such as O, N and H. Unfortunately, application of this technique on APPJs that are operating under realistic conditions for applications, i.e. in open air and with complex admixtures, is not straightforward. The highly collisional environment of APPJs means that collisional quenching of the laser-excited state becomes significant and needs to be taken into account. For well-controlled atmospheres and simple admixtures the effect can be estimated using quenching coefficients [4], however under realistic operating conditions the identity and density of the quenching partners is unknown due to the complexity of the plasma chemistry. An alternative is a direct measurement of the fluorescence decay on sub-nanosecond timescales. We present a picosecond TALIF diagnostic which uses a sub-ns laser (30 ps) and iCCD camera (200 ps), which allows us to measure the quenching-affected fluorescence decay rate directly and deduce absolute measurements of O and N density maps in the open-air effluent of an APPJ.

3. Power measurements

Measurements of the power dissipated in the plasma are of critical importance not only for further developing our understanding of APPJs, e.g. via comparison with modelling, but also in applications, e.g. for the optimisation of energy efficiency. Conceptually, measuring power in a radio-frequency (rf) circuit is relatively straightforward; however in practice it often turns out to be difficult to perform these measurements due to the small powers dissipated and the mostly capacitive nature of the load. We present a flexible, 'post-matching' technique that is capable of providing accurate measurements of power dissipated in rf-driven APPJs. This diagnostic is subsequently used to investigate the efficiency of the production of reactive O and N species for different rf excitation frequencies (13.56 MHz - 40.68 MHz).

4. Acknowledgments

The authors acknowledge support from the UK EPSRC (EP/K018388/1 & EP/H003797/1)

5. References

[1] D. Shaw et al., Plasma Sources Sci. Technol. **25** (2016) 065018.
[2] A.M. Hirst et al., Br. J. Cancer **112** (2015) 1536.
[3] A. West et al., Plasma Sources Sci. Technol. **25** (2016) 02LT01.
[4] E. Wagenaars et al., Plasma Sources Sci. Technol. **21** (2012) 042002.

Microhollow cathode discharges on silicon devices

R. Dussart[1], R. Michaud[1], V. Felix[1], A. Stolz[1], O. Aubry[1], P. Lefaucheux[1] , S. Dzikowski[2], V. Schulz-von der Gathen[2], L.J. Overzet[3]

[1] *GREMI, Univ. Orleans - CNRS, 14 rue d'Issoudun, BP 6744, 45067 Orléans, France*
[2]*Experimental Physics II, Ruhr-Universität Bochum, 44780 Bochum, Germany*
[3]*PSAL, University of Texas at Dallas, Richardson, TX 75080-3021, USA*

DC Microhollow cathode discharges have been produced on silicon platforms through different gases such as He, Ar and N_2. Silicon cathodes were investigated first, but induced many instabilities. Other materials deposited on the silicon were also tested and show much different behaviours. The microplasmas were optically and electrically characterized. The microreactors were also characterized after operation by SEM observations. Some new geometries were also tested to allow the injection of higher currents and powers (up to 1 W per microdicharge). By inversing the polarity, a quite different behaviour was evidenced that will be discussed as well.

1. Introduction

DC Microhollow cathode discharges (MHCD) were first introduced in the mid 90's [1]. Due to their dimension and their large surface to volume ratio, the produced microplasma remains cold and can stably operate at atmospheric pressure in the normal regime provided the cathode area is not fully utilized [2]. Microhollow cathode discharges on silicon platforms were first studied by J. G. Eden's group [3]. Silicon processing intensively developed for microelectronic devices offers many opportunities to design new, original and efficient devices to produce high density microplasmas.

An array of 1064 microplasmas using an etched silicon cathode could be completely ignited [4]. Unfortunately, the device operation is unstable and produces many current spikes that significantly damage the microcavities and lead to device failure. The mechanism responsible for this unstable operation and short lifetime was investigated [5]. In this paper, we discuss different possibilities to enhance the stability of microdischarges made from silicon wafers.

2. Experiment

A microreactor is schematically represented in Fig. 1. A ballast resistor is used to limit the current.

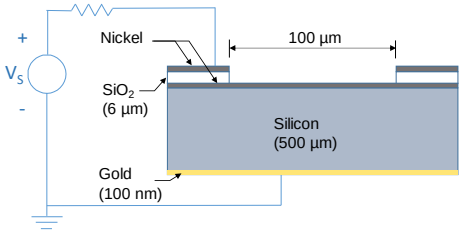

Figure 1: Schematic of a microdischarge reactor

In this particular configuration, the silicon cathode was covered by a metal thin film (nickel in this example). More than 15 individual process steps are necessary to create such a structure. The devices were then tested in 3 different gases: He, Ar and N_2.

3. Results

An example of a microdischarge operating in Argon (150 µm diameter cavity) is shown in Fig. 2. A very stable operation is obtained using the configuration shown in Fig. 1. The lifetime of the microreactor with a confined cathode is much longer when using nickel than with silicon. Other materials were also investigated. Interestingly, the same type of instability is obtained using a tungsten cathode as with silicon. Modifying the geometry, it was possible to inject a total power of up to 40 W in an array of 38 argon microplasmas.

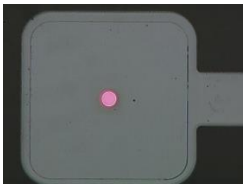

Figure 2: Single microdischarge operating in Argon.

In the case of inverted polarity, a bright spot appears in the middle of the cavity.

4. References

[1] K.H. Schoenbach *et al.,* Appl. Phys. Lett. **68** (1996) 13–15
[2] T. Dufour *et al.* , Appl. Phys. Lett. **93** (2008) 71508
[3] J.G. Eden *et al.*, J. Phys. D: Appl. Phys. **36** (2003) 2869–77
[4] M.K. Kulsreshath *et al.,* J. Phys. D: Appl. Phys. **33** (2012) 285202
[5] V. Felix *et al.*, PSST 25 (2016) 025021

Recent developments in probe diagnostics

C. Ionita[1], B.S. Schneider[1], S. Costea[1], J. Kovačič[2], M. Spolaore[3], V. Naulin[4], N. Vianello[3], J.J. Rasmussen[4], T. Gyergyek[2,5], R. Stärz[1,6], R. Schrittwieser[1]

[1]*Institute for Ion Physics and Applied Physics, University of Innsbruck, Austria*
[2]*Reactor Physics Department, Jožef Stefan Institute, Ljubljana, Slovenia*
[3]*Consorzio RFX, Padua, Italy*
[4]*Department of Physics, Technical University of Denmark, Kgs. Lyngby, Denmark*
[5]*Faculty of Electrical Engineering, University of Ljubljana, Slovenia*
[6] *Mechatronic Department, Management Center Innsbruck. A-6020 Innsbruck, Austria*

Plasma probes are well established diagnostic tools. The easiest and fastest accessible parameter is their floating potential. While the floating potential of a cold probe is not very significant, we report on probes with the floating potential close to or ideally equal to the plasma potential. Such probes can either be electron emissive probes or so-called electron screening probes (e.g. ball-pen probes). We have developed strong emissive probes and a new type of electron screening probe, the bunker probe. By arrays of such probes also the electric field can be determined.

1. Introduction

Plasma probes are simple and inexpensive with good spatial and temporal resolution. The easiest measureable parameter of a probe is its floating potential V_{fl}, which in case of a Cold Langmuir Probe (CLP) is of limited value since V_{fl} will regularly be more negative than the more important plasma potential Φ_{pl}.

We developed Plasma Potential Probes (PPP) the floating potential of which is close or even equal to Φ_{pl}. The best known are Electron Emissive Probes (EEP). Other types are the Ball-Pen Probe (BPP) [1] and the novel BUnker Probe (BUP) [2].

2. Plasma Potential Probes (PPP)

To shift the floating potential of a probe as close as possible to Φ_{pl}, (i) the inflowing plasma electron current must be compensated by an approx. equal emission current or (ii) the surplus of electron current must be screened off the probe until its magnitude roughly equals that of the ions. This is tantamount to making the probe's current-voltage characteristic (*IV*-trace) symmetric. Method (i) is realised in EEPs by heating the probe until sufficient electron emission; (ii) can only be attained in a strong magnetic field as in case of the BPP or the BUP.

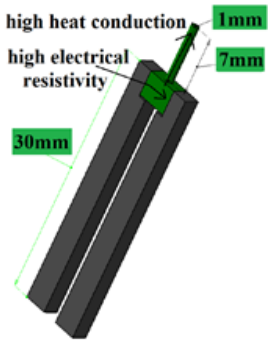

Fig. 1: Electron Emissive Probe

2.1. Electron Emissive Probes (EEP)

Our novel strong and robust EEP [3] takes favourable use of the basic properties of Highly Orientated Pyrolytic Graphite (HOPG). An indirectly heated HOPG pin is shown in Fig. 1. HOPG has strongly different values of electric resistivity and heat conduction in directions perpendicular to each other as indicated in Fig. 1.

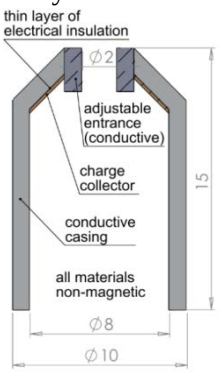

Fig. 2: Bunker probe

2.2. Electron Screening Probes (ESP)

For a BPP to work properly it must be quite exactly aligned perpendicular to the magnetic field ***B***. In contrast to that, our novel BUP (Fig. 2) floats on the plasma potential also for a much larger range of angles with respect to ***B***.

3. Acknowledgement

This work has been carried out within the framework of the EUROfusion Consortium and has received funding from the EURATOM research and training programme 2014-2018 under Grant Agreement No. 633053. The views and opinions expressed herein do not necessarily reflect those of the European Commission. This work was also supported by the Friedrich Schiedel Foundation for Energy Technology and the Commission for the Coordination of Nuclear Fusion Research in Austria (Austrian Academy of Sciences).

4. References

[1] J. Adamek et al. Czech. J. Phys. **55** (2005) 235.

[2] S. Costea et al., Rev. Sci. Instrum. **87** (2016), 053510.

[3] B.S. Schneider et al., Proc. Sci., on line: http://pos.sissa.it/archive/conferences/240/072/ECPD2015_072.pdf.

Electric field measurements in surface discharges in atmospheric air over solid and liquid dielectrics

M. Simeni Simeni[1], B.M. Goldberg[2], C. Zhang[3], K. Frederickson[1], W.R. Lempert[1], and I.V. Adamovich[1]

[1] *Department of Mechanical and Aerospace Engineering, Ohio State University*
[2] *Department of Mechanical and Aerospace Engineering, Princeton University*
[3] *Institute of Electrical Engineering, Chinese Academy of Sciences, Beijing, China*

Time-resolved and spatially resolved electric field is measured in ns pulse dielectric barrier discharges sustained in ambient air over solid and liquid dielectric surfaces. The measurements are done using ps four-wave mixing diagnostics. The results indicate significant electric field reduction following ns pulse breakdown, followed by electric field reversal as the applied voltage is reduced. After the discharge pulse, the electric field decays on microsecond time scale, due to surface charge neutralization. The present results yield quantitative insight into kinetics of ns pulse surface ionization wave discharges and provide detailed experimental data for validation of kinetic models of ns pulse surface discharges.

This work presents the results of temporally and spatially resolved electric field measurements in a nanosecond pulse discharge in atmospheric air, sustained between a razor edge high-voltage electrode and a plane grounded electrode covered by a thin dielectric plate or a by a layer of distilled water. The electric field is measured by picosecond four-wave mixing in a collinear phase-matching geometry, with time resolution of approximately 2 ns, using an absolute calibration provided by measurements of a known electrostatic electric field. In discharges over quartz plate and over liquid surface, the results demonstrate electric field offset on the discharge center plane before the discharge pulse due to surface charge accumulation on the dielectric from the weaker, opposite polarity pre-pulse. During the discharge pulse, the electric field follows the applied voltage until "forward" breakdown occurs, after which the field in the plasma is significantly reduced due to charge separation. When the applied voltage is reduced, the field in the plasma reverses direction and increases again, until the weak "reverse" breakdown occurs, producing a secondary transient reduction in the electric field. After the pulse, the field is gradually reduced on a microsecond time scale, likely due to residual surface charge neutralization by transport of opposite polarity charges from the plasma. Spatially resolved electric field measurements show that the discharge develops as a surface ionization wave. Significant surface charge accumulation on the dielectric surface is detected near the end of the discharge pulse. Spatially resolved measurements of electric field vector components demonstrate that the vertical electric field in the surface ionization wave peaks ahead of the horizontal electric field. Behind the wave, the vertical field remains low, near the detection limit, while the horizontal field is gradually reduced to near the detection limit at the discharge center plane. These results are consistent with time-resolved measurements of electric field components, which also indicate that vertical electric field reverses direction after the ionization wave.

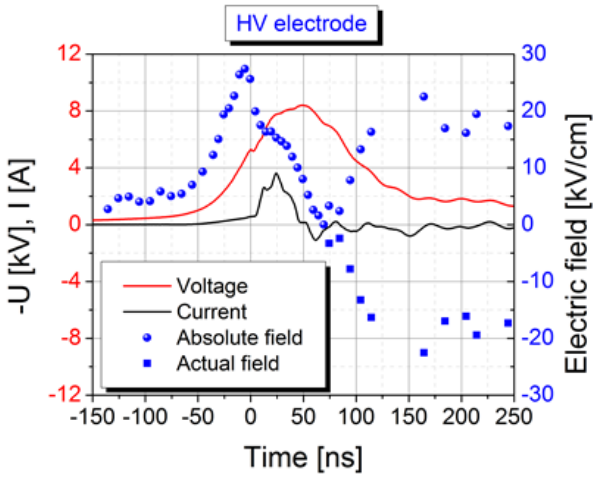

Figure 1. Time-resolved electric field measured in the negative polarity ns pulse discharge pulse over liquid water, on the discharge center plane ~ 100 μm below the high-voltage electrode.

Specific plasma phenomena in magnetron sputtering systems

P. Baroch, J. Vlček and J. Musil

Department of Physics and NTIS - European Centre of Excellence,
University of West Bohemia, Plzen, Czech Republic

The main aim of this work is to show recent developments and specific phenomena in the field of magnetron sputtering technology. In the first part we will focus on the basic principles of reactive HiPIMS method with a feedback pulsed reactive gas flow control and an optimized location of the reactive gas inlets providing the possibility to produce high-quality oxynitride films with a tunable elemental composition, structure and properties at very high deposition rates. In the second part we will focus on the dual magnetron sputtering systems which belong to advanced sputtering methods solving problems of disappearing anode and partially also arcing. Recently, a specific plasma drift has been discovered in the dual magnetron system with tilted magnetrons and we will discuss specifics, properties and consequences of this phenomenon for thin-films deposition.

High-power impulse magnetron sputtering (HiPIMS) methods currently constitute an intensively developing area of magnetron sputtering technologies. However, deposition of dielectric oxide coatings using HiPIMS at high-powers (a peak value of the target power density of up to several $kWcm^{-2}$ in a pulse) is challenging due to significant arcing on the target surface. To avoid this problem and to achieve high deposition rate of the films, our group has proposed a solution based on the reactive HiPIMS with a feedback pulsed reactive gas (oxygen and/or nitrogen) flow control and an optimized location (high-density plasma zone) of the reactive gas inlets in front of the target. It will be shown that this way it was possible to produce high quality Hf-O-N films with a tunable elemental composition, structure and properties at very high deposition rates ranging from 175 nm/min for HfN films to 230 nm/min for HfO_2 films [1]. The method is based on the following principles: i) intense sputtering of atoms from the target resulting in a substantially increased deposition rate, ii) very high degree of dissociation of both O_2 and N_2 molecules in a discharge plasma, resulting in a replacement of O_2 and N_2 molecules, which have very different reactivity with metal atoms on the surface of the growing films, by atomic O and N, which have similar reactivity, and iii) strong "sputtering wind" of the sputtered atoms resulting in a reduced flux of the reactive gas particles onto the target substrate.

In the second part we will focus on the phenomena occurring in the dual magnetron (DM). The DM is an advanced sputtering system which is effectively used for the deposition of thin films, particularly oxides and multiphase coatings [2]. Main advantages of this sputtering source lie in the suppression of arcing on the surface of the magnetron target and in the elimination of the disappearing anode effect, which is an issue in the reactive sputtering of electrically insulating oxides using a single magnetron. In this study we focus on the effect of the polarity of magnets on the performance of the DM, especially on the current-voltage characteristics and the deposition rates. A special attention will be devoted to the effect of the plasma drift [3] on the deposition process. This phenomenon occurs in the DM when the magnetrons are tilted as displayed in the Fig.1.

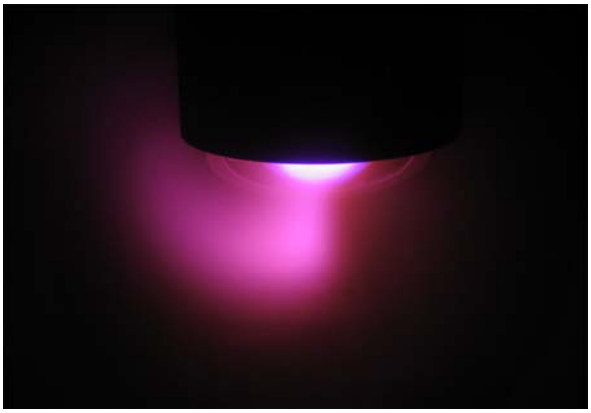

Fig.1. Side view photograph of the dual magnetron with closed magnetic field and tilted magnetrons.

References

[1] J. Vlček, A.Belosludtsev, J.Rezek, J.Houška, J. Čapek, R. Čerstvý and S. Haviar, High-rate reactive HiPIMS of hard and optically transparent HfO_2 films, Surf. Coat. Technol. 290 (2016) 58.

[2] P. Baroch, J. Musil, J. Vlcek, K.H. Nam and J.G. Han, Reactive magnetron sputtering of TiO_x films, Surface and Coatings Technology 193 (2005) 107-111.

[3] P.Baroch and J. Musil, Plasma Drift in Dual Magnetron Discharge - IEEE Transactions on Plasma Science 36 (2008) 1412-1413.

Topic number

Generating EUV light from tin plasma for chip manufacturing

O.O. Versolato[1]

[1] *Advanced Research Center for Nanolithography, Science Park 110, 1098 XG Amsterdam, The Netherlands*

Laser-produced tin plasmas are the prime candidates for the generation of extreme ultraviolet (EUV) light around 13.5 nm wavelength for nanolithography. It is our aim to understand this plasma at the fundamental level. I will present results on the plasma-pressure induced propulsion and hydrodynamic deformation of free-falling liquid-tin microdroplets as well as on charge-state-resolved measurement of highly charged tin ions using an electron beam ion trap.

Laser-produced tin plasmas are the prime candidates for the generation of extreme ultraviolet (EUV) light around 13.5 nm wavelength for nanolithography. This light is generated by atomic transitions in highly charged tin ions Sn^{8+}-Sn^{14+}. Due to the complicated electronic configurations of these charge states, thousands of atomic lines contribute to the emission of EUV light from the hot (~100 eV) and very dense (~10^{21} e/cm^3) plasma. It is our aim to understand this plasma at the fundamental level.

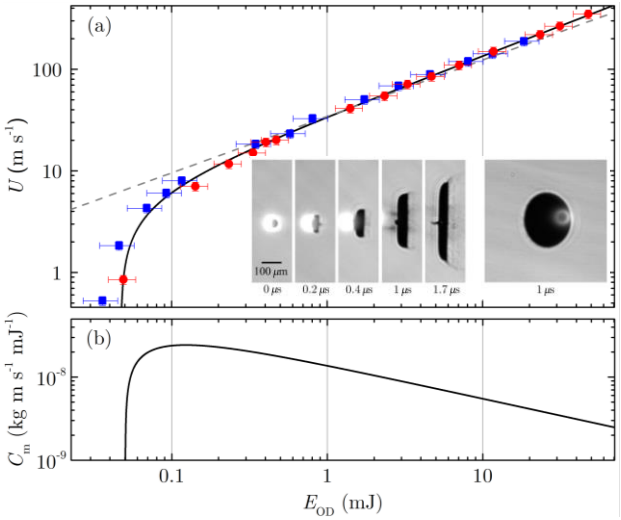

Fig. 1 (a) Propulsion velocity U of molten-metal microdroplets as a function of laser pulse energy E_{OD}. The inset shows shadowgrams of the expanding droplets. (b) Momentum coupling coefficient C_m.

I will present measurements of plasma-pressure induced propulsion and hydrodynamic deformation of free-falling liquid-tin microdroplets (see Fig. 1) by laser pulse impact [1]. These measurements, and the scaling laws obtained from them, serve as precision tests of state-of-the-art plasma simulation and theory predictions. To obtain a better understanding of the atomic processes within the laser generated plasma we performed charge-state-resolved measurement (see Fig. 2) of highly charged tin ions using an electron beam ion trap (EBIT). Combining the EBIT measurements with both the semi-empirical COWAN code as well as ab initio techniques for calculating the level structure, the optical spectra could be assigned [2,3]. We conclude that assignments of EUV transitions in the literature require corrections. EUV and optical spectra are measured simultaneously in the controlled conditions of the EBIT as well as in our microdroplet-based laser-produced plasma source, thus providing information on the contribution of Sn charge states to the EUV emission.

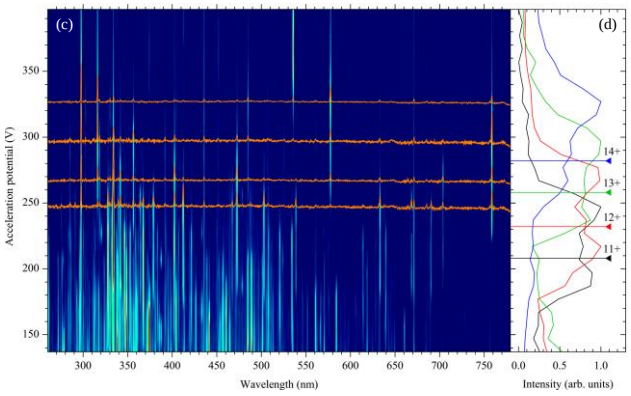

Fig. 2 (c) Composite spectral map from electron beam ion trap (EBIT) spectroscopy of highly charged Sn ions. (d) Fluorescence yield for each charge state as a function of the EBIT's electron beam acceleration potential.

[1] D. Kurilovich *et al*, Phys. Rev. Appl. **6** (2016) 014018

[2] A. Windberger *et al*, Phys. Rev. A **94** (2016) 012506

[3] F. Torretti *et al*, (accepted for publication in Phys. Rev. A) (2016) arXiv:1612.00747

Diagnosing negative ions using electrical probes

S. K. Karkari[1], A. Pandey[1], N. Sirse[2] and M. Turner[2]

[1] *Institute for Plasma Research, HBNI, Bhat village, Gandhinagar, Gujarat, India, Pin 382428*
[2] *Dublin City University, Glasnevin, Dublin-9, Ireland*

Unconventional application of hairpin and Langmuir probes has been demonstrated to quantify negative ion temperature and density in electronegative plasma. This includes the estimation of negative ion temperature based on floating potential of a cylindrical Langmuir probe and inferring negative ion density by resonance hairpin probe in conjunction with pulse laser photo-detachment method. The underlying principle behind these techniques shall be discussed along with experimental findings of plasma parameters in oxygen discharge.

1. Introduction

Electronegative plasmas are highly popular in semiconductor industries besides being used for producing energetic neutral beams for plasma heating in fusion devices. The negative ions presence in the discharge can dramatically influence the characteristic Bohm speed of positive ions entering the sheath and leaving the plasma boundary. The discharge impedance is also impacted due to negative ions. Thus quantification of negative ion parameters is important for characterization of negative ion sources besides being useful in the fundamental studies of negative ion plasmas in laboratory.

The conventional method to measure negative ion density is achieved by pulse laser photo-detachment technique [1]. This method relies on a detection probe to measure the photo-detachment current signal. Though this serves as a basic tool for the quantification of negative ions, however certain complication arises in magnetized plasmas. In this case, the detection probe when biased to electron saturation current severely depletes the plasma electrons in the magnetic flux tubes attached to the probe surface. Therefore estimates of plasma parameters are affected besides the probe introduce strong perturbation to the plasma.

2. Unconventional probing methods to measure negative ions

To overcome above limitation, unconventional probing methods have been developed based on resonance hairpin and cylindrical Langmuir probes.

2.1. Application of Hairpin probe

The hairpin probe is based on microwave technique and has been used for the detection of negative ions both inside and outside the photo-detachment region [3]. Experimental results have shown that the positive ions in the photo-detached channel are strongly depleted after the pulse laser beam has expired [4]. To address the above issue, a direct method of inferring negative ion parameters by hairpin probe has been developed. The negative ion parameters have been inferred by time modulating the dc sheath around the hair-pin prongs [5] with a train of rectangular voltage pulses applied to the hair-pin probe. Synchronous measurement of electron density provides the information of negative ion parameters around the hairpin.

2.3. Negative ion temperature from floating potential of cylindrical probe

Recently, floating potential of a cylindrical probe have been investigated as a function of electronegative parameters $\alpha = n_- / n_e$ and $\gamma = T_e/T_-$; [6]. A comparison of analytical curves of floating potential as a function of α, with γ as a free parameter enables to calculate T_- by tuning the value of γ to match with the floating potential obtained in experiment. Using this method, the negative ion temperature in oxygen discharge has been found in the range of 0.05 – 0.07 eV at operating pressures of 4.0 – 7.0 Pa.

3. References

[1] M. Bacal. Rev. Sci. Instrum, **71**(11) (2000) 3981

[2] S. K. Karkari, C. Gaman, A. R. Ellingboe. APL. **28** (2008) 071501.

[3] N. Sirse, S. K. Karkari, M. A. Mujawar, J. Conway, M. Turner. Plasma Sources Sci. Technol. **20** (2011) 055003

[4] J. Conway, N. Sirse, S. K. Karkari, M.M Turner. Plasma Sources Sci. Technol. **19** (2010) 065002

[5] N. Sirse, S. K. Karkari, M. Turner. Plasma Sources Sci. Technol. **24** (2015) 022001

[6] A. Pandey, S. K. Karkari. Physics of Plasma, **24** (2017) 013507

A point-like discharge, sustained by powerful radiation of terahertz gyrotron

A. V. Vodopyanov, A. V. Sidorov, S. V. Razin, A. G. Luchinin, A. P. Fokin, A. I. Tsvetkov, A. P. Veselov, M. Yu. Glyavin, S. V. Golubev

Institute of Applied Physics of the Russian Academy of Sciences, Nizhny Novgorod, Russia

We propose to use the discharge plasma sustained by terahertz radiation as a source of extreme ultrabviolet light for high-resolution lithography. Experimental studies of the breakdown sustained by terahertz waves in the nonuniform gas jet was performed on two cases: in pulsed mode - the radiation frequency of 670 GHz, pulse duration of 30 μs, power of 50 kW; in CW mode - the radiation frequency of 263 GHz; power up to 1 kW. The plasma density was measured from the Stark broadening of the line H_α. The radiation in the vacuum ultraviolet region was investigated using a calibrated PMT and filters, the radiation in the extreme ultraviolet investigated absolutely calibrated detector with filter sets.

Today micro- and nano- electronics industry requires a source of extreme ultra-violet (EUV) radiation with a wavelength of 13.5 ± 1 % nm for high resolution projection lithography. The power of the source must be at a level of 1 kW at the size of the emitting region of less than 1 mm. One of the most promising sources of EUV light is considered to be a source that uses a pulsed CO_2 laser radiation focused on a specially formed stream of droplets of tin with dimensions of the order of 0.1 mm. However, along with tangible achievements in these light sources have a number of fundamental flaws that do not allow us to consider the problem of creating a EUV light source to be solved.

We propose to use discharge plasma sustained by terahertz radiation as a source of EUV light for high-resolution lithography. In this report we discuss the experimental investigation of two types of EUV sources based on discharge sustained by powerful gyrotron radiation. An increase in plasma density with increasing frequency of the heating wave to the value of 10^{15} cm^{-3} and above makes a plasma resonance heating mechanism effective with small plasma size. The main idea of creating of a point discharge with high emissivity in the required wavelength band is the realization of a breakdown in a nonuniform gas jet with the scale of the inhomogeneity of the order of 1 mm. In this case, breakdown conditions fulfilled only in a small region of space and discharge cannot go beyond it [1-3].

In this work the experimental studies of the breakdown sustained by terahertz waves in the nonuniform gas jet was performed on two cases: in pulsed mode - the radiation frequency of 670 GHz, pulse duration of 30 μs, power of 50 kW; in CW mode - the radiation frequency of 263 GHz; power up to 1 kW. Figure 1 shows the photograph of the point-like plasma in that two cases. The plasma density was measured from the Stark broadening of the line H_α.

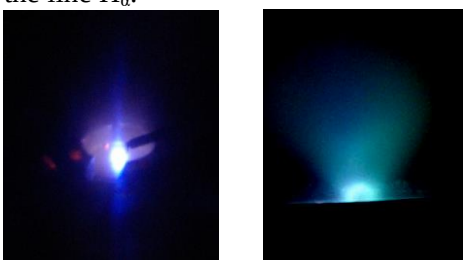

a) b)

Fig. 1. Photograph of the point-like plasma sustained by CW 263 GHz (a) and by pulsed 670 GHz focused beams

The radiation in the vacuum ultraviolet region was investigated using a calibrated PMT and filters, the radiation in the extreme ultraviolet investigated absolutely calibrated detector with filter sets.

The work was supported by Russian Science Foundation, project # 14-12-00609.

References

[1] M. Glyavin, S. V. Golubev, I. V. Izotov, et.al., Appl. Phys. Lett., vol. 105, no. 17, 2014.

[2] A. V. Sidorov, S. V. Razin, S. V. Golubev, et. al., Physics of Plasmas 23 (4), 043511

[3] M.Yu. Glyavin, S.V. Golubev, V.G. Zorin, et al, Radiophysics and Quantum Electronics, Vol. 56, Nos. 8–9, January, 2014.

Plasma and catalyst for the oxidation of NO_x

I. Jõgi[1], K. Erme[1], E. Levoll[1], J. Raud[1], E. Stamate[2]

[1] *Institute of Physics, University of Tartu, Tartu, Estonia*
[2] *Department of Energy Conversion and Storage, Technical University of Denmark, Roskilde, Denmark*

The removal of NO_x from the exhaust gases requires the oxidation of most abundant NO to NO_2 or N_2O_5. The oxidation can be done by non-thermal plasma but the efficiency is limited due to the back-reaction of NO_2 to NO by O radicals. Present contribution investigates the role of catalysts in the improvement of oxidation efficiency based on the stationary and time-dependent studies of the NO_x oxidation at different reactor configurations and experimental conditions. The plasma produced active oxygen species (O, O_3) were shown to play an important role in the reactions taking place on the catalyst surfaces while the exact mechanism and extent of the effect depended on the reactor configuration. The effect of catalyst at different experimental conditions was quantitatively described with the aid of analytical lumped kinetic models derived for the NO_x oxidation when the catalyst was directly in contact with plasma or only with the ozone.

1. Introduction

NO_x (NO, NO_2) produced in the burning of fossil fuels is a major threat to the environment [1]. The available adsorption or absorption based NO_x removal methods work efficiently when the most abundant NO_x constituent NO is oxidized to NO_2 or N_2O_5. The oxidation can be done by non-thermal plasmas which produce highly reactive oxygen species (O, OH, O_3). One of the main limiting factor for plasma oxidation of NO in O_2:N_2 mixtures is the back-reaction of NO_2 to NO by O radicals [2]. The presence of such back-reaction distinguishes the NO_x from organic compounds which are also often oxidized by plasma. The back-reaction can be suppressed by different means including the indirect treatment by ozone or the use of catalyst.

Present contribution investigates the role of catalyst in the plasma oxidation of NO_x. The investigation involved stationary and time-dependent studies of NO_x oxidation with different configurations of plasma and catalyst placement at varying experimental conditions. Furthermore, analytical lumped kinetic models incorporating effective reaction coefficients for NO_x oxidation were derived to quantify the effect of catalyst at different experimental conditions [3,4]. The results were mostly obtained in dry O_2:N_2 mixtures.

2. Main results

Stationary and time-dependent experiments with different binary metal-oxides placed either directly in contact with plasma or after the active plasma zone demonstrated that the metal-oxides could act both as NO_x adsorbents and oxidation catalysts.

With the catalyst directly in contact with the plasma, the back-reaction in gas phase remained important but the reaction balance was shifted towards the production of NO_2. The time-dependent changes of the NO_x concentrations suggested that the surface processes involved both the adsorption/disproportionation reactions of NO_2 [5] and reactions with plasma produced oxygen species. The importance of the latter process was also emphasised by the production of NO_2 on the catalyst surfaces previously treated by oxygen discharge.

The back-reaction can be avoided when the plasma is used indirectly for the production of ozone which then reacts with NO_x. In this configuration the catalyst enhanced considerably the oxidation of NO_2 to N_2O_5 [3]. The surface processes involved the decomposition of O_3 to surface bound oxygen species which then aided the oxidation of NO_2 to NO_3. Subsequent formation of N_2O_5 on the surface resulted also in the increased NO_x adsorption ability of tested metal-oxides.

Acknowledgements

The study was partially financed by Estonian Research Council (Grant nr. 585).

References

[1] K. Skalska, J.S. Miller, S. Ledakowicz, Sci. Total. Environ. **408** (2010) 3976.

[2] I. Jõgi, E. Levoll, J. Raud, Chem. Eng. J. **301** (2016) 149.

[3] I Jõgi, K. Erme, J. Raud, M. Laan, Fuel **173** (2016) 45.

[4] I. Jõgi, E. Levoll, J. Raud, Catal. Lett. **147** (2017) 566.

[5] L. Sivachandiran, F. Thevenet, P. Gravejat, A. Rousseau, Appl. Catal. B: Environ. **142** (2013) 196.

Pulsed electron beams for thin film deposition

M. Nistor

National Institute for Lasers, Plasma and Radiation Physics (NILPRP), Plasma Physics and Nuclear Fusion Laboratory, L22, P.O. Box MG-36, 7712 Magurele-Bucharest, Romania

In this work we present results on pulsed electron beams produced in a channel-spark discharge used for thin film deposition. The measured electron beam energy distribution is polyenergetic, having a high-energy electron component at the beginning of the applied high voltage fall and a dominant contribution of lower energy electrons increasing towards later times of the voltage fall. *In situ* diagnostics of ablation plasma produced in PED by fast imaging, optical emission spectroscopy and Langmuir probes showed that the kinetic energy of the species emitted by the target was roughly in the 10 to 60 eV range. These investigations led to the growth of high quality oxide thin films by the precise control of the PED parameters.

The discovery of the "pseudospark" gas discharge in 1979 by J. Christiansen and C. Schultheiss [1] has paved the way for many studies on pulsed electron beams and their application in pulsed-power switching, extreme ultraviolet sources for lithography, compact X-ray sources, microthrusters, high power microwave generation, etc. These pulsed electron beams are produced in low pressure gas discharges (10^{-3} -10^{-1} mbar) for applied voltages up to tens of kV. A pulsed electron beam, which propagates in a self-focused way due to the space-charge neutralization, has typical parameters: currents of tens - hundreds of A, pulse widths of tens - hundreds of ns, and energies up to tens of keV.

The channel-spark discharge [2] has been derived from the pseudospark one by replacing the floating electrodes from multigap pseudospark geometry with a dielectric tube, leading to a stable electron source for a low cost thin film deposition method: the pulsed electron beam deposition (PED). It has common features with pulsed laser deposition, i.e. the pulsed nature of process, the very anisotropic character of the ablation plume and the high energy of species, but uses a pulsed electron beam instead of a laser beam for ablating a target. Due to the specific electron-matter interaction, the range of materials that could be ablated has been extended to those that are transparent to laser wavelengths.

The knowledge of the electron beam energy distribution of the pulsed electron beams used in PED method plays a key role for an efficient ablation of the target surface and thus to the deposition of thin films. Experimental methods have been employed to determine electron beam energy distribution: self-biasing Faraday cup and X-ray radiation at the interaction of the electron beam with a target. Our measurements showed that in the channel-spark discharge the electron beam energy distribution is polyenergetic, spreading from hundreds of eV to the energy eU, where U is the applied high voltage and e is the electron charge. This distribution has a high-energy electron component (more than a few keV) at the beginning of the applied high voltage fall (U) and a dominant contribution of lower energy electrons increasing towards later times of the voltage fall. For U=16 kV, the voltage fall lasts 210 ns and the total beam current has a maximum value of 750 A, from which a current with a maximum value of 400A and pulse width of about 110 ns is carried by electrons having energy higher than 1.84 keV [3]. Tailoring the electron energy distribution function by variation of the discharge parameters has influenced the quality of grown thin films by PED.

In situ diagnostics of ablation plasma produced in PED by fast imaging, optical emission spectroscopy and Langmuir probes demonstrated that the kinetic energy of the species emitted by the target was roughly in the 10 to 60 eV range, leading to high surface mobility for these species. As a result, growth of stoichiometric and crystalline oxide thin films, even epitaxial films at relatively low temperatures, has been obtained. The tuning of the physical properties of thin films was possible by the precise control of PED growth conditions [4].

[1] J. Christiansen, C. Schultheiss, Z. Phys. A **290** (1979) 35

[2] G Müller, M. Konijnenberg, G. Krafft, C. Schultheiss, Science and Technology of Thin Film, World Scientific Publ. (1995) 89.

[3] M. Nistor, N.B. Mandache, J. Perrière, J. Phys. D: Appl. Phys. **41** (2008) 165205.

[4] M. Nistor, L. Mihut, E. Millon, C. Cachoncinlle, C. Hebert, J. Perrière, RSC Adv. **6** (2016) 41465.

Electron/molecular-cation collisions in cold plasmas: super-excited states at "zero" energy

J. Zs. Mezei[1,2,3,4], F. Colboc[1], Y. Moulane[1,5,6], N. Pop[1,7], S. Niyonzima[1,8], M. D. Epée Epée[1,9], O. Motapon [1,9,10], D. A. Little[11], F. Iacob[12], R. Boata[13], V. Laporta[1,11,14], R. Celiberto[14,15], K. Chakrabarti[1,16], E. Jehin[6], Z. Benkhaldoun[5], K. Hassouni[2], D. Benredjem[3], A. Faure[17], A. Bultel[18], J. Tennyson[11], I. F. Schneider[1,3]

[1]*Laboratoire Ondes et Milieux Complexes, CNRS, Université du Havre, Le Havre, France*
[2]*Laboratoire des Sciences des Procédés et des Matériaux, CNRS, Université Paris 13, Villetaneuse, France*
[3]*Laboratoire Aimé Cotton, CNRS, ENS Cachan and Université Paris-Sud, Orsay, France*
[4]*Instititute of Nuclear Research of the Hungarian Academy of Sciences, Debrecen, Hungary*
[5]*Oukaimeden Observatory, High Energy Physics & Astrophysics Lab., Cadi Ayyad Univ., Marrakech, Morocco*
[6]*Institut d'Astrophysique et de Géophysique, Liège, Belgium*
[7]*Department of Physical Foundations of Engineering, Politehnica University Timişoara, Timişoara, Romania*
[8]*Département de Physique, Université du Burundi, Bujumbura, Burundi*
[9]*Department of Physics, Faculty of Sciences, University of Douala, Douala, Cameroon*
[10]*University of Maroua, Faculty of Science, Maroua, Cameroon*
[11]*Department of Physics and Astronomy, University College London, United Kingdom*
[12]*Physics Faculty, West University of Timişoara, Timişoara, Romania*
[13]*Astronomical Institute of the Romanian Academy, Timisoara Astronomical Observatory, Timişoara, Romania*
[14]*Istituto di Nanotecnologia, CNR, Bari, Italy*
[15]*Dipartimento di Ingegneria Civile, Ambientale, del Territorio, Edile e di Chimica, Politecnico di Bari, Italy*
[16]*Department of Mathematics, Scottish Church College, Calcutta, India*
[17]*Université de Grenoble Alpes, CNRS, Inst. de Planétologie et d'Astrophysique de Grenoble, Grenoble, France*
[18]*Laboratoire CORIA, CNRS, Université de Rouen, Saint Etienne de Rouvray, France*

We will discuss the role of excited states in cold ionized media, as resonances in reactive collisions, and as initial states of the target in non-equilibrium regime.

Dissociative recombination (DR) [1,2]:

$$AB^+(N_i^+,v_i^+)+e^-\rightarrow AB^*,AB^{**}\rightarrow A+B, \quad (1)$$

the major recombination process in low pressure ionized gases, is often notably fast at "zero" (i.e. low) energy of the incident electrons, since it occurs via super-excited molecular states singly- (AB*) or doubly- (AB**) excited, embedded in the ionization continuum of the target ion. This process is competed by ro-vibrational and dissociative excitation:

$$AB^+(N_i^+,v_i^+)+e^-\rightarrow AB^*,AB^{**}\rightarrow AB^+(N_f^+,v_f^+)+e^-, \quad (2)$$

$$\rightarrow A+B^+(N_f^+,v_f^+)+e^-. \quad (3)$$

The use of the Multichannel Quantum Defect Theory [3] resulted in accurate state-to-state cross sections and rate coefficients, displaying a resonant character and a strong dependence on the target state. These features are particularly important for the collisional-radiative modeling of the cold ionized gases – Fig. 1 - in various environments - interstellar space, comets, planetary ionospheres, shock-waves in the entries of spacecrafts, ionic propulsion devices, industrial and edge fusion plasmas - and containing various cations - H_2^+, BeH^+, BF^+ [2,4], N_2^+[5], CO^+[6], SH^+, ArH^+, H_3^+[7], BF_2^+, etc.

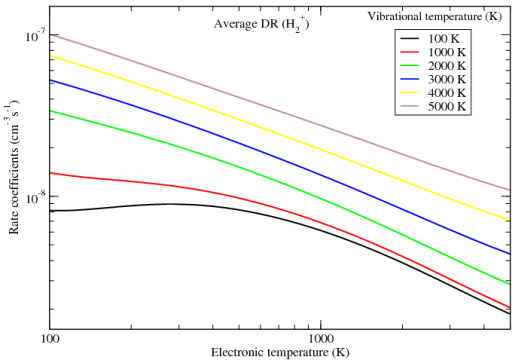

Fig.1. Maxwell rate coefficients for the Dissociative Recombination (DR) of H_2^+: dependence on the vibrational temperature of the ions.

References

[1] I. F. Schneider, O. Dulieu, J. Robert, *Proc. of DR2013: The 9th Int. Conf. on Dissociative Recombination: Theory, Experiment and Applications, Paris, July 7-12, 2013*, EPJ Web of Conferences **84** (2015).
[2] N. Pop *et al*, poster contribution to this conference.
[3] O. Motapon *et al*, *Phys. Rev. A* **90** (2014) 012706.
[4] V. Laporta et al, *Pl. Phys. Contr. Fusion* **59** (2017) 045008.
[5] D. A. Little *et al*, *Phys. Rev. A* **90** (2014) 052705.
[6] J. Zs. Mezei *et al.*, *Pl. Sour. Sci. Tech.* **24** (2015) 035005.
[7] I. F. Schneider *et al*, *Phys. Rev. A* **86** (2012) 062706.

Simultaneous vacuum UV and broadband UV-NIR plasma spectroscopy for LIBS improvement

P. Veis[1], J. Kristof[1, 2]

[1] *Department of Experimental Physics, Faculty of Mathematics, Physics and Informatics, Comenius University, Mlynská dolina F2, Bratislava 842 48 Slovakia*
[2] *Graduate School of Science and Technology, Shizuoka University, Johoku, Hamamatsu, 432-8561 Japan*

LIBS (Laser Induced Breakdown Spectroscopy) of light elements was investigated. As a spectrum of some light elements has not enough emission lines in UV-NIR range, such as B, C, P and S, determination of the electron temperature from Saha-Boltzmann plot is very difficult or impossible. Our aim, improvement of the precision of the electron temperature determination by broadening of emission of UV-NIR range up to VUV range allowed observing more emission lines and very often neutral, single ionized and also double ionized. Precision of the electron temperature of other elements such as Si, Ge, Zn was also studied. Ions abundance evolution of the elements allowed us to find the best experimental conditions for generation of the double ionized ions in LIBS plasma.

1. Introduction

LIBS is an analytical method, which determines elemental composition of materials based on atomic emission of spark created by a laser beam focused on the surface. For light elements as *B, C, P* and *S* important characteristic spectral lines are few and appear in VUV range only [1]. Including VUV, in addition to conventional UV-NIR range yields in more reliable data set for Saha-Boltzmann (S-B) plot, which helps to quantify light elements more precisely using calibration free LIBS.

Heavy elements, such as tungsten have plenty lines in UV-NIR, but their overlap makes the S-B unprecise. Therefore the detection of double ionized W III lines in VUV proves to be advantageous [2].

2. Experiment

2.1. Experimental Set-up

LIBS measurements were realized under low pressure (1330 Pa) He and Ar atmosphere for various delays after the laser pulse to ensure narrow emission lines and observation of all three ionization degrees (neutral - double ionised). Plasma was generated by Nd:YAG laser (Quantel) operating at 266 nm (4-th harmonic) - see Figure 1.

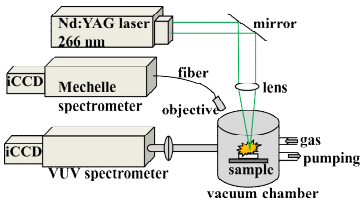

Figure 1. Experimental Setup.

Plasma emission was recorded simultaneously by two spectrometers: broadband UV-NIR echelle type spectrometer (230 nm – 950 nm, ME 5000, Andor) and VUV one (114-295 nm, McPherson), both equipped with iCCD camera (iStar, Andor).

2.2. Results

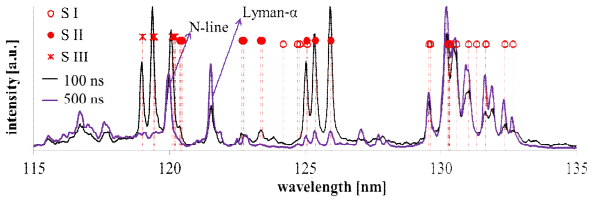

Figure 2. VUV spectra 300 and 500 ns after laser pulse.

The UV-NIR spectra of sulphur doesn't contains neutral S I lines. The VUV spectra allows to observe lines from different degree of ionisation, S I-III lines at 100 ns delay and S I-II lines at 500 ns delay (Figure 2). Clear line detection from three degree of ionisation (S I-III) allows us to determine electron temperature in the early state of the plasma plume (100 ns, Figure 3) and that leads to precise determination of sulphur concentration in a sample. LIBS of other elements (Si, Ge, Zn) was also studied.

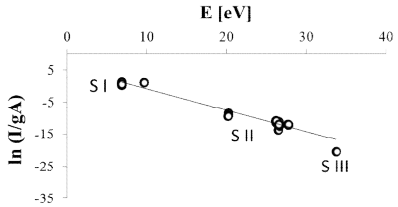

Figure 3. Saha-Boltzman plot of Sulfur.

Acknowledgement: This work has been supported by SRDA (No. APVV-15-0641).

3. References

[1] J. Jašík, J. Heitz, J. D. Pedarning, P. Veis, Spectrochimica Acta Part B 64 (2009) 1128.

[2] M. Pribula, J.Kristof, A. Hakola, P. Veis et al, Physica Scripta T167 (2016) 014045.

Simulation of glow discharge electrolysis for material processing in liquid

F. Tochikubo

Department of Electrical and Electronic Engineering, Graduate School of Science and Engineering, Tokyo Metropolitan University, Tokyo, Japan

In glow discharge electrolysis, the liquid-phase reactions are induced by electrons/ions irradiation of the liquid surface from the plasma. In this work, we carried out numerical simulation of glow discharge electrolysis, which consists of atmospheric-pressure dc glow discharge and electrolyte solution connected in series between parallel plate metal electrodes, based on fluid simulation. The calculated glow discharge facing the liquid is essentially the same as that generated between metal electrodes. In the liquid, electric double layer with approximately 10 nm width was reproduced in front of metal electrode while no electric double layer was observed at plasma-liquid interface. We found that the liquid-phase chemistry is strongly affected by the electron/positive ion irradiation of the liquid surface from the glow discharge, especially in the thin region from the liquid surface.

1. Introduction

Atmospheric-pressure dc glow discharge with liquid electrode is applied for material processing such as metallic nanoparticles generation [1-2]. This system is considered as glow discharge electrolysis (GDE) at atmospheric pressure. In this system, the reactions in liquid are induced by the electrons/ions irradiation of the liquid surface from the liquid-phase thin layer at the plasma-liquid interface. Therefore, it is necessary to clarify the transport of charged and neutral species both in gas and liquid. In this work, we carried out one-dimensional numerical simulation of atmospheric-pressure GDE.

2. Simulation model

The simulation model for GDE is shown in Fig. 1. A glow discharge in atmospheric-pressure helium with 1 mm gas-gap is connected with NaCl solution with 1 mm depth in series. Both the glow discharge and the liquid regions were calculated based on fluid model using continuity equations for charged/neutral species coupled with Poisson equation. Boundary conditions at plasma-liquid interface is important to determine the characteristics of GDE. However, the information on the reactions at plasma-liquid interface is very limited, therefore, we assumed the following simple model: electron irradiation of the liquid surface from the plasma generates hydrated electrons: negative ion irradiation also generates hydrated electrons: any positive ion irradiation causes the generation of H^+ and OH through charge transfer collision: neutrals dissolve in the solution.

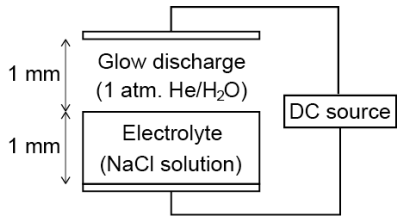

Fig.1. Model for glow discharge electrolysis.

3. Simulation results

The structure of atmospheric-pressure dc glow discharge is essentially the same as that calculated between two metal electrodes. Fig. 2 shows the ion distributions in liquid with glow discharge cathode. Very narrow negative charge layer with strong electric field is formed in the region of roughly 10 nm from metal anode. In front of the glow discharge cathode, we could not find the large difference in the concentrations between Na^+ and Cl^-. The incident electrons become hydrated electrons in the liquid, and react with other species. In the present case, hydrated electrons generate OH^- by the reaction with H_2O. Therefore, plenty of OH^- is generated close to the liquid surface, and local pH becomes approximately 10. The hydrated electron works as reductant. For example, hydrated electrons reduce the metal ions such as Ag^+ to synthesize Ag nanoparticles in liquid.

This work is partly supported by Grant-in-Aid for Scientific Research (B) from JSPS (No. 15H03584).

References

[1] D. Mariotti, R.M. Sankaran, J. Phys. D **43** (2010) 323001.

[2] N. Shirai, S. Uchida, F. Tochikubo, Jpn. J. Appl. Phys. **53** (2014) 046202.

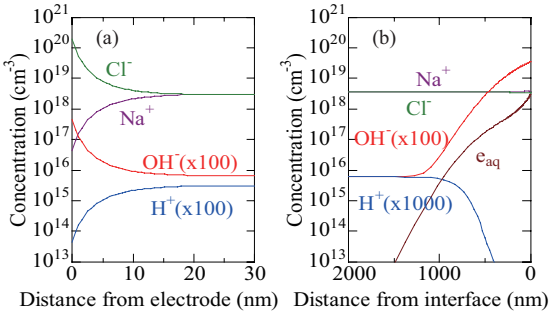

Fig. 2. Spatial distribution of ion species in the liquid in front of (a) metal anode and (b) glow discharge cathode.

Topic number
17, 14

Atmospheric pressure plasmas for agriculture, medicine and surface technology

J. Pawłat[1], P. Terebun[1], M. Kwiatkowski[1],
K. Hensel[2] Z. Machala[2], Z. Kovalova[2], K. Kučerová[2], B. Tarabová[2], M. Janda[2]
A. Starek[3], M. Budzen[3], A. Sujak[3]

[1] *Institute of Electrical Engineering and Electrotechnologies, Lublin University of Technology, Poland*
[2] *Faculty of Mathematics, Physics and Informatics,Comenius University, Bratislava, Slovakia*
[3] *Faculty of Production Engineering, University of Life Sciences, Lublin, Poland*

An atmospheric pressure plasma jet and glidarc reactors were used to enhance the seed germination, disinfect non-heat resistant surfaces and to increase wettability of selected polymeric materials. Selected reactive oxygen and nitrogen species (RONS) were measured for plasma generators operating in different modes: Transient Spark, Mini Glide-arc and Dielectric Barrier Discharge Jet to find optimal operational conditions for selected biomedical and agricultural applications. E. coli was selected as a model microorganism for biodecontamination comparative tests.

1. Introduction and experimental set-up

Different types of discharges could be taken into account for biomedical, material and agricultural applications. This work summarizes selected experimental results in above fields, obtained with Mini Glide-arc (GA), Dielectric Barrier Discharge Jet (BDB), radio frequency (RF) plasma jet and Transient Spark (TS) [1-4].

2. Results and conclusions

Paper is primary choice for antibiotic sensitivity tests (disc diffusion method). Radio frequency plasma jet with central electrode inside the nozzle, working with mixtures of oxygen, nitrogen, air with helium or argon was tested to decrease the surface contact angle of cellulose based paper platform using Kruss DSA25E goniometer. The highest change: decrease of surface contact angle from 96^o to 22^o after 60 s treatment was observed using mixture of helium and nitrogen. Experiments confirmed significant influence of the distance between the treated sample and reactor nozzle, especially for treatment times larger than 15 s.

After 30s application of DBD plasma jet working with helium gas and admixture of air caused average decrease of the contact angle for acrylonitrile-butadiene-styrene from 75^o to 42^o, for polypropylene homopolymer from 82^o to 45^o, and for high impact polystyrene from 90^o to 48^o o, respectively.

GA reactor was used for pre-sowing stimulation of *Lavatera thuringiaca* L. seeds. Five groups of seeds characterized by a different exposition times (1, 2, 5, 10 and 15 minutes) as well as untreated control were used. The highest germination parameters were obtained for seeds stimulated with plasma for the exposition times of 2 and 5 min.

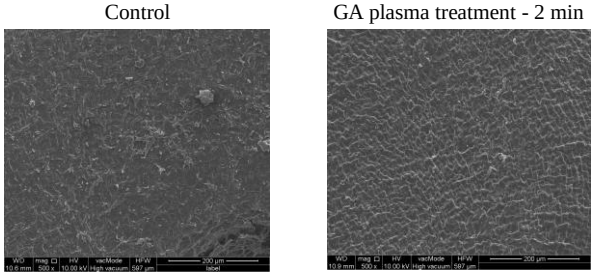

Fig. 1. SEM photos GA plasma treated seeds of *Lavatera thuringiaca* L., zoom 500x.

Germination capacity reached 60% and germination energy was 54.5% comparing to 36.25% and 30% for control, respectively. SEM photos (Fig. 1) indicated visible changes of the seeds' surface, however, distinguishing changes in the water contact angle measurement on the surface of the seeds were not observed. Measurements of RONS were performed in gas and liquid phase for selected plasma generators operating in different modes

3. References

[1] M. Janda, V. Martišovitš, K. Hensel, Z. Machala, Plasma Chem. Plasma Proc., **36** (2016) 767.
[2] J. Pawłat, EPJAP **61(2)** (2013) 1-11.
[3] J. Pawłat, M. Kwiatkowski, P. Terebun, T. Murakami, IEEE Trans. Plasma Sci., **99**, (2015) 1-7.
[4] J. Pawłat, M. Kwiatkowski, P. Terebun, J. Diatczyk. J. Phys. D **49** (2016) 374001.

This work was supported by COST Action TD1208, Slovak Research and Development Agency APVV-0134-12, Slovak grant agency VEGA 1/0918/15, KONNECT CATPLAS, and LUT research found.

Electron interactions for plasma diagnostics and modelling

P. Papp, J. Országh, Š. Matejčík

[1] *Department of Experimental Physics, Faculty of Mathematics, Physics and Informatics, Comenius University in Bratislava, Bratislava, Slovakia*

The role of low-energy and high-energy electrons in discharges and plasma is well known. In the Electron Plasma Processes Laboratories (EPPL) at the Comenius University in Bratislava we are studying the low-energy processes on atoms, molecules and clusters in gas-phase. Electron ionisations, excitations and corresponding dissociative processes are measured by the means of mass spectrometry and optical emission spectroscopy, as well as a theoretical interpretation of results with quantum chemical calculations is being done. Most recently Plasma-Enhanced Chemical Vapour Deposition (PECVD) and Focused Electron Beam Induced Deposition (FEBID) precursors were studied using crossed electron/molecular beams techniques and theory.

1. Introduction

The EPPL at the Comenius University in Bratislava are dealing with mass spectrometric studies of electron *e* ionisation and dissociative ionisation reactions of molecules *M* and clusters:

$$e + M \rightarrow M^+ + 2e \quad (1)$$

$$e + M \rightarrow X + (M\text{-}X)^+ + 2e \quad (2)$$

electron attachment and dissociative electron attachment studies to the molecules and clusters:

$$e + M \rightarrow [M^-]^{\#} + 2e \quad (3)$$

$$e + M \rightarrow [M^-]^{\#} \rightarrow X + (M\text{-}X)^- + 2e \quad (4)$$

electron induced fluorescence studies via excitation of atoms and molecules and in dissociative excitation of the molecules:

$$e + M(A) \rightarrow M^*(C) + e \rightarrow M^*(B) + e + h\upsilon \quad (5)$$

$$e + M(A) \rightarrow M^*(C) + e \rightarrow X^*(B) + (M\text{-}X) + e \rightarrow X^*(A) + (M\text{-}X) + e + h\upsilon \quad (6)$$

where *X, (M-X)* represent neutral fragments of the molecule, *M**, *X** represent excited states of molecules or fragments in different electronic states.

These studies (1-4) cover measurements of the ionisation functions of the molecules (partial cross sections), determination of the reaction threshold for the reactions and the corresponding bond dissociation energies, mainly on molecular targets relevant to plasma technology, nano technology and radiation chemistry (metal-organic compounds, alkenes, halogenated compounds, amino acids) [1]. The non elastic interactions (5-6) of electrons with atoms and molecules produce emission spectra of atoms, molecules recorded at different electron energies and absolute excitation-emission cross sections, being analyzed by UV/VIS optical spectrometer [2].

2. Results

Last few years a great effort of EPPL has been applied to understand the elementary processes of low-energy electron interactions with precursor molecules relevant to nano-technology [1-5]. We have studied several precursors available for deposition of Fe, Co, Cu, Zn, Ni, Si or W layers. The most extensive studies have been performed with the $Fe(CO)_5$ precursor; with electron induced ionisation (1,2) and dissociative electron attachment (3,4) to understand the fragmentation of ionised $Fe(CO)_5$ and its decomposition to Fe^+ and Fe^- respectively; with electron induced fluorescence the excitation thresholds and Fe and CO emission bands. Most recently the gas-phase experiments were upgraded to cluster measurements of this compound to reveal the behaviour of electron ionisation and electron attachment of a precursor in larger environment.

3. Acknowledgments

Financing of this work was by the Slovak Grant Agency VEGA 1/0417/15. This work was supported by the Slovak Research and Development Agency, project Nr. APVV-15-0580. This project has received funding from the European Union's Horizon 2020 research and innovation programme under grant agreement No 692335.

4. References

[1] M. Lacko, P. Papp, K. Wnorowski, Š. Matejčík, Eur. Phys. J. D **69** (2015) 84.

[2] A. Ribar, M. Danko, J. Országh, J.F.F. da Silva, I. Utke, Š. Matejčík, Eur. Phys. J. D **69** (2015) 117.

[3] S. Engmann, M. Stano, P. Papp, M. J. Brunger, Š. Matejčík, O. Ogólfsson, J. Chem. Phys. **138** (2013) 044305.

[4] P. Papp, S. Engmann, M. Kučera, M. Stano, Š. Matejčík, O. Ogólfsson, Int. J. Mass. Spectrom. **356** (2013) 24.

[5] S. Engmann, M. Stano, Š. Matejčík, O. Ogólfsson, Angew. Chem. Int. Ed. **50** (2011), 9475.

Gas-liquid interfacial plasmas for novel gene transfer systems

T. Kaneko[1], S. Sasaki[1], K. Takashima[1], T. Sato[2], M. Kanzaki[3]

[1] *Department of Electronic Engineering, Tohoku University, Sendai, Japan*
[2] *Institute of Fluid Science,Tohoku University, Sendai, Japan*
[3] *Department of Biomedical Engineering, Tohoku University, Sendai, Japan*

Gas-liquid interfacial atmospheric-pressure plasmas are medically utilized for highly-efficient and minimally-invasive gene transfer systems, where the various kinds of plasma-induced stimulations could affect the transfer efficiency. In an attempt to identify the dominant factors for enhancing the gene transfer, we focus on reactive species and measure the concentration and distribution of the plasma-produced reactive species in liquid using two types of plasmas; "plasma jet in contact with liquid" and "micro plasma in liquid (in-liquid plasma)". We have revealed a positive correlation between the transfer efficiency and concentration of the short-lived reactive species such as $^{\bullet}OH_{aq}$. Furthermore, it is found that the duration of $^{\bullet}OH_{aq}$ production by the in-liquid plasma is longer than that by the plasma jet, and accordingly, the higher transfer efficiency is realized by the in-liquid plasma compared with the plasma jet irradiation.

1. Introduction

Non-equilibrium atmospheric-pressure plasmas (APPs) in liquid or in contact with liquid, i.e., gas-liquid interfacial atmospheric-pressure plasmas (GLI-APPs), have attracted much attention as a novel technology, which provides new physical and chemical effects on the surface of the liquid and the exotic reactions are expected in the liquid. Using the GLI-APPs, several applications have been developed in material science such as nanoparticle synthesis, surface treatment of nanomaterials, while in life science such as medicine, agriculture, and biology.

Recently, GLI-APPs are medically utilized for highly-efficient and minimally-invasive gene transfer systems [1-3], where the various kinds of plasma-induced stimulations could affect the transfer efficiency. In an attempt to identify the dominant factors for enhancing the gene transfer, we focus on reactive species, which are classified into three categories in terms of the life-span: long-lived (e.g. H_2O_2) and short-lived (e.g. $^{\bullet}OH$, $O_2^{\bullet-}$) reactive species, and investigate the functions of the plasma-produced reactive species in liquid on the cell activity such as cell-membrane permeability [4,5] using two types of plasmas; "plasma jet in contact with liquid" and "micro plasma in liquid (in-liquid plasma)".

2. Experimental Results and Discussion

First, we developed a plasma jet whose plume is in contact liquid using low frequency (frequency: 8-10 kHz, voltage: 5-12 kV) with Helium gas flow, which was exposed to the biological buffer at a controlled thickness. To evaluate the spatial mapping of liquid phase OH radicals ($^{\bullet}OH_{aq}$) and plasma-induced effect on the gene transfer, the gelling reagent containing terephtalic acid (TA) and adherent cells with gene-simulated fluorescent dye (YOYO-1) are prepared, respectively. It is found that $^{\bullet}OH_{aq}$ which reaches to gelling reagent decreases with an increase in liquid thickness (<1 mm), and the plasma-induced YOYO-1 transfer is found to decay markedly with liquid thickness. Furthermore, the center-localized distribution of $^{\bullet}OH_{aq}$, which is resulting from the center-peaked $^{\bullet}OH$ distribution in the gas phase region, corresponds with the distribution of the transferred cells by plasma irradiation.

Second, we generated in-liquid plasma by applying a pulse power (voltage: 1.5 kV, pulse width: 10-100 μs, current:0.2-2.8 A) to micro-scale thin electrode in the biological buffer. Here, indirect plasma irradiation (IPI) method was employed to eliminate factors except for products in liquid for a clarification of cell response mechanism. The transfer efficiency using in-liquid plasma is found to be much higher than that using plasma jet. Furthermore, it is observed that the duration of $^{\bullet}OH_{aq}$ production by the in-liquid plasma is longer than that by the plasma jet.

These results suggest that short-lived reactive species such as $^{\bullet}OH_{aq}$ is likely one of the dominant factors responsible for the plasma-induced YOYO-1 transfer, and the higher transfer efficiency is relevant to the longer duration of $^{\bullet}OH_{aq}$ production using the in-liquid plasma compared with the plasma jet irradiation.

[1] S. Sasaki, et al., Appl. Phys. Express **7** (2014) 026202.
[2] T. Kaneko et al., Biointerphases **10** (2015) 029521.
[3] S. Sasaki, et al., Sci. Rep. **6** (2016) 25728.
[4] S. Sasaki, et al., J. Phys. D: Appl. Phys. **49** (2016) 334002.
[5] T. Kaneko et al., J. Clin. Biochem. Nutr. **60** (2017) 3.

Pulsed Laser and Sputtering Deposition of Optical Materials

M. Chaker[1]

[1] *INRS-Energie Matériaux Télécommunications, 1650 Boul. Lionel-Boulet, Varennes, Qc, Canada*

We used Pulsed Laser Deposition and Sputtering to synthesize advanced materials in the form of thin films with tailored properties. In this presentation, we will mainly focus on two materials, namely calcium-barium niobate (CBN) that show excellent electro-optical properties and vanadium dioxide (VO_2) that presents a reversible insulator-to-metal transition. Capitalizing on our in-depth characterization of such films, we were able to optimize their properties and to explore their use for various applications, including high performance electro-optical waveguide modulators based on CBN films and smart radiator device (SRD) based on VO_2 films for the passive thermal control of microsatellites.

1. Introduction

Innovation in materials science and engineering resides in our ability to design new materials with tailored properties (electrical, optical, magnetic, etc.) by controlling their microstructure. One of the most powerful means to uniquely arrange matter at such scale is to use plasmas due to their unique ability to provide simultaneously a variety of particles such as ions, neutral atoms and radicals. In this presentation, we will focus on the synthesis of two specific materials in the form of thin films, namely calcium-barium niobate (CBN) and vanadium dioxide (VO_2) using Pulsed Laser Deposition (PLD) and sputtering.

2. Results

Calcium barium niobate ($Ca_xBa_{1-x}Nb_2O_6$) in the form of thin film is a promising material for integrated electro-optical (EO) device applications, due to its unique EO properties (EO coefficient of 130 pm/V) and high Curie temperature (above 250°C). We successfully used PLD to grow high quality CBN epitaxial thin films on various substrates (MgO and NSTO). These films show both low surface roughness and out-of-plane lattice parameters comparable to that of CBN bulk material. An advanced patterning method using a nickel hard mask and a chlorine inductively coupled plasma was also developed. Combining PLD grown films and patterning, waveguides with smooth and nearly vertical sidewalls were fabricated and characterized. In addition, highly (001)-oriented CBN thin films were grown on MgO by Radio-Frequency magnetron sputtering. Close-to-bulk film stoichiometry ($Ca_{0.28}Ba_{0.72}Nb_2O_6$) was obtained for an O_2 fraction of 5% in the deposition chamber. At the annealing temperature of 1000ºC, (001) oriented thin films were achieved with lattice parameter in the c-direction and a chemical composition very close to that of the bulk. The refractive index of the films is 2.21 at λ = 630 nm and a strong second harmonic signal can be generated nonlinearly in the films [1]. This overall work represents a significant step towards the integration and the potential use of CBN films for high performance electro-optical waveguide modulators.

Vanadium dioxide (VO_2) is a “smart” material that undergoes a reversible insulator-to-metal transition (IMT), characterized by a dramatic increase of both its conductivity and reflectivity in infrared and terahertz (THz) ranges of wavelengths when the temperature is increased above 68°C. In a series of studies, our group has investigated the physics governing the IMT of VO_2 thin films [2] and explored new application opportunities [3-4]. For example, we demonstrated that by incorporating VO_2 films in an appropriate multilayer structure, it was possible to achieve VO_2-based smart coatings responding to the temperature by adapting their thermal emittance to radiate more heat at high temperature and less at low temperature. This behavior is quite interesting for application as smart radiator device (SRD) for the passive thermal control of microsatellites.

3. References

[1] S. Vigne *et al.*, Opt. Mater. Express **5** (2015) 2404.

[2] V.R. Morrison *et al.*, Science **346** (2014) 445.

[3] N. Emond *et al.*, Appl. Phys. Lett. **107** (2015) 143507.

[4] N. Emond *et al.*, Appl. Surf. Sci. **379** (2016) 377.

Direct kinetic simulation of nonlinear plasma waves and Hall thruster discharge plasmas

K. Hara [1]

[1] *Department of Aerospace Engineering, Texas A&M University, College Station, Texas, USA*

Plasma instabilities and oscillations play an important role in many plasma applications ranging from wave- and beam-plasma interactions to plasma propulsion. In order to investigate such nonlinear plasma phenomena, we have developed a direct kinetic (DK) simulation, in which the velocity distribution functions are directly obtained by solving kinetic equations such as the Vlasov equation in a discretized phase space, i.e., physical and velocity space. One advantage of a DK method is that the numerical noise inherent in particle methods is essentially eliminated. We employed the DK simulation to investigate plasma-wave interactions, including electron plasma waves, ion acoustic waves, and trapped particle instabilities, and the low-frequency ionization oscillations in the discharge plasmas of Hall effect thrusters.

1. Background and Motivation

Two main plasma simulation techniques that have been developed include fluid and kinetic models. Fluid models solve the conservation equations for macroscopic quantities, including the density, bulk velocity, and energy. On the other hand, the first-principles gas kinetic equations, such as the Vlasov and Boltzmann equations, are solved to obtain the distribution functions in kinetic models. One of the most popular is particle methods, in which computational "macroparticles" are used. However, the statistical noise inherent in the particle methods may alter the physical oscillation signals if the number of macroparticles is not sufficient.

We have developed a grid-based kinetic simulation, called the direct kinetic (DK) method, which is an alternative to particle-based kinetic models such as particle-in-cell (PIC) method. As the kinetic equations are hyperbolic partial differential equation, we employ a finite-volume method using Monotonic Upwind Scheme for Conservation Laws (MUSCL) framework with the Arora-Roe limiter, which preserves conservation and positivity of the distribution functions.

The DK method has been tested against plasma-sheath theory with and without secondary electron emission, Landau damping, and nonlinear plasma wave theories for Langmuir and ion acoustic waves. It is also benchmarked with a PIC simulation in the Hall thruster discharge plasma. [1] We developed a hybrid-kinetic simulation, in which ions are solved using a kinetic (DK or PIC) simulation while a fluid model is used for electrons, and showed that DK simulation is useful for ionization oscillations.

2. Key Results

I will focus on the two nonlinear phenomena that we investigated using a DK method.

First, we performed kinetic simulations of the trapped particle bunching instability in nonlinear plasma waves. [2] We have shown that the trapped particles in traveling potential wells experience a bunching instability and form a bunch in the phase space depending on the initial trapped particle distribution. The growth rates obtained from the numerical simulation are in good agreement with the theoretical predictions.

Second, low-frequency (10-30 kHz) ionization oscillation, also called the breathing mode, in Hall effect thrusters is investigated. Although this phenomenon has been often observed in experiments and numerical simulations, the mechanism of excitation and damping of the breathing mode was not fully understood. We have employed a hybrid-DK method and showed a qualitative agreement of the discharge current oscillations between experiments and numerical simulations. [3] Furthermore, we developed a perturbation theory of ionization oscillations by accounting for the perturbation of electron energy, which was neglected in the conventional predator-prey type formulation. [4] From the numerical results and the perturbation theory, we have concluded that the electron heat transfer mechanism plays a significant role in the mode transition of the ionization oscillations.

3. References

[1] K. Hara, I. D. Boyd, and V. I. Kolobov, Phys. Plasmas **19**, 113508 (2012)
[2] K. Hara, T. Chapman, J. W. Banks, et al., Phys. Plasmas **22**, 022104, (2015)
[3] K. Hara, M. J. Sekerak, I. D. Boyd, and A. D. Gallimore, J. Appl. Phys. **115**, 203304 (2014)
[4] K. Hara, M. J. Sekerak, I. D. Boyd, and A. D. Gallimore, Phys. Plasmas **21**, 122103, (2014)

Rotating spoke instabilities in standard and wall-less Hall thrusters: Experiments and PIC simulations

S. Mazouffre, L. Grimaud, S. Tsikata, K. Mathyash, R. Schneider

[1] *CNRS – ICARE, 1c Avenue de la recherche scientifique, 45071 Orléans, France*
[2] *Ernst-Moritz-Arndt University, Greifswald, D-17487, Germany.*

This work reports on the examination on rotating plasma inhomogeneities, also called rotating spokes, in the discharge of a low-power Hall thruster. Rotating structures have been observed by means of high-speed imaging and time-resolved LIF spectroscopy for two configurations of the thruster: the standard configuration and the wall-less configuration in which the plasma discharge is unbounded. Numerical simulations based on a 3D PIC model support the experiments.

Rotating plasma inhomogeneities are observed in various types of magnetized low pressure plasma discharges created in a crossed electric and magnetic field configuration. Over the past ten years, such structures, often termed "rotating spokes", have been experimentally investigated e.g. in plasma devices like magnetrons and Hall thrusters. There is a great deal of interest in studying rotating plasma structures for mainly two reasons. Firstly, such instabilities seem to be a very general phenomenon in low-pressure plasma discharges of which the origin is not yet fully understood. Secondly, these large-scale low-frequency rotating instabilities certainly play a role in the transport of charged particle. As a consequence, they probably influence both the characteristics and the performances of plasma devices and plasma technologies like thin-film deposition and spacecraft propulsion.

In this contribution we experimentally examine the properties of low-frequency (a few kHz) rotating plasma instabilities in the discharge of the low power ISCT200 Hall thruster. The latter is a versatile 200 W-class Hall thruster using permanent magnets for generating the magnetic field instead of helical magnetizing coils. Two different configurations of the ISCT200 have been employed in this study. The standard (ST) one rests upon a magnetic barrier perpendicular to the cavity walls. The unconventional wall-less (WL) configuration allows to entirely shift the plasma discharge outside the cavity, then eliminating wall processes such as secondary electron emission and sputtering. The two versions, however, share many common features: the channel geometry is the same, walls are made of $BN\text{-}SiO_2$ ceramic, the magnetic field is produced by SmCo magnets, a porous compound serves as propellant gas injector and a heated cathode with a disk-shaped LaB_6 emitter provides the necessary electron current for maintaining the discharge and neutralizing the ion beam. In ST configuration, a ring anode is placed at the back of the channel whereas in WL configuration, a gridded anode with circular holes is placed at the cavity exit plane.

The main objective of this work is to characterize the physics and the dynamics of rotating plasma structures in the E×B discharge of a 200 W-class Hall thruster operating with xenon by means of two diagnostic techniques. High-speed camera imaging has been used to capture the rotating spoke motion and transformation for various thruster operating conditions. Image processing with sophisticated algorithms allows to determine the rotation velocity, direction and frequency, the plasma structure shape and sizes and the mode number.
Time-resolved LIF spectroscopy in the near infrared has been employed to record the temporal evolution of the Xe^+ ion azimuthal velocity component during the rotation of a plasma inhomogeneity. Here, a novel photon counting approach has been developed to enable measurements without externally stabilizing the discharge. The following points will be presented and discussed: the determination of the properties of such structures (velocity, frequency, domain of existence) and correlation with longitudinal instabilities such as breathing oscillations, the impact of the discharge voltage, propellant mass flow rate and cathode heater current on the properties of the rotating spokes, clarifications as to the origin of the rotating inhomogeneities, time evolution of the ion velocity distribution function in the course of a spoke rotation, and finally a critical comparison of the features of rotating structures in conventional and wall-less Hall thrusters. Experimental results are supported by outcomes of numerical simulations carried out with a 3D PIC model.

Dynamic of HiPIMS Plasmas

A. von Keudell, C. Maszl, W. Breilmann, Julian Held,
V. Schulz-von der Gathen, A. Hecimovic

[1] *Institut für Experimentalphysik II, Ruhr-Universiät Bochum, Bochum, Germany*

The dynamic of high power pulsed magnetron plasmas is analysed using various diagnostics ranging from optical emission spectroscopy, probe diagnostics to mass spectrometry. It shown that structure formation in these plasmas is driven by the Simon-Hoh instability leading to the appearance of rotating spokes along the racetrack of the magnetrons. The plasma parameters in these rotating ionization zones are measured using time resolved optical and mass spectrometry. It is shown that the energy distribution of the ions reaching the substrate are directly connected to the appearance of the spokes. The underlying mechanisms are discussed to explain the good performance of HiPIMS plasmas for material synthesis

1. General

High power impulse magnetron sputtering (HiPIMS) plasmas are characterized by a high degree of ionization and a very energetic metal growth flux leading to superior material properties. Power densities at the target of several kWcm^{-2} are realized by using short pulses of 10 to 200 µs and duty cycles of a few percent only.

Many studies focus on unraveling the dynamic of a HiPIMS plasma. The intense sputter wind in a HiPIMS pulse causes gas rarefaction after a time span of 10...30µs after the onset of the plasma pulse. At target power densities above 1 kW cm^{-2}, localized ionization zones, so-called spokes, are observed which rotate along the plasma torus with a typical velocity of 10 km s^{-1}. It is assumed that the localized ionization zones correspond to regions of high electrical potential, and are, therefore, the source of an energetic group of ions of typically few tens of eV in the growth flux on the substrate. The spoke pattern depends on target material, plasma gas, power density and pressure. By adding a reactive gas such as oxygen or nitrogen to a HiPIMS plasma specific oxides and nitrides can be deposited on the substrate.

The analysis of the plasma parameters of this dynamic plasma pulses is very demanding because two time scales need to be taken into account: the first is the pulsing of the discharge with a duty cycle of a percent of less, the second is the dynamic of the plasma evolution during each pulse itself, where the current is rising from zero to over 100 A for a 2" target and the spokes form dynamically. Therefore, an elaborate triggering scheme is developed, to trigger the optical diagnostic as well as the mass spectrometer to the presence of the ionization zone in the direct line of sight to the diagnostic.

By using Stark broadening of hydrogen lines, the electron density inside the spokes can be determined to 10^{14} cm^{-3}. By inserting probes into the magneton target, the modulation of the target current by the traveling ionization zones of 30% could be determined. The synchronized mass spectra show that the energetic ions are uniquely connected to the presence of the spokes. This can be explained by the occurrence of a Simon-Hoh instability which modulates the electrical potential in the plasma and thereby the energy of the ejected ions.

2. References

[1] W. Breilmann, C. Maszl, A. Hecimovic, A. von Keudell, J. Phys. D (accepted) (2017)
[2] A. von Keudell, A. Hecimovic, C. Maszl, Contrib. Plasma Phys. **1**, 9 (2016)
[3] A Hecimovic, C Maszl, V Schulz-von der Gathen, M Böke and A von Keudell, Plasma Sources Science and Technology **25**, 035001 (2016)
[4] A. Hecimovic, V. Schulz-von der Gathen, M. Böke, A. von Keudell, Plasma Sources Science & Technology **24**, 045005 (2015)
[5] W Breilmann, A Eitrich, C Maszl, A Hecimovic, V Layes, J Benedikt, A. von Keudell, J. Phys. D **48**, 295202 (2015)

Special Session Lectures

Challenges in the modelling of reactive plasmas: limitations and opportunities in global modelling

A. R. Gibson[1,2]

[1] *York Plasma Institute, Department of Physics, University of York, Heslington, York, YO10 5DD, UK*
[2] *LPP, CNRS, Ecole Polytechnique, UPMC Univ. Paris 06, Univ. Paris-Sud, Observatoire de Paris, Université Paris-Saclay, Sorbonne Universités, PSL Research University, 91128 Palaiseau, France*

The use of global models in various forms is commonplace in the low temperature plasma community in large part because of their computational simplicity, which leads to short solution times and relative ease of interpretation. However, the penalties paid for a short solution time are often the loss of spatial and temporal information on the system of interest. In some applications, these variations could be considered negligible, but in others, they are crucial in defining the properties of the plasma. In this contribution, a perspective will be given on the limitations of global models, mainly from the point of view of temporal and spatial averaging. Specific examples of global models developed to circumvent these limitations will be presented along with a further perspective on the opportunities presented by such approaches for the field of global modelling, particularly with a view to improving comparisons with experimental measurements.

1. Introduction

Global models are often the first step undertaken by researchers aiming to understand complex variations in plasma properties under the change of a given external parameter. The low degree of computational complexity involved in these models allows for studies of systems inclusive of complex gas mixtures and reaction mechanisms, which are significantly more difficult using higher dimensional models. The lack of spatial dimensions and analytical complexity additionally simplifies the analysis of the results of the model allowing complex phenomena to be identified even in models inclusive of large reaction mechanisms.

2. Overcoming spatial and temporal averaging

The spatially and temporally averaged assumptions inherent in the most basic global model approaches present clear limitations when applied to many experimental systems, meaning that comparisons between global models and experimental results are often difficult. However, several works have demonstrated that it is possible to extend the basic global model approach to more complicated experimental systems while maintaining computational simplicity provided that the dominant physical properties of these systems are understood [1, 2, 3].

This contribution will discuss examples where the assumptions of spatial and temporal homogeneity inherent in global models limit the understanding of important phenomena in certain physical systems and how these limitations can be overcome while maintaining computational simplicity [4].

A further perspective will be given as to the opportunities presented to the field of global modelling by such approaches. Particular emphasis will be given to how these approaches may improve comparisons between global models and experimental results for systems that cannot be reasonably viewed to be spatially or temporally homogenous.

Acknowledgements

This work has been done within the LABEX Plas@Par project, and received financial state aid managed by the 'Agence Nationale de la Recherche', as part of the 'Programme d'Investissements d'Avenir' under the reference ANR-11-IDEX- 0004-02. Funding through UK EPSRC (EP/ K018388/1) and the York-Paris Low Temperature Plasma Collaborative Research Centre is also acknowledged.

References

[1] E. Kawamura, M. A. Lieberman, A. J. Lichtenberg, P. Chabert, C. Lazzaroni, Plasma Sources Sci. Technol., **23**, (2014) 035014.

[2] K. Niemi, T. Gans, D. O'Connell, Plasma Sources Sci. Technol., **22**, (2013) 032001.

[3] E. Despiau-Pujo, P. Chabert, Plasma Sources Sci. Technol. **18** (2009) 045028

[4] A. Hurlbatt, A. R. Gibson, S. Schröter, J. Bredin, A. P. S. Foote, P. Grondein, D. O'Connell, T. Gans, Plasma Process Polym, **14** (2017)

Challenges in the modelling of plasma-surface interactions

Vasco Guerra[1] and Daniil Marinov[2]

[1] *Instituto de Plasmas e Fusão Nuclear, Instituto Superior Técnico, Universidade de Lisboa, Lisboa, Portugal*
[2] *imec, Kapeldreef 75, 3001 Leuven, Belgium*

This contribution briefly addresses some current challenges in the modelling of plasma-surface interactions. Different types of models focus on different time and length scales and have specific challenges of their own. From the shorter to the longer scales, these formulations include atomic level simulations, kinetic Monte Carlo algorithms (KMC) and deterministic descriptions. The biggest challenge, however, resides perhaps on how to include the detailed information of atomic scale simulations into reliable and effective models that can be easily incorporated in simulations of realistic systems. A key role can be played by the KMC methods, currently under expansion, as their intermediate degree sophistication places them in a perfect position to help bridging this gap.

1. Statement of the problem

Modeling of plasma-surface interactions is a multi-scale problem. At the lowest level lies the detailed atomic-scale description of the elementary acts of adsorption, desorption, diffusion, and reactions on the surface. Despite the huge progress in recent years on the computation of potential energy surfaces from density functional theory and their use in classical molecular dynamics (MD), there is still a substantial discrepancy in the time and length scales of what is practically feasible in terms of calculation time at the atomic level and the time and length scales involved in a real system [1]. Another challenge to MD calculations is to accurately account for excited states, electromagnetic fields, charged particles and photons.

At the next, mesoscopic, level, plasma-surface interactions can be modelled using stochastic kinetic Monte Carlo (KMC) algorithms [2]. KMC algorithms do not solve explicitly the master equation for a given system, but instead numerically simulate the underlying Markov process. Efficient algorithms describing NO and O_2 recombination in silica were recently presented [2], opening the door for a significant development of this approach. However, these models lack a truly predictive power, as they need as input the energy barriers for each elementary step and other physical parameters.

The KMC approach can be further coarse-grained to derive models adopting a deterministic description (DD), where surface kinetics is formulated in terms of fractional coverages of different types of adsorption sites, simulated by a system of reaction-rate differential equations. The main advantage of this mesoscopic approach is its simplicity and computational efficiency, which allows the straightforward coupling to gas phase chemistry in reactor-scale simulations and in computational fluid dynamics. However, compared to KMC, it does not account for spatial correlations and cannot handle easily probabilities that depend on the local configuration of the system, characterize fluctuations and relies on additional assumptions regarding the treatment of physisorbed species [2]. The incorporation of a description of surface modification under plasma exposure is another critical step for further development of both KMC and DD models.

To bridge the gap between the sophistication of MD and the effectiveness of the DD remains perhaps the biggest challenge of all. In this context, KMC simulations play a central role: on the one hand, they can incorporate the information coming from ab initio simulations regarding binding energies, energy barriers and dynamic surface modifications; on the other hand, they can be used to validate and benchmark DD models and the underlying approximations [2]. A combination of KMC and ab-initio calculations was already used for predictive modeling of real catalytic systems [3], but the application of this combined approach with generality remains another important challenge. A description of KMC methods and examples of application will be given at the conference.

Acknowledgments: VG was partially supported by the Portuguese FCT, Projects UID/FIS/50010/2013 and PTDC/FIS-PLA/1420/2014 (PREMiERE)

2. References

[1] E.C. Neyts, Plasma Chem. Plasma Process. **36** (2016) 185. E.C. Neyts and P. Brault, Plasma Process. Polym. **14** (2017) 1600145.

[2] V. Guerra and D. Marinov, Plasma Sources Sci. Technol. **25** (2016) 045001. D. Marinov, C. Teixeira and V. Guerra, Plasma Process. Polym. **14** (2017) 1600175.

[3] M. Stamatakis, J. Phys.: Condens. Matter **27** (2015) 013001.

Topic number

Challenges in the kinetic modelling of electrons and ions in gaseous and liquid matter

R. D. White[1], D. Cocks[1,2], G. Boyle[1], M. Casey[1], N. Garland[1], D. Konovalov[1], J. de Urquijo[3], M. J. Brunger[2], R. P. McEachran[4], S. J. Buckman[4], S. Dujko[5], Z. Lj. Petrovic[5]

[1] *College of Science and Engineering, James Cook University, Townsville 4810, Australia*
[2] *School of Chemical and Physical Sciences, Flinders University, Adelaide, 5001, Australia*
[3] *Research School of Physics and Engineering, The Australian National University, Canberra, 0200, Australia*
[4] *Instituto de Ciencias Físicas, Universidad Nacional Autónoma de México, 62251, Cuernavaca, Mor., México*
[5] *Institute of Physics, University of Belgrade, Pregrevica 118, 11080 Belgrade, Serbia*

Modelling of electron and ion induced processes in plasma medicine and radiation damage is reliant on accurate self-consistent sets of cross-sections for electrons in tissue. These cross-sections (and associated transport theory) must accurately account not only the charged particle-biomolecule interactions but also for the soft-condensed nature of tissue. In this presentation, we report on recent swarm experiments for electrons in gaseous water and tetrahydrofuran using the pulsed-Townsend experiment, and the associated development of self-consistent cross-section sets that arise from them. We also report on the necessary modifications to the transport theory and gas-phase cross-sections required to accurately treat electron transport in liquids. The accuracy of the ab-initio theory is highlighted through comparison of theory and experiment for electrons in liquid Ar/Xe.

1. Introduction

Accurate modelling of electron and ion transport in plasmas, plasma-liquid and plasma-tissue interactions is dependent on (i) the existence of accurate and complete sets of cross-sections, (ii) an accurate treatment of electron/ion transport in these phases, and (iii) accurate description of other processes e.g. localization (trapping), bubbles, etc.

Modelling of electron/ions transport in gases, liquids and soft-condensed matter is considered through appropriate generalisations of Boltzmann's equation to account for spatial-temporal correlations present in liquids including self-trapping of electrons into bubble states, and combined localised-delocalised nature of transport. Unified solutions of Boltzmann's equation for electrons and ions are made within a multi-term framework, avoiding the well-known restrictions associated with the 'two-term' approximation.

2. Self-consistent electron-biomolecule cross-section sets

The accuracy and completeness of electron-biomolecule cross-section sets can be assessed by comparison of calculated transport coefficients with those measured using a pulsed-Townsend swarm experiment of de Urquijo and co-workers. In this presentation we will present results from our recent studies of electrons in water, as the natural surrogate for human tissue. In addition, while DNA is currently not convenient to study, tetrahydrofuran (THF – C_4H_8O) has been investigated as a close analogue for low-energy electron interactions with 2-deoxyribose, a sugar that links phosphate groups in the DNA backbone.

3. Electron transport in dense atomic gases and liquids

As detailed above the treatment of electron transport in liquids involves distinctly more complicated physical processes than in the gas and crystalline phases. The randomness assumption inbuilt in the treatment of gases is no longer present, and neither is the long-range order generally present in crystalline materials. Rather in liquids there exists some short range order, where the scattering centres are spatially and temporally correlated. The impact of the screening of the electron interaction potential within the liquid is treated using an ab-initio solution of the Dirac-Fock equation, with a fully non-local treatment of exchange and accurate multipole polarisability in the electron-atom potential. We should emphasize that there are no adjustable parameters in the calculation [1]. In the presentation we will highlight our results for the transport of electrons in liquid argon and liquid xenon. Furthermore, we will highlight our preliminary results for electron capture into bubble states for atomic liquids [2].

[1] G J Boyle, R P McEachran, D Cocks, and R D White. J. Chem. Phys. , 142:154507, 2015
[2] D Cocks and R D White. arXiv:1602.07834v1

Challenges in PIC Modeling: Electromagnetic Description and Resonance Phenomena

Thomas Mussenbrock

Brandenburg University of Technology, D-03046 Cottbus, Germany

This contribution provides an overview over applications of low-temperature plasmas for which new aspects of PIC modeling have to be taken into account. These new aspects come with a number of numerical as well as conceptual challenges, three of which are electromagnetic effects, resonance resonance effects, and plasma chemistry at high pressure.

Boltzmann's equation is certainly the most fundamental description of low-temperature plasmas. It is in fact imperative to take it seriously when particle systems are not in thermal equilibrium. [1] This holds in particular for low-pressure plasmas. It has been also recently shown that kinetic effects even occur in atmospheric pressure plasmas. Under certain conditions electrons show strong non-Maxwellian behavior. [2] The energetic behavior of electrons is of course directly related to the ongoing plasma chemistry which makes low-temperature plasmas so useful. [3] Whenever accurate information about the energy distribution of particles in a non-equilibrium plasma is needed, e.g., to calculate the fundamental transport properties of particles or the rates for elementary collision processes, a kinetic approach is mandatory.

A number of different kinetic approaches for directly solving Boltzmann's equation have been developed and used. One of these methods is particle-in-cell (PIC) coupled to Monte-Carlo collisions. [4 - 7] In this method super-particles in a Lagrangian frame – each of which represents millions of real physical particles – are followed in continuous phase space whereas particle densities and current as velocity moments of the distribution functions are calculated on Eulerian grid points. The basic PIC method itself is intuitive and quite simple to implement. It consists of just four fundamental procedures: i) integration of the Newton's equations of motion for the particles, ii) assignment of charges and currents to the numerical field grid, iii) calculation of the fields on the grid points, and iv) interpolation of the fields from the grid to the particle positions. This straightforward and conceptually simple approach is probably one reason for its popularity, particularly in the low-temperature plasma simulation community.

Although the PIC approach is more than 60 years old and quite straightforward – as briefly described above –, its development has not been completed. With the today's amazing applications of plasmas, new challenges in the context of numerical plasma simulation using PIC pop up. This contribution is intended provides an overview over a limited number of applications of low-temperature plasmas for which new aspects of PIC modeling have to be taken into account. These new aspects come with numerical as well as conceptual challenges, three of which are electromagnetic effects, resonance effects, and plasma chemistry at atmospheric pressure [8 - 10].

References

[1] J.J. Duderstadt and W.R. Martin, Transport Theory (Wiley, 1979)
[2] D. Eremin, T. Hemke and T. Mussenbrock, Plasma Sources Sci. Technol. **24**, 044004 (2015)
[3] A. Fridman, Plasma Chemistry (Cambridge University Press, 2002)
[4] M.M. Turner, Phys. Plasmas **13**, 033506 (2006)
[5] J.M. Dawson, Rev. Mod. Phys. **55** 403 (1983)
[6] C.K. Birdsall and A.B. Langdon, Plasma Physics via Computer Simulation (McGraw-Hill, 1985)
[7] R.W. Hockney and J.W. Eastwood, Computer Simulation using Particles (Hilger, 1988)
[8] D. Eremin, T. Hemke, R.P. Brinkmann, and Thomas Mussenbrock, J. Phys. D: Appl. Phys. **46**, 084017 (2013)
[9] S. Wilczek, J. Trieschmann, D. Eremin, R.P. Brinkmann, J. Schulze, E. Schuengel, A. Derzsi, I. Korolov, P. Hartmann, Z. Donkó, and T. Mussenbrock, Phys. Plasmas **23**, 063514 (2016)
[10] D. Eremin, T. Hemke, and T. Mussenbrock, Plasma Sources Sci. Technol. **25**, 015009 (2016)

Advances and Challenges in Fluid Flow Models of Low-Temperature Plasmas Flows

J.P. Trelles[1]

[1]*Department of Mechanical Engineering, University of Massachusetts Lowell, Lowell, United States of America*

Fluid flow models are essential tools for the analysis of low-temperature plasma (LTP) systems, especially in industrial application contexts. These models rely on the continuum approximation to describe the diverse range of chemical and thermodynamic nonequilibrium conditions inherent in LTPs. Numerical solutions face compound challenges found in other fields, such as nonlinearity of equation coefficients, resolution of large property gradients, instabilities and turbulence. These challenges are addressed by advanced methods designed for multiphysics and multiscale problems. Representative results of the use nonequilibrium fluid flow models for industrially relevant LTP systems are presented, which depict the challenges faced and approaches for their solution.

1. Introduction

Low-temperature plasmas (LTPs) are at the core of diverse applications, such as materials processing, chemical synthesis, and medicine. The wide range of particle densities and energies in LTPs makes fluid models especially appealing for their description. The interaction of LTP with processing media, such as a gas stream or solid surface, leads to a chemical and thermodynamic nonequilibrium conditions. Such interactions also present complex coupling among fluid dynamics, heat transfer, chemical kinetics, and electromagnetic phenomena.

2. Challenges

Numerical solutions of LTP fluid models face severe challenges found in other fields, including:

- Resolution of large solution field gradients, due to, e.g. boundary layers, sheaths, or shocks, which are often conducive to instabilities and turbulence.
- Handling of highly nonlinear equation coefficients and source terms result of constitutive relations, chemical reactions, Joule heating, etc., which produce numerical stiffness and limit convergence.
- Consistent coupling of multiphysics model requirements, from the fulfilment of the solenoidal constraint of magnetic fields to the coupling between pressure and velocity fields in low-speed flows.

3. Advances

The above challenges are addressed by advanced numerical methods for multiphysics and multiscale problems. Stabilized and Variational Multiscale (VMS) methods exemplify the state-of-the-art among such methods, as evidenced by their use in commercial multiphysics software (e.g. Comsol) and their use in diverse fields, including plasma flows. Fig. 1 shows representative results of their use for the simulation of an arc torch, the core component in plasma spray; and the free-burning arc, a canonical model for the analysis of electric welding [1, 2].

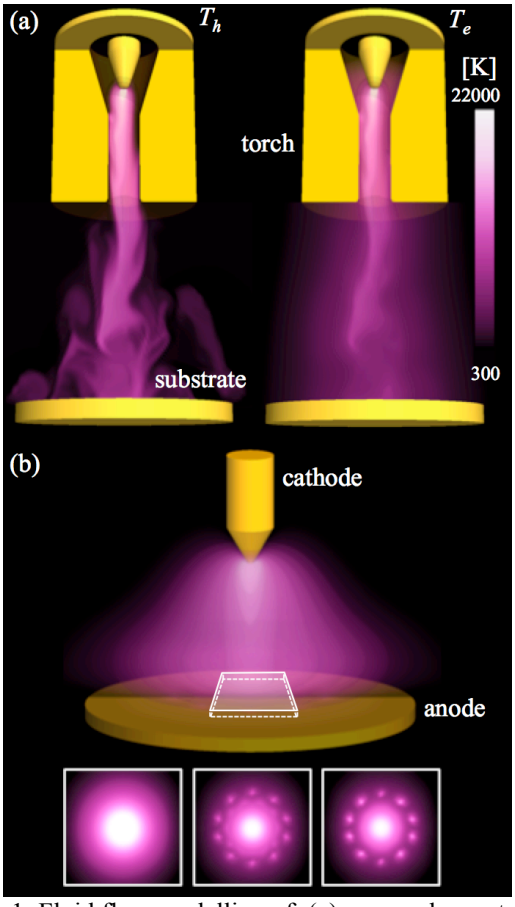

Fig. 1: Fluid flow modelling of: (a) an arc plasma torch showing nonequilibrium between heavy-species (T_h) and electron (T_e) temperatures, and (b) a free-burning arc, depicting the emergence of self-organized anode spots.

4. References

[1] J.P. Trelles, S.M. ModirKhazeni, Comput. Methods Appl. Mech. Engrg (2014) 282, 87-131.

[2] J. P. Trelles, Plasma Processes and Polymers (2016) 14 (1-2), 1600092.

Oral Contributions

Electron temperature of thruster plume plasma in far field

Boris Vayner

Ohio Aerospace Institute, Cleveland, Ohio 44142, USA

Voluminous arrays of data were obtained experimentally for various types of plasma thrusters operated in diverse chambers, and common conclusions were accepted: electron temperature decreased with distance from thruster orifice and increased with the background pressure decreasing. Plume plasma electron temperature is a very important parameter for evaluating the interactions between spacecraft elements and thruster plume. All measurements performed in vacuum chambers indicated rather low electron temperatures (0.5-2 eV) in the far field while computer simulations and measurements in space (one only) pointed to significantly higher temperatures (3-6 eV). The physical mechanisms of electron cooling in far field were not understood because of seemly collisionless electron gas in a vessel. It is shown in current paper that electron cooling in plasma chamber is caused by creation of potential barrier near walls, and this barrier originates from self-organization of electrically neutral plasma.

1.**Introduction**

In order to perform tests in vacuum vessels one needs to know the parameters of the plume plasma in very far field. There are two complimentary approaches to the search for a solution to this problem: 1) performing extensive computer simulations; 2) measuring plasma parameters in ground chambers. These two approaches are mutually intertwined, but the results are frequently contradictive. Generally speaking, plume plasma parameters in a chamber and space are different: backpressure of neutral gas and vessel's walls influence on plasma density, plasma potential, and electron temperature. The quantitative characteristics of these differences for any thruster depend on chamber dimensions and pumping speed [1]. The comprehensive study of all these factors was performed earlier. Background pressure (Xenon) varied from 3.5 μTorr to 73 μTorr. The electron temperature variations at the distance of 1 m from thruster exit plane (at the angle of 50 deg from axis) were determined within the range of 1-2 eV for floating thruster and 0.9-1.3 eV for thruster grounded. The electron temperature increased with pressure decreasing, and measurements error was estimated at 20%. In order to establish adequate test conditions the influence of a test arrangement on plume plasma parameters was analyzed and some criteria for appropriate ground test conditions were presented.

2. Ground experiments

The effect of backpressure was studied for P5 Hall thruster in a quite large chamber with a diameter of 6 m and length of 9 m. Two sets of measurements were performed at xenon background pressures of 3.6 μTorr and 11 μTorr. Probes were positioned at the distance of 1 m from exit plane, which was equal to seven thruster diameters approximately (D_0=148 mm). Certainly, ion current density was decreased about two times with increased pressure, and electron number density demonstrated dependence on pressure with factors of 2-4. Electron temperature varied within the range of T_e=1.2-1.6 eV, and no correlations were established between electron temperature and neutral gas pressure. Plasma properties of Electron Cyclotron Resonance (ECR) thruster in the near field (2 cm from exit plane) were investigated. Electron temperature decreased with increasing flow rate: T_e=2.5-3 eV at $\dot{m} = 20\,sccm$, and T_e=1.3-2.3 eV at $\dot{m} = 36\,sccm.$ These results were obtained in fairly large chamber (D=2.2 m, L=7.9 m), and they confirmed that low electron temperatures were caused by processes inside the thruster but not the influence of background gas pressure.

Plasma plume properties of the cluster of four BHT-200 Hall thrusters were measured at the distances comparable with assembly dimensions. Somewhat higher electron temperatures were recorded in far field for 1.5 kW Hall thrusters (PPS-100ML and PPI).

3. **References**

[1] B. Vayner. XXXIth ICPIG, July 14-19, 2013, Granada, Spain

Topic number: 5

A computational chemical kinetics study of a supersonic microwave plasma for CO_2 dissociation

V. Vermeiren, A. Berthelot, A. Bogaerts

Research group PLASMANT, Department of Chemistry, University of Antwerp, Belgium

Past experiments have reported[1] a record high energy efficiency (up to 90%) for plasma based CO_2 dissociation by means of a supersonic microwave discharge. So far, no detailed description of the chemical processes, occurring in such reactor, has been reported. In this work, we study these processes by means of a chemical kinetics model, elucidating the crucial role of the asymmetric vibrational modes of CO_2. This model uses flow values, calculated by the commercial software package COMSOL, as input parameters for the chemical kinetics model. The study is performed over a range of specific energy input values, by varying both the flow rate and the applied microwave power.

1. Introduction

Microwave sustained discharges have gained increasing interest as a possible pathway in the reduction of anthropogenic CO_2 emission[2]. Their non-equilibrium nature allows for a very efficient excitation of the asymmetric vibrational modes, leading to dissociation[3,4].

Very promising experimental results have been reported with a supersonic microwave discharge, in which the flow passes through a Laval nozzle[1]. In this setup, the flow passes through a convergent-divergent nozzle, which creates a desired pressure drop in addition to a supersonic flow velocity.

So far, no computational chemical kinetics study has been reported, explaining the underlying chemistry for such type of discharge, using a pure CO_2 gas.

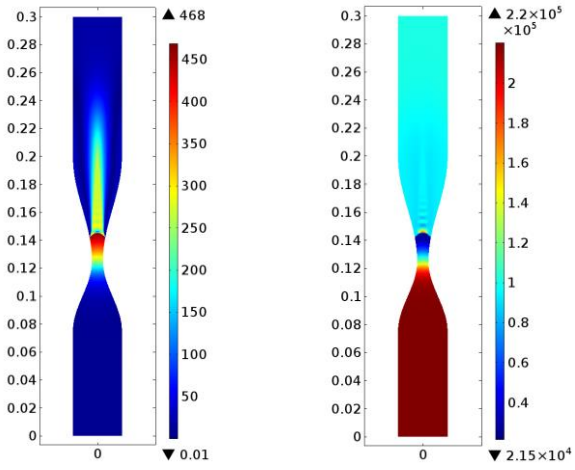

Figure 1: Calculated velocity magnitude [m/s] (left) and absolute pressure [Pa] (right) profiles for a total input pressure of 2 atm.

2. Methodology

This computational study is performed by a 0D chemical kinetics model, using the code ZDPlaskin[5]. The model solves various balance equations for the different plasma species, providing the evolution of the species densities through the reactor. The Electron Energy Distribution Function is calculated at every computational point by a built-in Boltzman solver, called BOLSIG+[6].

The chemistry set which is used in this work is based on the work of Kozák et al[3,4]. It takes into account all the CO_2 asymmetric mode levels up to the dissociation energy of 5.5eV, together with 4 effective low-lying symmetric stretching and bending mode levels.

3. Results

In figure 1, we show the calculated values for velocity and pressure when applying a total pressure of 2 atm on the inlet. The results show the characteristic pressure drop after the nozzle, followed by a shockwave, as is also experimentally observed for a similar setup[1,4].

4. References

[1] Asisov R. I., Vakar A.V., Jivotov V.K., Proc. of the USSR Academy of Sciences, **271** (1983).

[2] Fridman A., Plasma Chemistry, Cambridge University Press (2012).

[3] T. Kozák and A. Bogaerts, Plasma Sources Sci. Technol. **23**, 4 (2014).

[4] T. Kozák, A. Bogaerts, Plasma Sources Sci. Technol. **24**, 1 (2015).

[5] Pancheshnyi S., Eismann B., Hagelaar G. J. M. and Pitchford L. C. Computer Code ZDPlasKin www.zdplaskin.laplace.univ-tlse.fr (2008).

[6] Hagelaar G.J.M. and Pitchford L.C., Plasma Sources Sci. Technol. **14**, 722 (2005).

Quantitative Evaluation of High-Energy Oxygen Negative Ion Flux in DC Magnetron Sputtering of Indium-Tin-Oxide

H. Toyoda, H. Bae, T. Suyama, K. Setaka, H. Suzuki

Departament of Electrical Engineering and Computer Science, Nagoya University, Nagoya, Japan

Particle flux of high-energy (~a few 100 eV) negative ions from indium-tin-oxide target in DC magnetron plasma is evaluated quantitatively, using calorimetric method. Spatial profile of heat flux from the target is measured and localized heat flux originated from high-energy O^- ion is observed. From an O^- kinetic energy of 240 eV measured by an energy-resolved mass spectrometer, O^- particle flux of $2x10^{18}$ ion/m^2s is obtained.

1. Introduction

Indium Tin Oxide (ITO) is popular material as a transparent conductive film because of its low resistivity and high optical transmittance greater than 80%. So far, ITO films are used in many industrial applications, such as solar cell, touch panel, flat panel display, image sensor, and so on.

During the sputter deposition of ITO films, various species are coming to the film depositing surface such as high energy negative ion, positive ion or electrons. To give an insight into the key species for the film quality degradation, we have investigated sputter deposition of ITO films using a magnetron sputter device where 40 MHz VHF power is superposed to conventional DC power [1], reducing kinetic energy of high-energy oxygen negative ions. However, previous studies related to high-energy O^- ions did not mention absolute value of particle flux impinging on the surface, as far as we know. In this study, particle flux of high-energy O^- ions is quantitatively evaluated using calorimetric method.

2. Experimental Set-up

In the experiment, Ar gas is introduced into a cylindrical chamber (30 cm in diameter, 28 cm in height) at a pressure of 0.4 Pa. DC power (<250 V, <0.3 A) is applied to a magnetron sputtering ITO target (12 cm in diameter). A ring-shaped plasma of a 2 cm in radius is produced. A sheathed thermocouple is installed at a target-thermocouple distance of 10 cm. Heat flux is measured from an initial temperature increase rate of the thermocouple after turning on the plasma. To measure radial profile of the heat flux, the thermocouple is movable parallel to the target plate. To discriminate between isotropic heat flux originated from the plasma surrounding the thermocouple and anisotropic heat flux coming from the target, a small shield plate is installed in the vicinity of the thermocouple. Rotating the thermocouple with the shield plate, angle-resolved heat flux is measured and the heat flux originated from the high-energy O^- ions is evaluated.

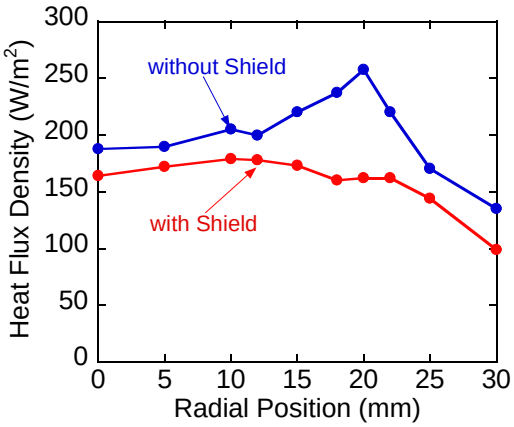

Fig. 1. Radial profile of heat flux with and without heat shield.

3. Results and discussion

Figure shows radial profile of heat flux with and without the shield plate at a discharge current of 0.3 A. With the shield plate, heat flux monotonically decreases with the radial position. Without the shield, however, local increase of the heat flux at a radial position of 2 cm, *i.e.*, just below the magnetron ring, is observed. From space-resolved mass spectrometry, localized high-energy O^- ion at the magnetron-ring radius has been also observed, and considering this fact, the peak of heat flux is considered to be due to the high-energy O^- ions. From the absolute heat flux measurement from O^- ions and O^- ion energy measurement by the energy-resolved mass spectrometer, particle flux of $2x10^{18}$ ions/m^2s is obtained taking account for energy loss by backscatter of surface-neutralized O^- ion and re-sputtering of ITO film by high-energy O^- ions.

Reference

[1] H.Toyoda: J. Vac. Soc. Jpn. **51** (2008) 258.

Modelling the chemical and electrical impact of lightning in the upper atmospheric plasma of planetary atmospheres

F.J. Pérez-Invernón[1], F.J. Gordillo-Vázquez[1] and A. Luque[1]

[1] *Instituto de Astrofísica de Andalucía (IAA), CSIC, Granada, Spain*

The electromagnetic field created by terrestrial lightning discharges has a chemical and an electrical impact in the plasma existent in the upper atmosphere, producing Transient Luminous Events (TLEs). We extend previous models of the impact of quasi-electrostatic field (QE) in the terrestrial mesosphere produced by cloud-to-ground (CG) lightning discharges, providing the community with new tools to interpret observations from spacecraft. In addition, we use a Finite Difference Time-Domain (FDTD) model to investigate possible TLEs existence in the atmosphere of giant planets caused by lightning-emitted electromagnetic pulses (EMP). Finally, we apply these models to the case of Venus to investigate the mesospheric optical signature produced by hypothetical Venusian intra-cloud (IC) lightning, proposing an indirect method to determine the existence of lightning discharges in Venus from the Japanese spacecraft Akatsuki, orbiting Venus since December 2015.

1. Impact of quasi-electrostatic field

The QE field produced by lightning induces glow discharges in the upper atmosphere. We have developed a 2D model to investigate the detailed chemical impact and transient optical emissions produced by lightning discharges in the upper atmospheres of the Earth and Venus.

On Earth, we extend the vibrational model proposed in [1]. We study the temporal density evolution of 136 species interacting through 1090 kinetic reactions under the influence of a QE field created by CG discharges. We predict the geometry of the resultant mesospheric optical emissions, and extract physical information from brigthness measurements of the Lyman-Birge-Hopfield (LBH) band, second positive and first negative systems of nitrogen.

On Venus, we define a chemical scheme composed by 27 species interacting through 79 kinetic reactions [3]. We calculate the expected mesospheric optical signature of hypothetical Venusian lightning, obtaining a transient increase in the OI (557 nm) green airglow emissions, observable from Akatsuki spacecraft.

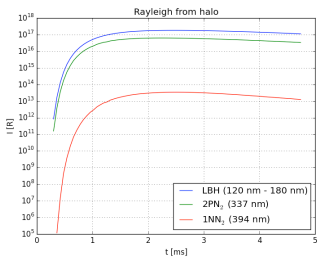

Figure 1: Emission brightness caused by a terrestrial CG lightning with a Change-Moment-Change of 350 C km.

2. Impact of EMP pulses

Terrestrial lightning discharges originate EMPs that can excite the plasma of the upper atmosphere, producing fast (< 1 ms) optical emissions known as elves. The discovery of these emissions could provide new useful information about extraterrestrial atmospheres.

We have developed a 3D FDTD model to solve the Maxwell equations in the atmospheres of giant planets and Venus, using an Intra-Cloud (IC) lightning discharge as a source. This solver is coupled with Langevin's equation for electrons and with a chemical scheme for each planet (Jupiter, Saturn [2] and Venus [3]). We study the influence of lightning channel inclination, background magnetic field and atmospheric composition.

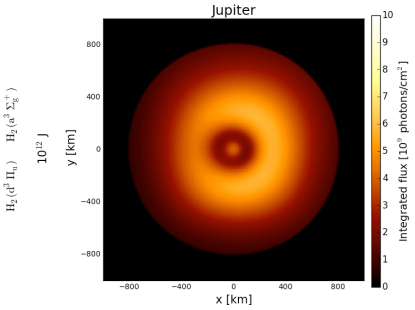

Figure 2: Predicted optical emissions in the upper atmosphere of Jupiter as seen from a spacecraft caused by EMP originated by a vertical lightning discharge.

3. References

[1] Gordillo-Vázquez, F. J. (2010). JGR. 115(A5).

[2] Luque, A., Dubrovin, D., Gordillo-Vázquez, F. J., Ebert, U., Parra-Rojas, F. C., Yair, Y., & Price, C. (2014). *JGR*, *119*(10), 8705-8720.

[3] Pérez-Invernón, F. J., Luque, A., & Gordillo-Vázquez, F. J. (2016). *JGR*, *121*(7), 7026-7048.

Kinetic study on gas discharge plasma generated by focused microwaves

Wei Yang, Qianhong Zhou, Zhiwei Dong

Institute of Applied Physics and Computational Mathematics, Beijing, China

Gas discharge plasmas generated by μs-pulse focused microwaves are investigated. The model is based on a self-consistent solution to Helmholtz equation for microwave field, particle continuity equations, and the energy balance equations, coupled with plasma kinetics. Two recent experiments were studied: a. sub-Megawatt (MW) X-band 9.4 GHz microwave breakdown in 200 Pa nitrogen; b. MW-class W-band 110 GHz microwave breakdown in 1~100 Torr air. In case a, the tracked density of electronic states $N_2(C^3\Pi_u)$ agreed with the measured intensity from second positive system (SPS) of optical emission spectroscopy (OES). In case b, the simulation results reproduced the dependence of nitrogen vibrational and translational temperature on microwave fields and air pressure measured by OES. The underlying mechanisms for above coincidences were unveiled.

1. Introduction

The microwave gas breakdown has applications in beamed energy propulsion, stand-off detection, and plasma heating in ITER. While the focused microwave beam was usually used in the experiments, the theoretical predictions generally used the model of plane electromagnetic (EM) wave. However, the discharge parameter is sensitive to the spatial field amplitude. The difference between plane EM beam and focused beam used in experiments should be noted, especially in the study of energy deposition into gas breakdown plasma.

We develop a plasma fluid model to study the gas discharge plasma generated by focused microwaves. The model calculates the particle densities, electron temperature, nitrogen vibrational T_v and translational temperature T_g, and is time dependent with microwave transmission and reflection considered in the Helmholtz wave equation. Here we studied two recent experiments: a. sub-MW X-band microwave breakdown in 200 Pa nitrogen [1]; b. MW-class W-band microwave breakdown in 1~100 Torr air [2]. The plasma decay in the afterglow is also investigated. The following just shows some important results, and more will be reported in the conference site.

2. Results and discussions

2.1. X-band microwave breakdown in nitrogen

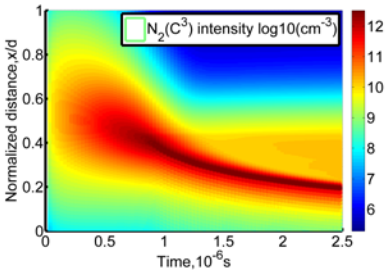

Fig. 1. Spatial and temporal distribution of excited states.

The spatial and temporal behaviour of particle density for excited states $N_2(C^3\Pi_u)$ during pulsed microwave discharge in nitrogen is shown in Fig. 1. The spatial position of density peak moves upstream toward the microwave source (x=0), accompanying the propagation of plasma electrons. The diffusion ionization front of plasma electrons impact neutral gases and generate excited states during its path toward microwave source. The de-excitation processes of quenching higher level excited states and optical transition emission result in generation of lower level excited states. The spatial integral of $N_2(C^3\Pi_u)$ density shows similar trend with the previously measured intensity of SPS [1].

2.2. W-band microwave breakdown in air

The dependences of T_v and T_g on gas pressure are shown in Fig. 2 near the breakdown threshold. The dependence of T_v on gas pressure from 1~100 Torr shows a Paschen-type curve. The vibrational excitation is strongly dependent on electron density, reduced electric field, and the microwave plasma interacting time duration [3]. The T_g shows a monotonic decrease with pressure, and the fast gas heating is attributed mostly to the available thermal energy in quenching of electronic excited states.

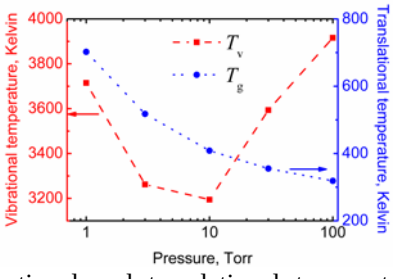

Fig. 2. Vibrational and translational temperature as a function of gas pressure near breakdown threshold.

3. References

[1] M. Mesko, Z. Bonaventura, P. Vasina, *et al.*, Plasma Sources Sci. Technol. **15** (2006) 574.

[2] J. S. Hummelt, M. A. Shapiro, and R. J. Temkin, Phys. Plasmas **19** (2012) 123509.

[3] W. Yang, Q. Zhou, and Z. Dong, Phys. Plasmas **24** (2017) 013111.

Topic number

Fuzzy nanostructure growth on precious metals by He plasma irradiation

S. Kajita[1], T. Nojima[2], Y. Tomita[2], N. Ohno[2], N. Yoshida[3], M. Yajima[4], T. Akiyama[4], T. Yagi[5]

[1] *IMaSS Nagoya University, Nagoya, Japan*
[2]*Graduate School of Engineering, Nagoya University, Nagoya, Japan*
[3]*Research Institute for Applied Mechanics, Kyushu University, Fukuoka, Japan*
[4]*National Institute for Fusion Science, Toki, Japan*
[5]*National Institute of Advanced Industrial Science and Technology, Tsukuba, Japan*

By helium plasma irradiation to precious metals including rhodium (Rh) and ruthenium (Ru), it was found that fiberform nanostructures were formed on the surface. By scanning electron microscopy and transmission electron microscopy analysis, helium bubble growth inside the fuzzy structures were observed. It was likely that the fuzzy structures were easily formed by He plasma irradiation on Rh and Ru because the shear modulus was high similar to tungsten.

1. Introduction

It was found in plasma material interaction in fusion devices that helium (He) plasma irradiation leads to the formation of fiberform fuzzy nanostructures on tungsten surface [1]. The incident ion energy and surface temperature are important parameters to control the surface morphology changes. Furthermore, the He plasma irradiation leads to the nanostructure formation on various metals including titanium, nickel, molybdenum and so on [2]. Because the nano-structurization of metallic material are important for industrial application including for catalysis and photocatalysis, it would be of interest to further investigate the He plasma irradiation effects on other metals as well which were not used for irradiation experiments. In this study, we conducted He plasma irradiation on precious metals including rhodium (Rh) and ruthenium (Ru).

2. Experiments

He plasma irradiation was conducted in the linear plasma device NAGDIS-II, in which high density (~10^{19} m^{-3}) He plasmas can be produced in steady state. Rh and Ru samples were prepared by a magnetron sputtering device. The sample was negatively biased, and the surface temperature was increased by the bombardment of He ions. The surface temperature was measured by a radiation thermometer. Figure 1 shows a typical scanning electron microscope (SEM) micrograph of the He plasma irradiated Rh surface. The incident ion energy was ~45 eV, the surface temperature during the irradiation was ~700 K, and the He ion fluence was 1.1x10^{26} m^{-2}. It was found that fiberform nanostructures were formed on the surface. By transmission electron microscope (TEM) observation, elongated bubbles were observed in the fiberform structures. We also conducted He plasma irradiation on Ru sample. Fiberform structures were also observed on Ru sample which was exposed to the He plasma at the surface temperature of 920 K, the incident ion energy of ~45 eV, and the fluence of 2.4 x10^{26} m^{-2}. The shear modulus of Rh and Ru at the room temperature was 150 and 173 GPa, respectively, and the values were comparable to that of W (161 GPa). It is likely that nanostructure formation tends to take place when the shear modulus is high [3] such as Rh and Ru.

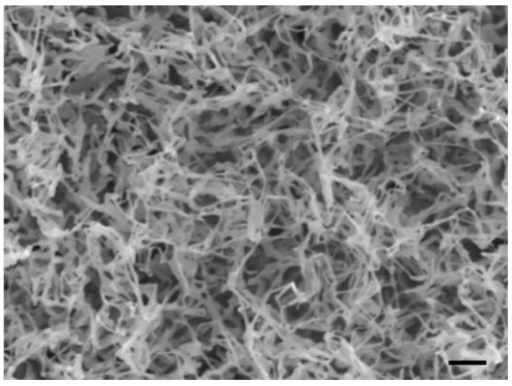

Figure 1: SEM micrographs of He plasma irradiated Rh surface. The length of the bar is 200 nm.

3. References

[1] S. Takamura, N. Ohno, D. Nishijima, and S. Kajita: Plasma Fusion Res. **1** (2006) 051.

[2] S. Kajita, T. Yoshida, D. Kitaoka, *et al.*: J. Appl. Phys. **113** (2013) 134301.

[3] S. Kajita, T. Yoshida, N. Ohno, *et al.*: Sci. Rep.

Mineralization of 2,4-dichlorophenoxyacetic acid by plasma-ozonation

M. Magureanu[1], C. Bradu[2], V.I. Parvulescu[3]

[1] *Department of Plasma Physics and Nuclear Fusion, National Institute for Lasers, Plasma and Radiation Physics, Magurele-Bucharest, Romania*
[2] *Department of Systems Ecology and Sustainability, Faculty of Biology, University of Bucharest, Romania*
[3] *Department of Organic Chemistry, Biochemistry and Catalysis, Faculty of Chemistry, University of Bucharest, Bucharest, Romania*

A pulsed corona discharge in contact with liquid combined with ozonation was investigated for the degradation of 2,4 dichlorophenoxyacetic acid (2,4-D), a widely used herbicide. The target compound was completely eliminated after 30 min treatment. The reaction rate constant for 2,4-D removal by plasma-ozonation was 194.5 x 10^{-3} min^{-1}, more than twice the value obtained by ozonation alone. Within 60 min over 90% mineralization was obtained, which represents a significant improvement as compared to O_3 alone. The chlorine balance demonstrates the absence of chlorinated by-products after 30 min treatment. An attempt to improve energy efficiency revealed the beneficial effect of shortening discharge pulse duration.

Pesticides are commonly detected in various water bodies and thus threaten aquatic species [1]. Various advanced oxidation processes are studied for elimination of these chemicals, and among them ozonation is considered one of the most promising, but the main drawback is poor mineralization [2,3].

In this work, non-thermal plasma generated in a pulsed corona discharge above liquid is combined with ozonation, with O_3 produced in the discharge. This combination proved efficient for the removal of other chemical compounds from water [4]. The target compound chosen for this study is 2,4-D, a widely used herbicide, often detected in surface and ground water and sometimes in drinking water [5].

The experiments were carried out using a pulsed corona discharge above liquid (multiwire-plate geometry) in series with a cylindrical ozonation reactor [4]. The 2,4-D solution (25 mg/L, 330 mL) was continuously circulated between the two reactors and the effluent gas from the plasma was bubbled into the solution contained in the cylinder.

The removal of 2,4-D is completed after 30 min treatment in the plasma-O_3 system (Fig. 1a) and the rate constant (194.5x10^{-3} min^{-1}) is more than twice the value obtained for O_3 treatment alone (88.2x10^{-3} min^{-1}). The mineralization degree is assessed from the elimination of TOC (total organic carbon). TOC removal reaches over 90% after 60 min plasma+O_3 treatment, much superior to the mineralization by O_3 alone (56%) (Fig. 1b). The results prove the major role played by other plasma-generated oxidants, besides O_3, in the degradation of 2,4-D.

Reducing discharge power by shortening the pulse duration did not affect the degradation, and thus results in lower energy costs.

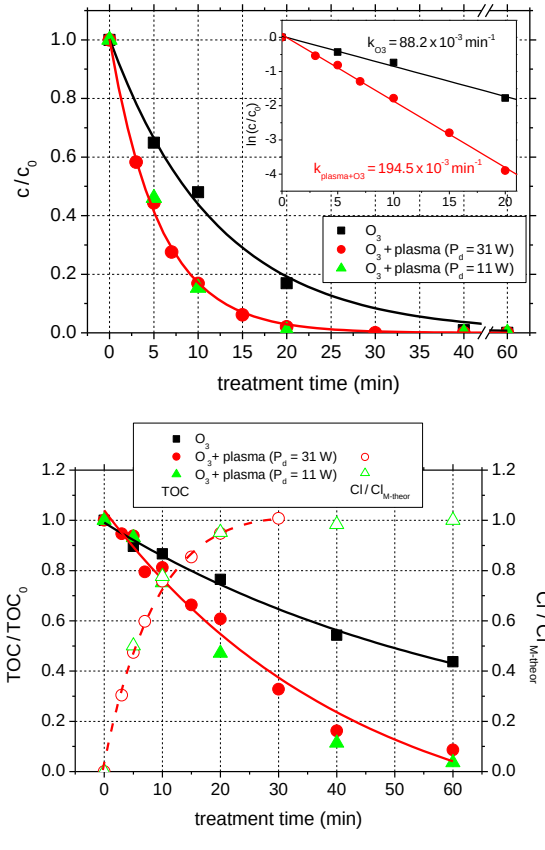

Fig. 1. a: Degradation of 2,4-D; b: Mineralization and dechlorination of 2,4-D solution during ozonation and plasma+O_3 treatment with plasma powers of 11 and 31 W

[1] L.H. Nowell et al., Sci. Total Environ. **476–477** (2014) 144

[2] K. Ikehata and M.G. El-Din, Ozone: Sci. Eng. **27** (2005) 83

[3] S. Chiron et al., Water Res. **34** (2000) 366

[4] M. Magureanu et al., Chemosphere **165** (2016) 507

[5] D.B. Donald et al., Environ. Health Perspect. **115** (2007) 1183

Ultrafast Laser Diagnostics to Interrogate High Pressure, Highly Collisional Plasma Environments

E. V. Barnat[1] and A.Fierro[1]

[1] *Sandia National Laboratories, Albuquerque, NM 87185-1423, USA*

The implementation and demonstration of laser-collision induced fluorescence (LCIF) generated in atmospheric pressure helium environments is presented in this communication. As collision times are observed to be fast (~ 10 ns), ultrashort pulse laser excitation (< 100 fs) of the 2^3S to 3^3P (388.9 nm) is utilized to initiate the LCIF process. Both neutral induced and electron induced components of the LCIF are observed in helium afterglow plasma as the reduced electric field (E/N) is tuned from < 0.1 Td to over 5 Td. Under the discharge conditions presented in this study (640 Torr He), the lower limit of electron density detection is ~ 10^{12} e/cm^3. Spatial profiles of the 2^3S helium metastable and electrons are presented as functions of E/N to demonstrate the spatial resolving capabilities of the LCIF method.

Diagnostics play a key role in assessing our understanding of processes that occur in low-temperature plasmas by benchmarking predictive capabilities as well as through discovering otherwise unexpected behaviors. As the perceived landscape of low-temperature plasma science evolve and challenges become more complex (high densities, shorter lifetimes, more reaction pathways), a broad range of diagnostic capabilities are needed to provide a sufficiently complete picture of the plasma. Therefore, new methods need to be developed and made available to facilitate research efforts of the low-temperature plasma community. In this presentation, we described continued efforts to further the state-of-the-art in plasma diagnostics.

To further the develop of the laser-collision induced fluorescence (LCIF) method [1] for use in such plasmas, a 640 Torr helium discharge, in a point-to-point configuration (Figure 1a) is studied. A key and potentially transformative element of the ongoing effort is the utilization of short pulse (~100 fs) laser to perform the initiation of the LCIF process (Figure 1a). For the presented data, LCIF is observed for 10 ns, starting ~ 1 ns before laser excitation.

To demonstrate the ability of the of the LCIF method to interrogate spatial and temporal evolution of a plasma, the evolution of a 640 Torr helium afterglow plasma in response to a 250 ns high-voltage excitation event (Figure 1b) is studied. It is observed that two excitation fronts are present during the formation of the plasma channel and that behind these fronts resides regions of higher electron density. As the electron density builds, the velocity of the front launched from the cathode (lower electrode) accelerates due to increased localized E/N. The successful development of the

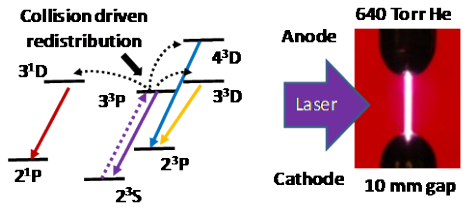

(a)

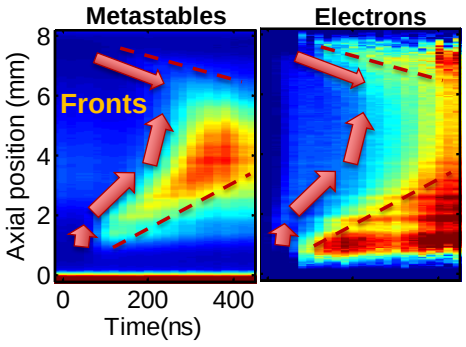

(b)

Fig. 1 – (a) Laser-collision induced fluorescence concept and set-up utilized in studies. (b) Spatial and temporal evolution of helium afterglow plasma in response to 250 ns voltage pulse.

LCIF method in atmospheric pressure plasma environments will be presented in an upcoming fast-track communication [2].

This work was supported by the Office of Fusion Energy Science at the U.S. Department of Energy under contracts DE-AC04-94SL85000 and DE-SC0001939.

[1] E. V. Barnat and K. Frederickson, Plasma Sources Sci. Technol. **19** (2010) 055015.
[2] E. V. Barnat and A. Fierro, J. Phys. D (accepted)

Effects of plasma-facing materials on the negative ion (H-/D-) current extracted from an ECR plasma source

S. Béchu[1], F. Biggins[1], J. Angot [1], S. Aleiferis [2], P. Svarnas [2], Yu. A. Lebedev[3], V. A. Shakhatov[3], A. Bès [1], L. Bonny [1], D. Fombaron [1], A. Simonin [4], A. Lacoste [1]

[1] *LPSC, Université Grenoble-Alpes, CNRS/IN2P3, F-38026 Grenoble, France*

[2] *High Voltage Lab., Electrical & Computer Engineering Dept, University of Patras, Rion-Patras, Greece*

[3] *Topchiev Institute of Petrochemical Synthesis, Russian Academy of Sciences (TIPS RAS), Moscow, Russia*

[4] *CEA, IRFM, F-13108 St Paul lez Durance, France*

The possibility of enhancing the extracted negative ion (H-/D-) current due to plasma-surface interactions on selected materials (potential alternatives of Cs in NBI for tokamak), is herein demonstrated. Current results, from plasmas sustained at a few mTorr by ECR dipolar plasma sources, as obtained with laser photodetachment at 1064 nm, demonstrate that, when tungsten material faces plasma it induces an obvious enhancement of the negative ion density. An extracting system using magnetic cores and three cooled electrodes are used to evaluate effects of the material itself and its relative position in the plasma, on the extracted current. The influence of the dimensions and geometry of the extracting aperture on the beam intensity, are also studied.

1. Background

The ignition of fusion reactions in future reactors requires the injection in the bulk plasma of high-energy high power deuterium neutral beams (34 MW of 1 MeV D° beams on ITER, the international tokamak). These systems, called neutral beam injectors (NBI), are based on the acceleration of intense deuterium negative ion (NI) beams, followed by a neutralization in D_2 gas. These injectors require caesium to reach the demanded current intensity of 55 A. Despite its high efficiency to increase the negative ion extracted current, caesium induces a potential contamination of the accelerator resulting in high voltage breakdowns Hence, an alternative material becomes mandatory to achieve the negative ion current specifications of NBI designed for ITER.

2. Collaborations

LPSC has a long collaboration with CEA-Cadarache (in charge of French scientific research on NBI) searching for alternatives to Cs as a negative ion enhancers. LPSC operates electron cyclotron resonance (ECR) plasma at low power intake (up to 0.2 kW), while High Voltage Laboratory (Patras) investigates identical ECR plasma at higher power (up to 1 kW). Collaboration with the Topchiev Institute (Moscow), allows the development of optical emission spectroscopy diagnostics, as essential for considering plasma-surface interactions.

3. Experimental setup

ROSAE-III is a stainless steel cylindrical plasma reactor [1] (152 mm in diameter and 214 mm long) developed at the LPSC. It is operated with dipolar plasma sources [2] at low pressure (< 25 mTorr). A cylindrical wall-coverage of borosilicate glass (Pyrex™, 5 mm thick), tapped with two circular plates made of the same material, can be housed in ROSAE III. Hence, hydrogen plasma can be confined in a chamber of either low (γ_H = 0.005; Pyrex™ at 280 K) or moderate (γ_H = 0.1-0.5; stainless steel) recombination coefficient. Studied materials are mounted on the Pyrex™ surface to face the H_2/D_2 plasma. Absolute negative ion density has been already measured inside ROSAE-III by laser photodetachment at 1064 nm. Furthermore, recently, an extracting device has been designed, following 3D modelling (COMSOL software [3]), and it is being implemented for measurements of the negative current extracted from the plasma. It consists of three cooled electrodes. Two magnetic cores are used to prevent electrons from being co-extracted with negative ions.

4. Results

The above experimental device should validate recent results of photodetachment measurements that shown a significant enhancement, by a factor 2.5, of the negative ion density in the bulk plasma when tungsten coverage is used. It will not only allow to assess the effect of the materials nature (tungsten, tantalum, and graphite) on the extracted currents but also to determine its best location with respect to the extracting aperture to maximize the negative ion current.

5. References

[1] S. Bechu et al., Phys. Plasmas. **20**, (2013).

[2] A. Lacoste et al., Plasma Sources Sci. T **11**, 407 (2002).

[3] https://www.comsol.fr/

Application of plasma-bullet propagation to hydrophilic treatments of an interconnected porous scaffold

M. Oshiro[1], T. Shirafuji[1], K. Orita[2], Y. Hirakawa[2], H. Toyoda[2]

[1] *Deparment of physical Electronics and Informatics, Graduate School of Engineering, Osaka City University, Osaka, Japan*
[2] *Department of Orthopedic Surgery, Graduate School of Medicine, Osaka City University, Osaka, Japan*

An atmospheric pressure plasma jet employing dielectric barrier discharge of helium gas is known to be a source of plasma bullets, which propagate in high-purity helium gas channels. A plasma bullet propagates to the direction independent of gas-flow direction, and nicely separated when they encounter branches of gas channels. We have applied these characteristics of plasma bullets to hydrophilic treatment of internal surfaces of an interconnected porous scaffold. The scaffold employed in this work is a hydrophobic treated glass filter with a thickness of 3.15 mm and a pore-channel diameter of 160-250 μm. Plasma bullets injected from one side of the scaffold have penetrate it and ejected from the other side. Water permeability of the scaffold has been markedly improved after the treatment with the plasma-bullet penetration.

1. Introduction

Atmospheric pressure plasma jets (APPJs) have been widely used for various surface treatments. Its unique nature involving "plasma bullets" [1] may be used for the treatment of internal surfaces of an interconnected porous scaffold used in bone-regeneration. There are few reports which discuss utilization of plasma bullets for such treatment, while there are extensive works using low pressure plasma [2] or those using an APPJ as a simple jet [3].

2. Experimental Setup

We have irradiated a helium APPJ to a hydrophobic treated glass filter, instead of expensive HA or β-TCP, of which thickness and pore channel diameter are 3.15 mm and 160-250 μm, respectively.

3. Results and discussion

Figure 1 show time-evolution of plasma bullets on *the back side* of the APPJ-irradiated glass filter, which indicates that the bullets penetrate the glass filter and exit out of its back side. Figures 2(a) and 2(b) show that water permeability of *the back side* of the glass filter before and after the treatment for 10 min. We can see marked improvement in water permeability of the hydrophobic glass filter after the treatment. These results indicate that the internal surfaces of the hydrophobic glass filter have become hydrophilic by propagation of plasma bullets.

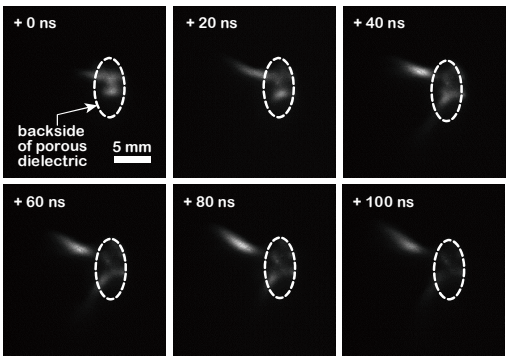

Fig. 1 Propagation of plasma bullets ejected from the glass filter.

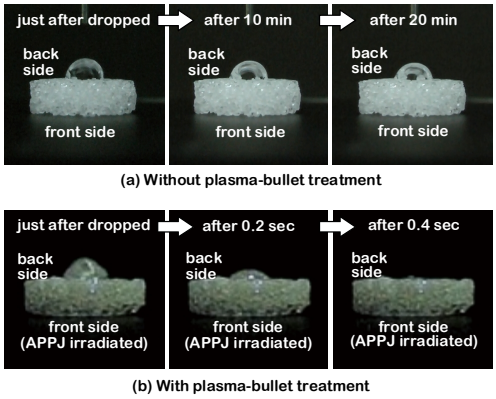

Fig. 2 Water permeability of the glass filter before and after the plasma-bullet treatment.

Acknowledgements

This work was partly supported by JSPS MEXT KAKENHI Grant Numbers 15H03585 and 15K13391.

References

[1] M. Teschke et al, IEEE Trans. Plasma Sci. **33**, 310 (2005).
[2] D.-S. Lee et al, J. Phs. D **45**, 372001 (2012).
[3] I. Trizio et al, Plasma Process. Polym. **12**, 1451 (2015).

Bubble formation in the discharge between planar and needle electrodes via laser ablation-induced cavitation bubble

K. Sasaki and Y. Takahashi

Division of Quantum Science and Engineering, Hokkaido University, Sapporo, Japan

We observed the formation of a bubble in the discharge process between needle and planar electrodes. A unique experimental condition was that a cavitation bubble, which was induced by liquid-phase laser ablation, was positioned between the electrodes. When the distance between the needle electrode and the gas-liquid boundary of the cavitation bubble became close, we observed the formation of an additional bubble from the tip of the needle electrode. The discharge occurred when the needle electrode and the cavitation bubble was connected by the additional bubble. It should be emphasized that the bubble formation was not induced by the Joule heating of water, since we observed the bubble formation even when the current through the electrode was negligible.

1. Introduction

The discharge processes in bubbles in water attract much attention recently, but the physics of the discharge in a bubble has not been fully understood yet. In addition, we also have insufficient understanding about the effects of electromagnetic fields on the formation processes of bubbles in water. In this work, we observed the bubble formation from the tip of a needle electrode which was connected to a high-voltage power supply. A unique point of the present experiment is that the needle electrode faced the gas-liquid boundary of a laser ablation-induced cavitation bubble.

2. Experiment

A titanium plate, which was electrically grounded, was installed in water, and it was irradiated by focused Nd:YAG laser pulses from the normal direction. A needle electrode, which was connected to a high-voltage power supply, was placed at a distance from the ablation point. The irradiation of the laser pulse induced a cavitation bubble. The cavitation bubble had the dynamics of the expansion, the shrinkage, and the collapse, but the tip of the electrode was separated from the gas-liquid boundary of the cavitation bubble even when the bubble size became maximum.

3. Results and discussion

Figure 1 shows shadowgraph pictures and the waveforms of the voltage and the current. We employed a pulsed power supply in this experiment, and the high voltage was switched on at a delay time of T_0=267 μs after the irradiation of the laser pulse. Figure 1(a) shows the shadowgraph picture at this timing. The shadows of a hemispherical cavitation bubble and the needle electrode are seen in Fig. 1(a). After the spiky displacement current, a conduction current of approximately 20 mA passed from the needle electrode to the grounded titanium plate. At a

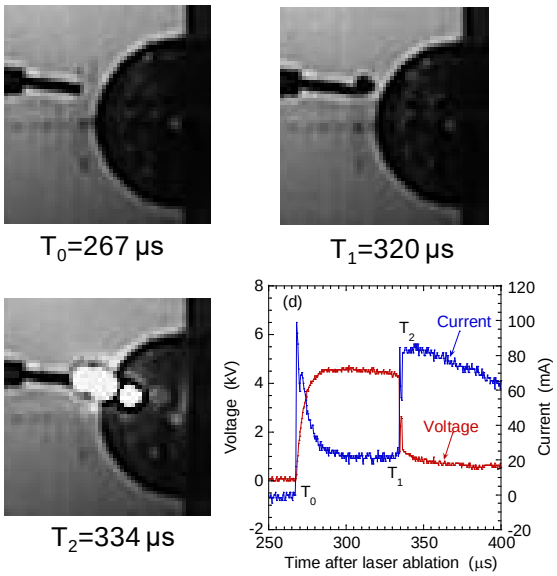

Fig. 1 (a)-(c) Shadowgraph images observed at various delay times, and (d) voltage and current waveforms.

delay time of T_1=320 μs, we observed the formation of a bubble from the tip of the needle electrode, as shown in Fig. 1(b). The bubble was lengthened toward to gas-liquid boundary of the cavitation bubble. The discharge between the needle electrode and the titanium plate occurred at a delay time of T_2=334 μs, when the bubble connected the cavitation bubble and the needle electrode, as shown in Fig. 1(c). It is noted here that a similar bubble formation was observed even when we employed an alumina target. Since the conduction current was negligible in the case using the alumina target, it is considered that the bubble formation was not caused by the Joule heating of water.

Measurement of the CH rotational temperature in DBD discharges in CH_4/CO_2/He mixtures and simulation of the gas temperature

N. Pinhão[1], J. Branco[2]

[1] *Instituto de Plasmas e Fusão Nuclear, Instituto Superior Técnico, Universidade de Lisboa, Lisboa, Portugal*

[2] *Centro de Ciências e Tecnologias Nucleares, Instituto Superior Técnico, Universidade de Lisboa, Lisboa, Portugal*

This work is dedicated to the measurement of the CH rotational temperature on micro-discharges in an atmospheric pressure DBD plasma in CH_4/CO_2/He mixtures. The rotational temperature is obtained from the optical emission of the CH ($A\ ^2\Delta$ - $X\ ^2\Sigma$) transition. The discharge is produced either by an ac or fast pulse generators. The CH rotational population shows a bimodal distribution with a high temperature tail and thermalized body. To evaluate if the rotational temperature is a good indication of the gas temperature, we have computed the gas temperature profile for a given input power through the simultaneous solution of the heat and Navier-Stokes equations. The modeling values are consistent with the rotational temperatures obtained.

1. Introduction

Non-thermal plasmas have been used for the conversion of methane/CO_2 mixtures into synthesis gas (CO/H_2) and higher hydrocarbons. In order to understand the chemical kinetics and build reliable models for these mixtures, it is necessary to know the gas temperature of the micro-discharges. Previous studies on CH_4 and CH_4/CO_2 mixtures [1] using the CH ($A\ ^2\Delta - X\ ^2\Sigma$) transition have found rotational temperatures, T_r, between 50-200 degree higher on the micro-discharges than the volume averaged gas temperature. In this work we study the influence of the specific energy input, the dilution in helium, and the type of power supply on T_r. In order to assess the gas temperature distribution on the reactor and compare with the T_r, we build a model for the gas and heat fluxes along the reactor taking into account the input power, the chemical energy efficiency and the energy losses to the surrounding air.

2. Experimental set-up and modeling

The experimental system is described in [2]. It is a cylindrical DBD reactor powered by three type of generators: a sinusoidal generator with frequencies of 5-20 kHz and two pulse generators: (i) a solid state switch producing 1.2 µs width rectangular pulses with 80 ns raise time and repetition rate of 2-10 kHz and, (ii) a drift step recovery diode generator producing pulses with <4 ns rise time, 10 ns FWHM and repetition rate of up to 3.5 kHz. The CH rotational bands were monitored with a mini-optical spectrometer with a 1.7 nm resolution and cooled to -10 ºC. The numerical results were obtained with the Elmer multi-physics FEM code coupling the Navier-Stokes and the heat equations. The power input corresponds to the experimental values.

3. Results

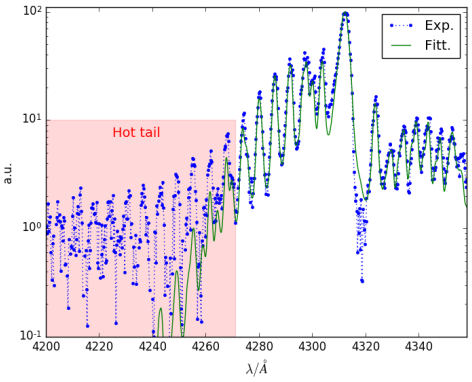

Figure 1: CH spectra showing the hot tail. Points: experimental results; lines: fit with LIFBASE

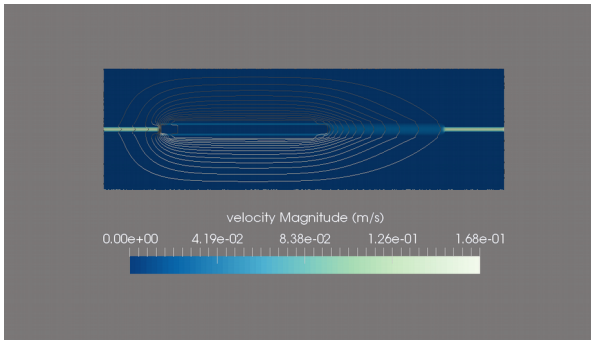

Figure 2: Color scale: Gas velocity on the reactor; Contour lines: temperature distribution from 300 K to 580 K with steps of 25 K

3. References

[1] J. Luque, M. Kraus, A. Wokaun, K. haffner, U. Kogelschatz and B. Eliasson *J. Appl. Phys.* **93** (2003) 4432-4438.

[2] N. Pinhão, A. Moura, J.B. Branco and J. Neves *Int. J. Hydrogen Energy* **41** (2016) 9245

Acknowledgments: This work was funded by Portuguese FCT – Fundação para a Ciência e a Tecnologia, under project UID/FIS/50010/2013.

Realistic 3D Particle Modelling of Discharge Inception near Ice Particles and other Dielectric Objects

C. Rutjes[1], J. Teunissen[1,2], U. Ebert[1,3]

[1] *Centrum Wiskunde & Informatica, Amsterdam, The Netherlands*
[2] *Centre for Mathematical Plasma-Astrophysics, KU Leuven, Leuven, Belgium*
[3] *Eindhoven University of Technology (TU/e), Eindhoven, The Netherland*

Prior to streamer formation, when the numbers of charged particles in the relevant region are still relatively low, a fluid discharge model is not appropriate. We have developed a particle model to study the initial phase, specifically the stochastic nature of positive streamer inception near dielectrics and other surfaces. The model is motivated by lightning initiation near ice particles in thunderclouds, but can be applied more generally to jitter in discharge inception. The model is designed such as to easily continue with 3D streamer simulations in the Afivo framework. This enables the first 3D streamer simulations that start with realistic initial distributions of electrons and ions.

1. Problem setting

In thunderstorms, streamers (as precursors for lightning leaders) can be initiated from hydrometeors (droplets, graupel, ice needles, etc.). These hydrometeors locally enhance the thundercloud electric field to values above electric breakdown; the initial electrons in the humid air of the cloud may be provided by extensive air showers [1]. Typically, streamers are modelled with a deterministic fluid model (i.e. drift-diffusion-reaction coupled with Poisson), which is now possible in full 3D with the Afivo framework [2].

However, under typical subcritical conditions electrons will only multiply in regions of local field enhancement to values above breakdown that can occur near a dielectric object. For typical hydrometeors this region is at most of the order of a cubic millimetre. Hence only individual electron avalanches – with their intrinsically random nature – are entering the breakdown area sequentially. On these scales, a deterministic fluid description is not valid**.** Therefore, we have developed a stochastic particle model to study the behaviour of the system described above, to calculate the probability of streamer inception for a given hydrometeor, electric field and initial electron density.

2. The DIPIC3D code

The DIPIC3D (Discharge Inception Particle in Cell 3D) code is a further development of the code used in [3] and assumes that initially space charge is not important, enabling fast parallel computation of the particle dynamics in the electric field. The initial electric field can be loaded from third party software packages like COMSOL®. In addition, the code can project particles into cells of the octree grids in the Afivo framework [2], which includes adaptive mesh refinement (AMR), a geometric multigrid solver, shared-memory (OpenMP) parallelism and it supports output in Silo and VTK file formats. In this manner, space charge effects can be included in the later stage of the discharge evolution, but currently still excluding polarization, which is fair for ice where the dielectric constant for fields changing on the nanosecond scale is relativity low (~3 compared to ~90 for stationary fields).

3. Results

First results show that the discharge starts with great jitter and usually off the symmetry axis, demanding a stochastic approach in full 3D for streamer inception in realistic thunderstorm conditions. We will present the latest developments of the DIPIC3D code and discuss our simulation results. After publication, the software will be made available as open source.

4. Acknowledgments

C.R. acknowledges funding by FOM Project No. 12PR3041, and J.T. by postdoctoral fellowship 12Q6117N from FWO.

5. References

[1] A. Dubinova et al., *Prediction of lightning inception by large ice particles and extensive air showers,* Phys. Rev. Lett. **115** (2015) 015002.

[2] J. Teunissen and U. Ebert, *Afivo: a framework for quadtree/octree AMR with shared memory parallelization and geometric multigrid methods,* submitted to Comp. Phys. Comm., arxiv.org/abs/1701.04329.

[3] J. Teunissen and U. Ebert, *3D PIC-MCC simulations of discharge inception around a sharp anode in nitrogen/oxygen mixtures,* Plasma Sources Sci. Technol. **25** (2016) 044005.

Investigation of Ion Dynamics in Collisionless RF Sheath

Yunchang Jang[1], H.-J. Roh[1], N.-K. Kim[1], S. Ryu[1], Y. Jin[1], S. Shim[2], M. Choi[2], S. Jeong[2], J. Cho[2], D. Sung[2], Gon-Ho Kim[1].

[1] *Deoartment of Energy Systems Engineering, Seoul National University, Seoul, Korea*
[2] *Mechatronics R&D Center, Samsung Electronics Co., Ltd, Hwaseong, Korea*

It was invesigated that energy spread of ion energy distribution (IED) which is known as being governed by the dynamics of ion in RF sheath and the magnitude of RF voltage peak. Semi-analytic models was derived from concept of ion response time (τ_i) in previous study. However, the property of ion response time (τ_i) was not clearly understood. In this study, τ_i was investigated with varying RF period (τ_{rf}) in a low pressure Ar plasma. Experiment results revealed that the time scale of ion response time is determined by one of the ion plasma frequency (ω_{pi}) rather than the ion transit time across the sheath (τ_{ion}) in this high-density plasma.

1. Background

The dynamics of ion motion in the collisionless rf sheaths play an important role in the determination of the energy spread of ion energy distribution (IED) with varying RF. Miller et al. proposed the concept of ion response time (τ_i) to RF sheath voltage and assumed that ion thermal motion at sheath boundary determine IED [1]. Sobolewski et al. [2] represented that the ion energy broadness (ΔE_i) is in terms of the sheath voltage oscillation (V_{pp}) and τ_i/τ_{rf} as shown in Equation 1 by using Miller's theory.

$$\Delta E_i = eV_{pp}\left[1+\left(2\pi\right)^2 \tau_i^{\,2}/\tau_{rf}^2\right]^{-1/2} \qquad (1)$$

Previous IED analyses adopted this equation as a function of ion transit imte across the sheath (τ_{ion})/τ_{rf} with a correction factor to explain the experiments or simulation results of ion energy spread [3]. Specifically, the correction factor played important role in the analyses. In this study, we focused on what physics governs the correction factor, consequently defining the ion response time τ_i with RF voltage oscillation. Experimental data taken in the low pressure Ar plasma with various RFs were compared to Equation (1) with the time scale of τ_{ion} and time scaled of $1/\omega_{pi}$.

2. Experimental setup

Experiment were performed in an argon VHF-CCP at 20 mTorr which has the ratio of maximum sheath size to ion mean free path ~ 2. Various ranges of RF (from τ_i/τ_{rf} ~ 0.05 to τ_i/τ_{rf} ~10) were applied to bottom electrode to enhance the incident ion energy with very high frequency (VHF, τ_i/τ_{rf} ~10) which was applied on the top electrode (showerhead) to sustain plasma. One RF bias power was applied to bottom electrode alone. A commercial retarding field analyser (Impedans, Vertex V4.0.10) was employed to measure IED. Plasma density, electron temperature and plasma potential were measured by using RF compensated Langmuir probe.

3. Results and Discussion

Experimental results of ΔE_i to V_{pp} are summarized in Figure 1. It is compared with models under assumptions that ion response time is ion transit time (indicated by solid and dotted lines) or one of ion plasma frequency (indicated by dashed line). The dashed line is agreed well with the experiments results, implying that the ion energy arriving at surfaces is governed by the ion thermal motion at the sheath boundary. Consequently, it determines the initial condition of ion acceleration.

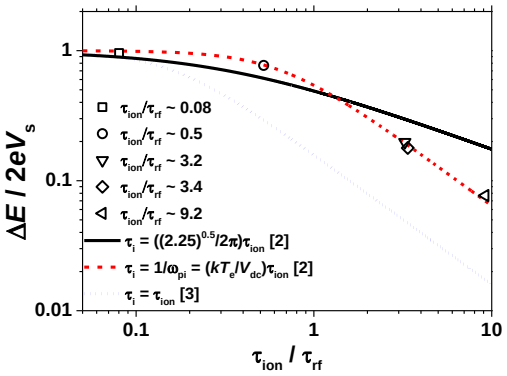

Figure 1. The ratio of ion energy broadness to sheath voltage magnitude as a function of τ_{ion}/τ_{rf} (symbols) for comparison between models (lines).

4. References

[1] P.A. Miller and M.E. Riley, J. Appl. Phys. **82** (1997) 3689.

[2] M.A. Sobolewski, Y. Wang, and A. Goyette, J. Appl. Phys. **91** (2002) 6303.

[3] A.C.F. Wu, M.A. Lieberman, and J.P. Verboncoeur, J. Appl. Phyis. **101** (2007) 056105

Acknowledgements

This work was partly supported by the Brain Korea 21 Plus Project (No. 21A20130012821) and Samsung Electronics Co., Ltd. (Project No. 0620-20160027)

Spectroscopic study of low pressure, low temperature H_2-CH_4-CO_2 microwave plasmas used for large area deposition of nanocrystalline diamond films

A. S. C. Nave[1], B. Baudrillart[2], S. Hamann[1], F. Bénédic[2], G. Lombardi[2], A. Gicquel[2], J. H. van Helden[1], J. Röpcke[1]

[1] *INP Greifswald, 17489 Greifswald, Germany*
[2] *LSPM CNRS UPR 3407 Université Paris 13, 93430 Villetaneuse, France*

In a distributed antenna array (DAA) reactor, microwave H_2 plasmas with admixtures of 2.5% CH_4 and 1% CO_2 used for the deposition of nanocrystalline diamond films have been studied by infrared absorption and optical emission spectroscopy techniques.

1. General

Although already more than two decades ago the feasibility of the deposition of nanocrystalline diamond (NCD) has been shown [1], the further development of this technology is still of great importance, in particular, as far the treatment of large substrates at relatively low temperatures is concerned. The physical properties of NCD are comparable to polycrystalline diamond (PCD), however, compared to PCD, NCD films are characterized by a very low roughness, which is independent on the thickness of the layers. A wider commercial use of NCD films has been limited so far (i) by insufficient adhesion properties to substrates and (ii) by the requirement of high substrate temperatures above 800 °C damaging sensitive substrates in the deposition process.

2. Experimental

In 2007 Latrasse and co-workers developed a new approach to provide high density microwave plasma sources for large area depositions while ensuring relatively low substrate temperatures below 400 °C. This new concept to realize a planar reactor comprises a 2-dimensional matrix of several single microwave plasma source elements without using magnetic fields [2]. Based on this 2-dimensional matrix approach of microwave antennas a 4 x 4 configuration has been successfully used to deposit uniform NCD films with very low surface roughness between 5 – 10 nm and a grain size in the range of 10 – 20 nm on a 4 inch wafer in 2014 [3].

The deeper understanding of the complex chemistry in H_2-CH_4-CO_2 microwave plasmas will be a crucial step for the further improvement of large scale NCD deposition at low substrate temperatures. In the present contribution optical emission spectroscopy in the visible spectral range has been combined with absorption spectroscopy (AS) in the mid-infrared spectral. For the latter one two different radiation sources have been used. Firstly, traditional lead salt lasers, since several decades employed in tunable diode laser absorption spectroscopy. Secondly, a new laser class, external cavity quantum cascade lasers (EC-QCLs), which up to now have only been used in limited cases in plasma diagnostics. In contrast to lead salt lasers EC-QCLs can be tuned over a spectral range greater than 100 cm^{-1} with a mode-hop free tuning range of the order of 80 cm^{-1}.

3. Results

Using AS the absolute concentrations of the methyl radical and of five stable molecules, CH_4, CO_2, CO, C_2H_2 and C_2H_6, were monitored in the reactor. Reliable information about the neutral gas temperature is a crucial precondition for the determination of concentrations of molecular species. Monitoring a variety of CO lines in the ground state and in three hot bands enabled an extensive temperature analysis providing novel insights into energetic aspects of the multi component plasma. An additional target was to derive fragmentation rates of the CH_4 and CO_2 precursors and their conversion rates to the reaction products. The influence of the discharge parameters power and pressure on the molecular concentrations was another focus of interest.

3. References

[1] D. M. Gruen, X. Pan, A. R. Krauss, S. Liu, J. Luo, C.N. Foster, J. Vac. Sci. Technol. A **12** (1994) 1491.

[2] L. Latrasse, A. Lacoste, J. Sirou, J. Pelletier, Plasma Sources Sci. Technol. **16** (2007) 7.

[3] H.-A. Mehedi, J. Achard, D. Rats, O. Brinza, A. Tallaire, V. Mille, F. Silva, C. Provent, A. Gicquel, Diamond Rel. Mat. **47** (2014) 58.

Control methods of RONS in Dielectric Barrier Discharge

Seungmin Ryu, Hyeongwon Jeon, Sangheum Eom, Jungwoo Yoon, Suk Jae Yoo and Seong Bong Kim

Plasma Technology Research Center, National Fusion Research Institute, Gunsan-city, Korea

Plasma in natural air condition can produce reactive oxygen and nitrogen species (RONS) simultaneously but ROS (Reactive Oxygen Species) and RNS (Reactive Nitrogen Species) has different application in the field of postharvest. ROS is a powerful disinfectant and RNS is an inhibitor of agri-food ripening. Therefore the production rate control of RONS is important. Frequency and flowrate of air can be methods of RONS concentration control factor. Applied frequency range was from 0.1 to 8 kHz and atmospheric air flow rate was from 0 to 20 l/m. The generation rates of O_3, NO and NO_2 were measured by the gas analysers. As external air flow rate was increased, the generation rate of O_3 was increased from 0 to 3.61 mg/min. In the contrary, the generation rate of NO was decreased from 0.21 to 0 μg/min. Frequency can control the production rate of RONS and optimum ozone and NO generation frequency was 3 and 8 kHz respectively.

1. Introduction

32% of all agri-food in the world was lost or wasted per year. The big two cause of food waste is rottenness by fungi and ripening by hormone. Ozone, OH radical, O radical, hydrogen peroxide are called as ROS and it is powerful disinfectant of fungi [1]. NO and NO_2 are called as RNS and considered as a key species in hormone-regulated processes [2]. Plasma discharge of air produces complex RONS but, only particular chemical reactive species might be useful to special purpose therefore, it is necessary to produce appropriate ROS or RNS. The flow rate and frequency was selected as affecting factors of RONS production rate.

2. Experimental Set-up

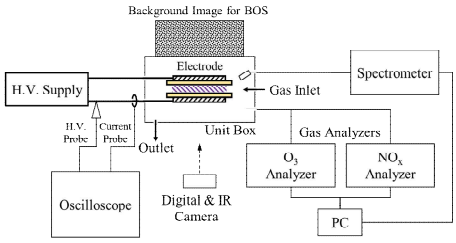

Figure 1. Experimental Set-up

Figure 1 shows the experimental set-up for measurements of electrical, optical and chemical properties of plasma discharge with different flow rate and frequencies.

3. Experimental Results

Figure 2 shows the results of ozone and NO concentration changes with different flow rates. As external air flow rate was increased, the generation rate of O_3 was increased from 0 to 3.61 mg/min. In the contrary, the generation rate of NO was decreased from 0.21 to 0 μg/min. Figure 3 shows the optimum frequency for generating maximum ozone or NO generation. 3 kHz is best to produce ozone and 8 kHz to nitric oxide.

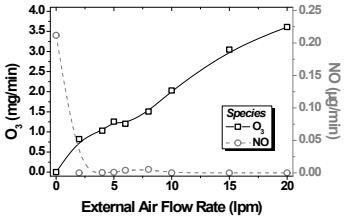

Figure 2. Generation rates of O_3 and NO by flow rates

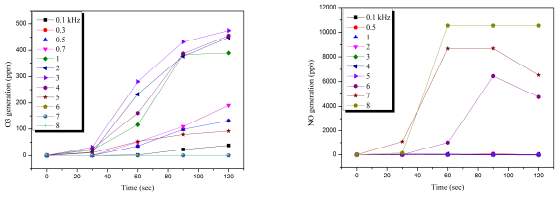

Figure 3. Concentration of O_3 (a) and NO (b) according to the frequency

4. Discussions

Frequency and air flow rate might be related to the plasma region bulk temperature. Temperature can be one key factor of RONS production and it is necessary to study further.

5. Acknowledgement

This work was supported by R&D Program of 'Plasma Advanced Technology for Agriculture and Food (Plasma Farming)' through the National Fusion Research Institute of Korea (NFRI) funded by the Government funds.

6. Reference

[1] S. Horvitz, M. J. Cantalejo, *Food Science and Nutrition*, **54** (2014) 312-339

[2] Lili Deng et al., *Postharvest Biology and Technology* **84** (2013) 9–15 -NO

Topic number 6

A novel non-invasive technique for detection and analysis of harmonics in Radio Frequency plasmas

A. Rawat, A. Ganguli, R. Narayanan, R. D. Tarey

Centre for Energy Studies, Indian Institute of Technology, New Delhi 110016, India

In this work, a new plasma diagnostic technique is proposed to analyze the harmonics generated in Radio Frequency (RF) discharges accurately using a Dual Directional Coupler (DDC). A careful and complete analysis not only determines the harmonics present in plasma, but also yields accurately the power in the *forward* and *reflected* waves of the fundamental and each harmonic generated in the plasma, which makes it a valuable plasma diagnostic tool. Apart from this, one can estimate the complex impedance and reflection coefficient at the plasma end for each harmonic as well as the fundamental. This non-invasive, calibrated experimental technique may prove useful in formulating a systematic model which enhances understanding of RF plasma heating at low pressures.

1. Introduction

In Radio Frequency (RF) discharges, two mechanisms of electron heating play crucial roles: (i) Ohmic heating at high pressures, due to electron-neutral collisions and (ii) Stochastic heating at low pressures, due to electron-sheath interaction [1, 2]. Due to the non-linear sheath behaviour, harmonics are generated in the plasma, which need to be considered for understanding how the RF power is coupled at low pressures. In this paper, a novel, non-invasive harmonic probe technique is presented that characterizes the plasma-generated-harmonics of a parallel-plate RF discharge using calibrated broadband Dual Directional Coupler (DDC). This technique determines the dominant harmonics produced by the plasma and yields accurately the ***forward*** and ***reflected*** power in the fundamental and harmonics.

2. Experimental Details and Methodology

The experiment is carried out in a 13.56 MHz, RF discharge system with parallel plate electrode geometry as shown in Fig. 1. The measured plasma densities are in the range 10^9 - 10^{10} cm^{-3} and electron temperatures in the range 1 - 2.5 eV. The experimental parameters varied are the RF power (25 - 60 W) and Argon gas pressure (10 - 80 mTorr).

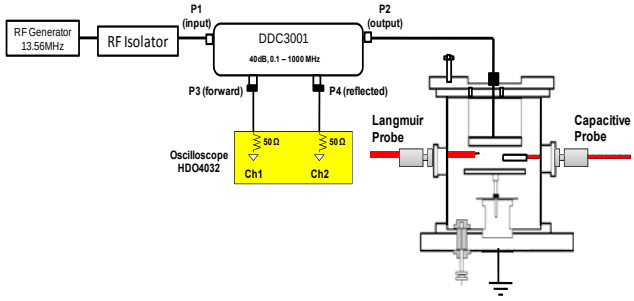

Figure 1 Experimental set up for harmonics analysis using DDC and Capacitive Probe.

A matching network was not used in the present experiments as its coupling capacitance allows the (plasma) load to develop a high DC self-bias voltage that can damage the DDC. However, an isolator has to be used to isolate the generator from the power flowing from the load to the generator.

The two DDC output signals yield the total forward (from the generator to the load) and reverse (from the load to the generator) power flow in the fundamental and the harmonics. The two output signals of the DDC are actually a superposition of the fundamental and harmonics produced by the plasma. The contribution of each frequency to the total signal is carried out by Fast Fourier Transform (FFT), from which other data like forward and reflected power, complex impedance at load etc. may also be determined for each frequency.

3. Results and Conclusions

While detailed results will be presented during the conference, the results indicate that among all the harmonics generated in the plasma, power content of the third harmonic (40.68 MHz) dominates in the present experiments. Since RF isolator absorbs all the harmonics generated from the plasma, this diagnostic gives way to characterize the different harmonics in a non-invasive manner. This precise information can be used to develop a better model for understanding power coupling in the low pressure regime.

4. References

[1] M. A. Lieberman and A. J. Lichtenberg, Principles of Plasma Discharges and Materials Processing, Wiley, New York, (1994).

[2] J. Schulze, Z. Donko, D. Luggenholscher and U. Czarnetzki, Plasma Sources Sci. Technol., **18**, (2009) 034011.

Active and passive optical diagnostics in a model HV circuit breaker

E.Panousis[1], P. Stoller[1], J.Carstensen[1], V.Teppati[1], R.Methling[2], St.Franke[2], S.Gortschakow[2]

[1] *ABB Corporate Research Center, ABB Schweiz AG, Baden - Switzerland*
[2] *Leibniz Institute for Plasma Science and Technology (INP), Greifswald - Germany*

We present results on the probing of an air arc in a HV circuit breaker model geometry using two distinct experimental techniques. First we apply Speckle imaging, an active refractive index based technique that yields quantitative information on the radial temperature distribution *T(r)* via a generalization of the Gladstone-Dale law [1]. Second, in a passive technique we use high speed video imaging of selected atomic (O-I) and ionic species (N-II) using appropriate narrow band filters. Post-processing the videos also allows to obtain *T(r)* based on the Fowler-Milner method [3] for the atomic emission. The results of the two techniques are found to be in good agreement.

1. Introduction and Experimental Set-Up

Optical diagnostics are a non-invasive means of probing the spatio-temporal evolution of key quantities (e.g. temperature) in the understanding of the phenomena in HV switching arcs: such experimental data are important for the benchmarking of CFD simulations that are used in the development of HV gas circuit breakers. The goal of the present work is to provide such validated data by employing two distinct optical diagnostic techniques and comparing their findings.

On the one hand we apply the Speckle interferometric technique [1] which probes the spatial derivative of the refractive index by illuminating the arc with a pulsed (20ns, 60kHz) Nd:YAG laser at 532nm. On the other hand we record the emissions of selected atomic and ionic lines with the use of a high speed video camera (1μs integration time, 20kfps) [2]. In both cases we record side-on images that are used for deriving 2D information by Abel inversion based on a rotational symmetry assumption. Furthermore, the temperature is estimated under an LTE assumption, that should be valid in the conditions here investigated.

The aforementioned methods are employed for the probing of a switching arc in a simplified circuit breaker model suitable for such optical diagnostic measurements [1]. The test object was operated in air at an exhaust pressure of 1 bar, while the arc was blown with quasi-constant pressure in the range of 3.5 to 8 bar. Sonic flow conditions in the arcing zone are thus ensured, while the interaction of the gaseous arc with the surrounding PTFE nozzle walls and CuW electrodes is negligible.

2. Results and Discussion

Fig. 1 shows the evolution of arc mantle and arc core diameters as a function of arc current (*I*) under a a constant blowing pressure of 8 bar. These are estimated both from Speckle measurements [1] as well as from measuring the luminous lateral extent of the corresponding video frames

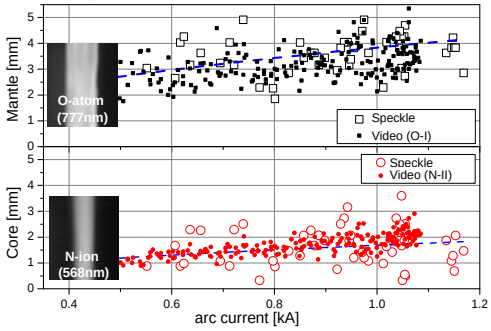

Figure 1: Current (*I*) dependence of arc mantle and core diameters. The dashed eye-guides correspond to a $\sqrt{I}$ law.

Fig. 2 shows the radial distribution of temperature as estimated by the Speckle technique and the O-I emission intensity using the method [3].

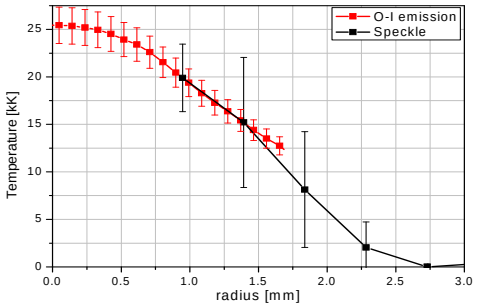

Figure 2: Radial distribution of temperature *T(r)* for a 1kA air arc at 3.5 bar blowing pressure.

We observe in both figures a good agreement between the two measurement techniques: validated measurements of a switching arc are thus obtained.

3. References

[1] P.C. Stoller *et al*, J. Phys. D: Appl. Phys., vol. 48, 015501, 2015

[2] R. Methling *et al,* Plasma Phys. Technol., vol. 2, 167-170, 2015

[3] R. H. Fowler, E. A. Milner, Roy. Astron.Soc. vol. 83, 403, 1923

Photoluminescence of plasma produced graphene quantum dots

S. Espinho, N. Bundaleska, J. Henriques, F. M. Dias and E. Tatarova

Instituto de Plasmas e Fusão Nuclear, Instituto Superior Técnico, Universidade de Lisboa, Lisboa, Portugal

Free-standing graphene sheets were synthesized using surface wave driven microwave plasmas, operating at 2.45 GHz stimulating frequency and at atmospheric pressure. A chemical treatment has been applied to cut the sheets and obtain small size, less than 10 nm particles, i.e. graphene quantum dots (GQDs) in an aqueous solution. The obtained suspension was then irradiated with soft UV light emitted by a commercial blue LED (λ = 410 nm). The photoluminescence of GQDs was evidenced by the rise of a broad peak at 510 nm, following the main one radiated by the LED. SEM and Raman analysis further confirmed the presence of GQDs in the suspension.

1. Introduction

Graphene quantum dots are nanometer sized fragments (< 10 nm) of graphene that demonstrate unique properties and show significant potential for many applications, ranging from energy storage and conversion, to optoelectronics and nano-medicine [1]. Their photoluminescence is one of their most promising properties for applications. However, the mechanism behind this phenomenon is not yet fully understood [2]. In the present work, free-standing graphene sheets were synthesized using microwave plasmas driven by surface waves at 2.45 GHz stimulating frequency and at atmospheric pressure as described in detail in [3, 4]. A chemical route has been applied to cut and reduce the size of the graphene sheets, so as to obtain GQDs in an aqueous solution.

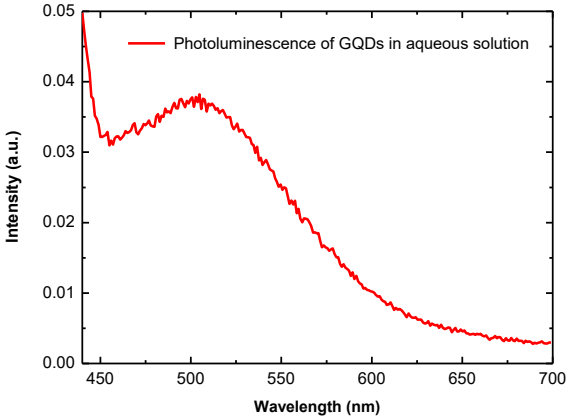

Figure 1. Photoluminescence of GQDs in aqueous solution, upon irradiation with a LED (λ = 410 nm).

2. Photoluminescence of GQDs

The GQDs were obtained in a suspension after the chemical treatment of the graphene sheets in acid environment under mild sonication for 15 – 20 h, followed by neutralization. The solution was then irradiated with UV light from a commercial blue LED. Optical emission spectroscopy measurements were performed with a Czerny-Turner spectrometer coupled to a photomultiplier for wavelengths between 300 – 700 nm. The photoluminescence of GQDs, although weak compared to the main peak of the LED at 410 nm, is evidenced by the rise of a broad peak centered at 510 nm (figure 1). Posterior SEM and Raman analysis confirmed the presence of GQDs in the obtained suspension. The observed photoluminescence is clearly originated by the GQDs in the solution, since no similar effect was observed upon irradiation of the LED on reference solutions containing graphene sheets as synthesized, i.e. without chemical treatment.

3. Final remarks

GQDs in an aqueous solution, obtained after the chemical treatment of plasma produced free standing graphene sheets, exhibited clear photoluminescence upon irradiation with a LED (λ = 410 nm). The effect is evidenced by the rise of a broad peak centered at 510 nm.

4. References

[1] M. Bacon, S. J. Bradley, and T. Nann. Particle & Particle Systems Characterization **31.4** (2014) 415-428.

[2] Zhu, Shoujun, et al. Nano Research **8.2** (2015) 355-381.

[3] E. Tatarova, et al., Journal of Physics D: Applied Physics **47.38** (2014) 385501.

[4] E. Tatarova, N. Bundaleska, J. Ph. Sarrette, and C. M. Ferreira, Plasma Sources Sci. Technol. **23** (2014) 063002.

Acknowledgements

This work was funded by the Portuguese FCT – Fundação para a Ciência e a Tecnologia, under project UID/FIS/50010/2013 and grant number SFRH/BD/52412/2013 (PD-F APPLAuSE).

Comparative cross-correlation spectroscopy study of positive and negative polarity transient spark discharge in ambient air

M. Janda[1], A. Sarani[2], T. Hoder[3], T. Gerling[2], R. Brandenburg[2], Z. Machala[1]

[1] *Faculty of Mathematics, Physics and Informatics, Comenius University in Bratislava, Slovakia*
[2] *INP Greifswald e.V., Greifswald, Germany*
[3] *Faculty of Science, Masaryk University, Brno, Czech Republic*

A streamer-to-spark transition in a self-pulsing transient spark (TS) discharge of positive and negative polarity in air was investigated using cross-correlation spectroscopy. The temporal evolution of the TS was recorded for several spectral bands and lines. The results enable the visualization of the different phases of discharge development. In positive polarity, we observed the primary and the secondary streamer, both propagating from the needle anode towards the plane cathode. In the negative polarity, the primary streamer propagating from the needle cathode was followed by the backward propagating streamer. The transition to the spark was not recorded due to relatively long (0.3-1.5 μs) and irregular streamer-to-spark transition phase.

1. Introduction

The transient spark (TS) is a dc-operated, self-pulsing filamentary discharge [1]. We optically explore the evolution of TS in ambient air in needle-to-plane geometry at mean pulse repetition rate ~2-3 kHz. Negative and positive needle polarity are compared. We used cross-correlation spectroscopy (CCS) that provides sufficient spatial and temporal resolution, high sensitivity, and is suitable for the investigation of randomly appearing discharges [2].

2. Results

The temporal evolution of the TS was recorded for several spectral bands and lines: the second positive system SPS of N_2 (337.1 nm), the first negative system FNS of N_2^+ (391.4 nm), and atomic oxygen (777.1 nm).

In the positive polarity, primary and secondary streamers are observed, both propagating from the needle anode towards the planar cathode (Fig. 1). During the primary streamer, the emission of the SPS dominates, but weak emissions of the FNS and O* are also observed. During the secondary streamer, only SPS emission is obtained. During the streamer-to-spark transition, the emission comes from the atomic lines and the FNS, but no SPS emission was observed.

In the negative polarity, the SPS emission propagating from the needle cathode towards the anode dominates during the initial discharge phase, similar as seen in Trichel pulses. When the SPS emission reaches the anode, the emissions of FNS and O* appear in the whole gap. In the SPS signal we observed another event moving towards the cathode (Fig. 2), assumed as backward propagating streamer.

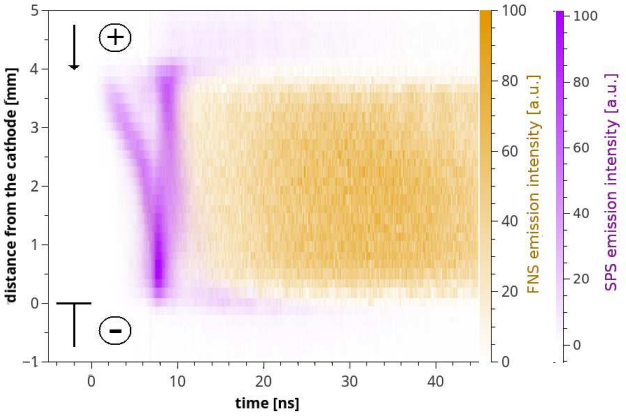

Fig. 1: CCS record of the TS evolution, positive polarity.

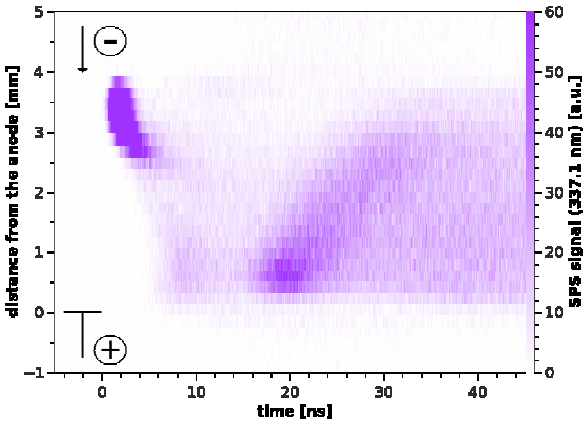

Fig. 2: CCS record of the TS evolution, negative polarity.

3. References

[1] M. Janda, V. Martišovitš, Z. Machala, Plasma Sources Sci. Technol. **20** (2011) 035015.

[2] T. Hoder, M. Cernak, J. Paillol, D. Loffhagen, R. Brandenburg, Phys. Rev. E **86** (2012) 055401.

Acknowledgement: Effort sponsored by the Slovak Research and Development Agency APVV-0134-12.

Topic number

In-flight modification of metallic nanoparticles by low pressure RF plasma

O. Kylian, A. Kuzminova, J. Hanus, M. Vaydulych, A. Choukourov, M.Cieslar, D. Slavinska, H. Biederman

[1] *Charles University, Faculty of Mathematics and Physics, Prague, Czech Republic*

Metallic nanoparticles were produced by means of a gas aggregation source based on DC planar magnetron with subsequent in-flight modification by auxiliary RF plasma operated either in Ar/O_2 or Ar/*n*-hexane working gas mixtures. It is shown that under appropriate conditions oxygen-containing auxiliary plasma is capable to oxidise metallic nanoparticles. In contrast, addition of an organic precursor resulted in the formation of a thin hydrocarbon plasma polymer shell around metallic nanoparticles and thus core@shell nanoparticles were successfully produced.

1. Introduction

Vacuum-based techniques have been gradually developed and studied for production of metallic nanoparticles (NPs) over many years. In particular, methods that utilize gas aggregations cluster sources (GAS) and are based on magnetron sputtering received much attention in recent years. GAS has the advantage of producing NPs in its volume so they reach the substrate in the form of a beam of already formed entities. This is a highly valuable feature for fabrication of nanocomposites as it enables an independent control of both the NP deposition and the growth of a matrix. Furthermore, modification of NPs prior they reach the substrate is in high demand for many applications that range from solar or fuel cells to the biomedical field. The main aim of this study is to investigate the possibility of in-flight plasma modification of metallic NPs produced by GAS.

2. Experimental

Metallic nanoparticles (Ti, Ag, Cu) were produced by means of a GAS based on a planar, water-cooled, 3-inch DC magnetron. Ar was used as a working gas whose pressure in the GAS aggregation chamber was set at 40 Pa. The magnetron current was chosen depending on the sputtering material in the range between 200 mA (Ag, Cu) to 400 mA (Ti).

Leaving the GAS, the NPs entered a glass tube equipped with an external circular electrode which served for the excitation of auxiliary RF plasma as is schematically depicted in Figure 1. Applied RF power was up to 10 W. Oxygen or *n*-hexane were added to the gas phase of the glass tube for in-flight modification of the NPs. The GAS/glass tube assembly was attached to the main deposition chamber where substrates were placed to collect modified NPs. The pressure inside the main deposition chamber was kept below 1 Pa.

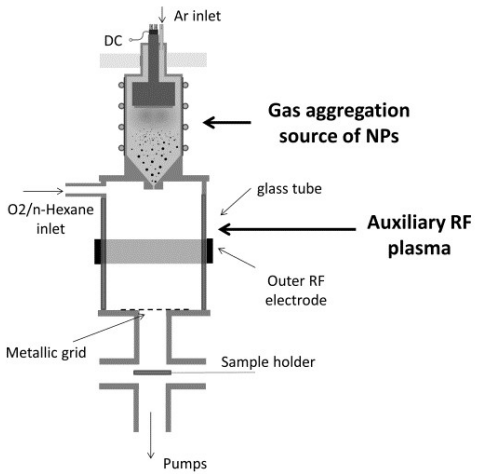

Figure 1. Experimental set-up

3. Results

Measurements of chemical composition (XPS), morphology (SEM, TEM) and optical properties (UV-Vis spectrophotometry) of produced NPs have shown that auxiliary RF plasma caused substantial changes in their properties as compared to NPs that were produced without RF plasma.

First, it was confirmed that presence of oxygen leads to rapid oxidation of produced NPs. In contrast, the use of *n*-hexane resulted in formation of few nm thick hydrocarbon plasma polymer shells around the metal NPs as confirmed by HRTEM. These results clearly showed the feasibility of this technique for in-flight modification of metallic NPs and opened the possibility to use such modified NPs as building blocks for fabrication of advanced functional coatings.

Acknowledgement

This work was supported by the grant GACR 13-09853S from the Grant Agency of the Czech Republic.

Effect of runaway electron preionization on discharge breakdown in air at atmospheric pressure: simulation study

Z. Bonaventura[1], O. Chanrion[2], A. Bourdon[3], F. Pechereau[4], F. Tholin[5] and T. Neubert[3]

[1]*Masaryk University, Faculty of Science, Department of Physical Electronics, Brno, Czech Republic.*

[2]*Technical University of Denmark, National Space Institute (DTU Space), Kgs. Lyngby, Denmark.*

[3]*LPP, CNRS, Ecole polytechnique, UPMC Univ Paris 06, Univ. Paris-Sud, Observatoire de Paris, Université Paris-Saclay, Sorbonne Universités, PSL Research University, 91128 Palaiseau, France*

[4]*CERFACS, 42 Avenue Coriolis, 31057 Toulouse, France*

[5]*ONERA, DMPH Department, 29 avenue de la Division Leclerc, 92322 Châtillon Cedex, France*

The runaway electron mechanism is of great importance for the understanding of the generation of X- and gamma rays in atmospheric discharges. Thermal runaway and the runaway electron avalanche discharge mechanisms are suggested to participate in the generation of Terrestrial Gamma ray Flashes. Thanks to development of both power supplies and diagnostic techniques, a number of experiments have been performed to study the discharges obtained using high voltage pulses with subnanosecond rise fronts. These discharges are also characterized by the presence of X-rays and runaway electrons. We use a 2D axisymmetric beam-bulk hybrid model, to study discharge breakdown appearing in a negative point-to-plane gap submitted to very high voltage pulse of 50 kV.

1. Introduction

The runaway electron mechanism is of great importance for the understanding of the generation of x- and gamma rays in atmospheric discharges [1]. Runaway electrons play also an important role for breakdown and discharge development in laboratory conditions [3, 2]. Both nanosecond discharges in an inhomogeneous electric field and atmospheric discharges are characterized by the presence of X-rays and runaway electrons [4].

2. Model and discussion

Negative streamer is simulated in a point-to-plane electrode configuration using a 2D axisymmetric hybrid beam-bulk approach [5]. Simulations are performed without pre-ionization or photoionization in order to emphasize the role of high-energy electrons. The discharge is initiated with a neutral gaussian plasma cloud composed of electrons and ions at rest in the vicinity of the pointed electrode. The results show the effect of high energy electrons on discharge development. While overtaking the discharge front, the high energy electrons pre-ionize the gas ahead and leave a trace of secondary seed electrons that in turn facilitate discharge propagation. As a result discharge with a support of fast electrons propagates significantly faster compared to discharge where the effect of fast electrons has not been considered, see figure 1.

3. Acknowledgements

This collaborative effort was supported by the European Science Foundation through the Research Networking Program: Thunderstorm effects on the atmosphere-ionosphere system (TEA-IS). This work has been done partially within the LABEX Plas@par project and has received financial state aid managed by the Agence Nationale de la Recherche as part of the programme "Investissements d avenir" under the reference ANR-11-IDEX-0004-02. ZB acknowledges support from the Czech Science Foundation research project 15-04023S.

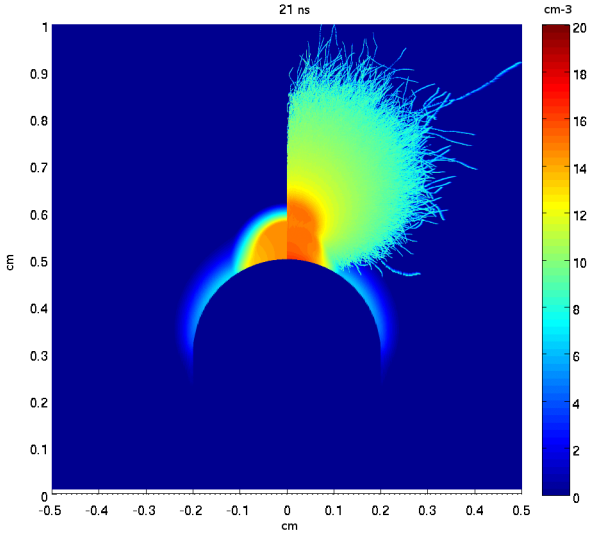

Figure 1: Negative streamer discharge onset close to the pointed electrode. Left: without runaways; Right: with runaways.

4. References

[1] J.R. Dwyer et al., Space Sci. Rev. **173** (2012), 133–196.

[2] E. Marode et al., Plasma Sources Sci. Technol. **25** (2016) 064004.

[3] P. Tardiveau, et al, J. Phys. D: Appl. Phys. **42** (2009) 175202.

[4] I. D. Kostyrya and V. F. Tarasenko, Plasma Physics Reports **41** 3 (2015) 269–273.

[5] O. Chanrion et al., Environ. Res. Lett. **9** (2014) 055003.

Flow characterization of the electro-thermal plume induced by nanosecond repetitively pulsed microplasmas

T. Orriere, N. Benard, E. Moreau, D. Z. Pai

Institut PPRIME (CNRS UPR 3346, Université de Poitiers, ISAE-ENSMA).
SP2MI – Teleport2 Bd Marie & Pierre Curie BP 30179, 86962 Futuroscope, France

The aim of this study is to describe the main characteristics of an electro-thermal plume produced by the interaction between a nanosecond repetitively pulsed microplasma generated between two tungsten electrodes and a DC biased metallic plate at a distance of 40 mm. The plume was studied by particle image velocimetry and Schlieren photography. The generated flow has a bi-planar topology and is characterized by both thermal and electrohydrodynamic flow. The impacts of the main parameters of the discharge are discussed, such as the pulse repetition frequency, plate distance and applied voltage. We will show how the properties at the micro-meter scale influence the generated flow.

1. Introduction

Non thermal plasmas generated in atmospheric air are useful in many research areas. Because of the complex composition of air, the selection of useful reactions and power management are difficult challenges. Furthermore, the presence of oxygen can cause strong heating and prevent the use of a more energetic and reactive discharge such as an arc or spark for certain applications. Nanosecond repetitively pulsed (NRP) discharges [1] can overcome these disadvantages by temporal control of the discharge regime and mean electron energy. These properties can be enhanced by adding surface interactions i.e. by confining the discharge to the micrometer scale. For materials applications, several configurations for the transport of reactive species from the plasma reactor to a substrate have been studied such as jets, sprays or just by placing the substrate in contact or near the discharge [2]. The aim of this study is to confine a NRP discharge to 200 µm in atmospheric air in a pin-to-pin configuration and investigate the impact of the presence of a DC biased electrode 40 mm away from the micro-plasma. The generated flow was analyzed by particle image velocimetry (PIV) and Schlieren photography.

2. Experimental setup

NRP micro-discharges were generated at atmospheric pressure in open air at room temperature between two tungsten electrodes sharpened to 280 µm radius of curvature and inclined at an angle of 45°. High voltage pulses, with 11-15 ns duration and up to 6 kV in amplitude were applied across this gap. For PIV, a laser was used to probe the flow at 16.25 kHz, with the beam shaped into a 1-mm thick laser sheet to illuminate seed particles.

3. Discussion

The presence of the plate with an applied potential of -14 kV or 14 kV placed near (i.e. at a distance of 5 to 40 mm from the microplasma) the microplasma generates an electrohydrodynamic flow. The velocity field in one dimension is presented in figure 1. The maximum flow velocity is not positioned along the central axis of the plume. We can identify the stagnation point on the plate along the center axis. The flow is not axisymmetric because the flow field is different in the perpendicular plane. After the presentation of some properties of the microplasma, the topology of the flow will be discussed further by presenting results with temporal resolution and better spatial resolution. The transport of the reactive plasma chemical species will also be discussed.

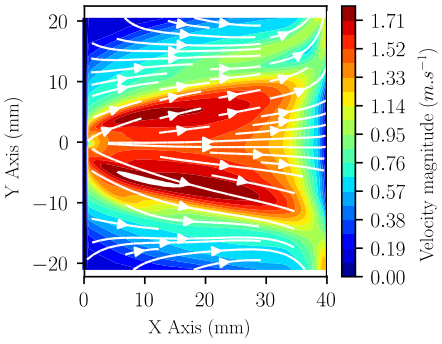

Fig. 1. Mean velocity field obtained over 6000 snapshots, the microplasma is placed at x = 0 mm and the plate at x = 40 mm

3. References

[1] D. Packan, Ph.D. thesis, Stanford University, 2003.

[2] D. Z. Pai, K. (Ken) Ostrikov, S. Kumar, D. A. Lacoste, I. Levchenko, and C. O. Laux, Sci. Rep. **3**, (2013).

Stark broadening of multiple Ar I lines as a diagnostics tool for transient welding arcs containing metal vapor

M. Kühn-Kauffeldt[1], J.-L. Marquès[2], J. Schein[1]

[1]*Institut for plasma technology and mathematics, Universität der Bundeswehr München, Neubiberg*
[2]*Institute for automation and control, Universität der Bundeswehr München, Neubiberg*

The aim of this work is to determine plasma parameters in Gas Tungsten Arc Welding (GTAW) and Gas Metal Arc Welding (GMAW) processes by using a combination of Stark broadened 696.54 nm, 738.40 nm, 763.51 nm and 794.8 nm Ar I lines. The line widths obtained from the measurements are correlated with results of other emission spectroscopy measurement techniques and Thomson Scattering carried out in the same processes [3]. Theoretical data available in the literature is compared to the obtained dataset for Ar I lines. It is used to discuss properties of the plasma and the influence of the metal vapor in the investigated processes. Moreover the usability of these lines as a diagnostic tool for simultaneous determination of electron densities and electron temperatures with current theoretical approaches is discussed.

1. Introduction

One of the most common industrial welding processes is GMAW. Due to a good process control in particular the *pulsed* GMAW process is interesting for industrial application. However it is not fully understood how the metal droplets and the resulting metal vapor interact in the plasma and thus influence the quality of the final join. Despite of a number of experimental investigations and modelling of the process that have been carried out so far, there is still a need for further experimental data in order to understand the physical processes within the arc and to obtain a reliable verification of its model [4]. Especially for aluminum as wire electrode only few emission spectroscopy investigations of electron temperature and density in the arc plasma have been carried out so far [1].

Stark broadening technique has been widely used to determine electron densities and temperatures in welding applications. Since species typically present in a welding process underlie to a quadratic Stark effect, line profiles have a temperature and electron density dependence. Thus several Stark broadened lines can be combined in order to determine temperature and density simultaneously. This method was applied in [8] using Ar I and Fe I lines.

However for welding processes, where Fe is not present, this method is not applicable. Theoretical data for broadening of different Ar I lines is available in the literature [6, 5, 2]. Thus it is desirable to develop a two line Stark broadening measurement method which uses Ar lines – a shielding gas typically used in many types of welding processes. Similar approach, which uses different line of the same element, was used to determine plasma parameters in a microwave discharge by [7]. The aim of this work is to evaluate the usability of multiple Ar I lies as a diagnostic tool for plasma parameter determination in GMAW processes.

2. Experimental setup

Stark broadening measurements were performed on two welding processes: GTAW with Argon and GMAW aluminum. For the simultaneous fine spectral resolution of a wide spectral range an Echelle spectrometer supplied with a CCD detector (Aryelle Butterfly 400, LTB Lasertechnik Berlin) was used. The light from the plasma volume with a cross section of 1 mm is collected by a fiber optic. In order to obtain a two dimensional signal different points of the plasma column are scanned along the horizontal arc axis.

3. References

[1] Sven Goecke. PhD thesis, Technische Universität Berlich, 2004.

[2] H. R. Griem. *Plasma spectroscopy*. New York: McGraw-Hill, 1964.

[3] M Kühn-Kauffeldt, J-L Marqués, and J Schein. *Journal of Physics D: Applied Physics*, 48(1):012001, 2015.

[4] A B Murphy. *Journal of Physics D: Applied Physics*, 43(43):434001, 2010.

[5] S Pellerin, K Musiol, B Pokrzywka, and J Chapelle. *Journal of Physics B: Atomic, Molecular and Optical Physics*, 29(17):3911, 1996.

[6] S. Sahal-Brechot, M.S. Dimitrijevic, and Moreau N. Stark-b database. http://stark-b.obspm.fr, 2014.

[7] J. Torres, M.J. van de Sande, J.J.A.M. van der Mullen, A. Gamero, and A. Sola. *Spectrochimica Acta Part B: Atomic Spectroscopy*, 61(1):58 – 68, 2006.

[8] S Zielinska, S Pellerin, K Dzierzega, F Valensi, K Musiol, and F Briand. *Journal of Physics D: Applied Physics*, 43(43):434005, 2010.

Topic number: 3

O atom kinetics in CO_2 pulsed glow discharges

A.S. Morillo-Candas[1*], B.L.M. Klarenaar[2], R. Engeln[2], A. Chatterjee[1], J-P. Booth[1], T. Silva[3], V. Guerra[3], O. Guaitella[1]

[1]*Laboratoire de Physique des Plasmas, Ecole Polytechnique-CNRS-Univ Paris-Sud-UPMC 91128 Palaiseau, France*
[2]*Department of Applied Physics, Eindhoven University of Technology, 5600 MB Eindhoven, The Netherlands*
[3]*Instituto de Plasmas e Fusão Nuclear, Instituto Superior Técnico, Universidade de Lisboa 1049-001 Lisboa, Portugal*
**Contact e-mail:* ana-sofia.morillo-candas@lpp.polytechnique.fr

O atoms play a key role in the efficiency of CO_2 plasma recycling processes because their reactions can either promote or reduce the conversion of CO_2. We have measured the O atom density and recombination probability by means of actinometry and TALIF and compared the results with the time evolution of CO measured by FTIR spectroscopy in pulsed glow discharge.

1. Introduction

Different strategies have emerged to deal with the excess of CO_2 emissions, whose increasing proportion in the atmosphere is the major cause of the global warming. One of these approaches is focused on CO_2 recycling, which is an initial step in building more complex organic molecules, such as energy-dense hydrocarbon fuels. In this regard, the dissociation of CO_2 to CO, as a first step, through the so called "vibration up-pumping mechanism" is believed to be the most efficient method, especially through the excitation of the asymmetric-stretch vibrational mode of CO_2 [1].

The dissociation of CO_2 results in the production of O atoms that can recombine into O_2, oxidize CO back into CO_2, or on the contrary dissociate further CO_2. O atoms therefore play a key role, beneficial or not for the efficiency of CO_2 conversion. To investigate the fundamentals of CO_2 plasma kinetics, a simple glow discharge powered with pulsed or modulated voltage is studied. This simple discharge allows to measure fundamental parameters such as the vibrational excitation of CO and CO_2 [2], the gas temperature and the electric field. This paper focuses on the measurement of O atom densities and recombination probabilities on the reactor wall and their comparison with CO production.

2. Experimental setup

The temporal evolution of the different species is studied by means of time-resolved *in situ* FTIR spectroscopy, actinometry and TALIF. The CO_2 plasma is ignited in a cylindrical Pyrex tube (2 cm inner diameter and 22 cm or 64 cm length) plasma reactor. Water circulating around the reactor allows control of the wall temperature between 5-50°C. Different gas flows (up to 50 sccm), pressures (millibar range), currents (10 to 50 mA) and pulse durations (millisecond range) were investigated.

3. Results

In actinometry experiments, the ratio of the intensities of O atom lines (at 777 nm and 845 nm) over Argon line at 750 nm were recorded and fitted obtaining the O atom recombination coefficient**.** The O atom characteristic decay time was found to be in the order of tens of milliseconds. Noticeable differences were observed in CO_2 compared to pure O_2, especially as a function of the wall temperature. The absolute O atom density was also obtained and compared with TALIF measurements. The time evolution of the dissociation fraction (ratio of CO over ($CO+CO_2$)) was determined under similar conditions by absorption spectroscopy (FTIR) and compared with the O atom density evolution. These results are analysed in light of a kinetic model [3].

4. Acknowledgments

This research is conducted within the LABEX Plas@par project, and received financial state support managed by the Agence Nationale de la Recherche, as part of the programme "Investissements d'avenir", reference ANR-11-IDEX-0004-02. V. Guerra and T. Silva were partially supported by the Portuguese FCT, under Projects UID/FIS/50010/2013 and PTDC/FIS-PLA/1420/2014.

5. References

[1] A. Fridman (2008), *Plasma Chemistry*. Cambridge University Press. 259–354.

[2] B.L.M. Klarenaar et al., contribution submitted to ICPIG (2017).

[3] T. Silva et al., contribution submitted to ICPIG (2017).

Cell death Mechanism on human colorectal cancer after PAM (Plasma Activated Medium) treatment

J. Chauvin[1,2], F. Judée[1], P. Vicendo[2], N. Merbahi[1], M.P. Rols[3], L.Gibot[3], M.Golzio[3], M. Yousfi[1]

[1]*LAPLACE, Université de Toulouse, CNRS, INPT, UPS, Toulouse 31000, France*
[2]*IMRCP, Université de Toulouse, CNRS, UPS, Toulouse 31000, France*
[3]*IPBS, CNRS, Toulouse 31000, France*

Cell death mechanism was investigated on HCT116 MCTS (Multi-Cellular Tumor Spheroids) with a luminescent analysis of the cell viability by measuring the Adenosine triphosphate (ATP) rate in cells. A fluorescence analysis was also conducted to investigate DNA damage, cell permeabilization and caspase detection as a mean to indicate apoptosis. After a several hours in Plasma Activated Medium (PAM) cells begin to detach from the MCTS as the level of ATP decreases. This loss in ATP can be attributed to the decrease in living cells. At the same time an increase in caspase intensity is occurring as well as cell permeabilization which are characteristic of apoptosis.

1. Introduction

Cold atmospheric pressure plasmas have received a growing interest in the past few years in the biomedical field and more precisely cancer treatment [1]. Recently, some studies used plasma activated medium (PAM) and have demonstrated an interesting effect on cancer cells like a decrease of cell proliferation [2], DNA damage [1] and apoptosis [3]. The main advantage of PAM is its possibility to be prepared in advance and then stored at the right temperature in order to be used later since the aqueous plasma byproducts can remain active up to several days [1].

The present work investigates the effect of PAM on HTC116 MultiCellular Tumor Spheroid and cell death mechanisms. MCTS is a model that mimics the 3D organization and the regionalization of a micro-tumor region. The medium was activated with a plasma jet based on a dielectric barrier discharge configuration excited by high voltage square pulse with a Helium gas flow fixed at 3L/min.

2. Results

The present work investigates cell death mechanism occurring in human colorectal cancer tumor spheroids after PAM treatment. Fig 1 shows light images of MCTS HCT116 spheroids after PAM treatment and a cell detachment is observed between 4-6H after treatment.

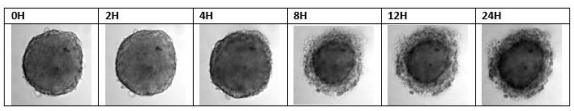

Fig 1. Light Images of MCTS HCT116 after PAM treatment.

In order to understand this cell detachment, early cell death mechanism was investigated. ATP levels were quantified and a rapid decrease as soon as in the first 30 min post-treatment was observed (Fig 2).

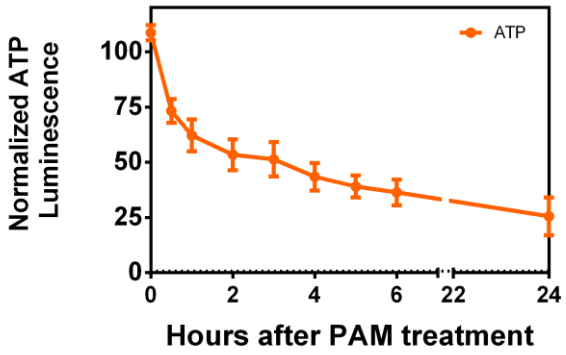

Fig 2. Normalized ATP luminescence evolution after transfer of MCTS into PAM (Cell viability evaluated by ATP luminescence).

DNA damages were also investigated and have previously been demonstrated to be linked to the presence of hydrogen peroxide inducing this cell detachment. [1]

Fluorescent analysis of cell permeabilization and apoptosis were conducted underlying apoptosis as the main cell death mechanism.

3. References

[1] F. Judée *et al*. *Sci Rep*, **22**, 21421 (2016)

[2] N. Hattori *et al*, *International Journal of Oncology*, **47**, 1655-1662 (2015).

[3] K. Torii *et al*., *Gastric Cancer*, **18**, 635-643 (2014)

Sensitivity analysis and uncertainty quantification for electric field determination in air from FNS and SPS intensity ratio

P. Bílek[1], A. Obrusník[1], T. Hoder[1], M. Šimek[2], Z. Bonaventura[1]

[1]*Department of Physical Electronics, Masaryk University, Fac. Sci., Kotlářská 2, 611 37 Brno, Czechia.*

[2] *Department of Pulse Plasma Systems, Institute of Plasma Physics, Academy of Sciences of the Czech Republic, Za Slovankou 3, 182 00 Prague, Czech Republic*

Frequently used method for the determination of electric field in air discharges is based on the measurement of the ratio of luminous intensities emitted by radiative states of $N_2(C^3\Pi_u)$ (second positive system) and $N_2^+(B^2\Sigma_u)$ (first negative system)[1, 2, 3]. This method is used for wide range of pressures from sea level pressures, where it is applied for example to investigation of dielectric barrier discharge, down to very low pressures at ionospheric altitudes for remote sensing of Transient Luminous Events, e.g., lightnings, sprites and blue jets. It is well known that quenching rates of $N_2(C^3\Pi_u)$ and $N_2^+(B^2\Sigma_u)$ determined by various experimental methods exhibit serious discrepancies. Therefore we aim to investigate the impact of uncertainties in values of these rates on electric field determined from FNS/SPS intensity ratio.

1. Problem description

In order to investigate densities of chemical species in air, we have implemented plasma chemistry model, which contains 617 processes for N_2:O_2 (80%:20%) mixture. Time evolution for plasma chemistry is solved in 0D for an electric field that represents passage of an ionization wave at a given point. We present uncertainty quantification and sensitivity analysis for the kinetic scheme for resulting intensity ratio of the FNS and the SPS. This analysis is based on the Elementary Effects (EEs) method invented by Morris [4]. The EEs reveal the most important reactions [5] at particular pressure conditions. As an example, the most important processes for FNS/SPS intensity ratio at sea level pressure are shown in table 1, figure 1 shows sensitivity plot for these conditions. Uncertainty quantification based on Monte Carlo methods will be applied to investigate the impact of uncertainties in values of rate coefficients and quenching rates on electric field determination from FNS/SPS intensity ratio.

Table 1: The key reactions for the ratio FNS/ SPS.

no.	reaction
10	$e + N_2 \longrightarrow N_2(C^3\Pi_u) + e$
28	$e + N_2 \longrightarrow N_2^+(B^2\Sigma_u) + 2e$
331	$N_2^+(B^2\Sigma_u) + N_2 \longrightarrow N_2^+ + N_2$
23	$e + N_2 \longrightarrow N_2^+ + 2e$
25	$e + O_2 \longrightarrow O_2^+ + 2e$
332	$N_2^+(B^2\Sigma_u) + O_2 \longrightarrow N_2^+ + O + O(1S)$
366	$N_2^+(B^2\Sigma_u) + N_2 + O_2 \longrightarrow N_4^+ + O_2$
130	$N_2(C^3\Pi_u) + O_2 \longrightarrow N_2 + O + O(1S)$
50	$e + N_2^+ \longrightarrow N_2^+(B^2\Sigma_u) + e$

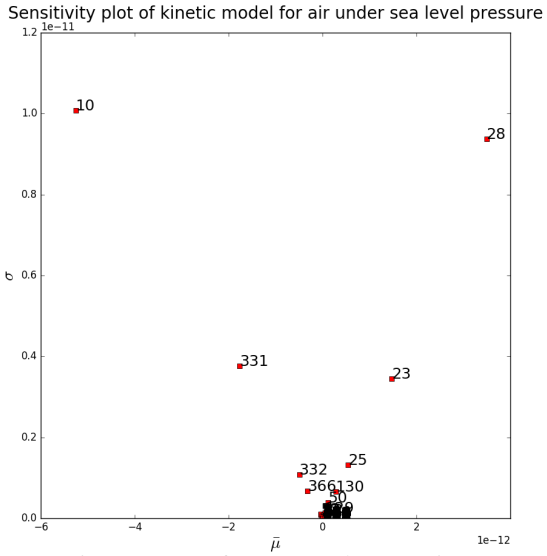

Figure 1: EEs for FNS and SPS ratio.

2. Acknowledgements

This research has been supported by the Czech Science Foundation research project 15-04023S.

3. References

[1] T. Hoder et al., Plasma Sources Sci. Technol. **25** (2016) 045021.

[2] Z. Bonaventura et al., Plasma Sources Sci. Technol. **20** (2011) 035012.

[3] S. Starikovskaia et al., J. Phys. D: Appl. Phys. **43** (2010) 124007.

[4] M. D. Morris, Technometrics **33** (1991) 161–174.

[5] M. M. Turner, Plasma Sources Sci. Technol. **25** (2015) 015003.

On the influence of ferroelectric materials in a packed-bed DBD reactor

A. Gómez-Ramírez[1, 2], R. Álvarez[2], F. J. García-García[2], A. Palmero[2], A. R. González-Elípe[2], J. Cotrino[1, 2]

[1] *Departamento de Física Atómica, Molecular y Nuclear, Universidad de Sevilla, Avda. Reina Mercedes, 42022 Sevilla, Spain.*

[2] *Laboratory of Nanotechnology on Surfaces, Instituto de Ciencia de los Materiales de Sevilla (CSIC-Uni. Sevilla), Sevilla, Spain*

This work reports a study of atmospheric pressure barrier plasmas using ferroelectric materials as packed-bed barrier instead of classical dielectrics. Electrical characterization of the discharge shows higher values of the current that increases non-linearly with the applied voltage when ferroelectrics are used. It contributes to enhance the efficiency of plasma-gas processes taking place in this kind of reactors.

Due to their outstanding properties, such as high electrical permittivity, piezoelectricity or pyroelectricity responses, applications of ferroelectric materials are spreading across different research areas. Recently, several authors have claimed the revolutionary character of ferroelectrics for future disruptive technologies, for instance in memory storage devices, transistors or surface acoustic wave applications [1]. In the field of plasmas, ferroelectrics have been integrated in plasma actuators [2] or as barrier materials in packed-bed discharge reactors, where it was found that they contribute to enhance the process performance in different plasma gas reactions [3, 4].

Trying to shed some light into the role of ferroelectrics to promote certain chemical reactions in atmospheric pressure plasma reactors, in this work we investigate the electrical behaviour of a parallel plate packed bed barrier discharge moderated by ferroelectrics instead of classical dielectric materials. Figure 1 shows a scheme of the reactor used. It consists of two parallel electrodes separated by a packed-bed barrier, which could be constituted by barium titanate ($BaTiO_3$) or lead zirconate titanate (PZT) pellets, both ferroelectrics, or by common dielectrics, as alumina or quartz. Several experiments were performed to compare the electrical response of the reactor filled with each one of these materials by varying both voltage and frequency, either in the absence or in the presence of plasma. The current through the plasma and the impedance of the whole system were analysed, and temperature was varied to check the performance of the ferroelectrics close to the Curie point. All measurements were carried out at atmospheric pressure.

Results showed a higher current when ferroelectrics were used, being the effect noticeable on both the frequency and the voltage domains. Furthermore, when increasing the voltage, measured current followed a strong non-linear response, which can be explained in terms of the dependence of ferroelectric permittivity with the voltage. These finding are used to explain the enhanced efficiency reported in ferroelectric packed-bed reactors operated under atmospheric pressure conditions.

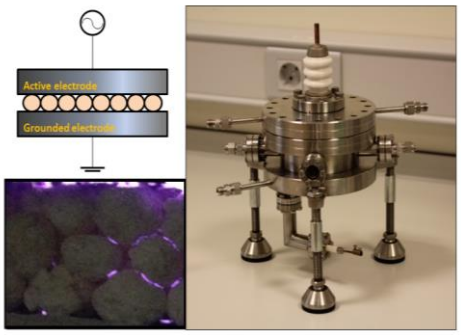

Figure 1. Scheme of the DBD reactor.

References

[1] A.I. Khan, K. Chatterjee, B. Wang, S. Drapcho, L. You, C. Serrao, S.R. Bakaul, R. Ramesh, S. Salahuddin, Nat. Mater. **14**, (2015) 182.

[2] M.J. Johnson, D.B. Go, Appl. Phys. Lett. **105**, (2015) 264102.

[3] A. Gómez-Ramírez, A.M. Montoro-Damas, M.A. Rodríguez, A.R. González-Elipe, J. Cotrino, Chem. Eng. J. **314** (2017) 311-319.

[4] A. Gómez-Ramírez, J. Cotrino, R.M. Lambert, A.R. González-Elípe, Plasma Sources Sci. Technol. **24** (2015) 065011.

Acknowledgements

We acknowledge financial support from Junta de Andalucía through the project P12–2265MO and from the European Regional Development Funds program (EU-FEDER) and the MINECO (project MAT2013-40852.

Topic number: 18

High Power Impulse Magnetron Sputtering: An overview on the benefits of ultra-short pulse operating mode

I.-L. Velicu[1], V. Tiron[2], G. Popa[1]

[1]*Faculty of Physics, Alexandru Ioan Cuza University of Iasi, Iasi-700506, Romania*
[2]*Research Department, Faculty of Physics, Alexandru Ioan Cuza University of Iasi, Iasi-700506, Romania*

This work highlights the benefits of operating the HiPIMS discharge in ultra-short pulse (< 10μs) mode, with the help of a comparative analysis on the results corresponding to the topological, structural and mechanical characterization of Cu thin films deposited by dcMS and HiPIMS. Operating the HiPIMS discharge with ultra-short pulses of 3μs, in the presence of an additional magnetic field, makes it possible to grow high-quality thin films, with low RMS surface roughness, high hardness to Young's modulus ratio, and low coefficient of friction. The additional magnetic field changes the plasma sheath's properties, improves the ion transport towards the substrate, leading to high metal ionized flux fraction and high deposition rates.

High Power Impulse Magnetron Sputtering (HiPIMS), an attractive physical vapour deposition technology, has revolutionized the abilities of magnetron sputtering, enabling new perspectives in thin films engineering, especially due to its dense plasma and high ionization degree of sputtered material.

The main aim of the present study was to make a step towards HiPIMS industrialization, trying to overcome its deposition rate drawback, which may have serious economic consequences for industrial process, to optimize its process and to enhance and tailor the properties of thin films deposited by HiPIMS / reactive-HiPIMS from a large variety of sputtering targets ($Fe_{73.5}Cu_1Nb_3Si_{15.5}B_7$, Ti, Ni, Cu, Zn, Ta, W etc.).

To fulfill the goal, we investigated the processes occurring at the target and substrate surface, as well as the target-to-substrate particle transport processes. Cathode voltage and current waveforms, fast imaging, tunable diode-laser induced fluorescence, tunable diode-laser absorption spectroscopy, time-resolved optical emission spectroscopy, time-averaged ion current of an electrical probe, energy-resolved mass spectrometry and deposition rate investigations were performed for this purpose.

The results of all our studies have led to the same conclusion: operating the HiPIMS discharge with ultra-short pulses (< 10 μs) offers several remarkable benefits: (*i*) enhancement of deposition rate (we found that in HiPIMS assisted by an external magnetic field created with a toroidal-shaped permanent magnet placed in front of a strong balanced magnetron, for some materials, the deposition rate is even higher compared with the case of conventional *dc* magnetron sputtering) [1]; (*ii*) possibility to control the ionization degree which allows to tune the properties of the films (density, adhesion, hardness, friction and roughness) [2]; (*iii*) stoichiometry preservation in the case of films sputtered from multi-elements targets. There are a few other benefits, worth mentioning, for the reactive HiPIMS discharge as: (*i*) hysteresis reduction; (*ii*) overcoming the problems related to the transition between metal and compound mode; *(iii)* avoidance of electric arc development; (*iv*) possibility to tune the composition and structure of elemental or compound (oxides, nitrides and oxinitrides) thin films [3].

To exemplify some of these benefits, the table below presents values of deposition rate (S), fraction of ionized metal species flux (Θ), RMS surface roughness (R), average grain size (D), hardness (H), and Young's modulus (E) corresponding to 800 nm nanocrystalline Cu thin films deposited by direct current magnetron sputtering (dcMS) and HiPIMS operated with ultra-short pulses of 3 μs in the presence / absence of an additional magnetic field (*m.f.*).

	S (Å/s)	Θ (%)	R (nm)	D (nm)	H (GPa)	E (GPa)
dcMS	5.8	3	12.1	11.3	2.6	119.6
HiPIMS	3.8	50	5.8	24.7	2.9	129.5
m.f.-HiPIMS	7.7	80	1.5	35.6	3.7	148.2

References

[1] I.-L. Velicu, V. Tiron, B.-G. Rusu, G. Popa, Surf. Coat. Technol. (2017) doi:10.1016/j.surfcoat. 2016.11.001.

[2] I.-L. Velicu, V. Tiron, C. Porosnicu, I. Burducea, N. Lupu, G. Stoian, G. Popa, D. Munteanu, Appl. Surf. Sci. (2017), doi: 10.1016/j.apsusc.2017.01.067

[3] V. Tiron, I.-L. Velicu, D. Stanescu, H. Magnan and L. Sirghi, Surf. Coat. Technol. (2017) doi: 10.1016/j.surfcoat.2016.11.087.

Free-standing graphene: synthesis and functionalization using plasma-based methods

A. Dias[1,2], J. Berndt[2], E. Kovacevic[2], C. Pattyn[2], T. Strunskus[3], J. Henriques[1], E. Tatarova[1]

[1] *Instituto de Plasmas e Fusão Nuclear, Instituto Superior Técnico, Universidade de Lisboa, Lisboa, Portugal*
[2] *GREMI UMR 7344, CNRS & Université d'Orléans, Orléans, France*
[3] *Institute for Materials Science - Multicomponent Materials, Christian-Albrechts-Universität zu Kiel, Germany*

In the present work, an atmospheric pressure microwave plasma-based method is used to synthesize free-standing graphene sheets (FSGs). The FSGs were then transferred to several types of substrates using different graphene suspensions. The results allowed to demonstrate the possibility to use graphene in future flexible nanodevices. Subsequently, the deposited graphene sheets were successfully N-functionalized and polymerized with aniline (ANI) using a capacitively coupled plasma at low pressure. The samples were characterized by transmission and scanning electron microscopy (TEM and SEM), Raman spectroscopy, X-ray photoelectron spectroscopy (XPS), near edge X-ray absorption fine structure spectroscopy (NEXAFS) and by contact angle technique.

1. Introduction

A critical requirement for the mass production of graphene is the control of the synthesis processes. So far, conventional methods used for the synthesis of these 2D materials present several drawbacks most importantly the quite limited control on the assembly process. Moreover, N_2 functionalization of graphene is one of the key topics in materials research, since functionalized graphene finds extensive application in polymer science and technology due to its extraordinary electrochemical properties (eg. polymer-graphene nanocomposites).

Therefore, the aim of this work is to find a simple method for the subsequent deposition and treatment of free-standing graphene sheets.

2. Experimental

At first an atmospheric microwave plasma was used to synthesize FSGs [1-5]. To this end, a hydrocarbon precursor was injected into the microwave plasma environment, where decomposition processes take place. The main part of the solid carbon is gradually dragged into the outlet plasma stream, where the graphene sheets assemble and grow. A power of 2 kW was applied, injecting Ar as background gas and ethanol as precursor with a ratio of 10:1. The collected FSGs (see Fig.1) are deposited using a simple dispersion method, which enable the deposition on various substrates. Distilled water and methanol were used as solvents in this process. Subsequently, N_2 plasma treatment [6] was performed to turn graphene into a hydrophilic surface, enabling for example the adhesion of biomolecules. The N_2 plasma treatment consists on placing the samples in a remote zone of a capacitively coupled plasma (CCP) for different processing times. A RF power of 8 W was applied at 13.56 MHz, while maintaining 0.1 mbar pressure in the chamber.

The same experimental set up was also used for the deposition of thin films onto the graphene flakes. These experiments were performed with aniline as a precursor for the thin film synthesis.

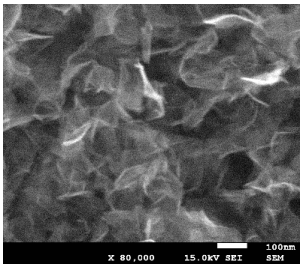

Fig 1 – SEM image of FSGs.

The resulting nanostructures were characterized by SEM and TEM, Raman spectroscopy, XPS, NEXAFS and contact angle measurements.

Plasma characterization was also performed by mass spectrometry and optical emission spectroscopy.

References

[1] E. Tatarova, A. Dias et al. Nova Science Publishers, ISBN: 978-1-63485-214-2 (2016).

[2] E. Tatarova, N. Bundaleska et al. Plasma Sources Sci. Technol. 23, 063002 (2014).

[3] E. Tatarova, J. Henriques, C.C. Luhrs, A. Dias, et al. Phys. Lett. 103, 134101 (2013).

[4] E. Tatarova, A. Dias et al. J. Phys. D: Appl. Phys. 47, 385501 (2014).

[5] A. Dias, N. Bundaleski et al. J. Henriques J. Phys. D: Appl. Phys. 49, 055307 (2016).

[6] E. Kovačević, J. Berndt et al. J. Appl. Phys. 105, 104910 (2009).

Acknowledgements

Work partially funded by Portuguese FCT - Fundação para a Ciência e a Tecnologia, under project UID/FIS/50010/2013 and grant SFRH/BD/52413/2013 (PD-F APPLAuSE) and by French Regional Research Agency through the project APR Capt'Eau and ARD PIVOT.

DBD plasma jet in helium, argon and nitrogen: energy balance and bactericidal activity

O. Stepanova[1], M. Pinchuk[2], A. Lazukin[3], O. Rybalchenko[1], O. Orlova[1], A. Astafiev[2], A. Kudryavtsev[1]

[1] *Saint Petersburg State University, Saint Petersburg, Russia*
[2] *Institute for Electrophysics and Electric Power of Russian Academy of Sciences, Saint Petersburg, Russia*
[3] *Moscow Power Engineering Institute, National Research University, Moscow, Russia*

The paper presents the experimental evaluations of bactericidal activity of dielectric-barrier discharge (DBD) plasma jets in helium, argon and nitrogen applied to *E. coli* cells freshly-inoculated on an agar surface in a grounded Petri dish. Sinusoidal high-voltage signals with the frequency of 7.5, 32 and 84 kHz were used to supply a plasma generator. The energy deposited into a discharge cell is distributed between a discharge region and a plasma jet. A balance of the energy changes with the varying of the voltage frequency. The effect of the energy balance of the system "DBD – plasma jet" on the dimensions and purity of the zones of bacterial inhibition has been considered. The biggest and the purest inhibition zones were obtained in the case of argon plasma jet. Inhibition zones formed under the nitrogen plasma jet have a heavy growth of bacteria near their boundaries. Helium plasma jets create relatively small, but pure inhibition zones.

1. Introduction

A dielectric-barrier discharge (DBD) plasma jet is usually formed in a noble gas flow which is passed through a discharge gap. Two distinct spatial regions, a main discharge and a plasma jet, can be distinguished [1]. The energy distribution between the two regions depends on whether a treated object is grounded or not. This paper presents the experimental evaluations of bactericidal activity of DBD plasma jets in helium, argon and nitrogen for the case of the grounding of an additional electrode which is located under a Petri dish with freshly-inoculated bacteria.

2. Experimental setup and procedure

To supply a DBD plasma jet generator, high-voltage sinusoidal power suppliers with a frequency of 7.5, 32 and 84 kHz were used. An electrical scheme of the experimental setup was equipped with the electrical parameters diagnostics. The energy deposited into the discharge and the energy transported to the Petri dish by the plasma jet was calculated using charge–voltage Lissajous figures. To investigate the effect of energy balance on the bactericidal activity of the plasma jet, *Escherichia coli* M17 cells freshly-inoculated on the agar nutrient medium in Petri dishes were used. The distance between the outlet of the discharge tube and agar surface was 10 mm. The duration of all treatments was 2 min.

3. Results

Bactericidal activity of the plasma jet was estimated according to the dimensions and purity of the zones of bacterial inhibition. Analysis was conducted for the zones which did not undergo heating up to the agar melting, so the modes of treatments by the jet which is close to the transition to an arc were excluded. The biggest (15-25 mm in a diameter) and the purest inhibition zones were obtained in the case of the argon plasma jet. But the argon plasma jet is easily transferred into the arc with the increasing of the voltage frequency. Inhibition zones formed under the nitrogen plasma jet are relatively large (about 15 mm on the average), but they have a heavy growth of bacteria near their boundaries - they are not pure. Helium plasma jets create small (maximal diameter is 10 mm), but pure inhibition zones. Various balances of the deposited energy have been obtained at the applying of voltages with different voltage frequencies. For example, for the helium plasma jet at frequencies of 7.5 and 32 kHz the energy deposited into the jet is higher than the amount of energy deposited into the discharge, whereas at 84 kHz this ratio is changed. For the argon plasma jet discharge energy is higher than jet's energy for the all analyzed values of voltage frequency.

The work was partially supported by Saint Petersburg State University (grant no. 0.37.218.2016) and the Russian Foundation for Basic Research (grant no. 16-08-00870).

4. References

[1] A. Shashurin, M. Keidar. Phys. Plasmas **22** (2015) 122002.

Efficacy of plasma-generated ozone in bioburden decontamination

M. Pajak[1], R. Barton[2], D. A. Diver[1], H. E. Potts[1,2], A. Smith[3]

[1] *School of Physics & Astronomy, University of Glasgow, Glasgow G12 8QQ, UK*
[2] *Anacail Ltd, Thomson Building, University of Glagsow, Glagsow G12 8QQ, UK*
[3]*Institute of Infection, Immunity and Inflammation, University of Glagow, Glasgow G12 8QQ, UK*

We show recent results of the efficacy of ozone, generated by cold plasma DBD discharge system, in the reduction of bioburden in various practical contexts. The patented plasma system is designed to generate ozone *in situ*, without endangering the operator, using the ambient air; in one configuration, the system can generate significant ozone concentrations in sealed packages from the outside, without compromising the seal. We demonstrate the performance of this system in a variety of contexts, with particular relevance to high level decontamination of medical devices, and also possible applications in disinfecting plumbing components. Only the plasma effluent impinges on the target: the plasma does not make contact. Our experiments show effective biocidal, virucidal, mycobactericidal and fungicidal treatments are possible, both *in* vitro and in realistic conditions.

1. Introduction

Cold plasma generation of ozone has a long history, primarily in water treatment plants as an alternative to chlorination [1]. Ozone is a very strong oxidising agent and consequently is an effective biocide. However, it is a difficult chemical to handle, because not only is it extremely hazardous to humans, it has a short half-life (a matter of hours at room temperature) and so must be generated on demand.

2.1 Plasma device

The novelty in our approach lies in the design of a plasma system that allows ozone to be generated inside sealed containers, but by an electrode system imposed from the outside [2]. In this system, there is no requirement to open the package for access, nor is any feedstock gas required. The electrode system attaches to the flexible package surface by suction, effectively making the package material an extra dielectric layer. Electric fields are expressed from the electrodes through the package to strike a low-energy plasma in the interior, which then generates ozone. The circulation of that ozone around the

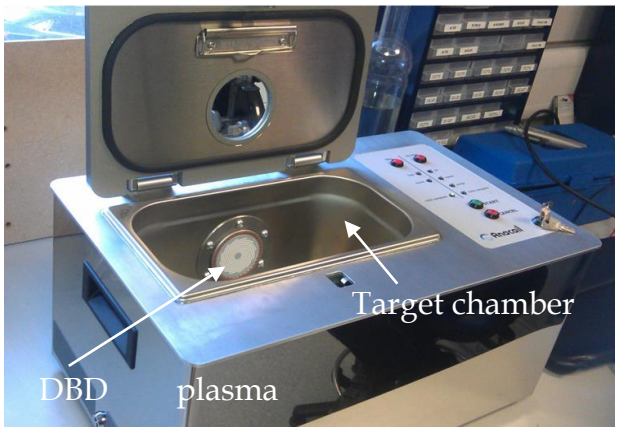

package interior ensures any target contained within is exposed to a powerful biocide. Typically, the ozone levels can reach in excess of 1000ppm in 20s, for 1 litre packages. The system used is shown in Figure 1: treatment targets are packaged and placed inside the chamber, attaching to the electrode plate via vacuum suction. Treatment cycles are generally 100s, with the target left for 1 hour before retrieval and testing: this allows the ozone to decay naturally, and prolongs the exposure of the bioburden to the ozone. This separation of plasma treatment time and the target dwell time is very practical: multiple, separate targets can be sequentially treated with a single plasma source, and the targets remain safely packaged whilst decontamination proceeds.

2.2. Results

In vitro testing under dirty conditions (3.0g/l bovine albumin + 3.0ml/l sheep erythrocytes: Efficacy as a biocidal, virucidal, mycobatericidal and fungicidal device was demonstrated by testing, via an independent accredited microbiological laboratory (BluTest [3]), petri dishes containing *Salmonella enteritidis* NCTC 13346, *Listeria monocytogenes* NCTC 7973, *Escherichia coli O157* NCTC 12900, *Clostridium difficile* NCTC 11209, Murine norovirus s99/RAW 264.7 cells, *Mycobacterium terrae* ATCC 15755, *Aspergillus brasiliensis ATCC 16404*. In each case, tests were done under dirty conditions and produced at least a 4 $\log_{10}$ reduction in viable organisms. Treatment of inoculated surrogate lumens (2mm, 1.5m) showed > 6 $\log_{10}$ reduction in *P. aeruginosa*, and aseptic storage exceeding 6 weeks.

3. References

[1] Gerrity D, Snyder S: *Ozone-Sci Eng* 2011, **33**(4):253-266.

[2] Patent: Plasma generation and use of plasma generation apparatus WO 2011055113 A1

[3] BluTest, Glasgow UK (UKAS No. 4597)

Topic number: 17

Surface-wave-sustained plasma for model biological systems treatment

E. Benova[1], Y. Topalova[2], P. Marinova[3], Y. Todorova[2], M. Atanasova[4], T. Bogdanov[5], I. Yotinov[2]

[1] *DLTIS, Sofia University, Sofia, Bulgaria*
[2] *Faculty of Biology, Sofia University, Sofia, Bulgaria*
[3] *Faculty of Physics, Sofia University, Sofia, Bulgaria*
[4] *Faculty of Mathematics and Informatics, Sofia University, Sofia, Bulgaria*
[5] *Department of Medical Physics and Biophysics, Faculty of Medicine, Medical University – Sofia, Bulgaria*

Surface-wave-sustained Argon plasma torch operating at 2.45 GHz was used for treatment of Gram negative and Gram positive bacteria as model biological systems to study the plasma bactericide effect. In special discharge conditions we are able to produce microwave plasma torch with gas temperature close to the room temperature eliminating in this way the heating of the treated object by the plasma. Such plasma can be used for direct treatment of living tissues and thermo-sensitive materials. The obtained results show good deactivation effect at direct plasma treatment of bacteria in agar and in bacterial suspension. This means that at such discharge conditions the microwave plasma torch can be used for direct *in vivo* treatment and disinfection.

1. General

Argon plasma torch is sustained by travelling electromagnetic wave excited by surfatron type wave launcher at 2.45 GHz. A solid-state microwave generator is used at low wave power (from 12 to 40 W) with 0 W reflected power. Argon gas flow does not exceed 3.2 l/min. At appropriate discharge conditions a stable plasma torch with low gas temperature can be produced (Fig. 1).

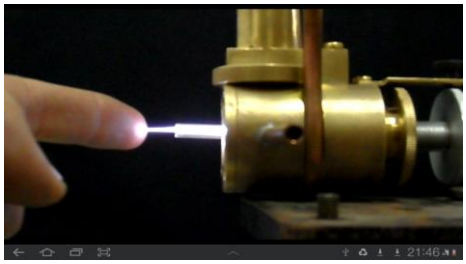

Fig. 1. Microwave Argon plasma torch with low gas temperature

The plasma torch is applied for direct treatment of microorganisms in agar and in bacterial suspension. Two model bacterial strains were used: *Pseudomonas sp. AP-9* as a suitable model of pathogenic Gram negative bacteria and *Brevibacillus laterosporus BT-271* as a suitable model of pathogenic Gram positive, spore-forming bacteria. In all experiments the treatment time is very short – less than 1 min.

2. Results and discussion

Thick layers of *Pseudomonas* with density from 2×10^7 to 6×10^9 cells/ml in agar plate were treated directly by the plasma torch at different wave power (14–22 W) and different treatment time (3–20 s). In Fig. 2 one can see well-presented completely sterilized zones with diameter depending on the wave power and treatment time. The later dependence is presented in Fig. 3.

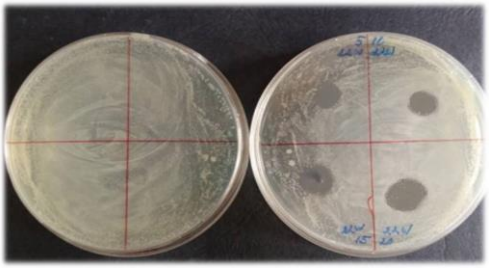

Fig. 2. Control (left) and plasma treated agar plates (right) with *Pseudomonas sp. AP-9*

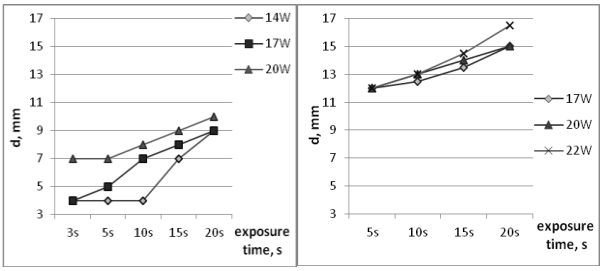

Fig. 3. Diameter of sterilization area at various wave power and treatment time at *Pseudomonas* concentration 6×10^9 cells/ml (left) and 2×10^7 cells/ml (right)

The diameter of the plasma torch is about 2 mm and that of sterilized zones can be more than 1 cm with no movement in radial direction during the treatment. The sterilization was complete, without any survived colonies and stable (confirmed by more than 168 hours monitoring).

Acknowledgements

This work was supported by Bulgarian Science Fund under Grant DH08/8 of 2016.

Investigation of the excited state population density of Xe plasma by active and passive spectroscopy

Dariya D. Krivoruchko, Alexander V. Skrylev

Moscow Institute of Physics and Technology, 9 Institutskiy per., Dolgoprudny, Moscow Region, 141701, Russian Federation

At preset paper the excited state concentrations distribution of a Hall Thruster (HT) at 300 W operating conditions was investigated by Laser Induced Fluorescence (LIF) and compare with results of passive diagnostics. The main challenge is that researching object is non-equilibrium low-temperature xenon plasma: $T_e \approx$2-100 eV, $n_i \approx n_e \approx 10^{11}$ cm^{-3} ,$n_0 \approx 10^{12}$ cm^{-3}, $r_D \approx 10^{-5...-6}$cm, that can't be describe in the network of classical plasma models. The necessity of the multilevel kinetic model is shown. Excited state population density of neutral atoms is at good agreement with passive method, however for ions due to its space anisotropy can't be measurement near thruster face using integral method. Stepwise ionization and excitation is observed for one charged Xe ions but not significant for neutral atoms.

1. Introduction & theory

Electrically powered spacecraft propulsions have a wide application in use with space vehicles. However, modern space-programs aims require thrusters those main characteristics such as: thrust, specific impulse and life time must be far beyond of currently available ones [1]. Thus researching of physical process of HT is still important. The excited state populations density (ESPD) is indicator of the presence defined process (ionization, excitation, transfer etc.) in the plasma and its parameters [2].

2. Experimental setup

Experiments are performed in the vacuum test facility – TMVC11 [3]. The work pressure is approximately 8×10^{-5} mbar. Pumping produces by Nd: YAG pulsed laser with wave length wide 192 – 2600 nm and with the output pulse energy from 1 to 400 mJ. Impulse duration is 5…9 ns. Measurements of the ESPD were made for points (volume of about 16 mm^3) all over the plane perpendicular to thruster axis in five positions on this axis (10 mm, 50 mm, 100 mm) and for 4 location of objective.

2. Results & conclusions

In this paper, we describe the results of a ESPD of Hall thruster in 3D by LIF compare with passive diagnostic method. We explored 10 transitions by LIF and more than 60 by passive diagnostics. The value of the measurements error is shown on the fig. 1. The results of ESPD for ions and neutrals are demonstrated on fig 2. Neutral atoms ESPD is comparatively homogeneous for different thruster region and state with good agreement with passive method. It can be described using one model (Collision–Radiative model). Ions ESPD not uniform at cathode area and near the thruster face and strongly depends on transitions that lead to divergence results of two method. In other words ones needs multilevel kinetic model for linking to excited state populations density and ion concentrations

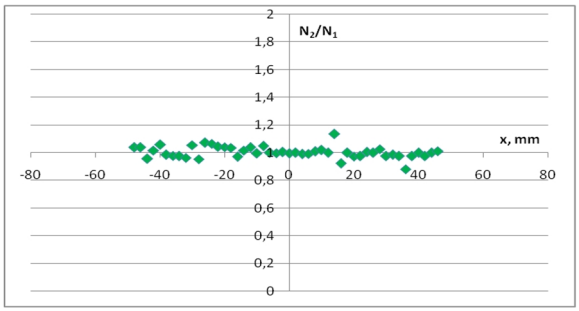

Fig.1. Measurements errors.

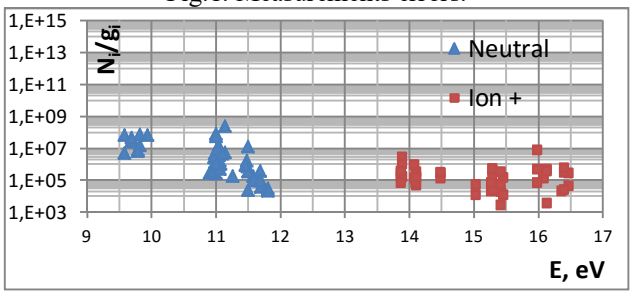

Fig 2. ESPD for ions and neutral atoms.

Classic model can be used for far plume region or for specific electron levels. Also was notice that ion ESPD is strongly not Boltzman.

3. References

[1] Griem H. Plasma Spectroscopy. — M.: Atomizdat, 1969. — 452 pages.

[2] Hani Kamhawi, Wensheng Huang et al. Overview of the Development of the Solar Electric Propulsion Technology Demonstration Mission 12.5-kW Hall Thruster, AIAA 2014-3898

[3] Krivoruchko D.D., Skrilev A.V. Skorokhod E.P. , Excited state population density and spontaneous emission probabilities XeI plasma of Hall Thruster , MAI proceeding, № 92, 2017.

AC electric arcs burning in and outside of the discharge channels of high voltage three-phase plasma torches

A. V. Surov, S. D. Popov, E. O. Serba, Gh. V. Nakonechny, V. A. Spodobin, A. V. Pavlov, A. V. Nikonov, O. M. Stepanova

Institute for Electrophysics and Electric Power of Russian Academy of Sciences (IEE RAS), Dvortsovaya emb. 18, 191186, St.Petersburg, Russia

Characteristics of AC electric arcs, burning in the experimental three-phase generators of thermal plasma are investigated. Part of the arc column is burning outside the device discharge channel. Arc currents were up to 85 A (rms), voltage drops were up to 3.3 kV. Average temperature of working gas exceeded 3000 K and in discharge zone temperature was above 8000 K.

1. Introduction

High-efficiency thermal plasma generators having a long life time of operation are required for plasma-chemical applications [1-3]. Electric arc plasma torches allow energy transfer to the working gas with high efficiency. Direct current (DC) plasma torches have been used for a wide range of applications [2]. However, the thermal efficiency of DC plasma torches as a rule does not exceed 80%. The operating cost is an important parameter for industrial applications, so achieving of a high efficiency is an urgent task. Industrial application of alternating current (AC) plasma systems is considered in [3]. IEE RAS conducts research on physics of gas discharge aimed at obtaining of the new data required for the development of high-efficiency thermal plasma generators. Experimental models of high-voltage plasma generators have been created. The thermal efficiency of plasma torches reaches 95%, the resource of continuous operation is up to 2000 hours [4]. The work is devoted to investigation of electric arcs in a variety of environments, burning in the split cylindrical channels and closes outside of the housing.

2. Experimental setup, methods and results

Experiments were conducted at the work of arc systems in the open space at atmospheric pressure and when working on the plasma chemical reactor. In figure 1 shows the schematic of experimental devices and photo of the torch with arc, burning outside of the discharge channels. The form of the arc quickly changes due to surrounding conditions where flows from channels are mixing. Video recording was conducted at speed 4000 fps. Measurements of the arc current and voltage drop on various parts of the arc column were carried out using the high voltage measuring system and multi-channel signal acquisition. To conduct extensive experimentation with halogen-containing gases and vapors under atmospheric and elevated pressure (upto 5 bar) a diagnostic chamber with windows was developed.

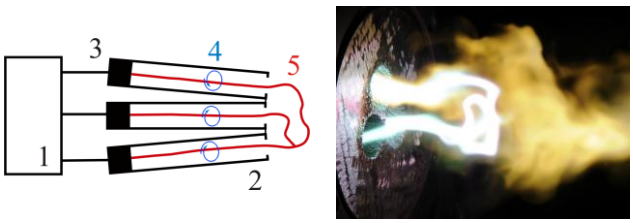

Fig. 1. Schematic of three-phase AC electric arc plasma system and photo of outside part of arc. 1 – power supply, 2 – cases, 3 – electrode, 4 – swirling gas flow, 5- arc.

Experimental studies of the high-voltage AC arcs, depending on the composition of the plasma-forming gas (air, CO_2, CH_4, steam and mixtures) and flowrate, parameters of the power source, influence of external conditions were carried out. Measurements of parameters of electric arcs with currents of 85 A (rms), the voltage drops to 3.3 kV (rms) are performed, dynamic characteristics are obtained. Average temperature of working gas exceeded 3000 K and in discharge zone temperature was above 8000 K.

3. Acknowledgements

The work is supported by RFBR grant 15-08-05909.

4. References

[1] Rutberg P.G., Kuznetsov V.A., Popov V.E., Bratsev A.N., Popov S.D., Surov A.V., Green Energy and Technology, **115** (2013) 261-287.

[2] J. Mostaghimi, M. I. Boulos Plasma Chem. Plasma Proc. **35** (2015) 421–36.

[3] L. Fulcheri, F. Fabry, S. Takali, V. Rohani Plasma Chem. Plasma Proc. **35 (**2015) 565–85

[4] A.V. Surov, S.D. Popov, V.E. Popov, D.I. Subbotin, E.O. Serba, V.A. Spodobin, Gh.V. Nakonechny, A.V. Pavlov, Fuel (2017), http://dx.doi.org/10.1016/j.fuel.2017.02.104

3D modelling of Negative Ion extraction in ITER-like NBI *via* massive parallel calculations

A. Revel[1,2], S. Mochalskyy[1], I.M. Montellano[1], Dirk Wünderlich[1], Ursel Fantz[1], T. Minea[2]

[1]*Max-Planck-Institut für Plasmaphysik, Boltzmannstr. 2, D-85748, Garching, Germany*
[2]*LPGP, Laboratoire de Physique des Gaz et Plasmas, UMR 8578, CNRS, Univ. Paris-Sud, Université Paris-Saclay, Orsay CEDEX, 91405, France*

Neutral Beam Injection (NBI) is one of the key elements for additional heating and current drive in fusion devices. The NBI system for ITER is based on the extraction and acceleration of negative ions (NI) produced in a low pressure plasma with complex 3D magnetic fields. The modelling of the extraction region is of high interest as it mostly determines the NI beam characteristics such as current density, emittance, etc. Modelling these very high electron density (~ 10^{17} m^{-3}) plasmas using Particle-in-Cell (PIC) simulations demands refined mesh and together with the 3D treatment huge computation resources to respect the stability criteria. The comparative results obtained by several numerical schemes are discussed and the main features of the NI beam are presented as issued from massive parallel calculations.

1. Introduction

The NBI for ITER is based on NI extracted from low pressure plasma ion source. A total current of 40 A will be further accelerated up to 1 MeV by a multi-grid, multi-aperture extraction system.

The RF prototype source for ITER corresponds to 1/8 size of the ITER source [1 *and references in*]. Understanding of the NI beam formation is of high importance for the optimisation of the beam optics. The beam divergence affects its focusing and can lead to serious power load on beam line components, and even to the failures of the system.

Moreover, plasma electrons are co-extracted together with NI. In order to reduce electron extraction, a bias potential is applied to the first grid, the plasma grid (PG), and additionally complex 3D magnetic fields are used. Hence, modelling of the extraction region is necessarily 3D to take into account this complex field topology.

2. Numerical modelling schemes

The ONIX code uses the Particle-in-Cell Monte-Carlo collision approach for modelling a part of the extraction region: a small volume surrounding a single extraction aperture. This volume extends each side of the PG, 2 cm in the plasma source and 1 cm outside. Details are given in [2].

The influence of the mesh size, of electron thermalization in the particle injection region and of different particle re-injection schemes, investigated by massive parallel simulations, are presented and discussed [3].

3. Results and discussion

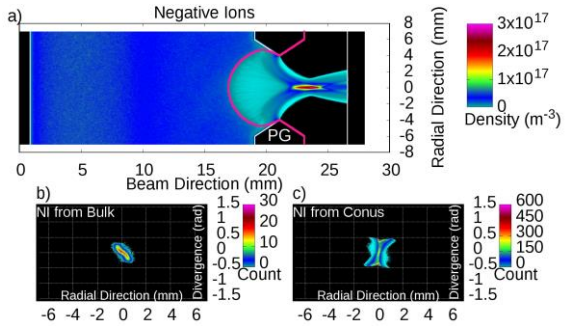

Fig.1. (a) Cross section of a NI beamlet obtained by ONIX with 4096 CPUs for the configuration of the prototype source; NI beam emittance for (b) NI coming from the plasma volume and (c) from the conical part of the PG.

Independent of the numerical schemes, the NI beam features (Fig. 1) are very alike. It comes out that the NI beamlet is composed of two NI ensembles: one is well focused and originates from the plasma volume. A second one originates from the chamfered wall of the aperture that provides an overfocused beamlet and dominates the current density.

4. References

[1] B. Heinemann *et al.* New Journal of Physics 19 (2017) 015001

[2] S. Mochalskyy *et al.* Nucl. Fusion 10 (2016) 106025

[3] A. Revel *et al.* Nucl. Fusion (2017) *to be submitted*

Poster Contributions

Topic number: 8

Similarity of gas discharges at low pressure in the gaps between two plane-parallel electrodes

Y. Fu, X. Wang, S. Yang, X. Zou, H. Luo

Department of Electrical Engineering, Tsinghua University, Beijing, China

The experiments show that the breakdown voltage of the gap between plane-parallel electrodes can be expressed with $U_b = f(p \cdot d, d/r)$ where p, d, r are gas pressure, gap length and electrode radius, respectively. It was proved that $U_b = f(p \cdot d, d/r)$ fulfils two necessary conditions for the similar discharges, which implies that $U_b = f(p \cdot d, d/r)$ is an expression of the similarity theorem in non-uniform electric field. There exist similar glow discharges in argon only when the scaled-down factor k for the two gaps is limited, which was explained that the forbidden processes such as the stepwise ionization and the inelastic collision of second kind violate the similarity of discharge as k increases. The Paschen's curves for the gaps with a same d but different r intersect as p rises, which was explained based on the mean free path length of the electrons inversely proportional to p and the electron impact ionization coefficient exponentially increasing with the electric field.

If two gaps are similar in geometry with all linear dimensions in proportion, they are called geometrically similar gaps. If the discharges in these gaps have same voltage-current characteristics, they are said to be similar. For the similar discharges, the physical parameters of the plasma in one gap are proportional to those in the other gap. Similarity of gas discharge enables us to use the known properties of the discharge in one gap to extrapolate the features of the discharges in the other geometrically similar gap for which the experimental studies may not be feasible or even possible.

Paschen's law, $U_b = f(p \cdot d)$, described the gas breakdown in uniform electric field. Townsend indicated that Paschen's law is just a special case of a more general similarity theorem which can be applied equally to the discharges in non-uniform fields if the discharges are dominated by the electron collision. In this paper, the results from the investigation of the discharge similarity in low-pressure gas between plane-parallel electrodes were presented.

It was found by experiments that the breakdown voltage of the gap depends not only on the product of gas pressure p and gap length d but also on the aspect ratio of the gas gap d/r where r is the electrode radius, *i.e.*, $U_b = f(p \cdot d, d/r)$. It was mathematically proved that $U_b = f(p \cdot d, d/r)$ fulfils two necessary conditions for the similar discharges in the non-uniform electric field, which implies that $U_b = f(p \cdot d, d/r)$ is an expression of the similarity theorem in the breakdown of a gap between two plane-parallel electrodes and confirms the Townsend's prediction that the general similarity theorem can be applied equally to the breakdowns in non-uniform fields.

It was also found by experiments that there exist similar glow discharges in argon only when the scaled-down factor k for two geometrically similar gaps is limited. By theoretical analysis, it was explained that the forbidden processes such as the stepwise ionization and the inelastic collision of second kind violate the similarity of discharge as k increases, which was verified by the numerical simulations of the discharges with or without these two forbidden processes taken into account.

The intersection of Paschen's curves for the gaps with a same gap length but different electrode radius was observed. While the breakdown voltage increases with the increase of the nonuniformity in the electric field of the gap at lower pressures, it decreases at higher pressures. The reason for the intersection of Paschen's curves was given based on the mean free path length of the electrons inversely proportional to the gas pressure and the electron impact ionization coefficient exponentially increasing with the electric field. The intersection of the Paschen's curves was qualitatively reproduced by numerical simulation.

The authors would like to thank the National Natural Science Foundation of China for supporting the research under contracts 51477087 and 51377095.

Development of ambient desorption/ionization source using ultrafast laser and nonthermal atmospheric pressure helium plasma jet for ambient imaging mass spectrometry

J. Y. Kim[1], E. S. Seo[1], H. Kim[2], D.-K. Lim[3], D. W. Moon[1]

[1] *Department of New Biology, DGIST, Daegu, Republic of Korea*
[2] *Division of Nano and Energy Convergence Research, DGIST, Daegu, Republic of Korea*
[3] *KU-KIST Graduate School of Converging Science and Technology, Korea University, Seoul, Republic of Korea*

We report a high spatial resolution ambient mass spectrometry (MS) system that allows us to sensitively image the live hippocampal tissue at ambient environment in the subcellular level. The method is based on an efficient desorption process by femtosecond (fs) laser assisted with nanoparticles and a subsequent ionization step by applying nonthermal plasma for ambient MS imaging. The desorption of molecules from live tissues was found to be greatly enhanced by the strong photothermal effect of gold nanorods and fs laser. The subsequent ionization process with nonthermal atmospheric helium plasma jets enabled production of sufficient amounts of molecular ions of important molecules from a live hippocampal tissue. Combining the ambient nanoPALDI with microscopic sample scanning, MS imaging with spatial resolution of 1.4 μm could be obtained with a sampling depth down to several tens of μm.

1. Introduction

Although ambient ionization mass spectrometry (MS) is a promising analytic technique for biological samples because of its ambient analytic process and no or minimal sample pretreatment [1-3], their applications are still limited due to the insufficient spatial resolution of several tens and hundreds micrometers. Here, we report a new ambient imaging mass spectrometric method with high spatial resolution based on gold nanorod assisted femtosecond laser desorption and subsequent non-thermal plasma induced ionization, termed ambient nanoparticle and plasma assisted laser desorption ionization (ambient nanoPALDI) MS.

2. Methods

Non-thermal helium atmospheric pressure plasma jets (APPJs) and femtosecond near infrared lasers are used as ambient sampling/ionization sources. The energetic light generated by femtosecond lasers focuses on a very small spot of the sample through the objective lens. At same time, non-thermal atmospheric pressure plasma jet device forms the plasma medium on the sample. The desorption of molecules from live tissues is found to be greatly enhanced by the strong photothermal effect of gold nanorods and femtosecond laser, and the subsequent ionization process with nonthermal atmospheric helium plasma jets enabled production of sufficient amount of molecular ions of important molecules from a live hippocampal tissue.

3. Experimental Results

Combined the ambient nanoPALDI with microscopic sample scanning, MS imaging with spatial resolution of 1.4 μm can be obtained with a sampling depth down to several tens of μm. The linear crater generated by ambient nanoPALDI on a hippocampal tissue is exceptionally sharp with the side wall width of around 1 μm and a flat plateau in the bottom. Gold nanorods are uniformly distributed over tissues by cellular uptake of live cells in tissues without any toxic effects and responsible for the high molecular ion intensity and the high spatial resolution. Our ambient nanoPALDI-MS effectively ablates the bulk molecular constituents down to at least several tens of μm while keeping the high spatial resolution which minimizes the sampling problem to represent the whole tissue. From the mouse hippocampal tissue, MS imaging of bio-molecules including monoacylglycerols, cholesterols, ceramides, fragments of sphingolipids and glycerophospholipids has been obtained.

4. Conclusion

A subcellular ambient image mass spectrometric system termed ambient nanoPALDI-MS is reported for live tissue analysis. It enables monitoring biological molecules without pretreatment and verify the molecular chemical properties, elemental compositions and chemical structures.

5. References

[1] R.G. Cooks, Z. Ouyang, Z. Takats, J.M. Wiseman, Science **311** (2006) 1566–1570.

[2] R.A. Musah, E.O. Espinoza, R.B. Cody, A.D. Lesiak, E.D. Christensen, H.E. Moore, S. Maleknia, F.P. Drijfhout, Sci. Rep. **5** (2015) 11520.

[3] M.-Z. Huanga, S.-C. Chenga, Y.-T. Choa, J. Shiea, Anal. Chim. Acta **702** (2011) 1–15.

Dynamics of a complex plasma measured with a 3D light field camera

V. Nosenko, M. Jambor, S. K. Zhdanov, H. M. Thomas

Institut für Materialphysik im Weltraum, Deutsches Zentrum für Luft- und Raumfahrt (DLR), D-82234 Weßling, Germany

The dynamics of a single-layer complex plasma crystal was measured by performing its three-dimensional (3D) imaging with a light field camera. To enrich the crystal's dynamics, the mode-coupling instability (MCI) was triggered in it by lowering the discharge power below a threshold. 3D coordinates of all particles in the crystal were extracted from the recorded video. All three fundamental wave modes of the plasma crystal were calculated from the particle velocity. In the out-of-plane spectrum, only the MCI-induced hot spots (corresponding to the unstable hybrid mode) were resolved. Both longitudinal in-plane and out-of-plane wave modes show profound anisotropy. The results are in agreement with theory and simulations and show that light field cameras can be used to measure 3D dynamics of complex plasmas.

A complex (dusty) plasma is a suspension of micron-size solid particles in a weakly ionized gas. Particles acquire high electric charges, interact with each other and their environment, and often form strongly coupled subsystems. The particles can be individually imaged in real time, which makes complex plasmas excellent model systems to study various generic phenomena in liquids and solids.

A long-standing challenge in the field of complex plasmas is accurate measurement of individual particles' 3D coordinates. 3D imaging methods used so far include stereoscopy, color gradient method, laser tomography, digital in-line holography. A recent development is using light field cameras for single-camera, single-shot imaging of 3D particle suspensions. In a light field camera, an additional array of microlenses is placed just in front of the image sensor; this allows to measure not only the intensity, but also the direction of the light oncoming on a microlens. Dedicated software uses triangulation to calculate all three coordinates of the imaged particles. In [1], a commercial Raytrix R5 light field camera was used to perform 3D imaging of a single-layer complex plasma crystal suspended in a rf discharge in argon. To enhance the out-of-plane oscillations of particles, the mode-coupling instability was triggered by lowering the discharge power below a threshold.

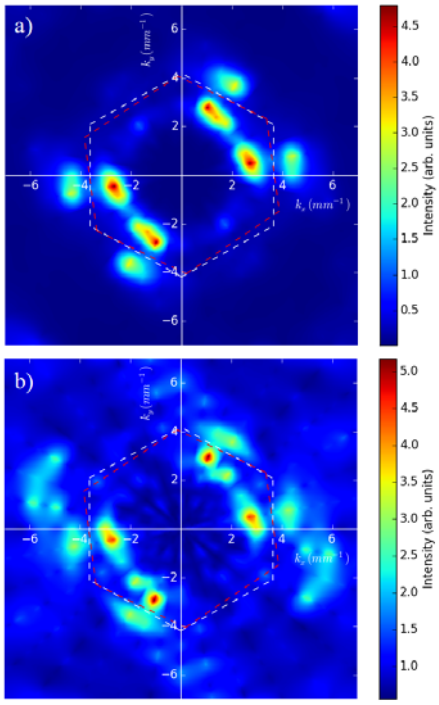

Fluctuation spectra of the particle velocity for a) longitudinal in-plane mode, b) out-of-plane mode. The white (red) dashed lines indicate the border of the ideal (real) first Brillouin zone. Both wave modes show profound anisotropy.

In this contribution, we present further analysis of the plasma crystal's wave modes calculated from the particles' 3D coordinates. The Fourier transform in space and time domains of the particle velocity was integrated over the hybrid mode frequency (in the range of 8.4-10.8 Hz), the result is plotted on the wave number (k_x, k_y) plane in the Figure. As is clearly seen, both wave modes show profound anisotropy. This result is consistent with a previous experiment, theory [2], and molecular dynamics simulations [3] and is explained by a shear deformation of the plasma crystal.

[1] M. Jambor, V. Nosenko, S. K. Zhdanov, H. M. Thomas, Rev. Sci. Instrum. **87** (2016) 033505.

[2] A. V. Ivlev, T. B. Röcker, L. Couëdel, V. Nosenko, C.-R. Du, Phys. Rev. E **91** (2015) 063108.

[3] I. Laut, C. Räth, S. Zhdanov, V. Nosenko, L. Couëdel, H. M. Thomas, EPL **110** (2015) 65001.

Simulation of Triode High Voltage Glow Discharge Electron Sources With Taking Into Account The Anode Plasma Parameters

I.V. Melnyk [1]

[1] *National Technical University of Ukraine "Igor Sikorsky KPI", Electronic Faculty, Electronic Devices Department, Kyiv, Ukraine*

This paper is devoted to describing the algorithm of simulation of triode high voltage glow discharge electron sources with including into consideration the parameters of anode plasma, such as the temperature and mobility of plasma electrons. For calculation of anode plasma parameters estimated relations for high voltage glow discharge have been used. The distinctive feature of proposed methodic of calculation is using of iterative algorithm, which allows to provide the calculations till obtaining the equilibrium between the force of electric field in the cathode-fall region and the force formed by the pressure of electron gas in anode plasma. Obtained results are very important to the experts in the industrial application of modern electron beam technologies.

1. Introduction

High Voltage Glow Discharge Electron Sources (HVGDES) are widely used in industry today for realizing complex technological operations of modern electron beam technology [1 – 3]. For effective control the stability of current of high-voltage glow discharge in such electron sources with low time-constant additional low-voltage discharge is used [4]. In the paper [4] the methodic of calculation of High Voltage Glow Discharge (HVGD) time parameters, based on defining of anode plasma distance through estimation the level of gas ionization by the fast beam and slow plasma electrons, as well as on the equation of discharge self-maintained, have been proposed. But main disadvantage of this method is necessity of using for such calculations important data about the temperature of electron gas in anode plasma and about mobility of electrons in it.

The improved iteration methodic of calculation of anode plasma parameters is proposed in this report.

2. Method of iterative calculation of the temperature and mobility of electron gas

For calculation the temperature of electron gas and mobility of electrons in anode plasma such estimative equations were used [5]:

$$T_e = \frac{eU_{ac}}{2k}\left[1+\sqrt{1+\frac{\pi e^2 m_i}{6m_e}\left(\frac{U_{ac}d_{cp}}{p_{a0}\overline{Q_{ea}}}\right)^2}\right], \qquad (1)$$

$$d_{cp} = \frac{p_{a0}\overline{Q_{ea}}}{U_{ac}}\sqrt{\frac{6m_e}{\pi e^2 m_i}\left(\left(\frac{2kT_e}{eU_c}-1\right)^2-1\right)}, \quad \mu_e = \frac{ap_{a0}d_{cp}}{U_{ac}}+b\,.$$

where T_e – temperature of electrons, μ_e – its' mobility, U_{ac} – acceleration voltage, d_{cp} – distance from the cathode to anode plasma, p_{a0} – residual pressure in the discharge gap, k – Boltzmann constant, $\overline{Q_{ea}}$ – average cross-section of dissipation of electrons on the atoms of residual gases, U_c – control voltage, a, b – empiric constants [4, 5].

Iterative calculation of plasma boundary position by the equation (1) and by the equations, obtained in paper [4], was provided, till the value of cathode-plasma distance dcp became equal in the both variant of calculations. Obtained calculation results for energetic efficiency of electron sources with considering nitrogen as operation gas for different values of control voltage are presented at Fig.

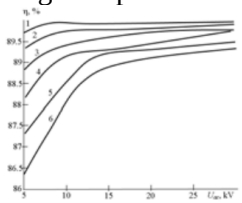

Fig. Calculated dependences of energetic efficiency of HVGDES on different acceleration voltage and control voltage: 1 – U_c = 80 V, 2–U_c = 70 V, 3 – U_c = 60 V, 4 – U_c = 50 V, 5 – U_c = 40 V, 6 – U_c = 30 V; p_{a0} = 0,5 Pa

3. Conclusion

Obtained results are mostly similar to presented in paper [4], difference nearly 15 – 20% is observed for the small and high values of control voltage. Therefore the main advantage of proposed iteration methodic is absence the reference to empirical data about the thermodynamic parameters of electron gas in anode plasma from the manuals [1, 5], which can be incorrect usually and must be strongly verified

3. References

[1] Novikov A.A. "High Voltage Glow Discharge Electron Sources With Anode Plasma", Moscow, "Energoatomizdat", 1983 (in russian).

[2] Feinaeugle P., Mattausch G., Schmidt S., Roegner F.H., Society of Vacuum Coaters, 54-th Annual Technical Conference Proceedings, Chicago, pp. 202–209, 2011.

[3] Mattausch G., Zimmermann B., Fietzke F., Heinss J.P., Graffel B., Winkler F., Roegner F.H., Metzner C., "Elektrotechnica and Electronica (E+E)", vol. 49, № 5-6, pp. 183–195, 2014.

[4] Melnik I.V., Radioelectronics and communication systems, Vol. 56, # 12, pp. 51 – 61, 2013.

[5] Raizer Yu.P. "Physic of Gas Discharge", Moscow, Nauka, 1987. (in russian).

Topic number 11

Investigation of arc binding to the hafnium cathode at atmospheric pressure

M. Kh. Gadzhiev, M. A. Sargsyan, D. V. Tereshonok and A. S. Tyuftyaev

Joint Institute for High Temperatures of the Russian Academy of Sciences - 13, bldg. 2 Izhorskaya str., Moscow, 125412, Russia

Our researchers present investigation of the argon and air arc binding to the hafnium cathode at atmosphere pressure. Working DC current is about several hundred amperes. Experiment was made on a plasmatron with a conical water-cooling cathode. Anode is presented by expanding copper channel. We assume that plasma of positive column is in LTE. It allows using the method of relative intensities for measurement of the electron temperature in positive column. Electron concentration is determined by the Stark broadening. Surface cathode temperature is measured by the high-speed camera which is used as a pyrometer. Obtained results are compared with the results for the pure tungsten, lanthanated tungsten (W-2% La_2O_3) and thoriated tungsten (W-2% ThO_2) cathodes.

Arc discharge is one of the widely used discharges in different areas such as metallurgy, surface treatment, welding etc. Understanding of plasma-physical processes creates opportunities for optimization of industrial plants [1, 2].

In this paper, we present results of the investigation of the arc binding to the hafnium cathode in argon and air at atmospheric pressure.

Experimental setup includes the cathode which is embedded in the copper water-cooling cathode holder and anode which is presented by the expending copper channel and vortex stabilization of the plasma torch [3, 4]. Working DC current was about several hundred amperes.

Assuming that plasma of positive column is in LTE creates an opportunity to use spectroscopy measurements for the electron temperature which is made by the spectrometer DFS-452. Electron temperature is determined by the method of relative intensities of the spectral lines from the same element and different ionization order. Electron concentration is determined by the Stark broadening. In argon plasma the spectral lines Ar II and Ar III were used with the wavelength 363.7 nm and 329.3 nm respectively.

Plasma parameters were measured at different distances from the cathode tip with the spatial step 0.1 mm.

A high speed black and white camera Phantom Miro M110 with the spatial resolution of about 25 micrometers was used for measuring the temperature distribution on the cathode surface. For the cancellation of the plasma stream we used an interface filter which is placed in front of the camera lens (for example for argon lens with an allowed bandwidth of 589 nm was used). Etalon tungsten lamp with a brightness temperature 2400 K was used to perform the calibrations.

All measurements were performed after some work time (tens minutes) of the plasma torch. Obtained plasma parameters are compared with the results (plasma temperature, electron concentration and cathode surface temperature) for the pure tungsten [4], lanthanated tungsten (W-2% La_2O_3) [3] and thoriated tungsten (W-2% ThO_2) [6] cathodes. Optimal plasma parameters for electric-arc technology can be obtained based on the comparison of the different results of particular discharge parameters.

Experimental part was supported by the Russian Foundation for Basic Research (no. 15-08-00404 A) and theoretical part was supported by the President of Russia Scholarship for young scientists (no. 3812.2016.1).

[1] Murphy A. B., Plasma Chem. Plasma Process., **35** (2015) 471.

[2] M.S. Benilov, M. Carpaij and M.D. Cunha, J. Phys. D: Appl. Phys. **39** (2006) 2124 2134.

[3] M.Kh. Gadzhiev, M.A. Sargsyan, D.V. Tereshonok and A.S. Tyuftyaev, EPL. **111** (2015) 25001.

[4] M.Kh. Gadzhiev, M.A. Sargsyan, D.V. Tereshonok and A.S. Tyuftyaev, EPL. **115** (2016) 35002.

Development and further improvement of a heat-treatment system using an arc driven by alternating magnetic field

K. Takeda

Professor emiritus of Akita Prefectural University, Uri-honjyo, Japan

Mechanical properties of a metal are modified by various heat treatments. A novel heat-treatment system is developed using a transferred arc which is driven by an alternating magnetic field imposed perpendicularly. The arc swings like a pendulum synchronizing with the change of the magnetic field. The amplitude of the arc motion and the distribution of the heat flow can be controlled by the flux density and the wave form of the imposed field. More than three times increase in Vickers hardness is obtained after the heat-treatment of carbon steel. Tiny melted spots are often scattered on the treated surface. Detailed observation reveals that the irregular movement of the anode spot results in such damage. Further study is required to understand why such irregularity occurs in the arc motion.

1. Development of the heat-treatment system

In an alternating magnetic field imposed to an arc perpendicularly, the anode root swings back and force as shown in Fig.1.

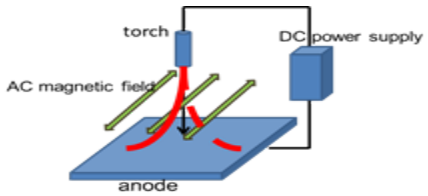

Fig.1 Schematic illustration of an arc driven by alternating magnetic field

The amplitude of the arc motion increases with the increase of the magnetic flux density. The heat flux distribution can also be controlled by changing the wave form of the alternating field. Considering these advantages, a novel heat treatment system has been developed.

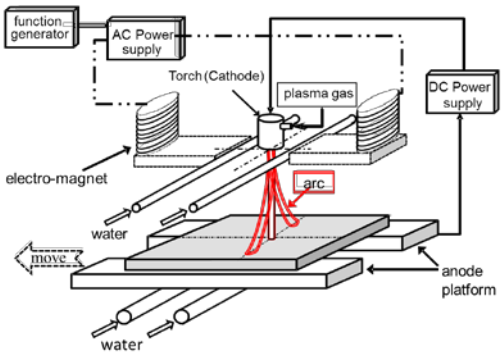

Fig.2 Arrngement of the developed heat treatment System [1]

The heat treatment device is composed of several systems. A transferred DC arc burns between a plasma torch and a work piece serving as an anode. The work piece travels in horizontal direction by a platform driving mechanism. Various magnetic fields can be produced by an AC current supply. After heating, the work piece is quenched from the back side of the plate by cooling water.

2. Result of the heat treatment for carbon steel

The carbon steel plate was heat-treated by the arc driven by an AC magnetic field with rectangular wave form at the frequency of 50Hz. Drastic increase of hardness was obtained as shown in Fig.3.

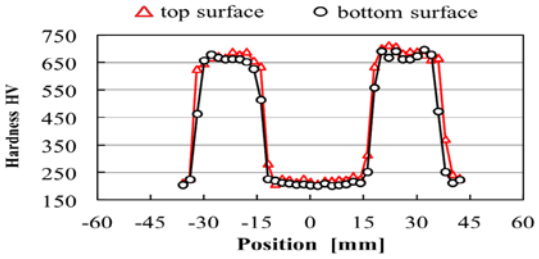

Fig.3 Hardness distributions after the heat treatment

3. Research for further improvement

Surface damage with many tiny spots was often found on the heat-treated work piece. The detailed observation of the arc motion revealed that irregular movement as shown in Fig.4 resulted in the surface damage. For further improvement, it is required to study how to prevent such irregular arc motion.

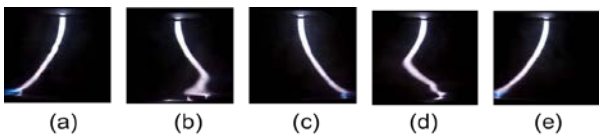

Fig.4 Irregular arc motion during one cycle of the imposed AC magnetic field

Reference

[1] R.Akiho, M.Sugimoto, K.Takeda, Y.Noguchi, T. Miura, Transaction JSME-C 79 (2013) 3979.

Topic number

Formation and annihilation of O_2^--ions in an oxygen discharge

D. A. Toneli[1], R. S. Pessoa[2], M. Roberto[1], J. T. Gudmundsson[3,4]

[1]*Technological Institute of Aeronautics, São José dos Campos, Brazil*
[2]*Paraíba Valley University, São José dos Campos, Brazil*
[3]*University of Iceland, Reykjavik, Iceland*
[4]*KTH Royal Institute of Technology, Stockholm, Sweden*

Depending on the pressure and power, the density of O_2^--ions can be close to the density of O^--ions and it can become an important species for the charge neutrality in the plasma. Here we study the main channels for formation and annihilation of O_2^--ions through a Volume Averaged Global Model in the pressure range from 0.5 – 100 mTorr. Results show that formation of O_2^- is a charge exchange dominated process; however, many reactions contribute to the loss of O_2^- and their contributions change in the range of pressure studied. For pressures below 2 mTorr, in a stainless steel cylindrical chamber, the loss of O_2^--ions is dominated by mutual neutralization of O_2^- and O_2^+. For an anodized aluminium chamber loss of O_2^--ions is dominated by detachment reactions between O_2^- and $O(^3P)$. The results also show the importance of the metastable states for the oxygen discharge.

Volume Averaged Global Model studies of inductively coupled oxygen discharges have shown that the mean density of O_2^--ions increases as pressure increases reaching values close to the mean density of O^--ions in the 100 mTorr range [1, 2]. Calculations were carried out for a stainless steel and anodized aluminium cylindrical reactor chamber with radius R = 15 cm and length L = 30 cm. The flow rate of oxygen feedstock is 50 sccm, the gas temperature is 600 K, and the absorbed power is 500 W. It was found that formation of O_2^- occurs mostly through charge exchange between O^- and $O_2(X^3\Sigma_g^-)$, $O^- + O_2(X^3\Sigma_g^-) \rightarrow O(^3P) + O_2^-$, in both stainless steel and anodized aluminium chambers. This channel remains the main channel for the formation of O_2^--ions even when changes in the electron energy distribution function are considered.

Figure 1 shows the reaction rates for the main reactions which have significant contributions to the O_2^- loss process. These reactions are shown in Table 1. The full reaction set used in the model can be found elsewhere [1]. Note that, for pressures below 2 mTorr, in a stainless steel chamber, reactions 5 and 6 are the dominant channels. In an anodized aluminium chamber, detachment reactions between O_2^- and $O(^3P)$ are the main channels for the O_2^- loss process. As the pressure increases, the reaction rates for reactions 1, 2, 3, and 4 increases. Thus, the loss process for O_2^- is not dominated by only one reaction, but many reactions contribute to it and the role of each reaction is heavily pressure dependent. These results also show the importance of the metastable states $O_2(a^1\Delta_g)$ and $O_2(b^1\Sigma_g^+)$ in oxygen discharges in particular at higher pressures.

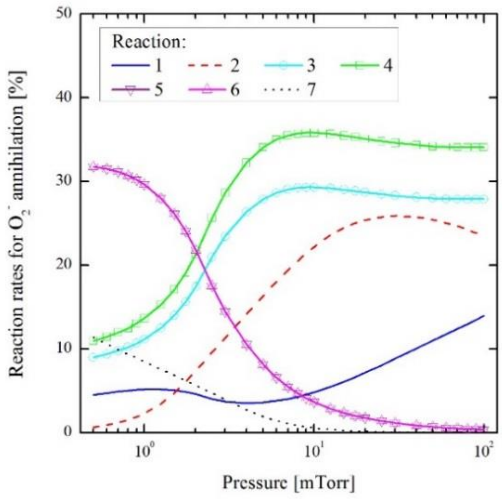

Figure 1. Reaction rates for O_2^- annihilation as a function of pressure for a stainless steel cylindrical chamber.

Table 1. Main reactions for O_2^- annihilation.

No.	Reaction
1	$O_2^- + O_2(a^1\Delta_g) \rightarrow e + O_2(X^3\Sigma_g^-) + O_2(X^3\Sigma_g^-)$
2	$O_2^- + O_2(b^1\Sigma_g^+) \rightarrow e + O_2(X^3\Sigma_g^-) + O_2(X^3\Sigma_g^-)$
3	$O_2^- + O(^3P) \rightarrow O_2(X^3\Sigma_g^-) + O^-$
4	$O_2^- + O(^3P) \rightarrow e + O_3$
5	$O_2^- + O_2^+ \rightarrow O_2(X^3\Sigma_g^-) + O_2(X^3\Sigma_g^-)$
6	$O_2^- + O_2^+ \rightarrow O(^3P) + O(^3P) + O_2(X^3\Sigma_g^-)$
7	$O_2^- + O^+ \rightarrow O(^3P) + O_2(X^3\Sigma_g^-)$

References

[1] D. A. Toneli, R. S. Pessoa, M. Roberto, and J. T. Gudmundsson. *J. Phys. D: Appl. Phys.* **48** (2015) 325202.

[2] D. A. Toneli, R. S. Pessoa, M. Roberto, and J. T. Gudmundsson. *J. Phys. D: Appl. Phys.* **48** (2015) 495203.

Luminescent spectra of noble gases and their binary mixtures under ion beam excitation

A.K. Amrenov, M.U. Khasenov

Nazarbayev University, National Laboratory Astana, Astana, Kazakhstan

Emission spectra of noble gases and their binary mixtures were measured under heavy ion beam excitation in the range of 200-1000 nm. Lines of p-s and d-p atomic transitions prevail in the gas spectra, bands of the third continuum of Ar, Kr and Xe were observed in UV region, strong bands of heteronuclear ionic molecules were observed in Ar-Xe, Ar-Kr and Kr-Xe mixtures. The presence of impurities leads to the appearance of N_2, N_2^+ bands, KrO, ArO, XeO excimer molecules' bands and atomic oxygen lines in the spectra. Radiation distribution among 2p-levels of atoms of noble gases was measured. Conclusions were made about mechanisms of level population in lasers on d-p transitions of noble gas atoms, 2p-1s-neon transitions.

Interest in the study of spectral-luminescent properties of low-temperature plasma excited by nuclear radiation stems to that fact that such plasma is an active medium of gas lasers with nuclear or beam pumping, scintillation detectors, as well as in spontaneous emission sources. Spectral-luminescent studies of noble gases excited by ionizing radiation began more than 50 years ago [1, 2]. The most detailed study was carried out by irradiation of dense gases with uranium fission fragments [3].

In this work, studies of spectral-luminescent characteristics of single component noble gases and binary mixtures excited by heavy ions are interesting from the standpoint of practical applications and were made under the same experimental conditions. The studies were conducted on the DC-60 accelerator [4]. Light was extracted through the quartz window located on the lid of the irradiation chamber. The spectrum of radiation was registered by compact QE65Pro and USB2000+ spectrometers; the relative spectral sensitivity of the installation was measured with the help of calibrated halogen lamp in the range of 400-1000 nm.

The continuous spectra of pure gases were presented by the "third continuum" of Ar, Kr and Xe, the weak band was observed in neon in the range of 200-370 nm. Strong bands of $ArXe^+$, $ArKr^+$ and $KrXe^+$ heteronuclear ionic molecules were observed in the binary mixtures of gases. The radiation of impurities is presented by N_2 and N_2^+ bands in helium and neon, N_2 bands in argon, KrO, ArO and XeO excimer molecules' bands near 557 nm, atomic oxygen lines in helium, neon, and argon. 2p-1s and 3d-2p (Paschen notations) transition lines prevail in atomic spectra.

Distribution of radiation intensity among atomic 2p-levels differs noticeably from the distribution of flow of the dissociative recombination of molecular ions among levels given at [5]. In less degree it is related to neon, the distribution of intensity is more uniform there. The significant part of the flow of Ar_2^+ dissociative recombination refers to the $2p_9$ level in argon, while about half of the radiation refers to $2p_2$ level. The half of radiation occurs from $2p_5$ level in xenon, there is only 4% of the flow of Xe_2^+ ion recombination at this level. Apparently, population of atomic 2p-levels of noble gases happens in cascade transitions from d-levels [6, 7], and the dissociative recombination of molecular ions with electrons is not the major process in population of 2p atomic levels of noble gases.

Table 1. Emission intensity distribution (in percentage) on the 2p levels of Xe in xenon and Ar-Xe, He-Xe with 1% of Xe and 0.8 kPa total pressure

P, kPa	$2p_5$	$2p_6$	$2p_7$	$2p_8$	$2p_9$	$2p_{10}$
0.27	56.0	8.0	4.3	16.8	7.4	6.4
0.53	47.2	8.6	4.4	19.8	7.6	11.3
0.81	41.6	9.1	3.6	23.0	7.9	13.7
Ar-Xe	3.8	9.4	10.5	3.5	4.8	66.9
He-Xe	1.2	42.7	1.4	11.7	9.1	33.4

References

[1] W.R. Bennett, Ann. Phys. **18** (1962) 367-420.

[2] R.J. De Young, W.R. Weaver, J. Opt. Soc. Am. **70** (1980) 500–506.

[3] V.V. Gorbunov et al., Proceedings of RFNC-VNIIEF, (2004) 148-185 (in Russian).

[4] B. Gikal et al., Physics of Particls and Nuclei Letters, **5** (2008) 642–644.

[5] V.A. Ivanov, Soviet Physics Uspekhi, **35** (1992) 17-36.

[6] M.U. Khasenov, Laser and Particle Beams, **32** (2014) 501-508.

[7] S.P. Mel'nikov et al., Lasers with Nuclear Pumping. Springer (2015).

Mode conversion characteristics of the electrostatic hybrid waves in a magnetized plasma slab

M.-J. Lee[1], G. Jung[1], Y.-D. Jung[2]

[1] *Depatment of Physics, Hanyang University, Seoul 04763, Republic of Korea*
[2] *Department of Applied Physics and Department of Bionanotechnology, Hanyang University, Ansan, Kyunggi-Do 15588, Republic of Korea*

Mode conversion characteristics of electrostatic hybrid surface waves due to the magnetic field orientation in a magnetized plasma slab have been investigated. The dispersion relations for the symmetric and anti-symmetric modes of hybrid surface waves are derived for two different magnetic field configurations: parallel and perpendicular. For the parallel magnetic field configuration, we have found that the symmetric mode propagates as upper-and lower-hybrid waves. However, the hybrid characteristics disappear and two non-hybrid waves are produced for the anti-symmetric mode. For the perpendicular magnetic field configuration, however, the anti-symmetric mode propagates as the upper-and lower-hybrid waves and the symmetric mode produces two non-hybrid branches of waves.

1. Theory and calculations

We consider a magnetized dusty plasma slab with the sharp boundaries at $x = 0$ and $x = L$ such that the characteristic length of plasma is much greater than the scale length of the inhomogeneity. Then, the specular reflection condition can be used as the boundary condition for the study of surface waves [1,2]. This boundary condition yields the dispersion equation for electrostatic surface waves propagating in the z direction in an isotropic plasma slab represented by [3]

$$1 + \frac{1}{\pi}\int_{-\infty}^{\infty} \frac{dk_\perp k_\parallel}{k^2 \varepsilon_l(\omega,k)} \left(\frac{1 \mp e^{ik_\perp L}}{1 \pm e^{ik_\perp L}} \right) = 0$$

where ω is the wave frequency, $k_\perp (= k_x)$ and $k_\parallel (= k_z)$ are the *x*- and *z*-components of the wave vector **k**, respectively, ε_ℓ is the longitudinal component of the plasma dielectric permittivity.

When the parallel magnetic field $\mathbf{B}_0 = B_0 \hat{\mathbf{z}}$ is applied to the boundary surfaces, the longitudinal plasma dielectric permittivity in dusty plasma for $kv_{T\alpha}, \omega_{cd}, \omega_{ci} << \omega << \omega_{ce}$ is obtained as follows [22]:

$$\varepsilon_{l,\parallel}(\omega, k_x, k_z) = 1 + \frac{\omega_{pe}^2 k_x^2}{\omega_{ce}^2 k^2} - \frac{\omega_{pe}^2 k_z^2}{\omega^2 k^2} - \frac{\omega_{pi}^2}{\omega^2} - \frac{\omega_{pd}^2}{\omega^2}$$

where $\omega_{p\alpha} = \left(4\pi n_\alpha q_\alpha / m_\alpha\right)^{1/2}$ is the plasma frequency of species α ($= e, i, d$ for electron, ion and dusty grain, respectively) and $\omega_{c\alpha} = q_\alpha B_0 / m_\alpha c$ is the cyclotron frequency of species $\omega_{c\alpha} = q_\alpha B_0 / m_\alpha c$.

Then the integral equation can be performed to derive the dispersion relation for the surface waves in the magnetized plasma slab.

2. Results

2.1. Symmetric mode

$$\left[\left(1 + \frac{\omega_{pe}^2}{\omega_{ce}^2} - \frac{\omega_{pi}^2 + \omega_{pd}^2}{\omega^2} \right) \left(1 - \frac{\omega_{pe}^2 + \omega_{pi}^2 + \omega_{pd}^2}{\omega^2} \right) \right]^{\frac{1}{2}} + \tanh\left[\frac{1}{2} F_\perp(\omega) k_z L \right] = 0$$

2.2. Anti-symmetric mode

$$\left[\left(1 + \frac{\omega_{pe}^2}{\omega_{ce}^2} - \frac{\omega_{pi}^2 + \omega_{pd}^2}{\omega^2} \right) \left(1 - \frac{\omega_{pe}^2 + \omega_{pi}^2 + \omega_{pd}^2}{\omega^2} \right) \right]^{\frac{1}{2}} + \coth\left[\frac{1}{2} F_\perp(\omega) k_z L \right] = 0$$

3. References

[1] A. F. Alexandrov, L. S. Bogdankevich, and A. A. Rukhadze, *Principles of Plasma Electrodynamics* (Springer, Berlin, 1984).

[2] Yu M. Aliev, H. Schlüter, and A. Shivarova, *Guided-Wave-Produced Plasmas* (Springer, Berlin, 2000).

[21] H. J. Lee and Y. K. Lim, J. Korean Phys. Soc. **50**, 1056 (2007).

Experimental and numerical study of a bubble plasma gas initiated by a wire explosion in a liquid

Z. Laforest, J.-J. Gonzalez, P. Freton

Université de Toulouse, UPS, INPT, LAPLACE (Laboratoire Plasma et Conversion d'Energie), 118 route de Narbonne F-31062 Toulouse, France

Applications, using electrical arc in liquid, increase with the use of pulsed energy of microseconds or nanoseconds. Some observed phenomena are common to those applications like the presence of a gas bubble surrounding the discharge. In order to understand the different mechanisms driving the bubble behavior, a numerical and an experimentation studies with a longer pulse of energy around 10ms were developed. The experimental results show an expansion and then a collapse of this bubble during the discharge. These observations linked to simulation results suggest some similitudes with the literature, such as the heating of the liquid and the gas by the discharge and a rise of pressure during the expansion of the bubble.

1. Overviews

Electrical arcs in liquids have many applications such as electrohydraulic discharges in water [1], nanostructures synthesis in various aqueous solutions [2] or oil circuit breakers [3]. Although the conditions on time and energy discharges are different for each of those applications, a gas bubble surrounds the arc. The aim of this work is to understand the mechanisms and phenomena driving the gas bubble with experimental and numerical approaches.

The experimental setup is composed of an electrical alimentation, a reactor and measurements. The electrical alimentation enables to generate a 10ms pulse current of a few kA. The reactor contains two tungsten plane electrodes of 1.6mm diameter immersed in the liquid. The area between the two electrodes is observed by a fast camera. In the same time, the electric discharge characteristics are measured by current and voltage probes.

A numerical model is also proposed to support the experimental results. The Fluent ANSYS software is chosen [4]. The VOF (Volume-Of-Fluids) model is adopted and completed with the change phase Lee's model [4].

2. Study cases

The experimental setup allows to change some parameters such as the inter-contact gap, the injected energy and power or the liquid environment. For example, a case in water liquid can be studied with a distance between the two electrodes of 3mm initially linked by a copper fuse wire of 100µm. The delivered energy for the electrical arc is 1kJ during 10ms. As other author observations [1-3][5], a gas bubble containing the electrical arc is observed. The simulation results show a global rise of the temperature as in Burakov et al. work [2] due to Joule effect and of the pressure as in Chen et al. work [1]. In our theoretical case, the central temperature and pressure can reach respectively 16kK and 15bars inside the bubble. Consequently, these characteristics lead to the bubble expand. When the injected energy is not sufficient, the gas is cooled and the pressure decreases. So after one phase of expansion, the bubble quickly collapses. This dynamic is also noted by others authors using different experimental conditions [3] like a shorter time of discharge [5].

3. Conclusions - Perspectives

An experimental setup and a theoretical model are developed to study the plasma bubble behavior in a liquid. In order to be able to discuss the bubble dynamic a parametric study is made changing the distance between the two electrodes, the nature of the liquid, the apply energy. All these results will be presented and discussed.

4. References

[1] W. Chen, O. Maurel, C. LaBorderie, T. Reess, A. DeFerron, M. Matallah, G. Pijaudier-Cabot, A. Jacques, F. Rey-Bethbeder, *Heat Mass Transfer* **50,** 673 (2014).

[2] V.S. Burakov, E.A. Nevar, M.I. Nedel'ko, N. V. Tarasenko, *Russ. J. Gen. Chem.* **85,** 1222 (2015).

[3] J. Slepian, T. E. Browne, *AIEE Transactions* **60**, 823 (1941).

[4] Ansys Inc. PDF Documentation, 15.0, *http://148.204.81.206/Ansys/readme.html* (2013).

[5] A. Claverie, J. Deroy, M. Boustie, G. Avrillaud, A. Chuvatin, E. Mazanchenki, G. Demol, B. Dramane, *Rev. Sci. Instrum.* **85,** 063701 (2014).

Influence of the radial plasma non-uniformity on the etch process

V. Georgieva, S. Tinck, A. Bogaerts

Research Group PLASMANT, Department of Chemistry, University of Antwerp, Antwerp, Belgium

SF_6/O_2 plasmas sustained in an inductively-coupled plasma (ICP) reactor are simulated by a hybrid model. An additional model based on the Monte Carlo method is used to simulate the Si etch rate and profiles. Extensive gas-phase and surface chemistry sets are developed. The reactive species fluxes control the deposition rate of the passivation SO_xF_y layer and the chemical etching, while the ion energy and angular distributions control the physical sputtering. It is found that the reactive species fluxes decrease, the ion energy range contracts and the ion angular distribution becomes wider, away from the wafer centre. The present research investigates the effect of the spatial variation in the plasma properties on the etch rate and profile.

1. Introduction

A radial uniformity in the plasma characteristics and in the neutral species densities is an important factor for achieving uniform etch rates [1]. It is well known that the radial plasma non-uniformity at the wafer is due to a combination of different factors, like an inhomogeneous magnetic field, pressure, reactor aspect ratio, applied power and bias, and the complex plasma chemistry typically used in material processing.

Computer modelling can be used for parametric investigation and improvement of the spatial uniformity. In the present work we apply the 2-dimensional Hybrid Plasma Equipment Model (HPEM) [2] to simulate SF_6/O_2 plasma sustained in an ICP reactor. The etch profile and rate are simulated by a Monte Carlo model [3]. The extensive gas phase (37 species) and plasma-surface (33 species) chemistry sets are developed based on a number of papers reporting cross-sections and reaction rate coefficients in SF_6/O_2 gas mixtures and plasma interaction with a Si surface.

2. Setup

We consider a typical ICP reactor operating at a pressure of 10 mTorr. The applied power and bias, and the O_2 content can be varied in order to find optimal operating conditions for etching. The ICP reactor geometry and an example of the calculated electron temperature, T_e, are presented in Figure 1.

3. Results

The fluxes of species with comparatively high density at the wafer are presented in Figure 2. It is clear that the degree of dissociation of SF_6 and O_2 has a radial maximum below the region of power deposition and its absorption by the electrons. The decrease of reactive species fluxes in the radial direction retards the etching. The research on the influence of the plasma uniformity at the wafer on the etch rate and profiles is ongoing.

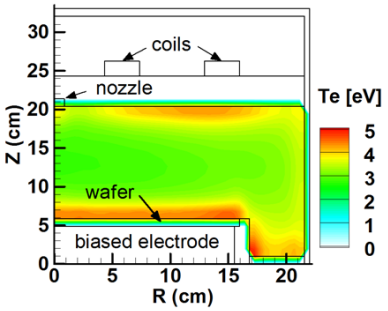

Fig.1. Calculated T_e for applied power 1 kW, bias 300 V, and 15% O_2 concentration in a SF_6/O_2 mixture, at a total gas flow rate of 100 sccm.

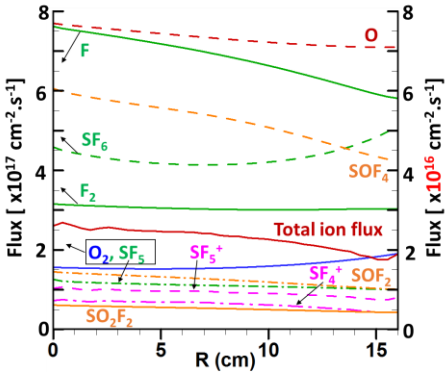

Fig. 2. Calculated species fluxes at the wafer surface. F, F_2, SF_6, SF_5 and O_2 refer to the left y-axis. The other species refer to the right y-axis. The operating conditions are the same as in Fig. 1.

4. References

[1] H. Sasaki, K. Nanbu and M. Takahashi. CP585, *Rarefied Gas Dynamics: 22nd International Symposium*, edited by T. J. Bartel and M. A. Gallis (2001), 262.

[2] M. Kushner, J. Phys. D: Appl. Phys. 42 (2009) 194013.

[3] R. J. Hoekstra, M. J. Grapperhaus, and M. J. Kushner, J. Vac. Sci. Technol. A 15, (1997) 1913.

Molecular Dynamics Simulation of Reaction Mechanism between Reactive Oxygen Species and Membrane Lipid Molecules in Moisture

S. Uchida[1], T. Yoshida[1], and F. Tochikubo[1]

[1] *Department of Electrical and Electronic Engineering, Graduate School of Science and Engineering, Tokyo Metropolitan University, Tokyo, Japan*

Plasma medicine is an attractive application of atmospheric pressure discharge. However, the atomic scale mechanism related to biological effects was not understood well. In the present work, reactive behavior of plasma radials with a membrane lipid in moisture was simulated using adaptive molecular dynamics. The dependence of chemical processes on radical energy was investigated. At low incident energy, oxygen atom did not penetrate to the water layer of some angstroms. The elemental reaction with water molecule produced two hydroxyl radicals, which finally changed to hydrogen peroxide. On the other hand, high energetic oxygen atom reached to phospholipid and combined with the part of choline. Then, most of incident energy dispersed in surrounding water.

1. Introduction

Medical applications of atmospheric pressure non-equilibrium plasma have been promoted on the basis of stable formation techniques. The biological responses by plasma irradiation must be initiated by the interaction between plasma radical and membrane molecule. However, the theoretical mechanism thorough the complicated reaction processes was not understood well. Recently, the structural change of stratum corneum was numerically clarified with reactive molecular dynamics [1]. In addition, surrounding water strongly affected the chemical reaction of radicals with DNA [2]. In the present work, we investigated the interaction between reactive oxygen species and membrane phospholipid in moisture using adaptive solvent molecular dynamics. The change in reaction processes on the irradiation direction and initial position of radical was also discussed.

2. Analytical method

In the present analysis, the direct contact of oxygen atom (O) to phosphatidylcholine (PC) in water was modeled as a basic interaction of plasma radical with biological membrane. The initial distance from O to PC was set to 6 Å. The incident energy of O was varied from 0 to 10 eV. The calculation time was 10 ps. The force field of each time increment was derived using a semi-empirical molecular orbital method (PM3).

3. Results and discussion

Figure 1 shows the trajectory of O at the irradiation to hydrophilic group of PC. At an incident energy of 0.1 eV, O could not penetrate deeply to water layer. The radical bound to H_2O at the vicinity of initial position. Then, two hydroxyl radicals (OH) were produced. Consequently, the direct combination of OH radicals generated H_2O_2. These are general processes between O and H_2O. On the other hand, high energetic O reached to PC. After colliding with PC, transient binding was occurred around the part of choline. The behavior was different from the dissolve process of PC in air. This result suggests that most of the incident energy of O was dispersed in the surrounding water.

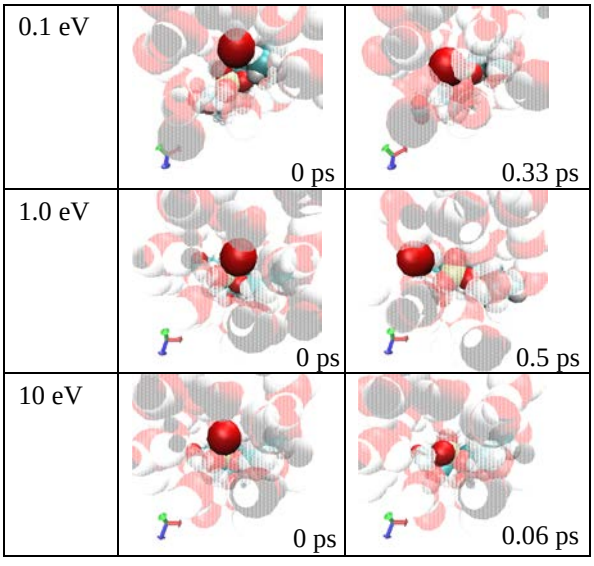

Fig1. Change in reaction processes between O and PC at different irradiation energies in water

References

[1] J. Van der Paal, C. C. Verlackt, M. Yusupov, E. C. Neyts and A. Bogaerts, J. Phys. D: Appl. Phys., 48, (2015) 155202

[2] R. M. Abolfath, P. K. Biswas, R. Rajnarayanam, T. Brabec, R. Kodym and L. Papiez, J. Phys. Chem. A, 116, (2012) 3940

Study of Coupling of 2.45 GHz Electromagnetic Waves with Dense Plasma in Strong Magnetic Field

S. Polosatkin[1,2,3], V. Batkin[1,2], A. Burdakov[1,2,3], I. Ivanov[1,2], P. Kalinin[1,2], I. Kotelnikov[1,2], K. Mekler[1], N. Melnikov[1,2], V. Postupaev[1,2], E. Sidorov[1]

[1] *Budker Institute of Nuclear Physics, Novosibirsk, Russia*
[2] *Novosibirsk State University, Novosibirsk, Russia*
[3] *Novosibirsk State Technical University, Novosibirsk, Russia*

Helicon discharge is one of the most suitable way for production of high-density low-temperature plasma. Helicon plasma sources, operating in the MHz frequency range and respectively low magnetic fields (0.01-0.1 T), capable to create plasma with density up to 10^{13} cm^{-3}. At the same time, next generation of linear plasma facilities for fusion requires production of plasma with density above this limit. Theoretical studies predict that such increasing of density can be achieved by application of powerful microwave sources of GHz range frequency. The paper presents first results of studies of coupling of 2.45 GHz radiation with low-temperature plasma column, created in strong magnetic field by external plasma source. Coupling efficiency (reflected-to-direct wave ratio) were measured for several types of antennas, and values of magnetic field and plasma density.

1. Experimental setup

Interaction of EM waves with plasma were studied on the GOL-3 facility, that represents 8-meter long solenoid with a magnetic field arranged from 0.3 to 4.5 T. Arc plasma gun, attached at the one end of the facility, produces plasma column with density up to $10^{14}cm^{-3}$. Diameter of the plasma can be varied from 0.5 to 4 cm by changing of relation between magnetic fields on the plasma gun and in the solenoid.

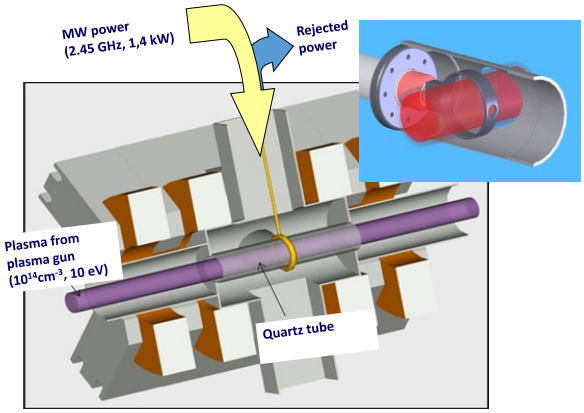

Fig.1 Configuration of the experiment. In the inset - screened ring antenna

Experimental study of EM wave interaction with plasma was performed in the special cell in the center of the facility. Microwave power was produced by 1.4 kW household 2.45 GHz magnetron, mounted in the R26 square waveguide. Magnetron is separated from antenna unit by ferromagnetic isolator to avoid influence of coupling efficiency to generation of microwave power. Direct and reflected power are measured by DD112 detectors from S-Team lab, mounted in the waveguide after isolator. Magnetron unit is connected to antenna by coaxial transfer line via specially designed waveguide-coaxial coupling unit.

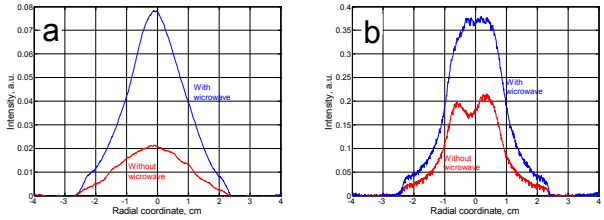

Fig.2 Profiles of plasma radiation in visible range with and without microwave power; a – magnetic field 0.3 T, b – magnetic field 1.7 T.

2. Results of experiments

Several types of antennas, including ring and horseshoe antenna with capacitive coupling, and screened ring antenna (fig.1, inset) were studied in experiments. Screened ring demonstrated best coupling efficiency – up to 30% for plasma density 10^{14} cm^{-3} and more than 60% for low-density (below 10^{14} cm^{-3}) plasma. Influence of microwave power to plasma was indentified on the images of plasma radiation taken by CCD camera. Profiles of plasma radiation across the plasma column are shown in Fig.4 for magnetic field 0.3 T (Fig. 3a) and 1.7 T (Fig.3b). Despite captured microwave power sufficiently less than power, released in the plasma gun, microwave cause valuable increasing of light emission and also transformation of the radial profile of emission.

3. Acknowledgments

This work was supported by Russian Foundation for Basic Research (project 15-02-06757).

Topic number 8

Formation of electrical potential profile in DC reflex discharge

G. D. Liziakin, A. V. Gavrikov, R. A. Usmanov, and V. P. Smirnov

Joint Institute for High Temperatures of the Russian Academy of Sciences, Moscow, Russian Federationde

In the paper reflex DC discharge in helium was explored. It was studied the effect of parameters such as magnetic field of 0.03 to 0.2 T, the pressure of 0.1-100 mTorr, discharge voltage of 0-1,2 kV, the distance cathode-cathode and cathode-anode on plasma column potential. It was shown that the dependence of the plasma column potential on pressure has two maxima. The position of the maxima was determined by the magnetic field. By single floating probe was measured radial profile of the plasma potential. Using a double probe was measured concentration and the electron temperature. The range of the potential oscillations of the plasma column in different modes was defined.

1. Introduction

The question about the formation of a defined spatial profile of the electric potential in the plasma is important in the plasma separation method of spent nuclear fuel [1]. The combination of electric and magnetic fields leads to spatial separation of «light» (m<160 u) and «heavy» (M~240 u) component of spent fuel. At the ends of the cylindrical chamber are the electrodes. To these electrodes is applied a negative voltage. A grounded vacuum chamber in conjunction with these electrodes forms a reflex discharge. This discharge generates a radial profile of the electric plasma potential. The work is devoted to the study of this profile.

2. Experimental setup and methods

We use single floating probe to measure plasma potential. Such measurement gives us a value with errors less than 10%. Electron temperatures and plasma density we measure by double probe method.

Schematic setup of the experimental facility is presented on Fig. 1. Cylindrical vacuum chamber (anode) 1 with diameter 856 mm has the length of 1900 mm. Helmholtz coils 2 are positioned coaxially with the chamber. The coils have inner diameter of 100 cm, and they stand at a distance of 50 cm from each other. Cathodes 3 are fixed on the chamber end planes on dielectric plates 4. We have used circular and ring shape cathodes. In addition, we have used superposition of them. Cathodes positioning on the opposite end planes is absolutely identical in all tests. In this connection hereafter in this text we will always discuss the electrodes positioning on one end plane only, having in mind that at the other end the layout is exactly the same. The plates screen the conductive chamber's end planes from the discharge gap. Thus, the cylindrical surface of the grounded chamber serves as a discharge anode.

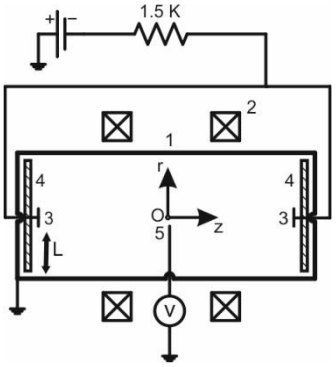

Fig. 1 Experimental setup

3. Results

Considered different geometries of the electrodes. Distance between anode and cathode is an important parameter, the smaller that distance is the lower is the electrostatic potential reproduced in the plasma volume. Increase of the discharge voltage up to 1.2 kV leads to the growth of the potential maximal value. However, at further increase of the discharge voltage, the plasma potential practically does not change. Varying the magnetic field value it is possible to change both – plasma potential and discharge current. Plasma potential monotonously grows with the growth of the magnetic field, and the dependence of the discharge current on the magnetic field has its maximum at B=40 mT. The value of plasma column potential is up to 800 V depends on conditions.

Acknowledegements

This work was supported by the Russian Science Foundation (project № 14-29-00231).

4. References

[1] V.P. Smirnov, A.A. Samokhin, N.A. Vorona and A.V. Gavrikov Plasma Phys. Rep. 39, (2013).

Gas temperature determination of non-thermal plasma jets from the collisional broadening of argon atomic emission lines

M. C. García[1, *], A. Rodero[1], A. Gamero[1] and C. Yubero[1]

[1]*Grupo de Física de Plasmas: Diagnosis, Modelos y Aplicaciones (FQM-136)*
Edificio A. Einstein (C-2), Campus de Rabanales. Universidad de Córdoba, 14071 Córdoba, Spain

We propose two new spectroscopic tools allowing gas temperature determination of non-thermal plasma jets, based on the measurement of the collisional broadening of two atomic emission lines, Ar I 750.39 nm and Ar I 842.46 nm, respectively. The gas temperature of a microwave non-thermal plasma jet was determined from them. Results were consistent with each other, and with those obtained from the rotational temperature derived from OH ro-vibrational band.

1. Introduction

In some technological applications, such as those related to plasma surface treatments or plasma treatment of liquids, a reliable determination of the gas temperature (T_g) in the plasma could be crucial. To control this plasma characteristic parameter becomes particularly relevant in biomedical applications. Optical Emission Spectroscopy (OES) techniques based on the analysis of molecular emission spectra are commonly used for T_g determination of plasmas sustained at atmospheric pressure. But, the use of molecular emission spectroscopy is not always easy: overlapping of bands, rotational population distribution of levels having a non-Boltzmann nature, wake emission of rotational bands, among others, can make difficult to obtain reliable values of gas temperature.

In this paper we propose two new spectroscopic tools for determination of gas temperature in non-thermal plasmas, based on the measurement of the collisional broadening of two argon atomic lines: Ar I 750.39 and Ar I 842.46 nm, respectively. The new methods have been used to measure T_g of an argon microwave jet open to the air. Values obtained using them, have been compared to the rotational temperatures derived from the OH ro-vibrational bands for validation.

2. Method

Lines Ar I 750.39 and Ar I 842.46 nm are very intense and can be almost always detected with a reasonably good signal-to-noise ratio, using appropriate detectors. They correspond to resonance transitions into both resonance levels s_2 and s_4 of the $3p^5 4s$ configuration of the Ar I system, and have a very high resonance broadening only dependent on the gas temperature. These lines also have a non negligible van der Waals broadening also depending on T_g.

For plasmas with gas temperatures under 2000 K, and electron densities lower than 10^{15} cm^{-3}, contributions of the Stark and Doppler broadenings to the whole line profile are negligible when compared to resonance and van der Waals ones. Under these experimental conditions, the total collisional broadening for these lines is then given by:

$$W_C(T_g) \approx W_W(T_g) + W_R(T_g) = \frac{C_W}{T_g^{0.7}} + \frac{C_R}{T_g} \qquad (1)$$

where constants C_W and C_R are characteristics for each line. Using expressions given by Yubero et al. in [1], and Ali and Griem in [2-3], respectively, we have calculated these constants for Ar I 750.39 and 842.46 nm.

The experimentally measured profiles of the lines (no self-absorbed), can be fitted to a Voigt shaped profile with a FWHM given by

$$W_V = \frac{W_C}{2} + \sqrt{\left(\frac{W_C}{2}\right)^2 + W_I^2} \qquad (2)$$

being W_I the instrumental broadening.

So, by measuring W_V, and knowing W_I, from eq. (2) W_C can be derived, and T_g determined.

Aknowledgements

The authors are grateful to Física de Plasmas: Diagnosis, Modelos y Aplicaciones (FQM-136) research group from the University of Córdoba and MINECO project MAT2016-79866-R for their technical and financial support.

References

[1] C. Yubero, M.S. Dimitrijevic, M.C. García and M.D. Calzada, Spectrochim. Acta B **62** (2007) 169.

[2] A.W. Ali and H.R. Giem, Phys. Rev. **140** (1965) 1044.

[3] A. W. Ali and H. R. Griem. Phys. Rev. **144** (1966) 366.

On the axial and radial streamer dynamics in dielectric barrier discharges

H. Höft[1], M. Kettlitz[1]

[1] *INP Greifswald, Felix-Hausdorff-Straße 2, 17489 Greifswald, Germany*

The temporal development of the discharge channel in axial and radial direction was investigated in pulsed dielectric barrier discharges (DBDs) in a 1 mm gap at atmospheric pressure using an iCCD and a streak camera system accompanied by a fast electrical characterisation. The analysis of the two-dimensional DBD structure together with the axial and radial propagation revealed an increasing DBD emission diameter with rising axial propagation velocity (cathode-directed streamer). The radial dynamics are slower compared to the axial propagation, i.e. the radial expansion velocity (~10^4 m/s) is approx. two orders of magnitude lower than the maximal axial propagation velocity (~10^6 m/s). In addition, the streamer diameter is smaller than the channel of the transient glow-like discharge, which is formed after the streamer has crossed the gap.

1. Introduction

Dielectric barrier discharges (DBDs) are a common tool to generate non-thermal plasmas at atmospheric pressure, which have a broad variety of applications [1]. Fundamental investigations on the DBD development, however, focus mainly on the axial dynamics, i.e. the propagation of the positive (cathode-directed) streamer and the subsequent transient glow phase. Therefore, this study is dedicated to both axial and radial breakdown dynamics. In addition, pulsed DBDs are proper test objects to study the radial dynamics of the streamer itself, because there are similar underlying breakdown mechanisms, and the streamer diameter is directly connected to the electric field strength [2].

2. Experimental set-up

A single-filament DBD arrangement (double-sided, half-sphere Al_2O_3 covered electrodes) with 1 mm gap was used [3]. The DBDs were driven by unipolar positive HV pulses with 10 kV amplitude and 10 kHz repetition rate at fixed pulse width of 10 µs in 0.1 vol% O_2 in N_2. Fast electrical, iCCD and streak camera measurements were performed to record the electrical characteristics as well as the spatio-temporal DBD development along and perpendicular to the discharge channel with sub-mm spatial and sub-ns temporal resolution.

3. Results

In figure 1, the two-dimensional emission structure and the corresponding spatio-temporal development in axial and radial direction are shown for a DBD at the falling slope of the HV pulse. The axial DBD characteristics feature the cathode-directed streamer propagation (v_{max} ~ 10^6 m/s) followed by the transient glow phase. The radial development is displayed at three positions in the gap; a different radial development is clearly visible, i.e. the slow expansion during the streamer propagation phase and the fast channel broadening after the streamer has crossed the gap (I,II). Directly in front of the cathode (III), no separation is visible, because the glow phase starts just when the streamer hit the cathode's surface.

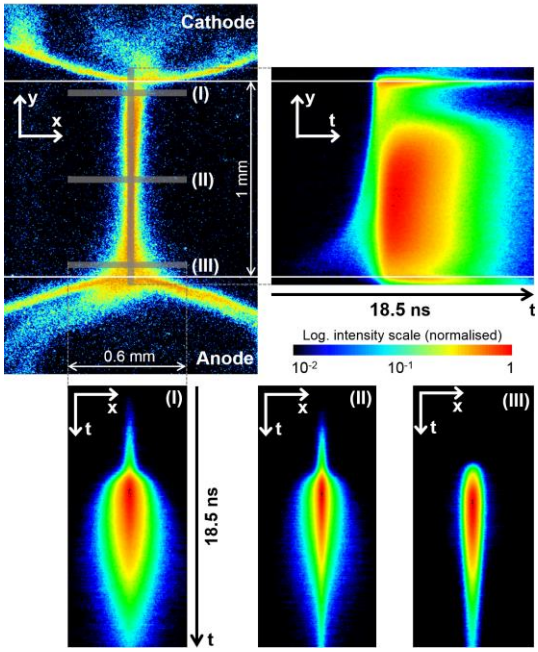

Figure 1: Two-dimensional emission structure (iCCD camera image, top left) and the corresponding spatio-temporal discharge development (streak camera images) along the axis and radially at positions (I) to (III) as indicated by grey bars in the iCCD shot.

4. References

[1] U. Kogelschatz, B. Eliasson, W. Egli, *J. Phys. IV France Colloque* **C4** 47-66 (1997).

[2] G.V. Naidis, *Phys. Rev. E* **79** 057401 (2009).

[3] M. Kettlitz, H. Höft, T. Hoder, S. Reuter, K.-D. Weltmann, R. Brandenburg, *J. Phys. D: Appl. Phys.* **45** 245201 (2012).

Coarse-Grained Simulation Method for Turbulent Nonequilibrium Plasma Flows

S.M. Modirkhazeni[1], J.P. Trelles[1]

[1]*Department of Mechanical Engineering, University of Massachusetts Lowell, Lowell, United States of America*

Nonequilibrium plasma flows in diverse applications often display instabilities and turbulence. The direct simulation of turbulent plasma flows is exceedingly expensive due to the large range of scales involved, which has motivated the development of coarse-grained simulation strategies. The Variational Multiscale-*n* (VMS$_n$) method is presented as a consistent and complete approach for the coarse-grained simulation of turbulent nonequilibrium plasmas. The method builds on the VMS framework and does not rely on the use of empirical or model/problem-specific parameters. Preliminary results confirm that VMS$_n$ produces significantly more accurate results than VMS, comparable with state-of-the-art approaches for other types of flow problems.

1. Introduction

Nonequilibrium plasmas are at the core of diverse applications, from materials processing to medicine. Thermodynamic nonequilibrium (NLTE) is generally a consequence of the interaction of plasma with processing media. This interaction also incites diverse types of instabilities and often leads to turbulence. The direct computational simulation of turbulent plasmas is often unfeasible due to the wide range of scales involved, which prompts the need for coarse-grained simulation approaches. Large Eddy Simulation (LES), the standard coarse-grained approach for turbulent incompressible flows, largely relies on assumptions not valid for plasmas.

2. Nonequilibrium plasma flow model

The NLTE plasma flow model, described in [1], is constituted by a coupled set of two-temperature (heavy-species and electrons) fluid conservation and electromagnetic equations. The model is treated as a single system of transient-advective-diffusive-reactive equations, which allows its straightforward extension to accommodate other plasma models.

3. Variational Multiscale-*n* formulation

The Variational Multiscale-*n* (VMS$_n$) method is a consistent and complete approach for the simulation of turbulent flows without the need for empirical or model/problem-specific parameters. VMS$_n$ is built on the VMS framework based on a variational decomposition of scales into *large* (grid-scale) and *small* (unresolvable) together with a residual-based approximation of the small scales [2]. A major challenge of VMS methods is the handling of the nonlinearity of the small scales, which VMS$_n$ addresses by a fixed-point procedure [3]. The n in VMS$_n$ indicates "nonlinear" or the level of approximation used, i.e., from $n = 0$ for the classical VMS method, to an exact description for $n = \infty$.

4. Method validation and next steps

Representative validation results are presented in Fig. 1 for the simulation of an incompressible turbulent free jet. The VMS$_n$ results show significantly improved accuracy than VMS and comparable to those by the dynamic Smagorinsky method, the state-of-the-art LES approach, but without empirical or model/problem-specific parameters. On-going efforts include the validation of the VMS$_n$ method with experimental data of the flow from a non-transferred arc plasma torch.

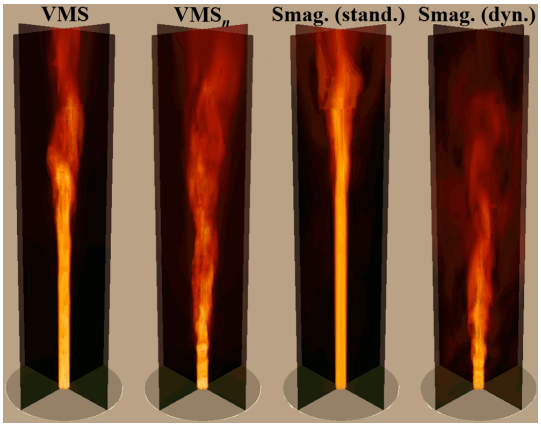

Fig. 1: Incompressible jet flow: instantaneous normalized velocity magnitude for different methods.

Acknowledgements: This work has been founded by NSF award PHY-1301935.

3. References

[1] J.P. Trelles, S.M. Modirkhazeni, Comput. Methods Appl. Mech. Engrg (2014) 282, 87-131.

[2] S.M. Modirkhazeni, J.P. Trelles, Comput. Methods Appl. Mech. Engrg (2016) 306, 276-298.

[3] S. ModirKhazeni, J. Trelles, 22nd Int. Symp. Plasma Chemistry, 2015.

Investigation of streamer propagation and discharge development on dielectric surfaces

M. Kettlitz[1], R. Klink[1,2], H. Höft[1], R. Brandenburg[1]

[1] *INP Greifswald, Felix-Hausdorff-Straße 2, 17489 Greifswald, Germany*
[2] *Robert Bosch GmbH, Daimlerstraße 6,71229 Leonberg, Germany*

Streamer propagation and discharge development on ceramic surfaces in nitrogen-oxygen gas mixtures at atmospheric pressure was investigated. It was possible to force the discharge to develop on the surface using pin electrodes attached directly to the dielectrics. The discharges were driven with unipolar square wave high voltages of 10 kV and 4.3 kHz. Ignition and discharge development on the surface were observed with ICCD and streak cameras. Images of single discharges showed a non-uniform and branched structure of discharge channels while accumulation over several events showed a propagation front rising from the electrode tip. The electrode polarity influenced the discharge dispersion and propagation velocity. Positive polarity of the metallic electrode (rising slope of the HV pulses) led to a cathode-directed streamer with higher propagation velocities than negative polarity (falling slope).

1. Introduction

Surface dielectric barrier discharges (SDBDs) create transient non-thermal plasmas [1-3] and are considerably used e.g. for gas flow control or surface modification [1]. Propagation of the discharge being in contact to a dielectric surface is not fully understood yet, but is of importance for the application of SDBDs. To get insight in this mechanism, a pin-to-pin arrangement was used to investigate single localized SDBDs on ceramics in a nitrogen-oxygen gas mixture.

2. Experimental set-up

The discharge arrangement consisted of a 1 mm thick alumina (AL_2O_3) plate with two metal pin electrodes on each side creating a 3 mm discharge gap (figure 1). One electrode was covered with silicone, thus plasma was generated only at one side. The electrode arrangement was inserted in a gas tight plexiglass cell and a gas flow of 100 sccm of 0.1 vol% oxygen in nitrogen was flushed through the cell. A unipolar square wave high voltage pulse of 10 kV at 4.3 kHz with a pulse width of 10 µs drove the uncovered electrode. The covered one was grounded. Fast current and voltage probes monitored ignition and discharge development on the surface. The uncovered pin electrode was observed optically with ICCD and streak cameras.

3. Results

During rising and falling slopes of the high voltage pulse, one discharge channel directly propagating along the gas-surface interface was formed. The discharges generated surface charges on the dielectrics, which led to a potential difference (i.e. polarity) to the pin electrode. The images of single discharges showed a non-uniform and branched structure of discharge channels while accumulation over several events showed the inception of the discharge at the electrode tip propagating off the tip.

Velocity measurements with the streak camera showed the slowing down of the discharge front within 1 mm from the tip and afterwards a moderate one on the dielectrics. The electrode polarity influenced the discharge dispersion and propagation velocity. Positive polarity of the uncovered electrode (rising slope of the HV pulses) led to a cathode-directed streamer with higher propagation velocities ($v_{max} \approx 5 \cdot 10^5$ m/s) than for negative polarity (falling slope). For negative polarity, the discharge was well localised at the electrode tip showing corona-like behaviour.

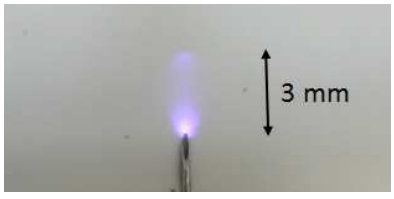

Figure 1: Photo of SDBDs on the ceramic surface.

4. References

[1] E. Moreau, R. Sosa, G. Artana *J. Phys. D: Appl. Phys.* **41** (2008) 115204

[2] H. Grosch, T. Hoder, K.-D. Weltmann, and R. Brandenburg, *Eur. Phys. J. D* **60**, (2010) 547–553

[3] Y. Akishev, G. Aponin, A. Balakirev, M. Grushin, V. Karalnik, A. Petryakov, N. Trushkin, *J. Phys. D: Appl. Phys.* **46** *(2013) 464014*

Ablated mass in high-voltage circuit breakers following the nature of electrode material

M. Courrege, J-J. Gonzalez, P. Freton

Laboratoire LAPLACE, Université Paul Sabatier – 31062 TOULOUSE cedex 9

In high-voltage circuit breakers (HVCB), the electrical arc created by the contacts opening, interacts with the device materials (PTFE walls and electrodes). The interaction of the arc with the electrodes leads to the presence of metallic vapours within the plasma due to ablation. These vapours greatly influence the behaviour of the arc as they modify the radiative transfer, as well as the plasma properties. We have been interested in electrode's composition. Indeed, depending of the electrode's material, the quantity of ablated metal differs changing the plasma behaviour. In this study two distinct electrode compositions: pure copper and copper-tungsten mixture are considered.

1. Introduction

During contact opening in HVCB, the arc interacts with the surrounding walls and the electrodes. The interaction with the Teflon nozzles (by radiation and conduction) must be considered as it allows the flow of gas to increase the pressure in the heating volumes. The PTFE wall ablation is taking into account in many models of arc in HVCB. In our study, we use the Christen's approach [1]. The second interaction which must be considered is related to the plasma with the electrodes. Due to its complexity and lack of experimental results this interaction is less considered in the literature. Its description requires the development of anode and the cathode models. In a thin layer near electrodes the plasma is out of equilibrium. Consequently, a hydrodynamic description is no longer suitable. To overcome the complexity of a kinetic approach, we chose to use Benilov's ablation model [2] to take into account the thin layer and the ablation of electrodes. It allows determining the properties at the layer/plasma boundary without resolving the non-equilibrium area.

A global description of the plasma with the electrodes interaction is realized using the @Fluent software. Depending on the current level vapours proportion change the plasma properties and the pressure increase in the heating volume.

2. Results

Considering pure copper electrodes we have previously studied the influence of the presence of metallic vapours on temperature field, radiation, electrical conductivity, on the ablated mass of PTFE or on the pressure rise in the heating volumes. In order to get closer to real configuration, we propose simulation results obtained with 20%Cu–80%W electrodes. We can see in the figure 1 versus time the copper mass ablated assuming a pure copper electrode and a Cu-W mixture. In the presented cases the alternative current is I=25kA.

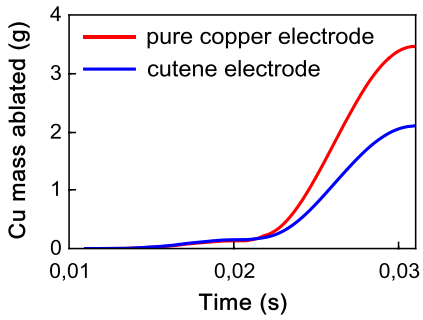

Figure 1: Copper quantity ablated from the electrode

Depending on the metallic vapours quantity the plasma properties are modified changing the HVCB behaviour. These results will be presented in a two dimensional (2D) configuration including pin and valve motions.

3. Conclusion

One transient turbulent 2D model is developed to describe the plasma behaviour in a HVCB. The interaction with the PTFE walls is considered (Conduction and Radiation by DOM and P1 models). The thin layers close to the electrodes are considered and the metallic vapour distribution calculated. Following the nature of the electrodes, the copper mass fraction field differs changing the plasma properties and the HVCB characteristics. These results will be presented and discussed.

4. References

[1] T. Christen. J. Phys. D: Apll. Phys. (2007).
[2] M.S. Benilov, S. Jacobsson, A. Kaddani, S. Zahrai. J. Phys. D: Apll. Phys. (2001).

Investigation of the RF power transfer efficiency of a planar ICP operated in Hydrogen

S. Briefi [1], D. Rauner [1, 2], U. Fantz [1, 2]

[1]*AG Experimentelle Plasmaphysik, Universität Augsburg, 86135 Augsburg, Germany*
[2]*Max-Planck-Institut für Plasmaphysik, Boltzmannstr. 2, 85748 Garching, Germany*

RF coupling efficiencies were investigated for low pressure low temperature hydrogen plasmas generated in a planar ICP. The measurements revealed that the power transfer efficiency η, defined by the ratio of RF power delivered by the generator to the power absorbed by the plasma, exhibits a peak for varying pressure and increases with higher power. Furthermore, η improves when the thickness of the dielectric window between the RF solenoid and the discharge chamber is reduced.

1. Introduction

An important task for optimizing low pressure processing ICPs is improving the transfer of the RF power from the RF circuit to the plasma. The power transfer (or coupling) efficiency η is defined as the ratio of the power delivered by the generator $P_{delivered}$ to the power actually absorbed by the plasma P_{plasma}. Two kinds of losses are imposed on P_{del} lowering η: losses due to ohmic heating in the RF network conductors and losses due to eddy currents that are induced e.g. in metallic parts of the vacuum system. In addition, operational parameters such as gas pressure, RF power and frequency but also the setup geometry influence the coupling efficiency [1].

Most investigations up to now focussed on rare gas plasmas but in many processing discharges, molecular gases are applied. Therefore, the investigations presented in this contribution were carried out in low pressure hydrogen discharges at pressures between 1 and 10 Pa.

2. Experimental setup and diagnostic methods

The experimental setup consists of a cylindrical discharge chamber with a height of 10 cm and a diameter of 15 cm. The planar solenoid which is connected to the RF generator (2 MHz, P_{max} = 2 kW) via a matching network is placed on top of the vessel. It is separated from the discharge by a quartz plate serving as dielectric window. Two different quartz plates can be installed: the first one has a thickness of 20 mm in order to withstand atmospheric pressure. This allows operating the solenoid in ambient air what is the standard setup of planar ICP's. In the second setup, the thickness of the quartz plate is reduced to 3 mm. As this plate cannot withstand atmospheric pressure, the coil is placed in an additional vacuum chamber.

Plasma parameters are obtained from a movable Langmuir probe and optical emission spectroscopy. The RF power delivered by the generator to the load is determined with an in-line V-I probe. An RF current transformer measures the RF current running through the plasma coil. With these quantities, the coupling efficiency η can be calculated [2]. It should be noted that impedance matching of the load to 50 Ω is always perfectly achieved for the presented measurements (i.e. $P_{reflected}$ = 0 W) by adjusting the variable capacitors in the matching unit.

3. Results and discussion

The measurements show that the RF coupling efficiency increases in general with higher RF power. At varying pressure, η exhibits a broad maximum between 3 and 5 Pa. These relative behaviours are also typical for ICPs operated with rare gases and can be explained with the variation of the electron density due to the change of RF power and with the change of the effective collision frequency of the plasma electrons at varying gas pressure [1, 2].

Installing the thin quartz plate increases the coupling efficiency significantly from around 45% to 70% at 5 Pa. The RF field magnitude drops rapidly with increasing distance from the coil. Therefore, much higher RF fields reach the plasma with a thin dielectric window what is beneficial for the coupling. In a next step, the influence of the RF frequency on η is going to be investigated.

Acknowledgements

The authors would like to thank the Deutsche Forschungsgemeinschaft (DFG) for their support within the project BR 4904/1-1.

References

[1] E. A. Kral'kina, Physics – Uspekhi 51, 493 – 512 (2008).

[2] J. Hopwood, Plasma Sources Sci. Technol. 3, 460 – 464 (1994).

Calculation of electron velocity distribution function under crossed electric and magnetic fields using a propagator method

H. Sugawara

Graduate School of Information Science and Technology, Hokkaido University, Sapporo, Japan

A propagator method (PM) to calculate the Boltzmann equation (BE) for the electron velocity distribution function (EVDF) in gas was extended for that under crossed electric and magnetic ($\boldsymbol{E}\times\boldsymbol{B}$) fields. Three-variable velocity space was divided into cells and the number of electrons in each cell was calculated with a three-dimensional memory array. The propagators to operate the intercellular electron transfers due to acceleration and collisional scattering were customized for the cell configuration and the electron acceleration particular to the $\boldsymbol{E}\times\boldsymbol{B}$ fields. Equilibrium EVDFs at some E/N and B/N values were obtained using a numerical relaxation scheme, and electron transport parameters derived from the EVDFs agreed with those obtained by a Monte Carlo (MC) simulation.

1. Introduction

In a PM [1] to solve the BE for the EVDF, velocity space is divided into cells and the number of electrons in each cell is calculated. While the EVDF under a dc $\boldsymbol{E}$ field is a two-variable function for its azimuthal symmetry, that under $\boldsymbol{E}\times\boldsymbol{B}$ fields is three-variable. Its calculation requires a huge memory capacity and the computational load is heavy. It was recent that computers became capable of such calculations. A prototype PM code for the EVDF under $\boldsymbol{E}\times\boldsymbol{B}$ fields was composed with customized propagators (Green's functions) to deal with intercellular electron transfers due to acceleration and collisional scattering. This report presents results of benchmark calculations.

2. Field model and PM configuration

In three-variable velocity space (υ, θ, ϕ) related to velocity $\boldsymbol{\upsilon} = (\upsilon_x, \upsilon_y, \upsilon_z)$ as $\upsilon_x = \upsilon\sin\theta\cos\phi$, $\upsilon_y = \upsilon\cos\theta$ and $\upsilon_z = \upsilon\sin\theta\sin\phi$ under $\boldsymbol{E} = (0, 0, -E)$ $(E > 0)$ and $\boldsymbol{B} = (0, B, 0)$, the (i, j, k)th cell was defined as the region of $\upsilon_{i-1} \le \upsilon < \upsilon_i$, $(j-1)\Delta\theta \le \theta < j\Delta\theta$ and $(k-1)\Delta\phi \le \phi < k\Delta\phi$. Here, $\upsilon_i = \upsilon_{1\mathrm{eV}}(i\Delta\varepsilon/\varepsilon_{1\mathrm{eV}})^{1/2}$, $\upsilon_{1\mathrm{eV}}$ is the electron speed associated with 1 eV and $\varepsilon_{1\mathrm{eV}} = 1$ eV. Desirable resolution depends on gas medium, E/N and B/N, where N is the gas molecule number density. The present PM adopted $\Delta\varepsilon = 0.01$ eV for 0–100 eV, $\Delta\theta = \pi/90$ and $\Delta\phi = 2\pi/360$ for SF_6 at $N = 10^{22}$ m^{-3}.

Electron acceleration $\boldsymbol{a} = (a_x, a_y, a_z) = \mathrm{d}\boldsymbol{\upsilon}/\mathrm{d}t = (\mathrm{d}\upsilon_x/\mathrm{d}t, \mathrm{d}\upsilon_y/\mathrm{d}t, \mathrm{d}\upsilon_z/\mathrm{d}t)$ by the $\boldsymbol{E}\times\boldsymbol{B}$ fields is dependent on $\boldsymbol{\upsilon}$ as $a_x = (e/m)\upsilon_z B$, $a_y = 0$ and $a_z = (e/m)(E - \upsilon_x B)$, where e and m are the electronic charge and mass, respectively. $\boldsymbol{a}$ is rotational around an axis in velocity space. The intercellular electron transfer due to $\boldsymbol{a}$ was evaluated as the integral of $\boldsymbol{\Gamma}\cdot\boldsymbol{n}$ over a cell surface, through which electrons move to the downstream neighbour cells. Here, $\boldsymbol{\Gamma}$ and $\boldsymbol{n}$ are the electron flux and the normal vector at the cell surface, respectively.

The collision propagator represents discontinuous changes of υ and θ at scatterings. Isotropic scattering was assumed for the collision propagator.

Table 1. Components $(\langle\upsilon_z\rangle, \langle\upsilon_x\rangle)$ $(10^4$ m s$^{-1})$ of the average electron velocity under the Hall deflection: υ_z, component of the $-\boldsymbol{E}$ direction; and υ_x, component of the $\boldsymbol{E}\times\boldsymbol{B}$ direction.

	Method	100 Hx	200 Hx	500 Hx
100 Td	MC	(6.39, 0.44)	(6.30, 0.86)	(5.79, 1.99)
	PM	(6.37, 0.43)	(6.29, 0.86)	(5.76, 1.96)
200 Td	MC	(11.44, 0.68)	(11.31, 1.36)	(10.59, 3.21)
	PM	(11.42, 0.69)	(11.31, 1.37)	(10.57, 3.22)
500 Td	MC	(23.89, 1.19)	(23.71, 2.36)	(22.68, 5.74)
	PM	(23.90, 1.20)	(23.74, 2.38)	(22.68, 5.74)

The EVDF was relaxed from a Maxwellian by applying the propagators to the EVDF using a numerical scheme like the Gauss–Seidel method. Components $\langle\upsilon_z\rangle$ and $\langle\upsilon_x\rangle$ of the average electron velocity under the Hall deflection were derived and compared with those obtained by MC simulations.

3. Results

Table 1 shows MC and PM results of $\langle\upsilon_z\rangle$ and $\langle\upsilon_x\rangle$ in SF_6 at E/N = 100–500 Td (1 Td = 10^{-21} Vm^2) and B/N = 100–500 Hx (1 Hx = 10^{-27} Tm^3). They agree with each other within discrepancies of a few percent.

4. Summary

A basic calculation scheme of the PM for EVDFs under $\boldsymbol{E}\times\boldsymbol{B}$ fields was established. Improvement of the precision via adjustment of resolution and further extension of the PM to real-space electron transport parameters are considered as succeeding work.

Acknowledgement

This work was supported by JSPS KAKENHI Grant Number JP16K05626.

Reference

[1] H. Sugawara, Plasma Sources Sci. Technol. (2017) (at press) doi: 10.1088/1361-6595/aa5d7f .

Topic number: 5

Gliding arc plasmatron for CO_2 splitting: A chemical kinetics modelling perspective

S. Heijkers[1], M. Ramakers[1], G. Trenchev[1], A. Berthelot[1], A. Bogaerts[1]

[1] *Research group PLASMANT, Department of Chemistry, University of Antwerp, Belgium*

Experiments show that the gliding arc plasmatron (GAP) has significant potential to split CO_2 in an energy efficient way. However, a detailed description of the most important chemical pathways in this type of reactor has not been elucidated yet. We therefore present a detailed chemical kinetics model for CO_2 in a GAP. The model results, such as CO_2 conversion and the resulting energy efficiency, are in very good agreement with experimental data, for different values of specific energy input. Both the model and experiments show that the obtained energy efficiency is quite promising (>20%) due to energy efficient vibration induced dissociation.

1. Introduction

Plasma technologies for converting CO_2 into value-added chemicals in an energy efficient way and at atmospheric pressure are highly wanted. The gliding arc discharge is one of these possible candidates[1]. A 0D kinetic model for the conventional gliding arc for pure CO_2 has therefore already been developed[2]. A significant amount of gas, however, passes the plasma without any conversion in the conventional configuration and the high current density causes strong electrode degradation[3]. To tackle these issues, reverse vortex flow stabilization was introduced[1],[3]. To the authors' knowledge, a full kinetic study of the GAP for pure CO_2 has not yet been conducted, which is thus presented here.

2. Methodology

We used a 0D chemical kinetics model, called ZDPlaskin[4] with the built-in Boltzmann solver, BOLSIG+[5]. The chemistry set is based on the original work of Kozak et al.[6] in which vibrational excitation till the dissociation limit of CO_2 is taken into account, and was recently updated by Koelman et al[7]. The dissociation cross section used in this study is the one proposed by Phelps, with 7eV threshold, suggested by Bogaerts et al. [8].

3. Results

In Figure 1, we show the calculated CO_2 conversion and energy efficiency. They are in very good agreement with the experimental results obtained by Ramakers et al. [9]. Both in the model and experiments, energy efficiencies greater than or equal to 23% were obtained. This is attributed to the large contribution of vibration induced dissociation (> 70%), followed by electron impact dissociation.

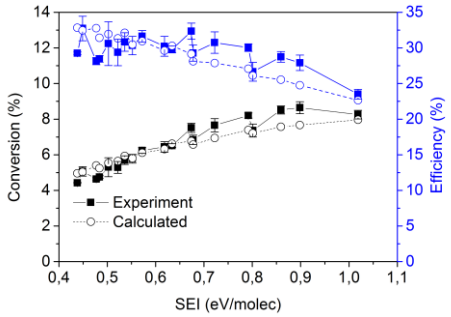

Figure 1: Calculated and measured CO_2 conversion (left y-axis) and energy efficiency (right y-axis) as a function of the specific energy input (SEI).

3. References

[1] T. Nunnally, K. Gutsol, A. Rabinovich, A. Fridman, A. Gutsol, and A. Kemoun, J. Phys. D. Appl. Phys. **44** (2011) 274009.

[2] S.R. Sun, H.X. Wang, D.H. Mei, X. Tu, and A. Bogaerts, J. CO2 Util. **17** (2016) 220.

[3] C.S. Kalra, Y.I. Cho, A. Gutsol, A. Fridman, and T.S. Rufael, Rev. Sci. Instrum. **76** (2005) 25110.

[4] S. Pancheshnyi, B. Eismann, G.J.M. Hagelaar, and L.C. Pitchford (2008).

[5] G.J.M. Hagelaar and L.C. Pitchford, Plasma Sources Sci. Technol. **14** (2005) 722.

[6] T. Kozák and A. Bogaerts, Plasma Sources Sci. Technol. **23** (2014) 45004.

[7] P. Koelman, S. Heijkers, S. Tadayon Mousavi, W. Graef, D. Mihailova, T. Kozak, A. Bogaerts, and J. van Dijk, Plasma Process. Polym. (2016).

[8] A. Bogaerts, W. Wang, A. Berthelot, and V. Guerra, Plasma Sources Sci. Technol. **25** (2016) 55016.

[9] M. Ramakers, G. Trenchev, S. Heijkers, W. Wang, and A. Bogaerts, Energy Environ. Sci. submitted (2017).

Topic number: 17

Mechanistic studies of H_2 production from H_2O using a low power Al/Al_2O_3 microplasma chip reactor

Z.S. Wiersma[1], Z. Dai[2], S.-J. Park[2], J.G. Eden[2]

[1]*Department of Chemistry, University of Illinois at Urbana-Champaign, Urbana, IL 61801, USA*
[2]*Department of Electrical and Computer Engineering and Laboratory for Optical Physics and Engineering, University of Illinois at Urbana-Champaign, Urbana, IL 61801, USA*

The transition to a H_2-based energy economy is considered an important step towards the alleviation of fossil fuel environmental effects. The current work demonstrates that plasmachemical water reactions within microplasma channels produce significant H_2. The mechanisms underlying these reactions are studied to optimize H_2 production efficiency. Chemical processes are characterized using a variety of gaseous measurement, optical characterization, and surface analysis techniques. The results demonstrate that the plasmachemical reactions deposit regular aluminium oxide and aluminium hydroxide structures along the walls of the microplasma channels. However, the electrical characteristics of the microplasma device are completely retained after more than 160 minutes of plasma reactions despite nanoparticle growth within the microchannels. Thus, microplasma chip reactors may have potential to aid the transition to a global H_2 economy.

Hydrogen is an ideal fuel because of its ultra-high energy density, lack of harmful combustion byproducts, and availability in common sources like water. However, H_2 lacks global adoption as a fuel because virtually all H_2 is synthesized from fossil fuels through expensive and energy-intensive industrial processes such as methane steam reforming.[1] Alternatively, small amounts of hydrogen can be made on-demand through water electrolysis, but this process is similarly energy intensive, requires high electrolyte concentrations, and its non-specific reactions can produce harmful reaction byproducts. As an example of non-specificity, water electrolysis can emit chlorine gas when chloride ions are present in solution.[2] Despite these limitations, the numerous applications of on-demand H_2 fuel encourages research to produce it at low cost and high efficiency.

Microplasmas are an emerging technology with promising potential for hydrogen production.[3] Microplasmas are micrometer-scale ionized gases. In contrast to traditional macroscale plasma apparatuses, microplasma chips use nanoporous materials with microscale channel dimensions to reduce dielectric breakdown voltages. These chips can operate at room temperature and pressure, and provide molecular excitation via weakly ionized nonthermal plasma.[4] Powers on the order of 1 W can excite nonthermal plasmas.[5]

Microplasma chips can produce H_2 on-demand at high efficiency and specificity using H_2O as fuel, as the current work demonstrates. The chips are modularly parallelizable, suggesting large amounts of H_2 can be created at high efficiency, and thus have significant industrial potential.[6] On-site hydrogen sources are needed for a wide variety of energy applications including hydrogen filling stations, fuel cells, and hydrogen energy storage.[7] Efficient and low power production of H_2 from H_2O would eliminate global dependence on fossil fuels.

References

[1] A. Iulianelli, S. Liguori, J. Wilcox, A. Basile, Cat. Rev., **58** (2016) 1-35.
[2] G. Chisholm, L. Cronin, Storing Energy: with Special Reference to Renewable Energy Sources, (2016) 315.
[3] C. Charles, Front.Phys., **2** (2014).
[4] J. Eden, S.-J. Park, J. Cho, M. Kim, T. Houlahan, B. Li, E. Kim, T. Kim, S. Lee, K. Kim, IEEE Trans. Plasma Sci., **41** (2013) 661-675.
[5] K.H. Schoenbach, K. Becker, EPJ D, **70** (2016) 1-22.
[6] O.K. Sung, J.G. Eden, IEEE Photon. Technol. Lett., **17** (2005) 1543-1545.
[7] A. Züttel, P. Mauron, S. Kato, E. Callini, M. Holzer, J. Huang, CHIMIA, **69** (2015) 264-268.

Internal Pressure Rise due to Arc under Insulating Oil in a Closed Vessel
-Fundamental Examination for Oil-filled Power Equipment-

T. Tadokoro[1], M. Kotari[1], T. Ohtaka[1] and M. Iwata[1]

[1] *Central Research Instituto of Electric Power Industry, Yokosuka, Japan*

When an arc fault occurs inside oil-filled equipment such as transformers in electric power systems, it heats the oil, thus generating flammable gas, and it causes dynamic increases in pressure, which can lead to a blowout. This paper reports a fundamental study on pressure rise due to an arc in a closed vessel containing air and oil. The pressure rises in the air and oil are measured under experimental conditions involving a 2.0-kA arc current, and 100-ms arc duration. The experimental results show that the arc decomposes surrounding oil to the flammable gas and the pressure oscillations vary in air and in oil. Our approximate pressure rise calculations considering oil flux are consistent with the experimental results.

1. Introduction

Electric power systems include oil-filled equipment such as transformers. When an arc fault occurs inside such equipment, the internal pressure increases, and this may result in blowout and other hazards. To clarify the arc fault phenomena, this paper reports a fundamental study concerning pressure rises due to an arc under insulating oil in a closed vessel.

2. Experimental conditions

Arc tests were carried out at the High-Power Testing Laboratory, CRIEPI, under the conditions listed in Table 1. The vessel used in the experiment (Fig. 1) contained the oil and a little air; the pressure rises were measured using pressure transducers located in the air and the oil. The arc was ignited by a fusing copper wire between the copper electrodes under the oil.

3. Results and discussion

The measured waveforms shown in Fig. 2 represent the arc current, pressure rise in air (*P*air), and that in oil (*P*oil), respectively. Every pressure rise peaks to about 200 kPa for the arc duration. The pressure oscillations in air and in oil have reversed phases. To discuss the differences in pressure oscillation, we calculated the approximate pressure for an oil flux. Assuming that flammable gas surrounding the arc compresses the air volume, an acceleration of the oil flow (α) can be calculated from *P*air. Based on this assumption, the pressure rise in oil (*P*cal) is calculated from the oil density (ρ), arc depth (D), and measured *P*air as follows:

$$P\mathrm{cal} = \rho D \alpha + P\mathrm{air} \quad (1)$$

Thus, it was observed that *P*cal is roughly consistent with the measured value except for several pressure peaks, the differences of pressure oscillation in air and in oil are attributed to oil flow.

Table 1. Experimental conditions.

Item		Condition
Power source (Short-circuit generator)	Test frequency	50 Hz
	Voltage / Current RMS	7.2 kV / 2 kA
	Arc duration	100 ms
Closed vessel	Shape	See Fig. 1
	Air / Oil volume	1.51 / 120 x10^{-3} m^3
Electrodes	Material / form	Copper / round bar
	Diameter / Gap length	5 mm / 5 mm

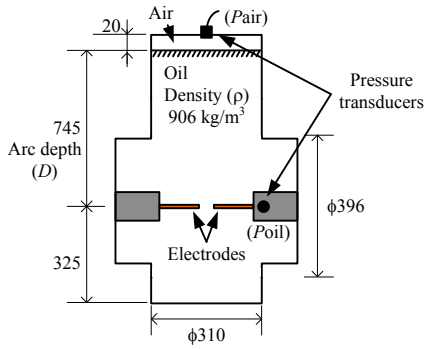

Fig. 1. Configuration of closed vessel. (Unit: mm)

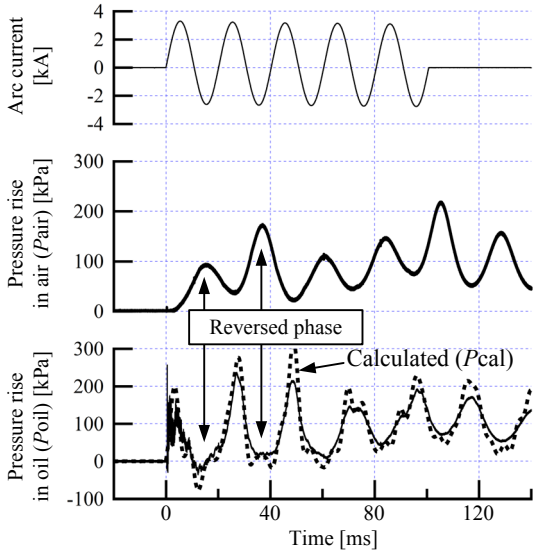

Fig. 2. Measured waveforms and calculated pressure rise in oil (*P*cal).

Effect of nitric oxide radicals on the proliferation of budding yeast

Masafumi Ito[1], Masashi Okachi[1], Jun-Seok Oh[1], Hiroshi Hashizume[2], Masaru Hori[2]

[1] *Department of Electrical and Electronic Engineering, Meijo University, Naogya 468-8502, Japan*
[2] *Institutes of Innovation for Future Society, Nagoya University, Nagoya 464-8603, Japan*

We have investigated the effect of NO radical treatment on the proliferation of budding yeast and optimized treatment conditions. NO and O_3 densities were measured using UV absorption spectroscopy and the proliferation was evaluated with microscope with cell-counting chamber. From these results, we observed around 20 % increase of the number of yeast cells at a NO density of $\sim 7 \times 10^{16}$ cm^{-3}.

1. Introduction

Non-thermal atmospheric pressure plasmas (herein referred to as plasma) are gaining importance to use in biology, medicine, and agriculture. [1] The plasma is a mixed of electrons, ions, photons and neutrals. Recent our studies were focused on the correlation between microorganisms and plasma generated neutral reactive species. [2] Here, we focused on NO which is a well-known molecule in biomedical application. For examples, it is known that the NO enables to improve signal transmission between nerves, maintaining blood pressure, supressing infection, and renewal tissue.

In this study, we report the effect of NO radical treatment on the proliferation of budding yeast and optimized treatment conditions.

2. Experimental

A commercially available atmospheric pressure plasma radical generator (Tough Plasma, Fuji Machine MFG Co., Ltd.) was used in this study. NO generated with mixture of O_2 and N_2 into buffered Ar (4 slm) through the radical generator. Flow rate of O_2 and N_2 was varied with a fixed total flow rate of 1 slm. The use of a large amount of Ar provides a high electron density on the order of 10^{16} cm^{-3}. [3] The gas channel at downstream of the radical source is bended where high energy photons are intercepted and the electrically grounded electrodes on the gas channel and the nozzle exit (0.5 mm × 16 mm) terminate charged species.

The 3ml-yeast suspension was prepared in a 38-mm diameter petri dish and treated with a fixed distance of 1 cm between the slit exit of the radical source and the surface of the liquid suspension. The cells in counting chamber were counted by using a microscope.

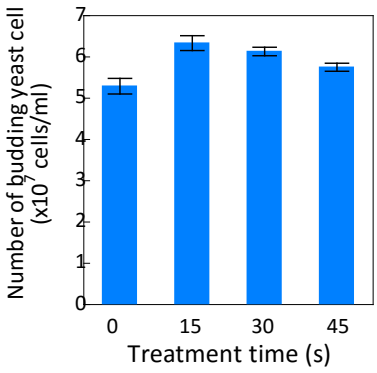

Fig. 1 Number of budding yeast cell was increased about 20% with NO treatment for 15 s. Cells were counted after incubation time of 48 h.

3. Results

Using UV absorption spectroscopy, we measured NO and O_3 densities, and decided a gas mixture condition, N_2 (30%)–O_2 (70%) in buffered Ar, to obtain high NO density but low O_3 density (lower than the detection limit). From our calculation, it was measure the NO density to be 7.27×10^{16} cm^{-3}. With this known NO density, we obtained 20% increase of number of budding yeast cell for 15 s treatment. While, longer treatment times up to 45 s, the cell counting results also showed large number of yeast cells compare to the untreated (t = 0, control) but smaller than 15 s.

This work was partly supported by MEXT-Supported Program for the Strategic Research Foundation at Private Universities (S1511021), JSPS KAKENHI Grant No. 26286072 and a project for Promoting Research Center in Meijo University.

4. References

[1] A. Fridman, Plasma Chemistry, Cambridge (2008).
[2] H. Hashizume *et al* Appl. Phys. Letts. **107** (2015) 093701.
[3] H. Inui *et al* Appl. Phys. Express **3** (2010) 126101.

Molecules Radicals and Ions produced in a N_2-H_2 CCP RF

N. Carrasco[1], D. Dubois[1], A. Chatain[1], L. Vettier[1], G. Cernogora[1]

[1] *LATMOS, Université Versailles St-Quentin, CNRS, 11 blvd d'Alembert, 78280 Guyancourt, France*

CCP RF discharges are well known to be sources of dusty plasmas. These plasmas are used to simulate the formation of organic solid particles in planetary atmospheres, as Titan with a N_2 CH_4 mixture. As a first step for understanding these plasmas, we study here the formation of molecules, radicals and positive ions in a N_2 H_2 CCP RF plasma. mixture. Radicals and positive ions are measured by in situ mass spectrometry. Neutrals are accumulated in a cold trap downstream the plasma. These molecules are measured, after warming the trap by mass spectrometry and IR absorption spectroscopy. . When mass spectrometry gives relative values of species abundances, IR absorption gives absolute values of the most abundant molecules. A focus is done on NH_3 , this molecule being produced as well in the discharge as by catalytic effect on the metallic wall of the discharge.

1. Introduction

A Capacitively Coupled Plasma in N_2-CH_4 mixture is used for the formation of dust to simulate the formation of solid aerosols in Titan's atmosphere. Details of this experimental device are described in details in [1]. The dissociation of CH_4 produces H_2 molecules. In order to understand the complex chemistry occurring in the N_2 CH_4 mixture, study of the N_2 H_2 mixture is developed as a first step.

2. Experimental device.

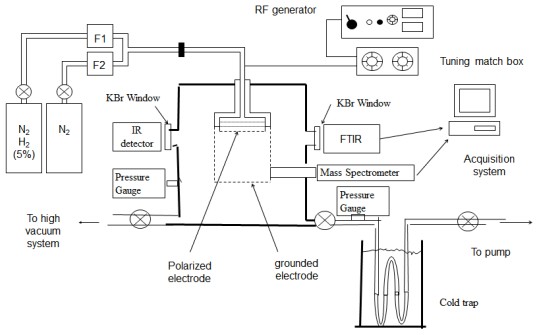

Experimental device

The CCP discharge is confined in a metallic cylindrical box of 13.6 cm in diameter. Two slots, diametrically opposed are managed in the cylindrical box. This box is placed into a 30 cm in diameter and 40cm height stainless steel reactor fitted with two KBr windows diametrically opposed. Gas mixture is injected continuously in the plasma and pumped with a rotary pump. The amount of H_2 in N_2 is tuned from 1 to 5%. Pressure in the plasma discharge is maintained at 1 mbar. Between the discharge and the pump, a trap cooled by liquid nitrogen condenses molecules produced in the discharge.

3. Measurements.

The neutral molecules, radicals and positive ions are measured using a mass spectrometer EQP Hiden placed in front of one of the slot.

After few hours of plasma run, the gas injection is turned off, valves upstream and downstream the cold trap are closed and the trap is slowly warmed up to the room temperature. Then the condensed gases are reinjected in the reactor.

The molecules densities are measured using a Nicolet 6700 Fischer FTIR spectrometer through the 40 cm of in diameter of the reactor [2]. Focus is done on the NH_3 molecule measured in the 967 cm^{-1} band. In our experimental conditions, the NH_3 density is on the order of 10^{12} cm^{-3}.

4- Perspectives

These results obtained are now to be compared with the modelling of the plasma in our experimental conditions. The major point is the relative contribution of volume reactions versus catalytic ones for the formation of NH_3.

5. References

[1] Alcouffe, G. , M. Cavarroc, G. Cernogora, F. Ouni, A. Jolly, L. Boufendi and C. Szopa (2010),. Plasma Sources Sci. Technol. 19(1): 015008.

[2] Dubois D., Carrasco N., Petrucciani M., Tigrine S., Vettier L *Neutral Chemistry in Titan's Ionospheric Simulated Conditions*, Dubois D., et al., DPS-EPSC 2016, Oct 2016, Pasadena, USA

Topic number: 9

H atom generation and loss kinetics in VHF plasmas

S. Nunomura[1], H. Katayama[2], I. Yoshida[3]

[1] *National institute of advanced industrial science and technology (AIST), Tsukuba, Ibarak, 305-8568, Japan*
[2]*Panasonic corporation, Kaizuka, Osaka 597-0094, Japan*
[3]*Photovoltaic Power Generation Technology Research Association Minato-ku, Tokyo 105-0011, Japan*

We study hydrogen (H) atom generation and loss kinetics in capacitively coupled low pressure H_2 plasma. The H atom density has been measured by using vacuum ultra violet absorption spectroscopy (VUVAS), under two different electrode setups: conventional diode (direct) and triode with an intermediate mesh (remote). In the triode setup, the H atom density is strongly reduced across the mesh electrode; it varies from 10^{12} cm^{-3} to 10^{10} cm^{-3} across the mesh. The fluid model simulations for VHF discharges have been performed to study the details of the H atom generation, diffusion and recombination kinetics.

A H atom is widely known to be reactive species, which reacts easily with other gas-phase species and various material surfaces. So, its reaction kinetics often plays key roles in plasma processing. So far, the H atom kinetics has been studied in "direct" plasma configuration. However, it is not studied for the "remote" plasma configuration that has advantages of less-ion bombardment and reduced surface charging.

Here, we study the H atom kinetics in capacitively-coupled very high frequency (VHF) discharges not only in direct (diode) configuration but also in remote (triode) configuration. The H atom density is experimentally determined from VUVAS [1]. The fluid model simulations of VHF discharges are performed to study the H atom kinetics.

Figure 1 show the meausrement results of the H atom density, n_H, in VHF H_2 discharges [2]. It is found that n_H is of the order of 10^{12} cm^{-3} in the discharge region, whereas it is of the order of 10^{10} cm^{-3} in the processing region under the remote configuration. For our mesh geometry, i.e., a mesh with 0.2 mm in thickness and 36% in aperture ratio, n_H varies two orders of magnitude across the mesh.

Figure 2 shows the simulation results. As shown Fig. 2(a), n_H is broadly peaked at the middle of the discharge region. The peak value is recognized to be ~1.0 x 10^{12} cm^{-3}, which is in good agreement with that measured by VUVAS in this study. The H atoms are generated mainly in the discharge region, via two processes: the electron impact dissociation (e + H_2 => e + 2H), as shown in Fig. 2(b), and the ion-molecule reaction (H_2^+ + H_2 => H_3^+ + H), as shown in Fig. 2(c). We also notice that in the processing region, the generation rate of the H atoms, g_H, is negligibly small. This is because the electron temperature is rather low compared with the threshold energy of the electron impact dissociation. As for the loss of H atoms, the electron attachment (e + H => H^-), shown in Fig. 2(d), is negligibly small, compared with the generation. The loss of H atoms is thus dominated by the surface recombination on the electrode. In the presentation, more details of experimental and simulation results are presented.

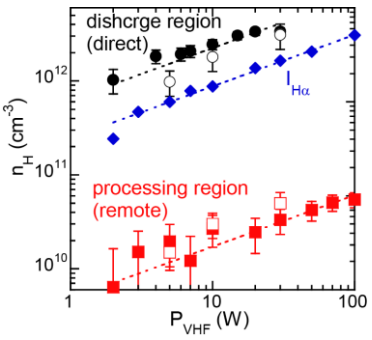

Fig. 1. H atom density, n_H, & Balmer emission intensity, $I_{H\alpha}$, vs. the discharge power, P_{VHF} at H_2 gas pressure of p = 0.3 Torr.

[1] S. Takashima, M. Hori, T. Goto and K. Yoneda, *J. Appl. Phys.* **89** (2001) 4727.
[2] S. Nunomura, H. Katayama and I. Yoshida, *Plasma Sources Sci. Technol.* **26** (2017) 055018.

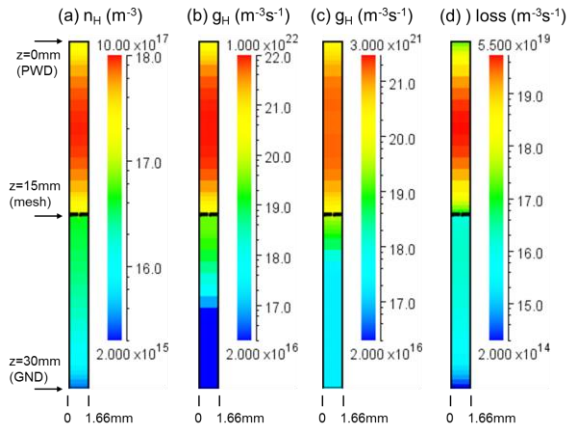

Fig. 2. Contour plots of hydrogen (H) atom related parameters [2]. (a) H atom density, n_H, (b) H atom generation rate, g_H, associated with the electron impact dissociation (e + H_2 => e + 2H) (c) H atom generation rate, associated with the ion-molecule reaction (H_2^+ + H_2 => H_3^+ + H) and (d) H atom loss rate due to the electron attachment, e + H => H^-. The simulation space includes two unit cells of the mesh structure in the horizontal axis of 0 – 1.66 mm.

Densities of active species in N_2/CH_4 afterglows with application to nitrogen and carbon doping of anatase nanocrystals and ALD TiO_2

A. Ricard[1], J.P. Sarrette[1], Y. Wang[2], Y.K. Kim[2]

[1] *LAPLACE, Université de Toulouse, CNRS, INPT, UPS, 118 route de Narbonne, 1062 Toulouse, France*
[2] *Departmentof Physics, Ajou University, Suwon 443-749, South Korea*

N_2 / 0-3$^0/_{00}CH_4$ microwave (HF) flowing afterglow emissions have been characterized by optical emission spectroscopy at pressure between 4 and 20 Torr in a tube of 18 mm internal diameter (i.d.) at constant flow rate (Q_{tot} = 0.5 slpm) and injected HF power (P_{HF} = 100 W). The N_2 1st pos at 580.4 nm and CN violet at 384.7 nm band system intensities were recorded along the tube in the late afterglow region. After calibration of the N atom density by NO titration, the absolute concentrations of N and C atoms were determined. The C-atom density shows a maximum value of 4.7 10^{13} cm^{-3} at 13 Torr for the N_2 / 0.04$^0/_0CH_4$ mixture. Anatase nanocrystals and ALD (Atomic Layer Deposition) TiO_2 samples were exposed to optimum afterglow conditions at temperatures ranging from 300 to 600 K. Surface-selective chemical modifications of TiO_2 samples are evaluated by XPS.

1. Introduction

In various applications such as photocatalysis, photovoltaics and sensors, the performance of TiO_2 is largely determined by the detailed chemical structure of the surface. For example, the introduction of nitrogen in TiO_2 can reduce the bandgap below 3.0 eV for a visible activity in photocatalysis. Nevertheless, the N-doped TiO_2 performance largely depends on the control of the nitrogen bonding structure and distribution between the surface and the bulk. In addition, carbon may also displace the lattice Ti to give C-doped TiO_2 which may show enhanced visible light absorption and photoactivity. However, the ultimate performance is strongly related with detailed bonding nature of carbon on the surface as well as within the TiO_2 matrix.

From this point of view, flowing afterglows at reduced pressure can be very useful because of their high concentrations in atoms and of their simplified chemistry, easily monitored through the operating parameters (pressure, gas flow rate, injected power).

The aim of the present study is to maximize the production of N and C-atoms in N_2/CH_4 afterglows and to expose anatase nanocrystals and ALD TiO_2 samples in optimal conditions. X-ray photoemission spectroscopy (XPS) is used to quantitatively evaluate the modifications induced on the extreme surface composition.

2. Results

In full late afterglow conditions, the N-atom gas phase chemistry is essentially reduced to the 3-body recombination process and the N-atom density [N] is related to the N_2 1st pos emission at 580nm I_{580} through relation (1):

$$I_{580} = k\,[N]^2, \qquad (1)$$

where the proportionality constant k can be obtained by NO titration [1]. Similarly, the emission intensity I_{385} of the CN violet system at 385 nm can be used to obtain the absolute C-atom concentration, once the N-atom density is known.

Varying the CH_4 amount (< 3$^0/_{00}$) and the pressure in the 4-20 Torr range, it is found that the [C]/[N] ratio shows a peak maximum for the N_2/0.4$^0/_{00}CH_4$ gas mixture and that a maximum [C] atom density of 4.7 10^{13} cm^{-3} is obtained at 13 Torr, with a corresponding N-atom density equal to 8.3 10^{14} cm^{-3}.

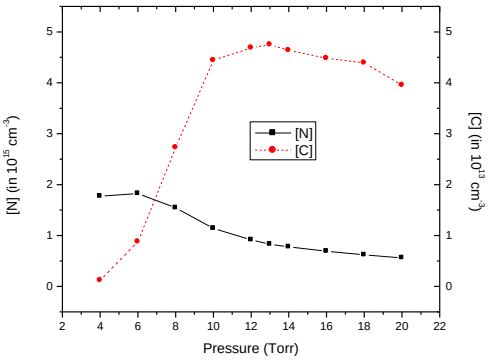

Pressure variation of N and C-atoms densities in the N_2/0.4$^0/_{00}CH_4$ late afterglow (0.5 slpm, 100 Watt)

Anatase nanocrystals and ALD TiO_2 samples were exposed in optimal afterglow conditions at temperatures ranging between 20 and 300°C and XPS analysis of the treated samples is in progress.

3. References

[1] H. Zerrouki, A. Ricard, J.P. Sarrette, Contrib. Plasma Phys. **54** (2014) 827.

Reduction of heat-fluxes during re-entry using magnetic fields

K. Lüskow[1], S. Kemnitz[2], G. Bandelow[1], J. Duras[3], D. Kahnfeld[1], P. Matthias[1], R. Schneider[1], D. Konigorski[4]

[1] *Institute for Physics, Ernst-Moritz-Arndt University of Greifswald, Greifswald, Germany*
[2] *Institute for Computer Science, University of Rostock, Rostock, Germany*
[3] *Department of Applied Mathematics, Physics and Humanities, Nuremberger Institute for Technology, Nuremberg, Germany*
[4] *Airbus Operations GmbH, Emerging Technologies and Concepts, Hamburg, Germany*

In wind-tunnel experiments a heat flux reduction was observed by applying magnetic fields. The underlying mechanism is still unexplained. One possible reason is the indirect effect of magnetic fields on the total heat flux. The application of magnetic fields influences the flux of electrons and ions, and through charge-exchange collisions also the dominant contribution of neutrals in the heat flux.

To reduce heat fluxes during re-entry one idea is to use magnetic fields that shield the spacecraft from the flux[1]. In 2002 the European Space Agency started an investigation on heat-flux mitigations by externally applied magnetic fields in partially-ionised argon-flows [2]. In these test experiments due to large differences between plasma density (~10^{17} m^{-3}) and neutral density (~10^{21} m^{-3}), most of the heat-flux is carried by neutrals. Therefore, it is not directly expected that it can be reduced by magnetic fields.

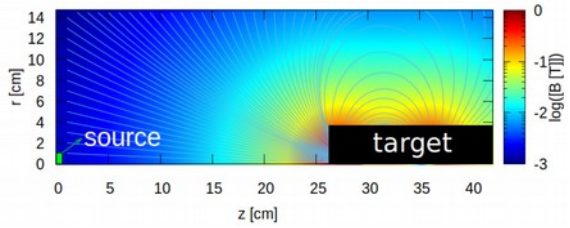

Figure 1: Magnetic field and simulation domain.

To study such scenarios the Particle-in-Cell method with Monte-Carlo collisions [3,4] was used. The simulation reproduces the heat flux reduction qualitatively. The magnetic field leads to a change in electron and ion density by affecting the trajectories of the charged particles through the Lorentz force. Magnetic field lines in the dipole-like field converge to the centre of the target. As particles are guided into this region a shield of high plasma density builds up in front of the target. Neutral transport is affected by charge exchange collisions with ions acting as a momentum sink for the neutrals and reducing the neutral axial velocity. By this, the resulting total neutral heat flux is reduced. Ion heat flux is increased only weakly, because the radial losses due to the magnetic field and turbulence get stronger. In addition, the simulation was verified against experimental spectroscopy using optical emission analysis. In the free stream region a loss of intensity for all wavelengths appeared, whereas in front of the target an increase of the intensity is observed. Both effects were in good agreement with the experiment.

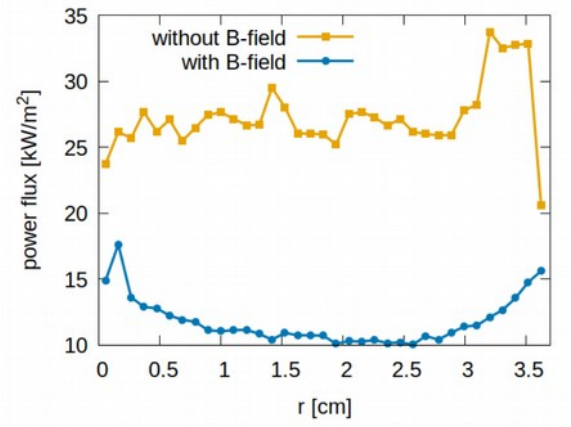

Figure 2: Simulated radial profile of the total heat flux onto the target.

A photo was simulated from the calculated optical emission spectrum. The simulation reproduces the observed optical effects when applying the external magnetic field. These effects are an overall red shift, a smaller bright emission region close to the arc jet exit and an emission region in front of the target.

[1] M.L. Blosser, NASA Technical Memorandum. **110296** (1996).

[2] A. Gülhan et. al., J. of Spacecrafts and Rockets. **46** (2009), 274-283.

[3] D. Tskhakaya et. al., Contributions to Plasma Physics. **47** (2007), 563-594.

[4] K. Matyash et. al., Contributions to Plasma Physics. **47** (2007), 595-634.

Topic number

Microcrater formation model under cathode spot plasma of a vacuum arc

G. A. Mesyats[1] and I. V. Uimanov[2]

[1] *P.N. Lebedev Physical Institute, RAS, Moscow 119991, Russia*
[2] *Institute of Electrophysics, UB RAS, Ekaterinburg 620016, Rissia*

A semiempirical hydrodynamic model based on the cellular structure of the cathode spot of a vacuum arc has been developed to describe the formation of a microcrater on the cathode under dense cathode spot plasma. In the context of a 2D axisymmetric problem statement of charge, heat, and mass transfer in a cathode, the formation of a crater on a copper cathode has been simulated. It has been shown that for the cell current ranging between 1.6 and 7 A and the time of current flow through a cell ranging between 15 and 60 ns, the crater diameter is 3–7 μm. In these cases, the current density at the center of a cathode spot cell is ~10^{12} A/m^2, and the average current density in a cell, determined using the crater diameter, is ~10^{11} A/m^2. The obtained results are in agreement with experimental data on the crater size, cathode spot lifetime, and cathode spot current density at near-threshold arc currents.

1. Introduction

According to numerous observations, any vacuum arc track on a cathode has a substructure of microcraters. Based on these observations, the ecton mechanism of the operation of a cathode spot (CS) was proposed [1]. The CS comprises an active area of a cathode, heated to above its melting temperature, and the adjacent dense CS plasma. The ecton model assumes a cyclic operation of individual CS cells having micrometer spatial dimensions and lifetimes of several tens of nanoseconds. Recently, some advances have been made in the theoretical study of the role of the liquid-metal phase in the initiation and operation of a CS cell [2–4].

2. Model description and Results

In the context of a 2D axisymmetric statement of the problem of the charge, heat, and mass transfer in a cathode, a semiempirical hydrodynamic model has been developed to describe the formation of a microcrater and the initial stage of the formation of liquid-metal jets in a cell of the cathode spot of a vacuum arc. The model includes experimentally obtained characteristics of the cathode spot plasma interacting with the cathode, such as the pressure exerted by the plasma on the cathode and the power dissipated in the cathode. The crater formation has been simulated for a copper cathode at a constant CS cell current. It has been shown that for the cell current ranging between 1.6 and 7 A and the time of current flow through the cell ranging between 15 and 60 ns, the crater diameter is 3–7 μm. The simulation predicted the maximum current density in the cell center equal to (1–3)·10^{12} A/m^2 for all calculation variants where the formation of a micrometer-size crater took several tens of nanoseconds. The mean current density in the cell determined in terms of the crater diameter is an order of magnitude lower, ~10^{11} A/m^2. These results are in agreement with experimental data [1] on the crater size, cathode spot lifetime, and cathode spot current density at near-threshold arc currents.

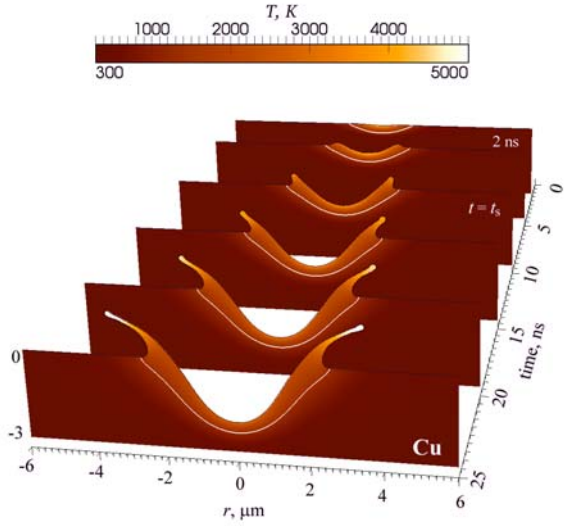

Fig. 1. Results of the numerical simulation of the micro-crater formation (Cu, i_c = 3.2 A, r_0 = 0.8 μm).

The work was performed under state assignment (theme No. 0389-2014-0005) and supported in part by the RFBR (grants Nos. 16-08-01099, 15-08-01648).

3. References

[1] G.A. Mesyats, *Cathode Phenomena in a Vacuum Discharge: The Breakdown, the Spark, and the Arc*. Moscow: Nauka, 2000.

[2] Mesyats G.A and Uimanov I.V., IEEE Trans. on Plasm. Sci., 43 (2015) 2241-2246.

[3] M. A. Gashkov, N. M. Zubarev,, O. V. Zubareva, G. A. Mesyats and I. V. Uimanov, J. of Exp. and Theor. Phys., 122 (2016) 776–786.

[4] M.A. Gashkov, N.M. Zubarev, G.A. Mesyats, and I.V. Uimanov, Pis'ma Zh. Tekh. Fiz., 42 (2016) 48–55.

Remote sensing of plasma phenomena in the upper atmosphere of the Earth by ground-based optical emission spectroscopy

F. J. Gordillo-Vázquez[1], M. Passas[1], J. Sánchez, A. Luque, O. Van der Velde[2], J. Montanya[2]

[1]*Solar System Department, IAA - CSIC, Glorieta de la Astronomía s/n, Granada, Spain*
[2]*Universitat Politècnica de Catalunya (UPC), C. Colom, 1, Terrassa, Spain*
**Contact e-mail:* vazquez@iaa.es

Remote sensing of the Earth mesosphere (50 - 90 km altitude) is difficult because it is too high for atmospheric balloons and usually too low for most satellite sensing. The occurrence of Transient Luminous Events (TLEs) in the upper layers of the atmosphere connected to lightning activity in the troposphere (0 - 14 km) can be now remotely sensed with GRASSP, the *GRanada Sprite Spectrograph and Polarimeter*, which can provide middle resolution (0.24 nm) spectra of transient plasma phenomena occurring in the mesosphere of the Earth. Spectra recorded with GRASSP can provide valuable information about key features of the mesosphere through remote sensing of such transient plasmas. We present preliminary results of gas temperatures and the degree of vibrational excitation of mesospheric air plasmas.

1. Introduction

The first and simultaneous spectroscopic campaigns of TLEs were carried out in the mid 1990s [1, 2], soon after the discovery of TLEs in 1989 [3]. These initial campaigns provided preliminary results on the optical emissions of TLEs corresponding to the first positive system (FPS) of $N_2(B^3\Pi_g) \rightarrow N_2(A^3\Sigma^+_u)$ in the visible and near infrared (NIR) spectral range (540–840 nm) recorded at standard video rate (30 fps) and at low (between 9 and 6 nm) spectral resolution.

More recently, in 2007, spectroscopic observations of sprite optical emissions between 640 nm and 820 nm provided information on the relative vibrational concentrations of the emitting electronic state $N_2(B^3\Pi_g, v')$ at different altitudes using higher video rate (300 fps) and higher spectral resolution (3 nm) spectrographs [4] originally designed for aurora spectroscopy [5].

The above mentioned sporadic TLE spectroscopic campaigns identified some of the key optical emissions from sprites (a type of TLE) and were even able to quantify some of the vibrational concentrations of the emitting levels in reasonable agreement with model predictions [6]. However, the best spectral resolution achieved to date is 3 nm and it is not enough to spectrally resolve the different low-lying vibro-rotational transitions of the FPS of N_2.

This contribution focuses on (1) the latest upgrades of the GRanada Sprite Spectrograph and Polarimeter (GRASSP), a ground-based medium-high spectral resolution spectrograph aimed at characterizing from ground the spectroscopic fingerprints of all sort of TLEs occurring in the mesosphere of the Earth and (2) the GRASSP 2015, 2016 summer-autumn TLE spectroscopic campaign in Europe when we got the first ever recorded high-resolution spectra of sprite halos and columniform and carrot-like sprites.

High-resolution spectra of TLEs recorded with GRASSP are a valuable tool to remotely probe the upper atmosphere of the Earth and extract information about the gas temperature and the distribution of vibrational levels of $N_2(B^3\Pi_g)$ underlying some of the transient optical emissions of TLEs.

GRASSP works at 0.24 nm spectral resolution covering the spectral range between 700 nm and 800 nm. The last version of GRASSP is currently installed in Castellgalí, Barcelona (Spain), it is aimed and operated manually by the operator from the UPC group on-site or operated remotely from IAA-CSIC in Granada.

GRASSP is already being used for systematic TLE spectroscopic surveys in Europe as part of the ground support for the future *Atmospheric Space Interaction Monitor* (ASIM) and the *Tool for the Analysis of RAdiation from LightNIng and Sprites* (TARANIS) space missions to be launch by the end of 2017 and 2018, respectively.

2. References

[1] S. B. Mende, R. L. Rairden, G. R. Swenson, and W. A. Lyons, (1995) Geophys. Res. Lett. **22**, 2633
[2] D. L. Hampton, M. J. Heavner, E. M. Wescott, and D. D. Sentman, (1996) Geophys. Res. Lett. **23**, 89
[3] R. C. Franz, R. J. Nemzek, and J. R. Winckler, (1990) Science **249**, 48
[4] T. Kanmae, H. C. Stenbaek-Nielsen, and M. G. McHarg, (2007) Geophys. Res. Lett. **34**, L07, 810
[5] T. J. Hallinan, H. C. Stenbaek-Nielsen, and C. S. Deehr, (1985) J. Geophys. Res. **90**, 8461–8475
[6] F. J. Gordillo-Vázquez, A. Luque, and M. Simek, (2011) J. Geophys. Res. (Space Phys) **116**, A09, 319

Metastable Molecules in O_2 Plasmas probed by High-Resolution Fourier Transform Absorption Spectroscopy

A.Chatterjee[1,2], J.P. Booth[1], O. Guaitella[1], N. De Oliviera[2] ,L. Nahon[2] ,C.M. Western[3]

[1] Laboratoire de Physique des Plasmas, CNRS, Ecole Polytechnique, UPMC Univ Paris 06, Univ Paris-Sud, Observatoire de Paris,Université Paris-Saclay, Sorbonne Universités, PSL Research University, F-91128 Palaiseau, Franc, [2] Synchrotron SOLEIL, Gif Sur Yevette, France; [3] University of Bristol, UK

DC glow discharges in pure oxygen were studied by high resolution (~10^6) VUV absorption spectroscopy using synchrotron radiation and a Fourier Transform Spectrometer. O_2(X), O_2 (a), O_2 (b) and ground state O atoms were observed, allowing their absolute densities to be determined as a function of gas pressure and discharge current.

1. Introduction

Electrical discharges in oxygen-containing gases are found widely in nature and are used for many industrial processes including etching, polymer stripping and surface cleaning as well as for sterilization and other biomedical applications. Metastable molecules (a $^1\Delta_g$ and b $^1\Sigma_g$) and atomic oxygen produced in such plasmas play a vital role in the plasma characteristics. Since they destroy O^- negative ions by associative detachment reactions, they have a strong effect on the plasma conductivity and reactivity. They are principally lost by reactions at the chamber walls, but the surface reaction coefficients are poorly known, limiting the predictive power of models.

Vacuum ultraviolet absorption spectroscopy is a promising technique for detecting these transient species. However, their VUV spectrum has not been measured since Ogawa et al. [2,3] in the 1970's. We have used the excellent spectral resolution (~10^6) and accuracy of the DESIRS VUV Fourier-Transform (FTS) branch at synchrotron Soleil [1] to revisit these measurements. Combining with spectral simulations we can identify the best transitions for future time resolved kinetic measurements on the monochromatic branch of the DESIRS beamline.

2. Experimental Setup

The DC discharge was excited in a 40cm long, 1.2 cm id Pyrex tube with water cooling and stainless steel electrodes and MgF_2 windows to transmit the VUV beam. The transmitted light in the region 120-170 nm is analysed with the FTS [1].

3. Results

Fig 1 compares our results with the spectra of Ogawa et al. O_2 X, a and b bands are observed, with high resolution, allowing the rotational temperature to be determined. The O_2 X and a state densities were determined using the data of Ogawa.

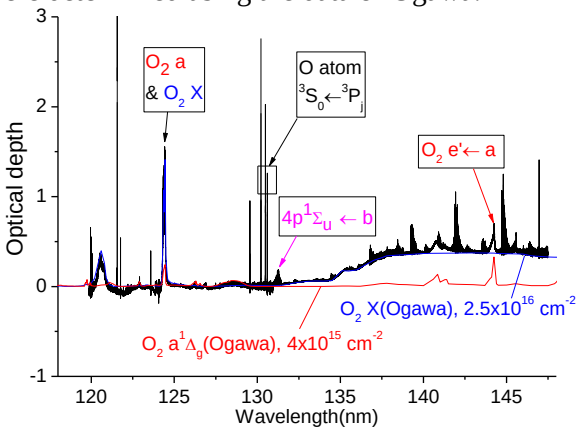

Fig.1. Absorption spectrum of 50 mA discharge, 10mBar He + 0.05mBar O_2

4. Conclusions and perspectives

New high resolution VUV absorption spectra for a $^1\Delta_g$ and b $^1\Sigma_g$ molecules and atomic oxygen are reported. In the future we will perform kinetic measurements using modulated current.

5. Acknowledgments

This research was conducted within the LABEX Plas@par project, and received financial state aid managed by the Agence Nationale de la Recherche, as part of the programme "Investissements d'avenir" under the reference ANR-11-IDEX-0004-02.

6. References

[1] N de Oliveira, M Roudjane, D Joyeux, D Phalippou, J-C Rodier & L Nahon, *Nature Photonics* 5, 149–153 (2011)

[2] S. Ogawa and M. Ogawa, *Canadian Journal of Physics*, **53**, (1975) 1845

[3]D.H. Katayama, S. Ogawa, M. Ogawa, and Y. Tanaka, *Journal of Chemical Physics*, **67**, (1977) 2132

Current Bearing Anti-Force Waves (Lightning Return Stroke)

M. Hemmati[1], J. Griffiths[1], M. Bowman[1]

[1] *Department of Physical Science, Arkansas Tech University, Russellville, Arkansas 72801, USA*

In our investigation of breakdown waves, we apply a one-dimensional, steady-state, three-component fluid model. The electrons are assumed to be the main element in propagation of the wave and the wave is considered to be shock fronted. Our set of electron fluid dynamical equations is composed of the equation of mass flux, equation of conservation of momentum, equation of conservation of energy, plus Poison's equation. For lightning return strokes, experimentally, few much larger than usual currents have been reported [1]; we intend to examine existence of such large currents; also, for return strokes, some researchers have suggested existence of a relationship between the peak current and wave speed values [2], we intend to find out its validity as well.

1. Model, Solution and Results

Anti-force waves are breakdown waves for which the electric field force on electrons is in the opposite direction of the wave propagation; however, the electron gas temperature is assumed to be large enough to sustain the wave motion. Following the shock front, there is a thin dynamical transition region referred to as the sheath region of the wave; where, the electric field starting with its maximum value at the shock front reduces to zero at the end of the sheath region, and the electrons, starting with an initial speed at the wave front, slow down to speeds comparable to those of heavy particles. For theoretical investigation of anti-force waves with a large current behind the shock front, we will use Hemmati et al.'s [3] modified set of electron fluid dynamical equations and the boundary condition on electron temperature at the shock front. In dimensionless variables, the equations are

$$\frac{d}{d\xi}[v\psi] = \kappa\mu\nu, \qquad (1)$$

$$\frac{d}{d\xi}[v\psi(\psi-1)+\alpha v\theta] = v\eta - \kappa v(\psi-1), \qquad (2)$$

$$\frac{d}{d\xi}[v\psi(\psi-1)^2+\alpha v\theta(5\psi-2)+\alpha v\psi-\frac{5\alpha^2 v\theta}{\kappa}\frac{d\theta}{d\xi}$$
$$+\alpha\eta^2] = 2\eta\kappa\iota\alpha - \omega\kappa\nu[3\alpha\theta+(\psi-1)^2], \qquad (3)$$

$$\frac{d\eta}{d\xi} = \kappa\iota - \frac{\iota}{\alpha}(\psi-1) \qquad (4)$$

$$\theta_1 = \frac{\psi_1(1-\psi_1)}{\alpha} - \frac{\kappa\iota}{\nu_1}. \qquad (5)$$

Where ν, ψ, θ represent non-dimensional electron number density, velocity and temperature; η, μ, ξ, ι, represent net electric field, ionization rate, position within the sheath region and current at the shock front; κ and α are wave parameters.

For lightning return strokes, experimental current values measured are generally in the 5-30 kA range; however, some, for example Rakov [1], has reported the highest recorded peak currents in Japan to be 280, 320 and 340 kA. Our dimensionless current, $\iota = 1$, represents an actual current value of 10 kA. We use a trial-and-error method to integrate equations 1-4 through the sheath region of the wave. Our solutions for a range of wave speeds, and also maximum current values possible for those wave speeds, meet the expected conditions at the trailing edge of the wave $(\psi_2 \to 1; \eta_2 \to 0)$. The following is a graph of the net electric field as a function of wave speed within the sheath region of the wave.

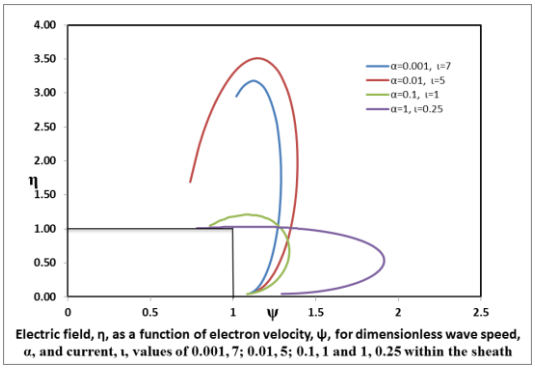

Electric field, η, as a function of electron velocity, ψ, for dimensionless wave speed, α, and current, ι, values of 0.001, 7; 0.01, 5; 0.1, 1 and 1, 0.25 within the sheath

For return strokes, in addition to existence of large currents, we also confirm existence of a relationship between the wave speed and peak current values.

2. References

[1] V.A. Rakov. 25th Int. Conference on Lightning Protection. (2000). 103-108.

[2] C.F. Wagner. AIEE Trans. Power Appar. Syst. 1968. 82:609-17.

[3] M. Hemmati, W.P. Childs, H. Shojaei and D.C. Waters. 28th International Symposium on Shock Waves, 2011, England.

Radiation study for DC and microware (mw) HID lamps

A. Sahab[1], M. Hamady[2], G. Zissis[3]

[1] *Solid Worx S.A.R.L, Sakr Building, Industrial Area , Roumieh Main Road, Lebanon*
[2] *Physics Department, Faculty of sciences, Beirut Arab University, Debbieh, Lebanon*
[3] *Université de Toulouse, UPS, INPT, LAPLACE (Laboratoire Plasma et Conversion d'Energie) 118 route de Narbonne, F-31062 Toulouse cedex9, France*

Advances in microwave and light source technology in the last decade have led to the most recent generation of highly efficient electrodeless discharge lamps. Such lamps are generally classified in the scientific literature as *electrodeless HID* (EHID) lamps, but currently they are often referred to as *plasma lamps.* The radiations of discharges sustained by a microwave (mw) electromagnetic field as well as discharges containing electrodes are discussed. The visible radiations are mainly important in light sources application while UV radiations are used extensively in water sterilisation.A 1D power balance model and ray-tracing method are both employed to calculated the radiations in these discharges.

1. General

In recent years, the use of an electrodeless light source excited by microwave electric fields has been widely used in our daily life and has attracted a great interest. The absence of electrodes provides greater flexibility in lamp design and the discharge is no longer limited by the narrow gap between the electrodes. In addition, the lack of inexpensive and efficient microwave power supplies has hampered the development of these lamps for many years. Pure Hg discharges are an ideal vehicle for a fundamental study, since the physical properties of mercury atoms have been well understood for many years.

2. Models

Zollweg [1] has deeply studied Hg DC discharges and has estimated the radiations of these lamps in different spectral range. The corresponding (same power) mw HID lamps are studied in this work. These discharges are considered to be excited by microwave electromagnetic fields in a cylindrical TM_{010} mode. A detailed theoretical analysis of these lamps was presented by Offermanns [2] and Waymouth [3]. We have already used in previous work [4] these analyses and obtained a representation of the temperature profile for DC discharges as well as for mw discharges.

3. DC and MW Discharges

Once the temperature profile for each lamp is known, the radiations in different spectral range are calculated using a model of radiation transport as in [4]. The obtained results for DC discharges at almost the same applied power are comparable with experimental results of Zollweg [1] as shown in Table 1.

Range (nm)	350-390	390-420	420-450	535-560	560-590
Model (W)	12.1	5.9	10.1	8.5	11.7
Zollweg (W)	14.4	7.5	10.7	12	15.2

Table 1: Radiations of each spectral range of the lamp

3. Results

We show in Figure 1 the increase in radiation as the applied electric power increases for both DC and mw discharges. The results show that the increase of radiation is almost linear with the applied power with a higher slope for DC discharge (blue line).

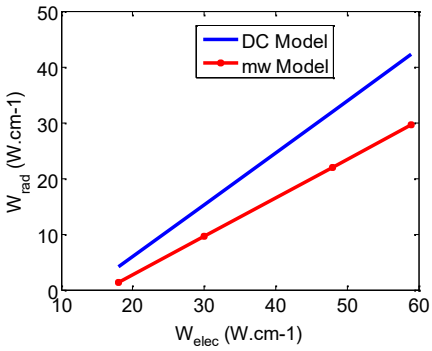

Figure 1: Variation of radiation with applied power

3. References

[1] Zollweg R J, Lowke J J and Liebermann R W,1975, *J. Appl. Phys.* **46** 3828-3838

[2] Offermanns S 1990 *J. Appl. Phys.***67** 115.

[3] Waymouth J F 1993 *Microwave Discharges: Fundamentals and Applications* Plenum Press, New York 427.

[4] M. Hamady, G. G. Lister, G. Zissis 2015 *Journal of Lighting Research and Technology*, DOI 10.1177/1477153515571678.

Flow Circulation and Ozone Concentration Generated by Plasma Actuator in a Closed Circuit Pipe

Youhwan Shin[1], Heon-Su Lee[2]

[1] *Center for Urban Energy Research, Korea Institute of Science and Technology*
[2] *Multifunctional Structural Composite Research Center, Korea Institute of Science and Technology*
Hwarangno 14-gil 5, Seongbuk-gu, Seoul 02792, Korea.
yhshin@kist.re.kr

This experimental research includes the characteristics of the flow generated by dielectric barrier discharge (DBD) plasma actuators installed on the wall inside a circular pipe as a closed circuit. We compare and discuss with the flow velocities and their distributions in the closed-loop tunnel at the various excitation voltages and frequencies applied to the actuators. We also observed the variation of the ozone concentrations with various conditions supplied to the actuators. The velocity magnitude of the air in the closed pipe decreases as the ozone concentration rapidly increases at first short time. Higher voltage excited to the plasma actuator makes its increasing rate grow steeper. However as time goes, the ozone concentration is saturated in a closed pipe and consequently it is independent on the electrode excitation voltage of the plasma actuator.

Abstract

Flow phenomena such as a separation on the surface wall or the leakage flow on the gas turbine blade tips normally cause flow losses. Therefore in order to increase some efficiencies related on the aerodynamic flow, they are needed to be depressed by the flow control. Plasma actuator can be used as one effective choice of the methods for active flow control, which has many advantages such as simple structure without moving parts and so on [1]. DBD plasma actuator induces parallel flow on the wall surface of the actuator by the interaction between plasma and neutral air particles.

As shown in Fig. 1, an experimental setup was arranged with single and multiple DBD actuators installed on a circular tube wall. The electrode is connected to high-voltage power amplifier (TREK 20/20C) excited by a function generator generating sine waves. The voltage and frequency ranges are 10~16 kV and 0.5~1.0 kHz respectively. Ozone concentrations were measured by USB New iStar ICCD Camera (Andor Technology) and analyzed by S/W, Andor Solis. Flow velocities were also measured at several radial positions inside the pipe by hotwire anemometry.

Ozone concentrations were measured for 20 minutes in a closed circular pipe under the operation of the plasma actuator as shown in Fig. 2. Firstly they dramatically increase for a short time, 300 seconds. Subsequently they gradually decrease to be saturated conditions. Higher excitation voltage applied to the actuators generates higher growing rate of them. The velocity magnitude in the pipe steeply decreases as the ozone concentration rapidly increases.

References

[1] G. Pechlivanoglou, C.N. Nayeri and C.O. Paschereit, Performance Optimization of Wind Turbine Rotors with Active Flow Control, Proceedings of ASME Turbo Expo. (2011) GT2011-45493.

[2] J. Malicet, D. Daumont, J. Charbonnier, C. Parisse, A. Chakir and J. Brion, Ozone UV spectroscopy. II. Absorption cross-sections and temperature dependence, Journal of Atmospheric Chemistry V.21 (1995) 263.

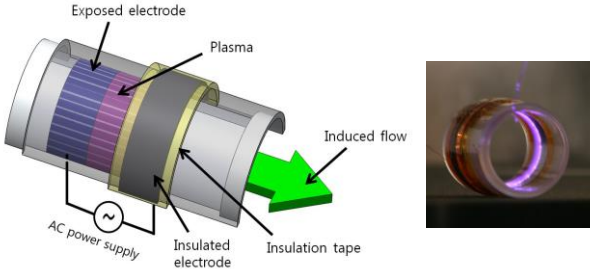

Figure 1 Schematic half view of a DBD plasma actuator on inner wall of a circular pipe

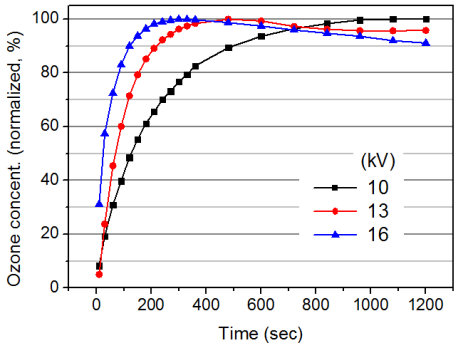

Figure 2 Ozone concentrations with different electrode voltages of DBD plasma actuators (1 kHz)

Optical measurement of meter-scale microwave line plasma under atmospheric pressure

H. Suzuki, Y. Tamura, Y. Inomata, and H. Toyoda

Graduate School of Engineering, Nagoya University, Nagoya, Japan

Meter-scale microwave line plasma is produced under atmospheric pressure using a loop-waveguide with a microwave circulator to suppress ununiformity of electromagnetic field inside the waveguide, and is investigated by an optical emission spectroscopy. Gas temperature and electron density of argon plasma are ~600 K and ~10^{20} m^{-3}, respectively, and are spatially-uniform in 80 cm in length.

1. Introduction

Recently, large-area surface treatment using atmospheric-pressure (AP) plasma attracts much attention due to its cost benefit and a variety of possibilities for industrial applications. As a new AP plasma source for large area processing, we have proposed a one-dimensionally long-scale AP microwave plasma source using a loop-waveguide system, where plasma uniformity is realized by suppression of standing wave inside the waveguide. Using this plasma source, spatially-uniform line plasma of 40 cm in length has been realized with helium gas and cw microwave power of 1.0 kW [1]. Furthermore, production of pure molecular gas line plasma inside a slot of 50 cm in length has been realized by improving the waveguide structure to increase power efficiency [2]. To apply this plasma source to industrial processing, understanding of the plasma characteristics such as spatial uniformity, gas temperature, plasma density and plasma-sustainment mechanism are important. In this study, plasma parameters are investigated by optical emission spectroscopy (OES).

2. Experimental Setup

A microwave source (2.45 GHz, power: <5.0 kW) is connected to the circulator through an impedance matcher. A slot antenna of 0.1 mm in gap width is cut along the modified ridge waveguide wall. Discharge gas (Ar: 14 slm) is introduced into the waveguide through small holes and is released through the slot. Plasma is produced inside the slot by applying microwave power. Spatiotemporal distribution of the plasma is investigated by a digital still camera and an optical multi-channel analyzer through an optical fiber. Gas temperature and electron density are measured from N_2 second positive band profile and Stark broadening of H_β spectrum, respectively. Microwave powers at the upstream and downstream of the slotted waveguide are monitored by crystal mounts.

3. Results and discussion

Firstly, the line plasma is produced with an input microwave-power of 500 W to a slot of 1.1 m in length. The emission intensity monitored by the digital camera is quite uniform and its spatial fluctuation is less than 8% in 80 cm around the slot center. Spatial profiles of the gas temperature and electron density are shown in Figure 1 and are uniform at ~600 K and ~10^{20} m^{-3}, respectively. These results suggest that meter-scale almost uniform plasma with low temperature and high plasma density is realized by using the plasma source.

Acknowledgement

This work was supported by JSPS KAKENHI Grant number JP16H03893.

References

[1] H. Suzuki et al.: Appl. Phys. Express **8** (2015) 036001.

[2] H. Suzuki et al.: 69th Gaseous Electronics Conference, 2016, NW3.7

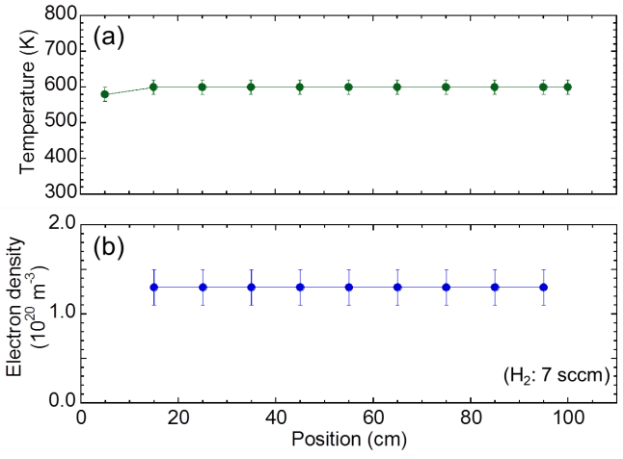

Fig. 1. Spatial distributions of (a) N_2 rotational temperature and (b) electron density along the slot.

Electronic response of a plasma-facing dielectric solid

F. X. Bronold, H. Fehske

Institut für Physik, Ernst-Moritz-Arndt-Universität Greifswald, D-17489 Greifswald

Based on the Poisson equation for the electric potential and two sets of spatially separated Boltzmann equations, one for the conduction band electrons and valence band holes inside the dielectric and one for the electrons and ions inside the plasma, we present a kinetic theory for the electronic response of a plasma-facing dielectric solid. It enables us to determine the quasi-stationary density and potential profiles of the electric double layer formed at the interface as well as the electron and ion fluxes maintaining it. To demonstrate the feasibility and the potential of our approach we present numerical results for collisionless double layers at silicon and silicon dioxide surfaces in contact with a hydrogen plasma.

The basic electronic response of a plasma-facing solid is the formation of the plasma sheath. It is the positive part of an electric double layer whose negative part is inside the solid. A stationary sheath develops if electron-ion generation in the plasma is balanced by electron and ion losses at or inside the wall. A complete kinetic modelling of the sheath has thus to contain not only the plasma physics of the positive part of the double layer but also the solid state physics of the negative part.

For a dielectric wall we developed such a synergetic approach [1] which we expect to be particularly useful for integrated microdischarges [2,3], in particular, when their miniaturization continues making thereby the length and time scales of the gaseous discharge comparable with the scales of the confining wall. Our approach is based on the Poisson equation and two sets of Boltzmann equations operating in disjunct half-spaces separated by a planar interface. One set is for electrons and ions inside the plasma and the other is for conduction band electrons and valence band holes inside the wall. The two sets are connected by quantum-mechanical matching conditions for the electron distribution functions, a semi-empirical model for hole injection due to neutralization of ions at the interface, and the matching conditions for the electric potential. Essential for the modelling is the merging of the space charge region with the neutral bulk plasma and the intrinsic or extrinsic bulk of the wall as well as the ambipolarity inside the wall leading to an electron-hole recombination condition.

The overall picture emerging from our kinetic modelling is a double layer whose positive space charge on the plasma side is balanced by a thermalized/trapped negative space charge inside the wall while the quasi-stationary electron and ion fluxes maintaining the double layer are limited by electron-hole recombination inside the wall. Numerical results for collisionless double layers formed at intrinsic and extrinsic silicon and silicon dioxide surfaces exposed to a hydrogen plasma (see Fig. 1 for the plasma-induced band bending in intrinsic silicon dioxide and silicon) show the feasibility and potential of our approach. Issues to be resolved before it can become quantitative for realistic interfaces will be discussed. – Supported by DFG through CRC/Transregio TRR24.

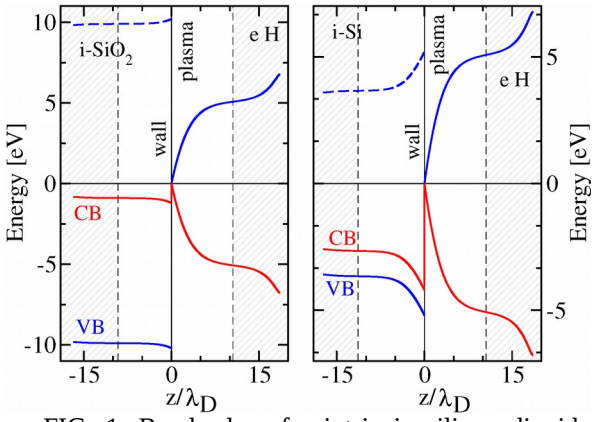

FIG. 1: Band edges for intrinsic silicon dioxide (left panel) and intrinsic silicon (right panel) in contact with a hydrogen plasma [1]. Inside the wall solid red (blue) curves are the edges of the conduction (valence) band while in front of it the curves give the potential energy of the electrons (ions). Dashed blue curves indicate the edges for the valence band holes. The distances from the interface at z=0 are measured in units of the wall's (plasma's) electron Debye screening length. The profiles inside the light grey regions have no direct physical meaning. They arise from implementing technically the physical boundary conditions for the double layer responsible for the band bending. The electron (ion) temperature of the plasma is 2 eV (0.2 eV).

References

[1] F.X.Bronold, H.Fehske, arXiv:1702.00644.

[2] J.G. Eden et al., IEEE Trans. Plasma Sci. **41** (2013) 661.

[3] M.K. Kulsreshath et al., J. Phys. D: Appl. Phys. **45** (2012) 285202.

Property of high-pressure Ar plasma induced by femtosecond laser

K. Tsuchida, N. Tsuda, J. Yamada

Dept. of Electronics, Aichi Institute of Technology
1247, Yachigusa Yakusa Toyota 470-0392 Japan

A femtosecond laser is focused at high-pressure Ar gas up to 100atm. An electron density and an electron temperature of are respectively measured at the focal spot. Dense plasma with an electron density of the order of 10^{25} - 10^{26} m^{-3} at focal spot is obtained. The initial electron is produced by multiphoton ionization because the laser intensity at the focal spot reaches 10^{13}W/cm^2. The electron density is calculated by cascade ionization and two-electron three-body recombination. The calculated results under 10atm are lower than the experimental results, because this theoretical calculation does not include effect of multiphoton ionization.

1. Introduction

When a nanosecond excimer laser was focused at high-pressure Ar gas up to 150atm, property of laser-induced plasma had been investigated. The laser intensity at the focal spot reached 10^{11} W/cm^2. An electron density at focal spot reached order of 10^{26} - 10^{27} m^{-3}[1], and an electron temperature reaches 10eV[2].

When high-pressure Ar gas up to 100atm is irradiated by femtosecond laser, electron density and electron temperature of laser induced plasma at the focal spot are respectively measured.

2. Experimental arrangement

The experiment arrangement of electron density measurement is shown in Fig. 1. The titan sapphire femtosecond laser is operated with a single shot operation. A pulse half width is 100fs, a wavelength is 780nm and a laser energy reaches 100mJ. The laser power is controlled by the ND filter. Electron density is measured by Mach-Zender interferometer. The Ar-ion laser is used as a probe laser source. The peak time of interferometric signal is measured. It is difficult to find out a turning point of interferometric signal at which the electron density reaches a maximum. Therefore, the peak electron density is estimated by extrapolating the observed electron density up to the time at which laser pulse is terminated.

3. Experimental results and discussion

Dense plasma with an electron density of the order of 10^{25} - 10^{26} m^{-3} at focal spot is obtained. The theoretical calculation of electron density and experimental results are shown in Fig. 2. The initial electron is produced by multiphoton ionization because the laser intensity at the focal spot reaches 10^{13}W/cm^2. The electron density is calculated by cascade ionization and two-electron three-body recombination. The calculated results under 10atm are lower than the experimental results, because this theoretical calculation does not include effect of multiphoton ionization. We are planning to report the electron temperature at the focal spot in the conference.

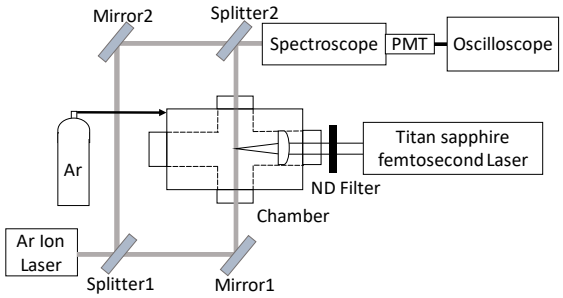

Fig.1 Experimental arrangement

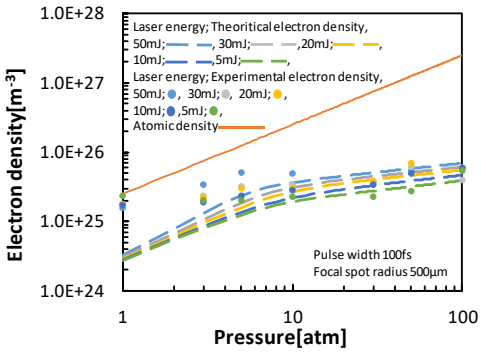

Fig.2 Electron density

4. References

[1] N.Tsuda, Y.Uchida, J.Yamada, Jpn. J. Appl. Phys., Vol. 36, Part 1, No.7B, (1997), pp.4690-4694.

[2] N.Tsuda, J.Yamada, Jpn. J. Appl. Phys., Vol. 38, No.6A, (1999), pp.3712-3715.

Simulating Ignition and Development of Cathode Spots in Vacuum Arcs

H. T. C. Kaufmann[1,2], M. D. Cunha[1,2], M. S. Benilov[1,2], W. Hartmann[3], N. Wenzel[3]

[1] *Departamento de Física, FCEE, Universidade da Madeira, Funchal, Portugal*
[2] *Instituto de Plasmas e Fusão Nuclear, Instituto Superior Técnico, Universidade de Lisboa, Lisboa, Portugal*
[3] *Siemens AG, Corporate Technology, Erlangen, Germany*

A detailed numerical model of individual cathode spots in high-current vacuum arcs is developed with account of all the relevant mechanisms. The spot is ignited and a crater is formed on the cathode surface. A jet of liquid metal in the direction of the plasma is formed and in certain cases the jet may detach from the cathode surface. No microexplosions (thermal runaway) are observed.

1. The model

A detailed numerical model of individual cathode spots in high-current vacuum arcs is developed. The model takes into account an "external" plasma (e.g., a plasma generated for arc triggering, a bulk background plasma, or a plasma cloud left over from a previous spot in the immediate vicinity) and the plasma produced due to ionization of the metal vapor emitted in the spot. Both kinds of plasma provide energy and momentum fluxes over the cathode surface. Ions from the external plasma enter the cathode space-charge sheath with Bohm's velocity and are accelerated in the direction of the cathode. The plasma produced in the spot is described by means of the model [1]. Melting of the cathode metal and motion of the melt are described by means of the heat conduction and Navier-Stokes equations.

2. Results

All phases of life of an individual spot on copper cathodes with microprotrusions and planar cathodes, are investigated. The spot is ignited by the action of the external plasma, provided that this action is sufficiently strong and not too short-lived. The metal in the spot is melted and the melt is accelerated toward the periphery of the spot, the main driving force being the pressure exerted by incident ions. In this way, a crater is formed on the cathode surface (Fig. 1). A jet of liquid metal in the direction of the plasma may be formed as well and in certain cases the jet may detach from the cathode surface (Fig. 1b). Vaporization and/or electron emission, as well as the convective heat transfer, are dominant mechanisms of cooling of the spot and solidification of the metal. No microexplosions (thermal runaway) are observed. The results seem to be in stark contrast with the popular concept of explosive emission.

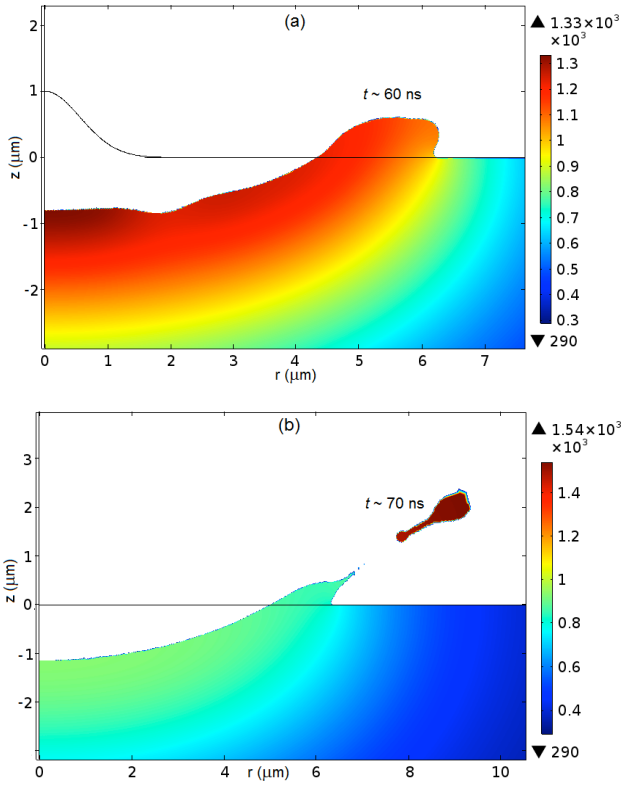

Fig. 1. Results of simulation for (a) cathode with a microprotrusion: solidification of the melt after extinction of the external plasma; and (b) planar cathode: formation of a jet and ejection of material occur after extinction of the external plasma. The colors denote the temperature distribution; the bar in K.

3. Acknowledgements

The work at Universidade da Madeira was supported in part by FCT of Portugal through the project Pest-OE/UID/FIS/50010/2013 and in part by Siemens AG.

4. References

[1] N.A. Almeida, M.S. Benilov, L.G. Benilova, W. Hartmann, N. Wenzel, IEEE Trans. Plasma Sci. 41, 1938 (2013).

Observation of the spin polarization of ^{87}Rb atoms during collisions with oriented metastable helium atoms

Victor Kartoshkin, Sergei Dmitriev, Nikolai Dovator, George Klementiev

Ioffe Institute, Politechnicheskaya 26, 194021 St-Petersburg, Russia

In the experiment on optical orientation in gas discharge we are the first to experimentally observe a magnetic resonance signal of $5^2S_{1/2}$ ^{87}Rb atoms by absorption of light from a helium lamp that was used to optically orient metastable 2^3S_1 ^{4}He atoms. The amplitude of the rubidium signal proved to be almost three orders of magnitude lower than the amplitude of the magnetic resonance of 2^3S_1 He atoms. It is shown that the anomaly in the amplitude ratios of the observed MR signals can be explained by the unidirectional action of two different factors (the presence of a large nuclear spin of rubidium atoms and depolarization of rubidium atoms between collisions).The theoretical explanation of the effect is presented.

1. Introduction

Optical orientation of atoms in gas discharge by polarized radiation is a powerful tool for obtaining spinpolarized atomic particles. Thus obtained polarized atomic particles have been used both to study various physical processes and for practical purposes.

2. General

Upon optical orientation of atoms in a Rb–He mixture under gas discharge conditions, polarization transfer between particles can occur in the following collisions:

$$Rb(5^2S_{1/2})\uparrow + He\,(2^3S_1)\downarrow\downarrow \rightarrow Rb^+(4^1S_0) + He(1^1S_0) + e^-\downarrow, \quad (1)$$

$$Rb(5^2S_{1/2})\uparrow + He\,(2^3S_1)\downarrow\downarrow \leftrightarrow Rb(5^2S_{1/2})\downarrow + He\,(2^3S_1)\downarrow\uparrow, \quad (2)$$

$$Rb(5^2S_{1/2})\uparrow + e^-\downarrow \leftrightarrow Rb(5^2S_{1/2})\downarrow + e^-\uparrow, \quad (3)$$

$$He\,(2^3S_1)\downarrow\downarrow + e^-\uparrow \leftrightarrow He\,(2^3S_1)\downarrow\uparrow + e^-\downarrow, \quad (4)$$

Here, the arrow denotes conventionally the direction of the electron spin of the particle.

As follows from (1)-(4), if the polarization transfer process between colliding particles involves the participation of metastable helium atoms, it is a result of collisional processes of two types-elastic and inelastic collisions. Thus, reactions (2)-(4) correspond to the elastic process, as a result of which the spin is transferred from one particle to the other, with the total momentum being preserved during collisions. At the same time, process (1) is an inelastic process. As a result of the collision of this type, the alkali atom is ionized (the Penning process) at the expense of the internal energy of the metastable helium atom (19.82 eV). As a result of collisions of this kind, the polarization is also transferred to an ensemble of alkali atoms.

Previously in works on optical orientation of atoms in alkali–helium plasma, indirect optical orientation of metastable helium atoms and electrons have been observed in the case in which Rb atoms were optically oriented by resonant radiation of a rubidium lamp. It follows from reactions (1)–(4) that a pattern of this kind should also be observed in the case of an experiment in which metastable helium atoms are optically oriented in the 2^3S_1 state, whereas the polarizations of rubidium atoms in the ground state and of electrons arise as a result of collisions with polarization transfer (by virtue of the symmetry of reactions (1)–(4) with respect to Rb and He atoms). However, experimentally, this has not been detected. This paper describes our successful attempt to observe magnetic resonance signals of polarized Rb.

3. Conclusins

Since the values of the nuclear and electron spins of the rubidium atom differ by tree times, upon the redistribution of the polarization between the electron and nuclear systems, the value of the electron polarization becomes considerably smaller compared to the polarization that was initially transferred upon collision. Subsequently, under the magnetic resonance conditions, the polarization of the hyperfine **F** level of the Rb atom is destroyed. In this case, a change in the electron polarization of the rubidium atom that the helium atom "senses" upon collision will also be small, since, as was noted above, the electron spin of the rubidium is considerably smaller than its nuclear spin. Therefore, as a result of these two processes, the change in the polarization transferred to rubidium will affect helium more than an order of magnitude more weakly than in the case in which both the registration and the pumping are performed using the light from the rubidium lamp.

Enhancement of catalytic activity and stability during PPC for total oxidation of TCE in humid air over Fe-doped cryptomelane.

S. Sultana[1], N. Nuns[2], P.Simon[2], J.-M. Giraudon[2], J.-F. Lamonier[2], N. De Geyter[1], R. Morent[1]

[1] Ghent University, Faculty of Engineering, Department of Applied Physics, Research Unit Plasma Technology, Sint-Pietersnieuwstraat 41, 9000 Ghent, Belgium
[2] Univ. Lille, CNRS, Centrale Lille, ENSCL, Univ. Artois, UMR 8181 – UCCS – Unité de Catalyse et Chimie du Solide, F-59000 Lille, France

Cryptomelane catalyst K-OMS-2 of ideal formula $K(Mn_7^{IV}Mn^{III})O_{16}$ is modified with Fe doping and has been previously used as catalyst in post-plasma catalysis (PPC) in the course of total trichloroethylene (TCE) oxidation in moist air (RH=15%). It was shown that adding iron to cryptomelane allows a better functioning of catalyst, consequently, combining with plasma significantly enhanced the catalytic performances (at 150°C). The issue we want to address herein is the effect of time on stream on the performance of Fe-doped cryptomelane in plasma assisted TCE oxidation. It is found that, next to enhanced catalyst activity, non-thermal plasma (NTP) remarkably improves the stability of the catalyst. A combined X-ray Photoelectron Spectroscopy (XPS) and Time of Flight-Secondary Ion Mass Spectrometry (ToF-SIMS) study on the fresh and used catalysts is in progress.

1. Introduction

The research of innovative technologies for VOC abatement is stimulated to accommodate the new stringent standards in terms of VOC emission. One emerging strategy is the coupling of 2 existing complementary technologies, namely here NTP and heterogeneous catalysis, to get a more efficient process for VOC removal in air.

In this study it is shown that Fe-doped (by co-precipitation: Fe-KOMS-2 and by a successive Fe(OH)x (x = 2; 3) precipitation: Fe/KOMS-2) cryptomelanes with the assistance of NTP are efficient candidates for the abatement of TCE (highly toxic chlorinated VOC) in terms of activity, selectivity and stability.

2. Results and Discussion

Our results shows that, initially Fe doped cryptomelane (solid red and green) (regardless the mode of Fe incorporation) exhibits excellent activity to decompose TCE compared to cryptomelane itself (fig. 1). A maximum obtained value of TCE abatement after 6 min is as follows: Fe-KOMS-2 (75.5%) > Fe/KOMS-2 (48.5) > KOMS-2 (22.6%). However, with prolonged operation time, the abatement of TCE decreases. Clearly, this phenomenon indicates catalyst deactivation either by chlorination or by blocking the active sites. Nonetheless, both undoped and doped catalysts (dashed lines) used in a PPC process remain strongly capable to abate TCE. The TCE removal efficiencies of the PPC processes with Fe/KOMS-2 and KOMS-2 catalysts are not affected by time on stream indicating an excellent catalyst stability. When using the Fe-K-OMS-2 as catalyst, TCE abatement slightly reduces by time on stream, however, it is noteworthy to stress that still a constant abatement of 83% is observed during at least 30 minutes.

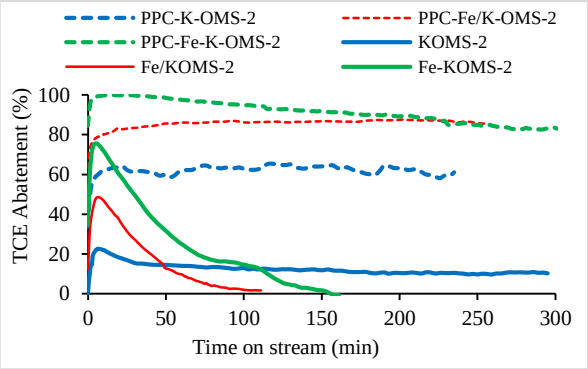

Figure 1: The effect of time on stream on the performance of the catalyst alone (150°C) and PPC (150°C and energy density 60 J/L) towards TCE removal for 3 catalysts.

3. Conclusion

These results prove that the combination of NTP with catalysts not only increases the catalytic activity but also allows to avoid, to some extent, the poisoning of catalytic sites resulting in an enhanced catalyst stability.

In order to better understand the different surface processes occurring in the course of the total TCE oxidation in PPC experiments, a detailed XPS and ToF-SIMS study on the fresh and used catalysts is in progress.

Study of Turbulent Particle Transport in ETG Dominated Plasma of LVPD

Prabhakar Srivastav[1], Rameshwar Singh[1], L. M. Awasthi[1], A.K. Sanyasi[1], R. Singh[2], and P K Kaw[1]

[1] *Institute for Plasma Research, Bhat, Gandhinagar, India-382428*
[2] *WCI Center for Fusion Theory, NFRI, Korea*

In present work we are studied plasma particle flux due to correlated fluctuation of plasma density and potential fluctuation in the background of target plasma of Large Volume Plasma Device (LVPD). The target plasma of LVPD have been characterized as ETG dominated region, by introducing an Electron Energy Filter (EEF). Radial profiles of turbulent particle flux and density - potential cross phase has been measured. It is observed that the net electrostatic flux is negative and is directed radially inward. Turbulent particle flux is predominantly electrostatic in spite of electromagnetic nature of excited turbulence . . The experimental cross phase angle and flux has been compared radially with theoretical counterparts resulting due to the non-adiabatic ion response because of the resonant interaction of the ions with the ETG mode, agrees well within 20%.

1. Introduction

Understanding turbulent plasma transport in magnetized plasma is a subject matter of great significance from the perspective of understanding plasma loss in fusion devices. Although, significant progress has been made in understanding physics of ion thermal transport over the past decade but various aspects of turbulent transport in electron and particle channel remains to be elucidated[1-2].

In this background, Large Volume Plasma Device (LVPD) ($length = 3\,m, dia. = 2\,m$) has successfully demonstrated unambiguous excitation of ETG turbulence, where plasma profiles characterized as $\nabla T_e \neq 0, \nabla n_e \approx 0, \nabla \phi_p \approx 0$ and $\eta_e = \frac{L_n}{L_{T_e}} > \frac{2}{3}$ by introducing an Electron Energy Filter (EEF)[3]. Radial profiles of turbulent particle flux (Γ) and density - potential cross phase,($\theta_{n-\phi}$) has been measured. It is observed that the net electrostatic flux is negative ($\Gamma_{es} \approx -10^{18} m^{-2} - s^{-1}$) and is directed radially inward. Turbulent particle flux is predominantly electrostatic in spite of nature of excited turbulence is electromagnetic ($\beta \approx 0.4$).

The particle flux maximizes when EEF is ON suggesting that the flux is due to ETG driven turbulence. Theoretically, net particle flux results when phase difference is, this agrees well with our observation. Turbulence intensity maximizes roughly at the location where particle flux maximizes.

The experimental cross phase angle and flux has been compared radially with theoretical counterparts resulting due to the non-adiabatic ion response because of the resonant interaction of the ions with the ETG mode, $k_\perp V_{thi} \sim \omega$, agrees well within 20%. Theoretical standpoint suggests that thermo-diffusive turbulent flux radially inward in the background of ETG [4]. Comparison of experimental results with theoretical model suggesting it as a thermo diffusive turbulent particle flux will be present in this conference.

2. References

[1] Coppi B and Spight C, Phys. Rev. Lett. 41 551(1978).

[2] Tang W et al. Phys. Fluids 29 3715 (1986).

[3] S. K. Mattoo, S.K. Singh, L.M. Awasthi, Phys. Rev. Lett. 108 255007(2012)

[4] R Singh, Hogun Jhang and P.H. Diamond, Phys. Plasmas 20 112506 (2013)

Analysis of the K-radiation structure for the determination of HED-plasma parameters and their spatial variations along the line of view

V. Bernshtam, E. Kroupp, A. Starobinets, O. Nedostup, Yu. Zarnitsky, Yu. Kuzminykh, and Y. Maron

Faculty of Physics, Weizmann institute of Science, Rehovot, Israel.

The spectral structures of the Heα and Lyα groups of lines are strongly dependent on the electron temperature in the plasma, on the plasma charge state composition, and the presence of fast electrons. We analyze the effect of the various parameters on the features of the spectral structures, and demonstrate methods to determine electron-temperature gradients in the plasma, and to infer bounds on the electron density. The analysis includes fits to the satellites emitted from plasmas of rather-different electron temperature, and discrimination of satellites due to inner shell excitations and ionizations. The analysis is applied to K-emission data obtained in our neon-puff Z-pinch experiment [1, 2]. As a result, we obtain quantitative estimates of the simultaneous contributions of plasmas of various densities and temperatures to the spectrogram.

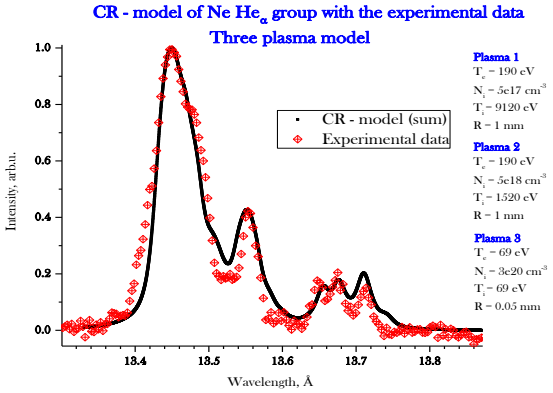

1. References

[1] Eyal Kroupp, Thesis for the degree of Ph.D., April 2004, Faculty of Physics, Weizmann institute of Science, Rehovot, Israel.

[2] E. Kroupp, D. Osin, A. Starobinets, V. Fisher, V. Bernshtam, I. Uschmann, E. Forster, A. Fisher, C. Deeney and Y. Maron, PRL 98, 115001 (2007)

Ecton processes in the generation of picosecond runaway electron beams

G. A. Mesyats [1]

[1] *Lebedev Physical Institute, Moscow, Russia*

The mechanism of the generation of runaway electrons and of the cutoff of their current in a gas discharge is considered. It is shown that the field emission current from the cathode microprotrusions in the discharge is enhanced due to ionization processes occurring in the cathode region. This hastens explosive electron emission, which lasts tens of picoseconds. Thus, the runaway electrons current pulse is similar in nature to the ecton process in a vacuum discharge.

It is well known from the physics of nanosecond pulsed electrical discharges in gases that if the energy acquired by electrons in the electric field is greater than the energy lost by them in collisions, the electrons become running away. In this case, the generation of runaway electrons (REs) is a pulsed process. However, the nature of these RE pulses still remains obscure [1–5].

As shown experimentally, the duration of the RE current pulse in a discharge between stainless steel electrodes in atmospheric air is $2.4\cdot10^{-11}$ s. A nearly triangular voltage pulse of rise time $t_0 = 1.5\cdot10^{-10}$ s and amplitude 160 kV was used. The RE current was equal to several amperes. The leading and trailing edges of the RE pulse, each lasting no more than $2\cdot10^{-11}$ s, are of different nature. We believe that the leading edge is due to the field emission (FE) current from cathode microprotrusions (CMPs) [6]. This current is enhanced due to ionization of the gas until explosive electron emission is initiated as a result of the Joule heating of CMPs during a time determined by the relation $j^2 t_1 = h$, where h is the specific current action for an electrical explosion of the cathode metal and j is the density of the electron current from the CMPs. For copper we have $h=4.1\cdot10^9$ (A·s) /cm^4 [7]; hence, using the Fowler–Nordheim formula, we estimate the FE current density at $t_1=2\cdot10^{-11}$ s as $j=1.4\cdot10^{10}$ A/cm^2. This corresponds to the electric field at the tip of an CMP $E=1.5\cdot10^8$ V/cm. Note that in Ref. 6, the time t_1 is estimated as $t_1=0.11t_0=1.6\cdot10^{-11}$ s. In vacuum, these extreme values of the parameters t_1, j, and E cannot be attained because of the electronic space charge effect [8]. In gases, this effect is not essential or even absent due to that the space charge is neutralized by the gas ions.

The electron emission mechanism changes after EEE: a cathode spot (CS) arises, and the intensity of electron emission from the spot quickly decreases as a result of energy loss. Assuming that a CS cools only due to heat conduction, we have $t_2=i^2/64\pi^2a^2h$, where a is the thermal diffusivity of the cathode metal [7]. For copper we have $a\approx1.2$ cm^2/s; thus, for the RE current i=1A, we obtain $t_2=1.8\cdot10^{-11}$ s.

The formation of RE pulses is similar to the formation of an electron butch (ecton) during a cycle of the CS operation in a vacuum arc [9]. The ecton processes in a vacuum arc take 10^{-9}–10^{-8} s.

Note that in our experiment, we have obtained historically high rates of rise of the electric field at CMPs: ~10^{19} V/(cm·s). Previously, it was supposed that the mechanism of the RE current cutoff is related to the plasma processes occurring in the electrode gap [3, 10]. In our opinion, this mechanism is governed by the emission processes taking place at the cathode. This concept seems to be more realistic in view of the very short times of the generation of runaway electrons and of the cutoff of their current.

1. References

[1] G.A. Mesyats, Yu.I. Bychkov, and V.V. Kremnev, Sov. Fiz. Usp. **15** (1972) 282.

[2] L.P. Babich, T.V. Loiko, and V.A. Tsukerman, Sov. Fiz. Usp. **33** (1990) 521.

[3] V.F. Tarasenko and S.I. Yakovlenko, Phys. Usp. **47** (2004) 887.

[4] G.A. Mesyats, M.I. Yalandin, A.G. Reutova, et al., Plasma Physics Reports **38** (2012) 29.

[5] S. Yatom, A. Shlapakovski, L. Beilin, et al., Plasma Sources Sci. Technol. **25** (2016) 064001.

[6] G.A. Mesyats, JETP Letters **85** (2007) 109.

[7] G.A. Mesyats, Pulsed Power, Kluwer/Plenum (2004).

[8] J.P. Barbour, W.W. Dolan, J.K. Trolan, et al., Phys. Rev. **92** (1953) 45.

[9] G.A. Mesyats, Phys. Usp. **38** (1995) 567.

[10] S.Y. Belomyttsev, I.V. Romanchenko, V.V. Ryzhov, and V.A. Shklyaev, Technical Physics Letters **34** (2008) 367.

Experimental and numerical study of electrical arc movement

J. Quéméneur[1], J-J. Gonzalez[1], P. Freton[1], P. Joyeux[2]

[1] *Université de Toulouse; UPS, CNRS, INPT; LAPLACE (Laboratoire Plasma et Conversion d'Energie); 118 route de Narbonne, F-31062 Toulouse cedex 9, France*
[2] *Hager Electro SAS, 132 boulevard d'Europe, BP3, 67210 Obernai, France*

The movement of an electrical arc between two parallel arc runners is studied by numerical and experimental approaches. The measurement setup and two methods to model the arc roots motion are presented alongside with a tool to determine the position of the arc using its light emission. The experiment consists in a simplified low-voltage circuit breaker (LVCB) chamber where voltage, current, pressure measurements and high-speed imaging are performed. 3-D computational fluid dynamic model based on the Fluent software is developed for the simulation of the arc in the same configuration as the experiment. Comparison between tests and modelling are presented.

1. Introduction

Electrical arc motion is a significant issue for several industrial applications such as breaking arcs, plasma torches, welding or in-flight lightning strike.

In LVCB the arc must be moved quickly from the opening contact to the extinction chamber. This improvement is mainly made by long empirical developments. Hence the industry is calling for predictive models. Here two numerical methods to simulate the arc movement are presented and compared to experimental results.

2. Experimental setup

LVCB have a complex design. For an easier study a rectangular arc chamber with two parallel iron electrodes is used. One of the lateral walls is transparent to allow high-speed imaging. The discharge can be ignited by contact opening or by a fuse wire. In order to get rid of the opening speed parameters the fuse wire ignition is used. The breaking current is a 50Hz sine wave up to 10kA.

3. Numerical model

A magneto-hydrodynamic model is developed to describe the plasma [1] and two different methods are used to calculate the arc motion:

In the first method named "Global Current Resolution Method" (GCRM), current density and heat transfer between the plasma and the metallic electrodes are solved neglecting the sheath mechanisms. This is an easy method to implement but it requires advanced calculation algorithms due to a strong difference of electrical conductivity between the two mediums. Therefore, calculation time is high.

In the second method, named "Mean Electrical Conductivity Method" (MECM), classical boundary conditions for anode and cathode roots [2] are used and applied where the electrical neighbouring conductivity of the plasma is the highest. Two arc roots can be specified on the same electrode.

4. Preliminary results & perspectives

A comparison between numerical and experimental results for the arc movement is presented Fig. 1. The good agreement validates the two methods used.

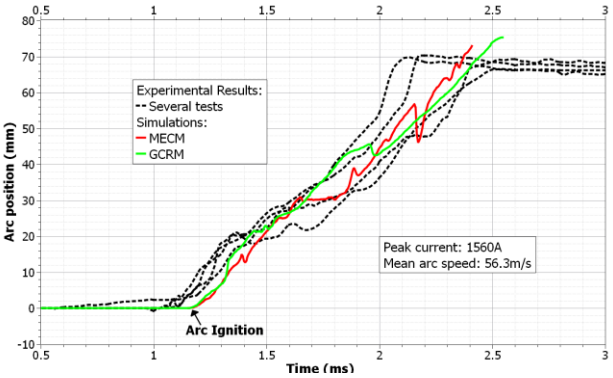

Fig.1: Experimental and simulated arc motion

With such tools we are able to investigate the parameters influencing the arc movement. To improve our model, description of the anodic [3] and cathodic [4] sheaths could be developed in order to allow a better description of arc commutation and calculation of the arc voltage.

5. References

[1] A. Gleizes, J-J. Gonzalez, P. Freton, J. Phys. D: Appl. Phys. **38** (2005) R153-183

[2] P. Freton, J-J. Gonzalez, A. Gleizes, J. Phys. D : Appl. Phys. **33** (2000) pp. 2442-2452

[3] F.Lago, J-J. Gonzalez, P. Freton, A. Gleizes, J. Phys. D: Appl. Phys. **37** (2004) 883-897

[4] M.S. Benilov, J. Phys. D : Appl. Phys. **41** (2008) 144001

Optimizing the CO_2 conversion efficiency in a low-pressure pulsed microwave plasma source

N. Britun[1], T. Godfroid[2], T. Silva[3], and R. Snyders[1,2]

[1] *Chimie des Interactions Plasma-Surface, Universite de Mons, Mons, Belgium*
[2] *Materia Nova Research Center, Mons, Belgium*
[3] *Instituto de Plasmas e Fusão Nuclear, Instituto Superior Técnico, Universidade de Lisboa, Lisboa, Portugal*

The CO_2 decomposition process in a pulsed 2.45 GHz microwave surfaguide discharge has been studied. The CO_2 conversion efficiency is found to be mainly affected by the plasma pulse repetition rate (at fixed applied power), along with the other discharge parameters such as the gas flow rate, residence time, etc. The electron and gas temperatures have been additionally studied using spectroscopic methods. A several time increase in the CO_2 conversion/energy efficiency points out on a crucial role of the pulsed plasma regime for better CO_2 conversion. The found effects are explained by the relevant energy relaxation mechanisms in the discharge, such as the electron-vibrational, vibrational-vibrational, and vibrational-translational ones.

1. Introduction

In spite of the numerous works devoted to plasma-based greenhouse gas conversion, related to microwave (MW) plasma [1], dielectric barrier discharge (DBD) [2], gliding arc plasma (GAP) [3], as well as those involving plasma catalysis, the effects of CO_2 conversion in the pulsed discharges are still far from being understood clearly. So far the beneficial role of plasma power modulation has been only demonstrated in the DBD case [4]. The present work studies the power modulation effect in MW surfaguide discharge, as a promising candidate for plasma-assisted CO_2 conversion.

2. Experimental

A surfaguide-type pulsed microwave plasma source has been used. The plasma was sustained by the electromagnetic waves with the filling frequency of 2.45 GHz, and modulated by nearly rectangular pulses with the repetition rate ranging from 0.01 to 2.5 kHz. The pulse duty ratio was mainly fixed at 50%. The discharge has been sustained in a quartz tube (14 mm in diameter and 31 cm long) in which the gas flow was regulated by digital mass flow controllers. The quartz tube has been cooled down by 10 °C flow of Si oil. More details are available in [1,5]. The optical emission actinometry [1] and two-photon absorption laser induced fluorescence (TALIF) techniques were used for monitoring the CO_2 conversion efficiency in our case [5].

3. Main results

In this work it was shown that the CO_2 conversion efficiency depends dramatically on the plasma pulse repetition rate. Up to a fourfold improvement in the CO production in the post-discharge (and thus in the CO_2 conversion rate) has been detected (see Fig. 1).

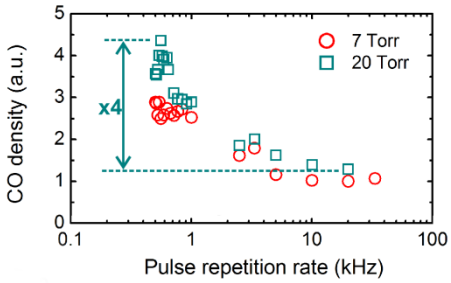

Fig. 1. Relative CO density in the post-discharge as a function of plasma pulse repetition rate.

It is also shown that the CO_2 conversion depends on the molecule residence time and the gas pressure. The electron temperature determined based on the Ar line ratio shows rather minor variations in the studied pulse frequency range, leading us to a conclusion that the vibrational energy exchange is the main reason for the observed effects. The estimates made for the electron-vibrational (e-V), vibrational-vibrational (V-V) as well as vibrational-translational (V-T) energy relaxation time point out on a primary role of vibrational excitation for CO_2 decomposition at long plasma pulse durations (low rep. rates), as well as its contribution to the gas heating via the V-T process. At the same time at high repetition rates these processes are less efficient due to shorter plasma pulse duration.

4. References

[1]. T. Silva, N. Britun, T. Godfroid, R. Snyders, Plasma Sources Sci. Technol. **23**, 25009 (2014).
[2]. S. Mahammadunnisa, E. L. Reddy, D. Ray, et al., Int. J. Greenh. Gas Control **16**, 361 (2013).
[3]. T. Nunnally, K. Gutsol, et al., J. Phys. D. Appl. Phys. **44**, 274009 (2011).
[4]. A. Ozkan, T. Dufour, et al., Plasma Sources Sci. Technol. **25**, 55005 (2016).
[5]. T. Silva, N. Britun, et al. Plasma Process. Polym. DOI: 10.1002/ppap.201600103 (2016).

Decay of radiation of the sliding surface discharge and the combined volume discharge

A. Kuznetsov[1], I. Mursenkova[1], I. Znamenskaya[1]

[1] *Faculty of Physics, Lomonosov Moscow State University, Leninskie Gory, 119991 Moscow,Russia*

The radiation decay of the sliding surface discharge and of the combined volume discharge with plasma electrodes lasting hundreds of nanoseconds in air have been studied experimentally by means of time resolved nanosecond ICCD imaging and streak diagnostics of the discharges development. Investigations were carried out at a voltage of 20-30 kV at air pressure of 2-160 torr. Analysis reveals the differences in the character of the radiation decay of two types of discharges. The radiation decay time of volume discharge decreases with increasing pressure at pressure of 10-100 torr. The decay time of the diffuse channels of sliding surface discharge is almost constant at pressure below 60 torr and increases at higher pressures.

1. Experimental setup and measurements

High efficiency contribution to gas heating during nanosecond discharge is used to control high-speed flow characteristics in aerodynamics [1-2]. In this work, the features of radiation of the sliding surface discharge [2] and the combined volume discharge [3] are investigated with nanosecond resolution using High-speed ICCD cameras of spectral range 380-880 nm (BIFO Company).

The experiments were conducted in the discharge chamber with rectangular channel [2, 3]. Sliding surface discharge of 30×100 mm^2 area consists of diffuse and bright channels moving over a dielectric surface [2]. Combined volume discharge occurs between two sliding surface discharges, which form two plasma electrodes at 24 mm distance between them. 20-30 kV voltage pulses initiated the discharges. The discharge current pulse had amplitude of ~1 kA and duration of ~200 ns. The radiation spectra were recorded using AVASpec-2048FT spectrometer in the range 174-1100 nm.

2. Results and discussion

The second positive system of molecular nitrogen (C→B) determines the main part of the spectra of the discharges. Volume discharge reveals the diffusive uniform radiation with duration of ~200 ns. Duration of diffuse part of sliding surface discharge close to 200 ns. The radiation of the bright channels lasts several times longer (Fig. 1) and increases with increasing pressure.

We have determined the decay time of radiation by processing the dependence of radiation intensity on time for two types of discharges (Fig. 1). Decay times of the radiation of volume discharge and diffuse radiation of the sliding surface discharge are close when pressure less than 100 Tor and have the value of ~40 ns. The radiation decay time of volume discharge decreases weakly when the pressure is rising. The decay time of the diffuse channels of the surface sliding discharge remains nearly constant when pressure is lower than 60 torr but increases significantly at higher pressures. This can be due to kinetic processes that lead to a population of the $C^3\Pi_u$ state of the nitrogen molecule.

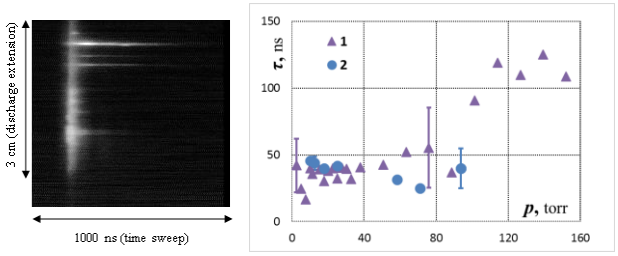

Fig. 1. Streak image of sliding surface discharge at pressure 76 torr (left); the decay time of the diffuse channels of surface sliding discharge (1) and the decay time of the volume discharge (2) (right). Voltage is 25 kV.

3. Acknowledgements

Russian Foundation for Basic Research supported this study, project No. 14-08-00777.

4. References

[1] D. Bayoda, N. Benard, and E. Moreau. J. Appl. Phys. (2015) 118.

[2] I.A. Znamenskaya, D.F. Latfullin, A.E. Lutsky, I.V. Mursenkova, Tech. Phys. Lett. 36 (2010) 795.

[3] I. Mursenkova, I. Znamenskaya, I. Ostapenko. Proc. of 31 International Conference on Phenomena in Ionized Gases (2013) 75_1.

Topic number: 18

Ball lightning as a key for the solution of an energy problem by means of muon-catalyzed fusion

A.G. Oreshko[1], A.A. Oreshko[2], T.B. Mavlyudov[1]

[1] *Moscow Aviation Institute, National Aerospace Research University, Moscow, Russia*
[2] *All-Russian Scientific Research Institute of Physical -Technical and Radiotechnical Measurements, Mendeleevo, Moscow region, Russia*

The main aim of the work is to develop a method for solving the problem of energy by using muons that are obtained by reacting of a ball lightning with a dense medium. On basis of experiments on the interaction of a ball lightning with a dense medium it was shown that in this case there is a generation of muons and muon neutrino, i.e. cascade process is realized, which is similar to the process in extensive air showers. The usage of ball lightning as a source of muons for muon-catalyzed fusion in reactors will improve conditions of operation and allow carrying out the nuclear fusion reaction at a lower temperature without insoluble problems which are characteristic of traditional methods of fusion.

As is known traditional methods of receiving of nuclear fusion reactions have a number of insoluble problems [1]. One of the main problems that have no solutions in the reactors with magnetic confinement is anomalous plasma transport on chamber walls. Anomalous transport of plasma is caused by an instability due to the charge separation and the formation of electrical domains – so-called domain instability [2]. Domain instability is a characteristic state of plasma in the presence of strong fields and high temperature. There is no methods in Nature for suppressing this instability. Therefore it is necessary to look for more simple and more efficient methods for successful solving the problem of nuclear fusion.

The analysis shows that the energy problem can be solved on the basis of the muon-catalyzed fusion. The concept of muonic catalytic fusion is one of most promising approaches to nuclear fusion. The only obstacle for muon-catalyzed fusion realization is the high cost of muons in existing devices for their obtaining. Existing giant sources of muons require considerable quantity of energy to produce muons. In the experiments it was established that the ball lightning has extremely high penetrating ability, i.e. phenomena of superpassability [3]. This phenomenon may be explained by multistage generation of particles due to interaction of high-energy protons of external shell of the ball lightning with dense medium [4]. An interaction of protons with atoms or molecules of dense medium causes appearance of neutral and charged pions. The decay of the pions is accompanied by appearance of either negative muons and muon antineutrinos or positive muons and muon neutrinos. The generation of muons at interaction of the ball lightning with dense medium makes it possible to use of them for nuclear fusion purposes. Only the cycle associated with the usage of negative muons represents the interest.

The analysis shows that the cheapest source of muons can be a ball lightning that interacts with the dense low temperature deuterium-tritium plasma. An electric power of facility to produce the ball lightnings "Prometheus" including system of control is equal to 5.4 kW, and its square is 6 m^2. An interesting application is a periodic injection of ball lightnings into the chamber of the reactor of nuclear fu-sion which was preliminary filled of plasma. The proposed method of nuclear fusion has a number of significant advantages compared to the existing methods. The method is based on real data obtained by the authors in the experiments on generation of ball lightnings. The suggested method of solution of the fusion problem requires an experimental validation. The cost of creating the demo version of nuclear fusion reactor based on muon catalysis is symbolic. A physical model of the reactor was created. Experiments were performed in water steam.

May be we should understand the expression P.L.Kapitza "Ball lightning is a small window in the great unknown world" as a hint to the effect that the ball lightning is a unique key to the solution of the problem of obtaining clean energy.

References

[1] G.J.Linhart, Quo vadis fusion? Nukleonika, **54** (4) (2009) 305-309.

[2] A.G.Oreshko, Proc. 41st EPS Conf. on Plasma Physics, Berlin (2014), P2.144.

[3] A.G.Oreshko, Journ.of Plasma Physics, **71** (3) (2015) 18 p.

[4] A.G.Oreshko, A.A.Oreshko, Proc. 43th EPS Conf. on Plasma Physics, Leuven (2016), P2.110 .

Negative ion mobility and ion-molecule reactions in O_2 with a trace amount of moisture

Y. Okuyama[1], K. Arai[2], S. Suzuki[2], H. Itoh[2]

[1] *National Institute of Technology, Tomakomai College, Hokkaido, Japan*
[2] *Chiba Institute of Technology, Chiba, Japan*

The mobility of negative ions was measured in O_2 while varying the H_2O concentration using a high-pressure ion drift tube with a point-plane gap acts as a negative ion detector. The H_2O concentration was monitored during the mobility measurement with a trace moisture analyser. Decreasing mobility were observed with increasing the H_2O concentration between 15 to 17000 ppb as 2.39, 2.31, 2.21 and 2.15 $cm^2/V{\cdot}s$. The mobility 2.39 $cm^2/V{\cdot}s$ is considered as O_4^-, and then O_4^- was converted to $O_2^-{\cdot}(H_2O)$, $O_2^-{\cdot}(H_2O)_2$ and $O_2^-{\cdot}(H_2O)_3$ by ion-molecule reactions. Thus, decreasing mobility could be interpreted as the variations of ion species by ion-molecule reactions which were reproduced by solving the continue equations using the modified rate coefficients.

1. Introduction

We have been measured negative ion mobility in O_2 at high-pressures using a high-pressure ion drift tube with a point-plate gap acts as an ion detector [1, 2]. At such high-pressures, the negative ion mobility is strongly affected by impurities although the concentrations of impurities are lower than a few ppm. In this paper, we describe the results of ion mobility measurement and ion-molecule reactions in O_2 with a trace amount of moisture.

2. Experimental set up

The measurement method used for negative ion mobility had already been described in previous papers [1, 2]. During the measurements, H_2O concentrations were monitored by a trace moisture analyzer (HALO-H_2O: Tiger Optics) whose principle is based on a cavity ring-down spectroscopy [3] using a light of which wave length is 1392.53 nm.

3. Results and discussions

Figure 1 shows the obtained mobilities and the corresponding relative intensities of ions calculated using the rate coefficients in zero dimension. The mobility 2.39 $cm^2/V{\cdot}s$ was observed in the range of H_2O concentration between 15 to 450 ppb which is considered as O_4^-. After that, the mobility is decreased to 2.31, 2.21 $cm^2/V{\cdot}s$ considered as $O_2^-{\cdot}(H_2O)$ and $O_2^-{\cdot}(H_2O)_2$ in the H_2O concentration 450 to 4600, 4600 to 17000 ppb, respectively. The mobility 2.15 $cm^2/V{\cdot}s$ considered as $O_2^-{\cdot}(H_2O)_3$ is also observed at the range of H_2O concentration between 12500 to 17000 ppb.

We considered the sequential progress of negative ions in O_2 with a little amount of moisture as shown in fig. 2. O_2^- having a mobility 2.17 $cm^2/V{\cdot}s$ [4] was never observed in our experiment because measurements were carried out around atmospheric pressure. In fig. 1 (b), the rate coefficients k_1, k_2 and k_3 reported by others [5-8] were used for the calculation. In contrast, other rate coefficients k_4, k_5 and k_6 were modified to fit in experiments because some of them were not sufficiently to convince us. The result is shown in fig.1 (b) as an example.

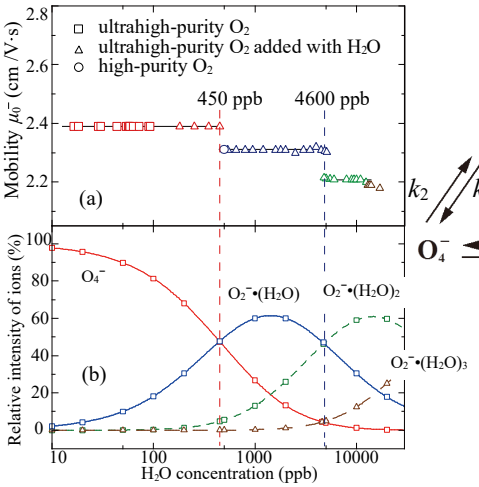

Fig. 1 Observed mobilities and their relative ion intensities against H_2O concentration.

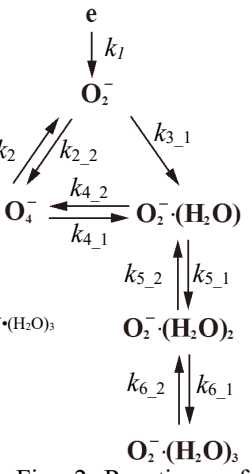

Fig. 2 Reactions of ions in O_2 with H_2O.

Acknowledgement

This work was supported by JSPS KAKENHI GRANT Number 16K18065.

4. References

[1] Y. Okuyama et al., J. Phys. D, 45, (2012) 195202
[2] Y. Okuyama et al., IEEJ Trans. FM, 133, (2013) 578−584 (in Japanese)
[3] H. Abe and K. Yamada, Sens. Actuators A, 165 (2011) 230-238
[4] R. M. Snuggs et al., Phys. Rev. A, 3 (1971) 477
[5] J. L. Pack and A. V. Phelps, J Chem. Phys, 44, 1870 -1883 (1966)
[6] L G McKnight and J Sawina, Phys. Rev. A, 4, 1043 (1971)
[7] J. D. Payzant and P. Kebarle, J. Chem. Phys, 56, 3482 - 3487 (1972)
[8] D. A. Parkes, Trans. Faraday Soc, 67, 711 (1971)

Comparative study on atmospheric-pressure plasma nitriding processes with pulsed-arc jet and barrier discharge

R. Ichiki[1], K. Kitamura[1], A. Maeda[1], R. Sannomiya[1], K. Yamanouchi[1], S. Chiba[1], M. Kono[1]
T. Onomoto[2], S. Akamine[1], S. Kanazawa[1]

[1] *Faculty of Engineering, Oita University, Oita, Japan*
[2] *Fukuoka Industrial Technology Center, Kitakyushu, Japan*

We have demonstrated nitrogen atom diffusion into steel surface using the atmospheric-pressure the atmospheric-pressure pulsed-arc (PA) jet and the dielectric barrier discharge (DBD). The elementary processes occurring in the two kinds of atmospheric-pressure plasmas proved to differ considerably; that is, the PA jet nitriding involves NH radicals as key radicals, while NH is not essential in the DBD nitriding.

1. Introduction

Plasma nitriding is one of the case hardening technologies for upgrading the mechanical properties of steel surface by nitrogen atom (N) diffusion. In industry, low-pressure plasmas are utilized for plasma nitriding. On the other hand, our group has developed atmospheric pressure plasma methods for nitriding to offer novel material processing to industry. For the present, we achieved nitriding with the pulsed-arc (PA) plasma jet [1] and the dielectric barrier discharge (DBD) [2]. In this paper, we discuss the chemical and physical differences of the two nitriding methods to understand the elementary process and technological potential of them.

2. Experimental

2.1. PA jet nitriding

The pulsed-arc is ignited inside the cylindrical electrode, where the pulsed voltage of 5 kV and several μs is applied to the inner electrode at 21 kpps. The operating gas is N_2/H_2 mixture at the flow ratio of 99:1. The afterglow (jet plume) is sprayed onto the steel sample at 530°C.

2.2. DBD nitriding

One of the planer electrodes is the sample electrode to be treated. The opposite electrode is fitted with an alumina barrier of 2.5 mm in thickness. The discharge gap is 1 mm. The ac voltage of 5.7 kV and 12.8 kHz is applied to the sample electrode to ignite DBD. The operating gas is N_2/H_2 mixture at the flow ratio of 9:1. The treatment temperature is 530°C.

3. Results and discussions

We have achieved to diffuse N atoms into steel surfaces by the both experimental procedures. Here, the thickness of the hardened layer, several 10 μm, is similar to the conventional nitriding of industrial use.

Fig. 1 shows the comparison of optical emission spectra from the two plasmas during the treatment. In the PA jet, the emission of NH is dominant, implying that NH radicals are actively produced. Besides, the NH emission is found to decrease with increasing H_2 addition to the operating gas. Moreover, we demonstrated that the diffusion amount of N into the steel is decreased by increasing H_2. These facts indicates that NH is the key radical in the PA jet nitriding.

On the other hand, we see that in the DBD, no NH peak appears, while N_2 2nd positive band is dominant. In addition, we have succeeded in DBD nitriding even without H_2 addition. These facts indicate that NH is not essential in the DBD nitriding. In addition, the N atom emission is not observed, implying that the active production of N is unlikely. We regard the dissociative adsorption of excited N_2 as a possible scenario of N diffusion.

This work was supported by JSPS KAKENHI Grant Number 15K17482.

4. References

[1] H. Nagamatsu *et al.*, Surf. Coat. Technol. **225** (2013) 26.
[2] K. Kitamura *et al.*, Proc. 21st Intl. Conf. Gas Discharge their Appl. (2016) 429.

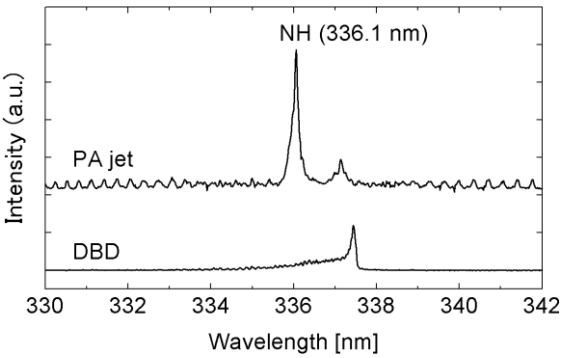

Fig. 1 Optical emission spectra of plasmas.

Characterization of carbon films by microwave-plasma assisted chemical vapour deposition in open-air system

H. Yagi[1*], S. Yudate[2], H. Motomura[2], M. Jinno[2]

[1]*Department of Industrial Innovation, Faculty of Collaborative Regional Innovation, Ehime University,*
[2]*Department of Electrical and Electronic Engineering, Faculty of Engineering, Ehime University,*
3 Bunkyo, Matsuyama, 7908577, Japan
(*) yagi@dpc.ehime-u.ac.jp

Reactive plasma has been generated under the open air condition by microwave excitation of a downstream flowing mixture of hydrogen and methane. The plasma torch having the shielding gas flow was employed to eliminate the effect from the atmospheric gas such as nitrogen and oxygen. The carbon films were deposited in the methane concentration about 10% (CH_4/H_2). The films have DLC properties from the Raman spectra. The intensity ratio of bonding energy $sp^2/(sp^2+sp^3)$ was 0.7. The films were smooth, flat and hard.

1. Introduction

In recent days, plasma phenomena and its process under atmospheric pressure have been widely researched. The plasma process under atmospheric pressure will be high in deposition/etching rate in spite of its controllability of plasma. If the process under atmospheric pressure realizes in "the open-air", the processing system becomes simple and the controllability of substrates such as the processing area and the handling of substrates, and also the processing rate becomes high in proportion to the pressure. But there are not enough data about the films deposited in the open-air condition. We researched about the influences of the atmospheric gas and the atmospheric pressure as the high pressure CVD process to the deposited films.

2. Instructions

2.1. Design of Torch

Experimental setup employed in this study is schematically shown in fig.1. Microwave power is supplied by a semiconductor generator at 2.45 GHz. The microwave is guided to the co-axial waveguide by a rectangular-to-coaxial line transition. The process gase mixed with hydrogen and methane were supplied through the gap between outer electrode and inner electrode to the end of nozzle. The plasma is torched between the end of inner electrode and the substrate caused by the high electric field between them. The shield gas of helium was supplied to separate between the plasma and the atmosphere.

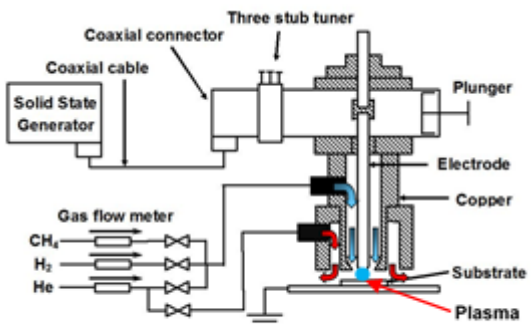

Fig.1 Apparatus of the plasma torch with the flow of shield gas.

2.2 Experimental conditions

Experimental conditions employed in the present study were as follows. The flow rate of CH_4, H_2 and He were 15 sccm, 150 sccm and 165 sccm, respectively. The incident power is 50 W, and the processing time was 10 min. The silicon and stainless steel substrates were used for the deposition, and the gap between the nozzle and the substrate was 1.0 mm.

3. Results

Fig.2 shows the Cls X-ray Photoelectron Spectrum of the film deposited on the stainless steel (JIS:SUS304). The intensity ratio of bonding energy $sp^2/(sp^2+sp^3)$ is about 0.7. The profile corresponding to C=O bond is found in the figure.

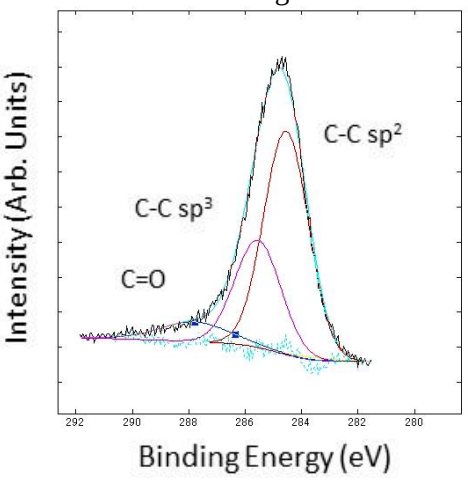

Fig.2 The Cls XPS of the film deposited on the stainless steel.

Ignition behaviour of atmospheric-pressure dielectric barrier discharges in argon with admixtures of hexamethyldisiloxane and tetramethylsilane

M. M. Becker[1], J. Philipp[2], A. K. Czerny[2], C.-P. Klages[2], and D. Loffhagen[1]

[1] *INP Greifswald, Felix-Hausdorff-Str. 2, 17489 Greifswald, Germany*
[2] *TU Braunschweig, Institut für Oberflächentechnik, Bienroder Weg 54 E, 38108 Braunschweig, Germany*

The impact of small admixtures of the precursors hexamethyldisiloxane and tetramethylsilane on the ignition behaviour of dielectric barrier discharges in argon at atmospheric pressure has been analysed by means of a time-dependent, spatially one-dimensional fluid model and measurements. A drop of the ignition voltage by about 60 % is found when adding up to 200 ppm of precursor gas to argon. Very good agreement between measured data and modelling results is obtained when assuming that 30 % of the collisions between excited argon atoms and precursor gas lead to Penning ionization.

Dielectric barrier discharges (DBD) represent the main approach for plasma-enhanced chemical vapour deposition (PECVD) processes and facilitate the scale-up for industrial processing. Silicon-organic coatings can be achieved by mixing precursors like hexamethyldisiloxane (HMDSO) or tetramethylsilane (TMS) to the carrier gas used by the DBD [1]. A detailed understanding of the impact of the precursor admixtures on the discharge properties like ignition voltage and energy consumption is highly important for DBD-based PECVD processing. Here, a fluid modelling approach is combined with measurements to analyse the impact of small admixtures of HMDSO and TMS to argon on the ignition behaviour of the DBD.

The investigations were performed by means of the time-dependent, spatially one-dimensional fluid-Poisson model for argon DBD reported in [2], which was extended by an appropriate reaction kinetics for HMDSO and TMS, respectively. The numerical studies are based on the experimental conditions described in [1]. A symmetric plane-parallel electrode configuration was used with a thickness of the dielectrics of 2 mm and a gap width of 1 mm. The discharge is driven by a sinusoidal voltage supply at 86.2 kHz. The ignition voltage was determined by a stepwise increase of the applied voltage until the discharge was ignited and covered the entire electrode area of 8 cm^2.

Results of the ignition voltage in dependence on the precursor concentration x are shown in figure 1. It has been found experimentally that the ignition voltage U_i of the considered argon DBD decreases by about 60 % with the admixture of HMDSO and TMS, respectively, in the range from 0 to 200 ppm. The modelling-based analysis of the ionization budget shows that the impact of Penning ionization processes mainly causes the observed decrease of U_i. Very good agreement between measurements and numerical results was obtained using rate coefficients for the collisions of precursor gas with excited argon atoms based on the works of Jauberteau *et al.* [3,4] and a fraction of 30 % of these collision processes leading to Penning ionization.

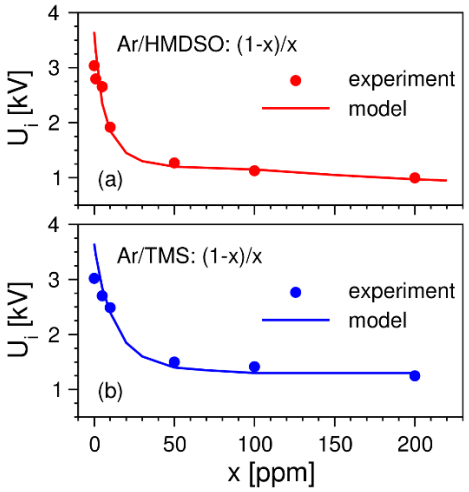

Figure 1: Ignition voltage in atmospheric-pressure argon DBD with admixtures of HMDSO (a) and TMS (b).

Acknowledgment

The work was supported by the German Research Foundation under grants LO 623/3-1 and KL 1096/23-1 as well as in the framework of the Collaborative Research Centre Transregio 24 “Fundamentals of Complex Plasmas”.

References

[1] J. Philipp *et al.*, Plasma Process. Polym. **13** (2016) 509–520.

[2] M. M. Becker *et al.*, J. Phys. D: Appl. Phys. **46** (2013) 355203.

[3] J. L. Jauberteau *et al.*, J. Phys. Chem. A **116** (2012) 8840−8850.

[4] J. L. Jauberteau *et al.*, Chem. Phys. Lett. **327** (2000) 351–358.

Water treatment using micro-bubble assisted three dimensionally integrated micro solution plasma

Y. Ishida, H. Masunaga, T. Shirafuji

Department of Physical Electronics and Informatics, Osaka City University, Osaka, Japan

We have performed water treatment for decomposing organic contaminants in water using micro-bubble assisted three-dimensionally integrated micro solution plasma (3D IMSP). The original 3D IMSP reactor without micro-bubble assistance cannot generate plasma when water to be treated has electrical conductivity of 200 μS/cm or higher. The novel micro-bubble assisted 3D IMSP reactor, on the other hand, can generate plasma in the water with electrical conductivity up to 500 μS/cm. Ignition and sustain voltages for plasma are also reduced. These results indicate that micro-bubble assistance brings about low-power consumption and extension of application area in water treatment by 3D IMSP.

1. Introduction

Plasma in liquid has attracted much attention because of their possible applications for solving water-related environmental issues. We have previously proposed a novel three-dimensionally integrated micro solution plasma (3D IMSP) reactor, which can generate a large amount of microplasmas in a porous dielectric material filled with a gas/liquid mixed medium [1]. However, 3D IMSP is not effective for the treatment of an aqueous solution with a high electrical conductivity [2], which was one of disadvantages of 3D IMSP.

In this work, we have introduced micro bubbles into the 3D IMSP reactor in order to treat water with higher electrical conductivity.

2. Experimental setup

We employed micro-bubble generator (Hack UFB, FB11) as a substitute of the liquid circulation pump used in our previous 3D IMSP reactor [1]. The aqueous solutions used for this experiment had electrical conductivities of 1, 10, 100, 200, 500, and 1000 μS/cm, which were prepared by mixing KCl with deionized water.

3. Results and discussion

Figure 1 shows effects of micro-bubble assistance on the operation of 3D IMSP. We can confirm that the micro-bubble assisted 3D IMSP reactor can generate plasma in the aqueous solution with electrical conductivity up to 500 μS/cm, while conventional 3D IMSP reactor cannot. Furthermore, micro-bubble assistance has an effect of reducing the ignition and sustain voltages of 3D IMSP as shown in Fig. 2, which means that we can suppress energy consumption for the water treatment by micro-bubble assisted 3D IMSP.

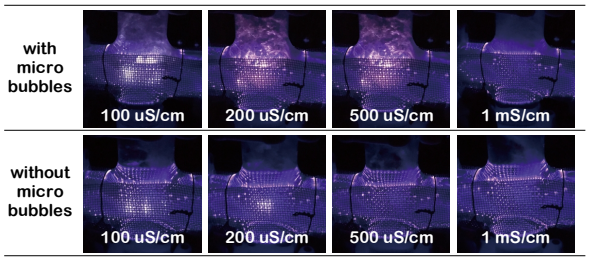

Fig. 1 Effects of micro-bubble assistance on the operation of 3D IMSP.

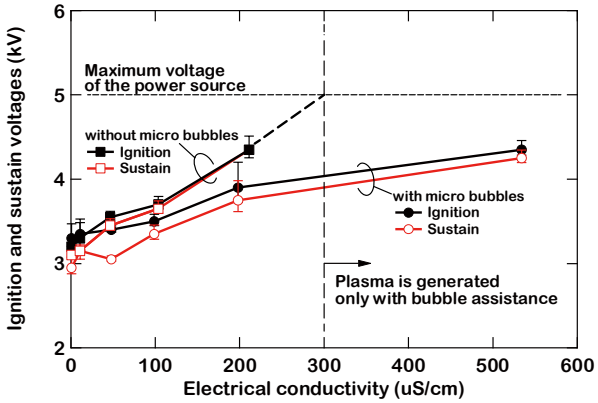

Fig. 2 Effects of micro-bubble assistance on the ignition and sustain voltages of 3D IMSP.

Acknowledgement

This work was partly supported by JSPS MEXT KAKENHI Grant Numbers 15H03585 and 15K13391.

References

[1] T. Shirafuji and Y. Himeno, Jpn. J. Appl. Phys. **52**, 11NE03 (2013).

[2] T. Shirafuji, J. Ueda, A. Nakamura, S. -P. Cho, N. Saito, and O. Takai, Jpn. J. Appl. Phys. **52**, 126202 (2013).

Solution-plasma synthesis of a gold-nanoparticle-containing polymer membrane on aqueous solution

Y. Nakamura[1], S. Azuma[1], T. Isshiki[2], T. Shirafuji[1]

[1] *Department of Physical Electronics and Informatics, Osaka City University, Osaka, Japan*
[2] *Department of Electronics and Systems, Kyoto Institute of Technology, Kyoto, Japan*

We have generated dielectric barrier discharge (DBD) of argon gas on $HAuCl_4$ aqueous solution for synthesizing gold nanoparticles. If we add gelatine to $HAuCl_4$ aqueous solution, we obtain a wine-red coloured membrane on the aqueous solution by the DBD. The membrane has fibrous structure composed of polymerized gelatine, which has been confirmed through optical microscope observation and infrared absorption spectroscopy of the membrane. In addition, we have confirmed that dispersed gold nanoparticles are incorporated in the membrane, which has been confirmed through energy dispersive X-ray spectroscopy of the membrane and transmission electron microscope observation of the edge of the membrane. Gold nanoparticles in the membrane are dense and have fairly uniform size distribution depending on the position in the membrane.

1. Introduction

Solution plasma can be used for various applications including nanoparticle synthesis and liquid treatment [1]. However, there are few reports on thin film formation using solution plasma [2]. In this work, we report that we can synthesize a free-standing and gold-nanoparticle-containing gelatine membrane by using dielectric barrier discharge (DBD) on aqueous solution.

2. Experimental setup

The aqueous solution was $HAuCl_4$ (0.3 mM) aqueous solution with gelatine. Gas gap was 2 mm. Applied voltage was bipolar pulse voltage (amplitude 4 kV, frequency 40 kHz, pulse width 4 μs). Typical discharge time was 10 min. Discharge gas was argon**.**

3. Results and discussion

A wine-red coloured membrane is formed on the surface of aqueous solution in contact with DBD as shown in Fig. 1. Infrared absorption spectra of the membrane and energy dispersive X-ray spectra have indicated that the membrane is made of polymerized gelatine and gold. Figure 2 shows a transmission electron microscope (TEM) image of the sample

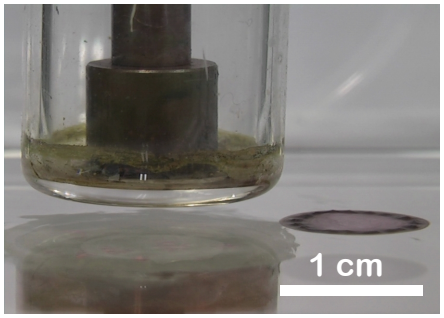

Fig. 1 The membrane formed on the $HAuCl_4$/gelatine aqueous solution by Ar DBD exposure.

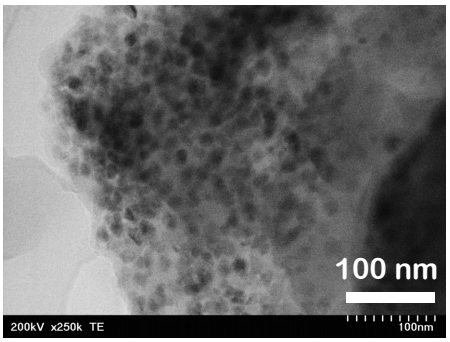

Fig. 2 A TEM image of the edge of the membrane.

taken from the outer edge of the membrane, which indicates that gold nanoparticles are formed in the membrane, and that they are dense and have uniform size distribution. Such size regulation may be explained in terms of immediate capture of reduced gold near the outermost edge of the laterally growing membrane. This method may be useful for preparing size-regulated nanomaterials because the particle size may be controlled by adjusting rates of reduction and membrane growth.

Acknowledgements

This work was partly supported by JSPS MEXT KAKENHI Grant Numbers 15H03585 and 15K13391.

References

[1] T. Shirafuji, J. Ueda, A. Nakamura, S.-P. Cho, N. Saito, and O. Takai, Jpn. J. Appl. Phys. **52**, 126202 (2013).

[2] H. Furusho, D. Miyamoto, Y. Nagasaki, K. Kitano, and S. Hamaguchi, J. Photopolym. Sci. Technol. **20**, 229 (2007).

Time- and space-resolved optical emission spectroscopy on dielectric barrier discharge of helium gas in contact with water

S. Kito, K. Obana, T. Shirafuji

Deparment of Physical Electronics and Informatics, Osaka City University, Osaka, Japan

We have performed time- and space-resolved optical emission spectroscopy on a dielectric barrier discharge of helium gas in a system consisting of a top metal syringe on a water surface. We have observed streamer propagation from positive to negative electrodes for both polarities of applied pulse voltages. After the streamer reaches the counter electrode, the discharge area has shown glow-like structure, which is composed of a positive column, a Faraday dark, and a negative glow, for both polarities. However, the negative glow formed on the water shows weaker emission intensity than the positive column, as opposed to the fact that a negative glow should show higher emission intensity than a positive column in the case of conventional glow-discharges in contact with a solid electrode. This can be attributed to electron attachment by dense water vapor on the water surface.

1. Introduction

Plasma in contact with liquid has attracted much attention because of its various potential applications [1]. However, characteristics of plasma in contact with liquid have not yet fully understood. Shirai and others have revealed static structure in a DC discharge on water [2]. In this paper, we report time evolution of structure in a DBD on water, which is observed by using time- and space-resolved optical emission spectroscopy (OES).

2. Experimental Setup

We applied time- and space-resolved OES on a DBD of helium gas on a water surface. The top electrode was a metal syringe to feed helium gas, and the bottom electrode was a planar surface of deionized water in a glass petri dish. The gas gap between them was 3 mm. Applied voltage was bipolar pulsed voltage (amplitude 1.2 kV, frequency 10 kHz, pulse width 4 μs).

3. Results and discussion

Figures 1(a) and 1(b) show the time- and space-resolved OES profiles for helium (587 nm) when positive and negative pulses are applied on the top electrode, respectively, in which a streamer propagates from the positive electrode to negative one. After the streamer reaches the counter electrode, the discharge area exhibits a glow-discharge-like structure composed of a positive column, Faraday dark, and negative glow. These are common features for both positive and negative polarity. However, the negative glow formed on the water surface shown in Fig. 1(a) has weaker emission intensity than the positive column as opposed to a conventional discharge on a metal electrode. This can be attributed to electron attachment by dense water vapor near the water surface.

Acknowledgements

This work was partly supported by JSPS MEXT KAKENHI Grant Numbers 15H03585 and 15K13391.

References

[1] P. Bruggeman and C. Leys, J. Phys. D **42**, 053001 (2009).

[2] N. Shirai, M. Nakazawa, S. Ibuka, and S. Ishii, Jpn. J. Appl. Phys. **48**, 036002 (2009).

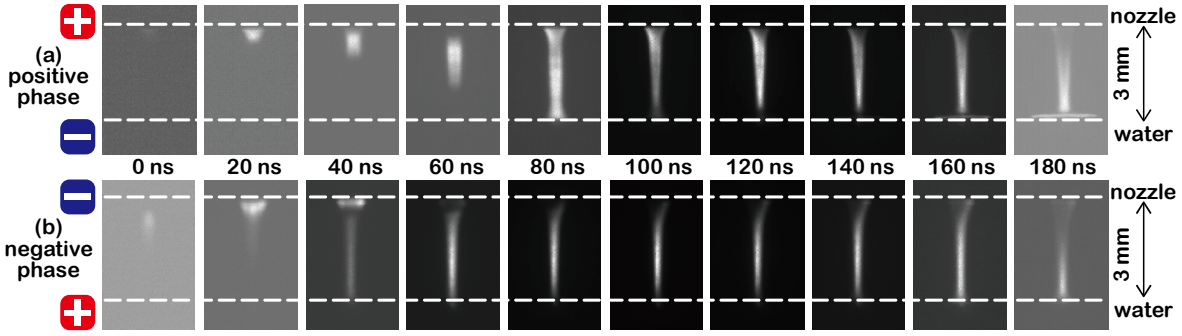

Fig. 1 Time- and space resolved OES profiles on a He plasma jet on water.

Diagnostics on aluminium dust explosion ignited by spark discharge

M. Sankhe[1], S. Bernard[2], S. Pellerin[1], P. Gillard[2], M. Wartel[1]

[1] *GREMI: Groupe de Recherches sur l'Energétique des Milieux Ionisés, UMR CNRS 7344, Université d'Orléans, France*

[2] *PRISME: Laboratoire Pluridisciplinaire de Recherche en Ingénierie des Systèmes et Mécanique Énergétique, UPRES 4229, Université d'Orléans, France*

Several companies are using flammable dusts in their manufacturing process and are sometimes faced with the risk of explosion that can cause tremendous catastrophe with human and material damage. Dust explosions can have many ignition sources but static electricity represents the largest cause of ignition. In this context we use spark discharge to ignite dust explosions for studying conditions and characteristics of dust explosions in order to prevent them. The main goal of this work is to provide ignition experimental data usable for combustion modelling such as the minimum ignition energy (MIE), the burning temperature, the ignition delay, the variation of electron density and the spark temperature.

1. Experimental device

To inflame aluminium powder we used a Hartmann tube which is a polycarbonate transparent cylinder fitted with two tungsten electrodes that are cerium doped, having a cylindrical shape with a diameter of 2.4 mm whose ends are tip shaped with an angle of 40°. Compressed air blower spreads the deposited metallic dust and the spark generator provides the discharge which inflames the dust.

2. Minimum Ignition Energy (MIE)

The spark discharge energy is correlated with the discharge duration and the Langlie test [1] is used to determine the inflammation probability of a dust cloud with the spark discharge energy. The determined MIE of 350 mg of aluminium powder with a mean particle diameter between 15 µm and 25 µm is equal to 15.13 mJ.

3. Pyrometric and spectroscopic temperatures

Pyrometric measured temperatures are close to 2600 K and correspond to the burning particles temperatures in the Hartmann tube. However spectroscopic measured temperatures using vibro-rotational lines of AlO are about 3000 K and correspond to gas molecules temperatures and are certainly representative of temperature in flame front.

4. Ignition delay

The spark discharge interacts with the flammable medium through an ignition delay during which all the chemical processes of heat transfer from the spark to the inflammable product take place. The ignition delay follows a parabolic evolution versus the dust mass concentration. The average value is around 25 ms.

5. Spark temperature

To evaluate the discharge energy, it is necessary to determine the spark temperature. The spark discharge duration is fixed to 100 µs. Optical emission spectroscopy is used for the acquisition of the WI emission lines from different zones of the arc. An Abel inversion was performed to set up a radial distribution of the measured emissivity by defining a cylinder of radius r whose axis corresponds to the inter-electrode axis. Spatial-time evolution of WI excitation temperature is given assuming excitation equilibrium and using Boltzmann plot.

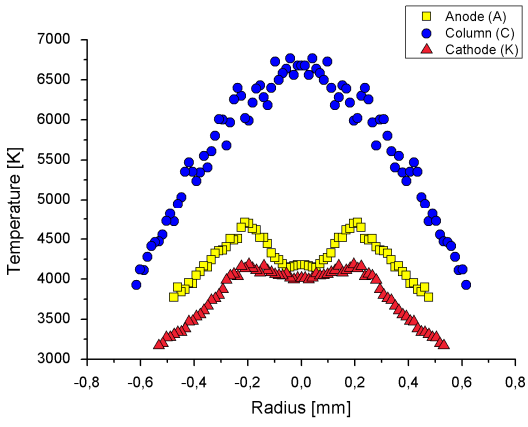

Figure 1 : Excitation Temperature at 50 µs

6. References

[1] S. Bernard & al. Statistical Method for the Determination of the Ignition Energy of Dust Cloud-Experimental Validation, Journal of lost prevention in the process industries, 23-3 (2010), 404-411.

Collisional-radiative model of iron vapour released in thermal arc plasma from molten electrodes

M. Baeva[1], D. Uhrlandt[1], A. B. Murphy[2]

[1] *Leibniz Institute for Plasma Science and Technology, Felix-Hausdorff-Strasse 2, 17489 Greifswald, Germany*
[2] *CSIRO Manufacturing, PO Box 218, Lindfield NSW 2070, Australia*

A collisional-radiative model for technological plasmas is set up. It considers the ground state and fifty effective levels of atomic iron, and one level for singly-ionized iron. The model provides the population of excited states of iron due to collisional and radiative processes. It is applied to a thermal argon arc plasma, in which iron vapour is released respectively from the molten steel anode in tungsten-inert gas and from the consumable iron electrode in a gas-metal welding arc. Input parameters are provided by magnetohydrodynamic simulations. The results clearly identify the conditions in the arc under which the atomic state distribution satisfies the Boltzmann distribution, with an excitation temperature equal to the plasma temperature or deviates from it.

Iron vapour is important in many arc plasma processes. The electronic structure of the iron atom is characterized by energy levels and ionization potential being lower than the energy of the first excited state of the shielding gas [1], i.e. iron atoms are more easily excited and ionized and can influence the radiative and electrical arc plasma properties. To obtain the population of excited states, cross-sections and transition probabilities for excitation and de-excitation, ionization and recombination, and radiative processes between the levels are required. However, there exists a drastic lack of data in the literature for iron atoms. Data obtained in the Opacity Project and the Iron Project is restricted to astrophysical applications [2]. For that reason, collisional data is described in the model by means of theoretical approximations [3]. Atomic transition probabilities data for allowed and forbidden transitions is critically evaluated and given in [4]. The net result of emission and absorption transitions between two levels is considered with transition probabilities modified by the optical escape factor. The model neglects the transport of excited atoms [5]. It is applicable to technological plasmas both in and out of local thermodynamic equilibrium (LTE). Magneto-hydrodynamic simulations of tungsten-inert gas and gas-metal welding arcs serve with input parameters.

The atomic state distribution (ASD) obtained for gas-metal tungsten arc is shown in Fig. 1. At low temperatures (a) observed respectively near the consumable electrode and the workpiece, the ASD deviates from the equilibrium one (straight line). Then, temperature determination from line intensity measurements can be inaccurate. Deviations from thermal equilibrium occur. In contrast, in the most of the central part of the arc column where the temperature is high (b), the excitation temperature and the plasma temperature are equal. The application of diagnostic techniques that are based on the assumption of LTE is better justified.

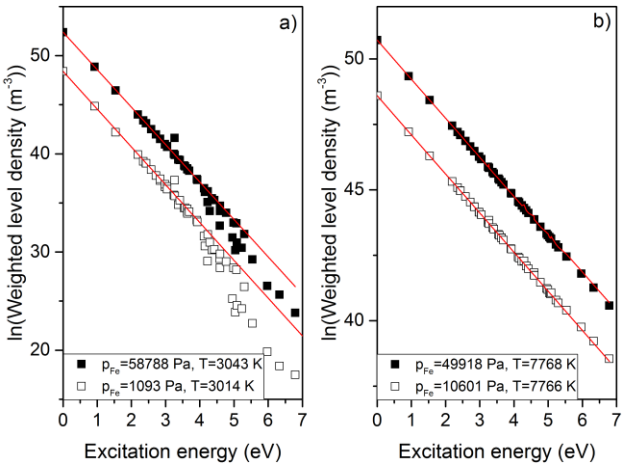

Fig.1 Atomic state distribution of iron at a) low and b) high temperatures in gas-metal welding arc plasma. In each case, results are shown for two iron partial pressures. The straight lines represent Boltzmann distributions.

The work was supported by DFG under Grant UH106/11-1.

References

[1] C.E. Moore, Atomic energy levels, vol. 2, Ntl. Bur. Stand. (US) Circ. 467 (1952, repr. 1971).

[2] D.G. Hummer et al, A&A, **279**, 298 (1993).

[3] L. Vriens, A.H.M. Smeets, Phys. Rev. A, **22**(3), 940 (1981).

[4] J. R. Fuhr, W. L. Wiese, J. Phys. Chem. Ref. Data, **35**(4), 1669 (2006)

[5] B. Van der Sijde et al, Beitr. Plasmaphysik, **24**, 447 (1984)

Topic number

Energy dependence of intensity ratio between nitrogen spectral lines of N II and N I from electrostatic discharge in air

T. Miura

National Institute of Occupational Safety and Health, Japan, 1-4-6, Kiyose, Tokyo 204-0024, Japan

For development of practical method to estimate energy of spark discharge in air without electrical measurements, dependence of spectral characteristics of light emission from the discharge on electrostatic energy was investigated. It was found that the relative light intensity of N II to N I increased with electrostatic energy in the region from 0.1 mJ to 10 mJ.

1. Introduction

For risk assessment of fires caused by spark, minimum ignition energy of the combustibles has been well evaluated using explosion apparatus, including a spark generator and a basic electric circuit with a capacitor, resistor, induction coil, and high-voltage supply. However, estimating the energy of an actual spark—such as a spark between an electrified human body and an ungrounded conductor—from the condition of an equivalent electric circuit is impossible in practice, even if the surface potential of the human body can be measured.

We has studied spectral characteristics of spark discharge in air. It was found that the relative intensity of the emission line from N II to that from N I increased with the initial electrostatic energy of the charged capacitor. In this study, dependence of their intensity ratio on electrostatic energy was measured in detail.

2. Experiment

A spark was generated in a gap between two spherical electrodes during the process of their approaching each other; one was grounded and the other was connected to a high-voltage charged capacitor. The electrodes were made of stainless steel, and their radius of curvature was 7 mm. The speed of approach was in the region between 0.5 and 5 mm/s. The room temperature was 24-27ºC, and the relative humidity was 30-60%. The maximum voltage was 6 kV. Capacities were varied from 47 to 1000 pF. Simultaneously discharge current was measured by means of current probe with digital oscilloscope and recoded.

3. Results and discussions

Figure 1 shows the typical spectrum of a spark due to a capacitor discharge in air. The spectrum shows emission lines from electronic excited nitrogen atoms (N I), monovalent positive ions (N II), and so on.

The intensity ratio of N II to N I was measured as a function of the electrostatic energy accumulated to the capacitor before discharge, as shown in Figure 2. The electrostatic energy was varied by changing the voltage of the capacitor. The intensities were obtained by integrating the spectrum's peak without any background.

As shown in Figure 2, the relative intensity of N II increased with the electrostatic energy of the capacitor. The current measurement implied that accumulated charge was almost discharged. A function between the ratio and the energy was found, although each voltage group has individual line.

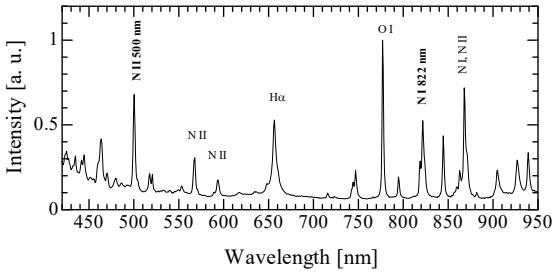

Fig.1. Emission spectrum of spark discharge (470 pF, 3.0 kV)

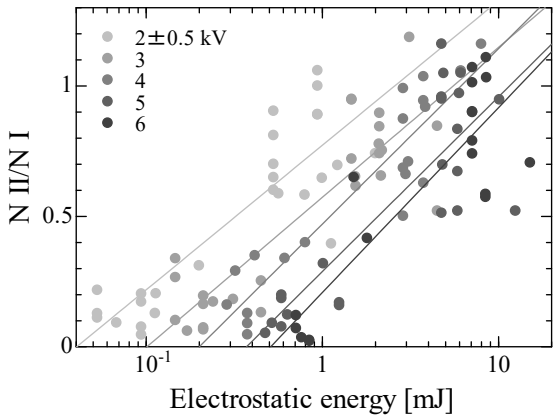

Fig.2. Relation between the relative intensity of the N II emission to the N I and the initial electrostatic energy of the capacitor, categorised by the applied voltages.

Simulating Propagation of Spots over Cathodes of High-Power Vacuum Circuit Breakers

M. D. Cunha[1,2], N. Wenzel[3], M. S. Benilov[1,2], W. Hartmann[3]

[1]*Departamento de Física, FCEE, Universidade da Madeira, Largo do Município, 9000 Funchal, Portugal*
[2] *Instituto de Plasmas e Fusão Nuclear, IST, Universidade de Lisboa, Portugal*
[3] *Siemens AG, Corporate Technology, Günther-Scharowsky-Strasse 1, 91058 Erlangen, Germany*

A model of an ensemble of a large number of spots on cathodes of high-power vacuum circuit breakers is developed by means of generalization of the concept of random walk of a single cathode spot in low-current vacuum arcs. The model is formulated in terms of a convection-diffusion equation governing the evolution of the distribution of spots along the cathode, taking into account the variation of the total number of spots with the arc current. A reasonably good agreement between the model and the experiment is found. The model can be used as a module of global numerical models of the interruption process in high-power vacuum circuit breakers.

1. The model

The motion of a spot on a cathode of a vacuum arc can be described as a random walk consisting of a sequence of displacements with a characteristic step length and a characteristic time interval, and with probabilities dependent on the spot location. The evolution of the probability of a spot to be at a certain position at a certain time instant is governed by the Fokker-Planck equation. Assuming that there is no interaction between individual spots and multiplying the above-mentioned equation by the total number of spots, we obtain an equation governing the evolution of the surface density of spots. Creation of new spots and extinction of existing ones is accounted for with the use of the assumption that the net local rate of creation of spots is proportional to the local density of those already existing. The proportionality coefficient is determined from the condition that the total number of spots at each moment conforms to the instantaneous value of the arc current, which is essential for the model to be applicable to high-power vacuum circuit breakers. The drift velocity is associated with the retrograde motion of the spots in a tangential magnetic field and was estimated from the experimental data [1] with the account of the effect of axial magnetic fields [2]. It is assumed that the spots are extinguished on reaching the boundary of the contact.

2. Results

The above-described model was applied to conditions of experiments [3, 4]. An example is shown in Fig. 1. The figure refers to the case of a cathode made of CuCr25 with a diameter of 40 mm operating under a sinusoidal current wave with frequency of 50 Hz and current peak of 7 kA, with variable axial magnetic field B_n. The agreement between simulation results and the experiment is reasonably good.

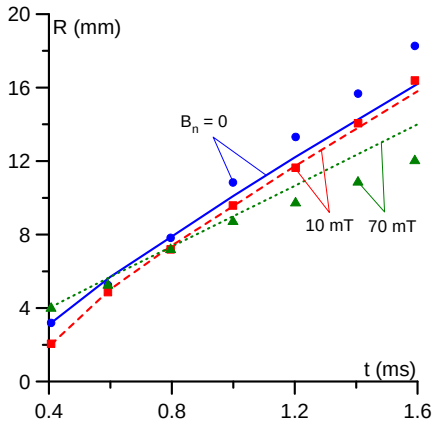

Fig.1 Time dependence of cathode arc root radius. Lines: modelling. Symbols: experiment [4, Fig. 12].

3. Acknowledgements

The work at Universidade da Madeira was supported in part by FCT of Portugal through the project Pest-OE/UID/FIS/50010/2013 and in part by Siemens AG.

4. References

[1] A.M. Chaly, K.K. Zabello and S.M. Shkol'nik, in Proc. 26th Int. Symp. Discharges Electr. Insul. Vacuum, vol. 1, pp. 229-232 (2014).

[2] A.M. Chaly and S.M. Shkol'nik, IEEE Trans. Plasma Sci., vol. **39**, no. 6, pp. 1311-1318 (2011).

[3] W. Hartmann, A. Lawall, R. Renz, M. Römheld, N. Wenzel, W. Wietzorek, IEEE Trans. Plasma Sci., vol. **39**, no. 6, pp. 1324-1329 (2011).

[4] X. Song, Z. Shi, C. Liu, S. Jia and L. Wang, IEEE Trans. Plasma Sci., vol. **41**, no. 8, pp. 2061-2067 (2013).

Astronomical radio-reception techniques for emission spectroscopy of molecular and short lived species in cold plasmas

I. Tanarro[1], B. Alemán[2,4], R. J. Peláez[1], V. J. Herrero[1], J. L. Doménech[1], P. de Vicente[3], J. D. Gallego[3], J. R. Pardo[2], K. Lauwaet[2], G. Santoro[2], J. A. Martín-Gago[2], J. Cernicharo[2]

[1]*Inst. de Estructura de la Materia, CSIC, Serrano 123, 28006 Madrid (Spain)* i.tanarro@csic.es
[2]*Inst. de Ciencia de Materiales de Madrid, CSIC, Sor Juana Ines de la Cruz 3, 28049 Cantoblanco (Spain)*
[3]*Observatorio de Yebes, IGN, Guadalajara (Spain),* [4]*IMDEA Materiales, Eric Kandel 2, 28096 Getafe (Spain)*

In this work we describe the proof of concept of the use of standard radio-astronomy receivers to conduct emission spectroscopy of different molecular precursors and products at room temperatures in low pressure plasmas. The goal is to obtain in laboratories valuable spectroscopic information on rotational transitions of molecular species of astrophysical interest at high spectral resolution. An inductively coupled RF discharge was employed to generate the plasma. OCS, CS_2 and O_2 were used as plasma precursors. The experiment was performed with the 33-50 GHz band HEMT detector available in the Observatory of Yebes (Spain), where the beam of its radio-telescope of 40 m diameter pointing towards the zenith was used as cold emission background.

1. Introduction

With the increasing use and continuous development of powerful radio-telescopes (like ALMA), spectral line surveys at mm and sub-mm wavelengths have enhanced tremendously the detection of stable molecules and transient species in interstellar molecular clouds and other astronomical regions. Evaluation of these data takes great advantage of laboratory information on the spectral fingerprints and reactivity of these species. In this work we describe the successful joint use of standard radio-astronomy High Electron Mobility Transistor (HEMT) receivers and plasma reactors for laboratory simulations of astrophysical observations.

2. Experimental set-up

The plasma was produced in a 25 cm diameter, 42 cm length SS vacuum chamber by an inductively coupled RF discharge (13.56 MHz) through a refrigerated Cu coil inserted axially. Upilex windows of 75 μm thickness were placed at both ends of the chamber. A differentially pumped mass spectrometer was used to identify the plasma precursors and stable products. Gas pressures ~ 10-30 Pa allowed stable plasma operation and produced similar column densities to those of typical interstellar clouds.

The radio-receiver operated in the 33-50 GHz spectral band, with 2 GHz bandwidth and 38 kHz spectral resolution. Data were acquired with a Fast Fourier Transform Spectrometer. A frequency switching method for background subtraction was used for stable gas detection, whereas turning on and off the plasma was most convenient to detect short lived species. Depending on the weather conditions, the background for emission measurements came from the antenna of the radio-telescope pointing towards the zenith (clear blue sky) or from a blackbody load of liquid N_2 (cloudy or rainy weather), implying 42 K or 77 K, respectively, at 45 GHz spectral frequency.

3. Results

OCS was selected for preliminary gas detection in the observing emission band, displaying maximum equivalent radiation temperatures of ~ 4 K. At the lowest pressure (5 Pa), its linewidth was due in part to thermal broadening and at the highest one (60 Pa), it was dominated by pressure broadening. OCS and CS_2 were selected as plasma precursors of the CS radical, which emits also in this region. It was routinely detected in different plasma conditions, with equivalent temperatures up to 3 K. O_2 discharges applied after sulphur deposition on the reactor walls by the previous S rich containing OCS and CS_2 plasmas allowed the surface generation of SO_2 and the detection of its rotational transitions in different bending vibrational states, v_2 = 0,1,2, the intensity of the transitions from upper levels increasing with discharge power.

The RF discharge didn't induce any electromagnetic spurious signals in the receivers, and astronomical detection of a SiO maser in the AGB star TX Cam showed identical results with plasma on and off.

In conclusion, these experiments confirm the viability of using standard radio-astronomy receivers to detect molecular and short lived species in gas simulation chambers based on plasma reactors.

Plasma sheath and pre-sheath in front of a ceramic wall: experimental and theoretical study

V. Pigeon, N. Claire, C. Arnas, L. Couedel

Aix Marseille Univ, CNRS, PIIM, Marseille, France

The sheath and pre-sheath in front of a ceramic wall (BNSi02), immersed in a low temperature plasma, are studied both theoretically and experimentally. Measurements were performed in a multipolar device using emissive probes and the laser induced fluorescence (LIF) diagnostic which shows an unexpected and significant flow of ions directed away from the wall toward the bulk plasma. The secondary electron emission (SEE) from the ceramic is assumed to be the cause of this phenomenon, since $BNSiO_2$ is known to be a strong emitter [1]. In order to explain experimental observations of the ceramic sheath, a kinetic model accounting for SEE, energetic electrons, thermal electrons and ions is being developed.

Plasma-wall interaction is a fundamental field of research in plasma physics for numerous applications. We are presently focused on a ceramic wall used in Hall thrusters ($BNSi0_2$), in which plasma-wall interactions are important in the combustion chamber sustaining issues and in the particle transport problematic.

The study presented in this poster aims to better understand the sheath and pre-sheath physics in the vicinity of a BNSiO2 wall sample**.** The sheath and pre-sheath are studied experimentally, while a kinetic model is developed to describe the sheath.

Experimental measurements are performed in the quiescent argon plasma of a multipolar device. Both the LIF and emissive probes are used to explore the ceramic sheath, measuring ion velocity distribution functions (IVDF) and the plasma potential, respectively. The results highlight an unexpected ion flow directed toward the plasma in addition to the wall-directed one as shown in Figure 1. It appears that these flows are slightly asymmetric regarding velocities, densities and consequently fluxes. These features cannot be explained by a monotonic sheath potential drop. Moreover, previous measurements performed in similar conditions in front of metals reported monotonic potential drop [2]. It indicates that metals and $BNSiO_2$ do not behave the same way when embedded in a plasma.

We have developed a kinetic model which takes into account the $BNSi0_2$ SEE characteristic coefficient, energetic electrons, thermal electrons and ions with finite temperature. It allows to calculate the variations of the potential and the densities along the sheath as a function of the energies and temperatures of the plasma species. The results are in good agreement with previous theoretical results describing sheaths in the presence of the previously cited species [3] (Figure 2). Furthermore, the model shows that a backward ion flow is incompatible with a monotonic sheath. Further improvements of the model will aim to verify the experimental results. Moreover, emissive probe measurements will be performed in the sheath, in order to avoid the strong laser light scattering at the ceramic surface.

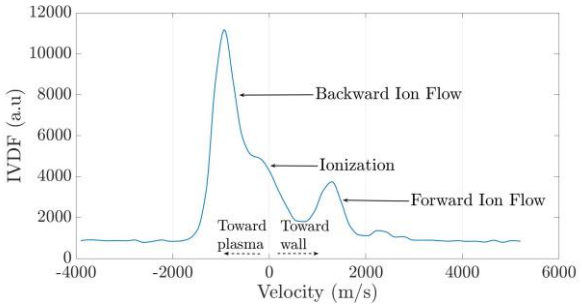

Fig. 1: IVDF at 1.5 cm from the ceramic wall sample

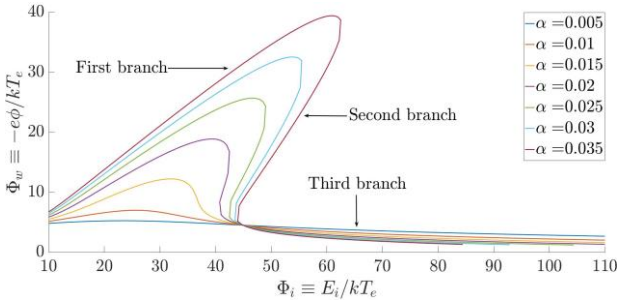

Fig 2: Wall potential variation vs impinging electron energy; α: relative energetic electrons concentration.

References

[1] T. Tondu, M. Belhaj and V. Inguimbert Journal of Appl. Phys. **110** 093301 (2011).

[2] N. Claire, G. Bachet, U. Stroth and F. Doveil Phys. of Plasmas **13**, 062103 (2006).

[3] S. Langendorf and M. Walker, Physics of Plasmas **22**, 033515 (2015).

Topic number: 5

Theoretical study of the influence of nitrogen admixture on plasma decay rate in argon dc afterglow

N. Dyatko, A. Napartovich

Troitsk Institute for Innovation and Fusion Research, Pushkovykh Str. 12, 108840 Troitsk, Moscow, Russia

In the present work the decay of plasma in a dc afterglow in pure Ar and Ar:N_2 mixtures was studied theoretically under the following conditions: discharge tube radius R = 1.5 cm, N_2 admixture α = 0.1%-1%, gas pressure P = 1 – 5 Torr, discharge current I = 20 – 50 mA. It was shown that the addition of nitrogen to argon led to a dramatic change in plasma decay scenario. One of the reasons is that the effective electron temperature in Ar+N_2 afterglow is rather high due to the second kind collisions of electrons with vibrationally excited molecules. As a result, the rate of plasma decay due to ambipolar diffusion is high, too. Another reason is that at the early stage of the afterglow (≤ 15 ms at P = 5 Torr) the loss of electrons and ions is noticeably compensated due to ionization processes with the participation of excited nitrogen atoms $N(^2P,^2D) + N(^2P) = N_2^+ + e$.

In the present paper, plasma parameters in a dc glow discharge and afterglow in Ar and Ar:N_2 mixtures were studied theoretically using the self-consistent 0-dimentional kinetic model [1]. The model included balance equations for charged species, a system of kinetic equations for populations of electronic states of Ar atoms, N_2 molecules and N atoms, a system of equations for the vibrational kinetics of N_2 molecules in the ground electronic state and an equation for the electric circuit. Rate coefficients for electron-induced processes were calculated from solution to the electron Boltzmann equation (with taking into account electron-electron and second kind collisions). The preliminarily estimated gas temperature was taken as a parameter.

The procedure of simulation was as follows. First, time-evolution of plasma parameters was calculated to come to steady-state discharge conditions (further it is characterized by the discharge current value I). Then, the applied voltage was set to zero and the time-variation of plasma parameters in the afterglow was calculated.

Electron concentrations calculated in the steady state discharge plasma (I = 20 mA, P = 1 Torr, 5 Torr) and in the afterglow are shown in fig. 1. According to the performed analysis, in pure Ar afterglow the electron temperature quickly (< 1 μs) relaxes to the gas temperature. The plasma decay is governed by recombination of electrons with molecular ions and ambipolar diffusion process, the contribution of the former process decreases with the decrease in the ion concentration.

In the discharge in Ar:N_2 mixtures the high degree of vibrational excitation of nitrogen molecules is achieved [1]. As a consequence, the effective electron temperature in the afterglow is also high [2] due to second kind collisions of electrons with vibrationally excited molecules. And high electron temperature in the afterglow results in the high rate of plasma decay due to ambipolar diffusion process. On the other hand, at early stage of the afterglow (≤ 15 ms, at P = 5 Torr) the loss of electrons and ions is noticeably compensated due to ionization processes with the participation of excited nitrogen atoms $N(^2P,^2D) + N(^2P) = N_2^+ + e$.

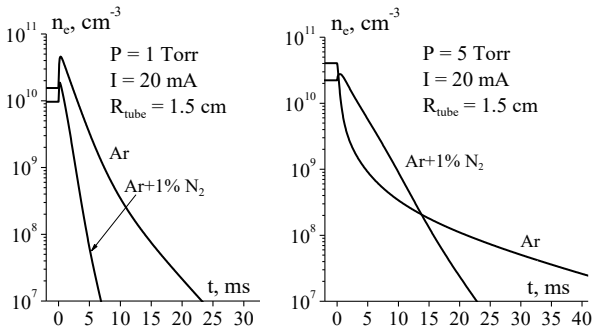

Fig. 1. Calculations. Electron concentration in the discharge plasma (t<0) and in the afterglow (t>0).

Naturally, the contribution of different processes to plasma decay rate depends on the gas pressure. It is seen in fig. 1 that at P = 1 Torr, the addition of N_2 to Ar leads to the significant increase in the decay rate. At P = 5 Torr the situation is more complex. In the beginning, the plasma in Ar afterglow decays faster and then slower than in Ar+1%N_2 afterglow.

This work was supported by the Russian Foundation for Basic Research, # 15-02-06191.

References

[1] N.A. Dyatko, Yu.Z. Ionikh, A.V. Meshchanov, A.P. Napartovich, K.A. Barzilovich, Plasma Phys. Rep. **36** (2010) 1040.

[2] S. Hübner, E. Carbone, J.M. Palomares, J. van der Mullen, Plasma Proc. Polym. **11** (2014) 482.

Topic number: 6

Experimental and theoretical study of radial profiles of the Ar metastable atom density in diffuse and constricted dc discharges

G. Grigorian[1], N. Dyatko[2], I. Kochetov[2]

[1]*St. Petersburg State University, St. Petersburg 199034, Russia*
[2]*Troitsk Institute for Innovation and Fusion Research, Pushkovykh Str. 12, 108840 Troitsk, Moscow, Russia*

In the present work the radial profiles of the number density of metastable Ar($1s_5$) atoms in a dc glow discharge in argon at intermediate gas pressures were studied both experimentally and theoretically under the following conditions: discharge tube radius R_{tube} = 2.0 cm, gas pressure P = 40 Torr – 100 Torr, discharge current I = 10 mA – 50 mA. For gas pressures under study a step-wise transition from diffuse to constricted form of discharge was observed after the discharge current had exceeded some critical value. Radial profiles were measured and calculated in diffuse as well as constricted discharges. Measurements were performed using optical absorption technic, and in calculations the self-consistent 1D axial-symmetric discharge model was used. Results of calculations were in a reasonable agreement with the experimental data.

It is known that at intermediate gas pressures the increase in the discharge current leads to the constriction of the positive column of the diffuse glow discharge. In most cases it looks like step-wise transition after the discharge current exceeds some critical value, herewith the transition is accompanied by the noticeable decrease in the electric field strength E in the positive column. The constricted positive column looks like a narrow bright cord at the discharge tube axis.

In the present work the radial profiles of the number density of Ar($1s_5$) metastable atoms were measured and calculated in the diffuse discharge as well as in the constricted discharge. Measurements were performed using optical absorption technic, experimental setup and procedure were nearly the same as in [1]. In calculations the self-consistent 1D axial-symmetric discharge model was used [2].

The measured $E(I)$ dependences and the calculated ones in argon discharge at P = 60 Torr are shown in fig. 1. One can see that, in this case, the measured critical current value for the step-wise transition from diffuse to constricted discharges is about 37 mA. The calculated $E(I)$ curve agrees rather well with the measured one.

In fig. 2 there are normalized radial profiles of the number density of Ar($1s_5$) metastable atoms. These profiles were measured and calculated in diffuse (I = 20 mA) and constricted (I = 50 mA) discharges. As one should expect, the profile of metastable atoms in the constricted discharge is essentially narrower than that in the diffuse discharge. The number densities of Ar($1s_5$) atoms measured at the tube axis are 8.53×10^{10} cm^{-3} (I = 20 mA) and 6.1×10^{11} cm^{-3} (I = 50 mA).

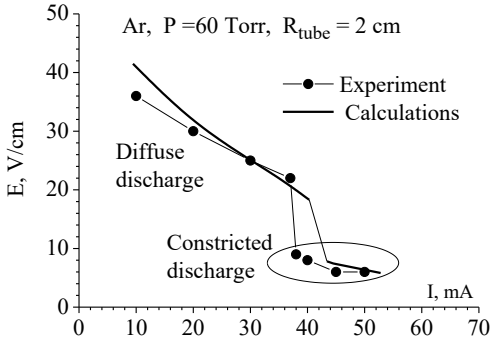

Fig. 1. Measured and calculated values of the electric field strength in the positive column.

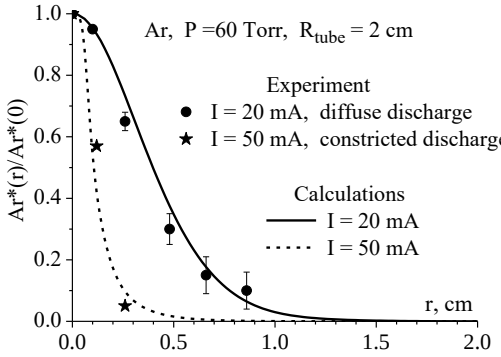

Fig. 2. Measured and calculated normalized radial profiles of Ar($1s_5$) metastable atoms.

This work was supported by the Russian Foundation for Basic Research, # 16-02-00861.

References

[1] G.M. Grigorian, N.A. Dyatko, I.V.Kochetov, J. Phys. D: Appl. Phys. **48** (2015) 445201.

[2] N.A. Dyatko, Yu. Ionikh, I.V. Kochetov, D. L. Marinov, A.V. Meshchanov, A.P. Napartovich, F.B. Petrov, S.A. Starostin, J. Phys. D: Appl. Phys. **41** (2008) 055204.

On the mechanism of retrograde motion of vacuum arc cathode spot in external magnetic field

S.A. Barengolts[1], V.G. Mesyats[1], M.M. Tsventoukh[2]

[1] *A.M. Prohorov Institute of General Physics RAS, Moscow, Russian Federation*
[2] *P.N. Lebedev Physical Institute RAS, Moscow, Russian Federation*

The physical processes that accompany the retrograde motion of the cathode spot of a vacuum arc in an external tangential magnetic field are considered based on the principle of maximum magnetic field. It is shown that the magnetic field causes an asymmetry in the plasma density distribution at the boundary of the plasma jet ejected from the cathode spot, but it has no effect on the physical processes that occur immediately in the spot. Cathode spot extinction is accompanied by ejection of plasma toward the site where the total magnetic field (the external field plus the self-magnetic field of the cathode plasma jet) is a maximum. At this site, a new spot is born. The velocity of the directed motion of a cathode spot in an external magnetic field increases with current mainly due to an increase in geometric size of the spot operation area.

The retrograde motion of the cathode spot of a vacuum arc in an external magnetic field parallel to the cathode surface is one of the most mysterious and difficult-to-explain phenomenon of vacuum discharge physics. The cathode spot motion opposite in direction to the Ampere force was discovered in 1903 by Stark [1].

When constructing a model describing the retrograde motion of the cathode spot of a vacuum arc, we will proceed from the principle of magnetic field maximum formulated by Kesaev[2]. Its essence is that the cathode spot motion is directed predominantly toward the site where the total magnetic field being the sum of the external magnetic field and the self-magnetic field of the cathode plasma jet is a maximum. In reality, the retrograde motion of a cathode spot is the initiation of new cathode spot cells mainly in the direction "retrograde" to the Ampere force. Analysis of the mechanism of initiation of cathode spot cells (that explosively emit ectons [3]) has shown that the main characteristic that determines the development of thermal instability of the cathode surface microscopic irregularities (on reaching a critical temperature T_{cr}) is cathode plasma density n_{pl} [4].

It is shown that immediately in the area of the cathode spot operation, the magnetic pressure is substantially lower than the gas-kinetic pressure and its effect shows up where the jet is compressed and, as a result, the plasma density increases.

When a cathode spot dies out, the current passed through it decreases abruptly, and so does the magnetic pressure produced by this current at the boundary of the plasma jet. This results in plasma ejection in the direction of cathode spot retrograde motion at the site where the total magnetic pressure was a maximum until the spot extinction.

The initiation of new cathode spots is probabilistic in nature and is determined not only by the plasma density, but also by the geometry and temperature of microirregularities whose explosion gives birth to new spots. We introduced the probability density function for the angle by which the cathode spot path deflects from the retrograde direction to the Ampere force:

$$f(\theta) = \frac{1}{2\pi} + \frac{B_e}{\pi B_s} cos(\theta), \qquad (1)$$

The velocity of the retrograde motion of a cathode spot is determined as

$$V_r \approx \frac{4RB_e}{\pi\tau B_s} \propto B_e, \qquad (2)$$

where R and τ are the space and time steps of the motion of a single cathode spot. For a second-type spot, these quantities are approximately equal to the spot crater radius and lifetime, respectively. According to our model, the increase in velocity of the directed motion of a cathode spot with arc current is determined mainly by the increase in crater size.

[1] J. Stark. Phys. Zeitschrift. **4** (1903) 440.
[2] I.G. Kesaev. *Cathode Processes in an Electric Arc* (Nauka, Moscow, 1968).
[3] G.A. Mesyats. IEEE Trans. Plasma Sci. **41** (2013) 676.
[4] S.A. Barengolts, D.L Shmelev, and I.V. Uimanov. IEEE Trans. Plasma Sci. **43** (2015) 2236.

Simulation of Plasma Processing with FPS3D

P. Moroz[1], D. J. Moroz[2]

[1]*US TDC, TEL Technology Center, America, LLC, Billerica, MA, USA*
[2] School of Engineering and Applied Sciences, *Harvard University, Cambridge, MA, USA*

Simulation of plasma processing via a Monte Carlo feature-scale simulator FPS3D is demonstrated by two very different examples: simulation of etching and implantation for the case of Ar/Cl_2 plasma, and simulation of atomic layer deposition with a cyclic process of dichlorosilane gas followed by the ammonia plasma. Comparison with experiments is provided.

1. Introduction - FPS3D.

Feature-scale simulations allow reasonably fast simulation of etching or deposition profiles. These simulations are many orders of magnitude faster that the higher accuracy MD methods. There have been many types of feature-scale simulators developed since the 1970s, and their capabilities differ significantly from each other.

FPS3D is a general software package designed to be applicable to any situation met by the semiconductor industry, be that etching, deposition, implantation, atomic layer processing, etc., or any combination of these. FPS3D uses a cellular model for representing solid materials, but that model goes well beyond the traditional approach. In FPS3D, each cell can contain different molecules and the number of molecules per cell is not fixed but rather is determined by the volume of the cell and by the size of molecules it contains. Also, FPS3D uses Monte Carlo pseudo-particles for representing all incoming fluxes. These particles are launched such that statistically they represent given angle-energy distributions of all relevant fluxes of species coming to the surface. Each particle typically contains many molecules, but preferably significantly fewer than the number of molecules in a full cell. Upon collision of such a particle with a solid material, the code determines a set of involved cells where interactions occur and computes the output on the basis of user-specified reactions.

FPS3D is free from many limiting assumptions of most other feature-scale simulators. For etching it allows simultaneously calculation or implantation, and for deposition, it allows materials to grow in accordance with their density, and in accordance with the actual sizes of participating molecules.

2. Two Examples of FPS3D Simulations

FPS3D can be applied to features of different scales ranging from nanometers[3] to microns[2]. By selecting proper sizes of material cells and incoming particles, the code obtains reasonable accuracy within reasonable calculation time.

2.1. Etching/Implantation with Ar/Cl_2 plasma

To setup surface reactions for the case of Ar/Cl_2 plasma etching of Si, FPS3D was run with the low ion energies of 35, 55 and 75 eV. Results of simulations were able to reproduce the experimental data[4]. High-aspect ratio etching often requires high-energy ions. We have used the same chemistry for the case with high energy Ar+ ions of 1.5 keV. Energetic ions penetrate deep into material, and sometimes could lead to plasma-induced damage. We simulated this process both in 2D and 3D.

2.2. SiN Atomic Layer Deposition with Cycles of Dichlorosilane and Ammonia Plasma

We considered a case of SiN ALD that uses cycles of dichlorosilane gas deposition followed by the nitration by ammonia plasma. This case is interesting because it results in the deposition of 1 ML only after two cycles. We believe that one of the main reasons for this is steric hindrance by SiH_2Cl_2 molecules. FPS3D is designed to take steric hindrance into account. This large molecule could cover two interaction sites on the surface, preventing those sites from interacting with other molecules until the large molecule reacts and reaction sites become accessible again. Results of simulations are compared with experiments[5].

References

[1] P. Moroz, D.J. Moroz, ECS Transactions, **50** 61 (2013).
[2] P. Moroz, D. J. Moroz, J. Physics: CS **550** (2014) 012030 (2014).
[3] P. Moroz, D. J. Moroz, to be published in Japan. J. Appl. Phys. (2017).
[4] J. P. Chang, A. P. Mahorowala, H. H. Sawin, J. Vac. Sci. Technol. **A 16**, 217 (1998).
[5] H. Goto, K. Shibahara, S. Yokoyama, Appl. Phys. Lett. **68**, 3257 (1996).

Determination of collisional quenching rate coefficients of metastable excited atoms Ar($^3P_2$) by Ar and H_2O

S. Suzuki[1], Y. Usui[1], H. Itoh[1] (Chiba Institute of Technology)

[1] *Department of Electrical, Electronic and Computer Engineering, Chiba Institute of Technology, Tsudanuma, Narashino, Chiba 275-0016, Japan*

We observed the transient current after turning off the UV light illuminating a cathode used to supply the photoemission current in a Townsend discharge to measure the effective lifetime of the metastable excited atoms Ar($^3P_2$). The diffusion coefficient of Ar($^3P_2$) in argon, the reflection coefficient of Ar($^3P_2$) at the electrode surface and the collisional quenching rate coefficient of Ar($^3P_2$) by ground-state atoms Ar($^1S_0$) were determined from the observed effective lifetime of Ar($^3P_2$). Moreover, the collisional quenching rate coefficient of Ar($^3P_2$) by H_2O was also determined.

1. Introduction

In this study, the three fundamental coefficients of metastable excited atoms Ar($^3P_2$) were determined by a non-spectroscopic measurement and curve fitting to theoretical values of the effective lifetime derived from the solution of the diffusion equation.

2. Experimental apparatus and method

Details of the experimental apparatus and the procedure used for numerical analysis have already been reported [1,2]. The purity of Ar gas used in the experiment was 99.999%.

3. Experimental results and discussion

In figure 1, the four solid lines show the observed effective lifetime τ_1 of Ar($^3P_2$) in Ar plotted against the gas pressure for different gap lengths. From the results, we determined the diffusion coefficient D_{m1} of Ar($^3P_2$), the collisional quenching rate coefficient k of Ar($^3P_2$) by Ar($^1S_0$) and the reflection coefficient R of Ar($^3P_2$) at the electrode to be 42.2±1.4 cm^2/s, (2.96±0.05)×10^{-15} cm^3/s and 0.13±0.02, respectively. The value of k is consistent with that reported by Molnar [3] and also with values previously obtained by spectroscopic measurement [4-7]. The temperature dependence of $k(T)$ was also derived as

k=3.9×10^{-7}exp(-5700/T) [300≦T≦343 K].

On the basis of the results, the experiments were extended to an Ar/H_2O(112 ppm) mixture and the preliminary results are shown in Fig. 1. The collisional quenching rate coefficient k' of Ar($^3P_2$) by H_2O was determined to be 2.3×10^{-10} cm^3/s, which is 10^5 times larger than the value of k. Our value k' was consistent with those reported by Bourene and Le Calvè [8] and Balamuta and coworkers [9, 10] of 1.84×10^{-10} cm^3/s and 2.16×10^{-10} cm^3/s, respectively, who described the generation of O, H and OH as the by-products of H_2O.

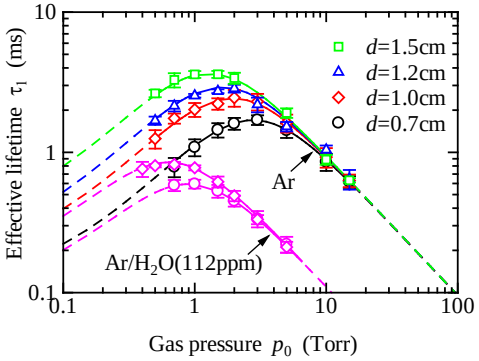

Fig. 1 Effective lifetime of metastable excited atoms Ar($^3P_2$) in Ar.

4. References

[1] S.Suzuki and H.Itoh, J. Phys. D: Appl. Phys. **49** (2016) 185202.

[2] S.Suzuki, H.Itoh, N.Ikuta and H.Sekizawa, J. Phys. D: Appl. Phys. **25** (1992) 1568-1573.

[3] J. P. Molnar, Phys. Rev. **83** (1951) 940-952.

[4] A. H. Furch and F. A. Grant, Phys. Rev. **104** (1956) 356-361.

[5] E. Ellis and N. D. Twiddy, J. Phys. B: At. Mol. Phys. **2** (1969) 1366-1377.

[6] A.V. Phelps and J. P. Molnar, Phys. Rev. **89** (1953) 1202-1208.

[7] R. A. Gutcheck and E. C. Zipf Bull, Am. Phys. Soc. **17** (1972) 395.

[8] M. Bourène and J. Le Calvé, J. Chem. Phys. **58** (1973) 1452.

[9] J. Balamuta and M.F. Golde, J. Chem. Phys. **76** (1982) 2430.

[10] J. Balamuta, M.F. Golde and Yueh-Se Ho, J. Chem. Phys. **79** (1983) 2822.

Topic Number: 17

Rate equation analysis of ROS/RNS in plasma-treated water

K. Takahashi[1], S. Kawaguchi[1], K. Satoh[1], H. Kawaguchi[1],
I. Timoshkin[2], M. Given[2], and S. MacGregor[2]

[1] *Muroran Institute of Technology, Muroran, Japan*
[2] *University of Strathclyde, Glasgow, UK*

The concentrations of H_2O_2, NO_2^-, and NO_3^- as reactive oxygen species and reactive nitrogen species in water, exposed to a pulsed discharge in nitrogen atmosphere, are calculated using rate equations coupled with acid-base equilibrium between NO_2^- and HNO_2 and a chemical reaction between H_2O_2 and HNO_2, considering the temporal variations of flux rates of H_2O_2, NO_2^-, and NO_3^-, which is estimated from measurement data in our previous work. Furthermore, the calculated concentrations are fitted to the measurement values. It is found that the calculated concentrations are in approximate agreement with the measured data. It is also found that the generation rates of H_2O_2, NO_2^- and NO_3^- are estimated to be 9.5×10^{-7}, 4.5×10^{-7}, and 2.5×10^{-7} M/s.

1. Introduction

In recent years, plasma-treated water, in which reactive oxygen species and reactive nitrogen species (ROS/RNS) dissolve, has gained increasing attention, because ROS/RNS in the plasma-treated water, such as H_2O_2 (hydrogen peroxide), NO_2^- (nitrite ion), HOONO (peroxynitrous acid), and NO_3^- (nitrate ion), and/or synergistic effects between these species play a key role in various applications such as disinfection [1] and plant growth promoting [2]. To selectively and/or effectively produce the ROS/RNS and utilize the plasma-treated water effectively and efficiently, it is important to clarify the generation process of the ROS/RNS; however, the generation process has not yet been clarified. In this work, we calculated the ROS/RNS concentrations in water, exposed to a pulsed discharge in nitrogen atmosphere, by solving rate equations coupled with acid-base equilibrium, and fitted the results to measurement values in our previous work [3].

2. Calculation methods and conditions

H_2O_2, NO_2^- and NO_3^- are produced in the water, and the pH of the water decreases with plasma exposure. NO_2^- is in acid-base equilibrium with HNO_2 (nitrous acid), and HNO_2 reacts with H_2O_2 to form NO_3^- as shown in Eq. (1) [4]; therefore, the concentrations of H_2O_2, NO_2^-, NO_3^-, and HNO_2 as functions of time t are expressed by rate equations as shown in Eqs. (2)-(7).

$$H_2O_2 + HNO_2 + H^+ \rightarrow NO_3^- + H_2O + 2H^+ \quad (1)$$

$$\frac{d[H_2O_2]}{dt} = F(t)G_{H_2O_2} - k[H_2O_2][HNO_2][H^+] \quad (2)$$

$$\frac{d[NO_2^-]}{dt} = F(t)G_{NO_2^-} \quad (3)$$

$$\frac{d[NO_3^-]}{dt} = F(t)G_{NO_3^-} + k[H_2O_2][HNO_2][H^+] \quad (4)$$

$$\frac{d[HNO_2]}{dt} = -k[H_2O_2][HNO_2][H^+] \quad (5)$$

$$[NO_2^-] = f_{NO_2^-}([NO_2^-]+[HNO_2]) \quad (6)$$

$$[HNO_2] = f_{HNO_2}([NO_2^-]+[HNO_2]) \quad (7)$$

Here, [M], $F(t)$, G_M, k, and f_M represent the concentration of product M, the time variation of flux, the generation rate of product M, rate constant, and the abundance ratio of product M, respectively. The time variation of flux is estimated from the differential coefficient of the measured concentration variations of NO_2^- and NO_3^-, and the abundance ratio is calculated from the pH of water, which is the measured data. The concentrations of H_2O_2, NO_2^-, and NO_3^- are calculated using the 4th order Runge-Kutta method, and fitted to the measurement values by varying G_M and k.

3. Results and discussion

The calculated concentrations of H_2O_2, NO_2^- and NO_3^- as functions of time are in approximate agreement with the measurement values. Therefore, NO_2^- is converted into HNO_2 under acidic conditions, and then HNO_2 reacts with H_2O_2 to form NO_3^-. It is found that the generation rates of H_2O_2, NO_2^- and NO_3^- for the plasma treated water are estimated to be 9.5×10^{-7}, 4.5×10^{-7}, and 2.5×10^{-7} M/s.

4. References

[1] A. Kojtari, T.K. Ercan, J. Smith, G. Friedman, R.B. Sensenig, S. Tyagi, S.G. Joshi, H-F. Ji, and A.D. Brooks, J. Nanomed. Biother. Discov. **4** (2013) 120.
[2] K. Takaki, J. HTSJ, **51** (2012) 64.
[3] K. Takahashi, K. Satoh, H. Itoh, H. Kawaguchi, I. Timoshkin, M. Given, and S. MacGregor, Jpn. J. Appl. Phys. **55** (2016) 07LF01.
[4] G. Merényi, J. Lind, G. Czapski, and S. Goldstein, Inorg. Chem. **42** (2003) 3796.

Topic number: 5

A modified fluid simulation of an inductively coupled plasma discharge with radio frequency bias considering heat transfer effect

Y. D. Jeong[1], Y. J. Lee[1], D. C. Kwon[2], H. H. Choe[1]

[1] *School of Electronics and Information Engineering, Korea Aerospace University, Goyang, Republic of Korea*
[2] *Plasma Technology Research Center, National Fusion Research Institute, Gunsan, Republic of Korea*

The plasma characteristics in an inductively coupled plasma (ICP) discharge with radio frequency bias (RF) were investigated. A two-dimensional axisymmetric structure was simulated by using a modified fluid model. Large and multi-size zones were used for the calculations of the Two-Term Boltzmann approximation electron energy distribution function (EEDF) and ion energy distribution function (IEDF) calculated by using spatial averaged plasma parameters. The energy and mobility of ion were calculated by using the IEDF at each zone. In addition, the heat transfer was considered. Voltage drop across the coils due to the reactance were considered that the capacitive field effect of the antenna was also considered. Effects of these application were analysed.

1. Introduction

Simulations for an inductively coupled plasma (ICP) Argon discharge with radio frequency (RF) bias for semiconductor device processes were conducted and plasma characteristics were investigated.

Although the fluid model, one of the models describing the plasma, has some accuracy problems, it provides relatively rapid computation and satisfactory solution for moderate pressure conditions [1-2]. The simulation model is based on this.

In this study, a two-dimensional axisymmetric structure was used for the simulation. Voltage drop of the antenna coil is considered and this effect was investigated. In addition, the electron energy distribution function (EEDF) was calculated. The EEDF is a dominant factor for determining plasma characteristics, since it is a key parameter in calculations of electron transport properties (e.g., the electron mobility, the electron diffusivity, reaction coefficients). Ion temperature and mobility were computed using particle tracing mechanism. The effects of these applications were studied.

2. Model description

To describe the electrons, the continuity, electron energy balance equation and drift-diffusion approximation were applied. Two-term Boltzmann approximation EEDF was applied to the model. The ion was calculated by adapting the continuity equation and the drift-diffusion approximation. The ion temperature and mobility were computed using the ion energy distribution functions (IEDFs). In addition, the energy and mobility of neutral species were considered. A block diagram for calculation of the ion temperature, mobility and the EEDF is shown Fig. 1.

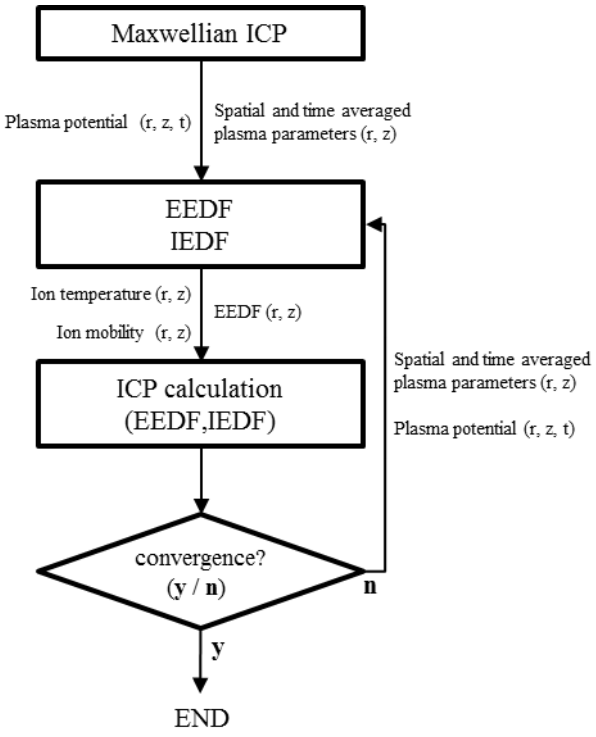

Fig. 1. A block diagram for calculations of the ion temperature, mobility and the EEDF.

3. References

[1] L. L. Alves, L. Marques, Plasma phys. Control. Fusion. 54 (2004) 124012.

[2] J. van Dijk, G. M. W. kroesen, A. Bogaerts, J. Phys D: Appl. Phys. 42 (2009) 190301.

Topic number: 6

A Spiral Microstrip-line Microwave Resonant Probe- for Measurement of Plasma Density

Ying-Chieh. Wu, and Keh-Chyang Leou

Department of Engineering and System Science, National Tsing Hua University, Hsinchu, Taiwan

In this study, a microwave probe (spiral probe, SP) based on a spiral shaped resonant structure is developed for plasma density measurement. The probe structure is a shorted microstrip transmission line operated at half-wavelength resonance. The characteristics of the probe is investigated by employing three dimensional electromagnetic numerical simulation analysis (HFSS, ANSYS Corp) where the plasma is treated as a dielectric with dielectric functions determined by plasma density, microwave frequency and collision frequency of electrons. In the simulation, the resonance frequency is extracted from the reflection spectrum. Simulation results show that a monotonic increase of the resonant frequency with the plasma density.

1. Introduction

The plasma density is one of the key parameters controlling the characteristics of plasma based processes. Thus, a non-invasive sensor, e.g., microwave-based ones, for monitoring, or even feedback control of the plasma density of plasma tools is highly desirable. One popular approach is the resonant-type microwave sensors, where a resonant structure is often employed and the plasma density is determined by the shift of the resonance frequency[1-3]. In our previous work, we have demonstrated a microstrip line microwave interferometer for monitoring of plasma density in plasma tools. In this study, a plasma density probe based on a spiral shaped microstrip microwave resonator, spiral probe (SP), is proposed. The structure of the probe and the measurement system are illustrated in Fig. 1. The probe is constructed by a shorted micro-strip transmission line operated at the half-wavelength resonance.[4] The characteristics of the probe have been investigated by numerical analysis using the High Frequency Structure Simulator (HFSS)[5].

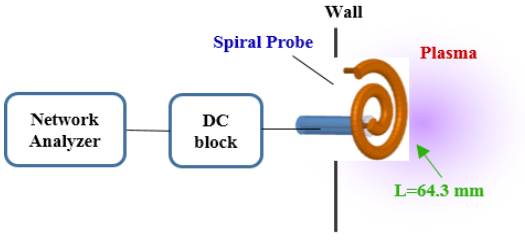

Fig. 1. Structure of Spiral-probe and experimental setup.

2. Simulation result

Figure. 2. shows the electric field distribution at the resonance for plasma density of $5x10^{10}$ cm^{-3}, illustrating the characteristics of half-wave resonance. Figure 3 depicts the microwave reflection spectra for different plasma densities, along with the dependence of the resonance frequencies on the plasma densities, showing a monotonic increase of the resonance frequencies with the plasma densities, as expected.

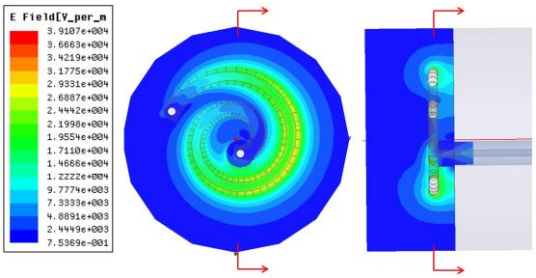

Fig. 2. The electric field distribution at resonance (2.71 GHz) for plasma density of $5x10^{10}$ cm^{-3}.

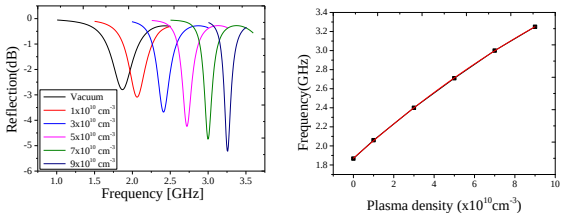

Fig. 3. HFSS simulation results: (a) microwave reflection spectra for different plasma densities, and (b) resonance frequency v.s. plasma density.

3. References

[1] M. Lapke, *et al.*, *Plasma Sources Sci. Technol.*, vol. 20, 2011.
[2] R. B. Piejak, *et al.*, *Appl. Phys.* vol. 95, 2004.
[3] T. Shirakawa and H. Sugai, " *Japan. J. Phys* 32, pp. 5129, 1993.
[4] A. Pandey, *et al.*, *Appl. Phys.* vol. 104, 2014.
[5] C. H. Hsieh, *et al.*, *Plasma Sources Sci. Technol.* vol. 24, 2015.

Topic number: 17

Emergency & critical care medicine for brain disease by irradiation / inhalation of atmospheric pressure plasma flow

T. Hirata[1], C. Kobayashi[1], H. Watanabe[1], S. Matsuda[1], S. Wakita[1], A. Mori[1], Y. Kudo[2], M. Iwashita[3]

[1] *Department of Medical Engineering, Tokyo City University, Tokyo 158-8557, Japan*
[2]*Department of Obstetrics and Gynecology, Hiroshima University, Hiroshima 734-8551, Japan*
[3]*Department of Obstetrics and Gynecology, Kyorin University, Tokyo 181-8611, Japan*

We performed to clarify the healing mechanism by which the irradiation / inhalation using atmospheric pressure (APP) plasma source promotes disease treatments such as burn healing, lung / heart disease treatment, bone regeneration, and cancer treatment. In this paper, the targeted disease treatment is functional recovery of hypoxic ischemic encephalopathy (HIE) by plasma inhalation.

Atmospheric pressure plasma (APP) are indispensable for sterilizing, disinfecting, decomposing hazardous materials, and modifying material surfaces. Clarifying the mechanisms of plasma technologies that are used in practical applications is of critical importance. Against this background, we are trying to clarify the healing mechanism by which the APP inhalation promotes disease treatments. [1-3]

The APP reactor with a coaxial structure is composed of a tungsten wire applied the high voltage inside a glass capillary that is surrounded by a grounded tubular electrode. The following conditions were applied pulse voltage: 5-8 kV; frequency: 1-5 kHz; helium (He) gas flow rate: 1 L/min; plasma irradiation time: 60-120 s.

The hypoxic ischemic encephalopathy (HIE) is a condition in which the brain does not receive enough oxygen. Although any injury and many health conditions can cause a lack of oxygen to the brain, there is no cure for HIE. We accomplished the experiment concerning the functional recovery of HIE by APP inhalation.

The rat HIE model used here involved ligating the common carotid artery with 3-0 silk to induce ischemia in the brain. The 7-day-old rats were allowed to recover for an hour and placed for 2 h in the infant incubator for hypoxia (oxygen (O_2): 8 %, temperature: 37°C). HIE model rats were anesthetized with sevoflurane, nitrous oxide (N_2O), and O_2 using an anesthesia device with a mechanical respirator. The 3-week-old rat HIE model were done the plasma inhalation for two weeks. The experimental conditions of the plasma inhalation are follows; Inhalation-1: plasma including O_2 gas and Inhalation-2: plasma including O_2 + N_2O gas. The rat's head and the brain were diagnosed by using X-ray computed tomography (CT). Here, the CT scanner for experimental animals (Latheta LCT-200, Hitachi, Ltd.) was used for the rat's head imaging.

According to the CT images of rat's brain, left brain in case of the Inhalation-1 is larger than that of Inhalation-2. The aneurysm, cerebral ischemia, and intricately shaped blood vessels were confirmed to the left brain. Especially, the cerebral ischemia makes a further trouble progressed so that not only causing the organization trouble at the cell level but also a rapid oxygen supply may generate a free radical such as super-oxides (OZ).

The APP including N_2O gases has the possibility of influencing the cerebral blood vessel. In addition, the condition of the cerebral ischemia is reported to be ameliorable by the promotion of the endothelial NOS (eNOS) activation in the brain cell.[4] Here, eNOS is a family of enzymes catalyzing the production of NO from L-arginine.

Therefore, it is thought that nitrogen oxides (NOx) such as NO, nitrite (NO_2), and nitrate (NO_3) produced from plasma source and N_2O gas can be expected of the improvement of the hypoxic ischemic encephalopathy.

3. Acknowledgments

The authors thank T. Yoshikawa, R. Tanaka, S. Shigekuni (Plasma Life-science Innovation Team, Department of Medical Engineering, Tokyo City University, Japan) for technical assistance. This study was supported by a Grant-in-Aid for Scientific Research on Innovative Areas (No. 24108010) from the Ministry of Education, Culture, Sports, Science and Technology (MEXT), Japan.

4. References

[1] T. Hirata, C. Tsutsui, A. Mori, T. Kanai, Y. Kudo, T. Izawa, M. Iwashita, XXXIIth International Conference on Phenomena in Ionized Gases (ICPIG), Iasi/Romania, (2015) P4.63

[2] T. Hirata, T. Kishimoto, C. Tsutsui, T. Kanai, A. Mori, Jpn. J. Appl. Phys. **53** (2014) 010302.

[3] C. Tsutsui, M. Lee, G. Takahashi, S. Murata, T. Hirata, T. Kanai, A. Mori: Jpn. J. Appl. Phys. **53** (2014) 060309.

[4] A. Sakamoto, S. T. Ohnishi, T. Ohnishi, R. Ogawa, Brain Res., 554 (1991) 186.

Excitation, recombination and dissociation of molecular cations by electron-impact in cold plasmas: Application to H_2^+, HD^+, BeD^+ and BF^+

N. Pop[1,2], J. Zs. Mezei[1,3,4,5], F. Colboc[1], Y. Moulane[1,6], S. Niyonzima[7], M.D. Epée Epée[8], O. Motapon[9], F. Iacob[10], R. Boata[11],V. Laporta[1], K. Chakrabarti[12], J. Tennyson[13], I.F.Schneider[1]

[1]*LOMC, CNRS, Univ. du Havre, France,* [2]*Politehnica Univ. Timişoara, Romania,* [3]*LAC, CNRS, ENS Cachan and Univ. Paris-Sud, Orsay, France,* [4]*LSPM, CNRS, Univ. Paris 13, France,*
[5]*INRHAS, Debrecen, Hungary,* [6]*LHEPA, Cadi Ayad Univ., Marrakech, Morocco,* [7]*Univ. de Burundi, Bujumbura, Burundi,* [8]*Univ. of Douala, Cameroon,* [9]*Univ. of Maroua, Cameroon,* [10]*West University of Timişoara, Romania*
[11]*Romanian Academy, Timişoara, Romania,* [12]*Scottish Church College, Calcutta, India,*
[13]*University College London, UK.*

Reactive collisions between electrons and molecular cations have a major role in the ionized gases kinetics. Using the Multichannel Quantum Defect Theory, cross sections and rate coefficients have been obtained for different reactions induced by electrons on H_2^+, HD^+, BeH^+ and BF^+ in natural, laboratory and industrial ionized media.

1. Introduction

Dissociative recombination (DR), (ro)vibrational excitation (VE) and de-excitation (VdE), and dissociative excitation [1,2]:

$AB^+(N_i^+,v_i^+)+e^- \rightarrow A+B$, $AB^+(N_f^+,v_f^+)+e^-$, $A+B^++e^-$,

are the dominant elementary processes in numerous cold ionized media. The Multichannel Quantum Defect Theory (MQDT) has been employed for computing state-to-state cross sections and Maxwell rate coefficients relevant for the kinetic plasma models.

2. Results

In order to model and diagnose *the low-temperature fusion edge plasmas*, a complete database for electron-impact collision processes is required for molecular species containing beryllium and hydrogen. We have expanded our studies on BeH^+ [3,4] to BeD^+ and BeT^+ cations. Figure 1 shows as an example the Maxwell rate coefficients for the lowest states (v_i^+= 0-5) of BeD^+, significantly dependent on the initial vibrational level of the molecular ion: Indeed, this figure illustrates the dominance of the DR, while the VdE, clearly higher than the VE, becomes progressively important for high initial vibrational levels of the target.

The electron impact processes on BF^+ are important in the *plasma ion implantation technique* [5]. The calculated rate coefficients have revealed that the vibrational transitions in this case are more important than the dissociative recombination.

And finally, in order to describe the chemistry of the *cold environments* involved in the history of the early Universe, in the *interstellar molecular clouds* and in the *edge of the fusion plasmas*, we have extended our most recent calculations on HD^+ [6] and H_2^+ [7] to higher energy, aiming to provide a complete state-to-state collisional data-base for the hydrogen molecular cations.

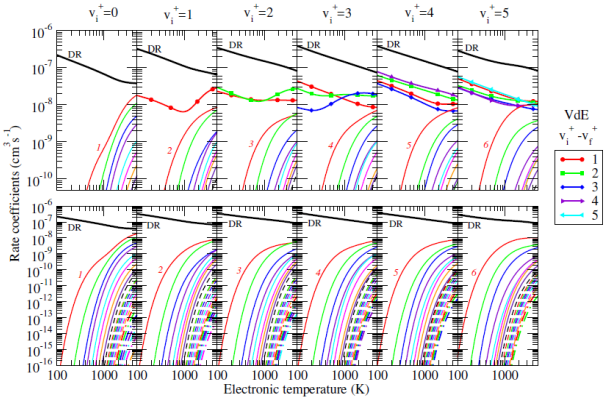

Fig.1. Dissociative recombination (DR, thick line), vibrational excitation (VE, thin lines) and vibrational de-excitation (VdE, symbols and thick lines) Maxwell rate coefficients of first excited (v_i^+ = 0-5) BeD^+ in its electronic ground state. For VE, since the rate coefficients decrease monotonically with the excitation, the lowest final vibrational quantum number of the target is indicated only, and the lower panels extend the range down to 10^{-14} cm^3/s.

In the case of the benchmark ions H_2^+ and HD^+, our reaction rates and cross sections have been thoroughly compared with those measured, mainly in the heavy-ion storage rings [2].

3. References

[1] I. F. Schneider, invited topical talk at this conference.
[2] I. F. Schneider, O. Dulieu, J. Robert, *Proceedings of DR2013: The 9th Int. Conf. on Dissociative Recombination: Theory, Experiment and Applications, Paris, 2013*, EPJ Web of Conferences **84** (2015).
[3] S. Niyonzima *et al.*, *ADNDT* (2017), in press.
[4] V. Laporta *et al*, *PPCP* **59** (2017) 045008.
[5] J. Zs. Mezei *et al.*, *PSST* **25** (2016) 055022.
[6] O. Motapon *et al*, *Phys. Rev. A* **90** (2014) 012706.
[7] M. D. Epée Epée *et al*, *MNRAS* **455** (2015) 276.

Topic number

Measurements of nitrogen and oxygen atom density in N_2/Ar sputtering plasma for fabrication of high-mobility amorphous In_2O_3:Sn films

Masaharu Shiratani[1], T. Takasaki[1], H. Wang[1], K. Matsushima[1], H. Seo[1], K. Koga[1], K. Takeda[2], M. Hori[2], and N. Itagaki[1]

[1] *Kyushu University, 744 Motooka, Nishi-ku, Fukuoka 819-0395, Japan*
[2] *Nagoya University, Furo-cho, Chikusa-ku, Nagoya 464-8603, Japan*

Aiming at clarifing effects of nitrogen on a-ITO film growth in N_2/Ar sputtering plasma, we measure absolute density of nitrogen and oxygen atoms in the plasma. X-ray diffraction analysis show that ITO film is changed from polycrystalline to amorphous by introducing N_2 into the deposition atmosphere. Electron Hall of a-ITO films increases from 14 to 55 cm^2/Vs with increasing N_2 /(Ar + N_2) from 1.5 to 5%, whereas the absolute density of nitrogen atoms in the plasma increases from 1.2×10^{10} to 7.9×10^{10} cm^{-3}. Since the nitrogen composition ratio of a-ITO films is almost constant for N_2 /(Ar + N_2) of 1.5–5%, adsorption/desorption behavior of nitrogen atoms on the growing surface probably brings about changes in film properties.

1. Introduction

Amorphous In_2O_3:Sn (a-ITO) has attracted attention because of the advantages such as surface smoothness, high etching rate, and low internal stress. However, the mobility of conventional a-ITO films, which are generally fabricated by lowering the deposition temperature (<150°C), is much lower than that of polycrystalline ITO films, limiting the use of a-ITO films in practical devices. We have recently developed a new fabrication method of a-ITO films with a high mobility of 61 cm^2/Vs. Here, aiming at clarifing effects of nitrogen and oxygen atoms on a-ITO film growth, we measure the absolute density of nitrogen and oxygen atoms by vacuum ultraviolet absorption spectroscopy (VUVAS) [2].

2. Experimental

ITO films were fabricated on quartz glass substrates at 150°C by radio-frequency (RF) magnetron sputtering. N_2 /(Ar + N_2) of 0–10% was used. The total gas pressure was 0.9 Pa. The supplied RF power was 100 W. Absolute density of nitrogen and oxygen atoms were measured by the VUVAS method.

3. Results and discussion

First, we performed X-ray diffraction analysis of ITO films fabricated at various N_2 /(Ar + N_2). The diffraction peak intensities of In_2O_3 (222) and (400) planes decreases with increasing N_2 /(Ar + N_2) from 0 to 0.65%, and finally there is no peak detected for N_2 /(Ar + N_2) ≥ 1.5%. Figure 1 shows the absolute density of nitrogen and oxygen atoms as a parameter of N_2/(Ar + N_2). The density of nitrogen atoms increases linearly from 1.3×10^{10} to 1.6×10^{11} cm^{-3} with increasing N_2 /(Ar + N_2) from 0 to 10%, whereas the density of oxygen atoms is in the range of 3.9×10^{9}–1.5×10^{10} cm^{-3}. These results suggest that nitrogen atoms inhibit crystallization and disorder the In_2O_3 bixbyte crystal structure, and thus leading to a-ITO films. Electron Hall mobility of a-ITO films increases from 14 to 55 cm^2/Vs with increasing N_2 /(Ar+N_2) from 3 to 5%, while the nitrogen composition ratio of the films is almost constant (10–11 atomic %). Therefore, the improvement in the mobility of a-ITO films for N_2 /(Ar + N_2)=3–5% is caused not by the nitrogen incorporation, but by the adsorption/desorption behavior of nitrogen atoms on the growing surface.

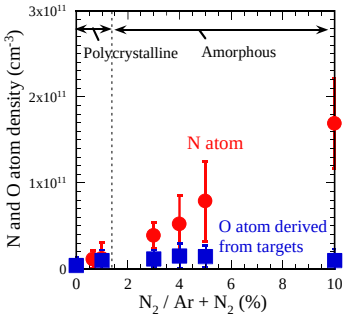

Fig. 1. Absolute density of nitrogen and oxygen atoms in sputtering plasma as a parameter of N_2 /(Ar + N_2).

4. References

[1] T. Takasaki, et al., Proc. 68th GEC/9th ICRP/33rd SPP 60, 9, GT1, 150 (2015).
[2] S. Takashima, M. Hori, T. Goto, A. Kono, M. Ito, and K. Yoneda, Appl. Phys. Lett. 75, (1999) 3929.

5. Acknowledgement

This work was supported by JSPS KAKENHI Grant Number 15H05431.

Topic number: 10

Time–space behaviour of barrier discharge ionization front in presence of 3D textured dielectric layer

I. Topala, G. Borcia

IPARC, Faculty of Physics, Alexandru Ioan Cuza University, Iasi, Romania

Atmospheric-pressure plasma represents particularly suitable technology for treating textiles. Nonetheless, fiber-based materials raise specific issues related to their surface processing, especially for woven materials, due to their particular 3D nature. In this respect, we are exploring the relation between the 3D structural characteristics of woven samples, the plasma parameters during sample exposure and the time–space evolution of the discharge, aiming to establish the role of the heterogeneous nature of the permeable samples, working as supplementary dielectric layer, in controlling the discharge, and thus the plasma processing efficiency. It results that such structures shift the behavior of the discharge and the plasma parameters, depending on the 3D characteristics.

1. Introduction

Woven materials are heterogeneous structures, from mechanical, electrical and chemical point of view, and may shift the behavior of the discharge and the plasma parameters during processing, depending on their 3D characteristics. Taking this into account, we are exploring the relation between the woven structural characteristics, the plasma electrical parameters during sample exposure and the time–space evolution of the discharge.

2. Experimental

The plasma is produced using DBD, in asymmetrical electrode arrangement [1]. The discharge is generated using positive voltage pulses with 5 kV amplitude, 5 kHz frequency, 100 μs width. The DBD parameters are established by electrical measurement. Then, a fast imaging technique using an ICCD was employed to complete the information on the plasma parameters and the time–space behavior of the ionization front.

3. Results and discussion

The voltage and current waveforms show two temporally distinct discharges, so-called primary and secondary discharge, respectively, associated to the HV rising and falling slope.

The current profile for the primary discharge, which ignites due to the externally applied electric field, is different in presence of different samples (Fig. 1), whereas the current profile for the secondary discharge, igniting by the so-called "memory effect", due to the charge deposited on the dielectric surface during the primary discharge, is similar for all samples.

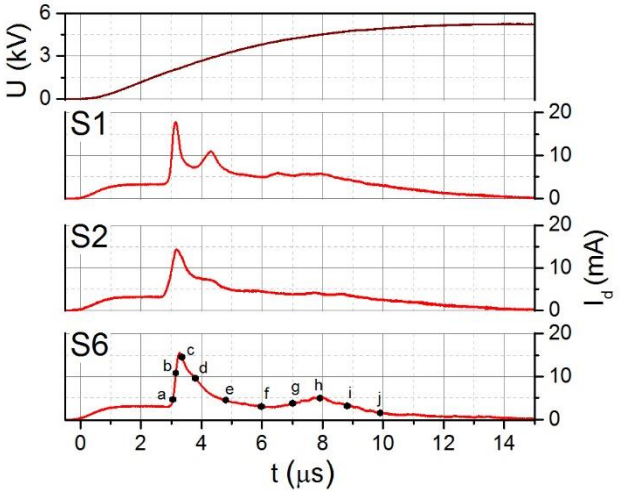

Fig. 1. Current waveforms in presence various fabrics during the HV rising slope.

The amplitude of the current pulse and the discharge energy vary for different samples, resulting that the aspects related to the permeability of the structure, due to its weaving characteristics, play the major role in the behavior of the discharge.

The total light intensity shows different distribution of the discharge regions, for the primary and the secondary discharge.

4. Acknowledgement

CASPIA project, Executive Agency for Higher Education Research Development and Innovation, Romania, PN-II-PT-PCCA-2013, grant 254/2014.

5. References

[1] G.B. Rusu, I. Topala, C. Borcia, N. Dumitrascu, G. Borcia, Plasma Chem. Plasma Process. **36** (2016) 341-354.

Topic number: 14

Air versus Helium atmospheric-pressure plasma for enhanced adhesion of woven textiles

G. B. Rusu, I. Topala, C. Borcia, G. Borcia

IPARC, Faculty of Physics, Alexandru Ioan Cuza University, Iasi, Romania

Atmospheric-pressure plasma treatment is used to improve the dyeing quality of woven structures. A comparison is carried out between inert gas and air atmospheric-pressure plasma, attempting to separate and analyze the physical and chemical plasma effects on the woven, under conditions where oxidation, hence chemical processes, likely superposes on the physical effect. This approach is useful in a context where the separation between combined cleaning – chemistry – roughness modification and their respective roles on the efficiency of the fabric dyeing procedure is more difficult. The results show that air–plasma treatment probably brings a supplementary component to the treatment outcomes, compared to He–plasma, although both treatments are conducting to improved adhesion properties of the woven, resulting in better quality of dyed fibers.

1. Introduction

Plasma treatment has developed markedly due to its potential environmental and efficient energy use benefits, in developing high-performance fiber-based materials.

Taking this into account, we studied the surface modification of synthetic woven textiles, using atmospheric-pressure plasma, for controlled adhesion, targeting improved dyeability, since dyeing is compulsory step for most textiles finishing, also aiming to explore the plasma capability to modulate the permeability of fabrics and the relation between the process parameters and the 3D weaving parameters of the fabrics.

2. Experimental

The reactor consists of a dielectric barrier discharge (DBD), in asymmetrical electrode arrangement. The treated fabrics are six types of commercial polyester woven, presented as raw materials, with different weaving parameters.

Processing is carried out for 30 s. Then, fabric dyeing is performed under industrial conditions, on untreated and plasma-treated samples. Moreover, two different dyeing temperatures are tested.

The materials are then analyzed by the usual wettability/wickability measurement, SEM and XPS, also by evaluation of color changes in the CIELAB color space.

The influence of the plasma treatment on the mechanisms at the interface between the material and a dye solution is established by a diffusion method. The measurement is carried out with the woven placed between two cells and the absorbance measurement is performed until equilibrium is reached in both cells.

3. Results and discussion

The enhanced adhesion properties of the plasma-treated samples are demonstrated by color analysis, with increased color intensity on plasma-treated samples, compared to untreated ones. Also, the air-plasma has demonstrably more pronounced effect on the color intensity, compared to the He-plasma.

The diffusion test is demonstrating the accelerated flow of the dye solution through the textured sample, for air-treated, compared to He-treated samples. The fluid is flowing at higher rate and the saturation of the flow, due to physical obstruction of the woven pores, is visibly limited for air-treated samples. This could suggest that a chemical effect is superposing on the physical cleaning effect of the He-plasma, conducting to better quality of the capillary channels. The plasma effect on loosely weaved structure is more limited, compared to denser structures.

Then, the process rates were evaluated, confirming that in case of the He-plasma treatment, the effect would be dominantly the physical one, whereas the strong modification of both rates for air-treated samples would imply that a chemical effect superposes on the physical one.

4. Conclusion

The results will be further exploited in developing large-scale set-up for air plasma operation, which obviously represents lower cost technological solution.

5. Acknowledgement

CASPIA project, Executive Agency for Higher Education Research Development and Innovation, Romania, PN-II-PT-PCCA-2013, grant 254/2014.

Electric field strength measurement by Stark polarization spectroscopy in diffuse helium-nitrogen barrier discharges

S. Nemschokmichal, R. Tschiersch, and J. Meichsner

Institute of Physics, University of Greifswald, Felix-Hausdorff-Street 6, 17489 Greifswald, Germany

Stark polarization spectroscopy is applied to a diffuse helium-nitrogen barrier discharge to measure the electric field strength. The splitting of the allowed and the forbidden line around 492.2 nm ($4^1D \rightarrow 2^1P^\circ$) as well as the shift of the allowed line are investigated. Both are compared to the electric field strength calculated from the ratio of the singlet lines at 667 nm ($3^1D \rightarrow 2^1P^\circ$) and 728 nm ($3^1S \rightarrow 2^1P^\circ$).

1. Introduction

Discharges in helium with molecular admixtures like nitrogen or oxygen are important for applications at atmospheric pressure because of their ability to produce radicals at low power requirements. For a better understanding of these discharges and to optimize applications, numerical simulations and their comparison with crucial discharge parameters of the experiment are necessary. One of the most important discharge parameter is the electric field strength, which can be determined by Stark polarization spectroscopy [1], and from the intensity ratio of the two singlet lines [2]. The combination of both methods allows a precise absolute calibration by Stark polarization spectroscopy, and a good spatial and temporal resolution by the intensity ratio method.

2. Experimental setup

The investigated discharge is ignited between to plane electrodes, covered by glass plates at a gap distance of 3 mm. The chamber is filled with a mixture of helium and 500 ppm nitrogen at 1 bar. A square wave voltage with a frequency of 5 kHz and an amplitude from 0.8 kV to 1.5 kV is applied. Under these conditions, a diffuse glow-like discharge develops.

The discharge emission is observed by a system consisting of a monochromator (0.75 m focal length, 1800 mm^{-1} grating) and a photomultiplier tube. The photomultiplier signal is amplified and recorded by an oscilloscope, allowing an averaging of up to 50000 signals. For low intensities, as for the Stark splitting line at 492.2 nm, a photon counting procedure is used to improve the signal-to-noise ratio.

3. Results

A typcial example of the Stark spectroscopy measurement is shown in figure 1 for three distances to the cathodic dielectric. Two characteristics are visible: Firstly, the emission maximum appears later for decreasing distance to the cathodic dielectric, which indicates the propagation of the cathode-directed ionizing front. Secondly, the forbidden line becomes more pronounced. Hence, the electric field strength increases towards the cathode, a cathode fall region forms. The limitations of this method are visible as well. The separation of the forbidden line is weak for low electric fields and a large background emission (probably first positive system of nitrogen) exceeds the forbidden line for later times. Therefore, the shift of the allowed line and the line ratio method are used to calculate the electric field for comparison.

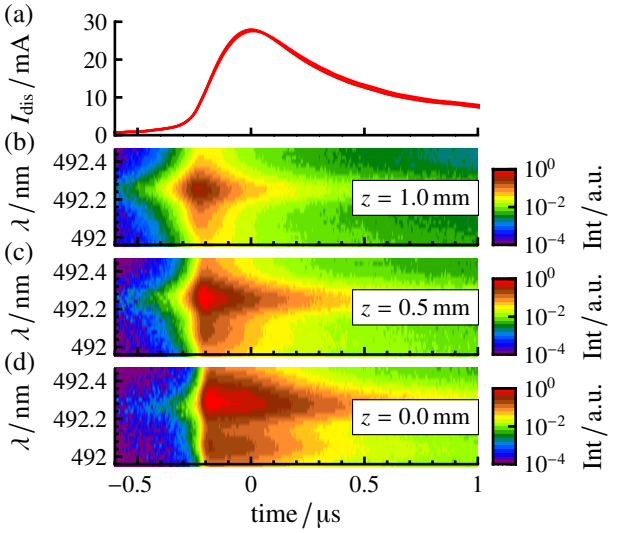

Fig. 1: (a) Discharge current and (b-d) spectrally resolved emission at 492.2 nm for three distances z from the cathodic dielectric.

References

[1] N Cvetanović, M M Martinović, B M Obradović, and M M Kuraica, *J. Phys. D: Appl. Phys.* **48** (2015) p. 205201.

[2] S S Ivković, G B Sretenović, B M Obradović, N Cvetanović, and M M Kuraica, *J. Phys. D: Appl. Phys.* **47** (2014) p. 055204.

Calcium phosphate film formation on TiN surface created by atmospheric-pressure plasma

R. Sannomioya[1], R. Ichiki[1], K. Hanada[2], S. Akamine[1], S. Kanazawa[1]

[1]*Faculty of engineering, Oita University, Oita, Japan*
[2] *Faculty of medicine ,Oita University, Oita, Japan*

We research improvement of biocompatibility of Ti alloy using atmospheric-pressure plasma nitriding. Four types of samples were immersed in simulated body fluid and the calcium phosphate formation on the surface was compared. As a result, the growth of calcium phosphate layer formed on the nitrided sample is the fastest among the samples. These results revealed that biocompatibility of Ti alloy nitrided by atmospheric-pressure plasma was improved.

1. Introduction

In recent years, new surface treatment methods have been developed in order to improve biological characteristics of biocompatible metals such as Ti alloy used in the medical field. Several studies have reported that TiN coating and nitriding of Ti alloy improved biocompatibility. For example, Lin *et al.* proposed that TiN layer can inhibit adhesive property of mutans streptococcus [1]. Moreover, Zhao *et al.* indicated that TiN layer improves adhesive property of osteoblast cells which synthesize bone [2]. In this study, we research improvement of the hard-tissue compatibility of Ti alloy nitride by pulsed-arc (PA) atmospheric pressure plasma jet. [3]

2. Experimental

2.1. PA plasma jet

The sample is Ti-6Al-4V (15×15×4 mm). The experimental system uses PA plasma jet. An external heater surrounds the quartz pipe to control the treatment temperature (1000˚C) so that the samples is uniformly heated. The operating gas is N_2/H_2 gas mixture at the flow ratio of 99:1. Low- frequency voltage pulses (5 kV, 1.2 A, 21 kHz) are applied to the internal electrode, and the external electrode is grounded. This nitriding method is spraying jet plume onto the sample.

2.2. Immersion test

To evaluate the formation ability of calcium phosphate in vitro, samples were immersed in simulated body fluid (Hanks' solution) at 37˚C for 10 days. In order to prove that nitrided sample have good biocompatibility, calcium phosphate formative ability of four types of samples (control, nitrided, high hydrophilicity, high surface roughness) are compared. In addition, samples are masked to determine formed layer, and thickness of film is measured by laser microscope.

3. Results and Discussions

After atmospheric-pressure plasma nitriding, the surface turned to the golden color, corresponding to TiN. Calcium phosphate formed on surface was proved by EDX analysis. Fig. 1 shows comparison of the four types of samples. The growth of calcium phosphate layer of nitrided sample is the fastest among the four samples. In addition, it is revealed that adhesion force of nitrided sample between calcium phosphate layer and substrate is improved. These results implied that atmospheric-pressure plasma nitriding has a high potential to improve the affinity of Ti alloy for osteoblast cells.

This work was supported by JSPS KAKENHI Grant Number 15K17482.

4. References

[1] N. Lin *et al.*, Appl. Surf. Sci. **258**, (2012) 7047.
[2] Y. Zhao *et al.*, ACS Appl. Mater. Interfaces **5**, (2013)1510.
[3] Y. Yoshimitsu *et al.*, Jpn. J. Appl. Phys. **54**, (2015) 030302.

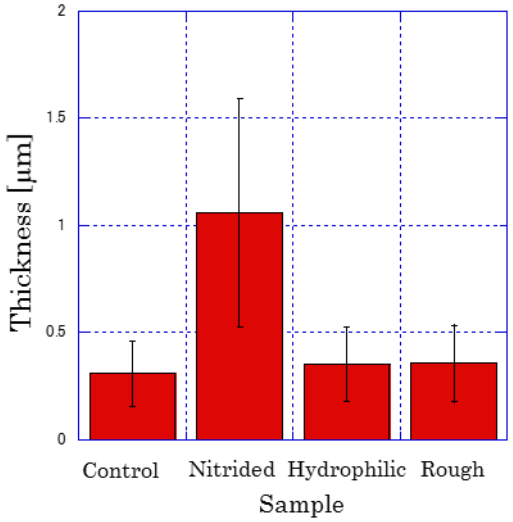

Fig. 1 Thickness of formed calcium phosphate.

Investigation on local formation of expanded austenite phase by atmospheric-pressure plasma jet

A. Maeda[1], R. Ichiki[1], R. Tomizuka[1], H. Nishiguchi[2], T. Onomoto[3]
S. Akamine[1], S. Kanazawa[1]

[1] *Faculty of Engineering, Oita University, Oita, Japan*
[2] *Research Promotion Institute, Oita University, Oita, Japan*
[3] *Fukuoka Industrial Technology Center, Kitakyushu, Japan*

We succeeded in forming expanded austenite phase (S phase) of stainless steel locally by atmospheric-pressure pulsed-arc plasma jet using N_2/H_2. We confirmed the formation of S phase from metallographic structure and XRD patterns. We found that surface hardness increases. This indicates that reduction of passivation film on stainless steel by hydrogen is successful.

1. Introduction

Austenite stainless steel is widely used for food processing equipments and chemical plants due to its good corrosion resistance. However, this steel does not have high hardness and wear resistance. Therefore, the wider application has been limited. To overcome the shortcoming, studies to form S phase on austenite surface has been carried out all over the world [1]. S phase is austenite phase that contains dense nitrogen. This phase has not only good corrosion resistance but also high surface hardness and wear resistance.

We need remove the passivation film of stainless steel surface to diffuse nitrogen. This film is removed by sputtering in low-pressure plasma nitriding. On the other hand, We have developed atmospheric-pressure plasma nitriding as unique technology [2]. However, it is impossible to sputter it in atmospheric-pressure plasma. Therefore, we attempted the use of hydrogen to reduce passivation film to form the S phase by the atmospheric-pressure plasma.

2. Experimental setup

JIS SUS304 (25×25×5 mm^3) was used as a sample. A ceramic heater was used to control treatment temperature to 425°C. N_2/H_2 mixed gas (N_2 97%, H_2 3%) is used as the operating gas. The pulsed voltage of 5 kV and 21 kHz was applied to the inner electrode and the generated jet plume is sprayed onto the sample surface. The duration is 2h.

3. Results and discussions

Metallographic structure of sample cross-section is shown in Fig. 1. The thin film is formed on the outermost surface.

XRD patterns of sample surface is shown in Fig. 2. Here, r is the distance from irradiation center. S and γ indicate the S phase and the base metal, respectively. We can obviously see S from r = 0 to 12 mm. The position of S shifts toward low 2θ with increasing r. This indicates that nitrogen concentration increases with r. This is probably attributed to that surface temperature and diffusion coefficient decrease with r. Moreover, intensity of S decreases with increasing r. This corresponds to that thickness of S phase decreases with r. Additionally, hardness test proved that surface hardness increases.

In conclusion, we succeeded in forming S phase by atmospheric-pressure plasma for the first time. This indicates that reduction of passivation film by hydrogen is successful.

This work was supported by JSPS KAKENHI Grant Number 15K17482.

4. References

[1] Y. Sun *et al*., J. Mater. Sci. **34** (1999) 4793.
[2] H. Nagamatsu *et al*., Surf. Coat. Technol. **225** (2013) 26.

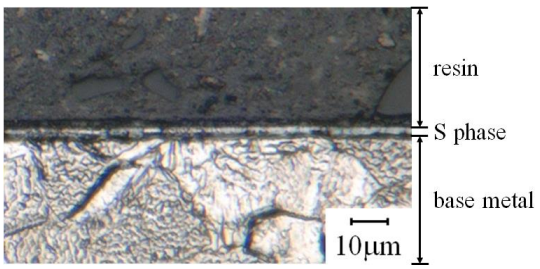

Fig. 1 Metallographic structure of sample cross-section.

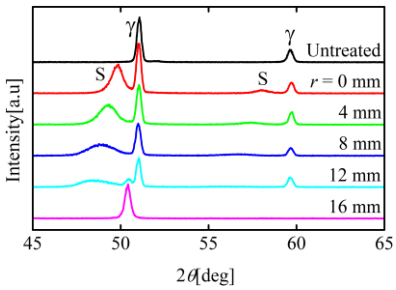

Fig. 2 XRD patterns of sample surface.

Surface charge measurements on different dielectrics in diffuse and filamentary barrier discharges

R. Tschiersch[1], S. Nemschokmichal[1], M. Bogaczyk[2] and J. Meichsner[1]

[1] *Institute of Physics, University of Greifswald, 17489 Greifswald, Germany*
[2] *Leibniz Institute for Plasma Science and Technology, 17489 Greifswald, Germany*

The presented work reports on the successful extension of the surface charge diagnostics via the electro-optic Pockels effect of a bismuth silicon oxide (BSO) crystal to dielectrics used in common barrier discharge configurations, such as borosilicate glass, alumina and magnesia. The focus is on the impact of these dielectrics on the diffuse discharge in helium due to different secondary electron emission coefficients, and on the importance of the surface charge memory effect for the re-ignition behaviour of self-stabilized discharge filaments operated in helium-nitrogen mixtures.

1. Introduction

Previously, we reported on the measurement of surface charges in barrier discharges (BDs) using the electro-optic Pockels effect of a bismuth silicon oxide (BSO) crystal [1,2]. It was shown that the surface charge morphology and dynamics determine the re-ignition behavior of the discharge and its lateral appearance, known as surface memory effect. The present work [3] makes this powerful method accessible to common dielectrics, e.g., borosilicate glass, alumina and magnesia. Fundamental issues are addressed such as the quantitative evidence of the surface memory effect, and the estimation of SEE coefficients for the different dielectrics using Townsend's criterion for the breakdown voltage.

2. Discharge configuration and diagnostics

The discharge is operated inside a plane-parallel electrode configuration shielded by dielectrics on both sides to the gas gap of 3 mm. At the pressure of 1 bar, the diffuse glow-like BD is driven by sine-wave voltage in helium and self-stabilized discharge filaments are operated by square-wave voltage in helium with 10 vol.% nitrogen admixture. Surface charges are measured on borosilicate glass, alumina or magnesia covering the electro-optic BSO crystal. The surface charge diagnostics is based on the change in polarization of light, induced by surface charges on the BSO crystal and detected by a CCD camera. Additionally, current-voltage characteristics as well as the spatio-temporal development of the optical emission from the discharge are measured.

3. Selected results

Figure 1 highlights the outstanding importance of the surface memory effect. In (a), a reduction of the feeding voltage amplitude from 3.2 kV to 2.2 kV causes the transition from arbitrary distributed to self-stabilized discharge filaments, revealed by the averaged surface charge density distribution $\sigma(x,y)$. Each surface charge spot significantly enhances the local electric field across the gas gap, as shown in (b) by the recalculated gap voltage distribution just before the breakdown. At the surrounding region, where no surface charges are present, the gap voltage amounts to 1.6 kV. However, at the center of the surface charge spot, the gap voltage is more than 1 kV higher. This difference in gap voltage distribution explains the periodic re-ignition of the discharge filaments at the same positions as well as the loss in lateral order when the feeding voltage amplitude exceeds about 3 kV.

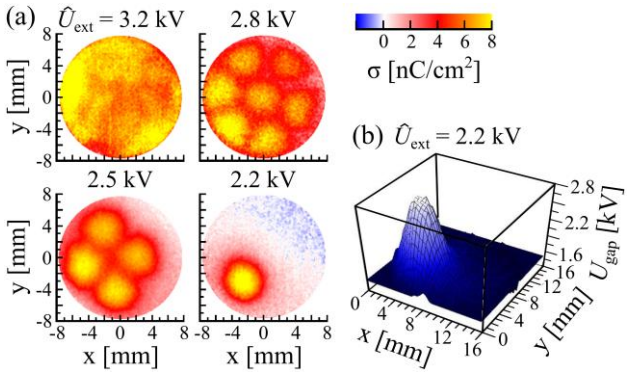

Fig. 1: (a) Surface charge density distribution $\sigma(x,y)$ after the filamentary discharge breakdown for different feeding voltage amplitudes U_{ext}, and (b) gap voltage distribution $U_{gap}(x,y)$. Borosilicate glass on top of the BSO crystal.

4. References

[1] M Bogaczyk, R Wild, L Stollenwerk and H-E Wagner, *J. Phys. D: Appl. Phys*. **45** (2012) 465202

[2] R Tschiersch, M Bogaczyk and H-E Wagner, *J. Phys. D: Appl. Phys*. **47** (2014) 365204

[3] R Tschiersch, S Nemschokmichal, M Bogaczyk and J Meichsner, *J. Phys. D: Appl. Phys*. **50** (2017) 105207

Direct synthesis of hydrogenated graphene using decomposition of hydrocarbons in plasma jet

R. Amirov, E. Isakaev, M. Shavelkina

Joint Institute for High Temperatures of Russian Academy of Sciences, Moscow, Russia

The synthesis of hydrogenated graphene using a high current DC plasma torch has been investigated. In the experiment the hydrocarbons with the working gas (helium, argon, nitrogen) have been introduced into the plasma jet, wherein heating and decompositions of components occurred in the plasma jet followed by condensation of the synthesis product. Products have been characterized by X-ray photoelectron spectroscopy, field emission scanning electron microscopy and Raman spectroscopy. Thermal stability and phase composition of products were evaluated by thermogravimetry and differential scanning calorimetry. It was found that by varying the parameters it was possible to achieve hydrogen to carbon ratio in final product up to 1:4.

1. Introduction

As a derivative of graphene, graphane is a nonmagnetic semiconductor with an energy gap formed by 100% hydrogenation of graphene with stoichiometry CH. Graphane opens new possibilities for the use of carbon based materials in applications involving manipulation of electronic properties, thermal conductivity, hydrogen storage, and magnetization. Graphane usually prepared in two steps by hydrogenation of graphene that was synthesized before.

2. Methods

For the synthesis of hydrogenated graphene in one step a high current DC plasma torch was used. In the experiment the carbon precursors (propane-butane, methane, acetylene) with the working gas (helium, argon, nitrogen) have been introduced into the plasma jet, wherein heating and decompositions of components occurred in the plasma jet followed by condensation of the synthesis product. The plasma torch electric power reached 40 kW. The main parameters were: varying pressure in the range from 150 to 730 Torr and gas flow rate. Products have been characterized by X-ray photoelectron spectroscopy, field emission scanning electron microscopy and Raman spectroscopy. Thermal stability and phase composition of products were evaluated by thermogravimetry and differential scanning calorimetry. Express - gravimetry (vario MICRO cube) method have been used to determine the elemental composition of synthesized product.

3. Results

Experimental results confirmed the possibility of hydrogenation of graphene in its synthesis. Figure 1 shows a typical SEM image of hydrogenated graphene structures that are morphologically identical to the structure obtained by the use of plasma afterglow [1]. Figure 2 presents Raman spectrum of the sample synthesized at 710 Torr using helium and propane-butane plasma. There are two characteristic peaks for graphane G (1581 cm^{-1}) and 2D (2692 cm^{-1}) [2]. D peak located at 1347 cm^{-1} appearing in graphene due to violation of the translational symmetry of the sp2 C-C bonds due to the formation of sp3 C-H bonds. Analysis of 2D peak form shows that the synthesized graphene structures are double-layer.

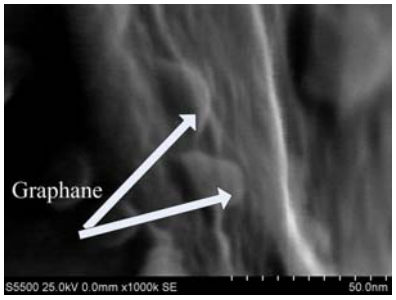

Figure 1. SEM image of graphane

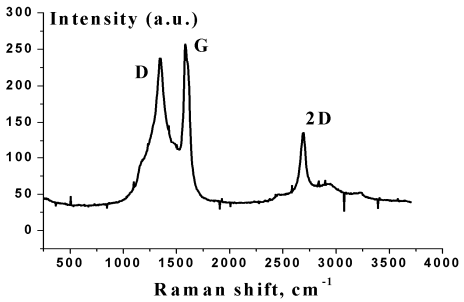

Figure 2. Raman spectrum of hydrogenated graphene

Direct method express - gravimetry found the ratio of the content of H:C in the samples. By varying the synthesis parameters it was possible to achieve hydrogen to carbon ratio up to 1:4.

4. References

[1] B Eren, D. Hug, L. Marot and et al. J. Nanotechnol. **3** (2012) 852.

[2] D.C. Elias, R.R. Nair, T.M.G. Mohiuddin and et al, Science, **323** (2009) 610.

Transport Characteristics of Reactive Oxygen Species in Cell Membranes with Molecular Dynamics - Superposition Effect of Electric Field -

R. Imai[1], S. Uchida[1], F. Tochikubo[1]

[1]*Graduate School of Science and Engineering, Tokyo Metropolitan University, Tokyo, Japan*

Reactive oxygen species generated by plasma irradiation have various medical effects to cell membranes. Efficient transport of reactive oxygen species into cells are essential for those appropriate regulations. Therefore, we focused on the electric field superposition effect during plasma irradiation. In present work, transport behavior of reactive oxygen species under electric field application was simulated using classical molecular dynamics. The threshold of channel formation was 0.4 V/nm, which corresponded to the general breakdown of biological membranes. The z-direction diffusion coefficient of reactive oxygen species greatly increased. The number of hydroperoxy raidcals penetrated into the channel was larger than that of hydrogen peroxide since hydroperoxy radicals accumulate at the interface between water and lipid.

1. Introduction

Recently, some stabilization techniques of atmospheric pressure non-equilibrium plasma have been established. Therefore, plasma medical science is rapidly developing as a new research field. In the field, it has been found that reactive oxygen species (ROS) generated by above plasma are important factors of various medical effects. However, polarized ROS have no significant membrane permeability [1]. We focused on the superposition effect of applied electric field during plasma irradiation. The similar process to electroporation would form water channels in cell membranes and promote the transport of ROS. In the present work, the deformation of cell membrane by electric field application was modeled with classical molecular dynamics. The influence of electric field on the diffusion coefficient of ROS was also discussed.

2. Analytical Method

In the present analysis, dipalmitoylphosphatidyl-choline (DPPC) was selected as typical phospholipid of cell membranes. The analytical membrane model was constructed with 128 DPPC and 3655 water molecules. We adopted force fields of GROMOS43A1-S3 [2] for lipid and SPC for water, respectively. 30 molecules of hydrogen peroxide (H_2O_2), hydroperoxy radical (HO_2) or singlet oxygen ($^1O_2$) were also involved in the membrane model. At first, we equilibrated the pressure, density and temperature of system as to be 1.05 bar, 1000 kg/m^3, and 323 K using Parrinello-Rahman and Nose-Hoover methods. Then, we performed MD simulations of 20 ns using a general software GROMACS 5.1.2. The strength of electric field was varied from 0.1 to 0.5 V/nm. The time step was set to 2.0 fs.

3. Results and Discussion

With respect to the electric filed strength, it was found that the threshold of channel formation was 0.4 V/nm. This value almost corresponded to the general breakdown of cell membranes. For example, Fig. 1 shows the transport dynamics of H_2O_2 at 0.5 V/nm. In this case, the channel formation time was 6.15 ns. As is shown in table 1, the z-direction diffusion coefficient averaged during 1 ns was 230 μm^2/s after channel formation. In comparison with the diffusion coefficient at non-electric field, it is clear that the membrane permeability of H_2O_2 was improved by the assistance of channel. On the other hand, HO_2 easily accumulated at the interface between water and lipid [1]. Consequently, most of HO_2 around membrane surface effectively flowed into the channel.

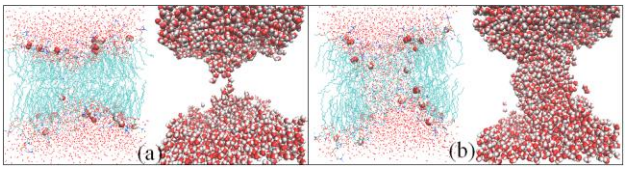

Fig. 1. Transport dynamics of H_2O_2 at 0.5 V/nm of electric field. The transient time is (a) 6.15 ns and (b) 6.75 ns. The right window of each figure represents only water molecules with VDW display style.

Table 1. Dependence of diffusion coefficient of ROS on electric field

Insert	0.5 V/nm [μm^2/s]	Non-electric field [μm^2/s]
H_2O_2	230	1.8
HO_2	279	6.2

4. References

[1] R. M. Cordeiro, *Biochim. Biophys. Acta* **1838** (2014) 438-444

[2] S. W. Chiu, S. A. Pandit, H. L. Scott and E. Jalobsson, *J. Phy. Chem. B* **113** (2009) 2748

A magnetized RF ion source for space propulsion applications

L. Dubois[1], F. Gaboriau[1], L. Liard[1], J.P. Boeuf[1]

[1] *LAPLACE, Université de Toulouse, CNRS, INPT, UPS, 118 Route de Narbonne, 31062 Toulouse, France*

In the framework of an innovative double stage Hall thruster concept, a new magnetized Inductively-Coupled Plasma (ICP) source with internal coil coupling is studied. The coil, inserted in a dielectric tube, is driven by a radiofrequency power supply. An internal magnet is introduced in the coil to confine the plasma. A RF compensated Langmuir probe is used to measure plasma parameters such as ion densities, electron temperatures, and electron energy probability functions. A parametric study is conducted by varying pressure (from 0.5 mTorr to 10 mTorr) and coupled power (from 50W to 200W). A capacitive probe is designed to quantify the capacitive coupling by measuring the radiofrequency plasma potential. Then, a particular focus is placed on the effects of the power supply frequency variation.

1. Issues of Hall thrusters

Hall thrusters are plasma sources that are known to deliver high ion ejection speed, which implies a very high specific impulse. However, since the same electric field provides electron energy for ionization and controls ion acceleration, thrust and specific impulse are closely linked.

In the next generation of satellites, electric propulsion will be used not only for orbit raising but also for station keeping. Thus, an important issue is to design versatile thrusters able to operate efficiently at high thrust and moderate specific impulse or high specific impulse and lower thrust.

2. Toward a double stage Hall thruster

The double stage Hall thruster concept allows to separate control of ionization and acceleration since ionization is provided in a separate plasma source while ion acceleration is performed through a magnetic barrier, as in a standard Hall thruster.

The concept of double stage itself raises practical and fundamental questions. Putting an ion source behind a magnetic barrier may lead to ion losses at the walls or large plasma instabilities [1]. Preliminary studies show that ion losses and instabilities can be minimized if the plasmas source is magnetically confined and placed as close as possible to the acceleration region.

In view of this, we have designed a new concept of double stage thruster. The ionization stage is an **ICP** source with a coil inserted in the central cylinder of the thruster [2]. A closed magnetic circuit is included to confine the plasma and reduce wall losses. This may provide a lower electron temperature and an increase of the electron density. A laboratory prototype based on this concept, called **ID-Hall** (**I**nductive **D**ouble-Stage **Hall** thruster) has been built and is being characterized.

3. Characterization of the ion source

Before integrating all parts of the system, an overall characterization of the plasma without a closed magnetic circuit is presented. The first results were obtained working with Argon using a cylindrical coil driven by a radiofrequency power supply. An internal magnet was added to confine the plasma. We used a RF compensated Langmuir probe and a capacitive probe for the diagnostics.

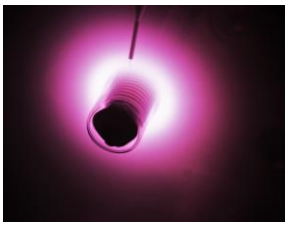

Fig.1: ICP magnetized plasma generated by the coil with internal magnet

In this presentation, we present the first results regarding the electronic densities, temperatures, energy probability functions, and efficiency of coupling. The pressure was varied from 0.5 mTorr to 10 mTorr and the coupled power from 50W to 200W. The influence of the static magnetic field intensity was studied in addition to the **impact of the power supply frequency**.

4. Acknowledgments

This work is supported by CNES. L. Dubois benefits from a PhD fellowship from the University of Toulouse.

5. References

[1] J.P. Boeuf, J. Appl. Phys. **121**, 011101 (2017)

[2] J. Arancibia Monreal, P. Chabert, and V. Godyak, Phys. Plasmas **20**, 103504 (2013).

Topic number: 5

Simulation Study of Radio Frequency Capacitively Coupled CF_4 Plasma Discharge – Hollow Cathode Effect

Chia-Yu Chen and Keh-Chyang Leou

Engineering and System Science Department, National Tsing Hua University, Hsinchu, Taiwan, R. O. C

Capacitively coupled plasma (CCP) sources have been widely used for material processing. In this study, carbon tetrafluoride (CF_4) CCP discharges have been investigated by fluid model numerical simulations (CFD-ACE+, ESI Corp.). The simulation model takes into account 12 gaseous species and 41 reactions, and the discharge is generated by a 27 MHz radio frequency power. Simulation results show that, for typical operation conditions the electron density is around 10^{15} - 10^{16} $1/m^3$ while the electron temperature is about 2 - 4 eV in the bulk plasma. The effect of a trench on the grounded electrode is also investigated. For a trench of dimensions smaller than 6 mm x 12 mm, simulation results reveal that there is a significant modification the spatial profile of the plasma density and flux density of important reactive species, as a result of the hollow cathode effect.

1. Introduction

Capacitively coupled plasma (CCP) sources driven by radio frequency power have been widely used for material processing, e.g., dry etching, plasma enhanced chemical vapor deposition (PECVD), and physical and reactive sputtering processes[1]. There have been also a great of interests to take the advantage of the plasma density enhancement by the hollow cathode effect to find tune the CCP discharge characteristics [2, 3]. In this study, numerical simulation analysis based on 2D fluid model (CFD-ACE+, ESI Corp) is carried out to investigate the effect of a trench in the grounded electrode of a 27 MHz CCP discharge. Both Argon (Ar) and Carbon tetrafluoride (CF_4) plasmas have been investigated for two structures, with and without trench.

2. Simulation results

Figure 1 shows the spatial distributions for basic plasma parameters, such as electron density, F and CF_3^+ number densities, for CF_4 CCP discharges of the two different structures. Figure 2 shows radial profiles for electron density at the center of the gap and the F flux incident on the powered electrode surface for the two cases. It is evident that, for the trench of dimension 6 mm x 12 mm, the density profiles of the important species become strongly modified by the presence of the trench, as a result of the hollow cathode effect. It is also interesting to note that the F flux density is enhanced by the hollow cathode effect by a factor ~2 for the entire radial profile, although the enhancement for the electron density occurs only at position beneath the trench. Simulation results also show that the effect of the trench is minimal for trenches of widths less than 4 mm. This is because the trench dimension would need to be greater than two times the sheath width for the hollow cathode enhancement to be effective[4].

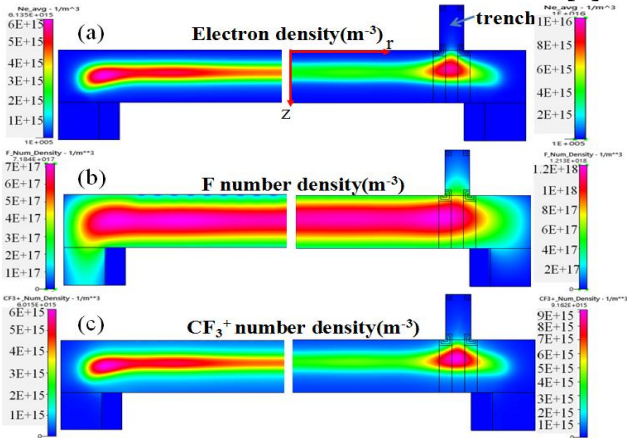

Fig. 1. Simulation results for The spatial profiles of (a) electron density (b) F number density (c) CF_3^+ number density, for the case without (left) and with (right) trench.

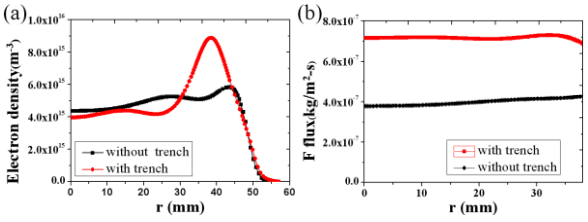

Fig. 2. Simulation results: radial profiles for (a)The electron density at gap center, and (b) F flux density arriving on powered electrode surface.

3. References

[1] M. A. Lieberman. and A. J. Lichtenberg., "Principles of Plasma Discharges and Materials Processing, Processing," (1994).

[2] T. Tabuchi, H. Mizukami, *et al.*, J. Vac. Sci. Technol. A 22 (2004)

[3] Y. Ohtsu, *et al.*, Phys. Plasmas. 23 (2016)

[4] Y. Ohtsu, *et al.*, J. Appl. Phys. 113 (2013).

Plasma activated water – stability and antimicrobial effect

I.E.Vlad[1], C. Martin[1], A.R. Toth[2], J. Papp[2], S.D.Anghel[1]

[1]*Faculty of Physics, Babeş-Bolyai University, M. Kogălniceanu 1, Cluj-Napoca 400084, Romania*
[2]*Faculty of Biology and Geology, Babeş-Bolyai University, Republicii 44, Cluj-Napoca 400015, Romania*

The interface region between plasma and water based liquids offers the perfect conditions for active chemical species like hydrogen peroxide, hydroxyl radical, nitrites and nitrates to be generated. The so formed molecules further diffuse in the treated samples, changing their physical and chemical properties. The current work records the changes induced by a He/Ar μ-jet discharge on distilled water samples. The electrical conductivity, pH value, nitric acid concentration and hydrogen peroxide concentration are measured immediately after treatment and for time intervals up to 21 days. A good stability of the plasma activated water can be observed. Furthermore, the antimicrobial effect of the plasma activated water is proved. The effects of the discharge gas, treatment time as well as storage time are all investigated.

1. Introduction

When plasmas and liquids interact, at the interface region between the two media specific chemical processes occur, producing modifications of the physical and chemical attributes of the liquids [1]. The so activated liquids have proven to hold special properties offering them the possibility of acting as chemical agents in several biological processes [1]. The current work proposes the application of plasma activated water (PAW) in bacterial decontamination and investigates the time evolution of the PAW characteristics as well as its antimicrobial character.

2. Experimental details and results

2.1. Water activation

The water activation by plasma treatment experiments were carried out using a low temperature atmospheric pressure μ-jet setup. It consists of a powered electrode (vertical needle - 0.6 mm i.d., supplied with at a sinusoidal voltage - 1.7 kV, 10.2 MHz) through which the discharge gas (He or Ar) is flown at a 0.3 l/min rate. The distilled water samples are placed 3 mm below the needle. The discharge is formed in the space between the electrode and the surface of the liquid. The treatment time intervals are up to 50 minutes. The physical and chemical properties of the PAW samples were measured immediately after treatment and for time intervals up to 21 days. During this period the samples were stored in closed containers at room temperature.

The pH, electrical conductivity, H_2O_2 and HNO_3 concentrations change strongly with the treatment time. After 50 minutes of treatment using the helium discharge the obtained values are: 1.79 pH units, 1747 μS/cm, 0.9 mM H_2O_2 and 3.6 mM HNO_3. Also, the discharge gas plays a substantial role in determining the final properties of the PAW samples. In the case of the Ar discharge, for the 50 minutes treatment time, the resulted quantities were: 2.19 pH units, 1269 μS/cm, 1.19 mM H_2O_2 and 2.6 mM HNO_3. The analysis of the water properties with the storage time revealed that the properties of the PAW remain stable in time for at least 21 days. For samples treated for 50 minutes with the He μ-jet the measured values after 21 days are: 1.9 pH units, 1820 μS/cm, 0.8 mM H_2O_2 and 3.6 mM HNO_3.

2.2. Bacterial decontamination

The antimicrobial effect of the PAW samples was investigated using *Staphylococcus aureus* (*S.aureus*) as test microorganism. An overnight bacterial culture grown in nutrient broth media was incubated for 24 hours with PAW in 1:1 volume ratios of growth media and PAW. The growth inhibition effect of PAW was estimated by measuring the optical density of the bacterial suspension at 620 nm. Control samples of bacteria incubated with 1:1 volume ratios of nutrient broth and distilled water and samples without dilutions of the nutrient broth were used.

The effects of the water treatment time, discharge gas and storage time were investigated. The PAW shows strong antimicrobial effects. The *S.aureus* sample incubated with the 50 minutes helium discharge treated water shows an OD value of 0.09 a.u. while the water control sample shows an OD value of 0.17 a.u., results that demonstrate a significant influence of the PAW.

3. References

[1] P.J. Bruggeman *et al.*, *Plasma Sources Sci. Technol.*, **25**, 5, (2016) 53002.

Theoretical study on plasma pattern formation and propagation during air breakdown by three intersecting microwave beams

Qianhong Zhou, Zhiwei Dong, Wei Yang

Institute of Applied Physics and Computational Mathematics, Beijing, China

Air breakdown by three intersecting high power microwave (HPM) beams is investigated by numerical solution of fluid-based plasmas equations coupled with the Maxwell equations. For three coherently intersecting HPM beams, interference-field maxima (form a triangular lattice) and minima are created in the intersecting region. The collisional cascade breakdown occurs only if the initial free electron appears or arrives in the vicinity of field maxima, where the free electron can be accelerated. A ball-like plasmoid grows around a field maximum (if there are seed electrons) until its density becomes large enough to diffract the incident field. When the plasma density is larger enough, it scatters the three waves and redistributes the interference pattern. Diffusion and ionization in the closest maximum field leads to the formation of new plasmoids. As time increases, the new plasmoids will form regular patterns and the plasma region enlarges.

1. Introduction

Microwave air breakdown has been extensively investigated since the 1940s. Previously, microwave air breakdown induced by single high power microwave (HPM) beam has been widely investigated[1-5]. However, relatively few studies existed on microwave air breakdown by intersecting microwave beams. Actually, two or more HPM beams are needed to satisfy the power requirement of applications. For example, many HPM beams are sent to the atmosphere with the help of ground-based antennas, in the beam crossing region, where the electric field is particularly large, a gas discharge is set up, i.e. an artificial ionized layer is formed.

In order to successfully use the air breakdown by crossing beams, it is necessary to have a clear understanding of which processes are involved and to what extent. Recently, we have studied microwave air breakdown in the region of two intersecting waves[6,7]. The plasma pattern formation and propagation by two waves is different from that by single wave.

In this paper, Air breakdown by three intersecting HPM beams is investigated by numerical solution of fluid-based plasmas equations coupled with the Maxwell equations. The detailed plasma pattern formation and propagation is investigated for different incident angles.

2. References

[1] Q. Zhou, Z. Dong, Appl. Phys. Lett. 98(2011), 161504.

[2] J. P. Boeuf, B. Chaudhury, G. Q. Zhu, Phys. Rev. Lett. 104(2010) 015002

[3] S. K. Nam, J. P. Verboncoeur, Phys. Rev. Lett. 103(2009) 55004

[4] A. Cook, M. Shapiro, R. Temkin, Appl. Phys. Lett. 97(2010) 011504

[5] V. E. Semenov, E. I. Rakova, M. Yu. Glyavin,G. S. Nusinovich, Phys. Plasma, 23(2016) 073109

[6] Q. Zhou, Z. Dong, Acta Phys. Sin. 62(2013) 205202

[7] Q. Zhou, Z. Dong, Pulsed Power& Plasma Science Conference, San Francisco, CA June 16-21, 2013

Production and study of a plasma confined by a dipole magnet: optical emission spectroscopy and electron energy distribution

Anuj Ram Baitha, Ashwani Kumar and Sudeep Bhattacharjee

Indian Institute of Technology, Kanpur, Uttar Pradesh: 208016

We report a table top experiment to investigate important physical processes in a plasma confined by a dipole magnet. A strong water cooled cylindrical permanent magnet, is employed to create the dipole field inside a vacuum chamber. The plasma is created by electron cyclotron resonance heating, using microwaves of 2.45 GHz. Visual observations (in terms of digital images) of the first plasma, including results of measurements of plasma parameters such as ion density and electron temperature, optical emission spectroscopy and electron energy distribution will be presented in the conference.

1. Introduction

Studies on the properties of a plasma confined by a dipole magnet has been of great interest in plasma physics, since a long time [1–2]. The dipole confinement concept was motivated by spacecraft observations of planetary magnetospheres [3-4]. It is of interest to investigate such a confinement scheme and resulting plasma behaviour in the laboratory. There have been large experiments using superconducting coils to understand underlying complex plasma processes in the dipole plasma [3-4].

In this work we report a compact table top experiment using a permanent magnet to investigate the properties of a plasma confined by a dipole magnet.

2. Experimental set up

In the present experiment, we employ a strong permanent magnet, having a surface magnetic field of ~ 6000 Gauss to create the dipole magnetic field. The magnet is suspended in free space from a top flange in a vacuum chamber and cooled by circulating chilled water. The plasma is heated by electron cyclotron resonance, using microwaves of 2.45 GHz and results in a beta of ~ 2%. The beta can be further increased by using dual frequency heating in the range 6 – 11 GHz using a traveling wave tube amplifier (TWTA), available in the laboratory. The wave powers can be widely varied from a few hundred watts (~ 300 W) in the CW mode to a few kilo watts (~ 7 kW) in the pulsed mode of operation. A schematic of the experimental setup is shown in Fig. 1.

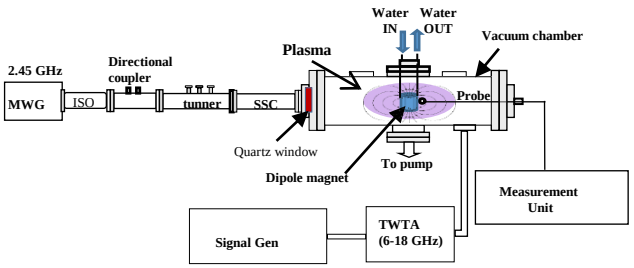

Figure 1. Schematic of the experimental setup SSC: Straight Section, ISO: Isolator, MWG: Microwave Generator.

3. Results

The dipole plasma has been successfully created and the resulting plasma density and electron temperature have been measured in the radial direction. In addition, we have measured the temperature anisotropy of the plasma in a direction parallel and perpendicular to the static magnetic field. We find that the plasma density is peaked a few centimetres away from the magnet and decreases as we go radially outward. The peak plasma density is ~ 1.8×10^{11} cm^{-3} and the electron temperature lies in the range 3 – 14 eV. In addition, optical emission spectroscopy and electron energy distribution function measurements will be presented in the conference.

4. References

[1] Hasegawa, Comments Plasma Phys. Controlled Fusion **1,** 147 (1987)

[2] Birmingham, T. J., Geophys. Res. **74**, 2169-2181 (1969)

[3] Yue Chen, Geoffrey D. Reeves & Reiner H. W. Friedel, Nature Physics **3**, 614 - 617 (2007)

[4] A.C Boxer, R. Bergmann, J.L.Ellsworth, D.T Garnier, J.Kesner, M.E Mauel and P.Woskov. Nature Physics **6**, 207-212 (2010)

Topic number: 14

Tuning the wettability of metallic surfaces by microwave plasma generated low energy noble gas ion beams

S. Chatterjee and S. Bhattacharjee

Department of Physics, Indian Institute of Technology, Kanpur, Uttar Pradesh: 208016, India

Metallic thin films of Cu have been irradiated with different inert gas ions (Ar^+, Kr^+, Ne^+) generated by an intense microwave plasma, in order to look at the changes in wetting behaviour of such irradiated films. Special attention is devoted to look at the static contact angle and contact angle hysteresis. Observations reveal an increasing trend of static, advancing and receding contact angles, indicating that the irradiation process precipitates a reduction in surface free energy which has been related to a change in dispersive intermolecular interaction due to implantation of noble gaseous elements with varying polarizability. The nanoscale roughness generated by this process has no impact on the static contact angle. However, the nominal hysteresis created may be attributed to the roughness according to Johanny-de Gennes theory.

1. Introduction:

Wettability is an important surface phenomena of a solid surface that is determined by the adhesive intermolecular forces between a solid and the liquid in contact [1]. Where there are conventional ways to tune wettability by engineering the surface roughness (the Wenzel regime), chemical texturing (Cassie- Baxter regime), and coating or by forming functionalized chemical groups, the present study looks at the possibility of controlling wetting behaviour of metallic surfaces (Cu) by implantation of inert gas molecules (Ar^+, Kr^+, Ne^+) in the near surface atomic layers. Since inert gas molecules do not form any chemical bond with metal, the system thus formed is heterogeneous in atomic length scales and hence has been termed as "atomically heterogeneous" system.

2. Experimental :

An intense microwave plasma based low energy ion source has been developed and employed in the experiment [2]. The wetting property has been characterised by contact angle and it has been measured by sessile drop method. The surface roughness is characterised by RMS roughness which is obtained by Atomic Force Microscopy (AFM) studies.

2.2. Results and discussions:

Figure 1 shows the variation of static contact angle of de-ionised water on Cu substrates irradiated with different ion beam species. It is observed that the substrate undergoes a transition from hydrophilic to hydrophobic nature indicating a reduction in surface energy.

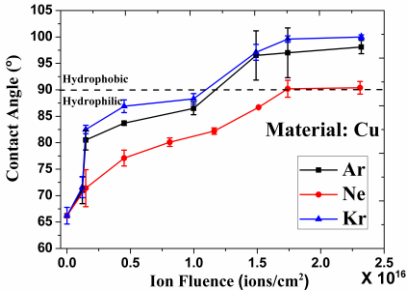

Fig. 1: Variation of water contact angle with fluence for different ion species

It is believed that the dispersive intermolecular force between the metal atoms is perturbed by the presence of inert gas molecule. The resultant surface energy is dictated by the polarizability of the implanted species. However, for real surfaces, the definition of a static, equilibrium contact angle is not unique and the possible values of contact angles are found to lie between the advancing and receding contact angles. We found that both these angles increase with beam fluence and a nominal hysteresis is induced by this process. AFM studies reveal that nanomeric rough surfaces are developed by the irradiation process, which has very little impact on the static contact angle, however, it is responsible for the nominal hysteresis according to the Johanny-de Gennes theory [3]. The details of the analysis will be presented in the conference.

3. References

[1] P.G. de Gennes., Rev. Mod. Phys. **57,** (1985) 827.

[2] A. Chowdhury and S. Bhattacharjee, J Phys. D: Appl Phys, **46**, (2013) 435304.

[3] J. F. Johanny and P. G. de Gennes, J. Chem. Phys, 81, (1984), 1.

Modeling of self-consistent mode formation in an electrostatic plasma lens

I. Litovko[1], A. Goncharov[2], A. Dobrovolskiy[2], A. Bugaev[3], V. Gushenets[3], E. Oks[3]

[1]*Institute for Nuclear Research NAS of Ukraine, Kiev, Ukraine*

[2] *Institute of Physics NAS of Ukraine, Kiev, Ukraine*

[3]*Institute of High Current Electronics, Tomsk, Russia*

Here we described the modeling of self-consistent mode formation in an electrostatic plasma lens under transport through it a wide-aperture, high-current, low energy, metal-ion plasma flow produced by a cathode arc discharge. When the negative potential applied on the central cylindrical lens electrode, a radial directed stream of energetic electrons is formed. The formation of the electric potential jump near the inner surface of the cylinder has been modelled. High-energy electrons appear near the inner cylindrical surface by secondary ion-electron emission under surface bombardment by peripheral flow ions. These energetic electrons can accumulate on axis and provide a mechanism for the plasma flow focusing. It has been shown that the presence of fast electrons in the volume of the plasma lens improves the propagating ion plasma flow.

New approach for devise a novel plasma technology for elimination of micro-droplets or their reduction to the nano-scale from the dense metal ion-plasma flow formed by erosion plasma sources (vacuum arc and laser produced plasma sources), without loss of plasma production efficiency was proposed and described in [1]. This approach is based on application of the cylindrical electrostatic plasma lens configuration for introducing in a volume of propagating along the axis dense low energy ion-plasma flow convergent toward axis energetic electron beam produced self-consistently by ion-electron secondary emission from internal cylindrical surface of plasma lens central electrode (see Fig.1)

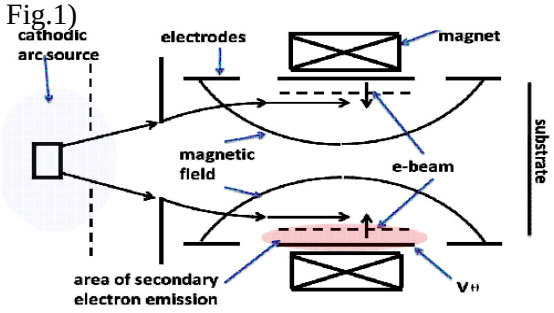

Fig.1. The scheme of model

Here we are modelling the transport through an electrostatic plasma lens of a wide-aperture, high-current, low energy, metal-ion plasma flow produced by a cathodic arc discharge. The lens consists from three electrostatic ring electrodes located in a magnetic field formed by permanent magnets. Modelling parameters were closed to experimental: the lens input aperture - 80 mm, the lens length 140 mm, the outer electrodes are ground and the central electrode voltage up to -3 kV. The plasma is a copper plasma with directed ion energy 20–40 eV, and the equivalent ion current is up to several amperes depending on the potential applied to the central lens electrode.

We modeled of electrical potential jump formation near the inner surface of the cylinder and appearance of self-consistent electron beam across the plasma flow. It is shown that beam is formed by double layer, appeared in a cylindrical channel of the plasma-optical system in crossed radial electrical and longitudinal magnetic fields. It is accelerated by electric potential jump. High-energy electrons appear near the inner cylindrical surface by secondary ion-electron emission at this surface bombardment by peripheral flow ions. Electrons are magnetized and ions are not magnetized. The electron mobility across a magnetic field is strongly suppressed. The electron movement along magnetic field is free up to region of electric potential jump. Under these conditions the magnetic field lines are equipotential up to region of electric potential jump. Thus, the magnetic field lines are equipotential inside flow. Then in space, filled with plasma, the electrical field is created, the form of which is approximately similar the structure of magnetic field lines. Because the electrons of the flow are magnetized, they in the field of the short coil are displaced to its axis, damping expansion of the flow due to electric field of plasma flow polarization. Thus, with increase of magnetic field the near axis density of flow increases. It is shown the energetic electrons accumulate on axis and provide ion focusing. Note that they can also provide additional energy pumping into system for reducing the micro-droplet component in the dense, low-temperature, metal plasma.

[1] A. A. Goncharov, Rev. Sci. Instrum., **87** (2016), 02B901

Activity of catalase enzyme in *P. tomentosa* seeds after direct plasma treatments and treatments with plasma activated water

N. Puač[1], N. Škoro[1], K. Spasić[1], S. Živković[2], M. Milutinović[2], V. Šašić[2], G. Malović[1] and Z.Lj. Petrović[1,3]

[1] *Institute of Physics, University of Belgrade, Pregrevica 118, 11080 Belgrade, Serbia*
[2] *Institute for Biological research "Siniša Stanković", University of Belgrade, B. despota Stefana 142, 11000 Belgrade, Serbia*
[3] *Serbian Academy of Sciences and Arts, Knez Mihailova 35, 11000 Belgrade, Serbia*

In this abstract we report on influence of direct and indirect plasma treatments on catalase enzyme activity in *Paulownia tomentosa* seeds. The direct treatment of the seeds was performed in low-pressure RF plasma system for different treatment times. After treatments these seeds were imbibed with distilled water. The other set of *P. tomentosa* seeds was imbibed with plasma activated water (PAW). PAW was produced by using atmospheric pressure plasma source in treatments with different durations. Seeds from both sets were exposed to the same conditions and after 5 days activity of catalase enzyme was measured. In comparison to the control sample, differences in the activity was observed both regarding direct and PAW treated seeds and regarding duration of treatments.

1. Introduction

Non-equilibrium low and atmospheric pressure plasmas can be efficiently used in stimulation of seed growth, increase of germination percentage and decontamination, breaking of dormancy or increase in the length of seed sprout. We have developed several low pressure and atmospheric pressure plasma systems for treatment of seeds and plant cells [1-3]. Here we will present the results obtained in treatments of *Paulownia tomentosa* seeds by non-equilibrium plasma that operates at low and atmospheric pressures. We have determined the germination percentage and activity of catalase enzyme for all treated samples and compared it to the control samples.

2. Results and discussion

Low pressure plasma treatments of seeds were performed in the cylindrically shaped RF plasma system that operates at 13.56 MHz reactor. The seeds were then imbibed with distilled water. Unlike low pressure plasma treatments where seeds were in direct contact with plasma, in case of atmospheric pressure plasma treatments we have treated distilled water (PAW) which was then used for imbibition of seeds. After the imbibition process seeds were exposed to red light for 5 min. In Figure 1 we show activity of catalyse enzyme 5 days after imbibition of water. The catalase activity for the treated samples is increased comparing to the untreated sample. This is in accordance with the observed increase in germination percentages obtained for this samples.

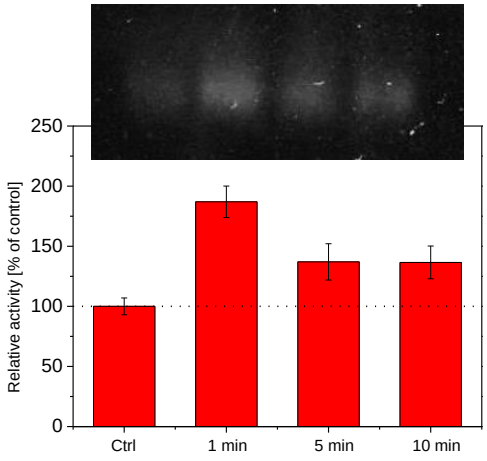

Figure 1. The activity of the catalase enzyme obtained by using native page. Data was obtained five days after the imbibition of water (distilled).

This work was supported by the MESTD of Serbia projects III41011 and ON171037.

3. References

[1] N. Puač, Z.Lj. Petrović, S. Živković, Z. Giba, D. Grubišić and A.R. Đorđević, *Plasma Processes and Polymers*, Wiley-VCH Verlag GmbH & Co. (2005).

[2] N. Puač, Z.Lj. Petrović, G. Malović, A. Đorđević, S. Živković, Z. Giba and D. Grubišić, *J. Phys. D:Appl. Phys.* **39** (2006) 3514-3519.

[3] N. Puač, S. Živković, N. Selaković, M. Milutinović, J. Boljević, G. Malović and Z.Lj. Petrović, *Appl. Phys. Lett.* **104**(21) (2014) 214106.

Topic number : 3

Growth of nano-tendril bundles on tungsten in impurity-rich helium plasmas

D. Hwangbo[1], S. Kajita[2], S. Kawaguchi[1], H. Tanaka[1], N. Ohno[1]

[1] *Graduate School of Engineering, Nagoya University, Nagoya, Japan*
[2] *Institute of Materials and System for Sustainability, Nagoya University, Nagoya, Japan*

Tungsten samples were irradiated with helium plasma which contains impurity gases to investigate the effect of impurity ions on the morphology changes under the sputtering dominant regime. The surfaces of the samples after irradiation were not uniform and the isolated nano-tendril bundles were found on the surfaces when the incident ion energy was higher than the threshold energy of sputtering by He ions. The size of the nano-tendril bundles were several tens μm and this was unexpectedly huge considering the sputtering effect under several hundreds eV of the incident ion energy. This result suggests that the impurity ions may work as an important source to form the isolated nano-tendril bundles.

1. Introduction

It is known that surface morphology changes occur on tungsten (W), one of the most promising candidates of divertor plate material in nuclear fusion devices, when exposed to helium (He) plasmas: nanostructures, so-called fuzz, are formed [1]. The growth mechanisms of the fuzz have been argued in several ways: surface migration by viscoelastic model [2] or adatom diffusion [3], or growth and burst of He bubbles under the surface [4].

It has been known that fuzz growth is affected with sputtering by impurity ions in He plasmas [5]. Here we examine the effect of impurity ions on the morphology changes on the W surfaces when the incident ion energy is higher than the threshold of He ions, It is demonstrated unexpected formation of nano-tendril bundles(NTBs) in impurity-rich He plasma irradiation is introduced.

2. Experimental setup

Experiments were performed in the linear divertor plasma simulator NAGDIS-II. He plasmas were produced in DC arc discharge with the typical electron density and temperature of ~1×10^{19} m^{-2} and ~5 eV, respectively. W samples were installed in the He plasma and biased negatively via a bipolar power supply to control the incident ion energy. The ion flux was in the range of 0.8 - 2×10^{22} $m^{-2}s^{-1}$. To compare the effect of sputtering by impurities, two different discharge conditions were set up by opening/closing the moving valve of turbo molecular pump near the end target of NAGDIS-II. By closing the valve, background pressure was changed from ~6×10^{-7} to ~2×10^{-6} Torr, meaning that the impurity level increased by factor of three. He gas flow was fixed in the range of 150-160 sccm.

3. Results and discussion

After the plasma irradiation with high impurity level condition, although the surfaces of samples were not covered with fuzz, isolated nano-tendril bundles were formed on the surfaces. As shown in Fig. 1, the sizes of the NTBs were over several tens μm, which was unexpectedly huge considering the present condition, such as 500 eV of incident ion energy. The remaining surface where the NTBs were not formed had no fuzz or tiny loops grown. Similar bundles were fabricated with the addition of RF modulation of the ion energy [6]. This result suggests NTBs can also be fabricated without ion energy modulation in the impurity-rich He plasmas.

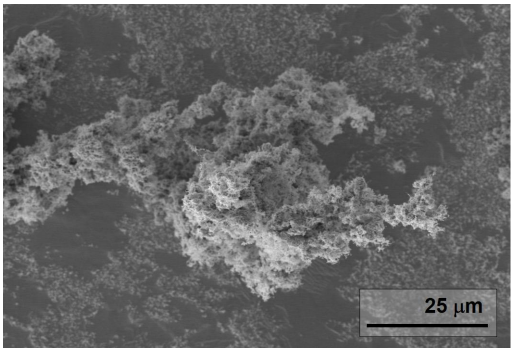

Figure 1. SEM micrograph of nano-tendril bundle with incident ion energy 500 eV.

References

[1] S. Kajita et al., Nucl. Fusion **49** (2009) 095005.
[2] S.I. Kracheninnikov Phys. Src. **T145** (2011) 014040.
[3] D. Trufanov et al., Phys. Procedia **71** (2015) 20.
[4] A.M. Ito et al., Nucl. Fusion **55** (2015) 73013.
[5] T.J. Petty et al., Nucl. Fusion **55** (2015) 093033.
[6] K.B. Woller et al., 26th IAEA FEC, MPT/P5-26, Kyoto, Japan, 2015.

State-by-state emission spectra fitting for non-equilibrium plasmas: OH spectra of surface barrier discharge at argon/water interface

J. Voráč, P. Synek, V. Procházka, T. Hoder

Department of Physical Electronics, Faculty of Science, Masaryk University, Kotlářská 2, Brno, Czech Republic

A novel method of state-by-state fitting of OH(A $^2\Sigma^+ \rightarrow$ X $^2\Pi$) spectra is introduced and applied to a special case of surface dielectric barrier discharge (DBD) in contact with water level. The resulting Boltzmann plot revealed three groups of OH(A $^2\Sigma^+$) - *hot group*, *cold group*, and group influenced by isoenergetic vibrational energy transfer OH(A $^2\Sigma^+$, $v'=1 \rightarrow v'=0$). The state-by-state fitting is incorporated in the *massiveOES* software package and available for free to the scientific community. The linearity of the problem ensures low computational demands - the whole fit for one spectrum takes few seconds on a usual office computer. The Boltzmann plot was extensively analysed, the three groups were decoupled and the of OH production pathways were investigated.

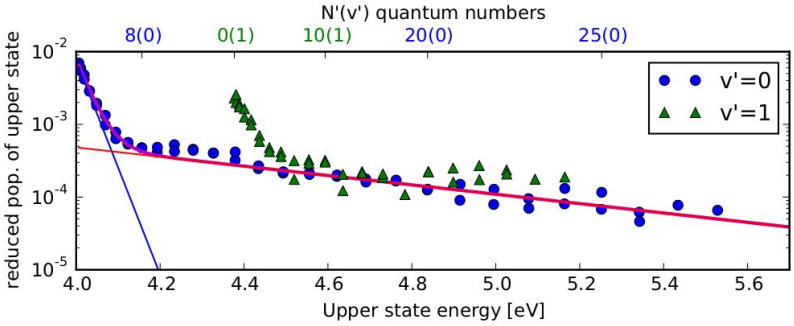

Figure: The population distribution of OH(A $^2\Sigma^+$) rotational states and two-exponential fit. The corresponding temperatures are $T_{rot}^{low} = 340 \pm 30$ K and $T_{rot}^{high} = 7800 \pm 550$ K.

Recently, the interest in discharges in contact with water increased enormously [1]. Often, the discharges are ignited in a noble gas and the atoms and water fragments are the only available spectral signature. In such cases, the spectrum of hydroxyl radical (OH) may seem attractive for neutral gas thermometry. This contribution brings an extensive analysis of OH(A $^2\Sigma^+ \rightarrow$ X $^2\Pi$) spectrum obtained on special case of kHz driven surface DBD in contact with water. As other groups, we have observed a spectrum that may be interpreted as a superposition of emission from several groups of OH. We have distinguished three groups - *cold group*, best observable for low N' quantum numbers, *hot group*, best observable for higher N' quantum numbers and the third group influenced by isoenergetic vibrational energetic transfer OH(A $^2\Sigma^+$, $v'=1 \rightarrow v'=0$), best observable for $9 \leq N' \leq 13$. The unusual accuracy of our Boltzmann plot (see the figure) was enabled by the novel method of state-by-state fitting. This approach combines spectral simulation and traditional Boltzmann construction procedure. A synthetic spectrum is simulated for each rovibronic upper state, including the instrumental broadening and matched with the measurement. Best-fitting linear combination is then searched for. This functionality was incorporated to the *massiveOES* software package [2,3,4].

Acknowledgements

This research was funded by the Czech Science Foundation project 16-09721Y and by the project LO1411 (NPU I) of Ministry of Education Youth and Sports of Czech Republic.

References

[1] P.J. Bruggeman et al. Plasma sources sci. technol. **25**.5 (2016) 053002.

[2] J. Voráč et al. Plasma sources sci. technol. **26**.2 (2017) 025010.

[3] J. Voráč et al. submitted to J. Phys. D: Appl. phys.

[4] massiveOES software package https://bitbucket.org/OES_muni/massiveoes

Charge transfer and ultra-fast imaging of the surface barrier discharge at argon/water interface

P. Synek[1], Yu. S. Akishev[2,3], A. Petryakov[2], N. Trushkin[2], J. Voráč[1], T. Hoder[1]

[1] *Department of Physical Electronics, Masaryk University, Brno, Czech Republic*
[2] *State Research Centre of Russian Federation, TRINITI, Moscow, Russia*
[3] *National Research Nuclear University MEPhI, Moscow, Russia*

We report on time resolved study of the charge transfer and 2D imaging of the surface barrier discharge emerging from liquid electrode in atmospheric pressure argon. Using a precise analysis of the constructed Q-V plots (Lissajous figures) the different modes of the barrier discharge are identified. Electrical signatures found in Q-V plots are linked to the optical appearances recorded by ICCD camera and the mechanisms are discussed. Special nanosecond gated camera enabling multiple expositions in a row for a single discharge event reveal the spatiotemporal development of the discharge luminosity. A light emission of an excited gas prior to the breakdown is detected as well as the subsequent contraction to the streamer-driven filament. The streamer-to-leader transition is evidenced, too.

1. Introduction

Recently, the water containing plasmas attach an intensive attention [1], mostly due to the emerging applications in plasma medicine or polymer surface treatment [2]. A special case of the discharge generation in contact with water is the surface barrier discharge, where one electrode is created by water. Water interface wetting the dielectric surface in gas atmosphere creates so called triple junction or triple line, where the Laplacian electric field can reach highly elevated values if a voltage source is used. As a consequence, transient plasma is generated at this interface. This phenomenon is considered a complication in electro-wetting devices or it can be favourable for polymer surface treatment, as shown in [2] and patented.

2. Experimental results and discussion

The discharge is driven by 100 kHz sine applied voltage and thus the pre-ionization plays an important role here. The applied voltage is connected to the embedded electrode in fused silica cuvette while the deionized water outside the cuvette is grounded. Precise electrical measurements enable the construction of Q-V plots – a charge-voltage phase space attractors describing the dynamical system [3]. Two different modes of the barrier discharge operation are identified. A low-power one, where the discharge is generated just at the triple-line, see in Fig.1, and a high-power one, where the surface of the cuvette is covered by streamer and leader channels. Special nanosecond gated camera enabling multiple short expositions in a row for a single discharge event reveal the spatiotemporal development of the discharge luminosity. The charge accumulation during the pre-breakdown phase is visualised on timescale of units of microseconds. Also a subsequent contraction to the streamer-driven filament is observed. The streamer-to-leader transition is evidenced, spreading the surface charge over a surface area of units of centimetres.

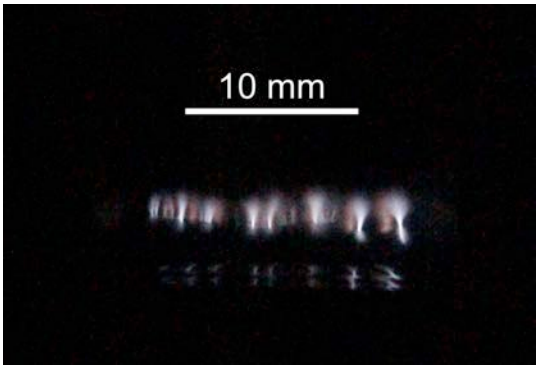

Fig.1: Discharge emerging in argon atmosphere at triple-junction consisting of argon/water/fused silica interface. The triple junction line is created by the elevated water interface wetting the fused silica cuvette. The micro-discharges are reflected at the water surface below.

3. Acknowledgements

This research was funded by the Czech Science Foundation project 16-09721Y and by the project LO1411 (NPU I) of Ministry of Education Youth and Sports of Czech Republic.

4. References

[1] P. Bruggeman et al. Plasma Sources Sci. Technol. **25** (2016) 053002
[2] D. Pavlinák et al. Appl. Phys. Lett. **105** (2014) 154102
[3] P. Synek, Yu. Akishev et al., J. Appl. Phys. to be submitted

Numerical study on the dynamics of He plasma jets with N_2 or O_2 admixtures

P. Viegas, A. Bourdon

LPP, CNRS, Ecole polytechnique, UPMC Univ Paris 06, Univ. Paris-Sud, Observatoire de Paris, Université Paris-Saclay, Sorbonne Universités, PSL Research University, 91128 Palaiseau, France

Simulations performed with a 2D fluid model address the study of the dynamics of Helium plasma jets in dielectric tubes with several admixtures of N_2 or O_2 and different geometrical set-ups, applied voltage waveforms and repetition frequencies, to compare with several experimental conditions. Recently different techniques have been developed to measure the electric field in plasmas jets. In this work, comparisons are carried out between simulations on the electric field measured by an external electro-optic probe and measurements based on the Pockels effect. The influence of different gas mixtures and species kinetics on the jet post-discharge is also addressed. Finally, for repetitive conditions, the influence of initial conditions of species densities and surface charge deposition for the next jet is studied.

1. Introduction

Recently, to tailor the generation of reactive species in plasma jets for biomedical applications, several research groups [1-3] have studied the use of admixtures (mostly O_2 and N_2) to the helium buffer. Furthermore, there exists also a recent interest for the consideration of electric field associated with the plasma plume delivery over tissues, with the development of several different measurement techniques of the electric field [4-7].

In this work, we present a numerical study on the dynamics of a Helium plasma discharge with N_2 or O_2 admixtures in a dielectric tube. At the tube exit, the mixing of helium with air is neglected. However, to be close to experimental conditions a grounded target is set at 1 cm from the tube exit. In this work, we focus on the calculation of electric field and its comparison with experimental results in different conditions (geometry, applied voltage, repetition frequency) for both positive and negative polarities and for different gas mixtures.

2. Numerical model and results

The simulations are performed with a 2D fluid model. In order to study the influence of different amounts of N_2 and O_2 admixture on the helium discharge dynamics, detailed kinetic schemes have been used.

We first compare time-resolved measurements using an electro-optic probe [4] and simulations of longitudinal and radial electric field components, as well as the creation of species such as He*, associated with plasma propagation in the dielectric tube and in the plasma plume. A good agreement is obtained on the dynamics of both components of the electric field during the ionization front propagation in the tube. After the arrival of the ionization front at the grounded target, a rebound of electric field is observed for both positive and negative polarities of the applied voltage. Interestingly, a first increase of the density of He* is observed behind the ionization front and a second increase is observed due to the electric filed rebound. Then, a detailed study of the influence of the geometry of the set-up (electrode inside or outside the tube, location of the target) is presented.

Second, we compare simulations with the technique of measuring the electric field through charge deposition on a dielectric surface perpendicular to jet propagation [6].

Finally, as in most experimental conditions, sinusoidal or repetitive voltage pulses are used, we have studied the post-discharge of a jet for different gas mixtures. The dependence on the gas mixture of the initial conditions at the breakdown of each jet is also obtained for different repetition frequencies. Focus is given to the densities of species left in the gas inside the tube between discharges, as well as to the surface charges left in the tube inner walls.

3. References

[1] S. Iseni, S. Zhang, F. van Gessel, S. Hofmann, B. van Ham, S. Reuter, K.-D. Weltmann and P. Bruggeman, *New J. Phys.* **16** 123011 (2014)

[2] B. van Gessel, R. Brandenburg and P. Bruggeman *Appl. Phys. Lett.* **103** 064103 (2013)

[3] A. Bourdon, T. Darny, F. Pechereau, J.-M. Pouvesle, P. Viegas, S. Iseni and E. Robert, *Plasma Sources Sci. Technol.* **25** 035002 (2016)

[4] T. Darny, C. Douat, V. Puech. J.-M. Pouvesle, S. Dozias and E. Robert, *Proc. of the 6th Int. Conf. on Plasma Medicine*, Bratislava, Slovakia (2016)

[5] A. Sobota et al., *Plasma Sources Sci. Technol.* **25** 065026 (2016)

[6] E. Slikboer, O. Guaitella and A. Sobota, *Plasma Sources Sci. Technol.* **25** 03LT04 (2016)

[7] G. B. Sretenovic, I. B. Krstic, V. V. Kovacevic, B. M. Obradovic and M. M. Kuraica, *J. Phys. D: Appl. Phys.* **47** 102001 (2014)

Gasification of crude glycerine: experimental and theoretical study

Q. Follador[1], D.M.G. Leite[1], A. Essiptchouk[2]

[1] *Instituto Tecnológico de Aeronáutica (ITA), São José dos Campos, SP, Brazil*
[2] *Instituto de Ciência e Tecnologia, São Paulo State University (UNESP), São José dos Campos, Brazil*

Biofuels industry produces demethylated crude glycerine on a large scale, which presents a potential raw material for the production of several high-benefit by-products. The aim of this work is to study the production of synthesis gas from crude glycerine via thermal plasma processing. The experiments were carried out at the plasma-chemical reactor operated at 33 kW. The mean operating temperature was ~1000K and the feedstock flow rate – 5 g/s. The concentration of H_2 and CO on the final gas were 34% and 24%, respectively, as measured by chromatography. The experimental results were compared with numerical simulation of the process, assuming the thermodinamical equilibrium conditions. This study shows that synthesis gas could be effectively produced from crude glycerol through the thermal plasma treatment.

The looking up for alternative energy sources has been proving, over the last years, that reducing the harmful effects, caused by the fossil fuels use, is a right way for improving of the human life quality. A plasma-chemical experimental system is used in this work for the study of biofuel plasma reforming. The system consists of a compact, water-cooled, plasma-chemical reactor working with a transferred arc at atmospheric pressure, a DC power supply, a glycerol supply system, a gas scrubber, and an exhaust fun for controlling of the inside reactor pressure. A mass-spectrometer and a gas chromatograph were used to quantify the components of the produced gases. In order to eliminate moisture before the quantitative analysis the sampling gas was conducted through condenser immersed in a thermostatic bath with the temperature -5°C.

In experiments, the crude glycerine with 15,5% of water and 1.9% of sulphur was used. The flow rate of feedstock was calibrated for 5×10^{-3} kg/s of crude glycerol. The arc current and interelectrode distance were adjusted to operate at power of 33 kW to maintain an average temperature inside the reactor at 1000±50 K during the tests. Small quantity of air, gasification agent, was added. Under these conditions, the sample of produced gas contained 34% of H_2 and 24% of CO with remainder compounds like carbon dioxide, methane, and lights hydrocarbons. In order to evaluate the reforming performance of the experimental system, it was quantified in terms of energy conversion efficiency (relation between the lower heating value of the synthesis gas and sum of the lower heating value of glycerine and the plasma torch power), which attains approximately 36%.

A numerical simulation of the process was carried out in a thermodynamic equilibrium approximation. The obtained experimental data corroborate well with the theoretical results and confirm the potential available in the plasma gasification process of crude glycerine.

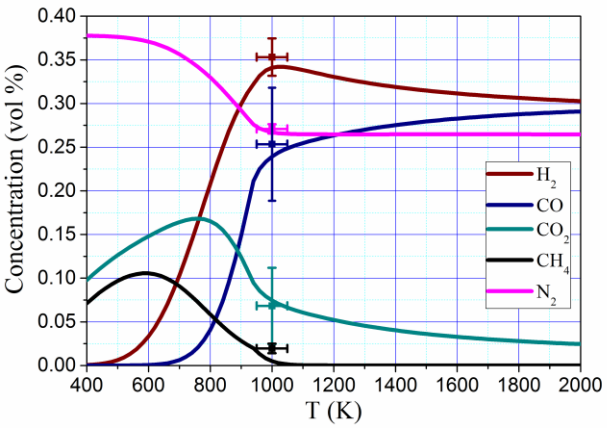

Figure. Numerical simulation (solid lines) versus experimental data (points)

A comparison with experimental works of different authors and methods, [1]-[3], indicates that the reforming process may be improved that requires more detailed studies together with a kinetic modelling.

We acknowledge FAPESP and CAPES for financial support of work.

[1] Tamošiūnas, A., Valatkevičius P., Grigaitienė V., Valinčius V., Striūgas N. J. Cleaner Production 130 (2016) 187

[2] Yoon S.J., Yun, Y.M., Seo M.W., Kim, Y.K., Ra, H.W., Lee, J.G., Int. J. Hydrogen Energy, 38 (2013) 14559.

[3] Zhu X., Hoang T., Lobban L.L., Mallison R.G., Chem Commun (2009) 2908

Bell's instability in the laboratory: pre-experiment simulation study

Chun-Sung Jao[1], Ye Chen[1], Matthias Gross[1], Gregor Loisch[1], Alberto Martinez de la Ossa[2], Jacek Niemiec[3],Jens Osterhof[2], Martin Pohl[1,4], Frank Stephan[1], Sergei Vafin[1,4]

[1] *DESY, Zeuthen, Germany*
[2] *DESY, Hamburg, Germany*
[3] *Institute of Nuclear Physics PAN, Krakow, Poland*
[4] *Institute of Physics and Astronomy, University of Potsdam, Potsdam-Golm, Germany*

The difusive shock acceleration is considered as a process to generate high energy cosmic ray particles. For efficient acceleration, magnetic field fluctuations stronger than the background interstellar field are indispensable in the upstream region of the shock. Bell's instability, a parallel electromagnetic instability driven by streaming cosmic rays, is a candidate for providing the required magnetic turbulence [1]. The properties of Bell's instability had been investigated with MHD studies and PIC simulations [1,2]. We attempt to develop an experiment for testing the saturation level and mechanism of Bell's instability in the laboratory. Here we would present the pre-experiment numerical investigations, based mainly on fully kinetic Particle-In-Cell simulations, that study physical conditions for the Bell's instability to occur in our laboratory experiment and its expected properties.

References

[1] Bell, A. R. 2004, MNRAS, 353, 550
[2] Niemiec, J., Pohl, M., Bret, A., & Stroman, T. 2010, ApJ, 709, 1148

High resolution infrared spectroscopy of ions of astrophysical interest: $H^{35}Cl^+$ and $H^{37}Cl^+$, investigated in a cold plasma

J. L. Doménech[1], I. Tanarro[1], Brian Drouin[2], V. J. Herrero[1], J. Cernicharo[3]

[1]*Inst. de Estructura de la Materia, CSIC, Serrano 123, 28006 Madrid (Spain)* i.tanarro@csic.es
[2]*Jet Propulsion Laboratory, California Institute of Technology, 4800 Oak Grove Drive, Pasadena, CA 91109-8099 (USA)*
[3]*Inst. de Ciencia de Materiales de Madrid, CSIC, Sor Juana Inés de la Cruz 3, 28049 Cantoblanco (Spain)*

In this work we have accurately measured the frequencies of an extensive set of vibration-rotation lines of the v = 1←0 band of $H^{35}Cl^+$ and $H^{37}Cl^+$ in the mid-IR at high spectral resolution, using a difference frequency spectrometer and a hollow cathode discharge reactor. We have also performed an extended and improved isotope independent fit with mm-wave, optical and infrared data. The chloroniumyl cation, HCl^+, was identified for the first time in space in 2012 with the Herschel Space Observatory. Now that the Herschel mission is over, IR observations from ground platforms at high spectral resolution can be an alternative and complementary tool to the mm and sub-mm observations, and a way to build up in the study of HCl^+ and other hydrides.

1. Introduction

The study of interstellar hydrides has received a great push in recent years, much of it due to observations like that of HCl^+ [1,2] from the Herschel Space Observatory. Since hydrides are some of the first molecules to form in space from atomic gas and molecular hydrogen, they provide invaluable information about the environment in which they are found. With the end of the Herschel mission, IR observations from the ground may be one of the few available means to further study this ion in space.

In this work we provide accurate wavenumber measurements of 183 vibration–rotation lines of $H^{35}Cl^+$ and $H^{37}Cl^+$, measured with a difference-frequency laser spectrometer in a hollow cathode discharge, and provide a new and improved global fit of vis-UV, IR and mm-wave spectroscopic data that will aid in future studies of this molecule [3].

2. Experimental set-up

The experimental set-up was described earlier [4]. It is based on an infrared difference-frequency laser spectrometer and a dc modulated hollow cathode discharge reactor with multipass White cell configuration (22.4 m optical path length). The discharge current was 325 mA, with 400 V rms between electrodes. A flowing mixture of ~ 1 mbar He with traces of HCl (<0.001 mbar) was used as gas precursor. The cathode was refrigerated by water or cold N_2. Double modulation in amplitude of the discharge and the laser at two different frequencies in the kHz range, and phase-sensitive detection at the sum frequency, allowed discrimination of absorptions due to longer lived species in the plasma and IR background removal.

The IR radiation was generated by mixing the outputs of an Ar^+ laser and a tuneable ring dye laser in a $LiNbO_3$ crystal contained in a temperature-controlled oven, covering without gaps the 1900–4300 cm^{-1} region with ~ 1 mW IR power. The accuracy (3σ) in the IR frequency was 10 MHz (3.3×10^{-4} cm^{-1}). The instrumental resolution was ~3 MHz (10^{-4} cm^{-1}), so the observed line widths were limited by the Doppler effect.

3. Results

The region studied spanned the 2337–2774 cm^{-1} interval. Atmospheric CO_2 absorption hampered detections at lower frequencies. The figure shows some absorption lines of $H^{35}Cl^+$ as observed and predicted (sticks and convolution with a Gaussian function 0.0055 cm^{-1} FWHM). A kinetic temperature ~400 K was obtained for spectra recorded with water cooling and ~270 K for those recorded with nitrogen cooling of the cathode.

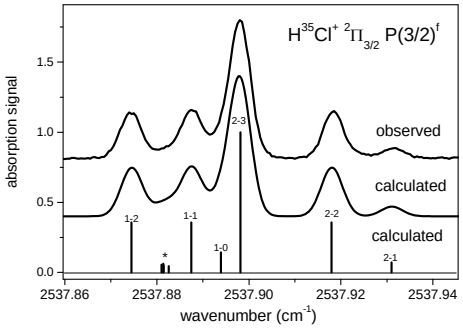

4. References

[1] DeLuca, M., et al. ApJL, 2012, 751, L37.
[2] Gupta, H., et al, ApJL, 2012, 751, L38.
[3] Domenech, J.L. et al. ApJL, 2016, 833, L32.
[4] Domenech, J.L. et al. ApJL, 2013, 771, L11.

Experimental and numerical study of arc commutation and restrikes in Low-Voltage Circuit Breaker (LVCB)

J. Quéméneur[1], J-J. Gonzalez[1], P. Freton[1], P. Joyeux[2]

[1] *Université de Toulouse; UPS, CNRS, INPT; LAPLACE (Laboratoire Plasma et Conversion d'Energie); 118 route de Narbonne, F-31062 Toulouse cedex 9, France*
[2] *Hager Electro SAS, 132 boulevard d'Europe, BP3, 67210 Obernai, France*

An experimental setup and a numerical model to investigate the breaking process in LVCB are presented. The influence of current level, contact opening speed, geometry of the chamber or the materials used for the electrodes are studied using current, voltage, pressure measurements and high-speed imaging. The experimental results are also used to develop a Computational Fluid Model (CFD) based on the commercial Fluent software. When validated, this model is used for a better explanation of experimental observations and can be used for predictions on new configurations that have not been tested. Yet, description of phenomena such as restrike or commutation implies the ignition of a new arc root on the electrode and therefore necessitates taking into account sheath physics and departure from thermal equilibrium. The work done toward such a predictive model of arc behaviour in LVCB will be revealed.

1. Introduction

LVCBs, and in particular Miniature Circuit Breakers (MCB), are classical apparatuses of electrical protection commonly found in houses or offices. When an electrical fault is detected, the LVCB opens its contacts, creating an arc. The arc then commutates on rails and moves toward the splitters plates where it loses its energy and extinguishes due to a current limitation [1]. In the meantime, an arc may appear in the contacts area because the gap is smaller and the gas still hot. This phenomenon, called back-commutation or restrike, causes delay in arc extinction and reduces the efficiency of the LVCB.

Understanding and predicting arc commutation is both a scientific and industrial challenge as a reliable simulation would reduce the need for prototype to be tested in a long and costly empirical development.

2. Experimental setup

To reproduce the current fault we use a capacitor bench that is discharged through and inductor to produce a 50Hz current sine wave up to 10kA. This current supply can be used to test either industrial LVCBs or our test apparatus presented in Fig.1. This setup is composed of a simplified arc chamber and a mechanism to achieve contact opening at a speed chosen between 2 and 8m/s with repeatability and synchronisation. Dedicated post-treatment tools have been developed in order to analyse the experimental data and conduct statistical analyses since breaking arc are rather chaotic.

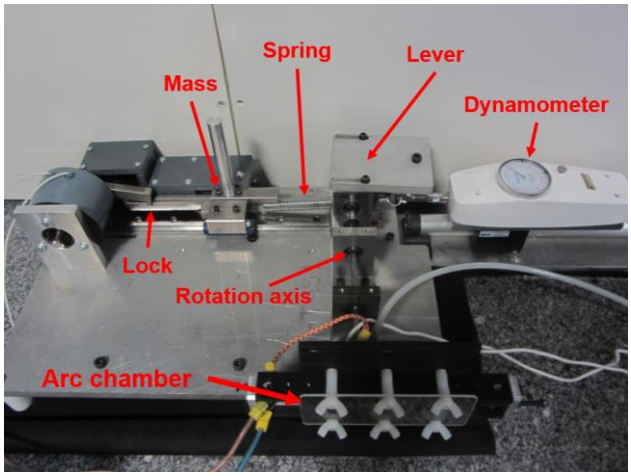

Fig.1: Experimental setup

3. Numerical model

A magneto-hydrodynamic model has been developed to describe the moving arc [2]. Several methods can be used and improvements have to be made in order to simulate commutation and to calculate the electrode fall voltage [3, 4]. Comparison between the behaviour of experimental and simulated arcs will be presented.

4. References

[1] P. Freton & J-J. Gonzalez, The Open Plasma Phys. J. **2** (2009) pp. 105-119

[2] B. Swierczynski & al., J. Phys. D: Appl. Phys. **37** (2004) pp. 595-609

[3] M.Lindmayer & al., IEEE Trans. Comp. Pack. Technol. **29** (2006) pp. 310-317

[4] M.S. Benilov, J. Phys. D: Appl. Phys. **41** (2008) 144001

Synthesis of titanium particles by RF atmospheric plasma jet: continuous mode vs. pulsed mode

A. Lazea-Stoyanova[1,*], V. Marascu[1,2], C. Stancu[1], G. Dinescu[1]

[1] *National Institute for Laser, Plasma and Radiation Physics, 409 Atomistilor street, 077125 Magurele, Bucharest, Romania*

[2] *Faculty of Physics, University of Bucharest, 405 Atomistilor, 077125 Magurele, Bucharest, Romania*

*Email: andrada@infim.ro

By controlling the particle synthesis process one can tailor specific particle's properties, namely size, shape, composition, surface area, etc. In our study titanium particles were obtained using a radio-frequency (RF) plasma jet that operates at atmospheric pressure, in continuous or pulsed mode.

Energy Dispersive X-ray Spectroscopy (EDS) investigations, optical and Scanning Electron Microscopy (SEM) analyses reveal that titanium spherical nano or micro-particles were deposited. The particle's structure, as investigated by Transmission Electron Microscopy (TEM), presents a surface oxide layer. The size, shape and density of the particles is influenced by the plasma parameters (power, frequency or duty cycle).

1. Introduction

In this contribution, we report the use of a RF atmospheric plasma jet to produce titanium particles by means of a gas-phase plasma method. It was found that adjusting the operating plasma mode it is possible to obtain titanium particles with sizes ranging from few hundreds of nm up to few microns. Moreover, tailoring the plasma parameters (power, frequency, duty cycle) particle's characteristics (size, shape and density) are changed drastically.

2. Experimental details and results

2.1. Experimental set-up

The schematic drawing of the set-up is presented by Figure 1 and was described in our previous papers [1].

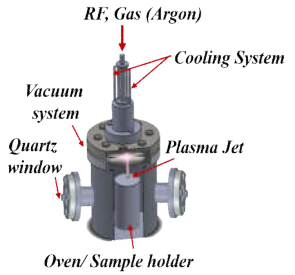

Fig. 1. Experimental set-up for titanium particles synthesis at atmospheric plasma jet

We highlight that titanium powered electrode, connected to a radiofrequency (RF) 13.56 MHz generator, is the starting material for the titanium particles. The particles were obtained using argon (1000 sccm and 5N purity).

Other parameters were: 20 mm the distance between the electrodes, 6 mm the distance between nozzle and Si substrate, 1 h exposure time, 70-200 W power and 1040 mbar operating pressure. When working in pulsed mode frequencies between 1-10 kHz and duty cycles of 20 up to 80% were used.

2.2. Results and conclusions

Spherical non-agglomerated titanium particles are obtained. Their size varies between 200 nm and ~3 μm and have a surface oxide surface layer.

In continuous plasma mode, the synthesis of titanium particles starts at 70 W and their size increases with increasing the RF power (Figure 2).

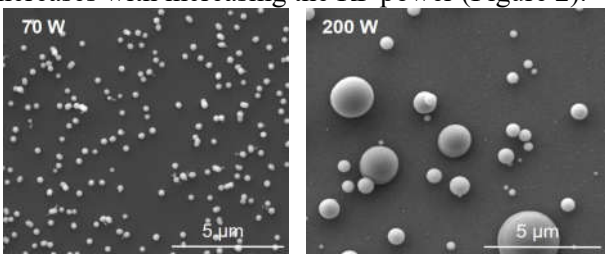

Figure 2. SEM image of titanium particles for 70 W (left) and 200 W (right, obtained in continuous plasma mode).

For pulsed mode, uniform size titanium particles are noticed mostly for high duty cycles (80%) and high frequency (10 kHz).

3. References

[1] A. Lazea-Stoyanova *et. al*, Plasma Processes and Polymers, Vol. 12, Issue 8, 705-709, 2015.

Acknowledgements: This work was supported by a grant of the Romanian National Authority for Scientific Research and Innovation, CNCS – UEFISCDI, project number PN-II-RU-TE-2014-4-2035 and by projects PN16470101-04. V. Marascu acknowledges the support in the frame EUROfusion Consortium, project 1-EU12 WPEDU-RO.

Mobility of Kr^+ ions in Kr for cold plasma modelling

C. Van de Steen[1,2], M. Benhenni[2], R. Kalus[1,3]

[1] *Center of Excellence IT4Innovations, VSB - Technical University of Ostrava, Ostrava, Czech Republic.*
[2] *Laboratoire Plasma et Conversion d'Energie, LAPLACE & UMR5213 du CNRS, Université de Toulouse, UPS, Toulouse, France.*
[3] *Department of Applied Mathematics, VSB - Technical University of Ostrava, Ostrava, Czech Republic.*

Mobilities of Kr^+ ions in Kr plasma are calculated for both states $^2P_{1/2}$ and $^2P_{3/2}$. Collision cross sections are calculated with quantum and JWKB method by using two different internuclear potential models. The collision cross sections are then used in an optimized Monte Carlo code to obtain mobility over a large range of reduced electric field. Kr^+ mobility values are compared to experimental and previously calculated ones found in the literature. This allows us to identify the most reliable potential model used to obtain cross section. Kr^+ mobility values and diffusion coefficient of this work can be used in kinetic models of low temperature plasma to quantify and improve the active species production for better usage in multiple fields.

1. Introduction

The krypton ion swarm data (reduced mobility and diffusion coefficient) are needed to optimise the plasma jet models in applications such as biomedical or spacecraft propulsion.

2. Potential

In this work, two internuclear Kr^+/Kr potential were used for cross section calculation. The first one (calculated by Kalus et al.[1]) was fitted with a cubic spline curve in order to obtain potential values for all internuclear distances. The other potential was obtained by Bonhommeau et al.[2] by fitting ab initio potential values calculated by Ha et al.[3]. Finally, spin orbit coupling was taken into account by using the Cohen-Schneider semiempirical model[4].

3. Method

Two methods were used to obtain momentum transfer cross section, namely quantum method and semiclassical method (using Jeffreys-Wentzel-Kramer-Brillouin (JWKB) approximation). From these cross sections, Kr^+ mobilities in Kr were obtained using an optimised Monte-Carlo method[5].

4. Results

Figure 1a shows that for $^2P_{1/2}$ state, when the Bonhommeau potential is used, a good agreement is observed between calculated and measured Kr^+ mobility in Kr with a maximum deviation of 3%. However for the $^2P_{3/2}$ state (Figure 1b), the deviation between calculated and measured mobilities is higher than in the case of $^2P_{1/2}$ state, reaching a maximum of 26%. Probably, further improvement of Bonhommeau potential will enhance the agreement with measurements.

The present work improves the agreement between calculated and measured mobilities as compared to previous calculations reported in reference [8].

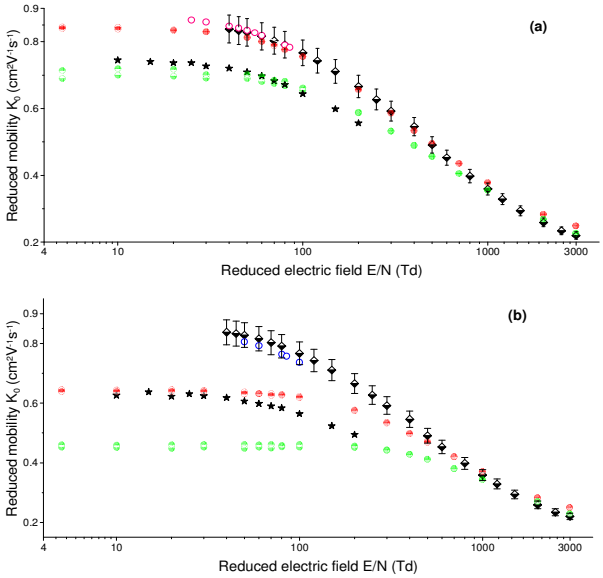

Figure 1: Standard reduced mobility K_0 in $cm^2V^{-1}s^{-1}$ of Kr^+ ions in $^2P_{1/2}$ (a) and $^2P_{3/2}$ (b) state in Kr gas at 293 K and 760 Torr. Exp. value: ○ $^2P_{1/2}$ [6], ○ $^2P_{3/2}$ [6] and ◆ not state resolved[7]. Reported calculation: ★ reference [8]. This work: JWKB method: ◒, ◓, quantum method: ◒, ◓ using potentials of references [1] and [2], respectively.

5. References

[1] R. Kalus et al., Chem. Phys. 294 (2003) 141.

[2] D. Bonhommeau et al., J. Chem. Phys. 124 (2006) 164308.

[3] T. H. Ha et al., Mol. Phys.101 (2003) 827.

[4] J.S. Cohen et al., J. Chem. Phys. 61 (1974) 3230.

[5] M. Yousfi, et al., J. Appl. Phys. 84 (1998) 107.

[6] H. W. Ellis et al., At. Mol. Nuc. Data Tab. 17 (1976) 177.

[7] H. Helm, J. of Phys. B 9 (1976) 2931.

[8] P. N. B. Neves et al., Nuc. Instr. Met. Phys. Res. A 619 (2010) 75.

Effect of non-thermal plasma on the germination and early growth of tomato seeds

M. Magureanu[1], D. Dobrin[1], M. Gidea[2]

[1] *Department of Plasma Physics and Nuclear Fusion, National Institute for Lasers, Plasma and Radiation Physics, Magurele-Bucharest, Romania*
[2] *University of Agronomic Sciences and Veterinary Medicine, Bucharest, Romania*

The influence of non-thermal plasma on tomato seeds has been investigated using a fluidized bed DBD reactor. The discharge was generated in air at atmospheric pressure and room temperature using sinusoidal voltage of 50 Hz frequency and 18 kV amplitude. It was found that plasma slightly enhanced germination rate and significantly influenced growth parameters. The roots and sprouts of plasma treated seeds were longer than those of the untreated samples, for treatment durations of 5-30 min. The effect is more pronounced for the root length. The most substantial increase was obtained for seeds treated in plasma for 5 min: the average root length was 2.88 cm, while for the control samples it was 1.01 cm.

Non-thermal plasma started to be investigated in the field of agricultural science as an alternative to traditional pre-sowing seed treatment. Early work on plasma treatment of seeds was carried out at low pressure, in RF and microwave discharges [1,2]. More recently, atmospheric pressure plasma started to be studied for this purpose [3,4]. Generally, it was found that seed germination was accelerated and plant growth was stimulated as a result of plasma exposure [1-4]. Various mechanisms are proposed to explain this effect, from modification of seed surface, influencing wettability and water uptake [2-5] to deeper changes affecting seed metabolism [3].

In the present experiments, tomato seeds were exposed to plasma generated in a dielectric barrier discharge (DBD) at atmospheric pressure, with high air flow (15 L/min), so that the seeds are held in suspension within the discharge zone. The expected advantage of this fluidized bed reactor is the more uniform treatment of the seeds due to their continuous movement in the plasma region. A coaxial DBD reactor was used, with sinusoidal voltage of 18 kV amplitude and 50 Hz frequency.

The distributions of plants as a function of their root and sprout lengths are shown in Fig. 1. The germination increased slightly as a result of plasma exposure: 68% - control seeds, 77% - seeds treated for 5 min. The roots and sprouts of plasma treated seeds (t=5-30 min) were longer than those of the control ones. The most substantial increase in length was obtained for seeds exposed to plasma for 5 min: the mean root length (MRL) was 2.88 cm as compared to 1.01 cm for untreated seeds and the mean sprout length (MSL) was 3.3 cm as compared to 2 cm for control seeds.

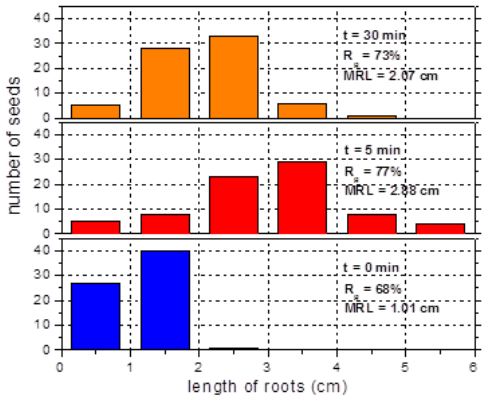

(a)

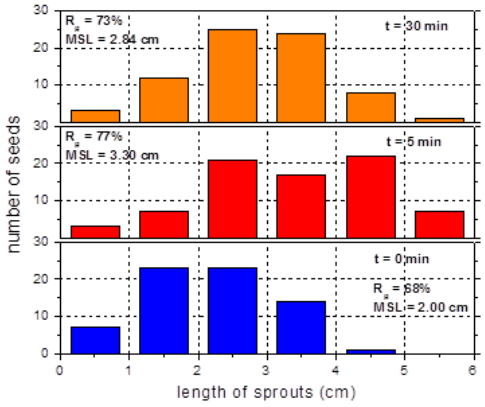

(b)

Fig. 1. Distribution of plants as a function of: (a) – root length; (b) – sprout length for control seeds (t = 0 min) and for seeds treated in plasma for 5 and 30 minutes

[1] S. Zivkovic et al., Seed Sci.Technol. **32** (2004) 693
[2] B. Sera et al., Plasma Sci. Technol. **10** (2008) 506
[3] T. Stolarik et al., Plasma Chem. Plasma Process. **35** (2015) 659
[4] D. Dobrin et al., Innov. Food Sci. Emerg. Technol. **29** (2015) 255
[5] E. Bormashenko et al., Sci. Rep. **2** (2012) 741

Analysis of secondary electron emission coefficients from Paschen curves using Monte Carlo simulations

T. Yoshinaga[1] and H. Akashi[1]

[1] *National Defense Academy of Japan, Yokosuka, Japan*

A Monte Carlo simulation and a simple one-dimensional analysis are applied to explore the possibility to evaluate the secondary electron emission coefficients for ions (γ_i) and photons (γ_p) concurrently. On the assumption that γ_i and γ_p are independent of the reduced field, those values are evaluated to reproduce the experimental Paschen curves for Ar and Ne. The effects of the initial electrons' energy and the reflection coefficient of the cathode are also studied. The values of γ_i and γ_p which reproduces the experimental Paschen curves in good agreement are obtained when the initial energy of Maxwellian distribution at 3.2 eV and the lower reflection coefficients at 0 or 0.1 are assumed.

Secondary Electron Emission (SEE) coefficient (γ) is one of the most important parameters in discharge phenomena since it determines the breakdown voltage (V_{bd}). A commonly used method to evaluate γ is based on the Townsend discharge criterion [1],

$$\gamma \cdot [\exp(\alpha d) - 1] = 1. \qquad (1)$$

Here, α is the first Townsend coefficient which is derived from V_{bd}, and d is the gap distance between the parallel plane electrodes. Since α is essentially a function of the reduced electric field (E/p), γ also depends on the discharge conditions. The SEE effects of other particles than ions would originate the dependency as well as the backward diffusion [2].

The purpose of the present study is to explore the possibility to derive γ for ions (γ_i) and photons (γ_p) concurrently from the experimentally obtained Paschen curves. A Monte Carlo (MC) simulation is applied to calculate the number of collision events for ionization (S_i), excitation to metastable states (S_{ms}) and to other permitted states (S_{ex}) per initial electron emitted from the cathode. From a simple one-dimensional analysis, which assumes no recombination and no reabsorption of photons, the particle fluxes of ions (Γ_i), photons (Γ_p) and metastable species (Γ_m) are estimated as follows,

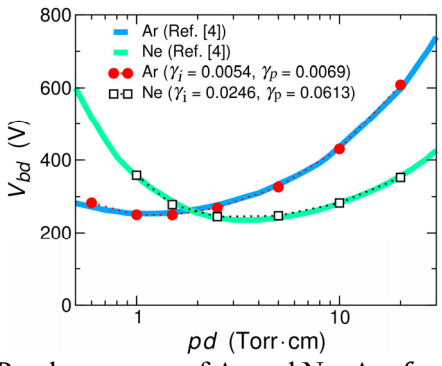

Fig. 1. Paschen curves of Ar and Ne. Ar: $f_{refl} = 0$ at 3.2 eV. Ne: $f_{refl} = 0.1$ at 3.2 eV

$$\Gamma_i = S_i = f_{eff} \cdot [\exp(\alpha d) - 1],$$
$$\Gamma_p = S_{ex}/2,$$
$$\Gamma_m = S_{ms} \cdot [1/\alpha d - f_{eff}/S_i].$$

f_{eff} is the fraction of initial electrons which escaped from the backward diffusion and penetrates into the discharge space. Instead of Eq. (1) the breakdown condition can be expressed as,

$$\gamma_i\Gamma_i + \gamma_p\Gamma_p + \gamma_m\Gamma_m = 1. \qquad (2)$$

Here, γ_m corresponds to the SEE coefficient for metastable species. Eight types of collision cross sections are included in the MC simulations [3].

The values of γ_i and γ_p are evaluated to reproduce the experimental Paschen curves of Argon and Neon [4] on the assumption that they are independent of E/p and that γ_m is equal to γ_i. The effect of γ_m is small compared with that of γ_i since Γ_m is less than 10 % of Γ_i. The effects of the initial electron energy distribution, which is assumed as the Maxwell distribution at 0.1, 0.32, 1.0, 3.2, and 10 eV, are considered as well as the reflection coefficient (f_{refl}) of the cathode at 0, 0.1, 0.2, 0.5, and 1.0. As a result, 3.2 eV produced the least square errors for both Ar and Ne, while f_{refl} at 0 and 0.1 produced the least square errors for Ar and Ne, respectively. Both of the fitted curves agree well with the experimental values as shown in Fig. 1. This result suggests that the consideration of γ_p in addition to γ_i can reproduce the V_{bd} characteristics. The concurrent estimation of γ_i and γ_p which are independent of the external discharge conditions such as E/p might be possible.

[1] G. Auday *et al*, *J. Appl. Phys.* **88** (2000) 4871.
[2] A. V. Phelps *et al*, *Plasma Sources Sci. Technol.* **8** (1999) R21.
[3] The Institute of Electrical Engineers of Japan, http://dpc.nifs.ac.jp/DB/IEEJ
[4] Radio Corporation of America, Electron Tube Design (1962) 792.

Plasma based N-graphene synthesis – *in-situ* and post treatment approaches

N. Bundaleska[1], A. Dias[1], E. Felizardo[1], J. Henriques[1], F.M. Dias[1], N. Bundaleski[2], O. M. N. D. Teodoro[2] M. Abrashev[3], J. Kissovski[3], U Cvelbar[4] and E. Tatarova[1]

[1] *Instituto de Plasmas e Fusão Nuclear, Instituto Superior Técnico, Universidade de Lisboa, Lisboa, Portugal*
[2] *Departamento de Física, Faculdade de Ciências e Tecnologia, Universidade Nova de Lisboa, 2829-516 Portugal*
[3] *Faculty of Physics, Sofia University, 1164 Sofia, Bulgaria*
[4] *Department for Surface Engineering and Optoelectronics F4, Jožef Štefan Institute, Ljubljana 1000, Slovenia*

Free-standing N-graphene sheets were synthesized by graphene post treatment in a low-pressure microwave N_2-Ar large-scale plasma reactor. The graphene sheets were placed in the remote plasma region, where they were treated for various durations and gas mixture compositions. Optical emission spectroscopy was used to diagnose the plasma source. The N-doped graphene sheets were analyzed by applying scanning and transmission electron microscopy, Raman, X-ray photoelectron, and Fourier-transform IR spectroscopy techniques. *In situ* synthesis of N-graphene was also achieved in a single step method by introducing N-containing precursor together with carbon precursor in the reactive microwave plasma environment at atmospheric pressure.

1. Introduction

N-graphene demonstrates outstanding electrochemical properties and shows better performance as catalyst than commercially available Pt-based electrodes [1-3]. Numerous methods for synthesis of N-graphene, such as chemical vapour deposition, bottom-up synthesis, wet chemical methods, plasma methods etc., which can be categorized into *in situ* and post-treatment approaches, were developed. In situ methods allow simultaneous graphene synthesis and N-doping, whilst in post-treatment previously fabricated graphene is further doped with nitrogen. In this study, plasma-based methods of N-graphene synthesis both in situ and post-treatment are presented.

2. Synthesis methods

In the frame of post-treatment N-graphene fabrication, free-standing graphene sheets were first synthesized using microwave argon plasma working at atmospheric pressure conditions. The method is based on injecting a carbon-containing precursor (ethanol) into the active plasma zone, where decomposition of ethanol into carbon atoms and molecules take place. Gas-phase carbon atoms/molecules diffuse into the colder zones and aggregate into solid carbon nuclei. The main stream of carbon nuclei is withdrawn into the outlet plasma zone, where the processes of assembly and growth take place. Selective synthesis of free-standing sheets is achieved via tailoring of the microwave plasma environment only. Afterwards, the produced graphene sheets are immersed into the remote plasma region of a low pressure N_2-Ar discharge. Raman and XPS analysis of the produced structures demonstrate that the doping level and type of functional groups attached to the graphene lattice can be controlled by changing the exposure time, while keeping the nitrogen percentage constant. The nitrogen atoms were incorporated into the hexagonal carbon lattice in pyridinic, pyrrolic and quaternary functional groups, mainly.

Microwave argon plasma working at atmospheric pressure was used to directly create N-graphene by passing through the active plasma environment ammonia solution in ethanol. This way the N-graphene sheets are synthesized in a single step by actively controlling the gas temperature and nitrogen/carbon atom fluxes.

3. References

[1] H. Choi, S. Jung, J. Seo, D.W. Chang, L. Dai and J. Baek Nano Energy **1** (2012) 534

[2] E. Tatarova, N. Bundaleska, J.Ph. Sarrette and C.M.Ferreira Plasma Sources Sci. Technol. **23** (2014) 063002

[3] A. Dias, N. Bundaleski, E. Tatarova, F.M. Dias, M. Abrashev, U. Cvelbar, O.M.N.D. Teodoro, J. Henriques J. Phys. D: Appl. Phys. **49** (2016) 055307

Acknowledgements

This work was funded by Portuguese FCT—Fundação para a Ciência e a Tecnologia, under Project UID/FIS/50010/2013, Project INCENTIVO/FIS/LA0010/2014, and grant SFRH/BD/52413/2013 (PD-F APPLAuSE).

Topic number: 8

Quantification of UV/VUV photon fluxes of hydrogen plasmas by spectroscopy and by collisional radiative modelling

U. Fantz[1,2], S. Briefi[2], R. Friedl[2], C. Fröhler[1], D. Rauner[1], D. Wünderlich[1]

[1]*Max-Planck-Institut für Plasmaphysik, Boltzmannstr. 2, D-85748 Garching, Germany*
[2]*AG Experimentelle Plasmaphysik, Universität Augsburg, Universitätsstr. 1, D-86159 Augsburg, Germany*

Photon fluxes are derived from absolutely calibrated UV/VUV spectroscopic measurements at a planar ICP discharge at 2 MHz in the pressure range of 1 Pa to 10 Pa. It is shown that the photon fluxes are comparable or even slightly higher than the ion fluxes onto a surface making it necessary to consider their impact for surface treatment processes. In order to predict photon fluxes for other parameters, collisional radiative modelling is used taking into account opacity effects of the Lyman lines. For the molecules ro-vibrationally resolved Corona models are used for deriving photon fluxes in different wavelength regions.

Hydrogen plasmas exhibit intense molecular and atomic radiation in the UV/VUV range. Besides the Lyman lines, the resonant Lyman (B–X transition) and Werner band (C–X transition) of the molecule are most prominent in the wavelength region 90 nm to 170 nm, partly overlapping each other [1]. The radiation of the continuum transition (a–b) in the triplet system is less intense but ranges from 120 nm to 600 nm with its maximum around 200 nm. In contrast to the radiation in the visible spectral range, the energy of the UV/VUV photons is much higher, ranging from several eV up to above ten eV. Hence, UV/VUV photon fluxes onto surfaces can become relevant for controlling surface treatment processes.

Previous investigations on photon fluxes and radiant power of UV/VUV photons in hydrogen and nitrogen plasmas for a cylindrical ICP [1] revealed that about 20% of the RF power delivered by the generator is radiated. The photon fluxes are in the range of 5×10^{20} $m^{-2}s^{-1}$ and thus close to the ion fluxes at the pressure of 3 Pa.

The present investigations focus on measurements in a planar ICP at 2 MHz and power levels up to 1 kW allowing for studying photon fluxes in the pressure range from 1 Pa to 10 Pa. Figure 1 shows that, at a pressure of 3 Pa, the photon flux in the VUV is distributed between the L_α line, the Lyman band (representing photons in the energy range of 6.5 – 9.5 eV) and the measured interval of the Werner band (photon energies between 9.5 eV and 10.3 eV) with slightly decreasing contributions. The measured values are compared to calculations based either on the collisional radiative model for the atoms (optically thin) or on ro-vibrationally resolved Corona models.

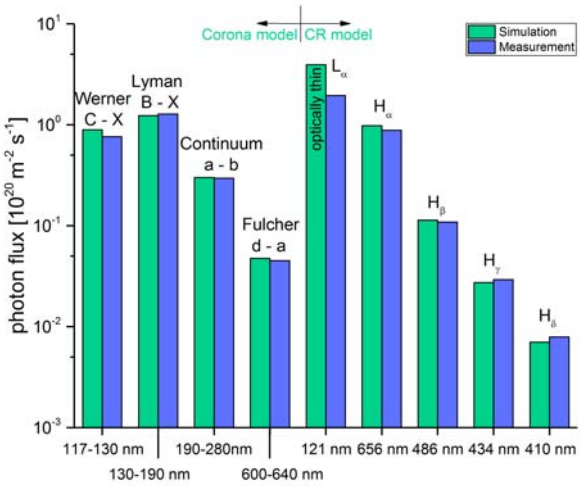

Figure 1. Photon fluxes measured in an ICP discharge at 3 Pa and 700 W RF power. Predictions obtained from CR (optically thin) and Corona modelling are also shown.

As the experiment is equipped with a RF phase-resolved voltage/-current measurement, the power coupled to the plasma and thus the RF efficiency can be quantified. The extension of the pressure range allows studying opacity effects. The predictive modelling capability of the collisional radiative models can be checked by comparison with measurements. Furthermore, the ro-vibrational Corona model for prediction of photon fluxes of the Lyman band is extended by considering the cascades from the EF-state.

Predictive modelling of photon fluxes are presented as well for a variation of electron density and temperature. The influence of the degree of dissociation is discussed.

References

[1] U. Fantz, S. Briefi, D. Rauner, D Wünderlich, Plasma Sources Sci. Technol. **25** (2016) 045006.

Radial and temporal density profiles of Ar($1s_5$) metastables in a nanosecond pulsed plasma jet impinging on different dielectric surfaces

K. Gazeli[1], G. Bauville[1], M. Fleury[1], O. Neveu[1], P. Jeanney[1], S. Pasquiers[1], J. Santos Sousa[1]

[1] *LPGP, CNRS, Univ. Paris-Sud, Université Paris-Saclay, 91405 Orsay, France*

We report on the radial-temporal distribution of Ar($1s_5$) absolute density in a cold nanosecond pulsed plasma jet impinging on ungrounded flat surfaces of different dielectric constants. The plasma was produced in the form of Guided Streamers (GSs) propagating through the argon gas channel at velocities of some 100s of km/s, reaching the surface in some 10s of ns and spreading on it. The influence of each surface on the Ar($1s_5$) absolute density radial and temporal profiles and on the GSs optical characteristics was evaluated for two gas flow rates, 300 and 400 sccm (standard cubic centimetres per minute). At these conditions, a diffuse discharge was established in contrast with the free-jet case (no target). This allowed reliable quantification of the Ar($1s_5$) radial density by means of a TDLAS setup and Abel-inverted profiles of the Ar($1s_5$) transversal density.

1. Introduction

Atmospheric Pressure Plasma Jets (APPJs) in the form of Guided Streamers (GSs) [1,2] are sources of abundant (re)active species, among which, various metastables. Metastables preserve their energies for relatively long time, contributing this way to the plasma reactivity, which is important for various applications. To map their absolute densities in He APPJs, Tunable Diode Laser Absorption Spectroscopy (TDLAS) has been applied [2]. Nonetheless, for Ar APPJs this technique must be applied wisely due to their filamentary nature in some cases [1]. This work is devoted to the measurement of the spatiotemporal density of Ar($1s_5$) metastables in an argon APPJ impinging on dielectric flat surfaces, for conditions which give a diffuse plasma, allowing a precise mapping of the absolute density in both axial and radial coordinates.

2. Experimental setup and results

A coaxial DBD reactor was employed to produce GSs in pure argon (flow rate range: 300−400 sccm) [1]. The reactor was driven by high voltage positive pulses (6±0.06 kV, 224±3 ns FWHM, 20 kHz). The dielectric targets (floating potential) were made of glass (ε_r≈4, see **Figure 1**) and alumina (ε_r≈9), and were placed 5 mm away from the end of the reactor's tube. At these conditions, diffuse discharges were established, allowing reliable application of TDLAS to measure the spatial (i.e., axial−z and transversal−y, see **Figure 1(a)**) and the temporal (over a voltage impulse) distribution of Ar($1s_5$). This was achieved by tuning the laser's wavelength to be in resonance with the radiative transition $2p_9$−$1s_5$ of the excited Ar at 811.531 nm. Emission spectroscopy and ICCD imaging were also performed. The reactor−target system was mounted in µm-stages (z and y displacement). The absorption was recorded along the z- and y-axis in steps of 0.5 mm and 10 µm, respectively.

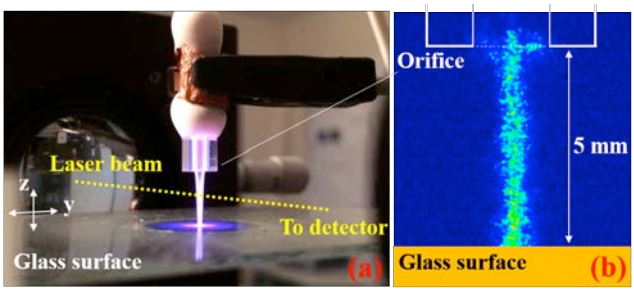

Figure 1. (a) Argon APPJ impinging on a glass surface (the laser beam in the TDLAS setup is illustrated in yellow) (b) ICCD image (3 ns gate) revealing diffuse discharge features.

The presence of the targets allowed the formation of diffuse discharges (see **Figure 1**). The transversal absorption profiles appeared well symmetric and reproducible. Thus, Abel inversion [2] was performed to map radial absolute density profiles at different z positions. Densities of some 10^{14} cm^{-3} were measured, depending on the gas flow rate, axial position and target material. Besides, the effective lifetime of Ar($1s_5$) varied between 50 and 400 ns, also depending on the operating condition. These results suggest that this device may be employed for the desorption of organic molecules present in trace amounts on the studied surfaces [1].

3. References

[1] X. Damany, S. Pasquiers, N. Blin-Simiand, G. Bauville, B. Bournonville, M. Fleury, P. Jeanney, J. Santos Sousa, *Eur. Phys. J. Appl. Phys.* **75** (2016) 24713.

[2] C. Douat, I. Kacem, N. Sadeghi, G. Bauville, M. Fleury, V. Puech, *J. Phys. D.: Appl. Phys.* **49** (2016) 285204.

Microwave capillary discharge as way to influence biological objects

A. G. Akopdzhanov[1], K.V. Artemyev[2]., N .N. Bogachev[1,2], A. M. Davydov[2], I. Yu. Egorova[3], N. G. Gusein-zade[1,2], I. A. Kossyi[2], N.L. Shimanowskii[1]

[1] *Medicobiologic faculyt, Pirogov Russian National Research Medical University (RNRMU), Moscow, Russia*
[2] *Prokhorov General Physics Institute of the Russian Academy of Sciences (GPI RAS), Moscow, Russia*
[3]*State Science Institution National Research Institute of Veterinary Virology and Microbiology of Russian Academy of Agricultural Sciences, Moscow, Russia*

We have studied microwave capillary discharge influence on culture of healthy and tumor cells. A experimental setup of microwave capillary discharge excite have been made. The discharge influenced the cell cultures. We have shown the possibility of local effects of the plasma filament on the viability of live cells with a high potential therapy for primary and secondary cancer formations. We used the culture of tumor cells Hela and prostate cancer and cell culture of fibroblasts as objects of our research. The authors assume the use of standard chemotherapy with plasma influence to increase the effectiveness of the therapy of cancer formations by rising the permeability of cell membranes.

We have studied microwave capillary discharge influence on culture of healthy and tumor cells. The experimental setup scheme of microwave capillary discharge treatment of cell cultures is presented on fig. 1. We have used the coaxial waveguide with the shortened central electrode (the inner conductor). The inner conductor is shorter than outer electrode (conductor) (2). The central electrode is hollow and also serves as a gas pipeline. The outer electrode (2) is grid with cells which size provides almost complete shielding of the microwave radiation and allows the discharge monitoring and measurement of its parameters. The discharge (4) was excited in a quartz capillary (3) which has been tightly fitted on the central electrode. The inner diameter of the quartz capillary is d_c=1-1.5 mm. The discharge influenced the cell cultures. Argon was used as a working gas in our experiments. The microwave radiation frequency was f=2.45 GHz. The microwave power in the pulse was P=2 kW. The pulse duration was ranged from 10 till 20 mcs and the pulse repetition rate was 50 Hz.

As shown in [1,2] the plasma torch generated contracted (diameter 200 μm) plasmoid (plasma filament) with electron concentration $n_e = 10^{16}$-10^{17} cm^{-3} in each pulse. The electron temperature was $T_e \approx 2$ eV.

We have shown the possibility of local effects of the plasma filament on the viability of live cells with a high potential therapy for primary and secondary cancer formations. We used the culture of tumor cells Hela and prostate cancer and cell culture of fibroblasts as objects of our research. MTT-test was used to evaluate the viability of cell cultures. The authors assume the use of standard chemotherapy with plasma influence to increase the effectiveness of the therapy of cancer formations by rising the permeability of cell membranes. This study is supported by Russian Science Foundation, project number 17-19-01583.

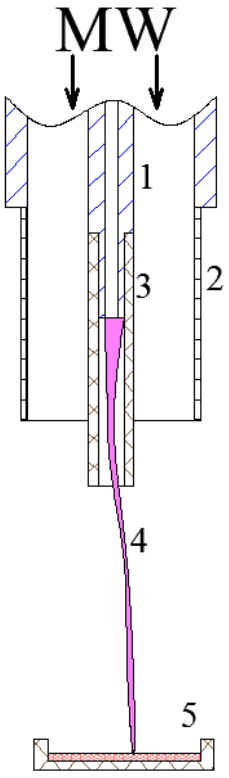

Fig 1. Scheme of experimental setup.

[1] S.I. Gritsinin, P.A. Gushchin, A.M. Davydov et al. Plasma Phys. Rep. (2013) 39: 644.
[2] S.I. Gritsinin, A.M. Davydov, I.A. Kossyi, Plasma Phys. Rep. (2015) 41: 591.

Diffuse discharges in helium and air: role of fast secondary electrons

N. Babaeva, D. Tereshonok, G. Naidis, E. Son

Joint Institute for High Temperatures Russian Academy of Sciences, Izhorskaya 13, Moscow 125412, Russia

We report on results from a computational investigation of nanosecond pulsed discharges in helium and air using a two-dimensional fluid and fluid-Monte Carlo simulations. Essential difference between discharges initiated in helium and air is observed. The diffuse discharge in helium is formed due to fast (but not runaway) secondary electrons as a result of ion bombardment of the cathode and Auger neutralization without any assumptions on the critical role of runaway electrons. Energetic secondary electrons emitted from surfaces are treated by the kinetic Electron Monte Carlo Module with account for elastic, inelastic and super elastic collisions. Conventional fluid equations describe the bulk electrons with relatively low mean energy.

1. Introduction

Diffuse discharges in atmospheric pressure air, helium and other gases in tube-to-plane gaps are initiated by short high-voltage pulses using cathodes of small radius of curvature. The diffuse forms of such discharges are usually attributed to gas pre-ionization by runaway electrons [1].

2. The model

We computationally investigated the formation of nanosecond pulsed discharges in helium and air using a two-dimensional fluid and fluid-Monte Carlo simulations. The model, *nonPDPSIM*, used in this paper is discussed in Refs. [2,3]. The discharge is ignited in a cylindrical chamber between a tubular and a plane electrode. The voltage pulse amplitude is 120 kV and the pulse rise time is 1 ns. For air (O_2^+ ions dominate) the energy of the beam of fast secondary electrons is 4 eV, for helium – 16 eV.

3.Results

The ionization sources S_{MC} produced by fast electrons and electron density in the conventional streamer with account for fast electrons are shown in figure 1. Tracks of electron avalanches in front of the streamer are clearly visible in figure 1b and 1e. These tracks follow the trajectories of sources S_{MC}. In air only a few avalanches produced by fast electrons are observed which do not overlap and thus cannot result in essential pre-ionization in the gap. The resulting discharge is shown in Figure 1c. In helium multiple overlapping avalanches produced by fast electrons are observed thus indicating the generation of the diffuse discharge. The resulting electron density is shown in figure 1f.

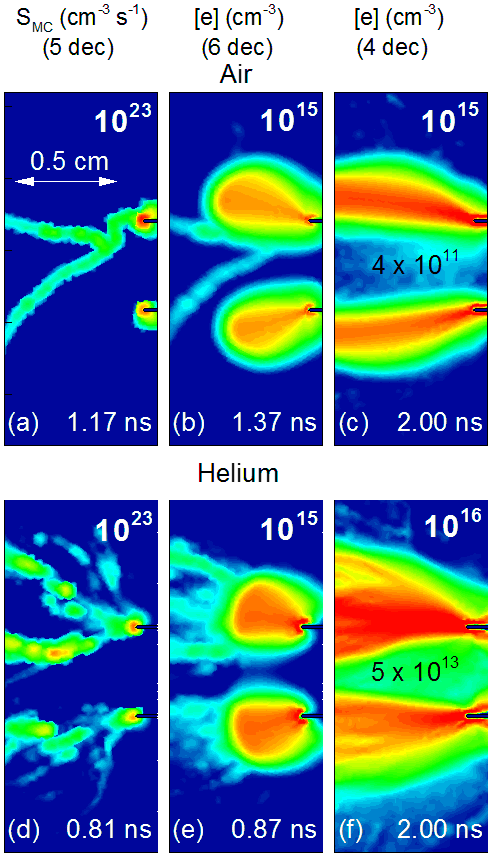

Figure 1. Ionization sources S_{MC} produced by beams of fast secondary electrons and resulting electron density in the evolving streamer shown for two time moments. (a,b,c) – air, (d,e,f) – helium.

4.Acknowledgements

The authors would like to thank Professor Mark J. Kushner for the elegant Electron Monte Carlo Module. This work is supported by the Russian Science Foundation (Project Number **14-50-00124**).

5. References

[1] T. Shao, C. Zhang, Z. Niu, P. Yan,V. F. Tarasenko, E. Kh. Baksht, I. D. Kostyrya, and V. Shutko, J. Appl. Phys.**109** (2011) 083306.

[2] N. Yu. Babaeva, D. V. Tereshonok, and G. V. Naidis, Plasma Sources Sci. Technol. **25** (2016) 044008.

[3] M. J. Kushner, J. Appl. Phys. **95** (2004) 846.

Reactive fluxes and ion activation energy to particulates in air and on dielectric surfaces

N. Babaeva

Joint Institute for High Temperatures Russian Academy of Sciences, Izhorskaya 13/2, Moscow, 125412, Russia

We report on a computational study of the intersection of plasma filaments in a dielectric barrier discharge with two small particulates suspended in air or residing on surfaces. The particulates are separated by a distant commensurate with the filament radius (140 μm). The particulates residing on the substrate surface can be totally or partially enveloped by the sheath formed beneath the positive filament and the substrate. Ion energies and fluxes incident on the particulate depend on dielectric properties of the underlying substrate material. Fluxes of photons, ions and radicals are recoded simultaneously with ion energy and angular distributions. By varying the dielectric constant of the substrate the energies of ions and fluxes of radicals can be controlled.

1. Introduction

We study the ion energy and angular distributions incident on dielectric curved surfaces of particles resulting from the intersection of a DBD filament with small particulates-bacteria suspended in air or residing on surfaces. In this contribution, the model *nonPDPSIM* is used [1,2]. The gas mixture is atmospheric-pressure humid air $N_2/O_2/H_2O$ = 79/20/1 at 300 K. The ion energies are simultaneously recorded along with the fluxes of photons, ions and reactive oxygen species.

2. Results and discussions

We show that the relative location of the particle with respect to the filament axis determines the asymmetry of treatment on a short plasma time scale. The particulates residing on the substrate can be partially or totally immersed in the sheath formed beneath the filament and the substrate. If the size of the particle residing on surface is smaller or commensurate with the width of the sheath region (which is typically 15-20 μm), the sheath may partially envelope the particulate. The electric field in the sheath can accelerate ions to energies as high as a few tens of eV. However, these ions arrive to the surfaces with grazing angles. In addition, the sheath region is depleted by electrons and ions as compared to the bulk. This fact is often ignored while considering the bacteria treatment with positive filaments in DBDs.

Ion and radical fluxes and ion energy and density incident onto the particulate may depend on dielectric constant of the underlying substrate materials (figure 1). By varying the dielectric constant of the substrate on which a particulate or bacteria reside the energies of ions and fluxes of radicals incident onto the surface can be controlled.

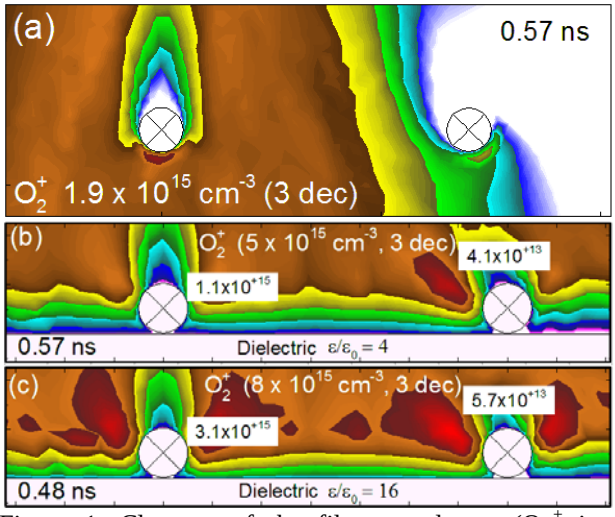

Figure 1. Close-up of the filament plasma (O_2^+ ions density) in vicinity of two particulates (20 μm diameter) suspended in air (a) and on the substrate surface with $\varepsilon/\varepsilon_0$ =4 (b) and $\varepsilon/\varepsilon_0$ = 16 (c).

Our investigation is relevant to the field of plasma medicine wherein the bacteria are treated for sterilization purposes. For this purpose, more study must be done on the size of particulate totally or partially enveloped by the sheath [3].

The work is supported by the Russian Foundation for Basic Research under Grant 17-52-53044.

3. References

[1] S. A. Norberg, E. Johnsen, M. J. Kushner, Plasma Sources Sci. Technol. **24** (2015) 035026.

[2] N. Yu. Babaeva, D. V. Tereshonok, and G. V. Naidis, Plasma Sources Sci. Technol. **25** (2016) 044008.

[3] N. Yu. Babaeva, Accepted for publication in Plasma Process. Polym. (2017).

Surface Properties of Polymer Films obtained by Atmospheric Pressure Plasma Jet on SAE 1020 Steel

L.L.G. Silva[1,2], N.A. Ferraz[1,2], V. Prysiazhnyi[2], K.G. Kostov[2]

[1] *Faculdade de Tecnologia de Pindamonhangaba – FATEC, Pindamonhangaba, SP, Brazil*
[2] *Faculdade de Engenharia de Guaratinguetá – FEG, Universidade Estadual Paulista – UNESP, Guaratinguetá, SP, Brazil,*

In this work polymer films were deposited on SAE 1020 steel by an atmospheric plasma jet system using hexamethyldisiloxane (HMDSO) monomer as polymerizing agent. Several experimental parameters, such as, deposition time, deposition mode (continuous deposition and deposition alternated with surface activation) and voltage waveform were varied. A decrease of the water contact angle from 98° up to 28° was observed for the samples without and with deposited film, respectively. As evidenced by SEM the polymer films exhibited a cauliflower structure, which can also influence the surface wettability. The results of electrochemical measurements presented a slight improvement of the corrosion potential and corrosion current density of SAE 1020 steel after the HMDSO film deposition.

1. Introduction

Nowadays there exist several methods to obtain polymer films for corrosion protection. However, in the most applications; the reactors are operated at low pressure, which requires an expensive vacuum system. Plasma deposition at atmospheric pressure has emerged as an alternative approach because it is economically favourable and environmentally friendly. However, still there are few studies about atmospheric plasma deposition on the metallic surface. Lommatzsch et al. grew HMDSO films on aluminium by using atmospheric plasma jet [1]. This work deals with the study of plasma jet deposition of HMDSO films on SAE1020 steel.

2. Experimental

The plasma jet system consists of a 18.0mm-diam Pyrex tube terminating with a horn-like nozzle, HV electrode placed inside it and a grounded electrode covered by glass table beneath the tube. Plasma was excited by an AC power supply operating at 19.0 kHz and voltage amplitude of 15.0 kVp-p. The device was flushed with 1.0 L/min argon flow and a mixture of air/monomer at flow rate of 0.1 L/min was introduced. Samples (12.5 mm diameter discs SAE 1020 steel) were exposed to plasma for 5 to 20 min. at a nozzle-to-sample distance of 6 mm.

3. Results and Discussion

The water contact angle decreased from 98° for the uncoated sample up to 28° for the coated sample. Therefore the HMDSO film deposition using plasma jet led to a hydrophilic surface. As evidenced by the Fig. 1 the film consists of cauliflower structures with many pores that allow spreading of the water drop.

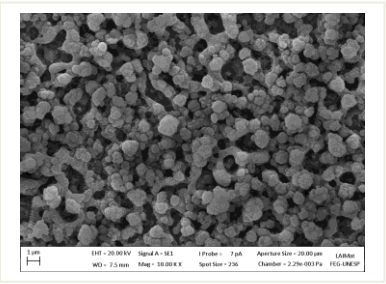

Figure 1: SEM image of HMDSO film (10,000 X)

As shown in the figure 2 the coated sample presented a nobler behavior because its corrosion potential is more positive (-0,59V) when compared to the standard sample (-0,62V). The same behavior was observed in the open circuit potential curves. The coated steel sample presented a corrosion current density of about 1.5 x 10^{-6} A/cm², which is slightly lower than the reference one.

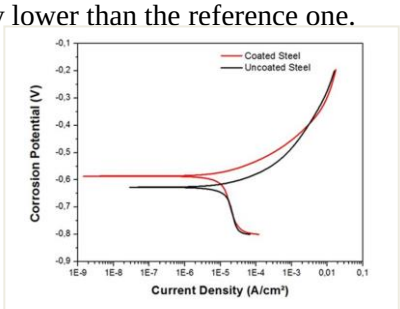

Fig. 2: Polarization curves of steel samples

4. References

[1] U. Lommatzsch, J. Ihde, Plasma Processes and Polymers. **6**, (2009) 642.

Near-cathode layers of arc discharges and diffuse mode of current transfer to cathodes of vacuum arcs

M. S. Benilov and L. G. Benilova

Departamento de Física, FCEE, Universidade da Madeira, Largo do Município, 9000 Funchal, Portugal
Instituto de Plasmas e Fusão Nuclear, Instituto Superior Técnico, Universidade de Lisboa, Lisboa, Portugal

Analytical results on integral characteristics of near-cathode arc plasma layers, available in the literature for different limiting cases, are revisited and modified where appropriate. A complete set of ready-for-use formulas for the whole range of conditions relevant for both vacuum arcs and arcs burning in ambient gases is given. As an example, the formulas are applied to analysis of spotless attachments of vacuum arcs to cathodes made of lead or chromium.

Under typical conditions of arc discharges, both in vacuum and ambient gases, the ion flux to the cathode surface is generated in a thin near-cathode plasma layer. A reasonably accurate description of this layer is of primary importance for understanding and modelling of arc-cathode interaction, which, in turn, is indispensable for understanding and modelling of both the cathode and the arc on the whole. What is needed to this end in the first place are not detailed distributions of plasma parameters in near-cathode layers, but rather integral characteristics relevant for modelling the arc-cathode interaction. In order to facilitate practical applications, results on these characteristics should preferably be delivered in the form of analytical formulas. A number of such formulas, derived under some or other approximations by means of different integral models, are available in the literature. Note that the integral models used in the derivation, while being simple, adequately reflect the most important physical processes and are sufficiently accurate.

The aim of this work is to revisit analytical results on relevant integral characteristics of near-cathode arc layers available in the literature for different limiting cases, to modify these results where appropriate, and to present a complete set of ready-for-use formulas for the whole range of conditions relevant for both vacuum arcs and arcs burning in ambient gases. The most important such characteristics are: electric field at the cathode surface (which is needed for evaluation of the electron emission current); currents of ions and plasma electrons reaching the cathode surface; and energy and momentum delivered to the cathode surface by the ion current, which play in important role in heating of the cathode to temperatures sufficient for electron emission and formation of cathode jets and droplets.

As an example, the derived formulas are applied to analysis of spotless attachments of vacuum arcs to cathodes made of lead or chromium. For both metals, the usual mechanism of current transfer to vacuum arc cathodes cannot sustain current densities of the order of 10^5-10^6 A m^{-2} observed in the experiment. The reason is that the electrical power deposited into the electron gas in the near-cathode space-charge sheath is too low.

It was hypothesized [1] that in such cases the electrical power is supplied to the electron gas primarily in the bulk plasma, rather than in the sheath, and a high level of electron energy at the sheath edge is sustained by electron heat conduction from the bulk plasma. The density of current of ions diffusing to the sheath edge from the quasi-neutral plasma was estimated with the use of the relation between the plasma pressure at the edge of the ionization layer and the equilibrium vapour pressure, derived in this work. The obtained values are comparable to the experimental current density, which supports the above hypothesis for both lead and chromium cathodes. The difference between the plasma pressure at the edge of the ionization layer and the equilibrium vapour pressure for the case of chromium cathode exceeds that for the case of lead cathode by about a factor of 2 and produces a stronger effect over the ion current. Note that the latter effect was disregarded in the previous analysis of spotless arc attachment to chromium cathodes performed in [1].

This work was supported in part by FCT of Portugal through the project Pest-OE/UID/FIS/50010/2013.

References

[1] M. S. Benilov and L. G. Benilova, *IEEE Trans. Plasma Sci*. (2015) **43**, 2247-2252

Steady equilibrium co-rotating dust vortices in a streaming sheared plasma

Modhuchandra Laishram[1], Devendra Sharma[1], and P. K. Kaw[1]

[1] *Institute for Plasma Research, Bhat, Gandhinagar, India, 382428*

Highly charged micron size dust particles suspended in a plasma often form clouds localized by electrostatic potential non-uniformities and gravitational field [1]. Force fields with nonvanishing curl in these clouds drive self-organized vortex flow motion [2] such that the setup replicates a wide range of volumetrically driven bounded natural and complex flow systems. Addressing their viscous fluid like regimes using 2D Navier-Stocks model allows to reveal various physical characteristics of a variety of volumetrically driven bounded flow equilibria and highly sheared vortex flows [3]. The 2D hydrodynamic formulation of the confined dust clouds and its nonlinear equilibrium solutions incorporating finite boundary effect shows a critical transition of the boundary flow from the laminar to a boundary layer separated (BLS) nonlinear regime. The scaling of boundary layer width $\Delta r^3 \propto \mu$, uniquely dependent on the kinematic viscosity μ in linear regime turn into velocity dependent form $\Delta r^2 \, (u_{\|} / L_{\|}) \propto \mu$ in the high Reynolds number nonlinear regime through a critical kinematic viscosity μ^*, influencing the velocimetric determination of the dust viscosity [4]. The nonlinear solutions recover development of vortex scales independent of finer structure in the boundary. The transition allows formation of sequence of corotating vortices separated by layers of high shear depending on varying depth-to-width called the aspect ratio (L_z/L_r) of the dust confined domain.

References

[1] Manjit, Sharma, and Prabal, Phys. of Plasma **22** 033703(2015).

[2] Laishram, Sharma, and Kaw, Phys. of Plasma **21** 073703(2014).

[3] Laishram, Sharma, and Kaw, Phys. Rev. E **91** 063110(2015).

[4] Laishram, Sharma, Prabal and Kaw, Phys. Rev. E** Accepted, Article in Press (February-2017).

Gas temperature distribution in cathode fall region of hydrogen Grimm glow discharge

M. Vasiljević[1], G. Majstorović[2] and N. M. Šišović[1]

[1]*University of Belgrade, Faculty of Physics, 11001 Belgrade, P.O. Box 44, Serbia*
[2]*University of Defence, Military Academy, 11105 Belgrade, Pavla Jurišića Šturma 33, Serbia*

Optical emission spectroscopy technique is used to measure gas temperature distrubition in cathode fall (CF) region of an abnormal type glow discharge operating in hydrogen at low pressure. For the gas temperature estimation, the Q branch of electronic transition $d^3\Pi_u^-, v'=0 \rightarrow a^3\Sigma_g^+,\ v''=0$ (Fulcher-α diagonal band) is recorded and analyzed in the cathode fall region of the Grimm type glow discharge. The rotational temperature of ground vibrational state $T_0(n', v')$ determined from the rotational population density distribution in an excited (n', v') vibrational state can be considered as a valid estimation of the ground state rovibrational temperatutre i.e. H_2 translational temperature T_{tr}.

1. Introduction

Within the growing number of applications original Grimm design glow discharge source (GDS) is successfully used as an excitation source for analytical spectroscopy of metal and alloy samples.

The knowledge of discharge parameters in CF region (the electric field distribution, excitation temperature, translational gas temperature T_{tr} of molecules etc.) is of particular importance for characterization of Grimm GDS.

Here, Fulcher-α diagonal band is recorded and analyzed in the cathode fall region of glow discharge in hydrogen for the gas temperature mapping.

2. Experimental

A detailed description of a modified Grimm GDS source and experimental setup is given in [1]. The experiment has been realized in hydrogen (purity 99.999%). The axial intensity distribution of radiation is observed side-on through the anode slot. The discharge tube was translated in steps d=0.125 mm. All measurements of molecular spectra are performed with an instrumental profile very close to Gaussian with full width-at-half-maximum (FWHM) of 0.014 nm in the second diffraction order. Signals from thermoelectrically cooled CCD detector (2048 × 506 pixels, pixel size 12 × 12 μm, -10 ºC) are collected and processed by PC.

3. Results and discusion

The temperature obtained from Q branch of Fulcher-α band may be considered as the most reliable for the temperature estimation, see details in Ref. 2. The Q branch lines of the electronic transition $d^3\Pi_u^-, v' \rightarrow a^3\Sigma_g^+,\ v''$ ($v'=v''=0$) are well resolved and have high enough intensities in the 595-645 nm wavelength region. So, Boltzmann plot technique is used for evaluation of rotational temperature T_{rot} (n',v') of the excited state. Within the framework of model discussed in [3], the temperature recalculated for the ground vibrational state $X^1\Sigma^+_g, v = 0$ is two times larger than the rotational temperature of excited states since the rotational constants for the upper and ground states are (30.364 cm^{-1}) and (60.853 cm^{-1}), respectively. The results obtained for gas temperature T_{tr} distribution along the CF region are presented in Figure 1.

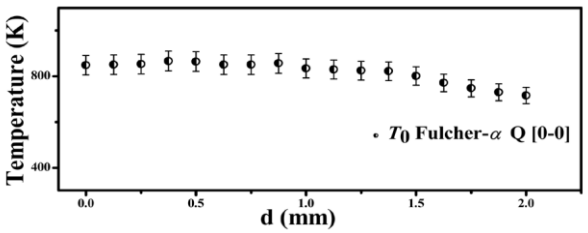

Figure 1. The axial distribution of gas temperature of the H_2 ground state $X^1\Sigma^+_g$. Experimental conditions: p = 4.5mbar; I = 13.4 mA; U= 775 V.

4. References

[1] G.Lj. Majstorović, N.V. Ivanović, N.M. Šišović, S. Djurović, N. Konjević. Plasma Sources Sci Technol. **22** (2013) 045015.

[2] G.Lj. Majstorović, N.M. Šišović, N. Konjević. Plasma Sources Sci Technol. **16** (2007) 750.

[3] S.A. Astashkevich, M. Käning, E. Käning, N. V. Kokina, B.P. Lavrov, A. Ohl, J. Röpcke. JQSRT **56** (1996)725.

Plasma-surface interaction, blister formation and hydrogen retention on ITER relevant materials

C. Quiros, G. Lombardi, J. Mougenot, M. Redolfi, K. Hassouni

LSPM-CNRS Université Paris 13, Sorbonne Paris Cité, F-93490 Villetaneuse, France

In this contribution we present a coupled approach diagnostics/modelling dealing with laboratory simulations of plasma-surface interactions in the frame of the ITER project. We made a focus on studying interaction between an hydrogen plasma and a surface of aluminum used as a surrogate to beryllium. In particular, the formation kinetics of blisters onto the surface was studied. The corresponding amount of hydrogen which diffused and is trapped in the material was quantified using a Molecular Rate Equation model.

1. General

Plasma-wall interactions present a serious concern in existing fusion reactors. Surface modification of PFC (Plasma Facing Components), dust formation and hydrogen retention are some of the problems that have to be resolved before achieving sustainable nuclear fusion. Beryllium (Be) is has been chosen as a first wall material due to its high thermal conductivity, low neutron activation, low Z and its affinity to oxygen. However it is a highly toxic material and it has to be handled with great caution. As proposed by [1,2] aluminum (Al) is a non-toxic proxy material to Be, which presents a similar behavior after plasma exposure. Its studies can therefore provide useful information that can be transposed to Be. However, their hydrogen isotope (HI) retention mechanisms are different. In this article, experimental and model results are first predicted for hydrogen retention and blister formation in Al. Next a numerical comparison between Al and Be retention will be exposed.

2. Experiments

The plasma reactor CASIMIR (Chemical Ablation, Sputtering, Ionization, Multi-wall Interaction and Redeposition) is used to partially simulate plasma wall interactions processes. This reactor relies on the ECR (Electron Cyclotron Resonance) principle to produce low pressure (10^3 mbar) and high-density plasmas (10^{11} cm^{-3}) [3]. Al samples were exposed to hydrogen plasma at different fluences with a flux of ~ $1.7x10^{20}$ ions/m^2s. After 6h of plasma exposure, corresponding to a fluence of ~$3.6x10^{24}$ ions/m^2, the Al surface shows a high density of blisters of approximately $2.9x10^{-4}$ blisters/μm as presented in Fig.1. The density of blisters doubles after the sample is exposed during 12h. The cross section images of these samples show large voids, of about 25-100 μm, under the blisters. These voids reach a depth of about 150 μm. There are also smaller voids, with a size of 1-5 μm, close to the surface of the sample.

3. Modelling

A macroscopic rate equations code has been used to simulate hydrogen retention in materials and bubble formation [4,5]. This code simulates the depth profile of hydrogen isotopes, the hydrogen concentration in the material and the temperature distribution in the exposed material. The code was initially developed to simulate HI retention in tungsten (W), however it has been extended for Al and Be and used to simulate the plasma conditions of CASIMIR. Three types of traps were used to simulate the experimental results on Al: vacancies, dislocations and bubbles. This numerical approach has been extended to Be and some differences on HI retention with Al are presented.

4. References

[1] L. Marot *et al*, Fusion Eng. Des. **88** 9-10 (2013) 1718-1721

[2] A. Kreter *et al*, Phys. Scr. **T159** (2014) 014039

[3] K. Ouaras *et al*, J. Phys. Conf. Ser. **591** (2015) 012029

[4] E.A. Hodille *et al*, J. Nucl. Mater. **467** (2015) 424-43

[5] C. Sang *et al*, J. Nucl. Mater. **463** (2015) 367-371

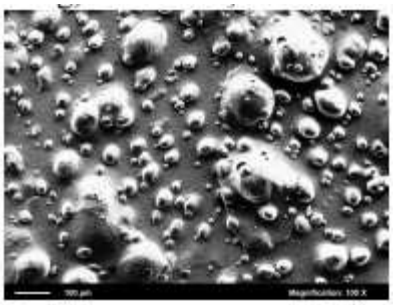

Fig. 1 SEM image of an aluminium target exposed to hydrogen plasma

Modelling heat dominated electric breakdown in air with adaptivity to electron or ion timescales

A. Agnihotri[1], W. Hundsdorfer[1,2], U. Ebert[1,3]

[1] *Centrum Wiskunde & Informatica, Amsterdam, The Netherlands*

[2] *Institute for Mathematics, Astrophysics and Particle Physics, Radboud University, Nijmegen, The Netherlands*

[3] *Department of Applied Physics, Eindhoven University of Technology, Eindhoven, The Netherlands*

We simulate heat dominated electrical breakdown in air in a short planar gap by coupling the discharge dynamics with the air dynamics. The electric discharge model is of diffusion drift reaction type for electrons, positive and negative ions, including secondary electron emission from the cathode. The air dynamics is modelled with the Euler equations and an energy balance equation for the heat. To follow the discharge dynamics over sufficiently long times, we derived a reduced model on the ion timescale from the full model on the electron timescale, and we switch to the reduced model when appropriate. We discuss in detail the implementation of a time-adaptive numerical scheme. We use this scheme to simulate the short and long time dynamics. As the electric discharge develops the air temperature rises due to Ohmic heating. The heated air expands, and the transport and reaction coefficients of the discharge change accordingly. We observe electric breakdown in an initially undervolted gap through a sequence of ionization waves.

1. Introduction

Gas heating in electrical discharges has been studied in the context of fast gas heating, plasma-assisted combustion, atmospheric lightning etc. The majority of simulation studies so far pertaining to gas heating in atmospheric pressure discharges have been performed in 0D or 1D approximation. The large difference in timescales between electron dynamics on the one hand and ion dynamics and gas movement on the other hand makes computations very expensive. Recently 2D axisymmetric simulations [1-3] have been published, but they are either only on the ion or only on the electron time scale. Here we overcome this limitation and study the long time dynamics.

2. Methodology

We simulate the dynamics in a short planar gap in 2D (r-z coordinates) with secondary electron emission where ionization grows due to Ohmic heating rather than through space charge dominated streamer breakdown. This dynamics is challenging to simulate as in the initial stage the electron dynamics has to be followed, and later on the much slower ion dynamics has to be resolved, and both have to be coupled to the hydrodynamics of the medium. We present a model on the time scale of ion motion, that is a reduced version of the full discharge dynamics; it is a generalization of the reduced model introduced in [4] where it was applied to study the transition from Townsend to glow discharge. Our calculations are adaptive in time, i.e., we switch between the full model on the electron time scale and the reduced model on the ion time scale as required. We also discuss possible numerical switching criteria.

3. Results

We developed and employed the 2D cylindrically symmetric model to simulate heat dominated electric breakdown in air. We observe a cyclic process whereby the positive ions hit the cathode, liberate electrons via secondary emission and these electrons feed the discharge channel by producing more electrons and ions via impact ionization. Ohmic heating causes the temperature of the gas to rise. Eventually, the heated gas expands resulting in electric breakdown near the discharge axis. Detailed results are submitted [5].

4. Acknowledgements

A.A. acknowledges financial support under the Computational Sciences for Energy Research (CSER) initiative by Shell and FOM (Dutch Physics funding agency) under project number 12CSER058.

5. References

[1] A. Agnihotri, W. Hundsdorfer and U. Ebert, Jap. J. Appl. Phys. **55** (2016) 07LD06.

[2] F. Tholin and A. Bourdon: J. Phys. D, Appl. Phys. **46** (2013) 365205.

[3] A. Komuro and R. Ono, J. Phys. D, Appl. Phys. **47** (2014) 155202.

[4] D. D. Sijacic, U. Ebert and I. Rafatov, Physical Review E. **71** (2005) 066402.

[5] A. Agnihotri, W. Hundsdorfer and U. Ebert, submitted to Plasma Sources Sci. Technol.

Complete and consistent set of electron-neutral scattering cross sections for carbon monoxide

Polina Ogloblina, Antonio Tejero-del-Caz, Vasco Guerra, Luís L. Alves

Instituto de Plasmas e Fusão Nuclear, Instituto Superior Técnico, Universidade de Lisboa, Lisboa, Portugal

This work proposes a complete and consistent set of cross sections for electron collisions with carbon monoxide (CO) molecules to be published in the IST-Lisbon database with LXCat. The set is validated by comparing swarm parameters, calculated using a two-term Boltzmann solver, with available experimental data. It is shown that for low values of the reduced electric field (E/N<2 Td) both rotational excitations and de-excitations mechanisms, as well as superelastic collisions with the first vibrational excited level, have to be taken into account in order to accurately predict the electron energy distribution function and the corresponding swarm parameters. The role in the calculations of the effective / elastic momentum-transfer cross section is also discussed.

1. Introduction

Carbon monoxide (CO) is one of the main constituents of Venus and Mars atmospheres [1]; it is the most abundant molecule observed in the interstellar space after hydrogen; and it is relevant in laboratory gas discharges for the production of syngas and the reforming of CO_2.

The study of the electron kinetics is essential to understand how the energy gained by the electrons from the applied field is transferred to the different heavy-particles. This work presents a complete and consistent set of electron-neutral scattering cross sections for carbon monoxide, to be soon included in the IST-Lisbon database with LXCat.

2. Description of the cross section set

The current set includes the elastic cross section, the cross sections for the excitation of 16 rotational states, 10 vibrational states and 7 electronic states, as well as the cross sections for dissociation, dissociative attachment and ionization. The cross sections are defined up to 1000 eV kinetic energy.

The elastic cross section is built in two steps: the mid- and high-energy regions are taken from [2], with small modifications; the low-energy region was re-calculated from an effective cross section in order to ensure consistency when rotational excitations are explicitly accounted for. Special attention is given to rotational excitation and de-excitation mechanisms, which can be very important at low reduced electric fields. Rotational cross sections are taken from [3]. Vibrational and electronic excitation cross sections are essentially taken from [2,4]; vibrational excitation is currently under revision, based in [5]. Finally, the dissociation, dissociative attachment and ionization cross sections are the same as in [4].

3. Results and discussion

The current set reproduces very well the available experimental swarm data. For example, figure 1 depicts the reduced Townsend ionisation coefficient.

Further results (not shown) reveal that it is essential to consider rotational excitation and de-excitation mechanisms, as well as superelastic collisions with the first vibrational level, to correctly describe the low field region (E/N<2 Td) at gas temperatures T_g≤300 K.

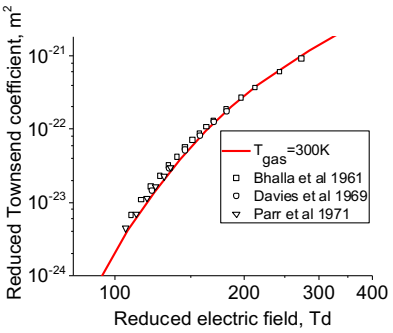

Figure 1. Comparison between calculated and measured reduced Townsend coefficient.

4. References

[1] L. Campbell, M. Allan, M. J. Brunger. J. Geophys. Res. **116** (2011) A09321.

[2] J. E. Land. J. Appl. Phys. **49** (1978) 5716.

[3] R. D. Hake, A. V. Phelps. Phys. Rev. **158** (1967) 70.

[4] Y. Itikawa. J. Phys. Chem. Ref. Data **44** (2015) 013105.

[5] R. Celiberto *et al*. Plasma Sources Sci. Technol. **25** (2016) 033004.

Acknowledgements: This work was partially supported by the Portuguese FCT, under Projects UID/FIS/50010/2013 and PTDC/FIS-PLA/1420/2014 (PREMiERE), and grant PD/BD/114398/2016 (PD-F APPLAuSE).

Human *Stratum Corneum Epidermidis* modification by means of atmospheric-pressure cold plasma treatment

D. Athanasopoulos, P. Svarnas

University of Patras, Electrical & Computer Eng. Dept., High Voltage Lab., 26504 Rion, Patras, Greece

In the frame of the emerging field of plasma medicine, the present work is devoted to human *stratum corneum epidermidis* modification by means of a sinusoidal-driven helium "plasma jet" (train of "guided streamers"). *Stratum Corneum* is the outermost layer of the epidermis and thus it plays the role of a barrier to protect the underlying tissues. Accordingly, and due to its composition, it exhibits highly hydrophobic nature and any drug delivery through skin is subjected to this barrier. Hereby, it is clearly demonstrated the possibility of increasing human *stratum corneum epidermidis* wettability as a function of the exposure time to plasma-induced reactive species.

1. Introduction

Plasma medicine is emerging world-wide as a new field of medical research, with special applications to dermatology. Towards this direction, human *stratum corneum epidermidis* (SCE) is here subjected to atmospheric-pressure cold plasma (APCP) treatment for increasing wettability.

SCE has the architecture of dead keratin filled cells in a lipid matrix [1]. Its thickness lies typically from 10 to 20 μm, and it functions to protect the underlying tissues. The wettability of human skin varies significantly depending on the anatomical site, the pre-conditioning (e.g. soap washing, water rinsing etc) [2] etc. However, clean human skin is hydrophobic, since it exhibits water contact angles (WCAs) up to 125 deg [2].

In this work, the wettability of SCE is reduced using a He APCP, sinusoidially driven at 10 kHz.

2. Experimental setup and specimens

The reactor used for APCP production and the plasma interpretation in respect to biological applications, have been presented elsewhere [3]. The SCE samples are from the breast of a 63-years old Caucasian female (BMI 27) and supplied from Biopredic International. Briefly, the samples are de-frozen, immersed in phosphate buffered saline, pH 7.4, rinsed gently by ultrapure water, and their surface is dried carefully under weak flow of Ar gas. The wettability of the samples is evaluated with WCAs (drops of 3 μl) due to a motorized drop shape analysis system (Krüss GmbH; EasyDrop). The experiments are realized in triplicates, providing mean values and standard deviations.

3. Results and Discussion

Fig. 1 depicts the SCE wettability evolution for increasing plasma treatment.

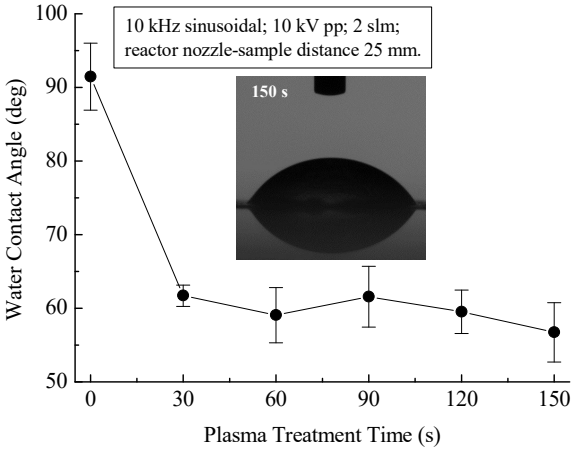

Fig. 1: Human *Stratum Corneum Epidermidis* wettability versus the exposure time to APCP.

Following XPS analysis (not shown here) and plasma probing [3], the WCA decrease down to 56 deg is attributed to surface functionalization induced by plasma-generated RONS.

4. Conclusions

APCP was here proposed as an efficient medium for SCE wettability increase, which in turns could be useful for therapeutic gel applications.

5. References

[1] C. L. Silva et al., Biochim. Biophys. Acta **1768** (2007) 2647-2659.

[2] M. E. Ginn et al., J. Colloid Interface Sci. **26** (1968) 146-151.

[3] P. Svarnas et al., Appl. Phys. Lett. **101** (2012) 264103.

Acknowledgments

D.A. acknowledge I.K.Y. (State Scholarships Foundation; NSRF 2014-2020) for financial support.

Controlling Atmospheric-Pressure Plasma Reactive Species Densities by means of Modulated Sinusoidal High Voltage

P. Svarnas[1], M. Mitronika[1], D. Athanasopoulos[1], E. Mitronikas,[2] K. Gazeli[1,3]

[1] *University of Patras, Electrical & Computer Eng. Dept., High Voltage Lab., 26504 Rion, Patras, Greece*
[2] *University of Patras, Electrical & Computer Eng. Dept., Electromechanical Energy Conversion Lab., 26504 Rion, Patras, Greece*
[3] *current address: Université Paris-Sud & Université Paris-Saclay, CNRS, LPGP, 91450 Orsay Cedex*

Audio-frequency sinusoidal high voltage is here modulated by square-wave signals, by means of a microprocessor-based power supply. The modulated voltage drives a single-electrode microplasma reactor using helium at atmospheric pressure as feedstock gas. The emissive species induced downstream the reactor nozzle are identified with UV-visible optical emission spectroscopy, and the influence of two modulating parameters (i.e. period and duty cycle) on the relative density of excited probe molecules is studied independently. It is clearly demonstrated that, under the present experimental conditions, both parameters have a profound effect on reactive species densities, and may thus control and enhance the plasma chemistry with an engineerable manner.

1. Introduction

For atmospheric-pressure plasma applications, numerous reports consider the role of the reactor design, driving voltage features (a.c. or pulsed d.c.), gas composition, and gas flow rate, in optimizing the density of various species. Differently, sinusoidal high voltage is here modulated by square-wave signals in respect to excited species densities.

2. Plasma and Diagnostic Setups

The setups employed here are extensively presented elsewhere [1]. Here, the distance between the single-electrode tip and the capillary tube exit is 30 mm and a novel power supply (commercialized by our group) is used (see **Fig. 1** and its caption).

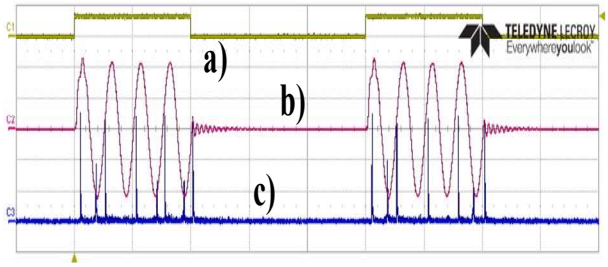

Figure 1: Representative oscillograms: a) square-wave modulating signal (TTL), b) modulated sinusoidal high voltage (9 kVpp; except the overshoot of each first cycle at 9.1 kVpp), and c) pattern of wavelength-integrated light impulses during "plasma bullet"-"guided streamer" propagation [1] (a.u.). The light is spatially-integrated over the first 5 mm in front of the reactor nozzle.

3. Results and Discussion

Fig. 2 shows how the relative density of an excited probe molecule – in terms of optical emission spectroscopy intensity (resolution 0.01 nm; integration time 2 s) – is affected by the modulating parameters. The linear increase vs. duty cycle is probably due to the increasing mean power (ionization/excitation) of the plasma. But, the sharp increase vs. frequency is still under investigation.

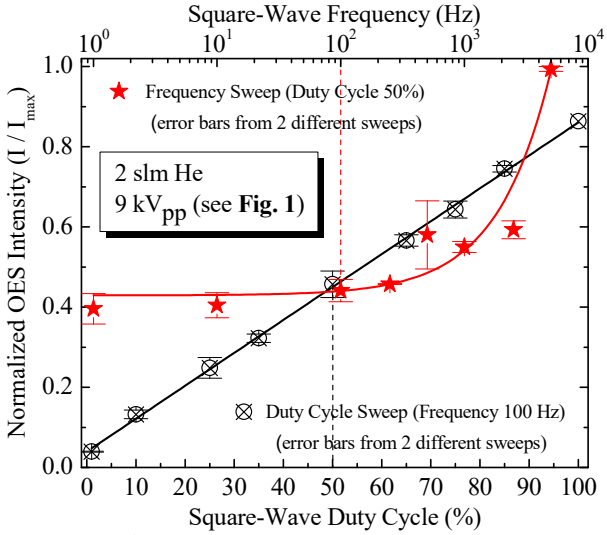

Figure 2: $N_2^*(C^3\Pi_u\text{-}B^3\Pi_g$; v'-v": 0-0) relative density.

4. Conclusions

Appropriately modulated sinusoidal high voltage is potentially a new way for controlling the chemistry of atmospheric-pressure plasmas.

5. References

[1] K. Gazeli et al., J. Appl. Phys. **114** (2013) 103304.

Acknowledgments

D.A. acknowledge I.K.Y. (State Scholarships Foundation; NSRF 2014-2020) for financial support.

Structure at the top of premixed burner flame with the superposition of pulsed dielectric barrier discharge

K. Sasaki and K. Zaima

Division of Quantum Science and Engineering, Hokkaido University, Sapporo, Japan

We investigated the transient phenomena in a premixed burner flame with the superposition of a pulsed dielectric barrier discharge (DBD). The length of the flame was shortened by the superposition of DBD, indicating the activation of combustion chemical reactions with the help of the plasma. We observed the modulation of the top position of the flame and the formations of local minimums in the axial distribution of the optical emission intensity of OH. These experimental results reveal the oscillation of the rates of combustion chemical reactions as a response to the activation by pulsed DBD. The cycle of the oscillation was 0.18-0.2 ms, which could be understood as the eigenfrequency of the plasma-assisted combustion reaction system.

1. Introduction

We have shown that the burning velocity is enhanced by superposing a dielectric barrier discharge (DBD) onto the bottom part of a steady-state premixed burner flame. The increase in the burning velocity is understood by the shortening of the flame length. However, it has been also observed that the flame length was not stationary. In this work, we report the transient change in the shape of premixed burner flame with the superposition of pulsed DBD.

2. Experiment

A premixed burner was fixed on a dielectric base plate. The side of the flame was covered with a quartz tube. A 10-mm-high aluminium electrode was attached on the outside of the quartz tube, and it was connected to a high-voltage power supply with an oscillation frequency of 1 kHz. The burner was electrically grounded. Asymmetric DBD was produced inside the quartz tube and was superposed onto the bottom part of the flame using this experimental configuration. The image of the optical emission intensity of OH from the top part of the flame were captured using an ICCD camera. In addition, laser-induced fluorescence (LIF) imaging spectroscopy was employed to estimate the spatial distribution of the ground-state OH radical density.

3. Results and discussion

Figure 1(a) shows the optical emission image of the top part of the flame in the absence of DBD, while we observed the optical emission images shown in Figs. 1(b)-1(k) in the presence of DBD at various phases of the applied voltage. We observed the temporal variation in the flame length in the presence of DBD. In addition, we observed the formation of local minimums in the axial distribution of the optical emission intensity. As illustrated by the oblique broken lines in the figure, the local minimums moved toward the upper side of the vertical direction at a constant speed. The propagation speed of the local minimums agreed well with the flow speed of the gas. The interval between the arrival times of the local minimums at the fixed position was approximately 0.18-0.2 ms, suggesting that the rates of combustion reactions become less efficient at the interval of 0.18-0.2 ms in the bottom part of the flame. The less efficient reactions may be caused by the overshooting of the rates of combustion reactions by the superposition of the pulsed plasma. Therefore, the interval of 0.18-0.2 ms could be understood as the eigenfrequency of the plasma-assisted combustion reaction system.

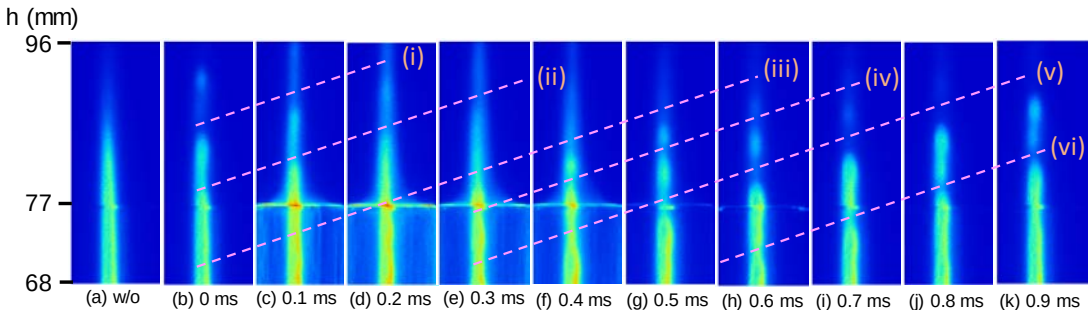

Fig. 1 Optical emission images of the top part of the flame observed in the absence (a) and presence (b)-(k) of DBD

Role of spectral region of discharge emission on initial electron generation for inducing surface discharge in air

Y. Kashiwagi[1]

[1] *National Institute of Technology, Kisarazu College, Chiba, Japan*

The present study clarifies the spectral region of discharge emission that is effective for triggering surface discharge in air. Light emitted from a bulk discharge generated between two needle electrodes irradiates a dielectric plate between two additional electrodes, inducing surface discharge. By changing the cut-on wavelength of an optical filter placed between the needle electrodes and the dielectric plate, the range of wavelengths that effectively generates the initial electrons that trigger the surface discharge is measured. The triggering probabilities change abruptly between 112 nm and 125 nm (9.9 - 11 eV), where oxygen and nitrogen emission lines are located. Thus, these lines play an important role in triggering surface discharge under the conditions used.

1. Introduction

Understanding the supply mechanisms of initial electrons is valuable knowledge because it is useful for both practical application and inhibition of discharge. This report investigates which discharge emission wavelengths are effective for generating the initial electrons that induce surface discharge.

2. Experimental setup and procedure

Figure 1 shows the experimental setup. Light emitted from a bulk discharge generated by needle electrode system Eb passes through an optical filter and irradiates the vicinity of an electrode Es, inducing surface discharge. The probabilities that the light emitted from the bulk discharge triggers surface discharge are measured for different filter cut-on wavelengths. The number of trials is 100 for each filter and the impulse voltage applied to Es is +30 kV, 0.7/80 μs.

3. Result and discussion

The results are shown in Figure 2. In the cases of no filter (w/o) and a 112-nm filter (MgF_2), the discharge probability is high. The probability rapidly decreases from 112 nm to 125 nm (CaF_2). Thus, the emission wavelengths of 112nm - 125 nm play an important role in triggering the surface discharge under the conditions used.

4. Conclusion

Several oxygen and nitrogen emission lines are located in this region [1]. Furthermore, the photoabsorption coefficient for O_2 in this range is relatively small only in several narrow regions [2]. Therefore, it is considered that the emission spectral lines between 112 nm and 125 nm (9.9 - 11 eV) play an important role in generating the initial electrons that lead to surface discharge in air.

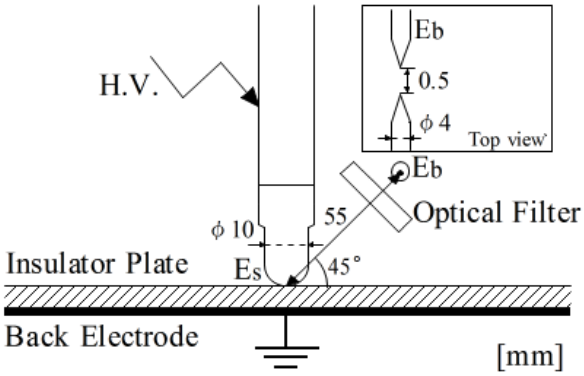

Fig. 1. Schematic diagram of the experimental setup. Surface discharge around Es is triggered by bulk discharge generated around Eb (perpendicular to the paper).

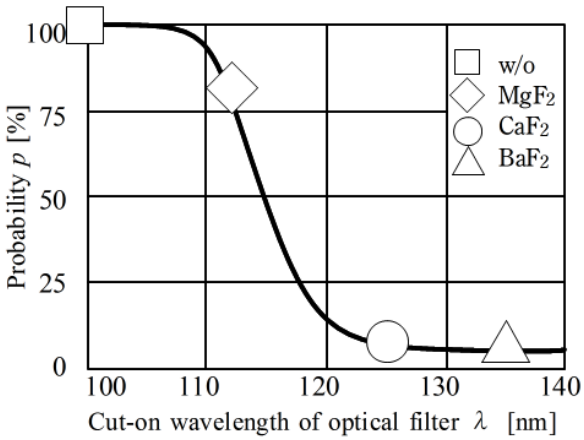

Fig. 2. Measured probability of triggering discharge on insulator plate by bulk discharge.

5. References

[1] T. G. Rogers, et al., IEEE Trans. on Plasma Science, 38, 10 (2010) 2764-2770

[2] K. Watanabe, et al., J. Chem. Phys. 21 (1953) 1026-1030

Study on the Generation Rate of Chemical Reactive Species in Dielectric Barrier Discharge depending on External Flow Rate

Sangheum Eom, Sung-Young Yoon, Changho Yi, Hyeongwon Jeon, Seong Bong Kim, Suk Jae Yoo and Seungmin Ryu

Plasma Technology Research Center, National Fusion Research Institute, Gunsan-city, Korea

The generations of chemical reactive species, such as O_3 and NO, were investigated in dielectric barrier discharge (DBD) plasma depending on different external air flow rates. The generations of O_3 and NO are a function of gas temperature in the plasma volume and the gas temperature can be affected by the air flow. The generation rates of O_3 and NO were measured using gas analysers and the gas temperature is assumed from the temperatures of electrode. The gas flow distributions were visualized using background-oriented schlieren (BOS) as the external air flow rate varies from 0 to 20 lpm. As the air flow rate was increased, the generation rate of O_3 was increased from 0 to 3.61 mg/min. In the contrary, the generation rate of NO was decreased from 0.21 to 0 μg/min.

1. Introduction

It is important to use appropriate chemical reactive species to obtain the effective results for specific applications. For example, O_3 has been explored for enhancement of agri-food preserving efficiency [1] and NO for prevention of agri-food ripening [2].

2. Experimental Set-up

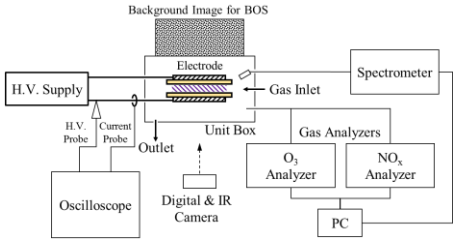

Figure 1. Experimental Set-up

The experimental set-up for measurements of generation rate is described figure 1. The generation rates of O_3 and NO were measured by using the gas analysers depending on the variation of external air flow rates from 0 to 20 lpm.

There are two method were performed to analysis of a correlation between the external air flow rate and gas temperature. Due to the limitation on the direct measurement of gas temperature in the plasma volume, the gas flow distributions were visualized by background-oriented schlieren (BOS) [3] and the temperatures of electrode were taken by IR camera.

3. Experimental Results

The generation rates of O_3 and NO, temperatures of electrode and visualizations of gas flow depending on the different external air flow rate were depicted as shown in the figure 2(a), 2(b) and 3, respectively. As external air flow rate was increased, the generation rate of O_3 was increased from 0 to 3.61 mg/min. In the contrary, the generation rate of NO was decreased from 0.21 to 0 μg/min.

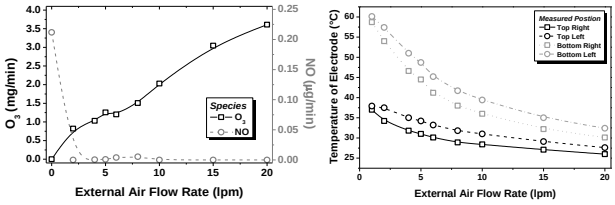

Figure 2. Generation rates of O_3 and NO (a) and temperature of electrodes (b)

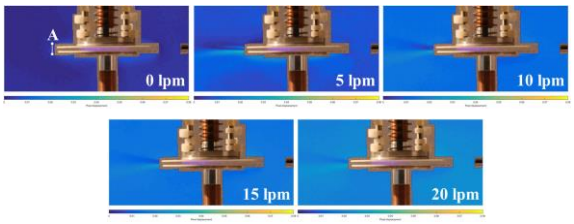

Figure 3. Background-oriented schlieren images

4. Discussions

In order to understand the influence of external air flow rates on the generation of O_3 and NO more precisely, follow-up research, such as simulation for numerical analysis, is needed.

5. Acknowledgement

This work was supported by R&D Program of 'Plasma Advanced Technology for Agriculture and Food (Plasma Farming)' through the National Fusion Research Institute of Korea (NFRI) funded by the Government funds.

6. Reference

[1] Horvitz S. and Cantalejo M. J., Crit. Rev. Food Sci. Nutr. **54** (2014) 312–39

[2] Eum H. L., Lee E. J. and Hong S. J., Kor. J. Hort. Sci. Technol. **32** (2014) 666–72

[3] Hargather M. J. and Settles G. S., *Hvac&R Res.* **17** (2011) 771–80

Time-evolution of $ONOO^-$ concentration in the water treated with air plasma and its relationship to the production of OH radicals

S. Miyamoto[1], K. Nishimoto[1], S. Imai[2], T. Shirafuji[1]

[1] *Deparment of physical Electronics and Informatics, Graduate School of Engineering, Osaka City University, Osaka, Japan*
[2] *Panasonic Corporation, Osaka, Japan*

We measured time-evolution of the concentration of $ONOO^-$ together with that of OH, O_2^-, NO_2^-, NO_3^-, and H_2O_2 in the water treated with air plasma for 60 min. The concentration of $ONOO^-$ was less than detection limit for the first 15 min and detected at 30 min or later, where the concentration increased from 6 to 9 μM. The concentration of OH simultaneously increased at around 30 min. These characteristics indicate that OH is supplied not only directly from plasma but also indirectly through formation of ONOO–, which suggests possibility of sustained release of OH in water treated with air plasma. Saturation in the concentration of NO_2^- and steep decrease in the concentration of H_2O_2 and O_2^- at around 30 min suggest that these species may play some roles to produce $ONOO^-$.

1. Introduction

Air-plasma treatment generates various RONS which include OH, O_2^-, $ONOO^-$, NO_2^-, NO_3^-, and H_2O_2. Among them, $ONOO^-$ has a unique nature of relatively long lifetime of 1.9 s at physiological pH and release OH radicals during its decomposition reaction sequences [1]. This feature may be used to deliver short-lifetime (~ ns) OH radicals to remote locations from a plasma/liquid interface. Thus, we have measured $ONOO^-$ together with the other RONS to discuss reaction mechanisms.

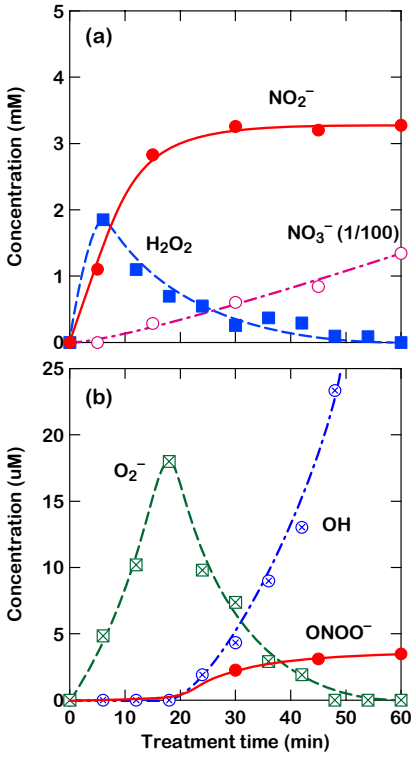

Fig. 1 Concentration of RONS in water measured as a function of air-plasma treatment time.

2. Experimental Setup

We treated deionized water using coaxial-type DBD, of which details have been reported elsewhere [2]. Treatment time was 60 min. We measured $ONOO^-$ by means of fluorescence spectroscopy using nitrative stress sensing pyrromethene dye (NiSPY-3, Goryokayaku, Japan) [3]. O_2^- and OH were measured using ESR. NO_2^- and NO_3^- were measured ion chromatography.

3. Results and discussion

Figure 1 show time-evolution in the concentration of measured RONS, $ONOO^-$ was not detected for the first 15 min, and appeared at 30 min or later. Its concentration increased from 6 to 9 μM for the last 30 min. OH radical appeared simultaneously at around 30 min. These characteristics clearly indicate that OH radicals can be supplied not only directly from plasma but also indirectly through formation of $ONOO^-$, which suggests possibility of susutained release of OH radicals in water treated with air plasma. Saturation in the concentration of NO_2^- and steep decrease in the concentration of H_2O_2 and O_2^- suggest that these species may contribute to produce $ONOO^-$.

Acknowledgements

This work was partly supported by JSPS MEXT KAKENHI Grant Numbers 15H03585 and 15K13391.

References

[1] J. S. Beckman et al, PNAS **87**, 1620 (1990).
[2] S. Imai et al, IEEE Trans. Plasma Sci. **43**, 2166 (2015).
[3] T. Ueno et al, J. Am. Chem. Soc. **128**, 10640 (2006).

Optical wave microphone measurements on pressure waves emitted from plasma jets

F. Mitsugi[1], S. Kusumegi[1], S. Aoqui[2], T. Nakamiya[3], Y. Sonoda[3], T. Kawasaki[4]

[1] *Graduate school of science and technology, Kumamoto University, Kumamoto, Japan*
[2] *Faculty of computer and information sciences, Sojo University, Kumamoto, Japan*
[3] *Industrial engineering department, Tokai University, Kumamoto, Japan*
[4] *Faculty of Engineering, Nippon Bunri University, Oita, Japan*

The aim of this research is to detect pressure waves that are emitted from plasma jets using an optical wave microphone technique and to analyse the frequency relationship between pressure waves and applied voltage waveform.

1. Introduction

Plasma jets have been expected to be used in various applications such as biomedical usage. There have been many reports on electrical and optical measurements about plasma jets. One of the important observations from practical point of view on what plasma jets emit is pressure waves because pressure waves can directly influence on targets or penetrate into liquid, tissues, and so on.

In this work, we utilized a fibered optical wave microphone, which works based on Fraunhofer diffraction of phase objects and improves upon a conventional optical wave microphone with regard to signal-to-noise ratio, to detect pressure waves generated inside He plasma jets with the electrode configuration of dielectric barrier discharge. The frequency of applied voltage dependence on the generation of pressure waves from plasma jets was investigated in different He gas flow rates. The distribution of pressure waves along radius direction of plasma jets at different distances downstream from the tip of the device was also discussed.

2. Results and discussions

It was obvious from the optical wave microphone measurement that pressure waves are emitted from plasma jets. Figure 1. shows the detected signals of pressure waves and its intensity distribution inside plasma jets operated at frequency of 2.8 kHz and 7 L/min. of He gas. The position of a series of the measurements was 5 mm downstream from the tip of a glass tube. The width of the pressure waves in He jet was estimated to be approximately 3 mm which corresponded to that of plasma plume. The pressure waves were completely degenerated and some pressure changes such as turbulence was detected at 20 mm downstream from the tip although plasma jet can be observable clearly at the position.

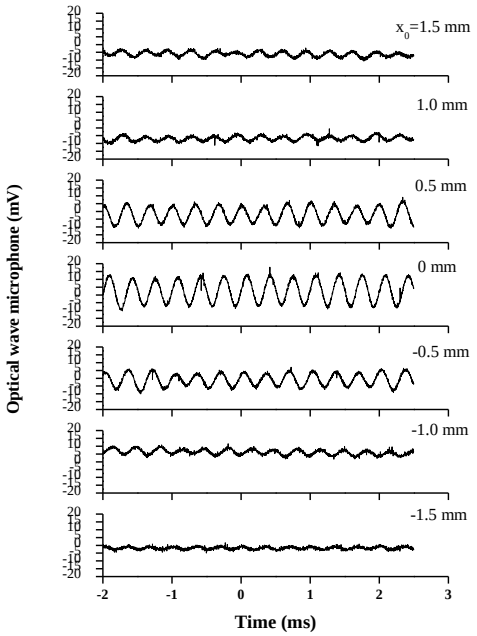

Fig. 1 Waveforms of detected pressure waves at different positions along radius direction. Plasma jets were operated at frequency of 2.8 kHz and 7 L/min. He gas.

3. Summary

Pressure waves were detectable with the optical wave microphone inside the plume of plasma jets.

4. References

[1] F. Mitsugi, T. Nakamiya, Y. Sonoda, T. Kawasaki, IEEE Trans. Plasma Sci., **44** (2016) 2759.
[2] F. Mitsugi, S. Kusumegi, T. Kawasaki, T. Nakamiya, Y. Sonoda, IEEE Trans. Plasma Sci., **44** (2016) 3077.

Dusty plasma structures in gas- metal vapor mixtures

M.K. Dosbolayev[1], A.R. Abdirakhmanov[1], T.S. Ramazanov[1] and S.A. Maiorov[2]

[1] *IETP, al-Farabi Kazakh National University, 71, al-Farabi av., Almaty, 050040, Kazakhstan*
[2]*Prokhorov General Physics Institute, Russian Academy of Sciences, Vavilov st. 38, Moscow, 119991, Russia*
merlan@physics.kz

In this paper the results of experimental study of the properties of the buffer and dusty plasma in mixtures of metal vapor and gas (Ar and He) are presented. Time characteristics (p=*f*(t); I=*f*(t)) of the gas discharge were obtained and analyzed. In addition, number of features of combustion of buffer discharge in a mixture of metal vapors and gas, and change of the properties of plasma-dust structures in it were identified.

1. Introduction

The discharge in mixtures of metal vapor with inert gases is commonly used in various practical applications: to create pulsed atomic lasers with high temperature active element to create discharge light sources.

Recently, technologies to produce nanoparticles from condensed metal vapors in different plasma environments leading to the formation of complex plasma are intensively tested.

Thus, there are two types of plasma of complex composition. Firstly, discharge in mixtures of metal vapor with inert gases. In this case, during discharge metal vapors do not agglomerate, and participate in the form of individual atoms and molecules. Since the metal atoms are easily ionized compared to the atoms of the gas, it is easier to ionize gas-discharge medium. Secondly, the metal vapors, for example during cathode material sputtering, entering the discharge zone of the cathode agglomerate and become part of the plasma as individual charged nano- and micro particles.

Effect of composition of gas on the characteristics of the dust formations was investigated in [1-3], where it is shown that the discharge in a mixture of different gases leads to a very significant change in the characteristics of both electronic and ionic plasma components. Moreover, the gas discharge characteristics can vary greatly even at very low concentration of impurities.

2. Results

Experiments were carried out in a vertical discharge tube in classic version. The procedure of the experiment is as follows: the discharge tube is filled with homogeneous gas and the initial value of pressure is set, it is usually p≈0.17 tor. In a few minutes discharge is ignited (Fig. 1, vertical dotted line on the left). The initial value of the discharge current is set so that during combustion of discharge cathode material is sputtered. This is evidenced by increase in pressure within the tube, the process continues relatively long time until the discharge is extinguished (Fig. 1, vertical dotted line on the right). The result is formation of discharge in mixture of cathode metal vapors and gas.

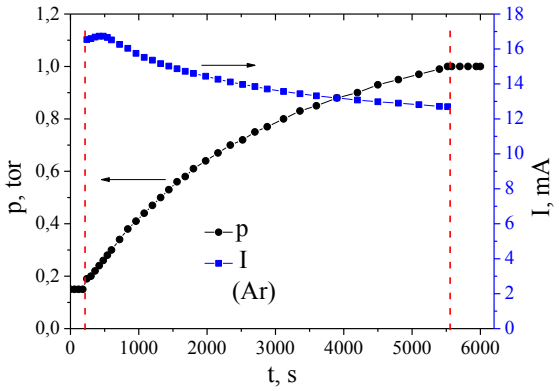

Figure 1. Time characteristics of the gas discharge (p=*f*(t); I=*f*(t))

So, the dust-plasma formations in a stratified glow discharge (first striation from the cathode) in pure gas and in mixture of pure gas and metal vapor were investigated. For characteristics of structural properties of dust formations pair correlation functions were also obtained.

3. References

[1] S.A. Maiorov, T.S. Ramazanov, K.N. Dzhumagulova, A.N. Jumabekov, M.K. Dosbolayev. Physics of Plasmas **15** (2008) 093701.

[2] T.S. Ramazanov, T.T. Daniyarov, S.A. Maiorov, S.K. Kodanova, M.K. Dosbolayev and E.B. Zhankarashev, Contrib. Plasma Phys. **51**, (2011) 505-508.

[3] M.K. Dosbolayev, A.U. Utegenov, T.S. Ramazanov, and T.T. Daniyarov, Contrib. Plasma Phys. **53**, (2013), 426 –431.

Topic number

STUDY OF PROCESSES OF DUST FORMATION IN TNER ON MODEL SET OF PULSED PLASMA ACCELERATOR

M.K. Dosbolayev[1], A.B. Tazhen[1], A.U. Utegenov[1], T.S. Ramazanov[1]

[1] *IETP, al-Farabi Kazakh National University, 71, al-Farabi av., Almaty, 050040, Kazakhstan*

In this work the results of the experimental investigation of dust formation after interaction of pulsed plasma flow with candidate material of thermonuclear reactor in PPA-30 are presented. Via Raman spectrometer it was revealed, that after interaction of plasma, the surface structure of graphite target becomes amorphous. Also in this experimental work, the materials with fractal surface as in tokamaks, which was appeared by the erosion, were obtained.

1. Introduction

Since the eighties of the last century, an interest in the creation of controlled thermonuclear fusion reactors with magnetic confinement has been actively developing for domestic and industrial using. Due to this, tokamak is the most perspective device for its implementation. It is known, that the main problem of realization of controlled thermonuclear fusion is the dust formation, which appears after interaction pulsed plasma flow with the components of reactor, placed inside the vacuum chamber. It has been established that the dust microparticles form layers in the form of films, which can be carried out of the chamber and, thus, be distributed in other systems of the reactor. Thereby, the accumulation of dust and precipitation of film in the volume of reactor play a negative role. First of all, it leads to instability of combustion of high temperature plasma and nucleation of breakdowns, secondly, to the capture and accumulation of tritium, which is a problem for safe of reactor operation and its economy [1]. Composition of particles includes materials of the first wall and other internal elements of structure, which are typically graphite, titanium, tungsten, beryllium and steel.

2. Results

The experiments were performed on a plasma accelerator PPA-30. Device consists of two coaxial electrodes, separated by an insulator. To investigate the dust formation after irradiation of the material with pulsed plasma flow, graphite plate was used. After the collision with the target of plasma flow, formed dust particles collected by separate container for further analysis (Figure 1). Analysis showed that the structure of obtained particles has a rough surface and the particle size varies in the range ~ 10-45 micron.

According to the Raman spectrum [2] it was revealed that the graphite surface is an inhomogeneous. The Raman spectrum of the defective area of the sample, which is characterized by an increase in the peak intensity of D, the total broadening of the peaks and the peak offset G in the high frequency region with a value of 1595 cm^{-1} suggests a certain degree of amorphous structure.

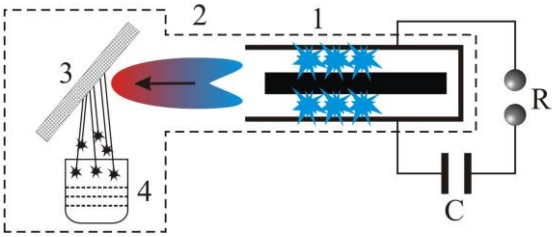

Figure 1. Principle schematic of the model experimental set-up. 1-system of electrodes, 2-plasma flow, 3-graphite plate, 4-container of separate.

3. Conclusion

Experimental results of study of processes of the dust formation on model set in IETP KazNU are shown. According to the results of synergetic analysis of erosion products, it was found that after interacting with pulsed plasma flow, the target surface becomes amorphous, which indicated the increasing of D peak in the Raman spectrum of the irradiated target.

4. References

[1] J.C. Flanagan, M. Sertoli, M. Bacharis et al. Plasma physics and controlled fusion. **57** (2015) 014037.

[2] J.R. Ferrero, K. Nakamoto, C.W. Brown. Introductory Raman Spectroscopy. Second Edition. Elsevier (2003).

Effect of accumulated charge desorption in atmospheric pressure dielectric barrier discharges

H. Akashi and T. Yoshinaga

Dept. of App. Phys., National Defense Academy, Yokosuka, Japan

Recently, atmospheric dielectric barrier discharges are widely applied to various fields, such as ozone generation, surface modification and so on. In dielectric barrier discharges, there are many parameters which affect to plasma significantly, so less attentions on interaction between plasma and dielectric surfaces. In the present paper, desorption of accumulated charges on dielectric surfaces is considered in atmospheric pressure dielectric barrier discharges using two dimensional fluid model. It is found that the waveforms of discharge current and voltage are similar to the results of no desorption case, however, electrons and ions in the vicinity of the dielectrics significantly increase with consideration of desorption, such as low secondary electron emission condition.

1. Introduction

Recently, atmospheric dielectric barrier discharges (DBDs) are widely applied to various fields, such as ozone generation, decomposition of toxics, surface modification, medical sterilization and so on. However, in dielectric barrier discharges, there are many parameters which affect to plasma significantly, such as dielectric materials and its thicknesses, geometries of electrodes, gas, gas pressure and gas mixtures, applied voltage waveforms, and so on. Less attentions on the interaction between plasma and dielectric surfaces and have been almost neglected. Golubovskii et al [1], simulated Atmospheric Pressure Townsend Discharges (APTG) using one dimensional fluid model. Recently, Itoh et al [2] also mentioned about desorption from dielectrics in DBDs. In the present paper, desorption of accumulated charges on dielectric surfaces is considered in atmospheric pressure dielectric barrier discharges using two dimensional fluid model [3,4] and the effect of desorption on DBD has been discussed.

2. Simulation model and Results

The present simulation model is the same as ref.[3,4]. 7.5kV and 200kHz sinusoidal voltage is applied to 760Torr Oxygen gas. Boundary condition at x=0, 0.6cm is periodical. And charges are accumulated on the dielectric surfaces. In the present paper, desorption from dielectric is considered.

Figure 1 shows the one cycle averaged spatial distributions of electron densities w/o and w/ the desorption effect. As shown in the figure*(a), electrons are locally generated and each high density regions consist of 5 filaments (streamers). However, with the considering desorption, high electron density regions are formed widely in x direction in the vicinity of the dielectrics. In the case of w/o desorption, electrons are recombine with ions on the dielectrics, but distributed on the dielectrics uniformly. In the case of w/ desorption, the accumulated electrons uniformly distributed on the dielectrics desorb gradually into the discharge space. As a result, total electron density in the discharge space becomes higher than conventional model. And only two kinds of streamers can be obtained with consideration of desorption case in spite of three without consideration of desorption case.

3. References

[1] Y.B.Golubovskii, et al, J.Phys. D: Appl.Phys. Vol.35, pp.751-761 (2002)

[2] H.Itoh et al, ESCAMPIG XXIII, Bratislava, Slovakia, p.192 (2016)

[3] G.Takahashi and H.Akashi, IEEJ Trans. FM, Vol.131, No.3, pp.205-210 (2011) (in Japanese)

[4] G.Takahashi and H.Akashi, IEEE Trans. PS, Vol.39, No.11, pp.234-235 (2011)

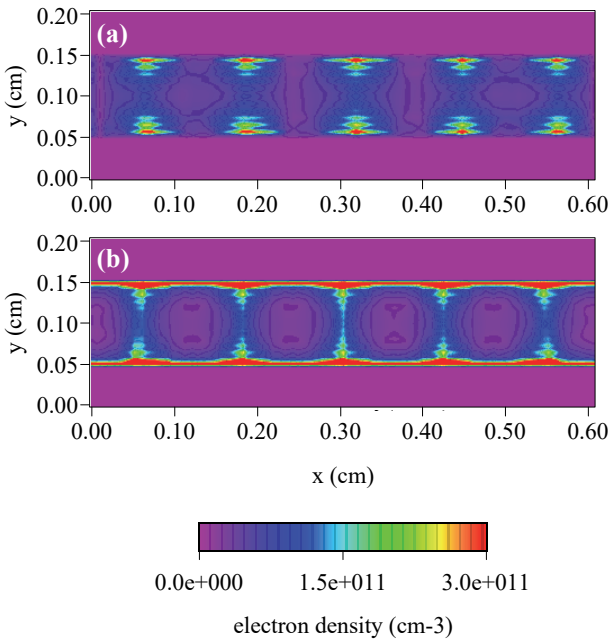

Fig.1. Spatial distributions of electron density (one cycle average). (a) without consideration of desorption. (b) with consideration of desorption.

Investigation of compositions in plasma-irradiated buffer evoking TRP-channel mediated calcium response

S. Sasaki[1], Y. Zheng[1], M. Kanzaki[2], T. Kaneko[1]

[1] *Department of Electronic Engineering, Tohoku University, Sendai, Japan*
[2] *Department of Biomedical Engineering, Tohoku University, Sendai, Japan*

Although plasma medicine is a rapidly emerging field and medical applications using non-equilibrium atmospheric pressure plasma are promising, the interaction mechanism between the plasmas and living cells remains unclear. In order to enhance understandings of the interaction, we focused on transient receptor potential (TRP) channel(s) on cell membrane as biological targets of APP-produced reactive species and investigated the concentrations of hydrogen peroxide (H_2O_2) and the potency of the reactive species for evoking calcium responses through TRP channel. The results suggest that the precursor(s) of H_2O_2 may be responsible for the APP-induced TRP-channel-mediated calcium responses.

1. Introduction

Plasma medicine is a rapidly emerging field, and a number of researchers have reported innovative applications of non-equilibrium atmospheric pressure plasma (APP) [1, 2]. While the fact that reactive species are key components of APP in the plasma medical treatment is now widely accepted, the interaction mechanism between the reactive species and living cells remains unclear. Because the first contact of the species with cells is considered to be just the membrane lipids or the membrane proteins, we have intensively investigated the APP-induced changes in cell membrane transports.

Thus, we experimentally showed that unclassified reactive species in APP-irradiated solution can trigger physiologically relevant Ca^{2+} influx through transient receptor potential (TRP) channel(s) on cell membrane [3]. However, it is still challenging to specify the key species and the key member of TRP family. Therefore, we tried to measure the APP-produced reactive species and the induced calcium response through TRP channels.

2. Experimental Apparatus

APP was generated using low frequency (LF) (frequency: 8 - 10 kHz, voltage: 5 - 12 kV) with Helium gas flow, which was exposed to the biological buffer. The plasma-irradiated solution was put on a hot plate (37°C) for a retention time t_r, and added to mouse fibroblast cells 3T3-L1 (indirect plasma irradiation) or added to hydrogen peroxide monitoring probe. Real-time changes in the amount of the intracellular calcium ion concentration ($[Ca^{2+}]_i$) were obtained using a calcium indicator fluo 4 and a confocal microscope.

3. Experimental Results and Discussion

Figure 1 shows that (a) the concentration of hydrogen peroxide (H_2O_2) in plasma-irradiated solution at varying t_r and (b)time course of changes in the average $[Ca^{2+}]_i$ of 3T3-L1 cells stimulated with plasma-irradiated solution at t_r = 30 s, 300 s, and 600 s. The concentration of H_2O_2 increased but the production rate decreased with time after APP irradiation, which indicating that APP-irradiated solution gradually lost the capacity to produce the precursor of H_2O_2 with time. As t_r increased, the APP-induced increase in $[Ca^{2+}]_i$ was lower. These results suggest that the precursor(s) of H_2O_2 is responsible for the APP-induced calcium response. In the presentation, I will show the result on the mechanism of not only calcium responses but also other membrane transports evoked by APP irradiation.

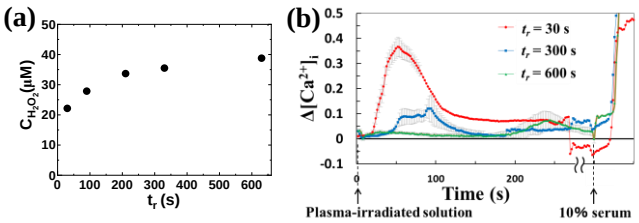

Fig. 1. (a) The concentration of hydrogen peroxide (C_{H2O2}) in plasma-irradiated solution at varying t_r and (b)time course of changes in the average $[Ca^{2+}]_i$ of 3T3-L1 cells stimulated with plasma-irradiated solution at t_r = 30 s, 300 s, and 600 s.

[1] G. Fridman, et al., Plasma Process. Polym. **5** (2008) 503.
[2] S. Sasaki, et al.: J. Phys. D: Appl. Phys. **49** (2016) 334002.
[3] S. Sasaki, et al., Sci. Rep. **6** (2016) 25728.

Topic number: 10

Comparative analysis of properties of helium and argon atmospheric pressure plasma jets

Y.A. Ussenov[1,2], A.S. Pazyl[1], A.K. Akildinova[1], M.K. Dosbolayev[1,3], M.T. Gabdullin[1], T. T. Daniyarov[1], T.S. Ramazanov[1,3]

[1] *Al-Farabi Kazakh National University, NNLOT, Al-Farabi, 71, 050040, Almaty*
[2] *Institute of applied science and information technologies, Shashkina, 40/48, 050038, Almaty*
[3] *Al-Farabi Kazakh National University, IETP, Al-Farabi, 71, 050040, Almaty*

This paper presents the results of studies of the structure, electrical, optical properties and temperature of the atmospheric pressure plasma jet in noble gases, such as helium and argon. The length and shape of the plasma jet at different gas flow rates and values of high voltage on the discharge electrodes were compared. Dynamic and static current-voltage characteristics on the basis of the oscillograms were also analyzed. Discharge spectra were obtained by optical emission spectroscopy method and compared for *He* and *Ar* gases. Temperature of treating surface (cupper plate) measured by thermocouple at different values of gas flow rate.

1. Experiment

Atmospheric pressure plasma jet on the basis of dielectric barrier discharge is a universal source of low temperature plasma [1,2]. In our experiments cold plasma was generated in the noble gas flow through a quartz tube. Two parallel cylindrical foils (electrodes) were attached to the quartz tube with length 80 mm, diameter 9 mm, an inner diameter of 7 mm. The distance between two electrodes was 15 mm. High voltage sinusoidal signal with a frequency f = 30 kHz was used. To register the current and the discharge voltage a high voltage probe (Tektronix P6015) and digital oscilloscope (Le Croy Wave Jet 354A) were used. The current is detected by low-voltage Le Croy probe and measuring resistor with resistance of 100 Ohms. The optical characteristics were measured by optical emission spectrometer Solar Systems.

2. Results

Series of experiments were performed to determine the optimal gas flow and to identify the optimal conditions for obtaining the longest plasma jet length. With increasing gas flow rate the plasma jet length is increased up to a certain value and then the value is decreased (Figure 1). The reason for such behaviour is transition of gas flow from laminar to turbulent regime at high gas velocities in the quartz tube [3]. The plasma jet length was also studied as a function of the applied voltage on the electrodes. To determine the surface temperature in contact with the plasma jet the copper plate and a thermocouple was used. The results showed a decrease in the treated copper plate temperature at higher gas flow. It is also revealed that the surface temperature in the contact with argon plasma much exceeds the temperature than in the case of helium. The emission spectrum was investigated for argon and helium at different discharge voltage and a fixed frequency and gas flow. In the both case results of optical emission spectroscopy of the plasma jet under atmospheric pressure indicates the presence of active chemical component and radicals as atomic oxygen, ozone, nitrous oxide and hydroxyl.

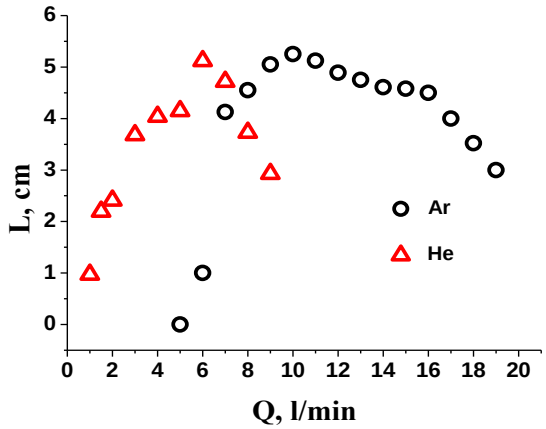

Figure 1. The dependence of plasma jet length on gas flow rate

3. References

[1] J. Winter, R. Brandenburg and K-D Weltmann, Plasma Sources Sci. Technol. **24** (2015) 064001.

[2] Y.A. Ussenov, T.S. Ramazanov, M.T. Gabdullin, M.K. Dosbolayev, T.T. Daniyarov, Kaz NU Bulletin. Physics series. **4** (55) 2015

[3] K. Gazeli, P. Svarnas, P. Vafeas, P. K. Papadopoulos, A. Gkelios, and F. Clément, Journal of Applied Physics, **114** (2013) 103304.

PECVD of DLC & N-doped DLC Thin Films for Biomedical Applications

Hyun-Jin Seo[1], Aiping Zeng[1], Sang-Hun Nam[1], Byungyou Hong[2], Jin-Hyo Boo[1]

[1]*Department of Chemistry, Sungkyunkwan University, Suwon 440-746, South Korea*
[2]*School of Electronic and Electrical Engineering, Sungkyunkwan University, Suwon 440-746, South Korea*

We have deposited pure diamond-like carbon (DLC) and nitrogen (N)-doped DLC thin films by plasma enhanced chemical deposition (PECVD) method. For bio-medical application test, nickel (Ni) nano particles have been electro-deposited on nitrogen-doped diamond-like carbon (N-DLC) thin film surface at potentials ranging from -1.1 V to -1.4 V vs Ag/AgCl in 0.1 M Na_2SO_4 aqueous solution containing 4 mM $NiCl_2$. Atomic force microscopy has been used to investigate the growth of the nano particles. The mean growth rate of the particles increases while the nucleic density decreases when the deposition potential becomes more negative. There is a tendency to obtain large particles at more negative potentials. The growth kinetics has been studied with the dependence of potentiostatic current density on the deposition time, and the growth mechanism has been explained by the cyclic voltammogram of N-DLC film electrode in the deposition solution.

1. Introduction

Metal nano particles deposited on highly boron doped diamond (BDD) thin film electrodes have been studied for electro-analysis application [1] because of the large potential window and low background current and inert surface with BDD electrodes. Recently, there is effect to replace BDD electrodes with nitrogen doped diamond-like carbon (N-DLC) electrodes, which have many chemical and mechanical properties similar to those of BDD thin film electrodes and can be deposited under easier conditions and have smoother surface because of amorphous structure [2]. Previously the authors [3] have reported that the nickel nano particles on N-DLC film possess catalytic function for glucose oxidation which indicates the potential application for direct glucose sensing.

In this work, the deposition potential has been studied to control the nucleic density of nickel nano particles deposited on N-DLC film electrodes. This work is the first step to optimize nickel nano particles on N-DLC film for bio-medical sensing.

2. Experimental

The N-DLC film was cut into 1.2 cm×1.2 cm squares for nano particle deposition and electrochemical testing. An O-ring fixture with an exposed area of Φ 7 mm was designed to seal the N-DLC film squares to service as working electrodes, and a platinum plate was employed as the count electrode opposite to the working electrode. An Ag/AgCl electrode with saturated KCl aqueous solution was taken as the reference electrode. The 3-D morphology of the nano particles deposited at different potentials is presented in Fig.1 and compared with that of as-deposited N-DLC film surface. The surface of as-deposited N-DLC film is very smooth at atomic scale. The nano particles presents the shape of rods, and they are sharp (pine-like) at the deposition potential of -1.1 V, while they become dull (corn-like) when the deposition potential gets more negative. The nano particles deposited at -1.1 V looks like jungles, while the particles are distantly separated at the more negative potentials.

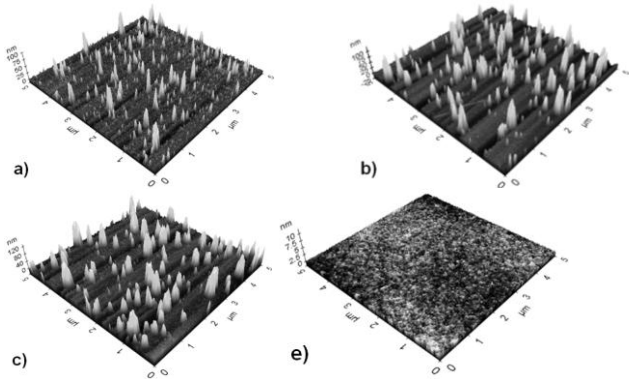

Fig. 1. 3-D AFM Images for the nickel nano particles deposited on N-DLC film surface dependent on the deposition potential: a) -1.1 V, b) -1.2 V, and c) -1.3 V, and compared with that for e) the as-deposited DLC film surface.

3. References

[1] K.E. Toghill, R.G. Compton, Electroanalysis **22** (2010) 1947.

[2] G. Adamopoulos, C. Godet, C. Deslouis, H. Cachet, A. Lagrini, B. Saidani, Diamond Relat. Mater. **12** (2003) 613.

[3] A. Zeng, C. Jin, S.-J. Cho, H. O. Seo, Y.D. Kim, D.C. Lim, D. H. Kim, B.Y. Hong, J.-H. Boo, Mater. Res. Bull. **47** (2012) 2713.

Anomalous nonlinear effects in a weakly ionized gas exposed to a strong shock wave

J.V. Triaskin[1], V.A. Pavlov[1]

[1] *Physics Department, St. Petersburg State University, 1, Ulyanovskaya str., Petrodvorets, 198504, St. Petersburg, Russia*

The patterns of exposure of the charged components to a strong shock wave in weakly ionized non-isothermal gas have been studied. The assumption of the ion sound is used for the plasma component. Computer simulation is based on the hypothesis of neglecting the action of the charged component perturbations upon the neutral gas component. The strong anomalous nonlinear effects are taking place. Joint competitive action of nonlinearity, dispersion, and dissipation is shown in formation of specific plasma «condensations» and «rarefactions». In a narrow range of shock wave speeds, the anomalous relaxation of plasma oscillations occurs behind the front. Essentially, it appears in the total ambipolar entrainment of charged components by a shock wave. This effect is the possible a result of strong nonlinear resonant (with the respect to shock wave speed) perturbation in the region ahead of the front.

1. Introduction

The interaction of neutral and charged gas components is in a high interest. This attention is caused mostly by aerospace applications as well as for exploring the nonlinear wave processes in the near-Earth space. In this work, the interaction of strong shock waves and supersonic bodies with low-ionized plasma is presented and discussed.

A motivation to the study is the discovery of the effect of anomalous supersonic flow of low-ionized plasma around a body in the absence of energy release ahead of the body [1]. Later, anomalous relaxation and instability of shock waves in gases were found in [2]. Generation of low-ionized gas-discharge non-isothermal plasma ahead of a body, streamlined by a supersonic flow, allows lowering the intensity of a strong shock wave [3]; this effect reduces the aerodynamic drag.

The essence of the phenomenon is the formation of a region with elevated concentration of charged particles ahead of the front of a shock wave at certain speed of the latter. This critical speed is defined by the electron temperature and ion mass. Laboratory experiments show the flow around a body by weakly ionized air to differ markedly from that by heated neutral air. The 'plasma effect' is manifested in distancing of the head shock wave from the body and lowering of its intensity.

2. Results

Under certain conditions, total 'destruction' of a shock wave is possible due to the presence of gas ionization ahead of the body. Analytical studies assumed rather far-reaching idealizations. Based on computer simulation [4], formation of a plasma precursor was shown to be possible ahead of the shock wave front – a soliton with a critical property: a non-monotonic resonant dependence of the soliton amplitude on the shock wave speed. The maximum perturbations develop at values of the shock wave speed in the range $c \approx (1.6 \div 2) \cdot u_s$, ($u_s$ is the ion sound speed).

In such situation, a sole, densest possible, local condensation of charged particles is formed in the precursor. The gas in the 'condensation' is not weakly ionized anymore, and charged particles can exert a reciprocal effect upon the neutral component and the shock wave. The 'competition' between strong nonlinearity and strong dispersion causes appearing of a sharp decrease of the soliton amplitude with the shock wave speed growing beyond critical value c. Previously similar effect have been found in [5] in hydrodynamic and called 'Houston's horse' effect.

3. References

[1] R.F.Avramenko, A.I. Klimov, Yu.L., Otkrytie No 007., (1986).

[2] G.Mishin, A.P.Rjazin et al., Tech.Phys.11, (1981), pp.2315-2324

[3] V.A. Pavlov, Yu.L. Serov. 3rd Weakly Ionized Gases Workshop, Norfolk, USA, (1999), AIAA-99-4852.

[4] V. A. Pavlov, Plasma Phys. Rep. 22, 167 (1996).

[5] V.A. Pavlov. Ya. V. Tryaskin. Journal of Applied Mechanics and Technical Physics, (2015), Vol. 56, No. 3, pp. 361–368.

Characteristics of recombination plasma in divergent magnetic field on the linear divertor simulator TPD-Sheet IV

T. Takimoto[1], R. Endo[1], A. Tonegawa[1], K. N. Sato[2], K. Kawamura[1]

[1]*Tokai University, 4-1-1 Kitakaname, Hiratsuka, Kanagawa, Japan*
[2] *Chubu Electric Power Co. lnc., 20-1, Kitasekiyama, Ohdaka, Aichi, Japan*

The relationship between recombination plasma and divergent magnetic field has been investigated on the linear divertor simulator TPD-Sheet IV. The divergent magnetic field was performed by individually controlling some stationary magnetic coils current and a magnet core. The neutral pressure in upstream and downstream (near the target) of the plasma (P_{up} and P_{down}) was measured by Baratron vacuum gauges. The peak value of the neutral pressure difference ($P_{down} - P_{up}$) depends on the magnetic field strength ratio (R_B) between the upstream and downstream. This peak characteristic was similarly confirmed even if the discharge current was different. It is suggested that the degree of magnetic field divergence has the optimal value to promote recombination.

1. Introduction

The divertor design for stable recombination plasma formation should be optimized to handle high heat and particle fluxes. Recently, a Super X divertor (SXD) is planned to accomplish an active neutral particles control to improve plasma confinement in the high-performance plasma for high power and a long pulse operation [1]. Both the divertor target geometry and the magnetic field design to be compatible with the high-performance plasma is one of key significant issues on stable recombination plasma.

Although there are a number of papers on the numerical simulation of the SXD configuration [2], very little is known about the experimental simulation of the SXD-shaped target on recombination plasma formation. Design studies about SXD-shaped target in the divertor plasma are not easily understood because three-dimensional geometry of the target in divertor plasma of tokamaks is complex. Therefore, in order to verify more accurate validity, it is necessary to investigate by basic experiments how divergent magnetic field exerts changes on the plasma. To be more specific, it is important to clarify the relationship between recombination plasma and divergent magnetic field.

We carried out the experiments for that on the linear divertor simulator TPD-Sheet IV [3]. The divergent magnetic field was performed by individually controlling some stationary magnetic coils current and a magnet core. It was measured the electron temperature and density of the plasma near the target by a Langmuir probe. The neutral pressure in upstream and downstream (near the target) of the plasma (P_{up} and P_{down}) was measured by Baratron vacuum gauges.

2. Results

In the experiment, the recombination plasma was generated by changing the gas flow rate. In the condition of the gas flow rate where the recombination plasma exists, a peak of the neutral pressure difference $\Delta P = P_{down} - P_{up}$ was observed. The peak is considered to indicate the degree of neutralization by recombination. Each peak showed different values depending on the magnetic field strength ratio between the upstream and downstream (R_B). Figure 1 shows the relationship between the pressure difference peak and R_B when the discharge current was 70 A and 40 A. Both discharge currents showed the characteristic that the pressure difference peaks became the maximum in a certain R_B. It was suggested that R_B (the degree of magnetic field divergence) has the optimal value to promote recombination.

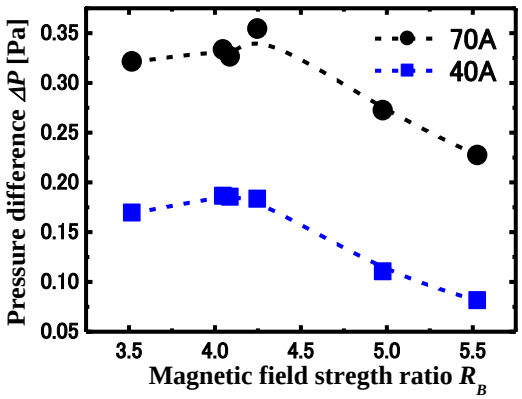

Fig. 1. The relationship between the pressure difference peaks and the magnetic field strength ratio when the discharge current is 70 A and 40 A.

3. References

[1] P. M. Valanju *et al.*: Fusion Engineering and Design 85 (2010) 46–52.
[2] E. Havlíčková *et al.*: Plasma Phys. Control. Fusion 57 (2015) 115001 (13pp).
[3] S. Tanaka *et al.*: Fusion Science and Technology, 63 (2013) 420-422.

Deposition of diamond-like carbon film using high power impulse magnetron sputtering

T. Ohta[1], A. Ishikawa[1], A. Oda[2], H. Kohsaka[3]

[1]*Department of Electrical and Electronic Engineering, Meijo University, Nagoya, Japan*
[2]*Department of Electrical and Electronic Engineering, Chiba Institute of Technology, Tsudanuma, Japan*
[3] *Department of Mechanical Engineering, Gifu University, Gifu, Japan*

Hydrogen-free diamond-like carbon film was deposited by using high power impulse magnetron sputtering in order to reduce the friction coefficient. The pressure dependence on the film structure was evaluated by using Raman spectroscopy.

1. Introduction

Diamond-Like Carbon (DLC) film has excellent material properties such as chemical stability, high hardness, low friction, and so on. In the tribology field, the DLC films are expected to be applied to sliding parts of cars due to its excellent features. The hydrogen-free DLC film can also realize the reduction of the friction coefficient [1]. A high power impulse magnetron sputtering (HiPIMS), which is applying a high voltage in a short time to the target due to promote an ionization of the target particles, realizes a smooth surface, good adhesion and a very dense film.[2] In this study, hydrogen-free DLC films was deposited using HiPIMS.

2. Experimental

The pulsed voltage of from 600 to 670V was applied to the target with the pulse duration of 50 μs and frequency of 500 Hz. Pure carbon target was used. The distance between the target and substrates were 50 mm. The gas flow rate of Ar was 100sccm and the pressure was change to be from 0.3 Pa to 3 Pa. Negative bias voltage of 100 V was applied to the substrate holder. Deposition time was 1 hour.

3. Results

Fig.1 shows Raman spectra of DLC film with various pressures. Raman spectra of DLC film was composed of two peaks of D(disorder) band at 1350 cm^{-1} and G(graphite) band at 1590 cm^{-1}. G band represents the graphite structure and D band represents the defect lattice. Raman spectra show the typical DLC film in the range of 0.3 to 1 Pa. However, graphite film was observed at 3 Pa. Fig.2 shows the intensity ratio of the D and G band (I_D/I_G) of Raman spectra as a function of pressure. I_D/I_G was estimated from the deconvolution of Raman spectra and represents relative sp2/sp3 composition ratio. I_D/I_G decreased with decreasing pressure up to 0.5Pa and then increased below 0.5 Pa. This result indicates that the sp3 structure in films increased with decreasing pressure due to ion bombardment. At below 0.5 Pa, however, the film was damaged by the large ion energy.

References

[1] N. Terayama, J. Plasma Fusion Res., 87, 548 (2011).
[2] A. P. Ehiasarian et al., Pure and Applied Chemistry, 82, 1247 (2010).

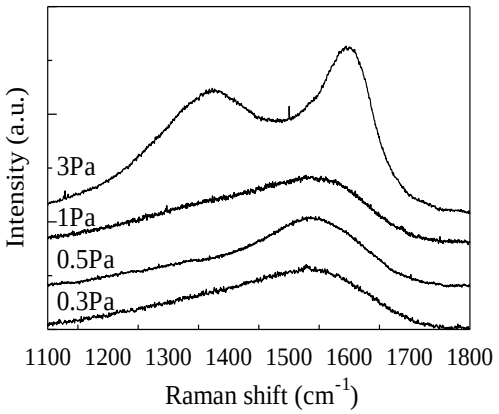

Fig. 1. Raman spectra with various pressures.

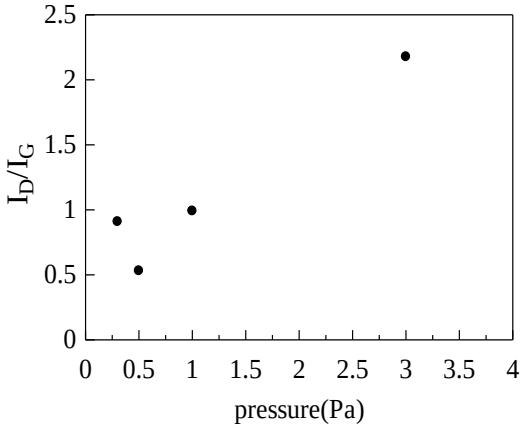

Fig. 2. I_D/I_G as a function of pressure .

Development of electric propulsion using ICR heating on TPD-Sheet IV

M. Nishimura[1], T. Takimoto[1], A. Tonegawa[1], H. Horisawa[1], K. N. Sato[2], K. Kawamura[1]

[1]*Tokai University, 4-1-1 Kitakaname, Hiratsuka, Kanagawa, Japan*
[2] *Chubu Electric Power Co. lnc., 20-1, Kitasekiyama, Ohdaka, Aichi, Japan*

The electric propulsion using an ion cyclotron resonance (ICR) heating on our experimental apparatus TPD-Sheet IV has been developed to control the thrust and specific impulse by manipulating RF powers for plasma production and ion heating. Ion acceleration of high density sheet plasma (~10^{18} m^{-3}) in divergent magnetic field by ICR is investigated. The RF electrodes are made of two parallel plates. The ion energy in the perpendicular direction was measured by a diamagnetic loop coil. The experimental condition is helium gas and discharge current 30~50 A. Ion energy in the perpendicular direction of the magnetic line increased by the ion-cyclotron resonance. Also, ions were accelerated along the axis of the magnetic line by divergent magnetic field.

1. Introduction

An electric propulsion system is one of the key elements in future space exploration projects and has been developed for various space missions. Development of a high power-density plasma thruster with a higher specific impulse and a larger thrust is prerequisite for a manned interplanetary space thruster [1]. Development of Variable Specific Impulse Magneto-plasma Rocket (VASIMR) engine proposed by NASA's Dr. F. R. Chang Diaz et al has proceeded. In this system, the thrust and the specific thrust are controlled freely by manipulating in powers for plasma production and ion heating and various engine operations according to the mission situation can be realized. [2]. The ion cyclotron resonance heating (ICRH) causes perpendicular direction ion heating, followed by the energy conversion from the perpendicular to parallel direction by divergent magnetic field. In the steady state plasma, experimental results of the ion heating have been reported in the low-density plasma (~10^{17} m^{-3}) by ICRH [3].

In this study, experimental of ion acceleration of high-density sheet plasma (~10^{18} m^{-3}) in the steady state by ICRH has been conducted on a linear plasma device TPD-Sheet IV. Since the thickness of the plasma sheet is small, which is about twice of an ion Larmor radius, efficient ion heating with relatively lower powers by using ICRH can be expected.

2. Experimental Setup

Shown in Fig.1, The TPD-Sheet IV device consists of the sheet plasma source, magnetic coils, radio-frequency (RF) heating part, a measurement part, end chamber, a vacuum exhaust. With a magnetic field power source (300 A, ~60 V) and nine coils, maximum magnetic field of 0.12 T can be generated in the heating region. Various magnetic field structures can be formed by using a small power source (300 A, ~10 V) for the two coils at z-axis direction end of the device.

The RF applying circuit consists of the RF power supply, a matching circuit and RF electrodes. The maximum output of the RF power supply is about 500 W. The RF electrodes is a parallel flat plate with a width of 60 mm and a length of 200 mm and experiments were conducted in the excitation frequency range of 200 to 600 kHz. The plasma is sandwiched between the two parallel plate electrodes.

The electron density and the electron temperature are measured by a fast scanning Langmuir probe. The ion temperature $T_{i\perp}$ and $T_{i//}$ are measured by the diamagnetic loop coil and a Faraday cup, respectively. The thrust measured was conducted by a target pendulum [3].

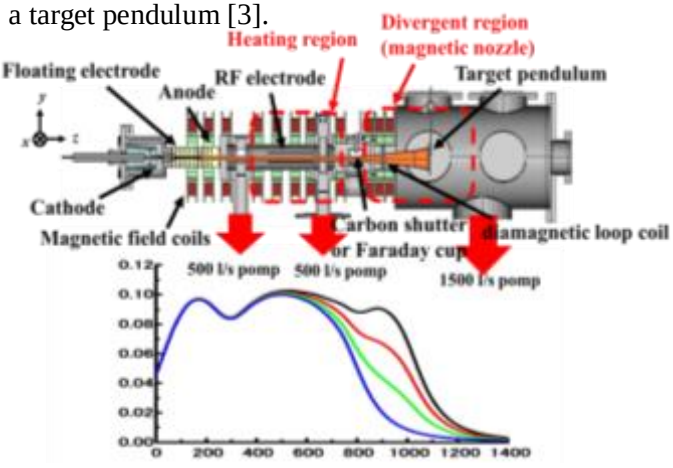

Fig.1. Schematic diagram of TPD-Sheet IV

3. References

[1] A. Ando, K. Takahashi, Y. Izawa, K. Suzuki, Y. Hoshino, IEPC-2013-338, 33th Int. Electric Propulsion Conference (2013)

[2] A. Ando, JAXA research and development report. JAXA-RR-09-003 (2010)

[3] T. Iijima, S. Hagiwara, Fusion Science and Technology. Vol.63, No. 1T, 417-419 (2013)

Development of a compact water-cooled surface wave plasma source for remote plasma processing

H. J. You, W. I. Choo

Plasma Technology Research Center, National Fusion Research Institute, Gunsan, Republic of Korea

A compact surface wave plasma source was newly developed for remote plasma processing such as chamber cleaning, dry etching(SiO_2, Si_3N_4, Silicon), photoresist stripping(SU-8), and decapsulation of microchips. The source was designed to be compact but to have high flow rate plasma generation and high gas decomposition rate so that it could bring higher radical generation, increased throughput, and uniform processing. In this presentation, we present results of microwave electric field simulations, and then we show experimental results on the source performances.

1. Introduction

As for cleaning process of unwanted deposits on processing chamber wall and its tooling, the most advanced cleaning method is so-called "remote plasma source cleaning(RPSC)". In the RPSC, input gases(i.e. NF_3) are supplied to a remote plasma source where they are dissociated into constituent atoms(F, N, F_2, and N_2), then the active species transported to the interior of the processing chamber. The first generation of remote plasma source was surfaguide-type microwave discharge since it has wide range of operating pressure and high rate of gas dissociation. However, the microwave source had some limitations on flow rate capability and hardware simplicity; The surfaguide discharge source used a dielectric tube as a discharge chamber, so the tube could not withstand some high level of plasma load. Also due to bulky set of supporting microwave hardware(tuning stubs, circulator/dummy load, and large-size high voltage power supply, it was difficult to have simple configuration and smaller footprint.

Therefore, the next generation of microwave remote plasma source should have higher flow rate capability and compactness, which allow for extendibility to faster, larger cleaning process and reduced complexity. In this presentation, a new compact microwave plasma source sustained by surface wave is introduced. We describe the design of the source and show the results of microwave electromagnetic simulations. Further, results of NF3 plasma experiments is given on plasma operation ranges and gas decomposition rates.

2. A Water-cooled Surface Wave Plasma Source

The source was designed to be compact but to generate high flow rate plasma with high gas decomposition so that it could result higher active species(radicals) generation and increased throughput. The above features were accomplished by an efficient microwave coupling and a water-cooled plasma region. As shown in Fig. 1, the microwave is fed by WR340 waveguide. High microwave field is coupled to a plasma region by a coupling rod that is intruded into the wide side of the waveguide inner wall. Plasma is mainly generated in a conical crucible-type alumina chamber. The conical end of the plasma chamber is made to be located in the opposite side of the waveguide and face with the coupling rod. The coupling rod is water cooled. The crucible plasma region is surrounded by an aluminium nitride(AlN) cover(shaped like a cap), and downstream plasma region is also by a tightly fitted aluminium(Al) jacket. Here, both surrounding structures are actively cooled by water again. Therefore, inside and outside of the waveguide, the plasma chamber can be efficiently cooled by the AlN cover and the Al jacket, respectively. It is worth noting that the microwave coupled to plasma region does not meet any obstacles like cooling media as previous surfaguide sources do. This is why the present source has efficient plasma generation.

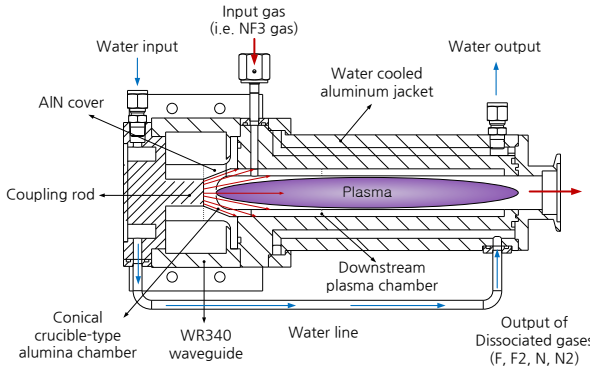

Fig. 1. A sectional view of the compact water-cooled surface wave plasma source.

It was found that the generated plasma can be sustained from 1 kW of microwave power with 10 slm NF_3 gas. Typically, higher power gives brighter plasma generation and higher gas decomposition. The measured decomposition rate was ranged from 80 to 99 % with 1-3 kW.

Retention and transmission of deuterium in tungsten on D-He mixture plasma

T. Hayashi[1], T. Takimoto[1], A. Tonegawa[1], Y. Matsumura[1], K. N. Sato[2], K. Kawamura[1]

[1] *Tokai University, 4-1-1, Kitakaname, Hiratsuka, Kanagawa, Japan*
[2] *Chubu Electric Power Co. Inc., 20-1, Kitasekiyama, Ohdaka, Aichi, Japan*

Effects of deuterium ‘(D) retention and transmission properties in the tungsten (W) material on D-He mixture plasma have been investigated on a linear plasma device TPD-Sheet IV. Used as sample is ITER grade tungsten. Titanium (Ti) target was placed on the back side of W target to investigate the retention and transmission properties. The amount of D retention in W increases with increasing the pure D plasma flux. On the other hand, the amount of D retention in W is nearly constant with increasing the D-He plasma flux. At the same time, the amount of the D retention in Ti increases with increasing the D-He plasma flux. It was found that the incident flux of D-He mixture plasma effects on the transmission of D in W.

1. Introduction

Tungsten (W) was chosen as a plasma-facing material in the ITER divertor region because of its high melting temperature, high thermal conductivity and low sputtering erosion yield. In the divertor, it is inflowing that hydrogen isotopes as fuel particles of unreacted besides helium ash. In the inflow to come a lot of fuel particles, there is also a fuel particles that result in accumulated and occluded in diverter material [1, 2].So it is important to understand the behavior of hydrogen isotopes in tungsten of the divertor wall material.

In this study, we have performed the irradiation experiments using deuterium and helium mixed plasma in order to investigate the effect of deuterium retention and transmission properties in the tungsten material by helium.

2. Experimental Setup

The samples were exposed to plasma in the linear divertor plasma simulator TPD-Sheet IV at the Tokai University. Either D plasmas, or He mixed D (D + He) plasmas was used. Samples were positioned at the end of the plasma column. Used as sample is ITER grade tungsten in the form of square plate with the thickness 1mm, was annealed to adjust the crystal grain boundaries. The deuterium transmission property of the tungsten material was investigated by the titanium plate which is mounted behind the tungsten as deuterium storage materials. The ion density in the D-He mixture plasma was measured by the omegatron mass analyzer.

3. Experimental Results

The retention property of deuterium with regards to the ion density ratio of helium is investigated. When the gas flow rate of the helium is increased, amount of deuterium in tungsten did not change and the amount of deuterium in titanium increased.

The retention property of deuterium with regards to incident flux is shown in Fig. 1. The amount of D retention in W increases with increasing the pure D plasma flux. On the other hand, the amount of D retention in W is nearly constant with increasing the D-He plasma flux. At the same time, the amount of the D retention in titanium increases with increasing the D-He plasma flux. It was found that the incident flux of D-He mixture plasma effects on the transmission of deuterium in tungsten.

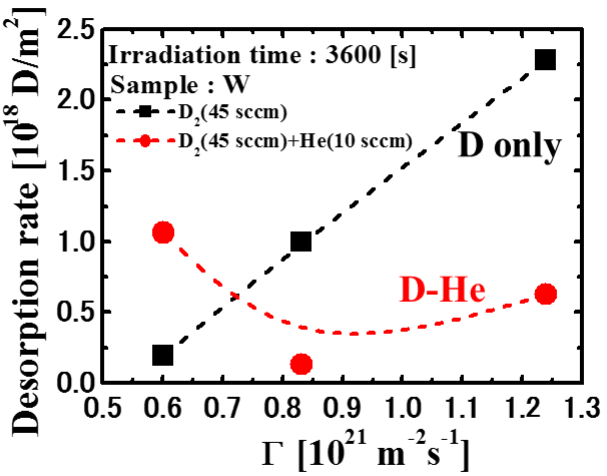

Fig. 1. Retention property of D_2 regarding incident flux

References

[1] J. P. Roszell, et al., Journal of Nuclear Materials, 438 (2013) S1084-S1087.
[2] R. Causey, et al., Journal of Nuclear Materials, 266-269 (1999) 467-471.

Antibacterial and non-fouling Cu/C:F nanocomposites deposited onto poly(ether-ether-ketone) folis

A. Kuzminova[1], J. Kratochvíl[1,2], O. Kylián[1], H. Langhansová[2], J. Lieskovská[2], J. Štěrba[2], V. Straňák[2], H. Biederman[1]

[1] *Charles University, Faculty of Mathematics and Physics, Prague, Czech Republic*
[2] *University od South Bohemia in České Budějovice, Faculty of Science, České Budějovice, Czech Republic*

The main aim of this study was investigation of antibacterial and biofouling properties of nanocomposites based on Cu nanoparticles produced by means of gas aggregation source of nanoparticles and embedded into hydrophobic fluorocarbon matrix deposited by low pressure RF magnetron sputtering. All biological tests were performed on nanocomposite coatings deposited on poly(ether-ether-ketone) foils used as substrate material. It is shown that such nanocomposites are capable to reduce by 5 orders of magnitude amount of *E. Coli* bacteria in solution within 6 hours of incubation as well as to maintain limited osteoblasts adhesion.

1. Introduction

Nowadays, polymers are applied in numerous ranges of industries comprising for example food packaging, medicine, aerospace and etc. This is connected with their low cost and favourable bulk properties. One of the relatively new and high-performance polymers is poly(ether-ether-ketone) (PEEK) that is considered as promising candidate for replacing metal implant components. However, similarly to other common polymers, PEEK possesses low biocompatibility, which limits its broader use. Because of this various methods were investigated to improve its surface properties such as for instance plasma treatment performed with aim to tailor its surface energy and biofouling.

Another issue that is in particular connected with body implants is possible colonization of their surfaces by bacteria that may lead to the formation of highly resistant biofilms and onset of infections. One possible strategy to lower probability of such undesirable events is coating of implants with antibacterial films. Probably the most studied antibacterial materials are the ones based on Ag nanoparticles. However, Ag at higher doses exhibit cytotoxicity and as it is readily accumulated in aquatic plants and animals its use appeared to represent serious environmental concerns. In this study, we therefore proposed to add antibacterial properties to PEEK foils by deposition of nanocomposites based on copper nanoparticles (NPs) embedded into a hydrophobic fluorocarbon matrix that in addition limits the adhesion of cells.

2. Experimental

Produced coatings had two layer structure (Fig. 1). PEEK foils were initially seeded by Cu NPs deposited by a gas aggregation source of nanoparticles. The films of Cu NPs particles were subsequently overcoated by C:F layer deposited by RF magnetron sputtering of PTFE target. The samples were characterised from the point of view of their morphology (AFM, SEM), chemical composition (XPS) as well as with respect to their biofouling and antibacterial activity. For the later *E. Coli* bacteria were selected as reference microorganism and the biofouling of produced nanocomposites was tested using .osteoblast cells.

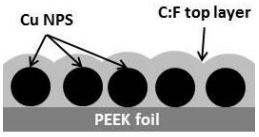

Fig. 1. Schematics of structure of prepared nanocomposites

3. Results

Biological tests showed promising antibacterial activity of prepared Cu/C:F nanocomposites that caused progressive reduction of *E. Coli* bacteria with incubation time. Moreover, it was found that both thickness of C:F overcoat layer and amount of deposited Cu NPs influence kinetics of bacteria reduction: the decline of bacteria count was more pronounced with increasing amount of Cu NPs and decreasing thickness of the top C:F coatings. For the highest amount of Cu NPs and the smallest thickness of matrix material in the nanocomposite 5-log reduction of bacteria capable to form colonies was observed after 6 hours of incubation in the bacteria solution. In addition, all samples showed non-fouling character.

Acknowledgement

This work was supported by grant GACR 16-14024S from the Grant Agency of the Czech Republic.

Topic number: 01

Electron collision cross section set of C_2F_4 gas

S. Kawaguchi[1], K. Takahashi[1], and K. Satoh[1]

[1] *Muroran Institute of Technology, Muroran, Japan*

Electron collision cross section set of perfluoroethylene (C_2F_4) gas is proposed in this work. The proposed cross section set consists of an elastic collision, two kinds of vibrational excitation, ten kinds of electronic excitation, ten kinds of ionization, and seven kinds of electron attachment cross sections. Electron transport coefficients, such as electron drift velocity, effective ionization coefficient, and longitudinal diffusion coefficient, in C_2F_4 gas and C_2F_4/Ar mixtures are calculated exactly by Monte Carlo simulation using the proposed cross section set, and those calculated transport coefficients are found to agree well with measured data. This confirms the reliability of the proposed cross section set.

1. Introduction

C_2F_4 gas has attracted attention as a substitution of CF_4 and *c*-C_4F_8 [1], which are used in the plasma etching of SiO_2 film and have high global warming potential. The electron collision cross section set of C_2F_4 gas was reported by Yoshida *et al*. [2] However, the values of electron drift velocity, longitudinal diffusion coefficient, and effective ionization coefficient calculated from the cross section set do not necessarily agree with measured data [2, 3]. Three partial ionization cross sections are included in the cross section set, but electron attachment cross sections are not. Furthermore, ten kinds of partial ionization [4] and six kinds of dissociative electron attachment cross sections [5], which are not included in Yoshida's s set, have been reported, so that these partial cross sections must be considered to increase the accuracy of cross section set.

In this work, detailed and reliable cross section set of C_2F_4 gas is proposed. The proposed cross section set includes the information on partial ionization and electron attachment cross sections obtained from the experiments [4, 5]. Electron transport coefficients in C_2F_4 gas and C_2F_4/Ar mixtures are calculated exactly by our Monte Carlo simulation [6] and the reliability of the proposed cross section set is confirmed by comparing the calculated transport coefficients with the measured data [2, 3].

2. Cross sections and simulation conditions

The proposed cross section set consists of an elastic collision q_{el}, two vibrational excitation q_{vib}, ten electronic excitaion q_{ex}, ten ionization q_i, and seven electron attachment q_a cross sections. The shape of q_{el} follows the data measured by Panajotovic *et al*. [7] For q_{vib}, two cross sections q_{v1} and q_{v2}, whose threshold energies are respectively 0.12 eV and 0.23 eV, are considered, based on measured electron energy loss spectra [7]. The shape of q_{v1} follows the integral cross section reported by Panajotovic *et al*. [7], and that of q_{v2} is estimated. For q_{ex}, ten kinds of cross sections theoretically calculated by Winstead and McKoy [8] are used, but q_{ex} for $^1B_{1u}$(V) and the others are multiplied by factors of 1.7 and 0.6, respectively. For q_i, partial cross sections related to the generation of $C_2F_4^+$, $C_2F_3^+$, $C_2F_2^+$, C_2F^+, CF_3^+, CF_2^+, CF^+, C_2^+, C^+, and F^+ follow the data measured by Haaland and Jiao [4]. For electron attachment, the yield curves of F^-, CF^-, F_2^-, CF_2^-, CF_3^-, and $C_2F_3^-$ by electron collision with a C_2F_4 molecule, measured by Illenberger *et al*. [5] are used as the shapes of q_a, and those magnitudes are estimated. Furthermore, q_a for the generation of $C_2F_4^-$ is added to fit calculated effective ionization coefficient to the measured data.

For simulating the behaviour of electrons in C_2F_4/Ar mixtures, the cross section set of Ar recommended by the institute of electrical engineers of Japan [9] is used, and electron collisions with C_2F_4 or Ar molecules are only considered. Reported differential cross sections [7, 10] are used to simulate electron scattering after the elastic collision with the C_2F_4 molecule exactly, and isotropic electron scattering is assumed after the other collisions.

3. Results and discussion

The calculated values of electron drift velocity *W*, effective ionization coefficient, and longitudinal diffusion coefficient in C_2F_4 gas are found to agree with the measured data [2, 3]. Furthermore, good agreement on *W* in C_2F_4/Ar mixtures between calculated and measured data [3] is found. This confirms the reliability of the proposed set.

4. References

[1] S. Takahashi *et al*., Jpn. J. Appl. Phys. **44** (2005) L781.
[2] K. Yoshida *et al*., J. Appl. Phys. **91** (2002) 2637.
[3] A. N. Goyette *et al*., J. Chem. Phys. **114** (2001) 8932.
[4] P. Haaland and C. Jiao, Air Force Research Laboratory Report, AFRL-PR-WP-TR-2001-2061 (2000).
[5] E. Illenberger *et al*., J. Chem. Phys. **103** (1995) 1406.
[6] S. Kawaguchi *et al*., Jpn. J. Appl. Phys. **55** (2016) 07LD03.
[7] R. Panajotovic *et al*., J. Chem. Phys. **121** (2004) 4559.
[8] C. Winstead and V. McKoy, J. Chem. Phys. **116** (2002) 1380.
[9] Y. Sakai, Appl. Phys. Surf. Sci. **192** (2002) 327.
[10] C. Winstead and V. McKoy, J. Chem. Phys. **122** (2005) 23404.

Topic number: 9

Dusty Plasma Manipulation via Driving Voltage Waveform Tailoring in an RF discharge

N.Kh. Bastykova[1], Z. Donko[2], S.K. Kodanova[1], T.S. Ramazanov[1], Zh.A. Moldabekov[1], M.K. Dosbolayev[1]

[1] *Institute of Experimental and Theoretical Physics, Al-Farabi Kazakh National University, Al-Farabi 71, Almaty, 050040, Kazakhstan*
[2] *Wigner Research Centre for Physics, Institute for Solid State Physics and Optics, Hungarian Academy of Sciences, Budapest 1525, Hungary*

The effect of the excitation waveform on the plasma properties and the equilibrium position of dust particles are investigated by using harmonic and alternating-phase waveforms that may as well include an additional DC component. Considerable changes of the plasma properties (density, temperature) in the case of alternating-phase waveforms are found. The electron dynamics and the position of the dust particles can be controlled by the change of the driving voltage waveform and the specific electric field configuration allows controlling the position of dust particles in the plasma.

1. Introduction

The manipulation of dusty plasma properties is of great interest both for the theoretical understanding of the fundamental characteristics of strongly coupled systems and for applications. A considerable progress has been made on the manipulation of dusty plasmas using lasers [1]–[2] and via modification of external electric and magnetic fields [3].

2. PIC/MCC simulation results

The discharge is described by particle-in-cell simulation incorporating Monte Carlo treatment of collision (PIC/MCC) processes [4]–[5].

We consider the following types of driving voltage waveforms (see Fig. 1), with an amplitude of $\phi_0 = 100\ V$:

1) harmonic RF voltage excitation:

$\phi(t) = \phi_0 \sin[2\pi f_{RF} t]$;

2) excitation of the discharge with alternating phase of the driving voltage with an additional DC bias, $\phi(t) = \phi_0 \sin[2\pi f_{RF} t + \sin[2\pi(2 \times f_{RF})t]] + \phi_{DC}$, where the phase of the RF voltage alternates as $\sin[2\pi(2 \times f_{RF})t]$, and ϕ_{DC} is the additional dc voltage.

In Fig. 2, the density profiles of the electrons and ions are shown for the three types of excitation waveform considered. The alternating-phase of the driving voltage leads to an increase of the electron and ion densities in the plasma due to the strong electron heating. The additional DC bias results in a decrease of the peak density and shifts the peak position of the density profiles toward the grounded electrode.

Combination of the two methods (the phase modulation and additional DC bias) gives more flexibility in realizing a control of the spatial profiles of electron (ion) density (temperature) and the forces exerted on dust particles [6].

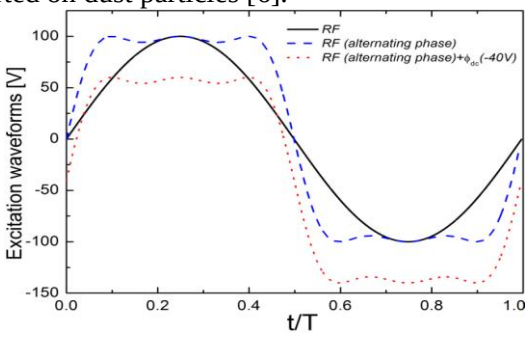

Fig1. Plasma excitation waveforms

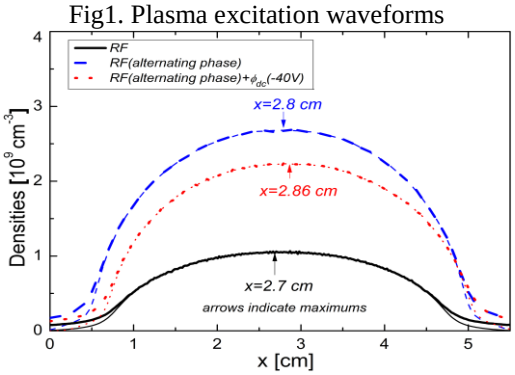

Fig2. Ion (thick lines) and electron (thin lines) density profiles for the different excitation waveforms considered.

3. References

[1] M. Bonitz, C. Henning, and D. Block, Rep. Prog. Phys., **73** (2010) 066501.

[2] V. Nosenko and J. Goree, Phys. Rev. Lett., **93** (2015) 155004-1.

[3] E. Thomas, Jr., B. Lynch, U. Konopka, et al, Phys. Plasmas, **22**(2015) 030701.

[4] Z. Donkó, Plasma Sour. Sci. Technol., **20** (2011) 024001.

[5] N. K. Bastykova, A. Zs. Kovács, et al., Contrib. Plasma Phys., **55**(2015) 671.

[6] N.Kh. Bastykova, Z. Donkó, S.K. Kodanova, et al IEEE Trans. Plasma Science, **44**(2016) 545.

Evidence of the paracetamol's aromatic ring breaking thanks to a non-thermal plasma

Y. Baloul[1], C. Colas[2,3], O. Aubry[1], H. Rabat[1], Benoit Maunit[2], D. Hong[1]

[1] *GREMI, UMR 7344 CNRS / Université d'Orléans, France*
[2] *ICOA, UMR 7311 CNRS / Université d'Orléans, France*
[3] *CBM, UPR 4301 CNRS / Université d'Orléans, France*

This study deals with the treatment of drug residue in aqueous media by using non-thermal plasma which may generate many oxidizing species, such as O, OH, O_3, H_2O_2, etc. More precisely, paracetamol solution was treated in a plasma reactor with multiple needle-to-plate structure. The treated solution was analyzed by high resolution mass spectrometry which allowed to determine with certainty several products, such as nitric acid and nitrate ion. But, further experiments, such as the use of labeled paracetamol, were necessary to identify other products like the dicarboxylic acid. The identification of this latter acid showed clearly that the non-thermal plasma enabled to break the paracetamol's aromatic ring.

The advanced oxidation process using non-thermal plasma (NTP) is a promising technique for the treatment of drug residue in aqueous media [1-2]. Indeed, many oxidizing species, such as O, OH, O_3, H_2O_2, etc. are produced by the NTP depending on their experimental conditions.

Our group works on the treatment of paracetamol ($C_8H_9NO_2$) in an aqueous medium by a NTP created in a multiple needle-to-plate reactor [3] and obtained about full degradation of paracetamol under specific conditions [4]. In order to determine the mechanisms of degradation, the treated solution was analyzed by high resolution mass spectrometry (HRMS) using a Q-TOF. Several products, such as nitric acid and nitrate ion, were easily determined with certainty, while others required further experiments as described partly in this communication.

In fact, this communication reports the identification of the dicarboxylic acid in treated solution, and so the evidence of the breaking of the aromatic ring of paracetamol by the NTP, through the investigation of the chemical species, of molecular mass of 199.0481, produced during the treatment. Indeed, the mass peak of high intensity at *m/z* = 198.0413, in negative mode (figure 1), corresponds to the ion having a condensed formula $C_8H_8NO_5^-$. A multitude of skeletal formulas can match the above condensed formula, but by taking into account the structure of paracetamol, only two of them are retained: tetraphenol which is an aromatic compound and dicarboxylic acid which has a broken aromatic ring. The skeletal formulas of these two latter spacies are shown in figure 2. In order to prove that the dicarboxylic acid was produced by plasma, labeled paracetamol with four Deuterium on aromatic ring was used during the degradation by NTP and studies have been made by HRMS and tandem MS technique. The details of these investigations will be presented at the conference.

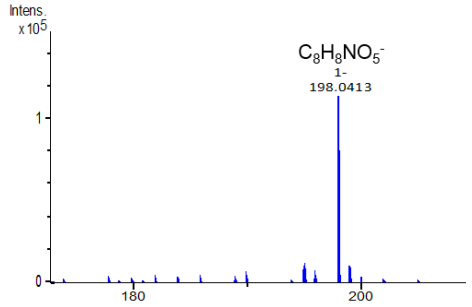

Figure 1. mass spectrum of a paracetamol solution treated by plasma.

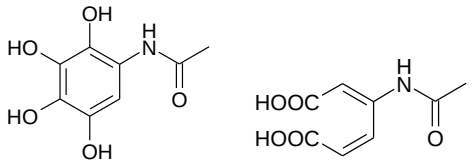

Figure 2. Tetraphenol and dicarboxylic acid skeletal formulas.

References

[1] B. R. Locke, M. Sato, P. Sunka, M, R. Hoffmann, J. S. Chang, Ind, Eng, Chem, Res, (2006), **45**, 882–905

[2] M. Magureanu, D. Piroi, N. B. Mandache, V. David, A. Medvedovici, C. Bradu, V. I. Parvulescu, Water Res, (2011), 45, 3407–3416

[3] Y. Baloul, H. Rabat, D. Hong, S. Chuon, and O. Aubry, IJPEST, (2016), **10**, 2, 102-107

[4] Y. Baloul, H. Rabat, C. Colas, B. Maunit, O.Aubry, D. Hong, HAKONE XV, September 11th–16th, 2016, Brno, Czech Republic

Combined electrical and optical diagnostics of surface discharges in high-voltage systems

R. Kozakov[1], M. Bogaczyk[1], S. Arumugam[2], S. Gortschakow[1]

[1]*Leibniz Institute for Plasma Science and Technology, Greifswald, Germany*
[2]*University of Rostock, Rostock, Germany*

Diagnostics of surface discharges in power apparatus during their initial stage is of great importance for the electric power generation and delivery system. The typical rise times of a single discharge event are of sub-nanosecond scale and represent a challenging task for measurements of the current pulse form due to signal distortion through the measuring circuit. In contrast to this, the optical signals do not suffer on the transmission line limitations and can be principally used for diagnostics. This work focusses on the precise measurements of both the electric current of an individual discharge and of its optical signal. It is shown that optical signals carry the same information as conventional electric methods, like e.g. phase resolved partial discharge diagrams.

1. Experimental setup

Two circular glass plates covered on one side with transparent conducting ITO layer were put together in a polyacrylics (PA) housing, as shown in Fig. 1. The gap between glass and PA surfaces is about 0.5 mm. The voltage was supplied by copper rings contacted with the ITO layers. One is connected with the grounded electrode, the other one is connected to the high-voltage power supply.

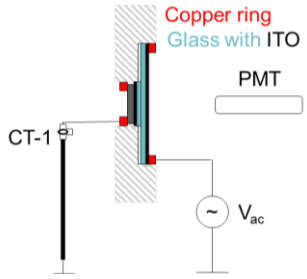

Figure 1: Experimental setup.

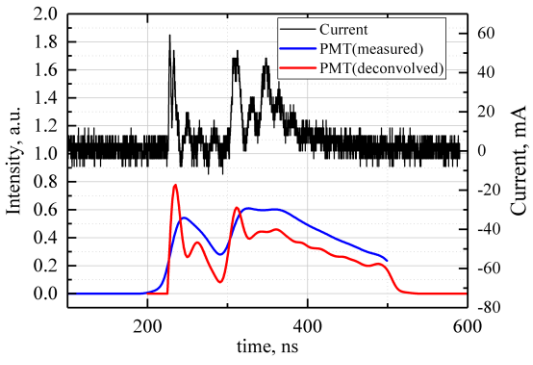

Figure 2: Measured profiles of electric current (black) and optical signal (blue and red curves).

Surface discharges could be observed in such arrangement, when a high voltage was applied (16 kV_{pp}, 50 Hz). The electric current was measured with a current transducer CT-1. Optical signals were recorded with the help of a photomultiplier (PMT).

2. Results

Typical measured profiles of the electric current and optical signal of a single discharge pulse are shown in Fig. 2. Three partially overlapping current pulses of a typical width of 20-50 ns can be identified. The corresponding optical signal exhibits widths of about 100-200 ns. For each current pulse, the apparent charge value was obtained by integration of the measured profile. Similar quantity

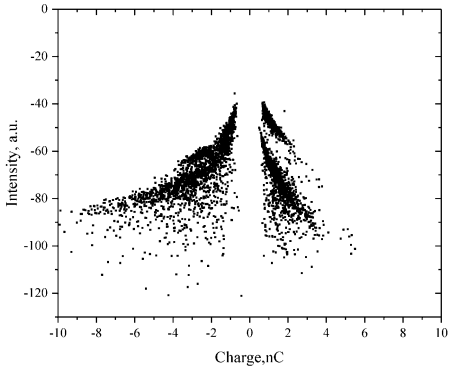

Figure 3: Correlation between charge transferred in single discharge and light intensity in the same discharge.

was calculated for optical signals by integration of the profiles resulting in intensity. The light intensity-charge diagram is shown in Fig.3. Here, the electrical signals and the corresponding optical emissions of 4000 subsequent current pulses were recorded simultaneously. Several structures were observed in this diagram, which are characteristics for this type of discharge. A further improvement in the description of the electric current by an optical signal can be achieved by application of signal deconvolution based on known regularization algorithms (see red curve figure 2).

Acknowledgements

The work was supported by German ministry for Education and Research, grant FKZ 03SF0476.

Topic number

Research on Active Species Production Mechanism of an Atmospheric He-Water Plasma Jet

J.J Liu[1], X.G. Wang[1], Z.Z Zhuo[1]

[1] *Department of Mechanical and Electrical Engineering, Guangzhou University, Guangzhou, Guangdong, 510006, P.R. China*

Abstract: The active species (OH, O and H_2O_2) in plasma play important role in bacterial killing and wound healing. Low gas temperature of plasma is another requirement while treating heat labile tissue. A DBD structured He-H_2O plasma jet can effectively produce OH and H_2O_2 with low gas temperature. In this paper, optical emission lines in plasma jet are measured, gas temperature, vibrational temperature, electron density and electron temperature are deduced from these lines. In conjunction with 2D neutral gas and 1D fluid model simulation, the production and loss mechanism of OH (A-X) is electron collisional dissociation and OH+OH→H_2O_2 reaction. Meanwhile, H_2O_2 production in saline solution indicates that the highest energy efficiency of H_2O_2 production is achieved with He/H_2O plasma jet in bullet mode when water vapor concentration is 1200ppm.

1. Introduction

Atmospheric plasma has attracted lots of attention due to its wide applications in bio-medicine, material, environment and chemical engineering.[1] With the development of plasma medicine, liquid-containing plasma can not only realize blood and tissue coagulation, necrotic tissue removal and kidney stone elimination [2] based on its physical effect, but also achieve low temperature treatment on many diseases, such as: wound healing, chronic and acute injury, cancer and tumour [3] due to its excellent chemical function.

Low temperature and abundant chemically reactive species are two main requirements for plasmas treating heat labile materials (live tissue, organic materials etc). A DBD structured He/H_2O plasma jet can effectively produce OH and H_2O_2 with low gas temperature. At present, some possible reactions to produce OH(A) and H_2O_2 are concluded, however, the main mechanism to produce OH(A)/ H_2O_2 and the influence of plasma working mode and water vapour concentration on their generation are still not clear. It is generally regarded that the accurate measurements of electron density and electron temperature play key role on the analysis of reactive species production mechanism. In this paper, the main generation and loss mechanisms of OH(A) and H_2O_2 will be found out by both experimental measurements of time-spatial distribution of OH(A) emission intensity, electron density and electron temperature and neutral gas/plasma fluid simulation at different working modes and water vapor concentrations.

2. Experimental setup

The schematic diagram of the experimental apparatus is shown in 0. The powered electrode is a capillary needle with inner and outer diameter of 0.8mm and 1.2 mm, where as a copper ring electrode and a stainless steel plate electrode are connected to the ground. The frequency of the applied voltage is 20 kHz. The outer and inner diameters of the glass tube are 2mm and 1.3 mm respectively. The axial distances between different electrodes are shown in 0. The working gas is a helium and water vapor mixture which is realized by mixing two channels of helium flow, one being a dry helium (99.996%) and the other being helium flowing through a water bubbling system. The total gas flow rate is 4slm, and the water vapor concentration is controlled by adjusting the ratio of the dry (F_{dry}) and moist helium (F_{moist}) flow rates. The optical emission spectra are measured at the plasma contact point on the surface of stainless steel plate.

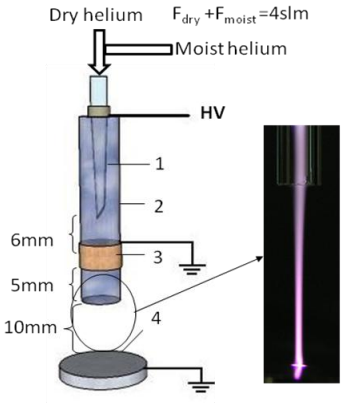

1-needle electrode, 2-glass tube
3-copper electrode, 4-stainless steel

FIG.1 SCHEMATIC EXPERIMENTAL SETUP

3. References

[1] K. Becker, A. Koutsospyros, S. M. Yin, C. Christodoulatos, N. Abramzon, J. C. Joaquin, G. Brelles-Marino, Plasma Physics and Controlled Fusion. **47**(2005) B513.

[2] P. Sunka, Physics of Plasmas. **8** (2001) 2587.

[3] M. G. Kong, G. Kroesen, G. Morfill, T. Nosenko, J. van Dijk, J. L. Zimmermann, New Journal of Physics. **11** (2009) 115012.

Topic number: 1

Simulation of prebiotic atmospheres by atmospheric pressure glow discharge generated in nitrogen-methane gas mixture

D. Trunec[1], V. Mazankova[2], L. Torokova[2], N. J. Mason[3]

[1] *Faculty of Science, Masaryk University, Kotlarska 2, Brno 611 37, Czech Republic*
[2]*Faculty of Chemistry, Brno University of Technology, Purkynova 464/118, 612 00 Brno, Czech Republic*
[3]*Department of Physical Sciences, Open University, Walton Hall, Milton Keynes MK7 6AA, United Kingdom*

We studied chemical reactions in N_2 + CH_4 mixture initiated by DC glow discharge. This experiment was designed to mimic prebiotic atmospheres. The content of CH_4 was set to 2%, the total pressure was set to 101 kPa and the gas temperature to 300 K. The composition of products from these reactions was studied by GC-MS and FTIR. A kinetic model for reactions in this mixture was developed. The influence of CO_2 admixture to N_2 + CH_4 was also investigated experimentally and theoretically. It was assumed in the model that 2% of nitrogen was dissociated to nitrogen atoms in the ground state, the CH_4 was fully dissociated into 90% of CH_3 and 10% of CH_2. This was taken as initial conditions for the calculations and the kinetic equations were solved numerically for time from 0 to 10 s.

1. Introduction

The gliding arc configuration of atmospheric pressure discharge has been shown to be a good mimic of processes in the prebiotic atmospheres [1]. The present work is focused on comparison of experimental data and data from kinetic model for chemical reactions in N_2+CH_4 gas mixtures and admixture of the carbon dioxide (CO_2) from 1% to 3 %. The neutral products generated in the discharge were identified and quantified by the means of the Fourier-Transform-Infra-Red spectroscopy (FTIR) and by Gas Chromatography Mass Spectroscopy (GC-MS).

2. Experimental set-up

The experimental set-up was in detail described in our previous studies [1]. An atmospheric pressure DC glow discharge was created between two stainless steel electrodes separated by a 2 mm gap. The discharge was operated at an applied voltage of 350 V and discharge current in range from 15 to 40 mA in pure nitrogen with 1–5 % of CH_4 (both gases having quoted purity of 99.995 %) with admixture of 1 and 3 % of CO_2 at the total flow rate of 50 sccm. The flow rates of all gases through the reactor were regulated using mass flow controllers..

3. Kinetic model

The kinetic model uses mainly the set of chemical reactions and their rate coefficients from Loison et al [2]. In our model 189 different particle types and 986 chemical reactions were taken into account. Also reactions with oxygen and oxygen containing species were involved in the model, although the calculations were performed firstly without any oxygen. The different initial conditions resulted in small changes in the product concentrations, however, the main discrepancies between the model and experimental results were not solved.

4. Results

The comparison of results from experiment and model is shown in Tab.1. The HCN concentration was calculated from the model in agreement with experimental data. The NH_3 concentration predicted by model is about three orders lower than in experiment. This can be caused by surface reactions which are not include in the model.

When from 1 to 3% of CO_2 was added to N_2 + CH_4 mixture, then only CO was detected additionally in the experiment and the production of HCN was increased. No other oxygen containing compounds were detected, however the model predicted creation of formaldehyde.

Tab. 1 Comparison of results from experiment and model.

	experiment (ppm)	model (ppm)
HCN	2000	1600
NH_3	1500	0.2
C_2H_6	n/a	400
C_2H_2	n/a	31

5. References

[1]L. Torokova, J. Watson, F. Krcma, V. Mazankova, N. J. Mason, G. Horvath, S. Matejcik. Contrib. Plasm. Phys., **55** (2015) 470.

[2] J. C. Loison, E. Hébrard, M. Dobrijevic, K. M. Hickson, F. Caralp, V. Hue, G. Gronoff, O. Venot, Y. Bénilan, Icarus, **247** (2015) 218.

Numerical modelling of high-pressure arc discharges: matching LTE arc core with the electrodes

M. Lisnyak[1], M. D. Cunha[2,3], J-M. Bauchire[1], M.S. Benilov[2,3]

[1] *GREMI, UMR 7344, Université d'Orléans, 14 Rue d'Issoudun, Orléans, 45067, France*
[2]*Departamento de Física, FCEE, Universidade da Madeira, Largo do Município, 9000 Funchal, Portugal*
[3]*Instituto de Plasmas e Fusão Nuclear, IST, Universidade de Lisboa, Portugal*

Numerical simulations of electric arcs burning in high-pressure gases are commonly performed by means of a model in which the arc plasma is assumed to be in local thermodynamic equilibrium (LTE). In this work, this model is supplemented with a self-consistent description of the interaction of the LTE arc bulk with the electrodes. This is done with the use of the equation of balance of energy in the non-equilibrium near-electrode layers that separate the LTE bulk from the electrodes. As an example, the developed model has been applied to a short free-burning arc in atmospheric-pressure argon in a wide range of arc currents, from 20 to 200 A. The simulation results have been compared with those from a model that does not rely on assumptions of thermal or ionization equilibrium in the bulk plasma, as well as with the experiment, and a good agreement was found.

Numerical modelling of high-pressure electric arcs is of high interest due to many industrial applications. The essential elements of the numerical models are interfaces separating the bulk plasma from the electrodes, which are supposed to provide a reasonably accurate description of the physics governing the plasma-electrode interaction.

The choice of the model of plasma-electrode interaction depends on the description of the bulk plasma being used. As far as the plasma-cathode interaction is concerned, self-consistent models exist for a fully non-equilibrium (NLTE) description and a two-temperature (2T) description, which takes into account different electron and heavy-particle temperatures but assumes ionization equilibrium. On the other hand, most works dedicated to simulation of high-pressure arc discharges employ the assumption of LTE. LTE models are significantly simpler than the NLTE and 2T models; their numerical realization is simpler, may rely on ready-to-use specialized software such as Equilibrium DC Discharge (sub)module of the Plasma module of commercial software COMSOL Multiphysics, and requires less computation resources. It is therefore highly desirable to develop a self-consistent method of matching solutions in the LTE bulk plasma and in the electrodes.

A self-consistent matching of an LTE bulk plasma with a cathode, proposed in this work, is based on the balance of energy in the near-cathode non-equilibrium plasma layer, which comprises a quasi-neutral ionization layer and a space-charge sheath [1]. The matching of an LTE bulk plasma with an anode is based on the balance of energy in the near-anode layer and on a pre-computed value of the so-called anode heating voltage.

The system of MHD equations is solved in the LTE bulk plasma. The heat conduction and current continuity equations are solved in the electrodes. Solutions in the different domains are matched through boundary conditions. The commercial software COMSOL Multiphysics is employed.

As an example, simulation results are reported for the conditions of experiment [2]: a free-burning 1 cm-long atmospheric-pressure argon arc with a rode tungsten cathode and a plane copper anode, the arc current varying from 20 to 200 A. The effect of the cathode shape on the arc temperature has been investigated as well.

The computed distributions of plasma parameters are compared with those obtained by means of the NLTE approach [3]. The current-voltage characteristic of the arc is compared with the experiment [2]. In both cases, a good agreement has been found.

The work at Université d'Orléans was supported by Zodiac aerospace and the work at Universidade da Madeira was supported by FCT of Portugal through the project Pest-OE/UID/FIS/50010/2013.

References

[1] M. S. Benilov and A. Marotta, J. Phys. D: Appl. Phys., vol. 28, no. 9, p. 1869, Sep. 1995.
[2] N. K. Mitrofanov and S. M. Shkol'nik, Tech. Phys., vol. 52, no. 6, pp. 711–720, 2007
[3] M. Baeva, M. S. Benilov, N. A. Almeida, and D. Uhrlandt, J. Phys. D: Appl. Phys., vol. 49, no. 24, p. 245205, 2016.

Behaviour of a short electric arc between bus-bars electrodes: numerical and experimental study

Marina Lisnyak[1], Moussa Chnani[2], Alain Gautier[2], Jean-Marc Bauchire[1]

[1] *GREMI, UMR 7344, Université d'Orléans, 14 Rue d'Issoudun, Orléans, 45067, France*
[2] *Zodiac Aero Electric, Zodiac Aerospace, 7, rue des Longs Quartiers, 93108, France*

The behaviour of the electric arcs between plane electrodes is in high interest due to their presence in industrial applications, such as low voltage circuit breakers. In this contribution, numerical simulations of an electric arc displacement are shown. The calculations are supported with experimental investigations. Magneto-hydrodynamic approach has been chosen for the arc description, while the plasma is assumed to be in local thermal equilibrium. The arc movement is realized by displacement of the electrodes attachments, which is determined experimentally. The calculations are performed using commercial software COMSOL Multiphysics. The simulation results have been compared with the experiment, and show similar arc behaviour.

1. Introduction

Study of the electric arc displacement between bus-bar electrodes is of high interest due to many industrial applications, such as low voltage circuit breakers (CB) [1]–[3]. Understanding of the arc displacement behaviour helps to predict and control successful switching capability of the CB. The interest of the present work is to investigate similar phenomena in the context of its appearance in electrical networks of aircrafts, while an arc fault takes place. In this work, numerical simulations of the electric arc are performed and supported with the experimental investigations.

System of magneto-hydrodynamic equations provides mathematical description of the electric arc phenomena, while the arc plasma is assumed to be in local thermal equilibrium (LTE). The complexity arises with the arc displacement description, while there is still no universally accepted opinion about the underlying mechanisms.

Numerically the model has been realized using the commercial software COMSOL Multiphysics®.

2. Results

A three-dimensional modelling of a moving arc between the bus-bars electrodes is performed. The size of the calculation domain is 60x60x30mm, including the bus-bar electrodes (copper) and surrounding gas (argon at 1 atm). The electrodes have a length of 40 mm, a square cross section with 3x3 mm, and the gap between them is 20 mm. The arc is supplied with a DC current of 200 A and 4 ms duration.

The initial values of a stationary arc with fixed positions have been used to obtain the time-dependent solution of the problem. The cathode attachment exists in spot mode, as the anode one, while the spot radius and the temperature is introduced in the model as fixed parameters. Arc displacement along the electrode is realized by displacement of the cathode and anode attachments with fixed velocity. The different arc behaviour is observed for different displacement velocities. The example of the simulation results is presented in figure 1 for the fixed arc displacement velocity 5 m/s.

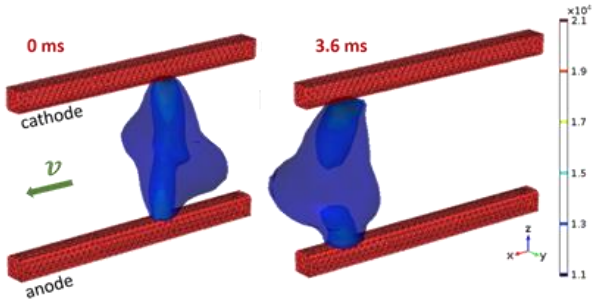

Figure 1: Temperature evolution (K) of the arc plasma.

The simulation results are supplied with the experimental investigations, which gives an estimation of the arc displacement velocity. High speed video-images of the arc emission have been compared with the computed arc temperature distributions and show similar arc behaviour.

3. References

[1] B. Swierczynski, J. J. Gonzalez, P. Teulet, P. Freton, and A. Gleizes, J. Phys. D: Appl. Phys., 2004.

[2] M. Lindmayer, E. Marzahn, A. Mutzke, T. Ruther, and M. Springstubbe, IEEE Trans. Compon. Packag. Technol., 2006.

[3] F. Yang et al., J. Phys. D: Appl. Phys, 2013.

Measurements and kinetic computations of electron transport parameters in CO_2 in an extended E/N range

I. Korolov[1], M.Vass[1], D. Loffhagen[2], N. Pinhão[3], Z. Donkó[1]

[1] *Institute for Solid State Physics and Optics, Wigner Research Centre for Physics, Hungarian Academy of Sciences, 1121 Budapest, Konkoly Thege Miklós str. 29-33, Hungary*

[2] *Leibniz Institute for Plasma Science and Technology, Felix-Hausdorff-Str. 2, 17489 Greifswald, Germany*

[3] *Instituto de Plasmas e Fusão Nuclear, Instituto Superior Técnico, Universidade de Lisboa, Lisboa, Portugal*

The transport coefficients of electrons (bulk drift velocity, longitudinal diffusion coefficient, and effective ionization frequency) in CO_2 have been measured under time-of-flight conditions over a wide range of the reduced electric field, 15 Td ≤ E/N ≤ 2660 Td, in a scanning drift tube apparatus. These parameters are compared to the results of previous experimental studies, as well as to results of solutions of the electron Boltzmann equation under different approximations and of Monte Carlo simulations. The experimental results extend the range of E/N in comparison with earlier studies. The computational results demonstrate the need for further improvement of the electron collision cross section data for CO_2 taking into account the present experimental data.

1. Introduction

The reduction of CO_2 emission is one of the key challenges for the next decades. One of the solutions may be the recycling of CO_2 to produce hydrocarbon-based fuels, and non-thermal plasma technologies can contribute to this challenge. It is crucial, however, to improve our knowledge on the fundamental properties, in particular electron collision cross sections and the electron transport parameters. For this purpose swarm experiments play an important role.

2. Experimental apparatus

We have developed [1] an experimental apparatus operating under time-of-flight (TOF) conditions to record "swarm maps" that show the spatio-temporal development of electron clouds. The bulk drift velocity W, longitudinal diffusion coefficient D_L and effective ionization frequency υ_{eff}, are obtained by fitting the experimental and theoretical forms of this electron swarm, assuming hydrodynamic conditions. From these data the effective (steady-state) Townsend ionization coefficient, α, can also be derived.

3. Numerical methods

The experimental results are supplemented by numerical modelling and simulation. In addition to Monte Carlo simulation, three different methods have been applied to solve the electron Boltzmann equation: (i) a multiterm method for spatially homogeneous conditions, (ii) a multiterm method for spatially inhomogeneous conditions, and (iii) a density gradient representation of the electron velocity distribution function. The CO_2 cross sections available on LxCat [2] were used.

4. Results

We found significant differences between the present and other published experimental data, with the numerical results for all cross section sets tested, demonstrating the need for further improvement of the CO_2 electron collision cross section data [3]. The figure below exemplifies these differences for D_L.

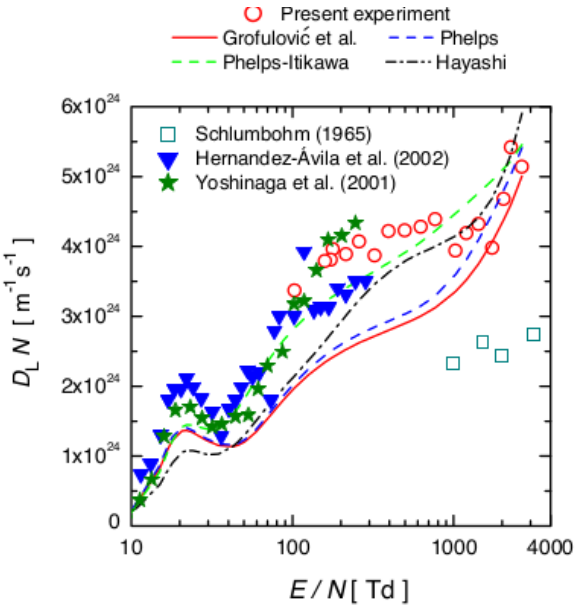

Measured values (symbols) of D_LN in comparison with values computed (lines) using different cross sections sets [2].

5. References

[1] I. Korolov, M. Vass, N. Kh. Bastykova and Z. Donkó, *Rev. Sci. Instrum.* **87** (2016) 063102

[2] http://www.lxcat.net

[3] M. Vass I. Korolov, D. Loffhagen, N. Pinhão, Z. Donkó. *Plasma Sources Sci. Technol.* (in print)

Acknowledments: This work was supported by OTKA/Hungary, via grant K105476, FCT/Portugal, under projects UID/FIS/50010/2013 and UID/FIS/PTDC/FIS-PLA/1420/2014 (PREMiERE). The studies were performed in the framework of the Collaborative Research Centre Transregio 24 ``Fundamentals of Complex Plasmas".

Transport properties of hot dense plasmas

S.K. Kodanova [1], T.S. Ramazanov [1], M.K. Issanova [1], E.E. Shokparbayeva [1]

[1]*IETP, Al-Farabi Kazakh National University, Almaty, Kazakhstan*

In this work the transport properties of non-isothermal dense plasmas were studied. Transport processes in dense plasmas were studied on the basis of the effective potentials using the Coulomb logarithm. These potentials take into consideration long-range multi-particle screening effects and short-range quantum-mechanical effects in two-temperature plasmas. The obtained results were compared with the theoretical works of other authors and with the results of MD simulations.

Investigation of transport properties of the dense plasma is a great importance for plasma physics, as well as for the problems of inertial confinement fusion (ICF), warm dense matter driven by heavy ion beams [1]. Experimental investigation of dense nonideal plasmas based on using of a shock wave compression, a high-power laser and an ion accelerator devices [1-2].

In presented work transport properties of hot dense, non-isothermal plasma are considered. One of the important values describing the transport coefficients of deuterium-tritium plasma is the Coulomb logarithm. The Coulomb logarithm is obtained on the basis of effective potentials. These interaction potentials take into consideration long-range many particle screening effects as well as short-range quantum-mechanical effects [3].

The Coulomb logarithm is determined by the center of mass scattering angle θ_c [4-5]:

$$\lambda_{\alpha\beta} = \frac{1}{b_\perp^2}\int_0^{b_{\max}} \sin^2\left(\frac{\theta_c}{2}\right) b db, \qquad (1)$$

$$\theta_c = \pi - 2b\int_{r^0}^{\infty} \frac{dr}{r^2}\left(1 - \frac{\Phi_{\alpha\beta}(r)}{E_c} - \frac{b^2}{r^2}\right)^{-1/2}, \qquad (2)$$

where $E_c = \frac{1}{2} m_{\alpha\beta}\upsilon^2$ is the energy of the center of mass, $m_{\alpha\beta} = m_\alpha m_\beta/(m_\alpha + m_\beta)$ is the reduced mass of the particles of kinds α and β (electron and ion); $b_\perp = Z_\alpha Z_\beta e^2/(m_{\alpha\beta}\upsilon^2)$, $b_{\min} = \max\{b_\perp, \lambda\!\!\!^{-}_{\alpha\beta}\}$ describes the minimum impact parameter, where is $\lambda\!\!\!^{-}_{\alpha\beta} = \hbar/\sqrt{2\pi m_{\alpha\beta} k_B T}$ is the thermal de Broglie wavelength.

For inertial confinement fusion applications, we have calculated diffusion and viscosity of deuterium-tritium plasma for density $\rho = 5\,g/cm^3$ and temperatures ranging from 2 to $10 eV$ using the Coulomb Logarithm based on effective potentials. Fig.1 show a comparison of the calculated data on diffusion and viscosity in a DT plasma with the theoretical results of other authors [6] such as finite-temperature Kohn-Sham density-functional theory molecular dynamics (QMD) and orbital-free molecular dynamics (OFMD).

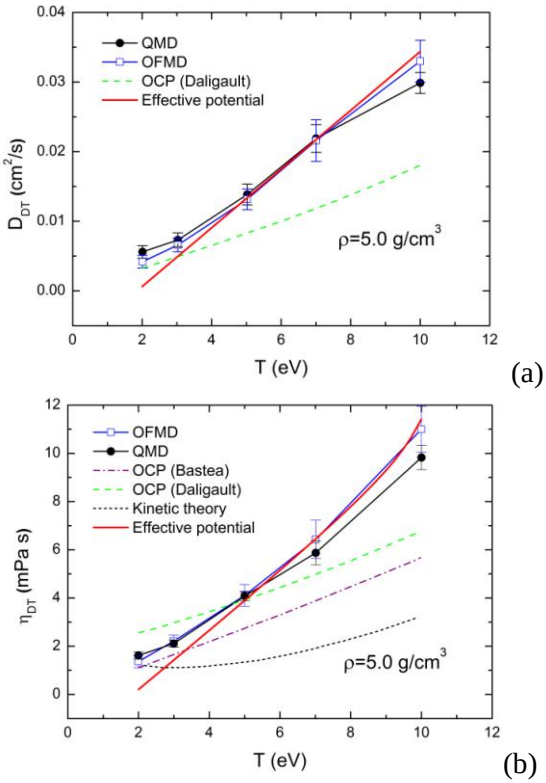

Fig. 1. The diffusion (a) and viscosity (b) coefficients for the DT plasma as function of temperature.

References

[1] V.E. Fortov et al. Physics-Uspekhi **51** (2) (2008).

[2] N.A. Tahir et al. Phys. Plasmas **18** (2011) 032704.

[3] T.S. Ramazanov, Zh.A. Moldabekov, M.T. Gabdullin. Phys.Rev. E **92** (20015) 023104.

[4] M.K. Issanova, S.K. Kodanova, T.S. Ramazanov, et al. LPB **34** (2016) 457-466.

[5] T.S. Ramazanov, et al. Contrib. Plasma Phys. **56** (5) (2016) 425-431.

[6] J.D. Kress, J.S. Cohen, D.A. Horner, et al. Phys. Rev. E **82** (2010) 036404.

Topic Number

Effects of Air, N_2, and CO_2 Plasma Irradiation to Seeds of Radish Sprouts, Potato and Soybean

Masaharu Shiratani, Thapanut Sarinont, Yosuke Wada, and Kazunori Koga

Department of Electronics, Kyushu University, 744 Motooka, Nishi-ku, Fukuoka 819-0395, Japan

We compare growth enhancement effects of air, N_2, or CO_2 plasma irradiation to seeds of radish sprouts, potato and soybean. Air and CO_2 plasma irradiation in a short duration of 3 min lead to growth enhancement of plants in a long term for radish sprouts and potato. The maximum average length is 1.42 and 1.14 times as long as that of control for radish sprouts and potato, whereas the length is nearly the same as that of control for soybean. N_2 plasma irradiation shows no effects indicating reactive oxygen species are key species for the plant growth enhancement.

1. Introduction

In recent years, a novel trend of plasma applications towards biomedical and agricultural areas has spread wide, because plasma can offer extracellular control of cell division, cell growth, and apoptosis.[1-6] Our previous study shows, for instance, that compared with non-treated seeds, air nonthermal plasma irradiated seeds lead to a 11-percent shorter harvest time, a 56-percent increase in total seed weight, and a 39-percent increase in the number of seeds harvested from the grown plants.[5] In this study, we investigated effects of plasma irradiation to seeds of radish sprouts, potato and soybean using air, N_2, or CO_2 plasmas.

2. Experimental

Experiments were carried out with a scalable DBD device described in elsewhere.[5] The discharge voltage and current were 9.2 kV and 0.2 A. Seeds of radish sprouts (*R. sativus*), potato (*S. tuberosum*) and soybean (*G. max*) were employed for plasma irradiation. 10 seeds for each species were arranged at 3 mm below the electrodes in chamber filled with air, N_2, or CO_2. After 3 min plasma irradiation, the seeds were cultivated using a water tray for radish sprout and soybean, and using soil for potato. The length of their stem was measured 7 days for beans and 30 days for potato and soybean after the onset of cultivation.

3. Results and discussion

Table 1 shows average length of plants 7 days cultivation for Radish and soybean, and 30 days for Potato after 3 min plasma irradiation in dry air, N_2 and CO_2. The length was normalized by that of control.. Radish sprouts has the maximum average length 1.42 times and 1.24 times longer than that of control for Air and CO_2, whereas that for N_2 is nearly the same as that of control. CO_2 plasma irradiation to soybean brings about slight inactivation. Average length of Radish and Potato were significantly greater by Tukey test, $P<0.1$ with air plasma irradiation than that control. These results clearly show that each species has its own unique response to plasma irradiation. Because N_2 plasma irradiation shows no effects, reactive oxygen species are key species for the plant growth enhancement.

	Ambient gas species		
Plants	**Air**	**N_2**	**CO_2**
Radish	142%*	98%	124%*
Potato	114%*	106%	108%
Soybean	96%	102%	84%

Table 1. Average length of plants 7 days cultivation for Radish and soybean, and 30 days for Potato after 3 min plasma irradiation in dry air, N_2 and CO_2. The length was normalized by that of control. N=10, * : $P<0.1$.

4. Acknowledgements

This work was partly supported by MEXT KAKENHI Grant Number 24108009 and JSPS KAKENHI Grant Number 16H03895.

5. References

[1] G. Fridman, et al., Plasma Proc. and Polym. **5** (2008) 503.
[2] S. Kitazaki, et al., Proc. IEEE TENCON (2010) 1960.
[3] S. Kitazaki, et al., Curr. Appl. Phys. **14** *(*2014*)* S149.
[4] T. Sarinont, et al., Arch. Biochem. Biophys. **605** (2016) 129.
[5] K. Koga, et al., Appl. Phys. Express **9** (2016) 016201.
[6] T. Sarinont, et al., Matr. Adv. (2017) doi.org/ 10.1557/adv.2017.178.

Nitrization of graphite during its interaction with nitrogen plasma jet

V.F. Chinnov, M.A. Sargsyan, D.I. Kavyrshin, A.V. Chistolinov

Joint Institute for High Temperatures of the Russian Academy of Sciences, Moscow, Russia

The results of spectral analysis of the nitrogen plasma jet and graphite surface interaction zone provide quantitative data on the effect of the surface and volumetric graphite nitrization on the component composition of plasma. The analysis was conducted with spatial and temporal resolution as the graphite sample was heated to the temperatures of 2500 – 3000 K. An experimental setup was designed and constructed that included a generator of high-enthalpy (H>20 kJ/g) argon, nitrogen and air plasma jets with a diameter of 8-20 mm and a partitioned calorimeter that is designed to measure the heat fluxes in the plasma-sample interaction zone. The measuring equipment used also included three high-speed video cameras, two fibre-optic spectrometers, one MS5204i spectrometer with a high-sensitivity matrix at its outlet.

1. Experimental set-up

As the plasma generator, a plasma torch with vortex stabilization and an expanding outlet channel is used, which provides a high flow performance, efficient heating of the working medium and low thermal losses into a water-cooled surface of the anode. Broad research and technological capabilities of such plasma torches are presented in [1]. The plasma torch with an expanding output electrode (anode) 6 or 10 mm diameter creates a downstream plasma jet with a temperature at the anode outlet of 10000 – 15000 K, which is defined by the plasma forming gas (argon, nitrogen, air) and the current arc that varies in 100-400 A range. The plasma jet outflows into the air atmosphere at a rate defined by the plasma forming gas flow rate and plasma density at the nozzle outlet. Heat-resistant sample (in this case graphite) is located on the plasma jet axis at a selected distance from the outlet section of the plasma torch. The graphite sample has a cylindrical shape with the bottom flat surface being mounted on an uncooled tungsten rods 2mm in diameter.

Spectral systems for longitudinal and transverse scanning of the plasma jet emission enable continuous monitoring of the emission spectra with a spatial resolution of 0.5 mm throughout the tests. Monitoring of spatial-temporal changes of plasma emission spectra is performed by scanning of the plasma jet's sharp image formed by lenses using spectrometers' fibre optic light guides. The detailed picture of changes in the near-surface region of the plasma is recorded with a scale of 1:1 on the high-speed camera and MS 5204i spectrometer with an Andor matrix camera at the spectrometer's outlet. The Andor camera records plasma's spectral intensity distribution along the vertical z axis near the sample's surface (0 – 5 mm above the sample's surface) and thermal radiation of the heated sample in the selected spectral range.

2. Experimental results

As shown by a comparison of the experimental spectrum with the model, vibrational and rotational temperature of cyanogen drop when approaching the surface of the sample and the relative concentration of cyanogen increases rapidly (Table. 1). The latter is probably due to the nitrization of the carbon that is released into a high-enthalpy nitrogen plasma stream during the destruction of carbon sample in the process C+N→CN, this process commences at high temperatures in both the gaseous environment around the sample and on the sample's surface [2, 3].

Table 1. Temperatures and relative plasma component concentration above the investigated graphite sample

Distance from the surface, mm	Vibrational temperature, K	Rotational temperature, K	Relative concentration of CN	Relative concentration of N2+
2	7800	5500	0,80	0,20
1	7500	5000	0,87	0,13
0	7000	5000	0,95	0,05

Another essential carbonaceous component that was observed in the surface region, is a strong spectral line C I 247,8 nm.

3. References

1. E.Kh. Isakaev, O.A. Sinkevich, A.S. Tyuftyaev and V.F. Chinnov, High Temp, **48** (2010) 97-125.

2. T. Suzuki, K Fujita, T. Sakai. J Thermophysics Heat Tr., **24** 3 (2010).

3. B. Vancrayenest and Douglas G. Fletcher. 9th AIAA/ASME Joint Thermophysics and Heat Transfer Conference 2006,

The movement of the optical inhomogeneities and the velocity of the plasma jet

V.F. Chinnov, M.A. Sargsyan, M.Kh. Gadzhiev, D.I. Kavyrshin, M.A. Khromov

Joint Institute for High Temperatures of the Russian Academy of Sciences, Moscow, Russia

Movement of the plasma jets during transient operation flow is accompanied by a large-scale turbulence, caused by twisting of the plasma flow needed to increase the resource life time of the cathode and the anode, the disruption of the boundary layer at the exit of the divergent nozzle of the plasma torch, the features of the current flow in the plasma jet and its binding to the electrodes, the roughness of the walls of the anode vortex channel, etc. When the plasma jet is registered by the video camera with high frequency $\nu \geq 1 \cdot 10^4$ Hz and low exposure time $\tau_e \leq 20$ μs, the "instant" structure of the turbulent flow can be obtained, with a typical size of turbulent moles of 5 – 10 mm, which is comparable to the radius of the jet. Therefore, in such flows the velocity measuring method could consist of measuring the velocity of plasma emission's optical inhomogeneities that are caused by the turbulization of the jet.

The proposed method of introducing a localized inhomogeneities in the plasma stream [1] consists of placing in the desired longitudinal coordinate along the diameter of plasma jet a source of plasma clumps, micro- and nanoparticles, that will move in the plasma stream without slipping and that will have a different luminous intensity when compared to the surrounding environment. The plasma stream with a temperature 7000 – 8000 K that is generated by the plasma torch is incident on the rod that is placed across the centre of the plasma stream. The formed sublimate moves away from the rod and forms fragments and clumps that are characterized by a bright luminescence, compact form and their weak change over time that allows to track the geometric centres or forefronts of these clumps. Optical inhomogeneities are recorded with one or two high-speed cameras, which with the necessary field depth, the scale of M = 1:5 and spatial resolution of 30-59 microns perform frame by frame video recording of the extended paraxial region of the stream with a frequency of $(0.5\text{-}10)\times10^4$ frames/s and selected exposure time τ_{exp} = 2-50 μs, which is determined by the luminosity of inhomogeneities and their velocity. The velocity of these clumps' forefronts was determined by the scale of their displacement from frame to frame, and the time length between adjacent video frames $\tau=1/\nu$, where ν – the frame rate.

Local measurements of the velocities of the microparticles that are ablated from the graphite rod's surface and are lying in the center plane can be accomplished by the synchronous illumination of this plane by "laser sheet" with a width of 1-1.5 mm and length of several diameters of the plasma jet, and front video registration of this plane. The pulse duration of a repetitively pulsed laser and the exposure time of the camcorder are selected in accordance with the luminance and diffusing capacity of the particles and the speed of their movement.

To test the effectiveness of this method a quantitative analysis was carried out on the results of high-speed video recording of optical inhomogeneities in the nitrogen plasma jet with a diameter of about 20 mm without the marker rod and with graphite, copper and tungsten rods with their diameters varying in 0.7 – 1.0 mm range. The aggregate value of the velocity of the plasma's "own" inhomogeneities and the velocity of inhomogeneities introduced by the rod that was placed at z = 20 mm in the zone z ≥30 mm have similar values and show a reduction in the speed of the plasma jet as it propagates downstream from 160 m/s at z=30 mm to 100 m/s at z = 70 mm.

To analyse the perturbing influence of the graphite sublimate on the temperature of the plasma jet a registration of the plasma emission spectra was performed at 1-2 mm downstream from the rod.

The first results of the use of optical inhomogeneities introduced into the stream by graphite rods for measuring the speed of the plasma jet, show the suitability of the proposed method and merit further development.

The work was partially supported by Russian Foundation for Basic Research (№ 16-08-00323)

[1] Russian Federation patent application №2016150439, МПК9 G 01 P 5/20, (2016).

Influence of humidity on formation of pulsed atmospheric pressure plasma streamers

N. Selaković[1], J. Voráč[2], N. Puač[1], G. Malović[1], P. Dvořák[2] and Z. Lj. Petrović[1,3]

[1] *Institute of Physics, University of Belgrade, Pregrevica 118, 11080 Belgrade, Serbia*
[2] *Department of Physical Electronics, Faculty of Science, Masaryk University, Kotlářská 2, Brno 611 37, Czech Republic*
[3] *Serbian Academy of Sciences, Knez Mihailova 35, 11000 Belgrade, Serbia*

Atmospheric pressure plasma jet (APPJ) falls into one of the most promising non-equilibrium low temperature plasma sources which are convenient for multiple applications. In order to achieve the best possible results in applications and explain the mechanisms that lead to the modification of the samples it is necessary to perform a detailed diagnostics of plasma source. Many studies showed that the low-frequency plasma jet's plume is made of fast pulsed atmospheric pressure plasma streamers (PAPS). In this study we show that the change in the concentration of water vapour within the tube, where the feeding gas flows, significantly affect the formation of PAPS.

1. Introduction

The expansion of low temperature atmospheric pressure plasma sources used in the treatment of heat-sensitive samples carries step forward in future bio technologies, methods of healing, etc. These kind of plasmas are particularly suitable for treatment of the samples that do not tolerate vacuum and, more importantly, they produce a huge number of reactive chemical species in its composition.

We have designed and performed detailed diagnostics of atmospheric pressure plasma jet sources with several types of electrode geometries [1]. It is shown that the formation and propagation of PAPS is influenced by electrode geometry, but also by the presence of the water vapour in the helium flow. The propagation of PAPS as a function of humidity of working gas was observed by using an ICCD camera.

2. Experimental set-up

In this experiment we used APPJ [2] that operates at 80 kHz and at 6.5 kV of applied voltage. We have used transparent PET foils coated with indium tin oxide as the powered and the grounded electrode (15 mm wide). The electrodes were wrapped around the Pyrex glass tube (O.D. 6 mm and I.D. 4 mm). As a feeding gas we have used 4 slm of helium and mixture of helium and water vapour. To perform humidity measurements within the flow tube we set up Vaisala DMT143 dewpoint transmitter in front of the glass tube. For PAPS evolution we set up the ICCD camera that recorded the discharge axially along the glass tube and the plume.

3. Results

During the active discharge (water vapour not added in mixture) we noticed that the humidity measured in the helium flow is decreasing and the concentration of H_2O molecules changes from 400 to 25 ppm**.** Around 100 ppm of H_2O we observe shorter range of PAPS. At the concentration of 30 ppm PAPS starts to lose its original shape and it becomes increasingly blurred. At concentration of about 20 ppm, the PAPS appear blurred. On the contrary, a high concentration of water molecules (above 1000 ppm obtained with mixture of helium and water vapour) creates a saturated environment in which discharge starts to be quenched.

This research has been supported by the MESTD Serbia, project III41011 and ON171037 and project LO1411 (NPU I) funded by the Ministry of Education Youth and Sports of the Czech Republic

3. References

[1] N. Puač, D. Maletić, S. Lazović, G. Malović, A. Đorđević and Z. Lj. Petrović Appl Phys Lett. 101 (2012) 24103 (2).

[2] D. Maletić, N. Puač, N. Selaković, S. Lazović, G. Malović, A. Đorđević and Z. Lj. Petrović Plasma Sources Sci. Technol. 24 (2015) 025006 (9pp).

Topic number

Decomposition of Acetic Acid Solution by Dielectric Barrier Discharge

K. Teranishi[1], K. Murata[1], M. Yonezawa[1], N. Shimomura[1]

[1] *Tokushima University, 2-1 Minamijyousanjima-cho,Tokushima 770-8506, Japan*

This study deals with the decomposition of an acetic acid solution by a water treatment reactor based on a dielectric barrier discharge (DBD) with a parallel plate electrode configuration. The treat water is supplied onto an electrode surface as a water film and exposed to the DBD. The total organic carbon of the solution is estimated to evaluate the decomposition of acetic acid by the DBD.

1. Introduction

Water treatment by discharge plasma is promising technology to decompose persistent organic pollutants by chemically active species produced in the plasma. Although a great deal of the water treatment reactor using discharge plasma has been actively developed with various configurations [1], [2], the authors have developed the water treatment reactor based on a dielectric barrier discharge (DBD) produced on a treat water surface [3]. In this work, an acetic acid solution, commonly used as an indicator of persistent organic pollutants, is treated by our reactor and the total organic carbon (TOC) concentration of the solution is measured.

2. Experimental setup

The water treatment reactor used in this study was previously presented in [3], of which the several parts were modified. The reactor has a parallel plate electrode configuration, consisting of a dielectric barrier, a ring-shaped metallic back electrode and a lower metal electrode. The dielectric barrier is a borosilicate glass plate with 75 mm in diameter and 1.1 mm in thickness. It has a hole at its centre for supplying the treat water. The ring-shaped metal electrode applying a high voltage is made of a copper tape with the inner and outer diameters of 28 and 51 mm, respectively. It is adhered on one side of dielectric barrier. The lower electrode is made of stainless steel whose diameter of the planer surface is 52 mm. It is movable in the vertical direction using a micrometer gauge and a stepper motor, which is capable of adjusting the gap distance automatically and precisely. With forming the water film on the lower electrode surface, the DBD is generated between the dielectric barrier and the treat water surface. An acetic acid solution of 20 mg/L in concentration is prepared as the treat water by dissolving a guaranteed reagent of acetic acid with pure water. Total amount of the treat water is 0.5 L, which is circulated by a water pump with a flow rate of 1.5 L/min. The TOC concentration is measured by a TOC analyser (TOC-L_{CSN}, Shimadzu Corp.) to evaluate the decomposition of acetic acid. Although the TOC concentration of the 20-mg/L acetic acid solution should be 8 mg_{TOC}/L, the TOC concentration before the plasma treatment become around 7.04–7.25 mg_{TOC}/L.

3. Experimental results and discussions

The acetic acid solution is treated for 2 hours with different gap distances of 1–2.5 mm. The results are shown in Fig. 1. Argon gas is fed into the reactor with a flow rate of 1.0 L/min. The initial discharge powers adjusted in an effort to be 1.7 W for all gap distances were within the range of 1.57–1.75 W. By 2 hours' treatment, the TOC concentration decreases for all gap distances. The consumption energy for 2 hours estimated from discharge power and treatment time is also indicated in Fig. 1. The consumption energy slightly becomes large with longer gap distance. However, the higher TOC reduction is observed with the shorter gap distance. These results indicate that the shorter gap distance is expected to effectively decompose the persistent organic pollutants.

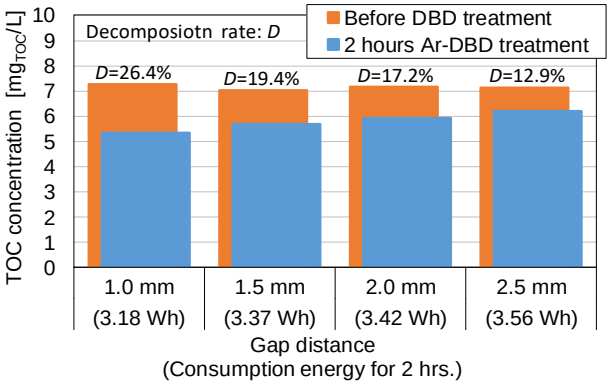

Fig. 1 TOC concentration of acetic acid before and after Ar-DBD plasma treatment for 2 hrs.

3. References

[1] N. Takeuchi *et al.*, *Jpn. J. Appl. Phys.*, **54** (2015) 116201.

[2] M. S. Jović *et al.*, *Chem. Eng. J.*, **248** (2014) 63–70

[3] K. Teranishi *et al.*, *32nd ICPIG* (2015).

Effects of the Driving Frequency on Generation of O_3, NOx in DBD plasma

Hyeongwon Jeon[1], Sangheum Eom[1], Hyewon Mun[2], Seong Bong Kim[1], Suk Jae Yoo[1] and Seungmin Ryu[1]

[1]*Plasma Technology Research Center, National Fusion Research Institute, Gunsan-city, Korea*
[2]*Department of Plasma Convergence Engineering, Kunsan National University, Korea*

The effects of driving frequency on generation of plasma reactive species were investigated in air plasma. The conventional dielectric barrier discharge(DBD) type plasma source and frequency tunable power were selected as a plasma generator. The frequency was considered as the main factor affecting the generation of plasma reactive species at air DBD plasma. The plasma reactive species, such as O_3, NO, NOx were measured with different frequency condition (operating range is from 100Hz to 8000Hz). Electrical and optical characteristics were additional measured. Experimental results show that the plasma reactive species are changed according to the frequency. It is considered that the plasma reactive species can be selectively generated through the frequency control.

1. Introduction

Air plasma application technology can be applied in various fields such as agri-food, environment, and energy. The O_3 and NOx are important chemical species of air plasma and these are utilized as a sterilizer. There are many ways to control plasma reactive species. The O_3 generation can be controlled through the driving frequency at the oxygen plasma source.[1] It is considered that O_3 and NOx can be controlled through the driving frequency at the air plasma.

2. Experimental Set-up

The experimental set-up for this study is shown in Figure 1.

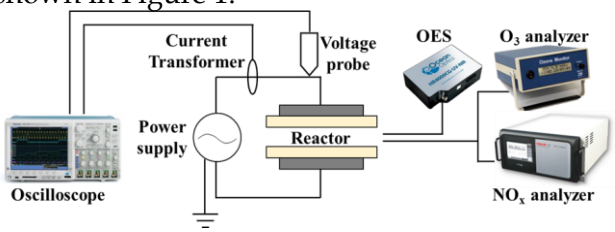

Figure 1. Experimental Set-up

A function generator and a high voltage amplifier were used to control the frequency. O_3 and NOx were measured using gas analyzers. Electrical properties were measured using an oscilloscope and optical properties were measured using OES.

3. Results and Conclusions

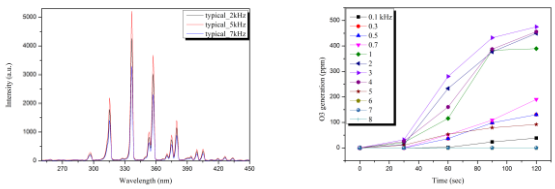

Figure 2. OES (a) and O_3 generation(b)

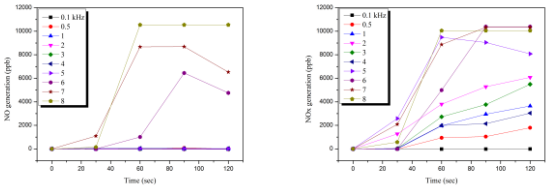

Figure 3. NO and NOx generation

As the frequency changes, the generation of reactive species is also changed. In this experimental condition, the O3 concentration increases with frequency and gradually decreases from 3kHz.(Fig. 2(b)) The NOx concentration steadily increases with frequency and is highest at 8kHz.(Fig. 3) As a result, it is considered that the generation of plasma reactive species can be controlled by frequency.

4. Acknowledgements

This work was supported by R&D Program of 'Plasma Advanced Technology for Agriculture and Food (Plasma Farming)' through the National Fusion Research Institute of Korea (NFRI) funded by the Government funds.

5. References

[1] Seung-Lok Park, Jin-Gyu Kim. J Korean Inst. IIIum. Electr. Install. Eng. Vol. 18, No.5 (2004) 146-150.

Continual radiation of H_2 and D_2 ($a^3\Sigma_g^+ \rightarrow b^3\Sigma_u^+$) induced by electron impact

J. Országh, M. Danko, M. Ďurian, Š. Matejčík

[1] *Department of Experimental Physics, Faculty of Mathematics, Physics and Informatics, Comenius University in Bratislava, Slovakia*

Electron induced fluorescence apparatus (EIFA) was used for examination of hydrogen and deuterium excitation by electrons at 14 eV impact energy with subsequent emission in spectral region between 200 – 700 nm. Relative excitation cross section for electrons with energy 0 – 100 eV was measured and compared at two separate wavelengths – 650 nm and 230 nm to confirm the radiation originates from the same deexcitation transition. The radiation of the continuum at wavelengths higher than 500 nm is shown for the first time in experimental studies. Deuterium spectral measurement was performed also at electron energy 14 eV in order to compare the results with hydrogen molecule observation.

1. Introduction

Motivation for this research is the application of the results in diagnostic of thermonuclear plasmas in tokamaks [1]. Hydrogen and deuterium plasma is produced in tokamak vessels, and the interaction of H_2 and D_2 molecules with low energy electrons (0 – 100 eV) is particularly important at the plasma edge.

2. Experiment

Hydrogen molecule has been examined in detail on EIFA. Spectra on several electron impact energies were obtained. In this work we present the spectrum at 14 eV (Figure 1) where only the continual radiation originating from the fluorescence transition H_2 ($a^3\Sigma_g^+ \rightarrow b^3\Sigma_u^+$) is observable. The spectrum was obtained with 0.4 nm optical resolution and it is given in relative scale dependent on the pressure inside the vacuum chamber (~10^{-4} mbar for H_2 measurements).

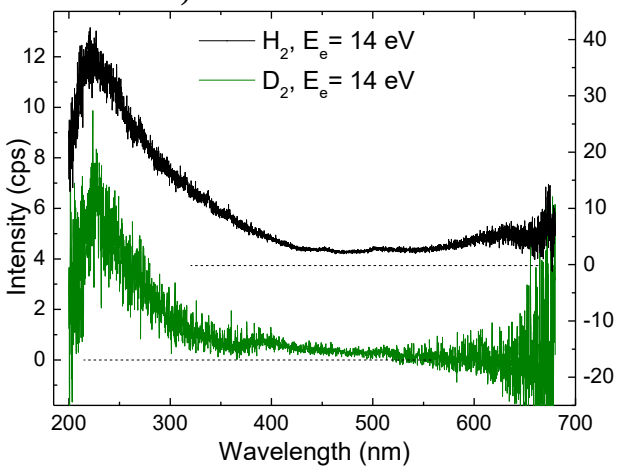

Figure 1. Emission spectrum of H_2 and D_2 at 14 eV electron impact energy originating from H_2 (black) and D_2 (green) ($a^3\Sigma_g^+ \rightarrow b^3\Sigma_u^+$) radiative transitions. The spectra were corrected for spectral response of the apparatus.

Deuterium spectrum at 14 eV was obtained for the comparison. The pressure in the reaction chamber during the D_2 measurements was slightly lower than the H_2 measurement (~5×10^{-5}mbar) which explains the lower signal – to – noise ratio in D_2 spectrum. In D_2 spectrum only the radiation of continuum is present, as well.

The second mode of measurement at EIFA is the excitation cross section measurement at fixed wavelength. The cross sections were measured at 230 nm and 650 nm. According to their identical shape and the threshold energies corresponding to 12.3±0.5 eV it is possible to suggest that both correspond to the bound – to – unbound transition, continuum radiation of H_2 ($a^3\Sigma_g^+ \rightarrow b^3\Sigma_u^+$).

3. Acknowledgements

This project has received funding from the European Union's Horizon 2020 research and innovation programme under grant agreement No 692335. This work was supported by the Slovak research and development agency project No APVV-15-0580.

4. References

[1] U. Fantz et al. Plasma. Phys. Contr. F. **43** (2001) 907.

Topic number: 5

Modelling of N_2-H_2 capacitively coupled radio-frequency discharges

M. Jiménez-Redondo[1], L. Marques[1,2], N. Carrasco[3], G. Cernogora[3], L. L. Alves[2]

[1]*Centro de Física das Universidades do Minho e do Porto, Universidade do Minho, 4710-057, Braga, Portugal*
[2]*Instituto de Plasmas e Fusão Nuclear, Instituto Superior Técnico, Univ. Técnica de Lisboa, Lisboa, Portugal*
[3]*Université Versailles St-Quentin, CNRS, LATMOS, 11 blvd d'Alembert, 78280 Guyancourt, France*

In this work, we present the results of simulations carried out for N_2-H_2 low pressure, low power capacitively coupled radio-frequency discharges, for amounts of H_2 up to 5%. Simulations are performed using a hybrid code that couples a two-dimensional time-dependent fluid module, describing the dynamics of the charged particles, to a zero-dimensional kinetic module, that solves the Boltzmann equation and describes the production and destruction of neutral species. The model accounts for the production of several excited states, and contains a detailed surface chemistry that includes recombination processes and the production of NH_x molecules. Simulations show that surface production of NH_3 plays a key role in the neutral and ion kinetics of the discharge.

1. Introduction

Capacitively coupled radio-frequency (ccrf) discharges in nitrogen-containing mixtures have been used in planetary studies to simulate, in laboratory environment, the reactivity of ionospheres. The present work is part of a research strategy, involving both simulations and experiment, to analyse the N_2-CH_4 ionospheric chemistry of Titan, the biggest satellite of Saturn. The first step was the study of ccrf discharges in pure N_2 [1], and now continues with the analysis of N_2-H_2 discharges.

2. Modelling

The simulations run at low pressures (0.6–1.2 mbar), for 30–100 sccm gas flows and 5–20 W coupled powers, in N_2-H_2 mixtures with hydrogen concentrations up to 5%.

The model consists of a hybrid code that couples a two-dimensional (*r*,*z*) time-dependent fluid-type module, which describes the transport of the charged particles, to a very complete zero-dimensional kinetic module for the nitrogen-hydrogen mixture. The fluid module solves the continuity and the momentum transfer equations for electrons, positive ions N_2^+, N_4^+, H^+, H_2^+, H_3^+, HN_2^+, NH^+, NH_2^+, NH_3^+ and NH_4^+, and negative ions H^- and NH_2^-, the electron mean energy transport equations, and Poisson's equation for the rf electric potential. The space-time map of the electron transport and rate coefficients are obtained from the electron mean energy profile, using the local mean energy approximation [1,2]. The kinetic module solves the two-term homogeneous and stationary electron Boltzmann equation (accounting for inelastic collisions from ground-state molecules and atoms, and inelastic and superelastic collisions involving vibrationally excited states) and the rate balance equations of the ground-state vibrational excited states of N_2 and H_2, the most relevant electronic excited states for N_2 and N, H, and the most important crossed-species NH_y (y=1-3) and N_2H_y (y=2-4) resulting from interactions within the N_2/H_2 systems [2,3]. An extended surface chemistry is considered, taking in account adsorption, surface association and heterogeneous reactions, which are key to the formation of NH_3. The electron impact chemistry of hydrogen has been updated using the latest set of cross sections available from the IST-Lisbon database of LXCat [4,5].

3. Results

Simulations show that significant amounts of NH_3 are produced in the discharge, with a high dependence on the parameters for the surface kinetics. The abundances of positive ions are greatly affected by the neutral composition, with NH_4^+ quickly becoming the major ion when sufficient NH_3 is present.

4. Acknowledgments

This work was partially supported by the Portuguese FCT under project UID/FIS/50010/2013.

5. References

[1] L.L. Alves et al, Plasma Sources Sci. Technol. **21** (2012) 045008.

[2] L. Marques, J. Jolly, L.L. Alves, J. Appl. Phys. **102** (2007) 063305.

[3] E. Tatarova et al, Plasma Sources Sci. Technol. **14** (2005) 19.

[4] L.L. Alves, J. Phys. Conf. Ser. **565** (2014) 012007.

[5] www.lxcat.net

Radiation trapping in non-equilibrium plasmas: matrix methods and its application to arcs and glow discharges

Yu. Golubovskii[1], D. Kalanov[1], V. Maiorov[1], M. Baeva[2], D. Uhrlandt[2], S. Gortschakow[2]

[1]*Saint-Petersburg State University, 7/9 Universitetskaya nab., St. Petersburg, 199034 Russia*
[2] *Leibniz Institute for Plasma Science and Technology, Felix-Hausdorff-Strasse 2, 17489 Greifswald, Germany*

Summary of recent experimental and theoretical studies by authors, related to radiation trapping in non-equilibrium plasmas is presented. A free-burning Ar arc and a constricted positive column of the Ar glow discharge were considered as plasma sources. Role of radiation trapping in formation of spatial distributions of excited species is demonstrated. Excited species densities and its radial distributions are determined by means of emission and absorption spectroscopy. Experimental data is compared with results of simulations. A new universal matrix method of radiation transport description in plasmas of arbitrary geometry, line shape and absorption coefficient is presented. The method is tested against existing matrix methods which are based on source symmetry.

1. Introduction

Processes related to radiative transfer with reabsorption play a significant role in non-equilibrium plasmas. Multiple approximate approaches were developed over the last decade, among them so called matrix method (reviewed in [1]) for plasma sources of certain symmetry. The latter allows for accurate treatment of the radiation trapping process within consistent collisional-radiative models [2].

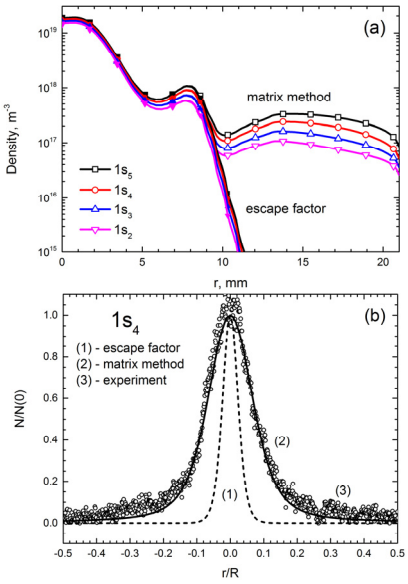

Figure 1: Density profiles of excited Ar atoms, obtained by means of matrix method and using escape factors: (a) free-burning arc; (b*)* constricted glow discharge.

2. Radiation transport and density profiles

Radiation transport equation for resonance atoms is solved in coupling with balance equations for other species. As Fig. 1 clarifies, correct description of radiation transport causes notable broadening of radial profiles of excited argon atoms, leading to an excellent agreement with experiment (Fig 1(b)).

3. Matrix method for arbitrary geometry

For an arbitrary 3D object the source geometry is discretized on a Cartesian voxel grid. Matrix coefficients, which describe a coupling between unit volumes, are computed using fast ray traversal algorithm [3]. Numerical scheme is efficiently parallelized for running on a graphical processing unit. As an example, solutions of the Holstein-Biberman equation for case of finite cylinder with point excitation source in the center using previously developed matrix approach and a new one are illustrated by Fig.2. Results are in a good agreement.

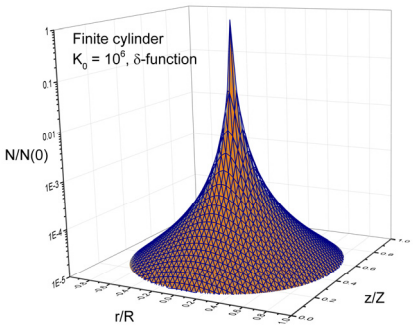

Figure 2: Solution of the equation with point excitation source in the finite cylinder. Orange – old matrix method, blue – ray tracing method.

4. References

[1] Yu. B. Golubovskii et al., Plasma Sources Sci. Technol. **22** (2013) 023001.

[2] Yu. B. Golubovskii et al., J. Phys. D. Appl. Phys. **49** (2016) 475202.

[3] J. Amanatides, A. Woo, *Eurographics* **87** (1987) 3–10

Uniform and strongly magnetized plasma using a Halbach array

O. Vasilovici[1,2], S. Costea[1], B.S. Schneider[1], R. Schrittwieser[1], C. Ionita[1]

[1]*Institute for Ion Physics and Applied Physics, University of Innsbruck, Austria*
[2]*Faculty of Physics, Alexandru-Ioan-Cuza University, Iasi, Romania*

For plasma confinement often magnetic fields are used, especially in fusion devices. Magnetic fields can either be produced by coils or by permanent magnets. Coils have the advantage of controlling the magnetic field strength by varying the current, but for high currents cooling systems have to be implemented. Permanent magnets can deliver magnetic flux into the airgap of a magnetic circuit without continuous consumption of energy and nowadays they are fully competitive with electromagnets for fields up to 2 T, and fields as high as 5 T can be produced in small volumes [1]. We present a way to produce magnetized plasma using a special magnet assembly, known as the Halbach array, which is able to produce a homogeneous magnetic flux density in a cylindrical volume. Electric probes were used to characterize this highly magnetized plasma.

1. Halbach array

An ideal Halbach array is a ring magnet where the polarization direction varies continuously along the circumference so that the magnetic flux increases inside and reduces or cancels outside. In practice, typical Halbach cylinders are built using discrete permanent magnets each with its own magnetization direction, approximating the Halbach distribution [2]. Choosing the orientation of each segment properly, the fields will add at the centre.

We have simulated the magnets' positions in order to obtain a uniform and homogenous magnetic field and the optimum cylinder bore diameter, using Quick Field v6.1 Student Edition software tool (Figure 1). The input parameters for the magnetic material were set according to the magnet's technical datasheet.

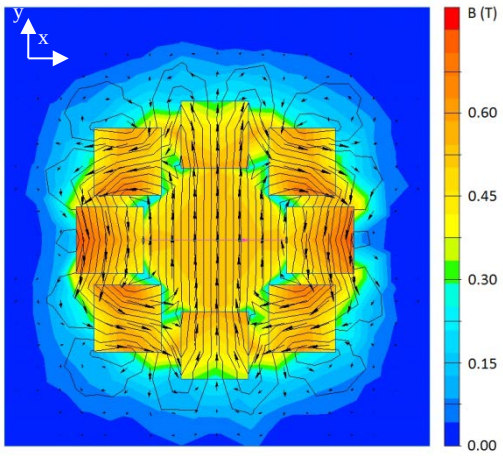

Figure 1: Magnetic flux simulation of experimental Halbach array.

2. Plasma device

To produce the magnetic field, we used 8 identical 50×15×15 mm $Nd_2Fe_{14}B$ cubic bar magnets. The perpendicular magnetic field strength ($\mathbf{B_y}$) was measured along the symmetry axis (Z) using a teslameter (Figure 2).

The plasma was created using two electrodes placed in such a way that the electrical field lines are parallel with the magnetic field (Figure 3). One electrode was grounded and the other was biased with negative voltages through a 2 KΩ resistor.

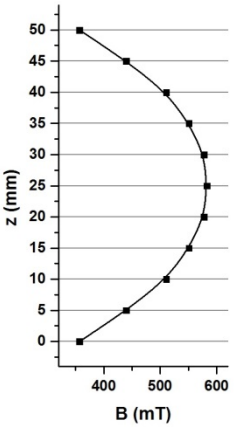

Figure 2: Magnetic flux distribution ($\mathbf{B_y}$) along the axis of the cylinder (Z axis).

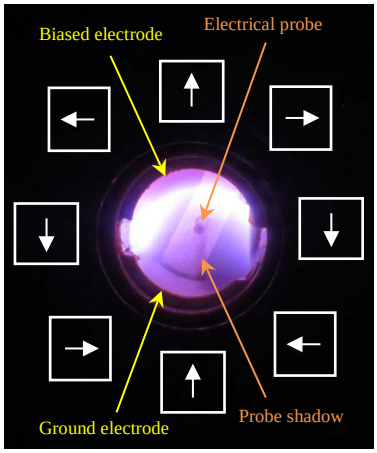

Figure 3: Plasma discharge inside Halbach array. White boxes with arrows represent the permanent magnets and their magnetic orientation.

3. Acknowledgement

This work was also supported by the CEEPUS network AT-0063.

4. References

[1] J.M.D. Coey, J. Magn. Magn. Mater. **248** (2002) 441–456

[2] C.K. Chandrana et al., J. Magn. Magn. Mater. **381** (2015) 396–400

Measurement of reactive species in Plasma Babbled-up Water affecting human cultured cells

J. Hosoda[1], T. Miyake[1], H. Kawano[1], M. Shimada[2], Y. Matsumura[3], H. Miyahara[1], A. Iwasawa[3], Y. Matsumoto[2], A. Okino[1]

[1]*FIRST, Tokyo Institute of Technology, Yokohama, 226-8502, Japan*
[2] *Advanced Nuclear Research, Tokyo Institute of Technology, Tokyo, 152-8550, Japan*
[3]*Division of Infection Prevention and Control, Tokyo Healthcare University, Tokyo, 141-8648, Japan*

As a method to introduce reactive species generated by plasma into water, plasma babbling method was proposed. In this method, it is possible to introduce reactive species into water effectively, compared with conventional method in which plasma is irradiated from above the liquid surface. By plasma babbling method, we measured ozone and hydrogen peroxide concentration in water with various plasma. Ozone was generated in oxygen and air plasma, and was 8.6 μM and 0.5 μM respectively. Also, hydrogen peroxide was generated at all kinds of plasma. Both ozone and hydrogen peroxide were measured the most at oxygen plasma. As measurement result, it was revealed that the amount and type of reactive species depend on kinds of plasma gas.

In recent years, atmospheric low-temperature plasma is being applied for medical fields. In addition, for the purpose of large capacity treatment, research about plasma-treated water in which plasma is introduced attracts a lot of attention[1]. However, to apply plasma for medical application, it is necessary to investigate the influence of plasma on living bodies. This main factor is considered to be reactive species such as ozone (O_3) and hydrogen peroxide (H_2O_2) generated by plasma. The amount and type of reactive species depend on kinds of plasma gas[2]. In this study, we investigated reactive species introduced in water by various kinds of gas plasma and the influence of them on human cultured cells.

As a method to introduce reactive species into the solution, we proposed a plasma bubbling method. In this method, the multi-gas plasma jet (PCT-DMFJ02, Plasma Concept Tokyo) is placed at the bottom of the container containing liquid. Then plasma is introduced as bubbles into the liquid directly. Therefore, the contact area between water and plasma is much larger than a conventional method in which plasma is irradiated from above the liquid surface. Thus, reactive species generated by plasma can be introduced into the liquid efficiently. In addition, since plasma is not influenced by ambient air, it is possible to specify reactive species derived from its own plasma gas. In this study, the water introduced reactive species by plasma bubbling method is called as Plasma Babbled-up Water (PBW).

After 200 mL pure water was babbled with argon, nitrogen, carbon dioxide, air and oxygen plasma at the plasma gas flow rate of 3 L/min for 5 minutes, ozone and hydrogen peroxide concentration in liquid were measured by absorption spectrophotometry. The results are shown in Fig.1. Ozone was measured in oxygen and air plasma, and the concentration was 8.6 μM, and 0.5 μM respectively. Also hydrogen peroxide was measured at all kinds of plasma. Both ozone and hydrogen peroxide were generated the most at oxygen plasma.

In the presentation, we will report the measurement results of reactive species other than ozone and hydrogen peroxide, and of reactive species in solvent other than pure water. In addition, influence of reactive species in PBW on human cultured cells will be reported also.

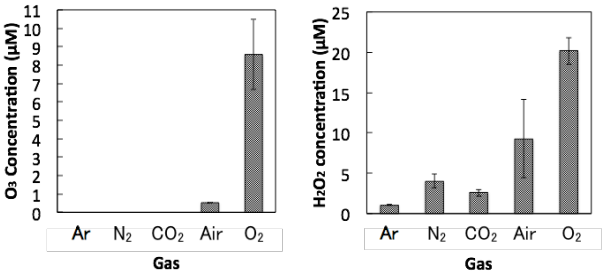

Fig.1: O_3 and H_2O_2 concentration at each Plasma Babbled-up Water

3. References

[1] K. Sato, K. Yasuoka, IEEE Trans. Plasma Sci., Vol.36, No. 4, pp. 1144-1145, Aug. 2008

[2] T. Takamatsu, K. Uehara, Y. Sasaki, H. Miyahara, Y. Matsumura, A. Iwasawa, N. Ito, T. Azuma, M. Kohno and A. Okino, *RSC Adv.*, Vol. 4, No. 75, pp. 39901-39905, Apr. 2014

Removal of supersonic ion singularity in radial Langmuir probe models

G.F. Regodón[1], J.I. Fernandez Palop[1], A. Tejero-del-Caz[2], J.M. Diaz-Cabrera[3], R. Carmona-Cabezas[1], J. Ballesteros[1]

[1] *Departamento de Física, Universidad de Córdoba, E-14071 Córdoba, Spain*
[2] *Instituto de Plasmas e Fusão Nuclear, Instituto Superior Técnico, Universidade de Lisboa, Lisboa, Portugal*
[3] *Departamento de Ingeniería Eléctrica, Universidad de Córdoba, E-14071 Córdoba, Spain*

It is well known that a singularity appears when the ions reach the speed of sound in an electropositive plasma. For cold ions, the singularity is at infinity, and so it poses no problem the numerical integration of radial Langmuir probe models. However, for warm ions the singularity typically occurs between the quasi-neutral plasma and the sheath. We have found that we can continuously join the solution at the plasma with the probe thanks to a careful analysis of the mathematical structure of the problem. The technique can be applied to different geometries and to electronegative plasmas as well. For the case of cylindrical Langmuir probes, we have derived potential profiles, ion population profiles and ion current to probe voltage characteristics. These results are used to refine diagnosis techniques by means of Langmuir probes in laboratory plasmas.

In the interest of obtaining the potential profile $\phi(r)$ around a Langmuir probe in electropositive plasmas one should solve **Poisson's equation**. In the case of cylindrical geometry, we have

$$\frac{1}{r}\frac{\mathrm{d}}{\mathrm{d}r}\left(r\frac{\mathrm{d}\phi}{\mathrm{d}r}\right) = -\frac{e}{\varepsilon_0}[n_+(r) - n_e(r)]. \quad (1)$$

The electron density $n_e(r)$ will be described by the Maxwellian distribution function, whereas the ion density $n_+(r)$ depends on the ion motion theory used. When using a radial motion theory**, the thermal motion of the ions introduces an additional term in the energy balance equation** [1], giving

$$\frac{1}{2}m_+v_+^2(r) + e\phi(r) + \frac{\kappa}{\kappa-1}k_BT_+\left(\frac{n_{+(r)}}{n_{e0}}\right)^{\kappa-1} = \frac{\kappa}{\kappa-1}k_BT_+, \quad (2)$$

where κ is the adiabatic coefficient of the thermal flow. As $v_+(r)$ is inversely related to the ion density through continuity equation, i being the ion current per unit length collected by the probe,

$$i = e2\pi n_+(r)v_+(r), \quad (3)$$

we get a polynomic equation in $n_+(r)$, with defining parameters r and $\phi(r)$, which should be solved in order to introduce its value into Poisson's equation. We have found that **this polynomial has two positive roots** that coalesce into one for certain values of the problem variables r and ϕ. We further found that one of the roots is valid in the plasma in the limit $x \to \infty$, where the ions are at rest, while the other root is valid in the sheath in the cold ions limit $T_+ \to 0$.

We have proved that the transition between these roots must occur, in the variable space (r, ϕ), in the curve where the two positive roots of the energy balance polynomial coalesce in a sort of bifurcation line, and that the only possible smooth and continuous crossing through the **regular singularity [2] where the ions reach the speed of sound** is tangent to that bifurcation curve. In figure 1 we show an example of solution of the potential profile.

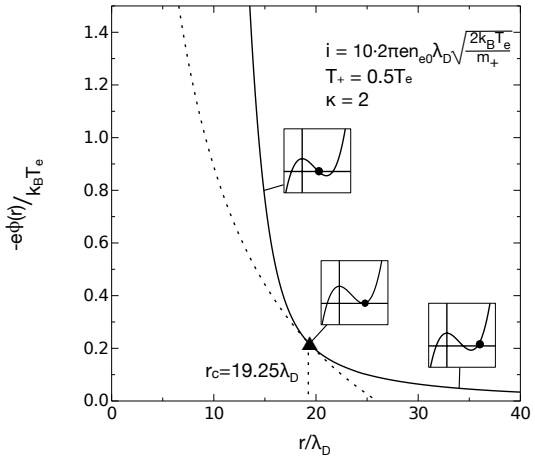

Figure 1: Potential profile and bifurcation curve solution. The small inserts are qualitative plots of the polynomic equation for $n_+(r)$.

This method is **valid for any ion temperature**. We indicate with a triangle the point where the speed of sound is reached. To the plasma or to the sheath we use the right energy balance polynomial root, as we mark with a dot in the inserts in the figure.

2. References

[1] J.I. Fernández Palop *et al* 1996 *J. Phys. D: Appl. Phys* **29** 2831.

[2] H.B. Valentini 1988 *J. Phys. D: Appl. Phys* **21** 311-321

Topic number: 4

Study of variation of hysteresis effects in self–excited amplitudes of a coaxial DC electrode system

R. Kumar[1], R. Narayanan[2], R. D. Tarey[2], A. Ganguli[2]

[1]*School of Basic and Applied Sciences, Shobhit University, Meerut–250110, U.P., India*
[2]*Centre for Energy Studies, Indian Institute of Technology Delhi, New Delhi - 110016, Delhi, India*

The paper analyzes changes in behaviour of self-excited oscillations resulting from extended plasma exposure in coaxial DC discharge plasma having a central powered anode. The role of the system asymmetry seems to play a role in triggering the oscillations. These oscillations are seen to undergo hysteresis effects with discharge current (I_d), showing a characteristic difference in the hysteresis shape as the system ages with plasma exposure. The shape change is from a hysteresis, with negligible amplitude shift post hysteresis (Type H4: bump-shaped), to a more generally observed one having a noticeable amplitude shift (Type H1: S shaped). Analysis tools such as phase maps, return maps, recurrence plots are used to characterize the variation of the observed changes in the oscillations and attempt to unravel the underlying physical mechanism to explain it.

1. Introduction

Observations of order-to-chaos-to-order transitions in the self-excited oscillations of plasma experiments have been reported [1, 2] earlier. In a study by Kumar *et. al.* [1], the associated order-to-chaos-to-order transitions have been correlated to a hysteresis in the amplitude of the floating potential fluctuations (V_f).

2. Experimental Setup

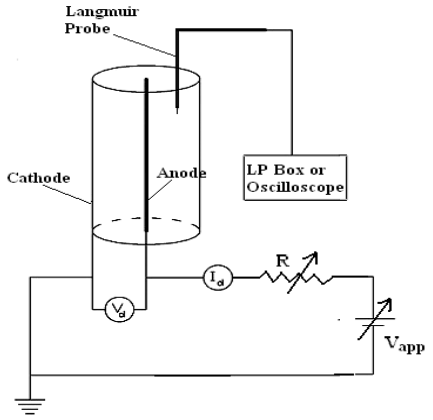

Fig 1: Schematic setup of coaxial DC plasma system

Experiments were carried out in a coaxial DC electrode (central anode diameter = 1.5 mm; outer cathode inner diameter = 48 mm) discharge system (Fig 1). A Langmuir probe, as seen in Fig 1, is used to measure the self-excited V_f oscillations.

3. Results and Discussions

Under certain operating conditions, hysteresis is observed in V_f amplitudes as a function of the discharge current (I_d) [1]. This amplitude hysteresis effect is observed between two Negative Differential Resistance (NDR) regions of the discharge characteristics (discharge current, I_d vs discharge voltage, V_d), which is also seen to undergo a hysteresis effect.

With plasma conditioning of several days one observes a flip in the forward-reversal paths of the I_d-V_d hysteresis. The plasma potential (V_p) is seen to be lower in the conditioned electrode discharges by about 30 V - 40 V. However, the more significant effect observed is modification of the behaviour of the self-excited oscillations also with the hysteresis flip in the I_d-V_d characteristics. For convenience, the unconditioned electrode is termed UE and the conditioned one is termed CE.

In the UE case, the hysteresis in the self-excited oscillations is to trigger higher amplitude oscillations in the forward path over a small range of I_d, reverting back to lower amplitudes at higher I_d (H1-type [3] or bump-shaped). However, in the CE case, the fluctuations show a characteristic change of state at higher I_d, *viz.*, a transition from low amplitude, high frequency oscillations to large amplitude, low frequency oscillations (H4-type [3] or S-shaped).

This abstract will present characteristic features of the variations in the two discharge cases using nonlinear dynamical analysis tools.

3. References

[1] R. Kumar, R. Narayanan, A. Prasad, Phys. Plasmas **21** (2014) 123501.

[2] M. Agop, D. G. Dimitriu, L. Vrajitoriu, M. Boicu, J. Phys. Soc. Jpn. **83** (2014) 054501.

[3] K. S. W. Sing, D. H. Everett, R. A. W. Haul, L. Moscou, R. Pierotti, J. Rouquérol, T. Siemieniewska, Pure Appl. Chem., **57 (**1985) 603.

Optical emission and mass spectrometric characterization of an atmospheric microwave plasma jet

J. Lo[1], L. Chauvet[1], C. Muja[1], L. Latrasse[2], Ph. Guillot[1]

[1] *Laboratoire Diagnostics des Plasmas Hors Equilibre (DPHE), Université de Toulouse, INU Champollion, Albi, France*
[2] *SAIREM SA,Neyron, France*

In this work, characterization of a surface wave discharge (SWD) in argon at atmospheric pressure generated by a surfatron device was performed by optical emission spectroscopy (OES), iCCD imaging and Time-Of-Flight Mass Spectrometer (TOF MS). The objective is to determine the spatial distributions of different species and evaluate different ions (TOF MS) generated by the source for different operating conditions.

Increasing interest in cold atmospheric pressure plasma jets (APPJ) has been observed during the last decade. Their applications are largely investigated in various fields such as nanomaterial synthesis [1], decontamination and sterilization [2], cancer treatment [3] or analytical chemistry [4]. Their ability to propagate in open air and to allow the formation of a rich chemical environment populated by ions, radicals and excited species make them promising versatile tool.

In this work, the surfatron plasma source (S-wave) is a compact source designed for industrial and laboratory applications which operates at atmospheric pressure. The plasma is generated in a dielectric tube (4 mm internal diameter and 6 mm external diameter placed within the source) by a solid-state microwave generator (200 W, 2.45 GHz). The microwave electric field propagates longitudinally at the dielectric/plasma interface. Hence, a plasma column is created and sustained with lengths varying as a function of the operating gas flow, microwave power and gas nature. In our case, the discharge gas is Argon maintained at 1 sl/min. The S-Wave plasma source is inductively coupled, thus only two tuning adjustments are provided to match the impedance. During operation, 0 W of reflected power is achieved using the integrated tuners. The source can be efficiently applied to the production of reactive/excited species.

Resolved spatial optical emission distribution measurements were performed with an optical spectrometer (HR2000+, Ocean Optics) and with an iCCD camera (PIMAX-2K-RB, Pearson Instruments). The optical measurements were performed with an iCCD camera coupled with filters to observe the spatial distributions of the main species emissions (argon, oxygen, nitrogen). The influence of the power will be presented and discussed. The presence of the ions created by the jet will be investigated with a Time-Of-Flight Mass Spectrometer (TOF MS).

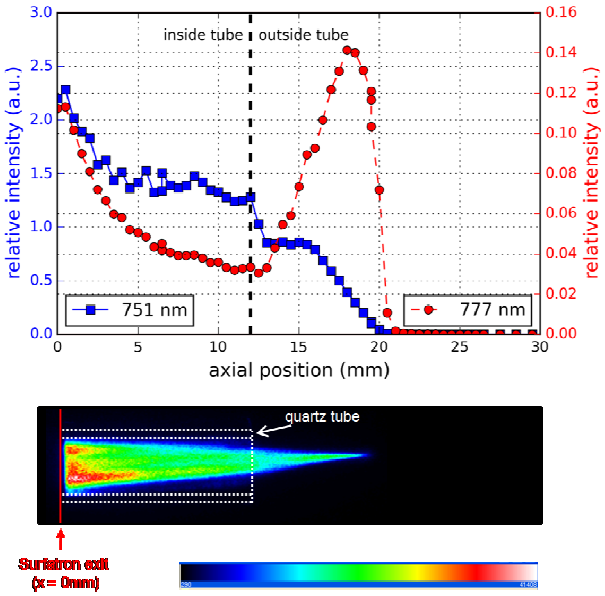

Figure 1: Intensities of argon (751 nm) and oxygen (777 nm) optical emissions as a function of axial position associated with iCCD camera imaging at 100 W power input, 1 sl/min argon.

References

[1] S. Yu, K. Wang, S. Zuo, J. Liu, J. Zhang, J. Fang, Phys. Plasmas, 22 (2015), 103522.

[2] E. Dolezalova, P. Lukes, Bioelectrochemistry, 103 (2015), 7-14.

[3] P.-M. Girard, A. Arabian, M. Fleury, G. Bauville, V. Puech, M. Dutreix, J. Santos Sousa, Sci. rep., 6 (2016).

[4] S. Martinez-Jarquin, R. Winkler, Trends in Analytical Chemistry, 89, (2017), 133-145.

Topic 1

Comparisons and scaling rules between $N+N_2$ and N_2+N_2 collision induced dissociation cross sections from atomistic studies

Fabrizio Esposito[1], Ernesto Garcia[2], Antonio Laganà[3]

[1] *Consiglio Nazionale delle Ricerche, PlasmiLab@Nanotec, Bari, Italy*

[2] *Departamento de Quimica Fisica, Universidad del Pais Vasco (UPV/EHU), Vitoria, Spain*

[3] *Dipartimento di Chimica, Biologia e Biotecnologie, Università degli studi di Perugia, Perugia, Italy*

Accurate modeling of air plasma chemistry, as in the case of aerothermodynamics or electrical discharges in air, needs elementary processes data with at least the specification of molecular vibration. Although this is presently well recognized in the literature, the associated heavy load of input data to handle can become an issue for both the dynamical and kinetic treatments. For this purpose we are developing some relationships between vibrationally dependent atom–diatom and diatom–diatom collision induced dissociation cross sections, and we show their successful application to the collisions of $N+N_2$ and N_2+N_2.

1. Scaling laws for collision induced dissociation

Quantitative knowledge of elementary processes involved in plasmas are key to successfully perform accurate kinetic simulations. The issue is the huge amount of data to treat, both in dynamical calculations and in kinetic simulations. The aim of this work [1] is to study collision induced dissociation detailed data in atom–molecule (AM) and molecule–molecule (MM) collisions involving nitrogen, obtained by molecular dynamics calculations, considering vibrational states in the range 10–50 and collision energy up to 10 eV, in order to formulate suitable scaling laws resulting in less expensive computational procedures and easier to handle treatments in kinetic simulations. It is shown that, while a direct substitution of MM dissociation cross sections with AM ones might be acceptable only at very high collision energy, scaling laws application allows to obtain quite good results on almost the whole energy range of interest. Two relations are developed in this work. The first one allows to obtain dissociation cross sections of MM(v_1,v_2) collisions, being v_1, v_2 respectively the initial vibrational states of the two molecules, from the corresponding MM(v_1,0), MM(v_2,0) dissociation cross sections. The second relation links the AM(v) cross section with the MM(v,0) one, as in fig.1. As a consequence, using both relations allows in principle to obtain any MM(v_1,v_2) dissociation cross section, provided AM(v_1), AM(v_2) cross sections are known. The advantage is clear, being a three-body dynamical calculation significantly less expensive than a four-body one. The possibility of a compact expression of the MM dissociation cross sections, expressed as a function of the AM ones, is also an advantage for the kinetic codes where those data are used. Rotation of the vibrationally more excited molecule can be included in the scaling. Work is in progress to extend these scaling laws to other collisional systems.

2. References

[1] F.Esposito, E.Garcia, and A.Laganà, Plasma Sources Science and Technology, **26** (2017) 45005 (doi:10.1088/1361-6595/aa5d27).

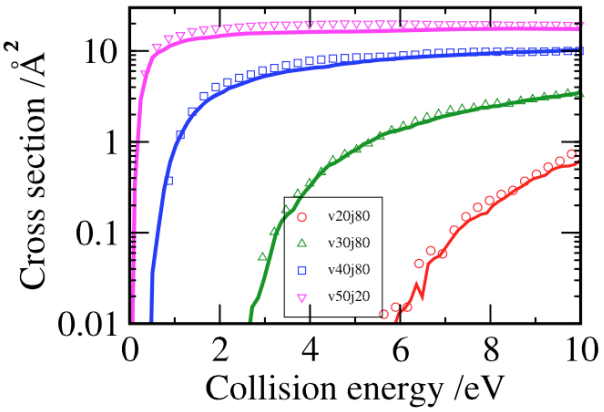

Fig.1. Comparison of computed molecule-molecule collision induced dissociation cross sections from the shown rovibrational states with corresponding values derived from atom-molecule ones.

Topic number

Investigation of collisional processes in dense semiclassical plasma

K.M. Turekhanova[1], D.S. Kaliyeva[1]

[1]*IETP, al-Farabi Kazakh National University, 71, al-Farabi av., Almaty, 050040, Kazakhstan*

Abstract: In this work we study kinetic processes of dense semiclassical plasma with the collective effect and screening. Collisional characteristics of plasma are obtained numerically by using several effective pseudopotential models with clear difference arising between them.

1. Introduction

Currently, a clear and accurate theoretical description of dense plasma remains an actual problem. Kinetic properties are the most important characteristics of dense plasma, the study of attract more and more interest. Finding the particle distribution function is one of the main problems in plasma physics. In work [1] the form of the particle distribution function determined by various parameters and processes. The main mechanism that determines the fastest part of the distribution function is the escape of electrons to the walls. Also, electron energy distribution functions have a rich structure induced by super elastic collisions between excited species and cold electrons. Super elastic vibrational collisions play an important role in affecting the electron energy distribution function in a wide range of the electric field [2].

2. Results

Due to the influence of external forces the particle distribution function deviates from the equilibrium leading to the change of the average energy and directional velocity of the particles and the distribution function, which depends on the velocity components. To describe this processes, the pseudopotentials was used that takes into account the charge screening at long distances and quantum effect of diffraction, which occurs in dense systems. As well, mean energy of the electrons was calculated by the Coulomb logarithm by using the distribution function in a strong field [3] for continuous collision cross section. The Coulomb logarithm determines by the scattering angle of particle in plasma. By solving the scattering angle of particle we got collisional characteristics of dense plasma such as scattering sections, free lengths and frequencies of particles on the basis of effective pseudopotential models. The results obtained in this work are compared with the results of other theoretical methods and computer simulations.

3. Conclusion

The tail of distribution function of particles in external electric field increases with the decrease of plasma density parameter when we take into account quantum mechanical and screening effects. This effect is possibly connected with decrease of the collision frequencies [4] and with the formation of some ordered structures in dense plasma.

4. References

[1] M. Capitelli, G. Colonna, O. De Pascale et al. Plasma sources science and technology. 18. 014014 (2009).

[2] L.D. Pietanza, G. Colonna, G. D'Ammando et al. Physics of Plasmas. 23. 013515 (2016).

[3] A.A. Kudryavtsev, L.D. Tsendin. Technical Physics. 44. 1290 (1999)

[4] T.S. Ramazanov, K.M. Turekhanova. Phys. Plasmas. 12. 102502 (2015)

Dependence of anode glow on surrounding geometry in a parallel plate glow discharge plasma

P. K. Barnwal, S. Kar, R. Narayanan, A. Ganguli, R. D. Tarey.

Centre for Energy Studies, Indian Institute of Technology Delhi, Hauz Khas, New Delhi, India, 110016

An intense anode glow is observed in a parallel plate glow discharge plasma (cathode to anode surface area ratio ≈ 90; cathode: grounded) that strongly depends on the surrounding geometry. The electrode system was placed inside a grounded vacuum vessel. The experiments were performed in three configurations: (a) when the discharge is allowed between the electrodes by covering them with a glass tube and mica discs at the ends, the anode glow appears only at low currents. (b) When a deliberate leak is introduced using smaller diameter mica discs that allow plasma to escape from the ends to reach the cathodic vacuum chamber, the anode glow is still formed at low currents, but a negative differential resistance (NDR) along with hysteresis appear in the *I-V* characteristics. (c) However, when the discharge is exposed to the whole chamber, the anode glow is present at high discharge currents also, although the NDR and hysteresis disappear.

1. Introduction

Anode glow may appear at low discharge currents to maintain the discharge [1,2] by formation of a potential double layer which accelerates the electrons near the anode, energizing them to energies above the ionization energy of the gas, which causes additional ionization near the anode. The present paper correlates the dynamics of anode glow with the system geometry at various discharge currents.

2. Experimental setup

The experimental setup consists of a cylindrical stainless steel chamber (inner diameter 150 mm and height 355 mm) in which two planar electrodes (grounded cathode (dia. = 76 mm) and anode (dia. = 8 mm)) were placed at a separation of 35 mm. A glass tube of inner diameter, 90 mm along with mica discs at the two ends, were used to cover the electrode system to isolate the plasma from the grounded chamber walls. The external circuit was completed through a variable DC power supply (1kV, 1A) and a variable ballast resistor. The argon gas pressure (p) was varied from 200 to 800 mTorr. The experiments were carried out in three different configurations: (a) the plasma discharge was completely isolated from the chamber walls; (b) a small gap was permitted between the glass tube and the electrodes (at both ends); (c) both glass tube and mica discs were removed and the discharge was left fully uncovered.

3. Results and discussion

Discharge characteristics (plot of discharge voltage (V) versus discharge current (I)) were observed at different gas pressures for all three configurations. In configurations (a) and (b), the anode glow appears at low currents ($\lesssim$ 2 mA) and its size and intensity are found to be linked to the slope of the *I-V* characteristics. More interestingly, an NDR with hysteresis is observed in the *I-V* characteristics in configuration (b). However, in configuration (c), the anode glow is present throughout, at all currents. Also, the size of the glow is larger and more intense than for configurations (a) and (b). Figure (1) shows the plasma snap shot for covered (Fig. 1a) and uncovered (Fig.1b) conditions.

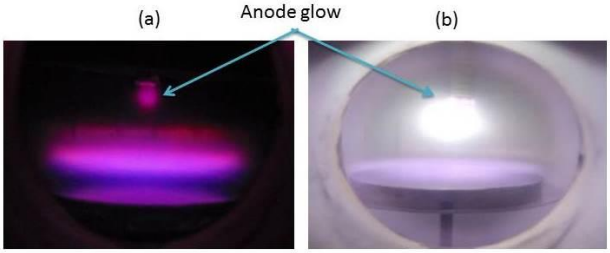

Fig. 1. Plasma snap shot at p = 400 mTorr for covered (Fig. a) and un-covered (Fig. b) (at I_d = 0.55 mA and 30 mA respectively).

The minimum discharge voltage required to sustain the discharge at 400 mTorr in configurations (a) and (b) is $V \approx 225$ V, which is greater than that for configuration (c), for which, $V \approx 180$ V. The detailed experimental results will be presented in the conference.

4. References

[1] K. G. Emeleus, Int. J. Electronics, **52** (1982) 407.

[2] B. Song, N. D. Angelo, R. L. Merlino, J. Phys. D Appl. Phys., **24** (1991) 1789.

Topic number

RF plasma simulation using semi-analytical sheath model

M. Miyashita[1]

[1] *Technology Reserch Center, Sumitomo Heavy Industries Ltd., Yokosuka, Japan*

We have developed a simulation technique to calculate sputtering etch rate distribution by accelerated energetic ions in radio frequency(RF) sheath within short computation time, in order to develop a high density and low metal contamination plasma source. The estimated sputtering etch rate distribution on the RF antenna cover qualitatively reproduced the experimental result.

1. Introduction

We have developed a plasma model according to the equipment in order to design the new device [1]. This paper focuses on the RF plasma source. A RF plasma source is expected as one of the plasma source with low metal contamination and high density. The plasma is sustained by providing RF power of 13.56MHz through U-shaped antenna in chamber. The RF antenna is isolated by dielectric cover from plasma. In design, the sputtering etch rate distribution on the RF antenna cover is important. However, expensive calculation cost is needed for RF simulation. We introduce a new model which does not resolve sheath thickness by interface problem.

2. Method

2.1. Interface Problem

The electronic fluid equation in plasma connects to usual Poisson equation in antenna cover and chamber with semi-analytical RF sheath model. This is so called interface problem. The calculation cost can be reduced for the mesh of the sheath area can be ignored. We have developed a hybridized discontinuous Galerkin method to deal with this interface problems [2].

2.2. Semi-analytical RF sheath model

A unified RF sheath model for wide frequency region is proposed in this report [3]. First of all, we investigated the mathematical property of this RF model by method of dynamical system. The phase space diagram reveals stability of the trajectory. Thus far, the calculation diverged because the surface of the dielectric is positively charging if large voltage condition is applied to the antenna on numerical simulation. We found this phenomenon is not a numerical divergence but a problem in the physical model.

2.3. Ion Energy Distribution Function (IEDF) and sputtering etch rate.

The ion energy distribution on the RF antenna cover can be estimated from the potential waveform. An approximation of ion energy distribution is described with convolution integral by Green function and sheath voltage wave form under the some simple assumption [4]. The IEDF can be gotten by inverse Fourier transformation. Finally, the sputtering etch rate distribution is calculated by using the estimated IEDF and sputtering yield. The calculated sputtering etch rate distribution on the RF antenna cover is compared with result of measurement.

3. Results and Discussions

Fig.1 shows the sputtering etch rate distribution on the RF antenna cover. The calculated result qualitatively reproduced the experimental result. The rate in the proposed method is relatively larger than the rate in the conventional single frequency model on the power supply side (0, 0.8m). In the near future, we will perform experiment by improved design using simulation technique.

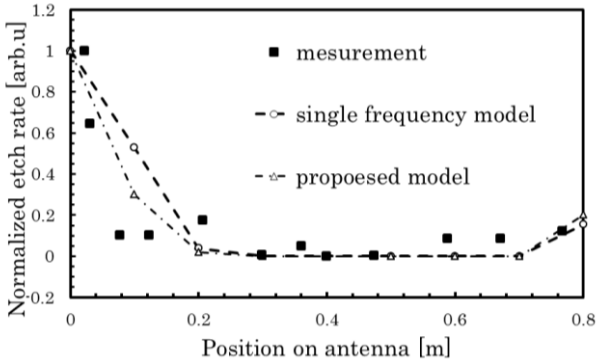

Fig.1 sputtering etch rate distribution on the RF antenna cover.

References

[1] M. Miyashita et.al. Frontier of Applied Plasma Technology Vol.5 No2 (2012) 79.

[2]M. Miyashita and N. Saito. arXive: 1701.00897v1 (2017).

[3]M. E. Riley. Sandia Report SAND95-0775 UC-401 (1995).

[4]Alan C. F. Wu et.al. J. Appl. Phys. 101 (2007) 056105.

Topic number 9

Study of ECR plasma expansion in diverging magnetic field geometry

A. Verma, A. Ganguli, R. Narayanan, R. D. Tarey, D. Sahu

Centre for Energy Studies, Indian Institute of Technology, Hauz Khas, New Delhi, India,110016

While considerable work has been carried out in Helicon thrusters, potential of ECR based plasma thrusters have yet to be explored. The present work therefore, attempts to explore the possibility of using ECR based plasma sources for such applications. The experiments were carried out by allowing the plasma produced by a small ECR source to expand into a bigger expansion chamber. Two expansion chambers with different dimensions were used to study the geometrical effect on plasma parameters during the expansion. It was observed that the electron density in the expansion chamber decreased along the axis, but the density and electron temperature variation scale length differ for the two chambers. The results indicate that in the smaller chamber plasma expansion is isothermal, while in bigger chamber, it obeys a polytropic law. An attempt has been made to understand the results in light of 1-D, gyro-averaged fluid equations.

1. Introduction

In recent years magnetized expanding plasmas have been studied widely because of their large span of application ranging from thrusters for space exploration [1] to ion beam production [2]. In the present paper behaviour of expanding magnetized ECR plasma has been studied.

2. Experimental setup

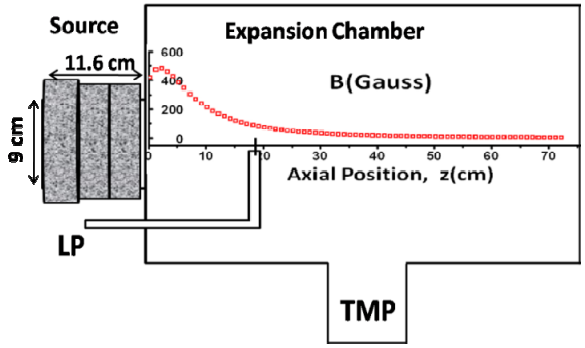

Figure 1 Experimental setup with B vs z plot

The experimental system shown in Figure1 uses a compact ECR plasma source (CEPS) [3] that consists of a small stainless steel source section (ID 9 cm × Length 11.6 cm), mounted coaxially onto a larger expansion chamber (stainless steel cylinder). Two expansion chambers of different sizes ((I) ID 15 cm × Length 37 cm; (II) ID 49 cm × Length 75 cm) were used. Ar plasma was produced using the ECR heating mechanism at 2.45 GHz microwave frequency. The CEPS uses ring magnets (concentric with the source chamber) to provide the magnetic field for the ECR as well as in the expansion region, which helps guide the plasma into the volume of larger expansion chamber. It is found that B falls exponentially in the expansion chamber with a scale length, L_m = 9.2 cm.

3. Results and discussion

Axial measurement of electron density n_e at 500W microwave power and Ar neutral pressure of 0.5 mTorr in the two expansion chambers were carried out and compared with magnetic field variation on axis. Moving away from the source n_e is seen to fall exponentially in both cases but with different scale lengths.

In setup I the density fall follows the magnetic field while in setup II the density decreases more slowly. Plots of $\log_{10}(T_e)$ vs $\log_{10}(n_e)$ show that the axial electron temperature variations are very different for the two set ups. From the thermodynamic relation for a polytropic process, $T_e/n_e^{\gamma-1}$ = constant, it is inferred that in setup I plasma expansion in the diverging magnetic field is isothermal ($\gamma_e \approx 1$) while in setup II it is no longer isothermal, but varies as given by the value, $\gamma_e \approx 1.22$.

Using gyro-averaged fluid equations that hold along a field line, it can be shown that the expansion along the field lines obeys the double-adiabatic equation of state and that the quantity $n_e^2/[B^2T_e] \approx$ constant. Experiments in setup I yield that n_e/B remain a constant along the field lines near the axis, implying isothermal expansion. However, in system II, n_e scales as B^s where $s<1$ and the expansion does not remain isothermal. Detailed analysis need to be done and will be presented in conference.

4. References

[1] C. Charles, *J. Phys. D. Appl. Phys.*,**42**, 16, (2009) 163001.

[2] W. Lu et.al, Rev. Sci. Instrum., **87**, (2016) 02A738.

[3] A. Ganguli et.al, *Plasma Sources Sci. Technol.*, **25**, 2 (2016) 25026.

LIBS technique, a useful tool for a rapid discrimination between meteorite and meteor-wrong

G.S. Senesi[1], P. Manzari[2], G. Tempesta[3], G. Agrosi[3], A.A. Touchnt[4], A. Ibhi[5], O. De Pascale[1]

[1] *CNR – Istituto di Nanotecnologia (NANOTEC) – PLasMI Lab, Bari, Italy*
[2] *Istituto Nazionale di Astrofisica - Istituto di Astrofisica e Planetologia Spaziali (INAF-IAPS), Roma, Italy*
[3] *Dipartimento di Scienze della Terra e Geoambientali (DiSTeGeo), University of Bari, Bari, Italy*
[4] *Department of Physics and Earth Sciences, University of Ferrara, Ferrara, Italy*
[5] *Petrology, Metallogeny and Meteorites Laboratory, University of Ibn Zohr - Agadir, Morocco*

In the last years meteorite hunting and business are increasing due to the high attention given to space materials studies and discoveries. In some cases, meteorites, in particular iron meteorites, sometimes can be confused with meteor-wrongs that may consist of artifacts or terrestrial rocks or minerals. With respect to traditional techniques used to analyze geological samples, laser induced breakdown spectroscopy (LIBS) shows significant advantages, including versatility, minimal destructivity, no carbon coating, low operating costs, rapidity of analysis and sensitivity to light elements. In particular, results of LIBS analyses showed no Ni presence in analysed fragments, thus confirming the high potentiality of this technique in discriminating a meteorite from a meteor-wrong.

Freshly fallen meteorites often stand out from the run-of-the-mill earth-rocks and typically show a fusion crust, i.e. a blackened, charred-looking exterior, which is the result of the meteor passage through earth atmosphere. Meteorite business is becoming progressively important in the Saharian area. For example, nowadays Morocco is one of the main exporters of meteorites in the world. Unfortunately, a number of natural or manmade objects exist, named "meteor-wrongs", which simulate some or all typical features of true meteorites, especially iron meteorites.

Visual methods used to identify a meteorite in the field are sometimes not fully exhaustive thus the use of sophisticated analytical laboratory techniques can be required to verify the extraterrestrial origin of especially iron meteorites. These techniques are generally based on the destructive and expensive analysis of the Ni content in the sample. In this study, some whole presumed meteorite fragments collected in a dry valley located half way from two villages, Imilchil and Agoudal, in the High Atlas Mountains in Morocco, where an iron meteorite named Agoudal was discovered recently [1], were analysed quantitatively by a portable double-pulse micro-laser-induced breakdown spectroscopy (DP-μLIBS) system associated with an optical microscope to verify if they were true meteorites [2]. The morphological and chemical analyses of the fragments were also validated by SEM-EDS.

No Ni presence resulted from LIBS analysis, which was confirmed by a further deeper SEM-EDS analysis and by chemical maps that showed the occurrence of spheroidal graphite. The microstructures were consistent with P bearing iron materials. These results suggested that the fragments studied consist of possibly ancient fragments of cast iron.

In conclusion, DP-μLIBS can represent a promising advanced analytical technique to obtain a fast and reliable chemical analysis able to discriminate between a true meteorite and a meteor-wrong.

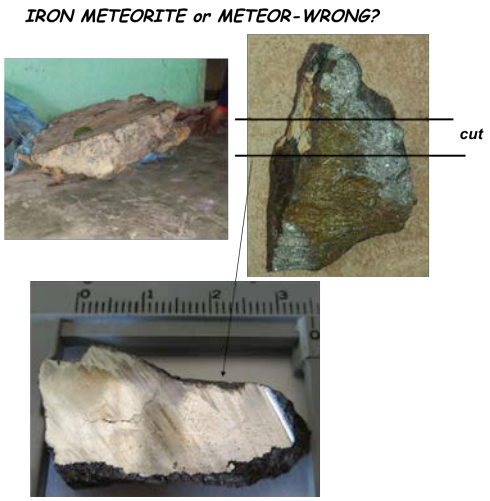

Fig. 1. Meteor-wrong fragment found in Morocco.

References

[1] H. Chennaoui Aoudjehane, L.A.J. Garvie, C.D.K. Herd, G. Chen, M. Aboulahris, 76th Meet. Meteoritical Soc. (Edmonton, Canada), (2013) 5026.

[2] G.S. Senesi, G. Tempesta, P. Manzari, G. Agrosi, Geostandards and Geoanalytical, **40** (2016) 533.

N_2 influence on the vibrational distribution of the asymmetric level of CO_2

L. Terraz[1], T. Silva[1], D. Nina[1], N. Pinhão[1], O. Guaitella[2] and V. Guerra[1]

[1] *Instituto de Plasmas e Fusão Nuclear, Instituto Superior Técnico, Universidade de Lisboa, Portugal*
[2] *LPP, Ecole Polytechnique, UPMC, Université Paris Sud-11, CNRS, Palaiseau, France*

Abstract: This work contributes towards a detailed kinetic model to study the plasma chemistry in CO_2-N_2 plasmas, in order to explore the possibility of admixing nitrogen to enhance CO_2 dissociation. A particular interest is dedicated to the pumping of the asymmetric vibrational mode of CO_2, considered as a promising way for the CO_2 dissociation at lower energy costs than by direct electronic impact. For this purpose, 0-D simulations are performed reproducing the conditions of the experiments lead in parallel at LPP. The input data of the simulations must comprise sets of reaction rates for the vibrational-translational exchanges (VT) and the vibrational-vibrational exchanges (VV) between N_2, CO_2 and the derived products. This presentation focus on the computation and the validation of these data sets and the first results obtained from a simplified kinetic model.

1. Introduction

Carbon dioxide dissociation is a way of both reducing one of the main greenhouse gases and providing a source of synthetic fuels, avoiding the carbon footprint and the restructuring problems linked to energy distribution. Non-equilibrium plasmas seem to be a very interesting medium to efficiently dissociate the CO_2 molecule, with reported energy efficiencies of about 45% under industrial conditions [1, 2]. This work explores the possibilities of admixing nitrogen to the CO_2 plasma to enhance the dissociation efficiency. The aim is to develop a kinetic model to study the plasma chemistry in CO_2-N_2 plasmas.

2. Discussion

The VT and VV reaction rates between CO_2 and N_2 molecules have been computed for the first vibrational levels, using a temperature power law which fits the results from previous experiments [3]. For the upper levels these rates have been scaled using the SSH theory [4]. In total, vibrational levels up to $v \leq 5$ for N_2, and $v_1 \leq 3$, $v_2 \leq 6$, $v_3 \leq 5$ for the symmetric stretching, bending and asymmetric stretching modes of CO_2, respectively, are taken into account in the model.

Figure 1 shows the time evolution of the population of the $CO_2(00^01)$ level in the afterglow of a dc discharge for p=5 Torr. The gas temperature profile in the afterglow and the initial densities of CO_2 molecules in the different vibrational modes are taken from experiments in a pure CO_2 dc discharge at a current I=50 mA. The results confirm the potential of N_2 addition to enhance the vibrational pumping of the CO_2 asymmetric mode, whenever the characteristic vibrational temperature of N_2 is larger than that of the CO_2 asymmetric mode.

3. References

[1] A. Fridman, Cambridge University Press (2008) 9, 54.
[2] G. J. van Rooij *et al.*, Faraday Discuss. **183** (2015) 233.
[3] S. Heijkers *et al.*, J. Phys. Chem. **C** (2015) 199, 12815-12828.
[4] T. Kozák and A. Bogaerts, Plasma Sources Sci. Technol. **23** (2014) 045004.

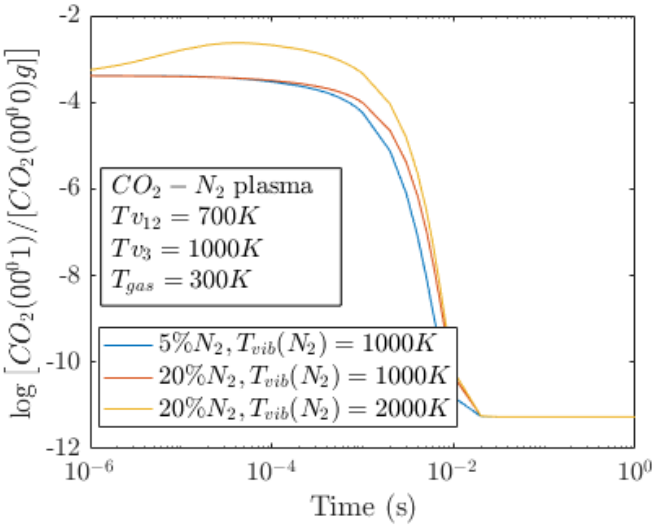

Fig.1: Time evolution of the population of $CO_2(00^01)$ level in a CO_2-N_2 afterglow, at 5 Torr, for different N_2 concentrations and vibrational temperatures.

Acknowledgments: This work was partially supported by the Portuguese FCT, under Projects UID/FIS/50010/2013 and PTDC/FIS-PLA/1420/2014 (PREMiERE). VG was partially supported by LABEX Plas@par under the project ANR-11-IDEX-0004-02.

Two-Dimensional Electron Density Distribution over Positive Primary Streamer Propagating in Atmospheric-Pressure Air

Y. Inada[1], R. Ono[2], A. Kumada[2], K. Hidaka[2], M. Maeyama[1]

[1] *Division of Mathematics, Electronics and Information Sciences, Saitama University, Saitama, Japan*
[2] *Department of Electrical Engineering and Information Systems, The University of Tokyo, Tokyo, Japan*

Elucidating the electron density of streamer discharges propagating in atmospheric-pressure air is critical for achieving a systematic understanding of the production mechanisms of reactive species. Using Shack-Hartmann type laser wavefront sensors with a temporal resolution of 2 ns, we carried out single-shot two-dimensional electron density measurements over positive primary streamers generated in a 13-mm air gap between pin-to-plate electrodes. The electron density over the positive primary streamers decayed in a range of 10^{15} cm^{-3} during the propagation. The decay time constant of the electron density in the primary streamer channels was estimated to be ～2 ns. The distribution widths of the electron density were in good agreement with those of the light emission, typically ranging from 0.8 to 1.5 mm.

1. Introduction

The electron density of streamer discharges propagating in atmospheric-pressure air is crucially important for systematic understanding of the production mechanisms of reactive species utilized in wide ranging applications such as medical treatment, plasma-assisted ignition and combustion, ozone production and environmental pollutant processing. However, electron density measurement during the propagation of the atmospheric-pressure streamers is extremely difficult by using the conventional localized type measurement systems due to the irreproducibility in the discharge paths. In order to overcome the difficulties, single-shot two-dimensional electron density measurement was conducted by using a Shack-Hartmann type laser wavefront sensor. The Shack-Hartmann sensors were applied to pulsed positive primary streamer discharges generated in an air gap.

2. Experimental setup and results

The temporal resolution of the Shack-Hartmann sensors was 2 ns, which was equal to the exposure time of the installed two ICCD cameras. The spatial resolution was determined by the pitch of the microlens arrays, which was 300 μm.

Pulsed positive streamer discharges were generated in a 13-mm gap installed in open air. The air gap was composed of a brass plate cathode and a stainless-steel pin anode, whose tip radius was 80 μm. Figure 1 shows voltage and current waveforms for the streamer discharge in atmospheric-pressure air. The voltage rise-rate was 0.83 kV/ns.

Figure 2 shows that the electron densities at 5 ns after streamer initiation ranged from 5 to 7×10^{15} cm^{-3}, while the electron density at the time of the streamer initiation was $8\text{-}9\times10^{15}$ cm^{-3}. In the process of streamer propagation, the electron density decreased with increasing time. On the other hand, the electron density widths distributed uniformly along the *y*-direction at the timing of the streamer occurrence and 5 ns after the streamer initiation. The decay time constant of the electron density in the primary streamer channels was estimated to be ～2 ns from the streamer propagation speed of 9×10^5 m/s. The half-maximum full-widths of the electron density distributions were in good agreement with those of the light emission profiles, typically ranging from 0.8 to 1.5 mm.

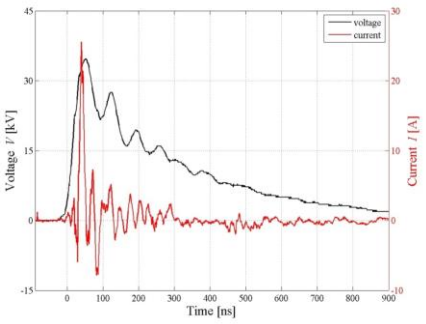

Figure 1. Current and voltage waveforms for air streamer discharge.

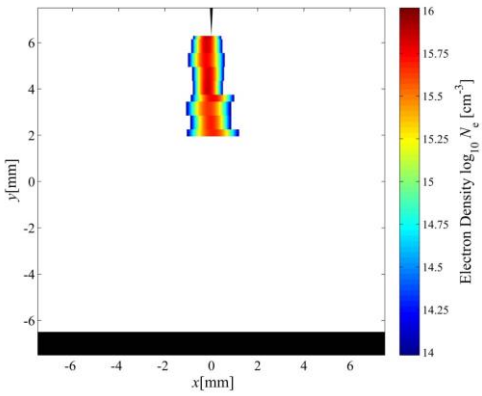

Figure 2. Two-dimensional electron density distribution at 5 ns after air streamer initiation.

Topic number 9

Characterization of ECR produced hydrogen plasma for H^- generation

P. Singh, R. Gaur, D. Sahu, R. Narayanan, A. Ganguli, R. D. Tarey

Centre for Energy Studies, Indian Institute of Technology Delhi, New Delhi, 110016

Experiments have been carried out in low pressures (≤1.5 mtorr) hydrogen plasmas in a vacuum chamber attached to a compact electron cyclotron resonance (ECR) source. The electron temperature and density, measured by a Langmuir probe, are seen to fall slowly along the axis away from the ECR source. Using the experimental data and a global model the density of different positive ion species, H^+, H_2^+, H_3^+ are estimated. It is found that H_3^+ is the dominant species at low pressures. It also turns out electron temperature plays a pivotal role in determining collisional energy loss. Work is in progress to determine the optimum conditions for H^- generation.

1. Introduction

Negative hydrogen ion (H^-) beams have great importance for neutral beam heating of fusion plasmas because they can be efficiently charge-neutralized to form neutral beams at particle energies of ~ 1 MeV [1]. In order for the scheme to be successful it is important that one be able to produce high density, robust, very-large volume hydrogen plasma over a large cross-section so that the required ion current (~ 30 – 40 amps over an area of 1sq.m.) can be extracted. To make such a technology viable and sustainable, it is important to be able to produce the starting hydrogen plasma extremely efficiently in terms of power input to the device. Since very few studies [2] exist on the characterization of non-equilibrium hydrogen plasma at low pressures, it becomes important to undertake such studies. In addition, most of the plasma sources for H^- production are RF based, whereas the present study is Electron Cyclotron Resonance (ECR) based.

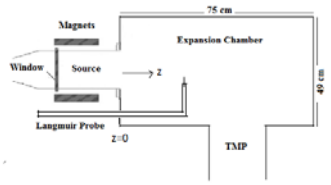

Fig.1 Schematic of Experimental Setup

2. Experimental Setup

Experiments were performed inside a stainless steel cylindrical chamber (length ≈ 75 cm, ID ≈ 50 cm) attached coaxially to a Compact ECR Plasma Source (CEPS) as shown in Fig. 1 [3]. The CEPS has a cylindrical plasma source section (ID ≈ 9.1 cm, length ≈ 11.5 cm) with coaxially arranged NdFeB permanent ring magnets. Microwaves at 2.45 GHz are used to produce plasma inside the CEPS. The magnetic field of the ring magnets not only provides the ECR magnetic field, but also penetrates the larger expansion chamber into which the plasma diffuses, guided by the magnetic field.

3. Results and Discussion

Experiments were performed at 0.5mTorr-1.5mtorr pressure and 200-1000W power. At 1mtorr pressure and 500W power it is found that the electron density (n_e) decreases slowly along the chamber axis from ≈ 4.0×10^{10} cm^{-3} (at z ≈ 15 cm) to ≈ 0.7×10^{10} cm^{-3} (z ≈ 60 cm), with the corresponding electron temperature (T_e) decreasing from ≈ 6.2 eV to about 2.7 eV.

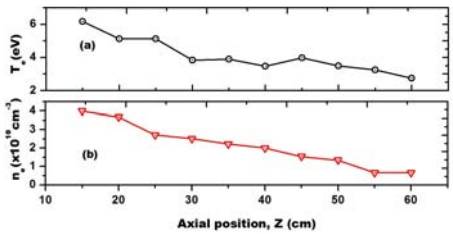

Fig.2 Variation of (a) Electron temperature and (b) density with axial position. Pressure ≈ 1 mtorr and power ≈ 500 W.

Taking T_e as input, a global model is used to determine the positive ion species in the plasma. Although n_e (Fig.2) is calculated assuming the positive ions are H^+, simulation from a global model indicates that different ion species, H^+, H_2^+, H_3^+ are present and at low pressure H_3^+ might be the dominant species. In that case n_e will be increased by a factor of 1.732. Further it was found out that if the neutral species is mostly H_2 rather than H, the collisional energy loss hence the input power to the plasma would need to be higher. Effort is under way to determine the optimum conditions for H^- production. Detailed results will be presented at the conference.

4. References

[1] M. Bacal and M. Wada, Appl. Phys. Rev., **2**, (2015) 021305.

[2] D. Sahu and S. Bhattacharjee, J. Appl. Phys., **112**, (2012) 063304 .

[3] A. Ganguli et al., Plasma Sources Sci. Technol., **25,** (2016) 025026.

Influence of dielectric barrier thickness on the reactor temperature of glass beads packed bed DBD reactor

S.K.P.Veerapandian[1], A.Nikiforov[1], C.Leys[1], N.De Geyter[1], J.-M. Giraudon[2], J.-F. Lamonier[2] and R.Morent[1]

[1] *Research Unit Plasma Technology, Department of Applied Physics, Faculty of Engineering and Architecture, Ghent University, Ghent, Belgium*

[2] *Unité de Catalyse et Chimie du Solide UCCS, UMR CNRS 8181,Université de Lille, Lille, France*

A glass beads packed bed dielectric barrier discharge (PBDBD) reactor is used in this work to study the effect of wall thickness of the reactor on the evolution of the reactor wall temperature and on the formation of by-products such as NO_x and ozone. The temperature of the reactor wall increases with increasing the input voltage. The formation of ozone decreases when the reactor wall temperature is 47±1˚C which results in the formation of toxic by-products such as NO_2. The maximum ozone concentration is obtained for the reactor with a wall thickness of 1.5 mm, which shows a lower increase in temperature for a particular input power. The maximum toluene removal efficiency of 60±4% is obtained for the PBDBD reactor with a wall thickness of 1.5 mm.

1. Introduction

The removal of low concentration volatile organic compounds (VOCs) from an air stream using non thermal plasma (NTP) technology such as PBDBD reactor is of great interest due to its cost and energy efficiency. The temperature of the reactor and the packing material increases with the input voltage and this influences the plasma discharge characteristics and thus the VOC removal efficiency and the formation of by-products.

In this work, the influence of the dielectric barrier thickness of the PBDBD reactor on the reactor wall temperature and formation of by-products such as ozone and NO_2 are examined.

2. Experimental

The PBDBD reactor used in this work is a cylindrical DBD reactor filled with borosilicate glass beads (ϕ 3 mm, ε_r = 4.6). The inner stainless steel high voltage electrode (powered by an AC power supply of 50 kHz) is placed along the axis and an iron mesh around the outer surface of the dielectric barrier acts as ground electrode. The different reactor wall thicknesses (w) used in this work are 1.5, 2.0 and 3.0 mm. Dry air polluted with 300 ppm of toluene is fed into the plasma reactor.

The formation of different by-products after plasma treatment is investigated with FTIR. The concentration of ozone in the outlet stream is measured using an UV absorption based ozone detector (Teledyne, Model 465M). The temperature of the reactor is measured using a thermocouple (Farnell, Type-K) attached to the reactor wall in the middle of the discharge region.

3. Results

The temperature of the reactor wall increases with increasing the input power for a particular reactor wall thickness. Figure 1 shows that the increase in temperature (ΔT) is the lowest for the reactor with lowest wall thickness (w=1.5 mm). Figure 1 shows that the ozone concentration increases with increase in specific input energy (SIE) and then decreases when the reactor wall temperature of is higher than 47±1˚C due to thermal dissociation of ozone[1] and thus formation of NO_2 increases[2] due to ozone generation stop.

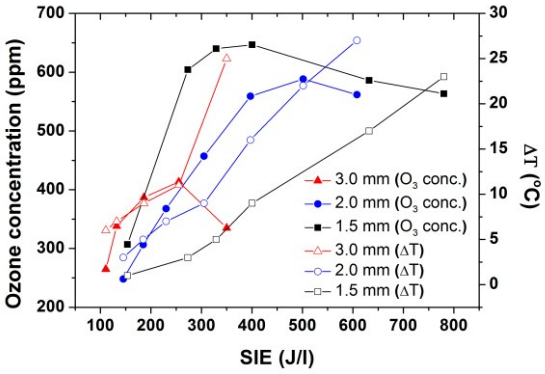

Figure 1. Ozone production (solid symbol) and increase in wall temperature (ΔT) after 10 minutes of plasma ignition (open symbol) as a function of SIE for PBDBD reactor of different reactor wall thicknesses (3.0 mm, 2.0 mm and 1.5 mm)

Thus the formation of ozone is higher for the reactor with wall thickness 1.5 mm as the increase in temperature for this reactor is lower for a particular input power. Also, the maximum toluene removal efficiency of 60±4% is obtained for the PBDBD reactor with the wall thickness of 1.5 mm.

4. References

[1] W. Mista and R. Kacprzyk, Catal. Today, 137 (2008) 345-349.

[2] S. Pekárek, Eur. Phys. J. D, 61 (2011), 657-662.

Electronegativity and negative ion kinetics in O_2 ICP during E-H transition

Th. Wegner[1,2], J. Meichsner[1]

[1] *Institute of Physics, Ernst Moritz Arndt University Greifswald, Greifswald, Germany,*
[2]*currently: Max Planck Institute for Plasma Physics, Greifswald, Germany*

Important plasma species, e.g., density of electrons, negative atomic oxygen ions, singlet metastable and ground state molecular oxygen as well as the electron and gas temperature were quantified using comprehensive plasma diagnostics. In particular, the negative ion kinetics was evaluated taking into account the O^- particle balance equation with the relevant rate constants from literature. During the E-H transition a continuous reduction of the electronegativity was observed over two orders of magnitude.

1. Introduction

Oxygen plasmas have been widely studied in experiment and simulation as a model system for electronegative plasmas. Furthermore, oxygen is used as reactive plasma processing gas in low or atmospheric pressure discharges to produce atomic oxygen and ozone as well as secondary reaction products in gas phase, e.g., OH, H_2O_2, NO_x. The interaction of these reactive species with materials is applied in plasma surface processing, e.g., surface oxidation/functionalisation, degradation and plasma etching. Here, we investigated experimentally inductively coupled radio frequency plasmas (RF ICP) in pure oxygen at low pressure using comprehensive plasma diagnostics. The changing plasma parameters during the E-H transition were systematically studied and the underlying species kinetics, in particular the negative ion kinetics, was evaluated.

2. Experimental

The configuration of the RF ICP at 13.56 MHz consists of a plane double spiral antenna of about 120 mm in diameter with 2.75 windings. The RF power up to 500W or coil voltage of about 8 kV was coupled to the centre connection, whereas the ground potential was applied at the two opposite ends of the coil. The coil was installed in a quartz cylinder immersed in the cylindrical vacuum vessel, [1].

The installed plasma diagnostics includes electric probe measurement, 160 GHz Gaussian beam microwave interferometry, emission and absorption spectroscopy, phase resolved optical emission spectroscopy (PROES) as well as laser photo detachment experiment, [2, 3].

3. Results

All plasma parameters, e.g., electron density and temperature, reveal a continuous E-H transition for pressures lower than 35 Pa. Here, a hybrid (E/H) mode was observed, that means the capacitive and inductive electron heating appears simultaneously in the RF cycle. The negative atomic oxygen ion density was determined by laser photo detachment experiment and the rate equation calculation. The electronegativity $\alpha=n_{O^-}/n_e$ during the E-H transition decreases from about 20 in the E-mode to 0.1 in the H-mode, see Fig.1.

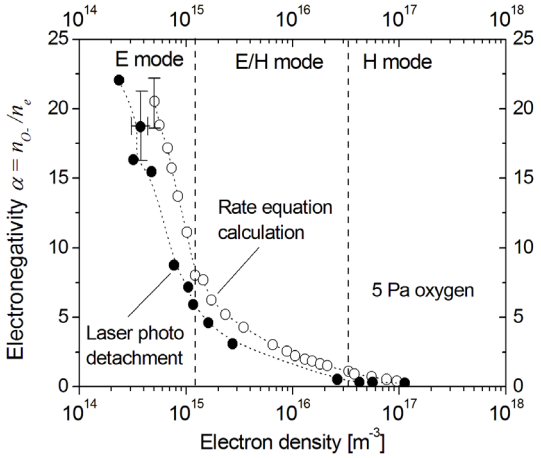

Figure 1: Electronegativity vs. electron density during E-H transition from O^- laser photo detachment experiment and O^- rate equation calculation.

The rate equation calculation for the negative atomic oxygen ion provides the dominant reaction channels for O^- generation and loss, respectively. These are for the E/H and the H mode the dissociative electron attachment reaction with $O_2(X)$ and $O_2(a^1\Delta)$ as well as the ion-ion recombination and the detachment with atomic oxygen.

4. References

[1] Th. Wegner, C. Küllig, J. Meichsner Contrib. Plasma Phys. **55** (2015) 728

[2] Th. Wegner, C. Küllig, J. Meichsner, Plasma Sources Sci. Technol. **26** (2017) 025006

[3] Th. Wegner, C. Küllig, J. Meichsner, Plasma Sources Sci. Technol. **26** (2017) 025007

Experimental Investigation of the Asymmetric Surface Dielectric Barrier Discharge Driven by AC/DC Voltage

F. Sohbatzadeh, H. Mahdavi, and M. Mehdipour

Department of Atomic and Molecular Physics, Faculty of Basic Sciences, University of Mazandaran, Iran.

The effects of AC and DC voltages on asymmetric surface dielectric barrier discharge were examined regarding to the offset voltage, surface charge deposition and induced electric wind velocity. The surface potential, the electric wind velocity and the produced thrust were measured. Our results showed that by increasing the DC voltage of the lower electrode, the surface potential increases and the electric wind velocity decreases. On other hand, by applying the AC voltage to the upper electrode and the DC offset to the lower one, higher wind velocity induces. The direction of the electric wind is independent of the applied voltages, but its magnitude and the surface potential depend on the amplitude and polarities of the applied voltage.

1. Introduction

The surface dielectric barrier discharge which is a common used method to generate atmospheric non-thermal plasma, was proposed for the first time by Roth *et al*. to apply in flow control applications [1]. It is composed of two asymmetric planar electrodes that one of them is exposed to the air and the other one is encapsulated by a dielectric layer [2]. The generated plasma in this structure can cause momentum transfer to the ambient gas. The resulting electric wind can modify the boundary layer properties. In this work, we investigate the effect of the AC and the DC offset voltages applied simultaneously to the lower and upper electrodes on the surface potential and the induced electric wind velocity.

2. Experimental setup and measurements

At first, a sinusoidal AC high voltage with 20 kV_{PP} at 5.5 kHz was applied to the upper electrode, while a DC offset simultaneously was applied to the lower electrode. Then the applied voltages were exchanged. The surface potential and the electric wind velocity measurements were carried out by using an electrostatic voltmeter probe and the pitot tube technique. A schematic picture of the experimental setup was shown in figure 1.

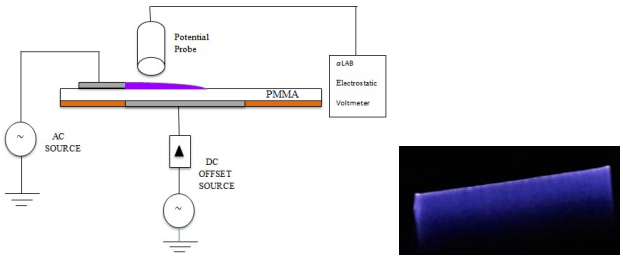

Figure 1: schematic picture of the electrical arrangement and the generated plasma.

3. Results

As shown in figures 2 and 3, by increasing DC offset voltages the magnitudes of the surface potential increases and the electric wind velocities decrease in downstream of the electrode. As can be seen in figure 2, the electric wind velocity and subsequently its extension for the negative DC offset were greater than the positive case. The sign of the potential was negative for the positive DC offset and always positive for the ground and the negative one. By changing the electrode voltages the electric wind velocity induced by the negative DC offset was very low with maximum value of about 2 m/s. This result was illustrated in figure 3. Moreover, the maximum thrust was obtained for the ground case, which was approximately 18 mN/m.

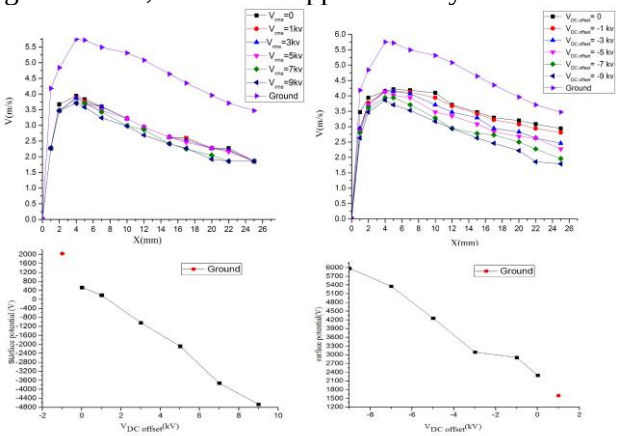

Figure 2: velocity and surface potential of the AC voltage applied to the upper electrode and positive(left)/negative (right) DC offset voltages to the lower one.

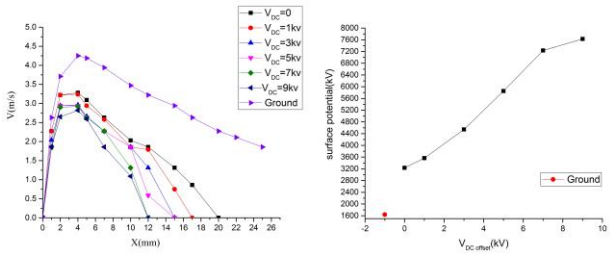

Figure 3: positive DC offset voltage applied to the upper electrode and AC voltage to the lower one.

4. References

[1] J. R. Roth, Phys. Plasmas **10** (2003) 2117.

[2] E. Moreau, J. Phys. D: Appl. Phys. **40(3)** (2007) 605–636.

Weakly ionized plasma effects on mitigation of shock waves

F. Sohbatzadeh, M. Mehdipoor and H. Mahdavi

Department of Physics, Faculty of Basic Sciences, University of Mazandaran, Babolsar, Iran.

In this work, shock wave modification by a DC glow discharge was investigated, theoretically. Numerical results showed that the electric field distribution has significant effects on shock front. Also, the electron temperature and their diffusion were found to be effective parameters on the plasmaaerodynamic. It was found that the plasma can deflect the incoming flow and modifies the structure of shock waves. The effect of the electric field strength was also examined in this work. Equilibrium and non-equilibrium assumptions for the plasma were examined to demonstrate heat and momentum transfer contributions in supersonic flow control.

1. Introduction

Since non- thermal plasmas generated in relatively low power input, therefore they are the appropriate discharges for use in aeronautic. Some authors believe that thermal effects [1] and transfer momentum to the incident fluid particles (neutrals) can modify the flow properties, locally [2]. Therefore, we will use a theoretical model to examine the physical mechanisms governing the plasma flow control for supersonic incident flow. We took a wedge geometry in which the plasma was created in front of the wedge by electrical discharge. The cathode electrode and anodes assumed to be positioned on the front and the side walls of the wedge, respectively. The DC voltage on the cathode was -10 kV. Here we assumed the electric field components as

$$E_X = \frac{E_0}{1+(a\xi)^2}, \qquad E_Y = \frac{\xi E_0}{1+(b\xi)^2} \qquad (1)$$

Where E_0 is electric field amplitude and $\xi = y/L$. Here L is cathode length and dimensionless parameters a and b are constant. a and b are either 1 or 0.7 depending on the cathode configuration such as flatness or sharpness.

2. Basic equation

We assumed a weakly ionized plasma that produced by the external electric field. Also, we assumed that the incoming flow having Mach number M=2.5 and p=0.175 atm. We used momentum transfer equation for electrons, ions and neutrals with taking into account of collision frequencies for electron-neutral, electron-ion, and ion-neutral interactions. We also employed the energy equation for each species. Some of our numerical analysis are as follows:

1- Thermal effect does not play a major role in the weakly ionized glow discharge.
2- The distribution of the electric field has more effect on the shock front position than the electric field strength
3- For higher values of the electric field, the electron temperature has not any significant effect on deflection angle of flow.
4- Incoming flow is deflected after interacting with the plasma.

Figure 1, shows the effect of the different electric field distributions on the shock wave angle. In figure 2, the change in attached shock by electric field distributions is seen. From figure 2, one can conclude that the electric filed distribution affects the shock properties significantly. It is also seen that the electric field strength has minor effect with respect to the field distribution.

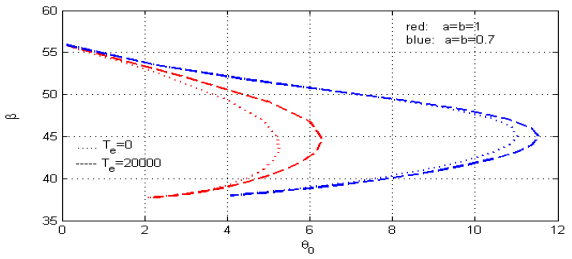

Figure 1. Shock wave angle β versus deflection angle by plasma, doted line with no electron density gradient and dashed line for T_e=20000 K for both electric field distributions a=b= 1 and a=b=0.7

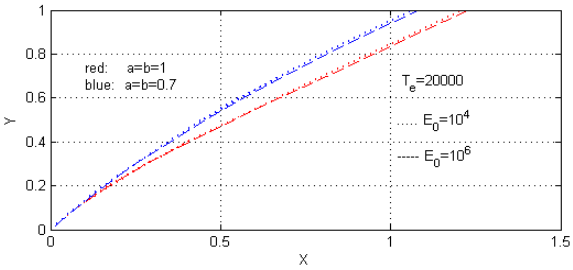

Figure 2. Attached shocks in the supersonic flow over a 15° wedge for different electric field distributions(red line: a=b=1 and blue line a=b=0.7), dot line 10^4V/m and dash line 10^6 V/m.

3. References

[1] L. Wang, Z.B. Luo, Z.X. Xia, B. Liu, X. Deng, Sci. China Tech. Sci. **55** (2012) 8:2225-40.
[2] S.P. Kuo, Steven S. Kuo, Physics of Plasmas, 12 (2005) 012315.
[3] M. Moisan, J. Pelletier, Physics of Collisional Plasmas, Springer, (2012).

The Characterization of Sputtered Nickel Oxide Thin Films by DC Reactive Sputtering for Application of an Electrochromic device

Won Chang Lee[1,2], Eun Chang Choi[1] and Byungyou Hong[1,2]

[1] *College of Information and Communication Engineering, Sungkyunkwan University, Korea*
[2] *Interdisciplinary Graduate School Program for Photovoltaic Specialists (IPPs), Sungkyunkwan University, Korea*

Nickel oxide (NiO) electrochromic thin films were prepared by dc reactive magnetron sputtering. The as-deposited optical property and electrochromic behavior strongly depended on the target operation mode and the substrate temperature. The films were deposited with substrate temperature from room temperature to 300 ℃. NiO films were investigated using X-ray diffraction, FE-SEM images and Hall effect measurements. The dependences of electrochromic properties on crystalline structure deposited from heated substrate temperature during dc reactive sputtering of NiO films were studied. The preferred orientation of NiO film change from (111) to (200) when the substrate temperature increased.

1. INTRODUCTION

Electrochromic materials enable dynamic control of the throughput of radiant energy and play a significant role in energy efficient "smart windows" by reducing the cooling and lighting cost of buildings [1]. Recently, nickel oxide (NiO) is of special interest because of high color contrast ratio, cyclic reversibility, durability and low cost [2].

The NiO film can be prepared by several methods such as sol-gel processing, chemical vapor deposition, thermal evaporation and sputter deposition [3]. Among these methods, dc reactive sputtering is used to deposit NiO film in this study.

2. EXPERIMENTAL DETAILS

NiO thin films were grown on the glass using dc reactive magnetron sputtering system from Ni target (4 inch in diameter, 99.9% purity) in a mixture of oxygen and argon gases. The distance between the target and the substrate was approximately 5 cm. The chamber was evacuated to a pressure below 5×10^{-6} Torr before deposition and working pressure was 1×10^{-2} Torr. The substrate was varied from room temperature to 300 ℃ in 50 ℃ step during deposition of the NiO films. To measure the electorhcormic properties of NiO films, in these case, NiO films were deposited on the indium tin oxide glass.

3. RESULTS AND DISCUSSION

The figure presents the XRD diffraction patterns of the samples prepared at different substrate temperature with dc power of 100 W. The diffraction peaks are observed at 2θ = 37.2° and 43.3° corresponding to (111) and (200) crystal planes of the cubic NiO phase, respectively.

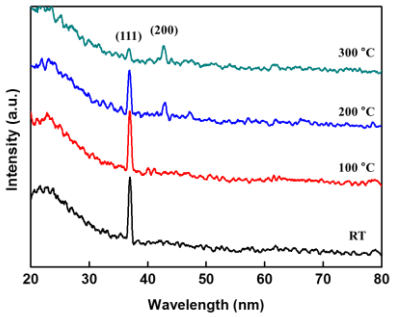

Fig. 1 XRD spectrum from the as-deposited NiO films prepared with different substrate temperature at dc power 100 W.

The electrical properties of NiO films are measured by the Hall effect measurement. The values of resistivity, mobility, Hall coefficient and carrier concentration are influenced by substrate temperature.

Also, the electrochromic properties of NiO films are measured such as cyclic voltammograms, response time and transmittance modulation between colored state and bleached state.

4. REFERENCES

[1] Ruben Baetens, Bjorn Petter Jelle and Arild Gustavsen. Solar Energy Materials and Solar Cells. **94** (2010) 87.

[2] Dhanaji S. Dalvi, Rupesh S. Devan, Raghunath S. Patil, Yuan-Ron Ma and Pramod S. Patil. Materials Letters. **90** (2013) 60.

[3] Hao-Long Chen, Yang-Ming Lu and Weng-Sing Hwang. Surface and Coating Technology. **198** (2005) 138.

Collisional-radiative modelling for multi-temperature plasma composition calculation

J Annaloro[1,2], Ph Teulet[1], A Bultel[2], Y Cressault[1] and A Gleizes[1]

[1] *Université de Toulouse, UPS, INPT, LAPLACE (Laboratoire Plasma et Conversion d'Energie), 118 Route de Narbonne, F-31062 Toulouse cedex 9, France.*
[2] *CORIA, UMR CNRS 6614, Université de Rouen, Site universitaire du Madrillet, BP 12, 76801 Saint-Etienne du Rouvray, France*

This paper concerns the calculation of multi-T argon plasma composition with a collisional-radiative model. This model takes into account a great number of electronic levels of Ar and Ar^+ and it is based upon an extended database of reaction rate coefficients (excitation/de-excitation, ionisation/recombination, spontaneous emission and radiative recombination). A particular attention is paid to problematic reactions with electrons in one side and only heavy species on the other: $Ar+Ar \rightarrow Ar+Ar^+ + e$. The detailed balance relations obtained for ionisation/recombination processes demonstrate the non-uniqueness of the multi-temperatures law of mass action. Plasma compositions exhibit abrupt densities variations associated to the transition between the domination of heavy particle reactions (low temperature) and the predominance of electron collisions (high T).

1. Introduction

Most of theoretical studies concerning thermal plasmas are achieved with the local thermodynamic equilibrium (LTE) assumption. However, it is clear that this assumption is not realised in some regions of the plasma (electrode sheaths, vicinity of walls and cold fringes) and for transient or low power arcs. Thus, electrons have a kinetic temperature T_e higher than that of the heavy species T_h ($\theta = T_e/T_h$).

There are 3 methods for the calculation of the plasma composition: The minimization of a thermodynamic function, the law of mass action or a CR model. They obviously all lead to the same results in the case of thermodynamic equilibrium but they strongly differ in non-equilibrium conditions, depending on the initial calculation assumptions. The more accurate technique to obtain the multi-T plasma composition is the CR model. Indeed, this approach allows avoiding the simplifying assumptions associated to the internal excitation modes (electronic, vibrational and rotational).

2. CR Model

The energy diagram of argon used in this study is taken from [1]: 379 electronic levels for Ar and the first 7 states for Ar^+. Thus, all possible transitions between levels until 32.2 eV above the ground state of Ar are taken into account (coherent with the temperature range considered i.e. T_e and T_h lower than 15000K). The CR model is thus formed of 387 nonlinear coupled ordinary differential equations. The DVODE library [2] dedicated to stiff problems is used to solve the system of equations. Direct reaction rate coefficients for inelastic collisions are calculated with the Drawin formalism [3-4]. Reverse rate coefficients are obtained from accurate detailed balance relations. Concerning radiative processes, radiative recombination rate coefficients are taken from [5] and Einstein coefficients from [1].

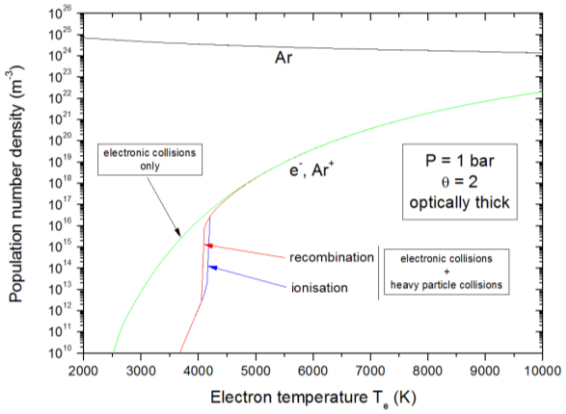

Figure 1. Argon plasma composition: influence of electron and heavy particle collisions

The argon plasma composition (optically thick case, $\theta = T_e/T_h = 2$) is given in figure 1. This result illustrates the influence of electrons and heavy particle collisions on the plasma composition.

3. References

[1] http://www.nist.gov/pml/data/asd.cfm
[2] P.N. Brown, G.D. Byrne and A.C. Hindmarsh SIAM J. Sci. Stat. Comput. **10** (1989) 1038
[3] H.W. Drawin Report EUR-CEA-FC383 (1966)
[4] H.W. Drawin and F. Emard *Phys. Lett.* **43A** (1973) 333
[5] J. Annaloro and A. Bultel *Physics of Plasmas* **21** (2014) 123512

Fabrication of transparent conductive films with Ag mesh patterns using a monolayer of polystyrene shperes

Eun Chang Choi[1], Won Chang Lee[1], Byungyou Hong[1]

[1] *College of Information and Communication Engineering, Sungkyunkwan University, Suwon, South Korea*

We show the fabrication of Ag mesh as a transparent conductive electrode using a polystyrene (PS) sphere template. To fabricate the Ag mesh pattern, monolayers of PS spheres with different diameters, such as 1, 3, and 10 μm, were investigated as a template. Since thick thickness and wide line width of Ag line degrade the transmittance, both heat pretreatment and wet etching are used to control the open ratio of Ag mesh films. The trade-off between transmittace and conductivity forces us to use larger diameter PS spheres. 10 micron PS spheres are chosen as the template for the Ps sphere monolayer, and the trasmittance and the sheet resistance are 70% and 15 Ω/sq . To improve the transmittance and conductivity of the films, we conducted O2 plasma treatment on the PS monolayer.

1. Introduction

All Thin transparent conducting films are crucial for liquid crystal displays (LCDs), flat panel displays, touch panels, organic light-emitting diodes (OLEDs), solar cells, smart windows, and other applications [1]. Currently, indium tin oxide (ITO), a transparent conducting oxide (TCO), is the industry standard due to its low resistivity (10^{-3}–10^{-4} Ω · cm) and high transparency in the visible spectrum (80%–90%). However, ITO has many disadvantages, such as rarity, high cost, possible exhaustion, process temperature limitations, and brittleness on a flexible substrate. In particular, as display technology moves toward flexible displays, ITO will become completely unsuitable due to its brittleness.

In this study, the transparent electrode with Ag mesh patterns is described. The monolayer of polystyrene (PS) spheres polystyrene spheres was prepared as a template to form the mesh pattern and coated with Ag ink. The heat pretreatment of PS monolayer and Ag wet etching processes can control the line of Ag mesh electrodes. We obtained Ag mesh films with 70 % transmittace and 15 Ω/sq sheet resistance. And, we conducted the O2 plasma treatment on the PS monolayer to improve the adhesion between Ag and substrate.

2.Experiments

We filled a water tank with deionized (DI) water. When a PS solution was dropped on the DI water, the PS spheres rapidly spread and self-assembled into a PS sphere monolayer on the DI water surface. After dropping a proper amount of PS solution, the monolayer was condensed by pushing it toward the wall using a bar. Finally, the transferred PS sphere monolayer on the PET substrate was dried by removing the DI water. Ag ink was dropped onto the surface of the PS sphere monolayer film. And then, the sample was heated on the hot-plate at 90 ℃ for 10 min. And, The PS was removed by immersing in toluene for 3 min. The Ag was cured in an annealing process at 140 ℃ for 10 min on a hot plate.

3. Result

We investigated that the heat pretreatment process of PS monolayer improve transmittance of the Ag mesh electrode.

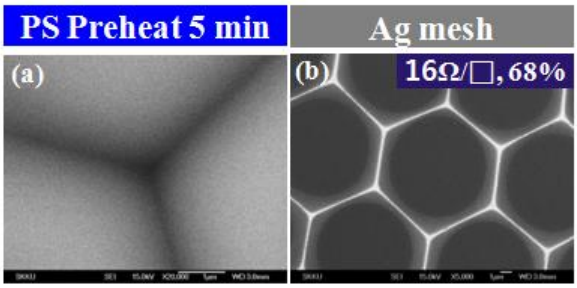

figure 1. FE-SEM images of (a) the PS sphere monolayer after heat treatment for 5 min, (b) the Ag mesh electrode fabricated using the preheated monolayer for 5 min.

4. Conclusion

We investigated that the heat pretreatment of PS monolayer and Ag wet etching processes can control electrical and optical properties of Ag mesh electrodes.

5. References

[1] Pang S, Hernandez Y, Feng X and M¨ullen K, Adv. Mater. **1** (2011) 23 2779.

Study of water treatment effects by a ball-lightning like discharge

Y. Takatori, H. Suzuki, K. Tokaji, Y. Inada, M. Maeyama

Graduate school of science and Engineering, Saitama University, Sakura-ku 255, Saitama, 338-8570, JAPAN

As for water treatment by a ball-lightning like discharge, we investigated the change of physical and chemical properties and the water treatment effect. The increase in the processing speed of the solution in the case of positive polarity was shown to be greatly influenced by ozone formation and dissolution by electrolysis around the upper electrode.

1. Background

The ball-lightning like discharge, a long living water plasmoid, first demonstrated by Egolov and Stepanov [1], has features of 1) long discharge duration of several 100 ms, 2) large spatial volume of diameter above 10 cm and 3) relatively low supply voltage of several kV. Also, it is reported by Maeyama et al. [2] that this discharge causes strong light emission originated from OH radicals over the discharge period rather than at the onset of the discharge, and that intensive water jet occurs above the water surface.

We had reported the preliminary relationship between the processing performance and the discharge condition for decomposition treatment of indigo-carmine solution [3]. As a result, the processing speed largely varies depending on the number of discharge and the polarity of the applied voltage. These facts are thought to be a result of the physical and chemical properties of the processing solution due to repeated discharges.

Therefore, in this study, we investigated the change of these properties of the solution and the water treatment effect, experimentally.

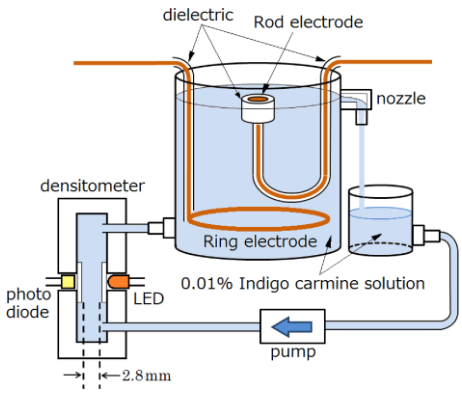

Fig. 1 Water treatment system with discharge electrodes

2. Experimental setup

Figure 1 shows the discharge device with the indigo-carmine densitometer. As diagnostics, we used a high speed camera, a spectrometer and measurement systems of various physical and chemical properties of the solution.

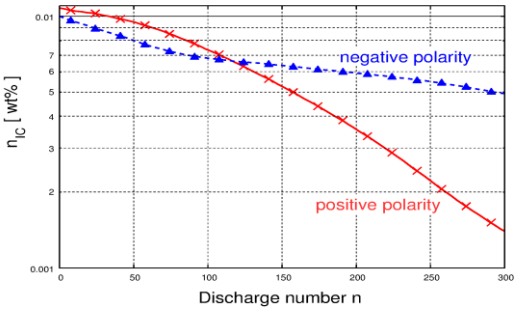

Fig.2 Changes of n_{IC} with different polarities

3. Experimental results

Figure 2 shows the change in the concentration of indigo-carmine n_{IC} by this discharge with different polarities. In the case of negative polarity, n_{IC} decreases exponentially in the early stage of treatment, but after that the rate of decrease deteriorates. As for the amount of dissolved O_2, which generally affects the processing rate, it remains unchanged 6 mg/L in both polarity cases.

The dissolved amount of ozone O_3 greatly varied depending on the polarity of discharge. In the case of negative polarity, it increased by about 0.1 mg / L at most after even 1000 discharges, but occurred in large amounts exceeding the measurement limit value of 5 mg / L at about 250 discharge times with positive polarity. From these results, it was shown that the increase in the processing speed of the solution in the case of positive polarity was greatly influenced by ozone formation and dissolution by electrolysis around the upper ring electrode.

3. References

[1] A.A.Egorov,et.al.:Tech.Phys.47(2002) 1584.

[2] M. Maeyama, et.al.: JPS Conf. Proc. 1(2014) 015076.

[3] M. Maeyama, et.al.: 21th Int. Conf. on Gas Discharges and their Applications (2016) 461.

Experimental studies of mechanisms of positive column constriction in argon and neon

Yu. Golubovskii[1], A. Siasko[1], D. Kalanov[1], V. Nekuchaev[2]

[1]*Saint-Petersburg State University, 7/9 Universitetskaya nab., St. Petersburg, 199034 Russia*
[2]*Ukhta State Technical University, Pervomaiskaia ul. 13, Ukhta 169300, Russia*

Paper presents latest results of experimental studies of positive column constriction in neon and argon. In particular, measurements of electric fields in neon and argon, densities and radial profiles of the excited states $2p^5 3s$ and $2p^5 3p$ in neon and $3p^5 4s$ and $3p^5 4p$ in argon (1s and 2p in Pashen's notation) were performed. Densities and radial profiles were obtained using classic method of emission and absorption spectroscopy and by line ratios method. The main role in constriction belongs to the nonlinear dependence of ionization rate on electron density due to a competition of the electron-atom and the electron-electron collisions. Basic regularities of the phenomenon and main distinctions of obtained results in constricted neon and argon discharges are discussed.

1. Introduction

Constriction is a phenomenon in gas discharge physics observed as abrupt formation of a thin bright cord with a growth of discharge current, which arises from a strong nonlinear dependence of the ionization rate on the electron density. The nonlinearity is related to a competition of electron-atom and electron-electron collisions during formation of an electron distribution function. As a result, this nonlinear dependence causes ionization instability in the radial direction with simultaneous constriction. Generalized experimental and theoretical knowledge of constriction in inert gases has been discussed in a review [1].

2. Experimental setup

A registration system consisted of a monochromator Acton SpectraPro 2300i. Radial scanning was performed with the high-speed camera pco.1200hs, so an instrumental function of the experimental setup was determined by a pixel size of the camera. Measurements were performed with a reduced gas pressure in argon tube of 98 Torr*cm and neon - filled cylindrical tube with pressure 90 Torr*cm. A second line source necessary for absorption measurements were 2 Torr ICP discharges in argon and neon.

3. Methods of spatial absorption measurements

Radial density profiles of 2s and 2p- states were first measured by classic absorption method. Theoretical description of the method can be found in [2]. For ICP plasma source a Doppler lineshape is assumed and a Voigt lineshape for the main source. The second method was a modified line ratios method, proposed in [3], which allows to determine densities and radial profiles of absorbing atoms by solving a system of emission flux ratio equations.

4. Results

Profiles of excited states in argon and neon measured in different lines show good agreement. Absolute density values of 1s-states in argon are lower than in neon and radial profiles in neon are wider. Distinctions in radial profiles are related to differences in dependencies of ionization rates on the electron density. Nonlinear dependence in argon is much stronger than in neon. Figure 1 compares measured radial profiles of 2p-levels.

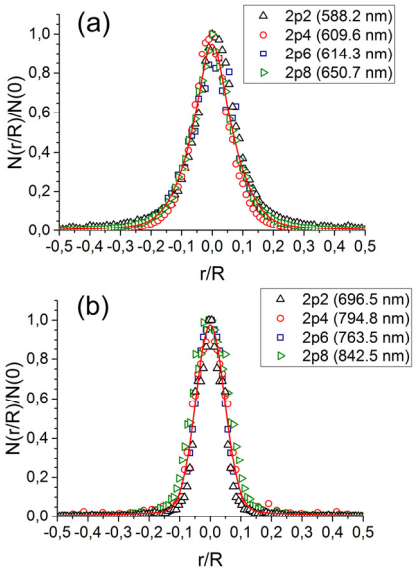

Figure 1. 2p profiles in neon (a) at i/R=40 mA/cm and argon (b) at i/R =17,4 mA/cm in selected emission lines.

5. References

[1] Y. B. Golubovskii et al., Plasma Sources Sci. Technol. **20** (2011) 53002.

[2] J. Loureiro, J. Amorim, *Kinetics and spectroscopy of low temperature plasmas*, Springer Int. Publ. (2016).

[3] M. Schulze et al., J. Phys. D. Appl. Phys. **41** (2008) 65206.

Dependence of double layer potential on the properties of anode spot plasma

Yuna Lee[1], Kyoung-Jae Chung[1], Y. S. Hwang[1]

[1] *Department of Nulcear Engineering, Seoul National University, Seoul, 08826, KOREA.*

The anode spot is successfully utilized to plasma ion source because of its high power efficiency with generating high plasma density near to aperture. It is important to figure out how to control the anode spot size at plasma ion source so as to enhance ion beam current. In this paper, we investigate the relationship among the anode spot size, bias current and operating parameters such as operating pressure and bias voltage. We find that properties of anode spot including its size is closely correlated with the double layer potential between the anode and the ambient plasma. The experimentally measured anode spot size show good agreements with the estimated one using particle balance between the production and loss of ions inside the anode spot.

1. Introduction

An anode spot plasma is localized high density plasma, generated in front of a small electrode biased positively with respect to the plasma potential of ambient plasma and distinguished with ambient plasma by a potential difference, called as double layer. We have proposed a new approach to produce high ion beam current using localized characteristics of anode spot plasma near the extraction aperture [1]. Recently, we found that the anode spot plasma size should be comparable to bias electrode in order to enhance the ion beam current with stable operation [2]. Song [3] proposed that the size of anode spot is proportional to the reciprocal of pressure and electron-impact ionization cross section of ionization potential. However, we experimentally observed that the length of anode spot is expanded by increasing the bias voltage even if operated at fixed pressure. In the present work, it is figured out that the relationship between changes of anode spot size and operating parameters such as operating pressure and bias voltage is explained in terms of double layer potential.

2. Experimental setup

The basic structure is the same as that used in our previous work [4]. The ambient plasma (argon, 10-100mTorr) is generated by inductive coupling with fixed RF power of 150 W at the frequency of 13. 56 MHz. The anode spot is generated in front of a planar electrode of 6 mm in diameter. A DC P/S drives the positive voltage in range of 0-100 V on the bias probe through a limiting resistor of 100 Ω. An axially movable Langmuir probe (D : 0.1 mm, L : 2.5 mm) is used to measure the plasma properties. Shapes and sizes of anode spot plasmas are recorded by a commercial digital camera.

3. Experimental Results and discussion

Measured plasma properties of ambient plasma and anode spot show that the anode spot expands with decreasing the double layer potential or increasing the operating pressure. Based on the experimental result, the length of anode spot is derived from the particle balance between ion production inside the anode spot and ion loss through the surface of anode spot. The estimated size of anode spot using the particle balance is comparable to the experimentally measured one which is determined by double layer potential variation with increasing bias voltage.

4. Conclusion

It is confirmed that not only the operating pressure but also the double layer potential has an influence on the determination of anode spot size. The present work is helpful to understand the relationship among the bias current, anode spot size and extracted beam current and also give an information about the operating parameters ranges of anode spot plasma ion source with stable operation

5. Acknowledgement

This work was supported by the technology innovation program (No. 10067509) funded by the Ministry of Trade, Industry & Energy (MI, KOREA).

6. References

[1] Y. J. Kim, D. H. Park, H. S. Jeong and Y. S. Hwang, Rev. Sci. Instrum. 77 (2006) 03B507.

[2] Yuna Lee, Kyoung-Jae Chung and Y. S. Hwang, Cur. Appl. Phys. 15 (2015) pp.1599-1605.

[3] B. Song, N. D. Angelo and R. L. Merlino, J. Phys. D: Appl. Phys. 24 (1991) 1789.

[4] Yeong-Shin Park, Yuna Lee, J. J. Dang, Kyoung-Jae Chung and Y. S. Hwang, Rev. Sci. Instrum.85 (2014).02A508.

Effect of discharge tube temperature on the density of N($^4S^o$) in a remote nitrogen plasma source

M. Shimabayashi[1], K. Kurihara[2], and K. Sasaki[1]

[1] *Division of Quantum Science and Engineering, Hokkaido University, Sapporo 060-8628, Japan*
[2]*Toshiba corp. resident at Imec, Kapeldreef 75, 3001 Leuven, Belgium*

We investigated the characteristics of surface nitriding of 4H-SiC using a remote nitrogen plasma to improve the carrier mobility of a SiC-based power transistor. Our previous report suggests the possibility of an efficient, low-damage nitriding process using the remote nitrogen plasma which has a high flux ratio of $N_2(A^3\Sigma_u^+)/N(^4S^o)$. In this paper, we tried to control the densities of reactive nitrogen species by heating the discharge tube. Quartz and p-BN tubes were employed for the discharge tube. We observed the increase in the N($^4S^o$) density with the discharge tube temperature between 20 and 600 ^{o}C. On the other hand, the N($^4S^o$) density was roughly independent of the discharge tube temperature when we employed a quartz tube.

1. Introduction

The control of the flux ratio of reactive species supplied from a reactive plasma is of importance in various plasma processing technologies to optimize their performances. We are investigating the characteristics of surface nitriding of 4H-SiC using a remote nitrogen plasma to improve the carrier mobility of a SiC-based power transistor. In a previous report, we pointed out a possibility of an efficient, low-damage nitriding process using the remote nitrogen plasma which have high flux ratio of $N_2(A^3\Sigma_u^+)/N(^4S^o)$ [1]. To realize the control of the flux ratio of reactive nitrogen species, we investigated the effect of the material of the discharge tube and its temperature. In this paper, we report the effect of the discharge tube temperature on the N($^4S^o$) density in the spatial afterglow region of the remote nitrogen plasma.

2. Experiment

The nitrogen plasma was produced by attaching a microwave resonator on the outside of a quartz or p-BN tube. The resonator was connected to a microwave power supply at 2.45 GHz. The microwave power was 100 W. The bottom side of the discharge tube was connected to a stainless-steel cylindrical chamber. The gas pressure was adjusted at 0.5 Torr by controlling the pumping speed. We attached a kanthal spiral wire on the outside of the discharge tube in the region between the microwave resonator and the stainless-steel chamber. The discharge tube was heated up to 600 ^{o}C by applying a heating power to the kanthal wire. The N($^4S^o$) density was measured in the spatial afterglow region by vacuum ultraviolet absorption spectroscopy. The distance between the microwave resonator and the measurement position was 12 and 13 cm when employing the quartz and p-BN tubes, respectively.

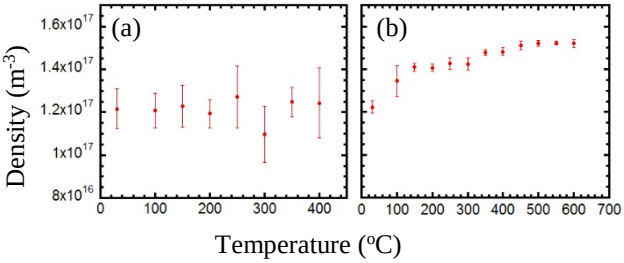

Fig.1. Relationship between density of N($^4S^o$) and temperature of (a) quartz and (b) p-BN tubes in the spatial afterglow region.

3. Results and Discussion

Figures 1(a) and 1(b) show the relationships between the N($^4S^o$) density and the discharge tube temperature when we employed a quartz and p-BN tubes, respectively. As shown in the Fig. 1(b), we observed the increase in the N($^4S^o$) density with the discharge tube temperature when we employed the p-BN tube. On the other hand, the N($^4S^o$) density was roughly independent of the temperature when we employed the quartz tube. Since the N($^4S^o$) density decreased with the distance from the microwave resonator, the result shown in Fig. 1(b) may be caused by the decrease in the surface loss probability of N($^4S^o$) on the surface of the p-BN tube at a high temperature. Another possibility is the production of N($^4S^o$) in the region between the microwave resonator and the measurement position due to collisions among vibrationally excited molecular nitrogen (the V-V pumping-up mechanism).

4. References

[1] M. Shimabayashi, K. Kurihara, and K. Sasaki, Jpn. J. Appl. Phys. **55** (2016) 036503.

Gas flow modifications by a kHz microsecond atmospheric pressure plasma jet

X. Damany[1], P. Viegas[2], S. Dozias[1], J-M. Pouvesle[1], A. Bourdon[2], E. Robert[1]

[1] *GREMI, UMR7344 CNRS Université d'Orléans, Orléans, France*
[2] *LPP, CNRS, Ecole polytechnique, UPMC Univ Paris 06, Univ Paris-Sud, Observatoire de Paris, Université Paris-Saclay, Sorbonne Universités, PSL Research University, 91128 Palaiseau, France*

In this work we present Schlieren images of a Plasma Gun discharge fed with several helium buffer admixtures (pure, O_2, N_2). It has been demonstrated that efficient gas flow channelling is observed with pure helium. Such gas flow channelling is also proven to be dependent on voltage polarity and frequency. Analysis of the role of molecular admixtures (N_2 or O_2) confirms the non-thermal nature of the effect and the potential crucial role of large negative ions. In order to get a better understanding of this effect, numerical simulations have been carried out to study the dynamics of formation of positive and negative ions in helium with various amounts of N_2 or O_2 admixtures. The influence of mixing the gases in the buffer or downstream is also studied.

1. Introduction

Atmospheric pressure plasma jets are effective for biomedical applications thanks to several factors but mainly due to reactive oxygen and nitrogen species (RONS). Yet, it has been shown that plasma jets change the gas flow, influencing RONS production and delivery. Several parameters have already been investigated with pure helium fed plasma such as pulse frequency, gas flowrate and voltage polarity [1]. Even though it sounds tempting to add O_2 or N_2 to enhance RONS' production, no study shows how it modifies the gas flow.

In this study we present Schlieren images of a Plasma Gun (PG) discharge fed with pure helium and then with admixture of O_2 and N_2. Gases were mixed in two different places: before and after the reactor. The collected images were compared to numerical simulation results of plasma jet propagation in conditions as close as possible to experiments.

2. Experimental Setup and modelling

PG is powered by µs duration voltage pulses. A conductive grounded metallic plate is placed 2 cm away from the glass capillary outlet in order to mimic PG operation for biomedical applications. A classic Z-Schlieren is used to reveal rare gas density gradients in ambient air. The simulations are performed with a 2D fluid model for plasma propagation with several He-N_2 and He-O_2 gas mixtures using detailed kinetic schemes [2,3].

3. Results

In pure helium, the gas flow structure was mainly controlled by voltage polarity and pulse frequency. There exists a limitation in frequency depending on gas flow, for example 500 Hz at 0,5l/min, below which it is impossible to channel the gas. With positive polarity, gas flow was disturbed above the target while with negative one, a well-defined channel was created. This behaviour has also been observed with neon and argon. Then Schlieren revealed that adding a small amount of O_2 was enough to deeply modify gas behaviour. It helped channelling the gas to the target in a well-defined way, even in positive polarity. In negative polarity both effects (polarity and addition of O_2) were working together, as an even smaller amount of O_2 was enough to channel the gas. Moreover, the more O_2 was added, the lower was the limitation of frequency. Hence a 100Hz-powered plasma managed to channel the gas thanks to a 2%-O_2 addition. It has to be noted that if mixing helium and O_2 in negative polarity is very effective, a too large amount of O_2 prevents plasma ignition. Nevertheless no difference with pure helium was observed when N_2 was mixed with helium. When O_2 was added downstream the reactor, the same behaviours have been observed even if the channelling was more effective with a mixture added upstream. The simulation results show the formation of positive and negative ions in several He-N_2 and He-O_2 gas mixtures, adding the admixtures in the buffer or downstream.

4. Acknowledgments

X.D. is supported by Inel Thermofisher Scientific/Centre Val de Loire PhD fellowship.

5. References

[1] E. Robert *et al., Plasma Sources Sci. Technol.*, vol. 23 **1** (2014) 12003

[2] A. Bourdon et al., *Plasma Sources Sci. Technol.* **25** (2016) 035002

[3] D.-X. Liu et al., Plasma Process. Polym. **7** (2010) 846

Atomic scale study of Al clustering and particle growth

N. Ning[1] and S. Khrapak[1]

[1] *Aix-Marseille University, CNRS, PIIM, 13390, Marseille, France*

Recent years, aluminium nanoparticles has attracted many attentions for a variety of applications, such as propellant [1], high capacity hydrogen storage materials [2], nanocomposite materials [3], and biomolecules detection [4]. The nanoparticle dimensions can be an important factor for a given application as the mechanical and electrical properties of a material is particle size related. While the real-time growing process is normally difficult to be observed directly, theoretical study becomes essential to provide a better understanding of particle growth kinetics and mechanisms. We are investigating Al clustering and Al particle formation by using Molecular Dynamic (MD) simulation based on empirical potential. Trajectory calculations were performed to predict rate constant of association reactions of Al clusters. We will also discuss the important parameters (such as temperature, cluster size, etc) which effect on reaction kinetics.

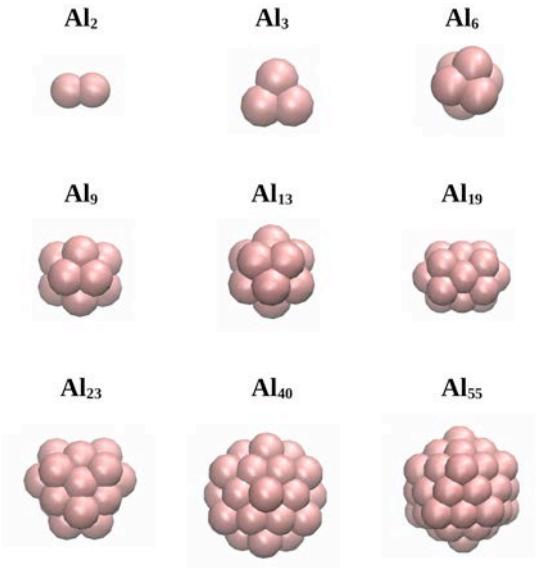

Figure 1. Visualization of geometry optimized aluminium clusters. It demonstrates global minimum configurations of involved Al clusters in this study.

1. References

[1] J.J. Granier, M.L. Pantoya, Combust. Flame **138** (2004) 373.

[2] P. J. Roach et al., Science **323** (2009) 492.

[3] O. Polonskyi et al., J. Mat. Sci. **49** (2014) 3352.

[4] M.H. Chowdhury et al., Anal. Chem. **81** (2009) 1397.

Computer simulation of ion stopping in a dense plasma by the Monte Carlo method

S.K. Kodanova [1], T.S. Ramazanov [1], M.K. Issanova [1], E.E. Shokparbayeva [1], S.A. Maiorov [2]

[1]*IETP, Al-Farabi Kazakh National University, Almaty, Kazakhstan*
[2]*A.M. Prokhorov General Physics Institute, Moscow, Russia*

In this work, the Monte Carlo method was used to simulate ion trajectories in a dense plasma of inertial confinement fusion. The results of computer simulation are numerical data on the dynamic characteristics, such as energy loss, penetration depth, the effective range of particles, stopping and straggling. By the results of the work the program of 3D visualization of ion trajectories in a dense plasma of inertial confinement fusion was developed.

Recently, a large number of theoretical and experimental studies of the physical processes that determine the construction of a thermonuclear target and the required parameters of a future driver carried out [1-2]. The calculation of thermonuclear target parameters for heavy ion inertial fusion requires adequate quantitative description of heavy ion interaction with the dense plasma in a wide range of parameters. Therefore, in order to know the properties of the dense plasma under different conditions, the most attractive way is a computer experiment. Computer simulation can answer many important questions, which are to be known to use the dense plasma.

Nowadays, there are various programs which allow us to carry out simulation of ion implantation process in solids without experiments. Simulation has some error and is not able to fully replace real experiments, but its results provide invaluable assistance in future research. The best-known programs are the SRIM (The Stopping and Range of Ions in Matter) [3] and Geant4 [4].

The main energy contribution of heavy ion beams in different types of fusion targets occurs in dense high-temperature plasma. Therefore, knowledge of free paths and energy input profiles of fast and heavy charged particles in the plasma will help to determine the characteristics of the thermonuclear target most precisely.

In this work, the Monte Carlo method is used for simulation of ion trajectories in a dense plasma of inertial confinement fusion. The main advantage of calculations by the Monte Carlo method is that they allows us to take into account any physical process directly, for example, local and non-local inelastic energy losses, binding energy between atoms, replacing collision, etc. Moreover, it is possible to obtain accurate solutions for multi-target and multi-layered complex geometry, which allows us to simulate actual interactions with the plasma ion beam. The paper considers the interaction of xenon ions in copper and beryllium, and iron ions in the mixture of deuterium, tritium and hydrogen at different energies.

The results of computer simulation are numerical data on the dynamic characteristics, such as energy loss, penetration depth, the effective range of particles, stopping and straggling. By the results of the work the program of 3D visualization of ion trajectories in a dense plasma of inertial confinement fusion was developed.

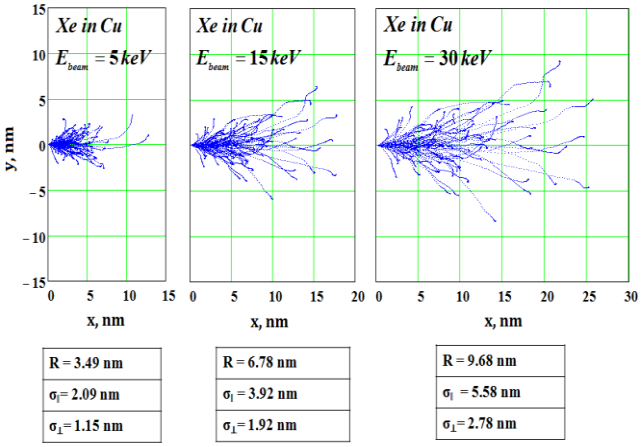

Fig. 1. The trajectories of the xenon ions in the copper: a) with an initial energy of $5 keV$, b) $15 keV$, c) $30 keV$. Figure shows the stopping range of the xenon ions depending on the energy in copper.

References

[1] T.S. Ramazanov, et al. Contrib. Plasma Phys. **56** (5) (2016) 425-431.

[2] D.H.H. Hoffmann, A. Blazevic, P. Ni et al. Laser and Particle beams **23**(2005) 47.

[3] J.F. Ziegler, M.D. Ziegler, J.P. Biersack. Nucl. Instr. Meth. in Phys. Res. B **268** (2010) 1818–1823.

[4] M.H. Mendenhall, R.A. Weller. Nucl. Instr. Meth. **227** (2005) 420-430.

Atmospheric pressure cold plasma driven Ni/γ-Al_2O_3 catalytic reactor for methanation of CO_2

L. Sivachandiran[1, 2], P. Da Costa[3], A. Khacef[1]

[1]*GREMI, UMR 7344, CNRS-Université d'Orléans, 14 rue d'Issoudun, BP 6744, 45067 Orléans Cedex 02, France.*
[2]*SRM Research Institute, Depart. of Chemistry, SRM University, Kattankulathur, Kancheepuram 603203 (D.t.), India.*
[3]*Univ Paris 6, UMR 7190 Sorbonne Univ-CNRS, Institut Jean Le Rond d'Alembert, 2 Pl Gare Ceinture, 78210, France.*

Hydrogenation of CO_2 to CH_4 was carried out using Ni/γ-Al_2O_3 catalysts coupled with non-thermal plasma dielectric barrier discharge reactor (NTP-DBD). The effect of gas temperature (22-400°C), plasma input power (25-35 W), and CO_2 to H_2 ratio on CO_2 conversion rate and CH_4 selectivity has been studied. It was evidenced that, compared to conventional thermal catalysis, plasma-catalysis coupling decreased the catalyst activation temperature, *i.e.* the CO_2 conversion, by 50°C. Furthermore, 10 wt% Ni/γ-Al_2O_3 catalyst has shown about 40% CO_2 conversion and 70% CH_4 selectivity.

Modernization, deforestation and overwhelmingly increasing world population are significantly increasing the atmosphere CO_2 level. Consequently, several methods have been developed to reduce the atmospheric CO_2 level. The conversion of CO_2 in other products has attracted much more attention, especially non-thermal plasma (NTP) for CO_2 conversion [1] and methanation [2].

In this study, thermal catalysis, plasma, and plasma-catalysis processes have been investigated for direct hydrogenation of CO_2 in a wide range of temperature, plasma input power and CO_2 to H_2 ratio. The NTP-catalytic reactor is a cylindrical DBD powered by sub-ns HV pulses with an amplitude up to 20 kV at frequency up to 500 Hz.

The nickel metal is doped on γ-Al_2O_3 beads (1.8 mm diameter, Sasol Germany GmbH) by wet impregnation method. Before each experiment, the Ni/γ-Al_2O_3 catalyst (1.5 g) was activated for 20 min at 400°C under H_2 (5%)/N_2 flow. The catalyst was placed in the centre of the plasma discharge volume. This configuration, stated as In-Plasma Catalysis (IPC), leads to two distinguished discharge configurations: gas phase streamer discharge before and after the catalyst bed, and surface discharge on the catalyst.

For all the experiments, the total gas flow rate was fixed as 620 ml.min^{-1}, unless otherwise mentioned. CO_2, CH_4, CO, and O_2 concentrations were followed using gas chromatography (μGC, MyGC-SRA).

An example of data obtained for plasma alone, catalysts alone (γ-Al_2O_3, 10 wt% Ni/γ-Al_2O_3), and plasma-catalyst systems is shown in Fig. 1. For the investigated temperature range γ-Al_2O_3 catalyst, whether used alone or coupled with plasma, has shown less than 2% CO_2 conversion. Indeed, Ni doping on γ-Al_2O_3 has significantly increased the CO_2 conversion. Thermal catalytic activity of 10 wt% Ni/γ-Al_2O_3 catalyst begins above 250°C, and about 55% of CO_2 conversion is reached at 300°C. Under the similar operating conditions, when 10 wt% Ni/γ-Al_2O_3 is coupled with plasma, the CO_2 conversion starts at lower temperature and 45% CO_2 conversion is reached at 250°C. The decrease in catalyst activation temperature can be correlated to synergetic effect of plasma-catalyst coupling.

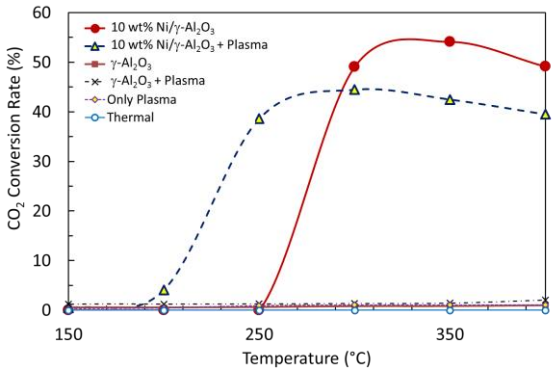

Fig. 1. CO_2 conversion rate as function of temperature (plasma conditions: 15 kV and 100 Hz).

It was evidenced that, without Ni doping on γ-Al_2O_3, CH_4 is not produced for all the investigated temperatures as reported in literature [3]. This implies that Ni doped on Al_2O_3 are mainly involved in CO_2 hydrogenation processes. It can be suggested that although plasma dissociates CO_2 but it does not induce the hydrogenation reaction. At 250°C, with or without plasma, 10 wt% Ni/γ-Al_2O_3 catalyst has shown 70% CH_4 selectivity. The decrease in CO_2 conversion and CH_4 production can be attributed to the catalytic partial oxidation of CH_4 to CO_2, CO, and H_2O at high temperature. In that case and at 300°C, the CO selectivity increased by a factor 2 when the combined plasma-Ni/γ-Al_2O_3 system is used compared to the Ni/γ-Al_2O_3 catalyst used alone (from 8 to 4%).

At a fixed temperature, the increasing of the plasma input power increase slightly the CO_2 conversion and CH_4 selectivity. However, the CO selectivity rapidly increases up to 10% (at 20 kV) evidenced the fact that the injected excess power probably promotes the CO formation from CO_2 and CH_4.

[1] D. Mei, X. Zhu, Y.L. He, J.D. Yan, X. Tu. Plasma Sources Science and Technology **24** (2015), 015011.
[2] L. He, Q. Lin, Y. Huang. Journal of Energy Chemistry **23** (2014), 587.
[3] E. Jwa, S.B. Lee, H.W. Lee, Y.S. Mok. Fuel Processing Technology **108** (2013), 89.

Topic number: 5

Development of the LisbOn KInetics (LoKI) tool

A. Tejero-del-Caz[1], D. Nina[1], S. Jacob[1], D. Gonçalves[1], M. Lino da Silva[1], L. Marques[1,3], N. R. Pinhão[1], C. D. Pintassilgo[1,2], V. Guerra[1] and L. L. Alves[1]

[1] *Instituto de Plasmas e Fusão Nuclear, Instituto Superior Técnico, Universidade de Lisboa, Lisboa, Portugal*
[2] *Departamento de Engenharia Física, Faculdade de Engenharia, Universidade do Porto, Porto, Portugal*
[3] *Centro de Física da Universidade do Minho, Universidade do Minho, Braga, Portugal*

This work presents the current status of development of LisbOn KInetics (LoKI), a computational tool to model non-equilibrium low-temperature plasmas, produced from different gas mixtures for a wide range of working conditions. LoKI comprises a Boltzmann module (LoKI-B) and a chemistry module (LoKI-C), coupled in a self-consistent way, yielding the electron energy distribution function, the electron swarm parameters, the concentrations of the various plasma species, and the corresponding gain/loss reaction rates. The tool can handle simulations including any gas mixture, accounting for the electronic, vibrational and rotational internal degrees of freedom of the atomic / molecular excited states present in the discharge.

1. Introduction

Predictability in plasma science and engineering based on fundamental modelling has been considered a requirement for the progress in the field, and the model-based design of plasma processes has been identified as a necessary capability to achieve industrial goals. Therefore, there is general agreement on the intellectual and technological importance of modelling low-temperature plasmas (LTPs).

Predictive tools for non-equilibrium LTPs should describe the kinetics of both electrons and heavy-species, the former responsible for inducing plasma reactivity and the latter providing the paths for industrial applications. Here, we focus on plasma-based environmental and biological applications, which have recently attracted the interest of pure and applied research. In this context, we have launched a research project for delivering a KInetic Testbed for PLASMa Environmental and Biological Applications (KIT-PLASMEBA), embodying a MATLAB® computational tool (LisbOn KInetics, LoKI) linked to a web-platform (KIT) containing state-of-the-art kinetic schemes.

2. Code implementation

LoKI comprises two modules (LoKI-B and LoKI-C) that can run self-consistently coupled or as standalone tools. The foundations for developing this tool were stablished years ago [1]. LoKI-B (to become open-source) provides the solution to the homogeneous two-term electron Boltzmann equation [2] (for a pure gas or a gas mixture, including first and second-kind collisions, as well as electron-electron collisions), using the LXCat open-access website [3] for obtaining electron scattering cross section data; LoKI-C gives the solution to the system of zero-dimensional (volume average) rate balance equations for the most relevant charged and neutral species in the plasma. The simulations can include any gas mixture, accounting for the electronic, vibrational and rotational internal degrees of freedom of the atomic / molecular excited states present in the discharge. On output, LoKI yields the electron energy distribution function, the electron swarm parameters, the concentrations of the various plasma species, and the corresponding gain/loss reaction rates.

The results are obtained either for a prescribed constant pressure, ensured by varying the gaseous mixture composition, or at fixed mass density. For stationary discharges, the reduced maintenance electric field is self-consistently calculated as an eigenvalue solution to the problem, under the assumption of quasi-neutrality.

3. Discussion and conclusions

LoKI is a user-friendly, scalable and upgradable tool. This work discusses its current status of development, presenting basic structure, evidencing functionality and introducing test cases along with first results of benchmarking against other codes. LoKI development will continue focusing on its graphical user interface and on the introduction of verification and validation procedures.

4. Acknowledgments

This work was funded by Portuguese FCT – Fundação para a Ciência e a Tecnologia, under projects UID/FIS/50010/2013 and PTDC/FISPLA/1243/2014 (KIT-PLASMEBA).

5. References

[1] Guerra V and Loureiro J, Plasma Sources Sci. Technol. **6** (1997) 373-385

[2] Alves L L, Plasma Sources Sci. Technol. **16** (2007) 557-569.

[3] www.lxcat.net

Vibrational excitation kinetics of CO_2 in a pulsed glow discharge

B.L.M. Klarenaar[1], R.Engeln[1], M.A. Damen[1], M.C.M. van de Sanden[1,2], A.S. Morillo-Candas[3], and O. Guaitella[3]

[1] *Department of Applied Physics, Eindhoven University of Technology, Eindhoven, The Netherlands*
[2] *Dutch Institute for Fundamental Energy Research, Eindhoven, The Netherlands*
[3] *Laboratoire de Physique des Plasmas, Ecole Polytechnique-CNRS-Univ Paris-Sud-UPMC, Palaiseau, France*

Excitation of the asymmetric stretch vibrational mode of CO_2 is believed to be crucial for an efficient plasma assisted dissociation of CO_2 to CO. Using time-resolved *in situ* Fourier Transform Infrared spectroscopy we gain insight in the vibrational dynamics of CO_2 in a pulsed glow discharge (5/10 ms on/off). FTIR measurements in a discharge at 5 mbar and 50 mA reveal excitation of the asymmetric stretch mode of CO_2, showing a vibrational temperature of 913 K versus a rotational temperature of 437 K, at 0.5 ms after plasma-on. Rotational temperatures measured using spatially and time-resolved rotational Raman spectroscopy correspond well to the FTIR results and show no significant temperature changes over the longitudinal axis of the reactor.

1. CO_2 reduction for renewable energy storage

Efficient reduction of CO_2 to CO is a key step in the process of storing renewable energy in the form of hydrocarbon fuels. This dissociation process is believed to be most efficient when selectively exciting the asymmetric stretch mode of CO_2. We study the vibrational dynamics of CO_2 by performing *in situ* Fourier Transform Infrared (FTIR) spectroscopy, as well as rotational Raman spectroscopy on a pulsed glow discharge. Since the discharge mechanisms of such a plasma are well known, a glow discharge is particularly suitable for a fundamental study on vibrational energy levels.

2. Setup and analysis for vibrational kinetics

The cylindrical plasma reactor (23 cm length, 2 cm diameter) is operated under flowing conditions (7.4 sccm CO_2) in the millibar range, with a pulsed 10–50 mA plasma current at 5/10 ms on/off. To study the vibrational dynamics by IR absorption, the reactor is positioned inside the sample compartment of an FTIR spectrometer (Bruker, Vertex 70). The step-scan operation mode allows the recording of spectra with a temporal resolution of 10 µs, well below the millisecond timescale of the plasma.

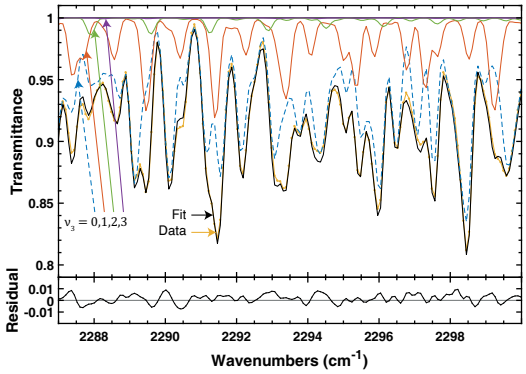

Fig. 1: IR transmittance data and fit of CO_2 at 0.5 ms after plasma-on, at 50 mA and 6 mbar. Absorptions from transitions with ν_3 = 0, 1, 2, and 3 are shown separately.

For the analysis we developed an algorithm to calculate and fit the transmittance spectra of CO_2 and CO, using the HITEMP-2010 database. Fit parameters include the rotational temperature, T_{rot}, the temperature of the fermi-coupled symmetric stretch (ν_1) and bending (ν_2) modes of CO_2, $T_{1,2}$, and the temperature of the asymmetric (ν_3) mode, T_3.

3. Analysis results, related to Raman spectroscopy

Fig. 1 shows a fit at 0.5 ms after plasma-on, giving T_{rot} = 437 K, $T_{1,2}$ = 459 K, and T_3 = 913 K. Hence, a clear asymmetric stretch excitation of CO_2 is observed, with respect to the other temperatures. Details on a kinetic model used to study these experiments are given in [1]. Furthermore, details on the important role and kinetics of O atoms in these discharges are given in [2]. Additional experiments are planned, to study the link between the measured vibrational excitation and CO_2 dissociation.

Time and spatially-resolved rotational Raman measurements are done to study the assumption made in the FTIR analysis, i.e. no temperature variations along the line-of-sight. Spatially, the measured T_{rot} does not significantly change, while temporally, it corresponds well to the IR fits. This affirms the validity of both measurement techniques and the reliability of vibrational temperatures resulting from the infrared absorption experiments.

4. References

[1] T. Silva *et al.*, abstract submitted to ICPIG 2017.
[2] A.S. Morillo-Candas *et al.*, abstract submitted to ICPIG 2017.

Comparison of two electric field measurement methods for a kHz microsecond atmospheric pressure plasma jet

X. Damany[1], G. Sretenović[2], S. Iséni[1], V. Kovačević[2], I. Krstić[2], S. Dozias[1], J.-M. Pouvesle[1], M. Kuraica[2] and E. Robert[1]

[1] *GREMI, UMR7344 CNRS Université d'Orléans, Orléans, France*
[2]*Faculty of Physics, University of Belgrade, Serbia*

Electric field associated with a kHz microsecond atmospheric pressure plasma jet has been measured using two different methods. The first one consists in an electro-optic probe allowing to measure the electric field outside the capillary in which propagates the plasma. The second one relies on Stark polarization spectroscopy on the 492.19nm line of helium. If the first one offers a nice time resolution, the second method has a better spatial accuracy but can be used only where light is emitted by the plasma. Thus these two methods complement one another and can even be compared depending on the conditions. If plasma is powered by a positive polarity voltage pulse both techniques are in good agreement. Nevertheless when negative polarity is used some discrepancies are observed.

1. Introduction

Atmospheric plasma jets are studied because of the wide range of applications they offers, especially in biomedical fields. They consist of an ionization wave propagating into a rare gas followed by a plasma channel [1]. If the role in biology of reactive oxygen and nitrogen species has been highlighted, other components of the plasma deserves more attention as transient electric fields (EF). This work focuses on the measure of these EF with two different methods based on Pockels effect [2] or Stark spectroscopy [3] for a Plasma Gun (PG) discharge. Depending on the situation both techniques can either be complementary or compared.

2. Experimental Setup

Plasma Gun consists in a vertically downward oriented capillary with an inner high-voltage electrode and an outer grounded one. Plasma is powered with µs-duration voltage pulses. First method to measure the EF uses an electro-optic probe (Kapteos), based on Pockels effect and made of a birefringent crystal in an alumina tube. The second technique, using Stark polarization spectroscopy of helium I 492.19nm line, has the advantage to be non-perturbative. A 1:1 image of the PG is created on the 70µm-wide spectrometer slit. The spectrometer contains two 1200 grooves.mm^{-1} gratings. In presence of strong EF, *i.e.* in this study only the one associated with the ionization wave, forbidden transitions become allowed, making appear a forbidden line in the spectrum. Moreover this line is shifted according to EF strength. Thus measuring the position of the forbidden line and the allowed one can allow to evaluate the EF strength.

3. Results

EFs in several situations have been investigated. In each one, EF measured by the spectroscopy in the plasma was compared with the one obtained thanks to the probe placed next to the capillary or the plume. If the plasma is powered with positive polarity voltage, both methods give results with a good agreement. For example, the transient EF was measured in the plume with a metallic grounded target 1cm away from the end of the capillary. The value given by the spectroscopy in the plasma was compared with the one obtained with the probe, placed 5mm away from the axis of the tube. Both methods gave a value around 10kV.cm^{-1}

Nevertheless, EF with a negative polarity voltage is not as easy to evaluate. Spectroscopy shows that the EF is weaker than with positive polarity voltage: 5kV.cm^{-1} instead of 9 for positive polarity in the same other conditions at the end of the capillary. Yet, electro-optic sensor finds comparable values of EF, around 10kV.cm^{-1} for both polarities near the end of the capillary.

4. Acknowledgments

This work was supported by the bilateral project PHD Pavle Savic 2016 (no 36216UA). X.D. acknowledges his grant funding Thermofisher Scientific INEL/Région Centre Val de Loire.

5. References

[1] E. Robert *et al*., Phys. Plasmas, **22** (2015) 122007.
[2] G. Gaborit *et al*., IEEE Trans. Plasma Sci., **42** (2014) 1265.
[3] G. Sretenović *et al*.. Phys. D. Appl. Phys., **47** (2014) 102001.

Atmospheric pressure plasma assisted preparation of ceramic submicron fibers

V. Medvecká[1], A. Zahoranová[1], D. Kováčik[1,2], M. Černák[1,2]

[1] *Department of Experimental Physics, Faculty of Mathematics, Physics and Informatics, Comenius University Mlynská dolina F2, 842 48 Bratislava, Slovakia*

[2] *CEPLANT, Department of Physical Electronics, Faculty of Science, Masaryk University Kotlářská 2, 611 37 Brno, Czech Republic*

Atmospheric pressure plasma generated in ambient air by Diffuse Coplanar Surface Barrier Discharge was used as an alternative to the conventional thermal sintering for the oxidation and removal of polymer matrix by the preparation of zinc oxide submicron fibers from polymer/precursor fibers. Morphology of fibers was observed by Scanning Electron Microscopy (SEM). Efficiency of removal of organics was studied by Energy-Dispersive X-Ray Spectroscopy (EDX). Changes in chemical bonds were investigated using Fourier Transform Infrared Spectroscopy (FTIR). Significant decrease of organics was detected and high porosity of fibers was observed after plasma exposure time in the order of minutes.

1. Introduction

Zinc oxide (ZnO) nanofibers, due to the unique electrical and optical properties, have attracted attention for applications in solar cells, gas and biosensors, transparent conductors, etc. [1]. Most common technique for preparation of ZnO fibers in submicron scale is thermal calcination of polymer/precursor fibers [2]. Due to the high temperature approach and long treatment times, conventional thermal calcination is economically and energetically demanding process.

Plasma assisted calcination (PAC) is a novel low temperature process of oxidation and removal of base polymer by non-thermal plasma [3,4]. In this work, special type of dielectric barrier discharge, so called Diffuse Coplanar Surface Barrier Discharge (DCSBD) [5,6], was used for PAC of *polyvinyl alcohol/zinc acetate*($PVA/Zn(O_2CCH_3)_2$) submicron fibers in ambient air.

2. Results and discussion

ATR-FTIR was used for characterization of specific chemical groups in the composite material before and after plasma treatment. Reduction of all major peaks related to PVA and zinc acetate indicate decomposition of the organic part of composite fibers.

The surface of fibers observed by SEM became after plasma calcination rough due to the removal of organics. Higher porosity of fibers can be advantageous in the application requiring high specific surface. However, DCSBD plasma does not cause breaking of fibers.

EDX measurements show decrease of carbon and increase of oxygen and zinc content. After 60 minutes of plasma treatment the atomic ratio of C/Zn decreased from 32.7 to 4.3 and O/Zn decreased from 18.0 to 6.1. Decrease of C/Zn atomic ratio indicates a very strong decline already in the first minutes.

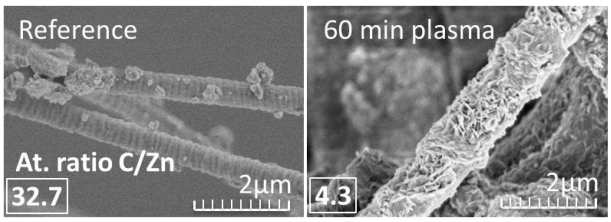

3. Conclusion

The presented results show availability of DCSBD-based atmospheric pressure plasma assisted calcination for preparation of inorganic submicron fibers. The low temperature approach and short treatment time of process are very attractive as pre-treatment method or alternative to conventional thermal calcination.

Acknowledgement: This project has received funding from the European Union's Horizon 2020 research and innovation programme under grant agreement No 692335.

4. References

[1] Z. L. Wang, J. Phys. Condens. Matter **16**, (2004), R829.

[2] J.-A. Park, J. Moon, S.-J. Lee, S.-C. Lim, and T. Zyung, Curr. Appl. Phys. **9**, (2009), S210.

[3] P. Baroch, J. Hieda, N. Saito, and O. Takai, Thin Solid Films **515**, (2007), 4905.

[4] H. Wang, H. Tang, J. He, and Q. Wang, Mater. Res. Bull. **44**, (2009), 1676.

[5] M. Černák, L. Černáková, I. Hudec, D. Kováčik, and A. Zahoranová, Eur. Phys. J. Appl. Phys. **47**, (2009).

[6] V. Medvecká, D. Kováčik, A. Zahoranová, M. Stupavská, and M. Černák, Mater. Lett. **162**, (2016), 79.

Plasma vs combustion in analytical chemistry: comparing the kinetics of DBD plasma and flame-based atomizers

A. Obrusnik[1], M. Mrkvičková[1], M. Talába[1], J. Kratzer[2], P. Dvořák[1], J. Dědina[2]

[1] *Department of Physical Electronics at Faculty of Science, Masaryk University, Brno, Czechia*
[2] *Institute of Analytical Chemistry of the CAS, v. v. i, Brno, Czechia*

In this contribution, we discuss the reaction kinetics in so-called atomizers, i.e. devices which are used in analytical chemistry to convert molecules of hydride forming elements to free atoms being subsequently detected by atomic absorption or fluorescence spectroscopy. It is known that the atomic hydrogen plays a key role during this process of volatile metal hydrides atomization, and it is produced in conventional atomizers by oxyhydrogen combustion. A logical alternative to the combustion-based atomizers is the DBD plasma, in which the energetic electrons can dissociate the hydrogen molecules directly. We compare the atomic hydrogen production and loss channels in the two respective devices with the help of validated numerical models. We also illustrate the role of advection on the chemistry and atomic hydrogen retaining.

We have previously developed a numerical model which combined a model of the background gas dynamics in full 3D coupled to a 0D kinetics model [1] and was implemented in COMSOL Multiphysics finite-element method package.

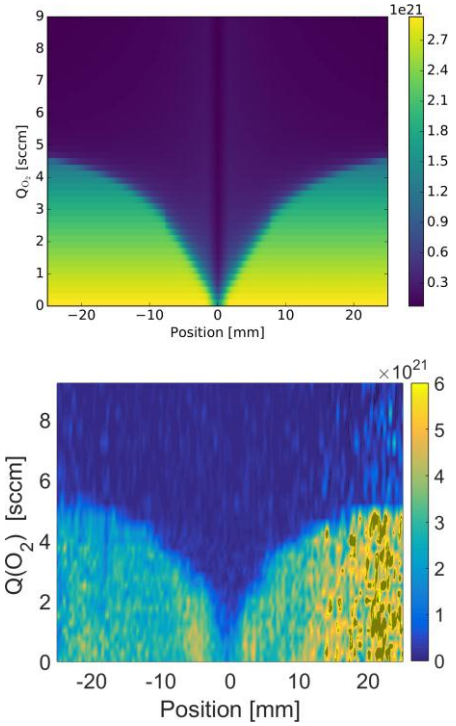

Figure 1: Benchmarking the model with TALIF measurements of atomic hydrogen density for different oxygen admixtures to the plasma.

The gas flow model solves the incompressible Navier-Stokes equation for the mixture of argon, hydrogen and oxygen, and includes diffusion of ambient air into the atomizer (which was, however, previously found to be negligible compared to the impurity of the laboratory gases). By integrating the velocity obtained from the gas dynamics model, we obtain information about spatially resolved gas residence time inside the atomizer which allows us to map the 0D kinetic model onto the 3D gas flow model, on the assumption of neglecting cross-streamline diffusion.

When the model is correlated with TALIF measurements (see figure 1), reasonable agreement is obtained, though it becomes apparent at some conditions [1], that the assumption of negligible cross-streamline diffusion is limiting and the transport of reactive species in this atmospheric-pressure plasma is both advection-driven and diffusion-driven. For this reason, we have begun developing a model which solves the gas flow and kinetics in full 3D geometry and is implemented in the OpenFOAM finite-volume method library which will also be presented and compared to the simpler model.

References

[1] P. Dvořák *et al. Concentration of atomic hydrogen in a dielectric barrier discharge measured by two-photon absorption fluorescence.* Plasma Sources Sci. Technol. **under review**

Acknowledgements

This work was supported by Czech Science Foundation (P206/17-04329S), Institute of Analytical Chemistry of the CAS, v. v. i. (project no. RVO: 68081715) and by project LO1411 (NPU I) funded by Ministry of Education, Youth and Sports of Czech Republic. AO is a Brno PhD Talent scholarship holder – funded by Brno municipality.

Effect of the magnetic field on formation of Cu nanoparticles during the magnetron sputtering in a gas aggregation source

M. Vaidulych[1], J. Hanuš[1], S. Kadlec[2], A. Marek[2], I. Khalakhan[1], O. Kylián[1], A. Choukourov[1], H. Biederman[1].

[1] *Department of Macromolecular Physics, Faculty of Mathematics and Physics, Charles University, Prague, Czech Republic*
[2] *HVM Plasma Ltd., Prague, Czech Republic*

In this study, the impact of the adjustable magnetic field on the formation of Cu nanoparticles (NPs) in the Gas Aggregation Source (GAS) of nanoparticles was investigated. It was found that the deposition rate of NPs passed through a maximum when decreasing the magnetic field from 83 mT down to 30 mT. The change in the deposition rate was furthermore accompanied by alteration of the size distribution and the shape of produced NPs. Spherical NPs with the size of 26±1 nm as well as cubic NPs with the size of up to 150 nm were successfully prepared.

1. Introduction

Over the last few decades, there was an increasing interest in efficient and wet chemical-free preparation of metal NPs by means of gas aggregation sources. Gas pressure and flow as well as magnetron current were recognized to be crucial parameters for tuning the structure, size distribution and yield of produced NPs. An impressive number of metallic nanoparticles (Ag, Cu, Ti etc.) were studied in terms of the influence of these parameters. Nevertheless, energetic conditions of the plasma can be also affected by the intensity of the magnetic field above the magnetron target, a parameter which has been given much less attention. Vernieres and co-authors studied the impact of the magnetic field (adjusted by thickness of the magnetron target) on the efficiency of the deposition of Fe NPs [1]. In their research, the intensity changed together with the shape of the magnetic field. In our work, we demonstrate an approach that conserves the shape of the magnetic field and thus allows studying the formation of Cu NPs solely by changing the field intensity.

2. Experimental

Cu NPs were deposited by means of a Haberland type GAS. The GAS was equipped with a specially constructed 81 mm planar magnetron that enabled the adjustment of the magnetic induction above the target from 30 mT to 83 mT. Variation of the field was performed manualy by changing the distance between the magnetic circuit and the target surface. A special circuit of permanent magnets was designed to provide the invariable shape of the magnetic field with different intesity.

3. Results

It was found that the deposition rate of Cu NPs, their size and shape can be indeed tailored by the intensity of the magnetic field. This is demonstrated for two selected values of magnetic field in Fig. 1, where are presented 3D maps of the deposition rate in dependence on pressure and magnetron power for a given magnetic field together with SEM images of produced NPs. As can be seen either spherical or bigger cubic NPs may be produced depending on the magnetic field.

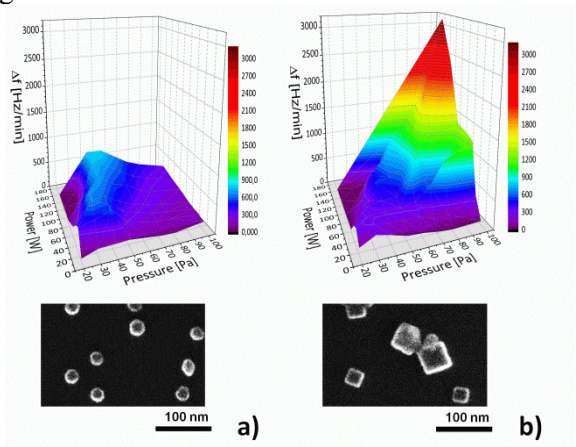

Fig. 1. Dependence of the deposition rate of Cu NPs on pressure and power with magnetic field of: a) 83 mT; b) 53 mT and examples of SEM images of produced NPs.

Acknowledgements

The work was supported by the grant SVV–2017–260444

4. References

[1] J. Vernieres, S. Steinhauer, J. Zhao and A. Chapelle et al., Adv. Funct. Mater. (2017) 1605328

Study of chemical modifications induced by an APPJ on an ultra-pure water target

C. Muja [1], L. Invernizzi[1], F. P. Sainct[1] and Ph. Guillot[1]

[1]*Laboratoire Diagnostics des Plasmas Hors Equilibre (DPHE), Université Toulouse, INU Champollion, Place de Verdun 81012 Albi, France*

Due to the increased oxidizing capacities of non-thermal plasmas, they are good candidates for wastewater chemical decontamination. The aim of this work was to assess the chemical changes produced by the exposure of a liquid to a plasma jet and to evaluate its capacity to decompose complex molecules such as pharmaceuticals. An asymmetric atmospheric pressure plasma jet was used to treat liquid samples and several colorimetric methods were used to assess the concentrations of nitrite, nitrate, ozone and hydrogen peroxide. Finally, samples containing acetaminophen (paracetamol) were exposed to the plasma jet and the concentrations following exposure were measured.

1. Introduction

In the last decades, the behaviour of pharmaceuticals in water cycle, raised concerns in both scientific and public media [1]. These molecules generally enter environment though wastewater, where can have negative effects on the ecosystem. Due to the increased oxidation capacity, non-thermal plasmas can potentially be used as oxidation agent for the treatment of polluted wastewater. The aim of this work was to characterize the chemical changes taking place inside the liquid exposed to plasma, with a special interest on reactive species generation. Finally, the capacity of the plasma jet to degrade pharmaceutical products was estimated using as model molecule the acetaminophen.

2. Material and methods

The experimental setup consists of an asymmetric plasma jet with the grounded electrode located on upper large area of the tube and the high voltage electrode on the narrow zone of the source. The discharge was initiated in a Helium-Oxygen mixture (0.2% O_2) at a flow of 2 $l.min^{-1}$. The high voltage power supply connected to the electrode provides a 6 kV voltage pulse at a frequency of 20 kHz.

The plasma jet is studied in contact with a liquid surface (Milli-Q water). Colorimetric assays were used to determine the concentrations of nitrate, nitrite, ozone and hydrogen peroxide in the liquid phase.

In order to assess the plasma jet capacity to remove complex molecules from water, several acetaminophen solutions were exposed to plasma. Following the exposure, the acetaminophen concentration was then measured using the Glynn and Kendal colorimetric method [2,3].

3. Results

Figure 1 shows the nitrite concentration as a function of the time of exposition to the plasma jet, for various pulse lengths. For treatment durations ranging from 0 to 5 minutes, the nitrite production is linear for all the pulse lengths tested. In the same time, for pulse lengths ranging from 0.5 µs to 1.5 µs the nitrite production increases with the pulse length but remains stable for 1.5 µs - 2,5 µs pulse lengths.

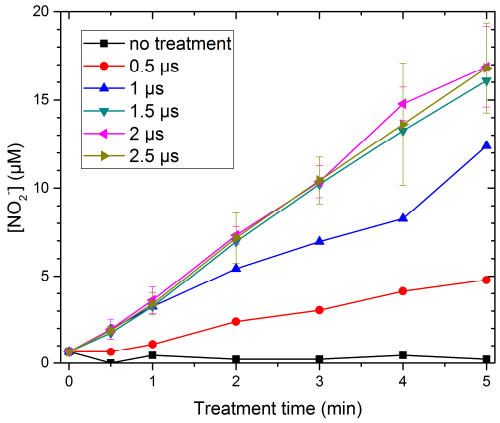

Fig. 1. Nitrite concentration in plasma treated water.

These results as well as the results concerning the other reactive species will be used to discuss the interaction of the plasma jet with the liquid, and the possible mechanisms that leads to the removal of complex molecules from water.

4. References

[1] Fent, K., *et al.* Aquatic toxicology, (2006).76(2)

[2] Glynn, J.P., Kendal, S.E. The Lancet (1975).

[3] Shihana, F., Dissanayake, D.M., Dargan, P.I., Dawson, A.H. Clin Toxicol (Phila) 2010 48(1) 42-46.

Numerical modelling of high-pressure arc discharges: computing anode heating voltage

N. A. Almeida, M. D. Cunha, and M. S. Benilov

Departamento de Física, FCEE, Universidade da Madeira, Largo do Município, 9000 Funchal, Portugal
Instituto de Plasmas e Fusão Nuclear, Instituto Superior Técnico, Universidade de Lisboa, Lisboa, Portugal

Two simple approaches to simulation of plasma-electrode interaction in high-pressure arc discharges are available in the literature: the so-called model of nonlinear surface heating, which is applicable for cathodes, and an approximate model based on the concept of electrode heating voltage, applicable for anodes. In this work, the anode heating voltage is computed for three plasma-producing gases (Ar, Xe, and Hg) in a wide range of plasma pressures, anode surface temperatures, and current densities. The results can be used for modelling the plasma-anode interaction in a wide range of conditions of high-pressure arc discharges. As an example, modelling is reported of interaction of arc plasmas with rod electrodes in both dc and ac arcs.

1. Anode heating voltage

It is known from the experiment that the power input Q from the plasma to anodes of high-pressure arc discharges is proportional to the arc current I: $Q = U_h I$, where the proportionality coefficient U_h (the anode heating voltage) may depend on the plasma-producing gas, its pressure, and the electrode material. For example, results of experiments with tungsten rod electrodes of different dimensions in an arc in argon at pressure of 2.6 bar are well described by this relation with $U_h = 6.24$ V [1].

The anode heating voltage may be theoretically evaluated by means of a suitable 1D numerical model of near-anode layers in thermal plasmas; e.g., [2, 3]. A few results have been calculated for conditions typical of UHP lamps: xenon or mercury plasmas at very high pressures (of the order of 100 bar) [2]. In this work, the anode heating voltage is calculated for a wide range of conditions: the plasma-producing gas is Ar, or Xe, or Hg; the anode material is tungsten (the work function 4.55 eV); the plasma pressure is atmospheric, $p = 1$ bar, or very high, $p = 100$ bar; the temperature of the anode T_w = 300, 1000, 3000 K for the atmospheric pressure and T_w = 1500, 2500, 3500 K for $p = 100$ bar; the current density varies in the range $j = 10^5$-10^7 A m^{-2}.

Calculations have been performed by means of the code [2] and another code, in which the original equations are solved without preliminary transformations. An example of results is shown in Fig. 1. The density q of energy flux from the plasma to the anode is governed primarily by the local current density j and varies approximately proportionally to j: $q = U_h j$. The computed anode heating voltage U_h is virtually independent of the anode temperature and close to 6 V for all the three gases for $p = 1$ bar. For $p = 100$ bar, U_h is close to 7 V for Ar, 6 V for Xe, and 9 V for Hg.

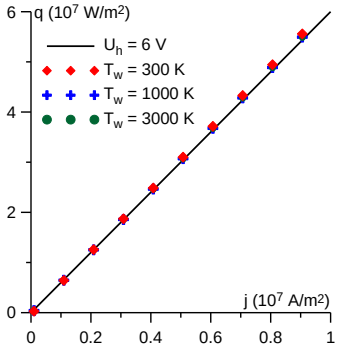

Fig. 1. Points: modelling, $p = 1$ bar, Ar. Line: $q = U_h j$ with $U_h = 6$ V.

2. Rod electrodes

As an example, computed values of the anode heating voltage are applied, jointly with the model of nonlinear surface heating for cathodes, to the modelling of interaction of arc plasmas with rod electrodes. A simple and free of empirical parameters model is developed, which is applicable to the anode and cathode dc regimes as well as ac regimes, provided no anode spots are present. The model is in good agreement in a wide range of conditions with the available experimental data.

3. Acknowledgements

The work was supported by FCT of Portugal through the project Pest-OE/UID/FIS/50010/2013.

4. References

[1] J. Mentel and J. Heberlein, J. Phys. D: Appl. Phys. 43, 023002 (2010).

[2] N. A. Almeida, M. S. Benilov, U. Hechtfischer, G. V. Naidis, J. Phys. D: Appl. Phys., vol. 42, no. 4, pp. 045210 (11pp), 2009.

[3] I. L. Semenov, I. V. Krivtsun, and U. Reisgen, J. Phys. D: Appl. Phys. 49, 105204 (2016).

Diagnostics of vicinity of thermal plasma jet by electric probes

O. Hurba[1,2], M. Hrabovský[1]

[1] *Institute of Plasma Physics AS CR, v.v.i., Prague, Czech Republic*
[2] *Charles University in Prague, Faculty of Mathematics and Physics, Prague, Czech Republic*

Electric probes and double probe have been applied to study an atmospheric pressure thermal plasma jet generated by the torch with water/argon stabilized arc. Different operation modes of the plasma torch were studied. Dependence of properties of the plasma jet on arc electric current, and argon content in the plasma was investigated. The area 9 - 33 cm from the plasma torch was investigated. Floating potential and the extent of conducting area were determined form the measurements. Plasma temperature and the plasma resistance corresponding to measured probe signals were evaluated.

Thermal plasma jets generated in dc arc torches are used in a number of plasma processing applications like plasma spraying, waste treatment and gasification of organics, reforming of hydrocarbons, and plasma cutting and melting. In all these applications the plasma flow interacts with treated material which is introduced into the jet or plasma flow impinges material surface.

The jet dimensions are determined by torch nozzle geometry and size, and by jet expansion in the space after plasma leaves the nozzle. The extent of region of plasma presence can be substantial larger than visible area of plasma jet. The presence of cold gas eddies inside the core of plasma jet, resulting from an entrainment of gas into plasma flow, has been well described [1]. However, little is known about possibility of ejection of plasma eddies from the jet into surrounding gas due to turbulences in the boundary between high velocity, low density plasma flow and steady colder gas surrounding the jet. Although the presence of plasma species around plasma jet can substantially influence interaction of treated material with plasma flow, the region surrounding plasma jet has not been sufficiently studied.

In this paper, electrical single and double probes were used for the investigation of a region surrounding thermal plasma jet generated in hybrid water/argon plasma torch [2]. Figure 1 presents boundaries of conducting region around plasma jet for several arc currents and flow rates of argon.

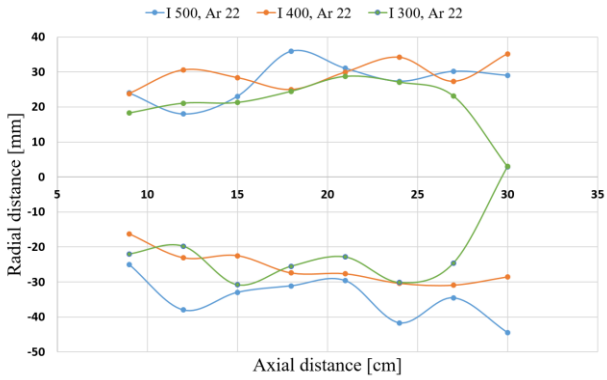

Fig. 1 - Conductive area of plasma torch in operating modes with flow rate of Ar = 22 slm

Floating potential and the plasma temperature corresponding to the probe signals have been evaluated from results of measurements.

Acknowledgement

The authors gratefully acknowledge support of the Grant Agency of CR under the project number GA15-19444S.

References

[1] E. Pfender, Thin Solid Films, 238 (1994) 228-241.

[2] M. Hrabovsky, V. Kopecky, V. Sember, T. Kavka, O. Chumak, IEEE Trans. on Plasma Science, TPS0333, 2004.

Investigation of optical emission in the plume of the Advanced Plasma Source in argon-oxygen mixtures

J. Harhausen, J. Wauer, D. Loffhagen, R. Foest

Leibniz Institute for Plasma Science and Technology (INP), Greifswald, Germany

Plasma ion assisted deposition employing the Advanced Plasma Source (APS) is an important tool for the production of high precision optical interference coatings. Present efforts focus on radiance monitoring of the plasma plume of an APS by optical emission spectroscopy (OES) to provide the basis for an advanced plasma control. In this contribution the electron density, plasma potential and electron energy distribution function in Ar/O_2 mixtures are determined using a Langmuir probe. Moreover, results of the optical emission of various argon 2p – 1s transitions and of oxygen atoms at 777 and 844 nm are presented. The measured radiance is compared to results of collisional radiative modelling.

In various optical applications like imaging, metrology or laser technology, interference coatings are required to provide specific spectral properties e.g. for lenses, mirrors or beam splitters. Plasma ion assisted deposition (PIAD) is commonly used to produce such optical coatings [1]. The knowledge of plasma properties promotes the control of the deposition process regarding accuracy and reproducibility.

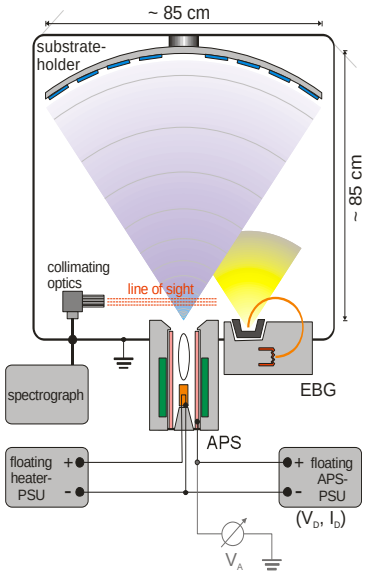

Fig. 1: Scheme of the box coater equipped with plasma source (APS) and diagnostics (OES).

An industrial PIAD box coater using an APS plasma source serves as experimental environment and is equipped with additional diagnostics (Fig. 1). OES provides data on the spectral radiance, and a movable Langmuir probe allows the determination of the plasma potential and electron energy distribution function (EEDF) at different heights above the APS [2].

Figure 2 shows typical results for an EEDF in an argon/oxygen gas mixture as a function of the total energy E_{tot} demonstrating the non-local character of the EEDF.

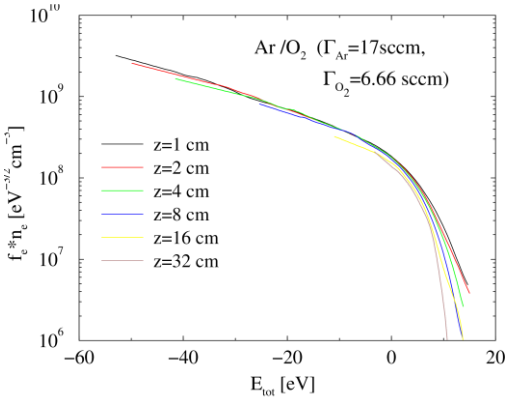

Fig 2: Measured EEDF in the plume of an argon oxygen plasma as a function of the total energy at various heights *z* above the APS.

In addition, the optical emission of various argon 2p – 1s lines and atomic oxygen lines (777 nm and 844 nm) near the plasma source was measured and the radiance was calculated. The measurements are related to results of a collisional radiative model of the plasma plume providing further possibilities to analyse the plasma properties and ultimately to control the plasma process at an elevated level.

Acknowledgment

This work was financially supported by BMBF under grant 13N13214.

References

[1] O. Stenzel et al., Appl. Opt. 56 (2017), C193.

[2] J. Harhausen et al., Plasma Sources Sci. Technol. **21** (2012) 035012.

Study on high flow rate F-radical generation by compact water-cooled surface wave plasma source for remote plasma cleaning process

W. I. Choo, H. J. You*

Plasmas Technology Research Center, National Fusion Research Institute, Gunsan, Republic of Korea

In this study, cleaning process experiments using a F-radical generated from a compact water-cooled surface wave plasma source were carried out in a process chamber. This is why it is called remote plasma source cleaning. It is essential process of improving performance. For quick cleaning, it is necessary to generate more F-radicals. The cleaning processes for the various $Si/SiO_2/Si_3N_4$, were investigated by varying the various process parameters, such as the NF_3 Gas flow rate, process temperature, microwave power. Stable plasma have been maintained in conditions of high flow rate (1 ~ 10 slm of NF_3) at low microwave power (1 ~ 3 kW). We present the result of the species emitted during cleaning was monitored by residual gas analysis (RGA), and the observed in the pressure and etch rate.

1. Introduction

A remote plasma source cleaning is used to clean residues of process steps using silicon in the semiconductor and display industry. And it is essential process of maintaining high throughput during the thin film deposition process and lowering the defect rate of refinement process and increasing productivity. Remote plasma source cleaning have been attempted and used by various methods using chemical reactions. The industry has moved from wet cleaning to *in-situ* plasma cleaning and, finally, to remote plasma cleaning. The first generation technology for remote plasma source cleaning used microwave and second generation of equipment used a toroidal RF plasma source. The third generation of equipment, also based on toroidal plasma technology, offers significant expansion in the process flow rate and pressure operating range, including the capability to operate on cleaning gases other than NF_3. Existing microwave remote plasma source cleaning to require complicated set-up where was not sufficient. Due to these shortcomings the microwave type has been low preference. But it can be operated in a wide area (10 mTorr to 760 Torr), and in this area it has a plasma density of 10^8 ~ 10^{15} ㎝$^{-3}$. Also have high electron temperature in terms of electron temperature and is efficient in dissociation and radical generation of molecular flow. In this research, it is an improved structure than existing surfa-guide type surface wave plasma discharge tube. It is improvements have been made on the cooling and microwave transmission efficiency. So overcome the problem of capacity and no loss of electromagnetic waves.

2. Experimental

The compact water-cooled surface wave plasma source is shown in Figure 1. F-radicals are generated by using the surface wave plasma source. The plasma is generated and continued by an electromagnetic wave electric filed formed into the waveguide. The apparatus of the cleaning system is shown in Figure 2. The decomposition rate of NF_3 was measured via RGA, and the pressure change before and after decomposition was investigated. Also, the observed in the etch rate of the sample. We intend to show the relationship of process temperature and substrate position to etch rate.

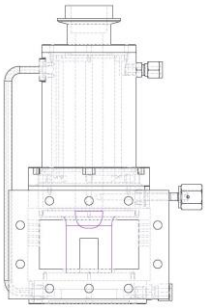

Fig 1. Structure of compact water-cooled surface wave plasma source

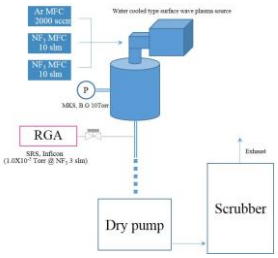

Fig 2. Schematic of compact water-cooled surface wave plasma source

Dependence of electrode materials and gaseous in serpentine plasma for nano particles preparation

S. Aoqui[1], F. Mitsugi[2], H. Kawasaki[3]

[1] *Department of Computer and Information Sciences, Sojo University*
4-22-1 Ikeda, Nishi-ku, Kumamoto, 860-0082, Japan
[2] *Graduate school of science and technology, Kumamoto University*
2-39-1 Kurokami, Chuo-Ku, Kumamoto, 860-8555, Japan
[3] *Department of Electrical & Electronics Eng., Sasebo National College of Tech., Okishin-machi 1-1, Sasebo, 857-117, Japan*

Gliding arc discharge is attractive discharge system that can control electrical consumption power under atmospheric pressure. Regarding this discharge, we named serpentine plasma. This plasma does not satisfy thermionic emission condition, but there is much characteristic. This plasma generates particles in atmospheric pressure environment. We investigated preparation of nano particle using various gas and electrode materials on atmospheric serpentine plasma system.

1. Introduction

Gliding arc discharge is attractive discharge system that can control consumption power under atmospheric pressure [1]. In our previous study, we showed that gliding arc discharge did not satisfy the requirements of normal arc discharge condition. In other words, the conditions of gliding arc discharge are not low voltage, high current. The gliding arc does not have thermionic emission condition in a fixed point on electrode. Depending on a shape of electrodes, gliding arc discharge may satisfy normal arc condition, but many cases are not so. In addition, it has been understood that the discharge strongly depended on a velocity of supplied gas. Therefore we named it 'serpentine plasma' as a name to distinguish from a normal arc discharge. Nano particles preparation using this atmospheric plasma was carried out. Also emission spectroscopy observation of plasma was carried out. We already confirmed that particles were generated in a vapour phase between the electrodes by a high-speed Infrared thermography. An image same as a visible region was got in an infrared region by the measurement of the interval that plasma maintained. Usually thermography does not enable plasma diagnoses because thermography observes the wavelength from 1μm to 1mm. Plasma does not often emit the infrared radiation of this wavelength area. This thing means that there were particles in the space between electrodes. We confirmed nano particles based on the electrode metallic element were generated in particular easily when only argon (Ar) was used for feeding gas in serpentine plasma.

2. Experiment

We used for serpentine plasma system with UV assistance and equipment for observation of electrical properties and dynamic behaviour. Two electrodes, which are made of iron, graphite or aluminium, are 100 mm height knife edge-shaped and their shortest gap was 5 mm. The electrodes were set inside an acrylic chamber that has an outlet on the top for gas exhaust. An inlet for gas supply to the chamber was placed at the bottom and at the centre between two electrodes. Ar, He, CH_4, CO_2 was used. The definition of discharge starting voltage in this work is the amplitude of applied voltage just before the start of discharge. Waveforms of applied voltage and discharge current were measured with a high-voltage probe and a current clamp, respectively. Both waveforms were captured with a digital oscilloscope. Time-resolved digital photographs for plasmas were recorded by a high-speed digital camera (Nobby Tech. Ltd., Phantom V.1210) with 10,000-100,000 fps with external trigger signal from a pulsed signal generator. Sampling of the particle to silicon substrate or stainless mesh which was installed in the gas exhaust aperture was carried out. The nano particles were analysed by Electron Beam 3D surface roughness analyzer (Elionix, ERA-8900FE).

3. Summary

Nano and micro size particles were confirmed on stainless steel mesh. However positive confirmation was not possible with silicon substrate. Flow rate of the gas was more than 10 l/min (maximum rate 50 l/min) therefore substrate heating will be necessary with a flat and smooth silicon substrate. Because gliding arc discharge system is extremely simple structure, and a power supply can apply it with a commercial power supply, low-cost nano particles preparation is enabled.

4. References

[1] J. Sperka et al. Materials Research Bulletin 54 (2014) 61–65

Fine Structure of Ionisation Patterns and Confinement of Energetic Electrons in Asymmetric Capacitive Radio Frequency Discharges

S. Wilczek[1], J. Trieschmann[1], J. Schulze[1,2], R. P. Brinkmann[1], Z. Donkó[3], T. Mussenbrock[4]

[1]*Department of Electrical Engineering and Information Science, Ruhr University Bochum, Bochum, Germany*
[2]*Department of Physics, West Virginia University, Morgantown, USA*
[3]*Institute for Solid State Physics and Optics, Wigner Research Centre for Physics, Budapest, Hungary*
[4]*Electrodynamics and Physical Electronics Group, Brandenburg University of Technology, Cottbus, Germany*

Geometrically asymmetric capacitively coupled radio frequency discharges (CCRF) are investigated by Particle-In-Cell (PIC) simulations. At low pressures, CCRF discharges promote strongly nonlinear dynamics and nonlinear electron resonance heating (NERH) is important. During sheath expansion, multiple electron beams are accelerated into the plasma bulk, which support the ionization process and frequently lead to the excitation of the plasma series resonance (PSR). At small gap sizes and low pressures, some of these beam electrons can reach the opposing sheath at different temporal phases without any collisions. Especially during sheath collapse, the confinement of these energetic electrons is inefficient, which influences the complete discharge.

Low pressure capacitively coupled radio frequency (CCRF) discharges are operated in a strongly non-local regime. In geometrically asymmetric discharges assuming cylindrical or spherical symmetry, the two opposing plasma sheaths (Fig.1: white lines) exhibit different nonlinear dynamics, e.g. in the sheath width and the sheath potential. The dynamics of such a geometrically asymmetric CCRF discharge are investigated by means of 1d3v Particle-In-Cell simulations. A spherical grid is implemented to obtain the geometrical asymmetry (including a DC self-bias). Cross-sections for electron-argon (elastic, excitation, ionization) and ion-argon (isotropic and backward elastic scattering) collisions are taken from the Phelps JILA database.

Most of the RF power is coupled into the plasma near the sheath at the driven electrode (situated at r = 20 mm). During sheath expansion (Fig.1: 10 < t < 25 ns), a bunch of energetic electrons is accelerated into the bulk region and undergo different scenarios. First, they collectively interact with bulk electrons and excite plasma oscillations (e.g. PSR). That is, cold bulk electrons are attracted back to the expanding sheath, which generates harmonics in the RF current. This process leads to the acceleration of multiple successive electron beams the number of which depends on the timescale of the local plasma frequency and the time of sheath expansion. Second, these multiple electron beams have enough energy to ionize the neutral gas, which is important to sustain the plasma. The color map plot of Figure 1 shows the spatio-temporal result of a very fine ionization pattern in an argon gas with an ionization threshold of 15.7 eV. This structure similarly represents the dynamics of all

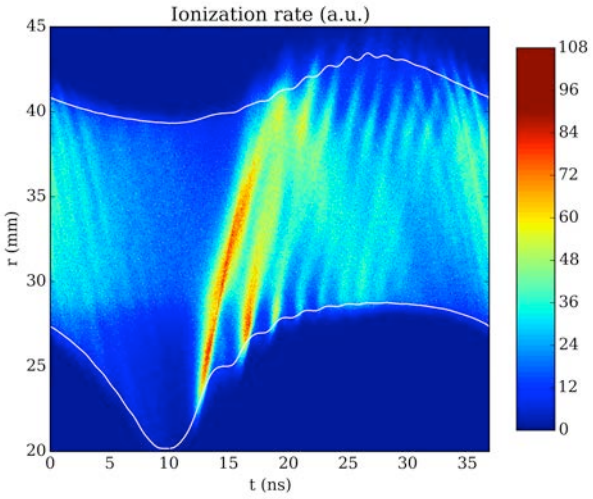

Fig.1: Ionization rate within one RF period. The white lines represent the sheath edges. The driving frequency is 27.12 MHz and the driving voltage is 700 V. The powered/grounded electrode is at r = 20/45 mm.

electron beams. Lastly, at low pressures the electron mean free path is frequently larger than the gap size. In this case, beam electrons can traverse through the discharge without hardly any collisions and interact with the opposing sheath (e.g. energetic electrons hit the sheath collapse, overcome the sheath potential and lose their energy at the wall). Especially the latter mechanism can lead to an inefficient confinement of energetic electrons, which strongly influences the discharge parameters (e.g. plasma density and ion flux). In order to obtain a better control of these mechanisms, different parameter variations (driving frequency, driving voltage, gap size, gas pressure) are studied.

Self-consistent modelling of spot patterns on anodes of DC glow discharges

M. S. Bieniek, P. G. C. Almeida, and M. S. Benilov

Departamento de Física, FCEE, Universidade da Madeira, Largo do Município, 9000 Funchal, Portugal
Instituto de Plasmas e Fusão Nuclear, Instituto Superior Técnico, Universidade de Lisboa, Portugal

Self-organized patterns of spots on a flat metallic anode in a cylindrical glow discharge tube are computed. A standard model of glow discharges is used, which comprises conservation and transport equations of ion and electron species, written with the use of the drift-diffusion and local-field approximation, and the Poisson equation. The computation domain is the near-anode region, separating the anode and the cylindrical discharge column. Multiple solutions, existing for the same value of discharge current and describing modes with different configurations of anode spots, and none at all, are computed in a wide range of currents by means of a stationary solver. At low currents the spots exhibit unusual forms with localized field and anode current density reversal.

1. Introduction

Beautiful regular patterns of bright spots on anodes of DC glow discharges have been observed for many decades; see references in [1]. Recently, such patterns were shown to be potentially useful for the treatment of cancer [2]. 2D spot patterns on glow anodes have been computed in [3], although not for a wide range of currents and apparently without a proper description of the discharge column.

Recently, self-organized spots and patterns on cathodes of arc and DC glow discharges have been described and systematically computed in terms of multiple steady-state solutions, which exist for the same values of the discharge current and describe modes associated with different spot patterns [1]. In this work, multiple solutions describing different modes have been for the first time computed for the case of an anode of a DC glow discharge.

2. Model and numerics

The reported results refer to a helium discharge under the pressure of 5 Torr, in a 1 mm-diameter cylindrical tube. The numerical model was the same as in [4]. Boundary conditions used for a metallic anode and a dielectric lateral wall were conventional ones. The height of the computation domain was 5 mm, which proved to be sufficient for an axially uniform column to be formed in a wide range of currents. The boundary conditions on the column side are zero normal derivatives of the charged particles densities and a constant value of axial electric field, related to the discharge current (a specified parameter). Axially symmetric and 3D solutions were computed by means of the Plasma module of COMSOL Multiphysics, employed in a nonstandard way permitting the use of a stationary solver.

3. Results

As an example, Figure 1 shows electron densty distribution on the anode. A regualr ring of spots is formed, similar to what was observed in the experiments (references in [1]).

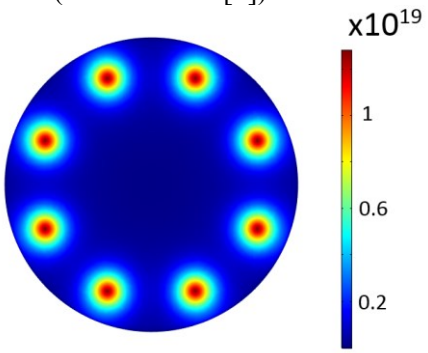

Fig. 1. Electron density on the anode. 0.01 A.

The modelling results differ from what is known from the theory and modelling of multiple modes on cathodes of arc and dc discharges: no pronounced N-shaped current voltage characteristic and no bifurcations have been observed; the spots assume a "mini-cathode" structure at low currents.

3. Acknowledgements

The work was supported by FCT of Portugal through the project Pest-OE/UID/FIS/50010/2013.

4. References

[1] M. S. Benilov, *Plasma Sources Sci. Technol.* (2014), **23** 054019.

[2] Z. Chen *et. al.*, arXiv:1701.01655, (2017).

[3] R. S. Islamov, *Phys. Rev. E* (2001) **64**, 046405.

[4] P. G. C. Almeida and M. S. Benilov, *Phys. Plasmas.* (2013), **20** 101613.

Rise time of Sabatier process using low pressure and low temperature plasma

Susumu Toko, Satoshi Tanida, Kazunori Koga, Masaharu Shiratani

Department of electronics, Kyushu University, Fukuoka, Japan

For reducing the loaded mass in rocket towards Mars, propellant production on Mars has attracted attention. Catalytic methanation of CO_2 is one way of production of the rocket propellant on Mars. Considering Mars environment of low temperature and low pressure, plasma process is superior to catalyst in the propellant production. Here, we carry out methanation of CO_2 using low pressure and low temperature plasma, and investigated dependence of rise time of CH_4 yield on H_2 flow rate. Based on the experimental results and rate equations, we discuss the methanation mechanism and deduce some key rate coefficients.

1. Introduction

Loaded propellant mass is important issue in planetary mission, because propellant mass accounts for 80% of total rocket mass. When return flights are required, loaded mass requirements are even more critical. Recently, in situ propellant production on Mars has attracted attention for returning journey from Mars to Earth. The Sabatier reaction is hydrogenation of CO_2 to CH_4.

$CO_2+4H_2 \rightarrow CH_4+2H_2O$, $\Delta H = -165.0$ kJ/mol. (1)

CO_2 is the dominant species in the atmosphere of Mars. H_2O could be electrolyzed to provide H_2 and O_2, with the O_2 acting as the oxidant for the rocket propellant and the H_2 being recycled [1].

Catalytic methanation is a major way of hydrogenation of CO_2 on Earth. However, Mars environment provides inappropriate conditions for catalytic methanation; catalytic methanation requires high temperature over 200°C and high pressure over 1.0×10^5 Pa, while the surface pressure on Mars is 750 Pa (135 times less than that on Earth) and the average temperature is very low of −63 °C [2]. Plasma process allows methanation under low pressure and low temperature conditions, employing high energy electrons in the nonequilibrium plasma ($T_e >> T_g$) to dissociate gas molecules and form reactive species [3]. Here, we carried out methanation of CO_2 using low pressure capacitive coupled plasma (CCP), and investigated dependence of rise time of CH_4 yield on H_2 flow rate FR_{H2}.

2. Experimental

Experiments were carried out using a low pressure CCP plasma reactor at ambient temperature. Plasmas were generated by applying 60 MHz RF power of 50 W. The electrode diameter was 34 mm and the distance between the electrodes was 10 mm. The pressure was 750 Pa. The CO_2 gas flow rate was 1 sccm and the H_2 gas flow rate was in the range of 6.0-21 sccm. The gas composition in the discharge plasma was measured with a quadrupole mass spectrometer (QMS, SRS QMS100).

3. Results and Discussion

Figure 1 shows time evolution of normalized CH_4 yield as a parameter of the H_2 flow rate. CH_4 yield rises more rapidly at higher H_2 flow rate. The rise time provides information of methanation mechanism. Using rate equations, we deduced the rate coefficients of decomposition reaction of CO_2 and H_2 and those of CH_4 generation reactions. I will discuss the methanation mechanism and will report some key rate coefficients.

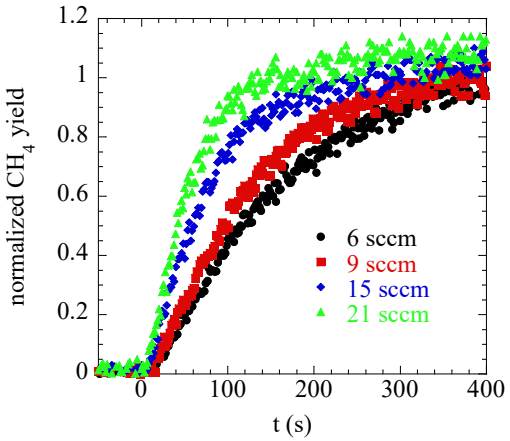

Fig. 1. Time evolution of normalized CH_4 yield as a parameter of H_2 flow rate.

This work was supported by JAXA and JSPS KAKENHI Grant Number 15J05441.

4. References

[1] K. P. Brooks, J. Hu, H. Zhu, and R.J. Kee, Chem Eng. Sci. 62 (2007) 1161.

[2] M. Kano, G. Satoh, and S. Iizuka, Plasma Chem. Plasma Process 32 (2012) 177.

[3] S. Toko, R. Katayama, K. Koga, E. Leal-Quiros, and M. Shiratani, to be published in Sci. Adv. Mater.

Suppression of Si-H_2 bond formation at P/I interface in a-Si:H solar cells deposited by multi-hollow discharge plasma CVD

Susumu Toko[1], Kazuma Tanaka[1], Kimitaka Keya[1], Takashi Kojima[1], Daisuke Yamashita[1], Hyunwoong Seo[1], Naho Itagaki[1], Kazunori Koga[1], and Masaharu Shiratani[1]

[1]*Kyushu University, Fukuoka, Nishi-ku Motooka 744, Japan*

Light induced degradation is the most important issue of hydrogenated amorphous silicon solar cells. A-Si:H films of a lower Si-H_2 bond density show less light-induced degradation. We have revealed existence of high-density Si-H_2 bonds within 60nm from P/I interface by Raman spectroscopy. These Si-H_2 bonds are originated from surface reactions of SiH_3; because the other origin, namely, cluster incorporation is considerably suppressed by a multi-hollow discharge plasma CVD (MHDPCVD) method. Substrate temperature dependence of I_{SiH2}/I_{SiH} shows the fine tuning the substrate temperature during initial stage of I-layer deposition is effective to suppress Si-H_2 bond formation at P/I interface.

1. Introduction

Light-induced degradation is the most important issue of hydrogenated amorphous silicon (a-Si:H) solar cells. By Raman spectroscopy, we have succeeded in detecting Si-H_2 bonds in cells, which are responsible for the light-induced degradation [1]. Here we have measured the hydrogen content ratio I_{SiH2}/I_{SiH} associated with Si-H_2 and Si-H bonds at P/I interface to identify high density region of Si-H_2 bonds and to suppress Si-H_2 bonds.

2. Experimental

Non-doped a-Si:H films (I-layer) were deposited on B-doped Si films (P-layer) with a MHDPCVD reactor [2, 3]. Pure SiH_4 was fed to the reactor at 84 sccm. The total pressure was 0.08 Torr. The discharge frequency and power were 110 MHz and 20 W, respectively. The substrate temperature was 170, 200, and 220 °C. The deposition rate was 0.0214 nm/s. Raman spectroscopy was carried out using HeNe laser light (λ= 632.8 nm). The penetration depth of HeNe laser light was more than 500 nm.

3. Results and discussion

Figure 1 shows dependence of I_{SiH2}/I_{SiH} on thickness of I-layer. I_{SiH2}/I_{SiH} decreases with increasing the thickness from 10 to 60 nm and it becomes constant for the thickness above 60 nm, indicating high density Si-H_2 bonds exist at P/I interface. These Si-H_2 bonds are originated from surface reactions of SiH_3; because the other origin, namely, cluster incorporation is considerably suppressed by the MHDPCVD method. To realize higher stability, suppressing Si-H_2 bond formation at P/I interface is important.

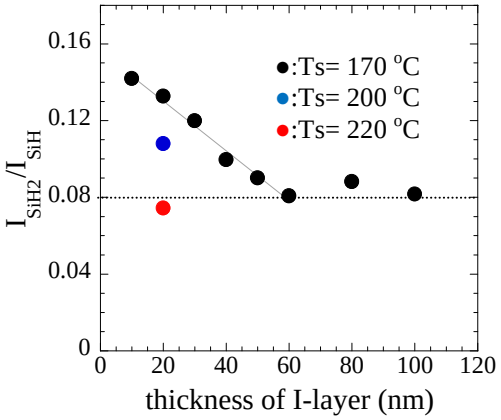

Fig. 1. Dependence of I_{SiH2}/I_{SiH} on thickness of I-layer and substrate temperature.

To realize such suppression, we have examined effects of substrate temperature on I_{SiH2}/I_{SiH}. I_{SiH2}/I_{SiH} decreases with increasing the substrate temperature from 170 °C to 220 °C. A precise turning the substrate temperature together with the deposition rate is effective to suppress Si-H_2 bond formation at P/I interface.

This work was supported by JSPS KAKENHI Grant Number 26246036 and 15J05441.

4. References

[1] T. Nishimoto, M. Takai, H. Miyahara, M. Kondo, and A. Matsuda, J. Non-Cryst. Solids **299-302**, 1116-1122 (2002).

[2] S. Toko, Y. Torigoe, W. Chen, D. Yamashita, H. Seo, N. Itagaki, K. Koga, M. Shiratani, Thin Solid Films **587**, 126 (2015).

[3] W. M. Nakamura, H. Matsuzaki, H. Sato, Y. Kawashima, K. Koga, and M. Shiratani, Surf. Coat. Technol. **205**, S241 (2010).

Segmented high voltage glow discharge for a controllable ion source

I. G. Vicente-Gabás, G. Mattausch, R. Blüthner

Fraunhofer Institute for Organic Electronics, Electron Beam and Plasma Technology FEP,
Winterbergstraße 28, 01277 Dresden, Germany
E-Mail: ignacio.vicente@fep.fraunhofer.de

A novel cylindrical ion source has been developed in order to produce an ion source, whose intensity can be easily controlled in each segment. It is possible to independently ignite each segment and, consequently, an inhomogeneous ion beam with the desired intensity can be extracted. Due to the wire anode configuration an electrostatic trap is built, within discharge electrons perform rosette orbits. This set up improves the electron lifetime and, accordingly, the ion production is enhanced which allows the discharge to be sustained down to 1 Pa. Finally, ions scape from the discharge through the extraction grid. In this contribution the latest investigations in a single plasma discharge segment will be presented.

1. Chamber geometry

The plasma chamber consists of two concentrically cylinders, the external one is a grid. Each section is defined by the volume included by two plates, which are built in perpendicular to the surface of both cylinders and in parallel to the radial axis. The plasma discharge is typically divided in five segments. The aforementioned structure is at ground potential. The anode is a tungsten wire built in parallel to cylinder´s axis of symmetry.

2. Segmented discharge

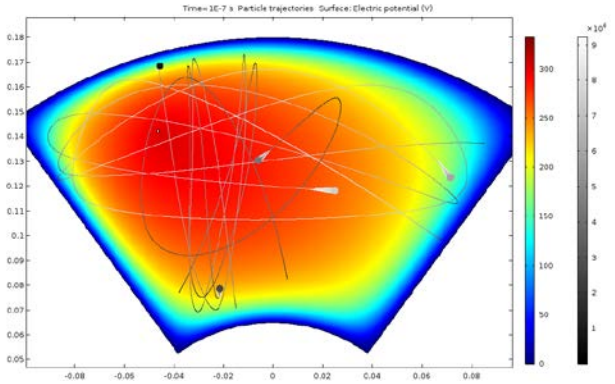

Fig 1. One segment discharge simulation. The colour scale represents the electric potential created by the discharge (max. 350 volts). The greyscale represents the discharge electron velocity (max. 9 10^6 m/s).

The segmented wire anode discharge developed by Fraunhofer FEP is based on McClure´s glow discharge [1]. The anode wire electric potential creates an electrostatic trap, which enhances the electron lifetime and, consequently, the ion production [2]. In Figure 1 discharge electrons movement inside the electric field, created by the plasma, is simulated. In Figure 2 is a picture of the experimental set up discharge. In Figure 3 ignition curves of a single segment are shown using helium and argon as working gas.

Fig 2. Picture of a single segment discharge experimental set up, with argon as working gas.

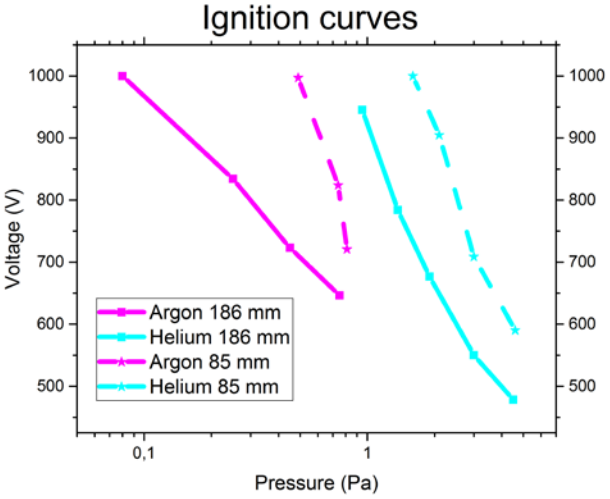

Fig. 3. Single segment ignition curves for argon and helium with two different chamber heights.

3. References

[1] G. W. McClure, "Low-pressure glow discharge" *Applied physics letters* ***2****, 12,* (1963).

[2] Makarov. "Why does a low-pressure wire-discharge exists self-sustained?" *Europhys. Lett, 74(3), 2006*

Experimental study of ns pulsed microdischarge arrays reactor in nitrogen

S. Kasri[1], G. Bauville[2], M. Fleury[2], K. Gazeli[2], J. Santos Sousa[2], S. Pasquiers[2], X. Aubert[1], G. Lombardi[1], L. William[1], C. Lazzaroni[1]

[1]*LSPM-CNRS Université Paris 13, Sorbonne Paris Cité, F-93490 Villetaneuse, France*
[2]*LPGP, CNRS, Université Paris Sud, Université Paris-Saclay, Orsay, France*

Advanced material deposition such as BN, GaN, … require the use of an efficient plasma source to produce N. To do so, we made use of a Micro Hollow Cathode Discharge (MHCD) technology [1] which generates an electron density in auto-pulsed mode up to 10^{16} cm^{-3} [2]. This value depends directly on the intensity of the current. To increase this intensity, a pulsed power supply was used. In order to deposit over a cm size substrate the source must be extended. Thus, we use an MHCD matrix. Experimental study through fast imaging and spectroscopy emission techniques of array of 7-MHCDs in nitrogen (N_2) has been realized.

1. General

The device is composed of an anode-dielectric-cathode sandwich drilled with a ps laser. An array of 7-MHCDs, with 400 µm in diameter for each MHCD is disposed at the junction between two chambers at different pressures. In chamber 1, the pressure is 50 mbar and the electrode is polarized negatively to favor the high production of nitrogen dissociation. In chamber 2, the electrode is connected to ground and the pressure is 3 mbar in order to limit the nitrogen recombination as illustrated in Fig. 1. Three windows for optical diagnostics are shown (W1, 2, 3). The ICCD is positioned perpendicularly to the MHCDs array, whereas the spectrometer is in front of the plasma jet.

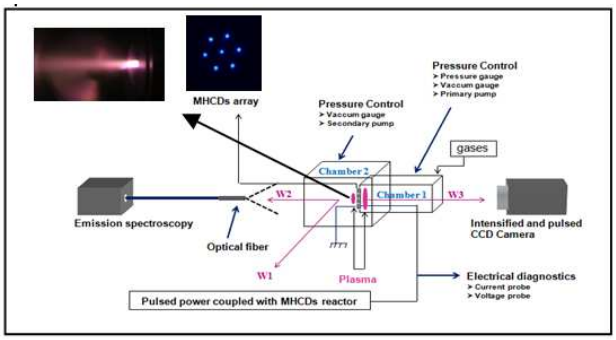

Fig.1. Experimental setup with pictures of the N_2 microplasma jet generated in the low pressure side.

2. Results

Discharge voltage, discharge current and energy per pulse and the corresponding frames of the discharge are shown in Fig. 2. Three main behaviors of N_2 microplasma are identified.

Step 1: the plasma is located on the sandwich throughout the negative pulse of current (0.5 mA) and voltage (800 V).

Step 2: at 1 µs the cathodic inversion occurs. The radiative zone moves at a speed of ~ 80 $km.s^{-1}$, which is typical of the velocity of a streamer.

Step 3: at the voltage decay, the overlapping jets are observed until disappearance, with a velocity of 100 $m.s^{-1}$, which corresponds to the gas velocity.

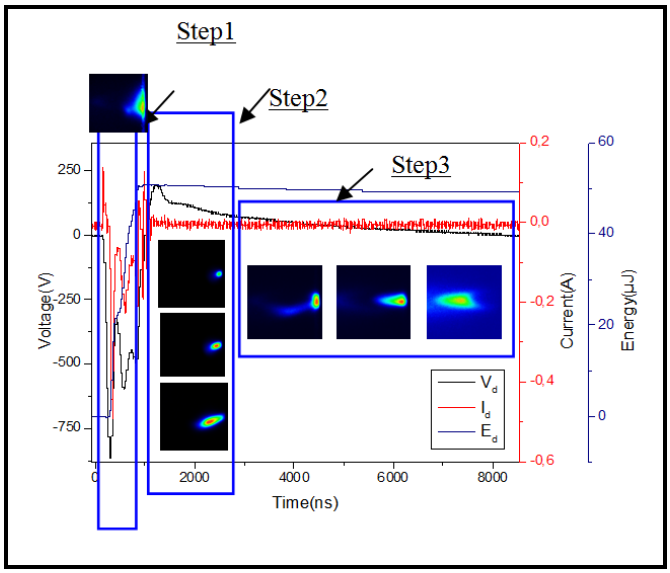

Fig.2. Main steps of the N_2 plasma propagation in the low pressure side of the reactor, including electrical signals

Using a fitting procedure of the second positive system of N_2 at 337 nm [3], we estimate the rotational temperature to be 850 ± 20 K, and the vibrational temperature equal to 3210 ± 200 K under the same conditions.

3. References

[1] K.H. Schoenbach *et al.*, Appl. Phys. Lett. (1996) **68**, 13-16

[2] C. Lazzaroni *et al.*, Eur Phys. J. D (2010) **60**, 555-563

[3] K. Gazeli *et al.*, J. Appl. Phys. (2015) **117**, 093302

Towards a fluid model for the streamer-to-leader transition in lightning channels

A. Malagón[1], A. Luque[1]

[1] *Instituto de Astrofísica de Andalucía (IAA), CSIC, Granada, Spain*

One of the still unknown phenomena involved in electric discharges is the streamer-to-leader transition. Here, as a first approach to investigate this transition, we present our recent steps modelling heating and gas expansion produced in streamer discharges, coupled to electromagnetic and air plasma chemistry. So far, we have applied this model to the mechanism of air heating and pressure perturbations present in sprite discharges, without losing sight of our final aim, i.e., to disentangle the streamer-to-leader transition in lightning channels by testing whether attachment instability leads to heating of air to a temperature high enough develop space stems.

Electric discharges are a very common phenomenon on Earth's atmosphere. However some of their features are still poorly understood. A sufficiently long electric discharge, such as a lightning channel, propagates along two phases. The first phase is known as "streamer phase" and consists in thin filaments of ionised air that advance due to a high electric field at their tip. The dominant process of ionisation is impact ionisation, involving electrons and the two major components in the air mass, which are nitrogen and oxygen. In the second phase called "leader phase", the electric current of the streamers has increased the air temperature highly enough so the thermal energy of the molecules present in the air is comparable to the ionisation potential of nitrogen and oxygen. The underlying mechanism whereby the streamer-to-leader transition occurs is not precisely known. High-speed observations show that in negative discharges, comprising 90% of cloud-to-ground lightning, this transition is not smooth but rather mediated by the formation of a "space leader", that is, an isolated hot segment within the streamer region. This space leader is connected to the main leader in a sudden jump and therefore one speaks of a "stepped leader". However, the origin of the space leader is so far unknown.

Here we present recent steps in the modelling of the streamer-to-leader transition, which requires coupling fluid mechanics, electromagnetism and air plasma chemistry. We discuss our work towards a model that solves Euler's equations (3 dimensions reduced to 2 by virtue of symmetry) coupled to electron drift using high-resolution finite volume methods for hyperbolic systems [1] implemented in the software package CLAWPACK. The drift of electrons is determined by a self-consistent electric field, which we obtain by solving Poisson's equation by means of off-the-shelf solvers. Our model also includes a selection of chemical reactions that have a relevant effect on the electron density in air, such as impact ionisation, attachment and detachment.

Besides the streamer-to-leader transition, our model can also be applied to the mechanism of air heating and pressure perturbations caused by sprite discharges in the upper atmosphere. We present here preliminary simulation results on this topic.

Our final aim is however to test the hypothesis that leader stepping results from an attachment instability that creates low-conductivity, high-field regions in a streamer corona, as recently discussed for sprites in [2]. With our detailed model for gas heating and expansion we will investigate whether the attachment instability leads to heating of air to a temperature high enough to develop space stems. A positive answer to this question would elucidate the physical mechanism of leader stepping.

[1] R.J. LeVeque. Finite Volume Methods for Hyperbolic Problems. Cambridge Texts in Applied Mathematics. Cambridge University Press, 2002.

[2] A. Luque, H. C. Stenbaek-Nielsen, M. G. McHarg, and R.K. Haaland. Srpite beads and glows arising from the attachment instability in streamer channels. J. Geophys. Res. (Space Phys), 121, 2016.

Sensitivity and uncertainty analysis of a kinetic model for CO_2 non-equilibrium plasmas

Marija Grofulović, Tiago Silva and Vasco Guerra

Instituto de Plasmas e Fusão Nuclear, Instituto Superior Técnico, Universidade de Lisboa, Portugal

This work is dedicated to the systematic investigation of the influence that uncertain rate constants have on model predictions. The kinetic scheme examined here describes CO_2 plasmas with a very complex vibrational kinetics model. Uncertainty of the rate constants models arise from the experimental errors or the approximate theories. To rank the most influential rate constants we used the Morris method, that is a One-At-a-Time design for the sensitivity analysis (SA). The output parameters that were traced are the densities of some species, *i.e.* $CO_2(001)$ and $CO_2(010)$ and the vibrational temperatures $T_{1,2}$ and T_3. The results show that the dominant e-V reactions are also the ones with larger contribution to the uncertainty of the output.

1. Introduction

Modelling low-temperature plasmas usually involves very complex chemistry models described by data that are measured or calculated with some uncertainty. In order to make the simulations of experimentally difficult or inaccessible conditions more credible, the influence of the input uncertainty on the output must be studied [1].

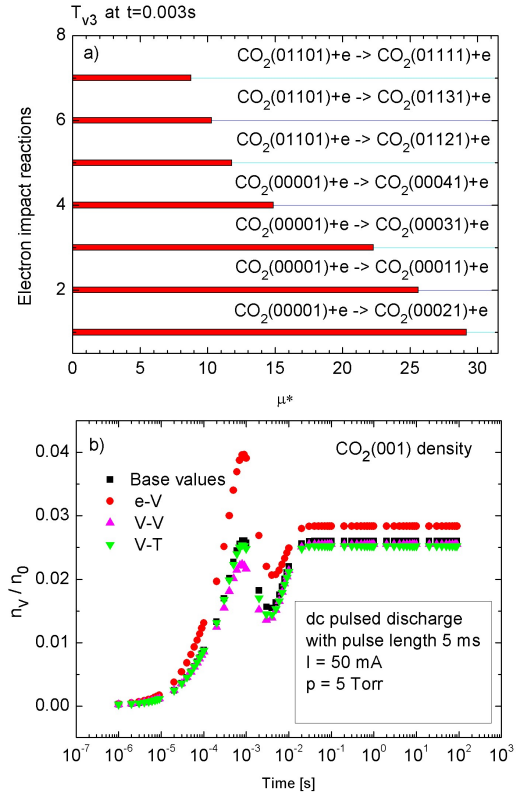

Figure 1 The result of SA, μ* [1] for the vibrational temperature T_{v3} a); and the simulation results using varied rate constants for e-V, V-V or V-T processes b).

A good example of such systems is CO_2 plasma. Recent interest in CO_2 conversion has set the goals for fundamental experimental research and plasma modelling. One particularity of these plasmas is the extended vibrational kinetics, which can comprise ~9000 vibrational levels in a full state-to-state description. In the present work, the SA was performed on a kinetic scheme describing a low excitation regime in CO_2, accounting for 72 individual vibrational levels and more than 1200 elementary processes. The operating conditions are well characterized experimentally, allowing the validation of the model presented in [2].

2. Results and discussion

The screening procedure used in this work, proposed by Morris [3], gives both the quantitative and the qualitative information on the influence of the input uncertainty. Figure 1a) shows that the e-V reactions contributing to the uncertainty of the T_{v3} are the ones populating the asymmetric levels from the ground state. Different simulation results for rate constants varied within the ascribed uncertainty are shown in figure 1b). The present analysis evaluates the level of model reliability, reveals the possible sources of model failure and therefore recommends directions for future improvement.

Acknowledgments: This work was partially supported by FCT, Projects UID/FIS/50010/ 2013, PTDC/FIS-PLA/1420/2014 (PREMiERE) and grant PD/BD/105884/2014 (PD-F APPLAuSE).

References

[1] M. M. Turner, Plasma Sources Sci. Technol. **24** (2015) 035027.

[2] T. Silva et al, contribution to ICPIG, (2017).

[3] M. Morris, Technometrics, **33** (1991) 161–74

Non-intrusive Method for Electron-Density determination in Low-pressure Microwave Plasma

A.Kais[1], J.Lo[1], L.Thérèse[1] and Ph.Guillot[1]

[1]*Laboratoire Diagnostics des Plasmas Hors Equilibre, Université de Toulouse, INU Champollion, Albi, France*

The power supplied by the plasma at the surface of a glass substrate is measured and calculated. The total contribution of the heating mechanisms is calculated according to the theories commonly used in the literature, and measured by exploiting the temperature curve variation in the heating phase (plasma on). The cooling mechanisms are leads by the conduction with the gas and the substrate holder, their contribution is measured using the temperature variation during the cooling phase (plasma off). Assuming that our plasma obeys the hypothesis of the corona balance, the Modified Boltzmann Plot (MBP) method is used to determine the electron temperature T_e. A correlation between the power deposited by the plasma and the results of the MBP is established. This correlation indicate that it is possible to estimate the electron density (n_e) without using the Langmuir probe.

1. Introduction

This work is dedicated to the determination of plasma electron-density without using the Langmuir probe (intrusive method which can be unhandy in some cases). The method developed allows to calculate the electron density by combining two non-intrusive methods: the temperature measurement [1] and the modified Boltzmann plot [2].

2. Experimental sut-up

This study was carried-out in a pure argon gas at pressure range of 10 to 30 *Pa*. Plasma is generated by a coaxial microwave plasma source (*Hi-Wave*) switched-on by a 2.45 *GHz* Solid State Generator which the power can vary from 1 to 200 *W*. The parameters of the discharge are measured by a double Langmuir probe (*Impedence Ltd*). The temperature time variations are measured by a *K-type* thermocouple. Optical Emission Spectroscopy measurements are performed by an *Avaspec 2048-2-Avantes* spectrometer with a resolution of 3 *nm*.

3. Experimental results

In this work, we will shown that P_{th}=P_m, where P_{th} is the calculated power at the surface obtained by summing the contributions of electron, ions and electron-ion recombination [3], and P_m is the total experimental power measured by exploiting the temperature curve variations. Thus, the following relation between P_m and n_e is established:

$$n_e = \frac{P_m}{A_s}\left[\sqrt{\frac{k_B T_e}{2\pi m_e}}\exp\left(\frac{e_0 V_{sh}}{k_B T_e}\right)(2k_B T_e + E_{ion}) + 0.3 k_B T_e \sqrt{\frac{k_B T_e}{M}}\frac{1}{2}k_B T_e \left|\ln\frac{2\pi m_e}{M} + 1\right|\right]^{-1} \quad (1)$$

One can see in this equation that electron density depends on one unknown parameter (T_e). The determination of T_e by the MBP method allows the calculation of the electron density. In equation 1, V_{sh} represents the sheath potential taken equal to $(k_B T_e/2e_0)(\ln(M/2\pi m_e)$, E_{ion} is the ionization energy of argon, M is the mass ion and A_s is the total substrate surface.

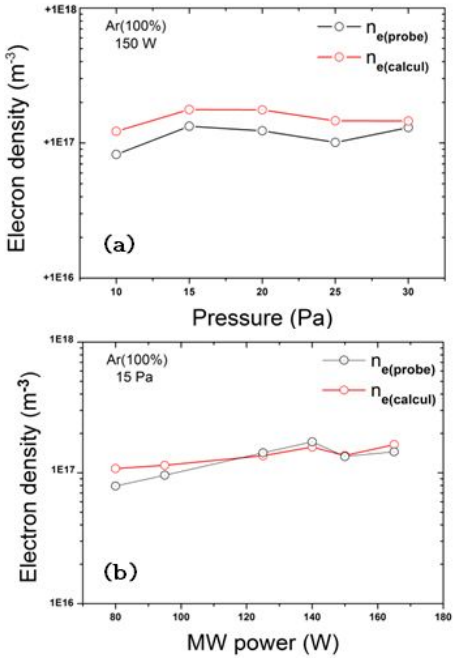

Figure 1: Electron density calculated from Eq.1 compared with Langmuir probe measurments: effect of the pressure (a) and the microwave power (b).

4. References

[1] H. Kersten *et al. Journal of Applied Physics* **87** (2000) 3637

[2] F J Gordillo-V'azquez *et al. Plasma Sources Sci. Technol.* **15** (2006) 42

[3] Daniel Lundin *et al. J. Phys. D: Appl. Phys.* **42** (2009) 7

Relaxation of electronic excitation in nitrogen discharge plasma at high specific deposited energy

N.D. Lepikhin[1], N.A. Popov[2], S.M. Starikovskaia[1]

[1]*Laboratoire de Physique de Plasmas (CNRS, Ecole Polytechnique, Sorbonne Universities, University of Pierre & Marie Curie-Paris 6, University Paris-Sud, Observatoire de Paris), France*
[2]*Skobeltsyn Institute for Nuclear Physics, Moscow State University, Moscow, Russia*

The energy relaxation from electronic degrees of freedom of molecular nitrogen excited by a capillary nanosecond discharge at high specific deposited energy and electric fields of 200-300 Td is investigated experimentally and numerically. The key role of pooling reaction between metastable $N_2(A^3\Sigma_u)$ states and quenching of $N(^2D)$ atoms by N_2 in the mechanism of fast gas heating at high specific deposited energy is demonstrated. The temperature dependence of pooling reaction rate constant was obtained based on the treatment of available experimental data.

1. Introduction

The knowledge of the channels of energy relaxation from electronically excited states is extremely important for the applications. This study is dedicated to the experimental and numerical study of the relaxation of electronic excitation and fast gas heating in pure nitrogen, excited by capillary nanosecond discharge at electric fields of E/N = 200-300 Td and specific deposited energy up to 1 eV/molecule.

2. Experiment setup

The nanosecond discharge was initiated in the capillary tube 1.5 mm of internal diameter and 70 mm in length, P = 27 mbar. High-voltage pulses of U = + 9.3 kV, 30 ns FWHM were used to initiate the discharge. For each initial pulse from the generator, typically three pulses with progressively attenuated amplitude separated by 250 ns were observed. A detailed description of the experimental setup and diagnostic techniques are presented in [1].

3. Results and discussion

The temporal evolution of gas temperature in nitrogen, excited by capillary nanosecond discharge, measured experimentally and compared with the one calculated numerically in 1-D axially symmetric model is presented in Fig. 1. The calculations were performed according to the model described in [1,2].

The observed fast increase of gas temperature in nitrogen (2200 K/μs, Fig. 1) demonstrates fast energy relaxation from electronic degrees of freedom. The pooling reaction between metastable $N_2(A^3\Sigma_u)$ states with 3.5 eV energy converted to translational energy [2] is found to be a dominate process responsible for the fast gas heating in pure nitrogen, as well as quenching of $N(^2D)$ atoms [3],

$$N(^2D) + N_2 \rightarrow N(^4S) + N_2(v), \qquad (1)$$

which becomes extremely important at high gas temperatures. The temperature dependence of pooling reaction rate constant, which used in the model, was obtained based on the treatment of the experimental data [4].

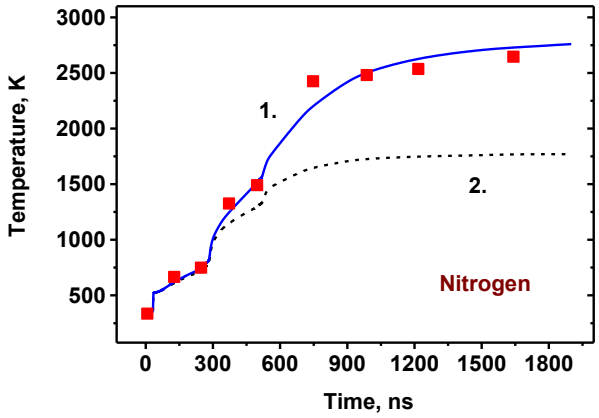

Fig. 1. Temporal evolution of gas temperature in nitrogen plasma at 27 mbar. Points – are experimental data, curves – are the results of calculations with (curve 1) and without (curve 2) the heat release in reaction (1).

Acknowledgements

The work was partially supported by French National Research Agency, ANR (ASPEN Project), LabExPlas@Par and French-Russian international laboratory LIA KaPPA and RFBR project No 17-52-16001.

4. References

[1] N. Lepikhin, A. Klochko, N. A. Popov and S. M. Starikovskaia, Plasma Sources Sci. Technol. **25** (2016) 045003.
[2] N. A. Popov, J. Phys. D: **44** (2011) 285201.
[3] B. Galvao et al. Phys. Chem. Lett. **4**, (2013) 229
[4] G. Stancu, M. Janda, F. Kaddouri, D. Lacoste, C. O. Laux, J. Phys. Chem. A **114** (2010) 201.

Control of charged species dynamics in atmospheric pressure plasmas using tailored voltage waveforms

A. R. Gibson[1, 2], L. Alelyani[1], S. Doyle[1], J. Bredin[1], J.-P Booth[2], J. P. Dedrick[1], T. Gans[1] and D. O'Connell[1]

[1] *York Plasma Institute, Department of Physics, University of York, Heslington, York, YO10 5DD, UK*
[2] *LPP, CNRS, Ecole Polytechnique, UPMC Univ. Paris 06, Univ. Paris-Sud, Observatoire de Paris, Université Paris-Saclay, Sorbonne Universités, PSL Research University, 91128 Palaiseau, France*

Precise control of the chemical kinetics in atmospheric pressure plasma sources is crucial for their full potential to be realised in a range of applications. Radio-frequency plasmas driven by multiple driving frequencies offer an attractive route to achieve such control. In this work, we demonstrate wide-ranging control of charged species dynamics in He/N_2 plasma jets at atmospheric pressure using tailored voltage waveforms. Experimentally we employ using Phase Resolved Optical Emission Spectroscopy to measure the time and space resolved electron dynamics. Further insight into plasma control is obtained through comparison with one-dimensional fluid simulations.

1. Introduction

Atmospheric pressure plasma sources have been researched extensively for a wide variety of applications ranging from biomedicine to sustainable chemical feedstock production. For any application of these plasma sources to achieve its full potential control of both charged and neutral species dynamics is of key importance. However, only limited control is possible in plasma sources operated with a single fixed frequency. In low-pressure plasma sources, enhanced control has been demonstrated by employing multiple driving frequencies. In this work, we investigate multiple frequency operation for control of radio-frequency (rf) driven atmospheric pressure plasma sources using experimental measurements and numerical simulations.

2. Experiment and simulations

The plasma source used in this study has the same critical dimensions as the "COST Reference Microplasma Jet" [1]. The source is driven by tailored voltage waveforms (TVW) consisting of a fundamental frequency of 13.56 MHz with up to five harmonics. Both "pulse-type" and "sawtooth-type" waveforms are investigated. The plasma is formed in a feed gas of He with small N_2 admixtures. In order to observe the time and space resolved electron dynamics in the plasma we apply Phase Resolved Optical Emission Spectroscopy (PROES).

The experimental measurements are complemented by 1D fluid simulations using the model discussed in detail in [2, 3].

3. Results

Experimentally, it is observed that the time and space resolved electron dynamics are strongly dependent on the number of harmonics constituting the driving voltage waveform. Significant differences are also observed in the electron dynamics in plasmas driven by "pulse-type" and "sawtooth-type" waveforms.

Simulations carried out under the same operating conditions demonstrate that this control of the time and space resolved electron dynamics results in control over the time and space averaged electron energy distribution function (EEDF). The simulations further show that this allows for control over the densities of both charged and neutral species in the plasma.

The wide range of control possible using this technique offers significant potential to tailor plasma properties in different gas mixtures for specific applications, which will be of importance for future applications of atmospheric pressure plasmas in industry and biomedicine.

Acknowledgements

This work has been done within the LABEX Plas@Par project, and received financial state aid managed by the 'Agence Nationale de la Recherche', as part of the 'Programme d'Investissements d'Avenir' under the reference ANR-11-IDEX- 0004-02. Funding through UK EPSRC (EP/ K018388/1) and the York-Paris Low Temperature Plasma Collaborative Research Centre is also acknowledged.

References

[1] J. Golda et al. J. Phys. D: Appl. Phys. **49** (2016) 084003.

[2] C. O'Neill, et al, Appl. Phys. Lett., **101** (2012) 154107

[3] J. Waskoenig, J. and T. Gans, Appl. Phys. Lett., **96** (2010) 181501

Parameters of tap water treated by cold plasma discharges over the surface and inside water

M. El Shaer, M. Mobasher, M. Habib, M. Samir

PEARLZ (Plasma & Energy Applications Research Laboratory, Zagazig), Faculty of Engineering, Zagazig University, Zagazig, Egypt

Cold plasma applications in many fields, as plasma medicine and plasma agriculture, involve discharges in air above water surface or directly inside water. We have measured parameters of tap water as pH value, ORP, conductivity and nitrate concentration for two types of discharges: pin-water surface DBD above water and pin to plate corona discharge inside water. In the first case, pH is nearly constant on the beginning of discharge time and decreases for longer time giving acidic water, while conductivity, ORP and nitrate concentration increase. For discharge inside water, pH remains constant, as well as conductivity, ORP and nitrate remains at normal level. From these results, we see that acidic medium needed for sterilization is better obtained by discharges in air outside water while for drinking water and agriculture, discharges inside water are more suitable.

1. Introduction

In plasma medicine and plasma agriculture different discharge schemes are applied outside or inside water [1]. This influences the physical and chemical properties of treated water. Two types of discharges are considered, pin-water surface dielectric barrier discharge (DBD) above water surface and pin to plate corona discharge inside water. During plasma treatment, tap water parameters as pH, ORP, conductivity and nitrate concentration are measured.

2. Experimental setup

Pin-water surface DBD occurs between a needle above water surface and a counter electrode placed outside the glass container bottom, as shown in Fig. 1-a. An AC signal of 5.7 kHz and 2 KV is used.

Needle to plate corona in water is made by discharging a single tri-plate Blumlein capacitor of 2 nF charged by DC high voltage, as shown in Fig.1-b. Water parameters as pH value and conductivity are measured using HI98129 meter, ORP by HI98120 meter and nitrate by test kit HI3874.

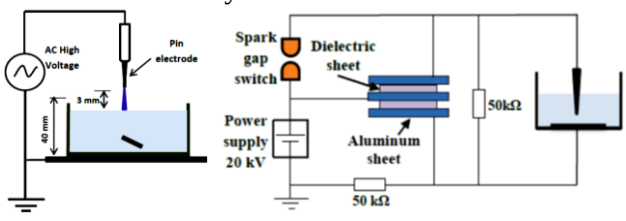

-a- -b-

Fig. 1, a- pin-water surface DBD, b- pin to plate Corona

3. Results

pH, conductivity, ORP and nitrate concentration for tap water under pin-water surface DBD outside water and pin to plate corona inside water are shown in Fig 2 -a and 2-b.

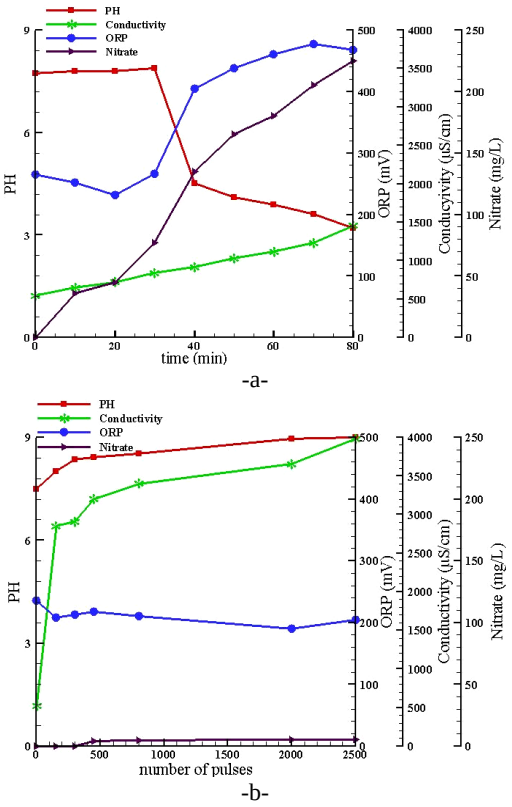

-a-

-b-

Fig. 2, water parameters for discharges outside water (a) and inside water (b)

4. Conclusion

Depending on applications requiring certain tap water parameters, we choose between discharge initiated in air outside water surface or inside water.

5. References

[1] P. Bruggeman, C. Leys, J. Phys. D: Appl. Phys. 42 (2009) 053001.

Understanding the electron and vibration kinetics in CO_2 plasmas

T. Silva[1], M. Grofulović[1], B. L. M. Klarenaar[2], O. Guaitella[3], R. Engeln[2], C. D. Pintassilgo[1,4] and V. Guerra[1]

[1]*Instituto de Plasmas e Fusão Nuclear, Instituto Superior Técnico, Universidade de Lisboa, Portugal*
[2]*Department of Applied Physics, Eindhoven University of Technology, The Netherlands*
[3]*LPP, Ecole Polytechnique, UPMC, Université Paris Sud-11, CNRS, Palaiseau, France*
[4]*Departamento de Engenharia Física, Faculdade de Engenharia, Universidade do Porto, Portugal*

This work contributes towards a detailed CO_2 kinetic scheme that describes the input and relaxation of vibrational energy in CO_2 plasmas. The vibrational energy exchanges in CO_2 discharges and post-discharges are investigated through a self-consistent model describing the time evolution of the population of individual vibrational levels of the $CO_2(X^1\Sigma^+)$ molecule. The different processes taken into account include the electron-vibration (e-V), vibration-vibration (V-V) and vibration-translation (V-T) energy exchanges. The model was validated by comparing the calculated densities of vibrationally-excited CO_2 molecules with experimental data obtained in a pulsed CO_2 glow discharge.

1. General and model description

The growing interest to plasma-based greenhouse gas decomposition requires the knowledge of the different kinetic mechanisms inherent in CO_2 discharges and post-discharges. To this purpose, we developed a kinetic scheme to describe the time-resolved densities of several CO_2 vibrational levels. More specifically, the rate balance equations for the creation and loss of the levels are investigated. The different processes taken into account include electron-vibration (e-V), vibration-vibration (V-V) and vibration-translation (V-T) energy exchanges. As a starting point, we have assumed a low excitation regime in which only a few CO_2 vibrational levels are excited, such as in pulsed discharges at low specific energy input and short pulse durations [1].

2. Results and discussion

To validate our model, the calculated concentrations of the CO_2 vibrational levels were compared with the experimental densities (obtained via time-resolved *in situ* Fourier Transform Infrared spectroscopy) in a low-pressure pulsed CO_2 DC glow discharge. The system under analysis operates with pressure p = 5 Torr, current I = 50 mA and a pulse width of 5 ms. More details about the experimental setup are given in [1]. As illustration of this analysis, Fig. 1 shows the calculated and measured results of the relative densities of the first vibrationally-excited CO_2 levels associated to the bending vibrational mode v_2 during the afterglow of the pulsed discharge. As one can see, there is a very good agreement between the calculated and experimentally determined densities, which is also extended to the population of the vibrational levels in the other modes and to the active discharge phase (not shown here).

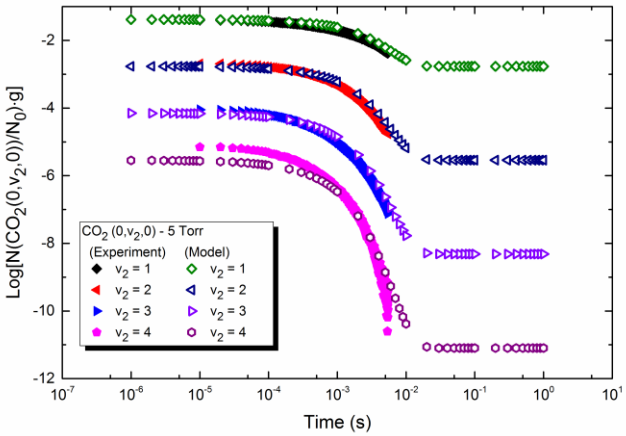

Fig. 1: Normalized density of the first CO_2 bending states during the afterglow of a pulsed DC discharge. Open symbols represent the calculations, while closed symbols the experimental data. N_0 and g represent the ground state density and statistical weight, respectively.

3. Acknowledgments

This work was partially supported by the Portuguese FCT, Projects UID/FIS/50010/2013 and PTDC/FIS-PLA/1420/2014 (PREMiERE). VG and RE have been supported by LABEX Plas@par receiving financial support managed by the Agence Nationale de la Recherche under the reference ANR-11-IDEX-0004-02.

4. References

[1] B.L.M. Klarenaar, R. Engeln, M.A. Damen, et al., contribution submitted to ICPIG, (2017).

Surface Functionalization of Fluoropolymers with Amino and Carboxyl Groups by Atmospheric Pressure Plasma Jets with Substrate Biasing

M. Nagatsu[1,2], and M. Kimpara[2]

[1] *Shizuoka University, Research Institute of Electronics, Hamamatsu 432-8561, Japan*
[2] *Shizuoka University, Graduate School of Integrated Science and Technology, Hamamatsu 432-8561, Japan*

Fluoropolymers are difficult materials to modify their surfaces because of the presence of strong C-F and C-C bonds. Surface modifications by low pressure plasma surface treatment have proven to be efficient, but it needs costly high-vacuum systems. In this study, the surface modification of fluoropolymer films with amino- and carboxyl-groups was performed by using atmospheric pressure plasma jet under negatively-biased substrate condition. Ion bombardment effect onto the polymer surface due to negative substrate bias will make dangling bonds and eventually improve the chemical modification on the surface. Functionalized surfaces were analyzed by XPS to confirm the breaking C-F bond and creating C-C or C=O bond. Fluorescence patterns where the fluorescent dyes connect specifically with the amino or carboxyl group, respectively, were clearly observed by fluorescence microscope.

1. Introduction

Fluoropolymers, such as polytetrafluoroethylene (PTFE), perfluoroalkoxy polymer (PFA), fluorinated ethylene-propylene(FEP), etc., have been widely used in various industrial fields, because of their excellent chemical, mechanical and electrical properties. In this study, amino- and carboxyl-group modification of fluoropolymer sheets was performed by using an atmospheric pressure plasma jet(APPJ) under a negatively-biased substrate condition.[1,2] With negative biasing, ion bombardment effect on the polymer surface will serve to modify the surface with functional groups more efficiently.

2. Experimental setup and results

In this experiment, PTFE films with a thickness of 50 μm or 1 mm were used. The PTFE film was fixed on the stage by a carbon tape and was masked by a Cu grid, as illustrated in Fig. 1(a). The APPJ plasma was generated by applying a high voltage of ±8 kV with a frequency of 5 kHz and duty ratio of 50% to the electrodes. Fluoropolymer films were modified by two types of functional groups by changing gas species. While He/NH_3 gas mixture was used for amino group modification, He/O_2 gas mixture was used for carboxyl group modification. Figs. 1(b) and (c) show fluorescent microscope images of PTFE surface after amino- and carboxyl-group modification, respectively. Fluorescence pattern shows clear modification in the maskless area. Figure 2 shows the XPS spectra of C 1s and N 1s of amino group modified PTFE surface. It is clearly seen that the CF_2 peak intensity dropped to generate C-C or C=O bonds after plasma treatment, and NH_2 at ~400 eV peak was appeared. The details of other experimental results will be presented at the conference.

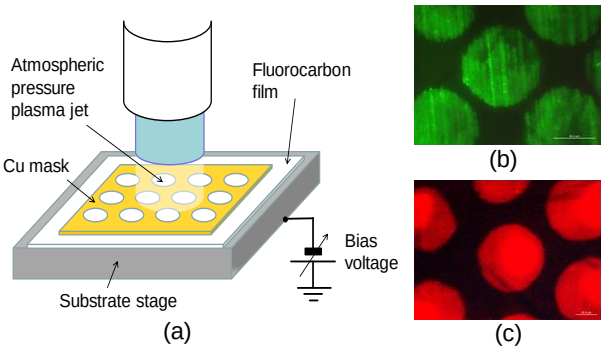

Fig. 1 (a) Experimental setup of APPJ, and fluorescence images of (b) amino group and (c) carboxyl group modification, respectively.

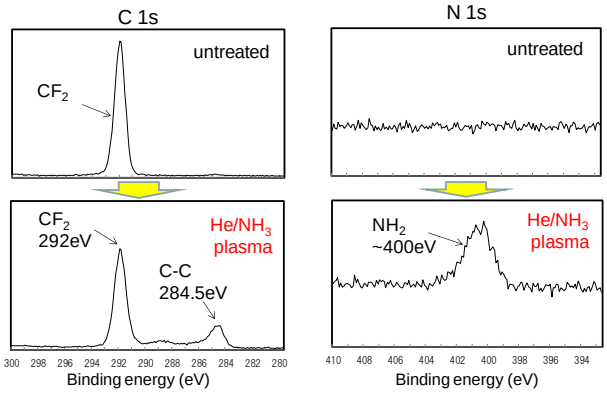

Fig. 2 XPS spectra of C 1s and N 1s for untreated and H/NH_3 plasma treated PTFE films.

References

[1] T. Abuzairi, M. Okada, Y. Mochizuki, N.R. Poespawati, R.W. Purnamaningsih, M. Nagatsu: Carbon 89 (2015) 208-216.

[2] T. Abuzairi, M. Okada, S. Bhattacharjee, M. Nagatsu, Appl. Surf. Sci. 390 (2016) 489-496.

Discharge properties in gas filled micro voids in XLPE material

S. Gortschakow, M. Bogaczyk, R. Kozakov

Leibniz institute for plasma science and technology, Greifswald, Germany

Micro voids belong to typical defects in medium voltage cross-linked polyethylene (XLPE) cables. Application of high voltage can causes micro discharges in the medium, which fills the void. Besides the liquid products, methane and ethylene are the major components in a void. Properties of the micro discharges in a dielectric encapsulated void of typical size 3-10 µm have been studied by time- and space-dependent numerical model in a wide range of pressures and applied voltages. Basic features of the model will be presented. Temporal evolutions of electrical properties, species densities are presented and discussed. Typical discharge duration of less than 1 ns has been found. The discharge development is characterized by fast propagating waves of ions and electrons, as well as pronounced deviation from quasineutrality. The role of various electron production mechanisms is discussed.

1. Introduction

Parasitic micro discharges in high voltage apparatus can lead to it destruction. Understanding of discharge phenomena is therefore of a great importance. Discharge behaviour in a micro void, typical defect of XLPE cable, is studied by a numerical model.

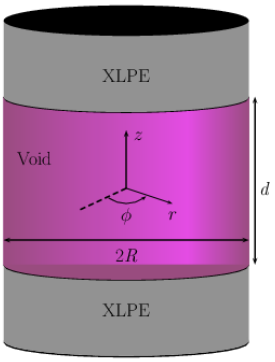

Figure 1: Schematic picture of discharge geometry.

2. Brief model description

The void is represented by cylindrical filament (Fig.1) with a length d=(3-10µm) and a radius R=d/2, encapsulated between two 1 cm thick XLPE specimens. The model [1] was adopted and extended for analysis. The plasma-chemical model of a discharge in methane or ethylene considers besides the electrons, neutral species and various positive and negative ions. Corresponding reaction rates and transport data were obtained by solution of electron Boltzmann equation. The model includes the surface emission [2] as possible electron production mechanism.

3. Example of results

Fig. 2 shows the spatio-temporal evolution of the electron density n_e and of the main ion density CH_4^+ in atmospheric pressure methane discharge. Clear differences in the species behaviour are obvious. Detailed explanation and discussion of this and other results of will be given in presentation.

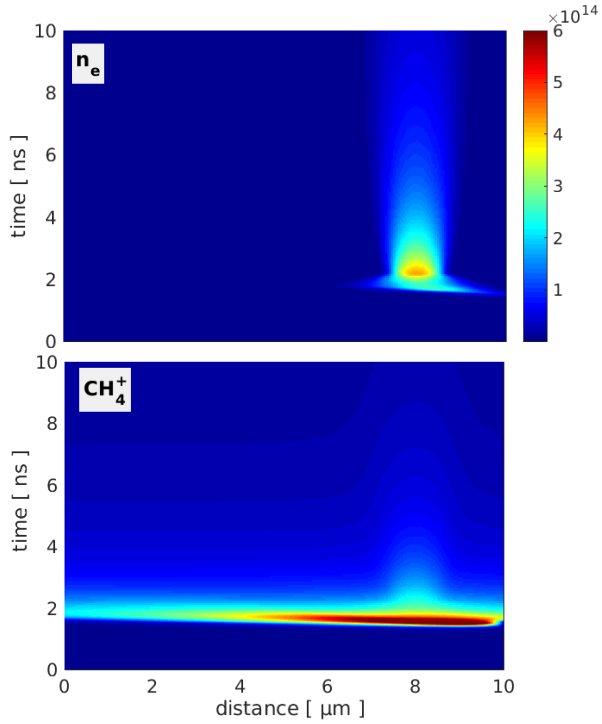

Figure 2: Spatio-temporal evolution of charged particles in methane.
P=1 bar, U_0= 20 kV. Cathode z=0, anode z=10 µm

4. Acknowledgement

The project is supported by German federal government (BMBF) by grant FKZ 03SF0476A.

5. References

[1] M. M. Becker et al., J. Phys. D: Appl. Phys. **46** (2013) 355203.

[2] L. Niemeyer, IEEE TDEI **2** (1995) 510.

Topic number

Effect of space charge on electron emission in vacuum

B. Seznec[1,2], Ph. Dessante[2], Ph. Teste[2], T. Minea[1]

[1]*LPGP, Laboratoire de Physique des Gaz et Plasmas, UMR 8578, CNRS, Univ. Paris-Sud, Université Paris-Saclay, Orsay CEDEX, 91405, France*
[2]*GeePs, Group of electrical engineering – Paris, UMR 8507, CNRS, CentraleSupelec, Univ. Paris-Sud, Sorbonne Universités, UPMC Univ Paris 06, Université Paris-Saclay, 91192 Gif sur Yvette CEDEX, France*

Vacuum electron sources exploiting field emission are generally operated in direct current (DC) mode. The development of nanosecond pulsed power supplies facilitates the emission of high density electron bunches. The breakdown levels are taken as the highest value of the voltage avoiding the thermo-emission instability. However, the space charge limits the performance of these electron sources by decreasing the electric field and consequently the thermo-field emission at the surface of the electrode. A comparative study of the space charge effect for different protrusions, operated in DC and pulsed modes for a given voltage, shows the decrease of the electron current by a factor of 2 with respect to its value in vacuum (no charge).

1. Introduction

Controlled electron emission in vacuum is very interesting for applications such as high frequency amplifiers, accelerators, etc. Most of the sources of electron emission are localized thermo-field emitters, known as micro-protrusions (MP), present on the surface of the cathode. The electric field is locally enhanced at the MP tip where initially the cold field-emission occurs. This current flowing along the MP leads to the MP heating by the Joule effect. Consequently, the temperature increases, facilitating the electron emission by the thermo-ionic effect. If the temperature of the MP tip reaches the melting temperature, the cumulative effects develop thermo-emissive instabilities and the breakdown can occur. In this work, we present the numerical analysis of the effect of the space charge on the electron emission and the breakdown voltage.

2. Numerical model

This theoretical work focuses on the description of the electron emission of a field emitter. The problem is reduced to a 2D axisymmetric time dependent model. The electron emission is given on the MP surface with the Murphy and Good approximation [1]. The MP surface temperature, the electric field and the work function (ϕ=4.3 eV for titanium (Ti)) are the inputs of the Murphy Good model. The MP temperature is governed by the Joule heating effect The Joule heating effect is induced by the current inside the MP. A complete description of this part of this model is given in [3]. The electric field is obtained as solution of Poisson equation. The electron density is determined from the mean number of emitted electrons filling each mesh during their flight.

3. First results

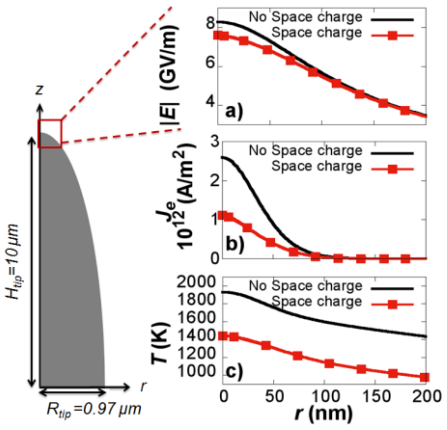

Fig.1. Electrical field (a), normal current density (b), and temperature (c) at the surface of the emission zone of a titanium elliptic MP for V_{cath} = -33.1 kV and d_{gap}= 0.2 mm with and without space charge.

For V_{cath} = -33.1 kV and d_{gap} = 0.2 mm, Figure 1.a shows a decrease (9 % at the tip) of the electric field at the MP surface when the space charge is considered. This decrease causes a reduction of the current density (2.5 times lower Fig 1.b) at the MP tip. As a consequence, the Joule effect is less important and the temperature at the surface decreases as well (Fig 1.c). Neglecting the space charge, the melting point ($T_{melting}$ = 1930 K for Ti) is reached whereas with the space charge considered, the maximum tip temperature is only 1400 K.

3. References

[1] E L Murphy *et al*. *Phys. Rev.***102** (1956) 1464
[2] W B Nottingham Phys. Rev.**59** (1941) 906
[3] B Seznec *et al*. J. Phys. D: Appl. Phys. **49** (2016) 235502

The memory effect of pulsed plasma jets in He, Ar and N_2

M. van der Schans[1], J.H. Savenije[1], L.C. van Mouche[1], M. van Ommeren[1], R.G.J. Jongen[1], W.L. IJzerman[1,2] and S. Nijdam[1]

[1] *Eindhoven University of Technology, Eindhoven, The Netherlands*
[2] *Philips Lighting, Eindhoven, The Netherlands*

When an atmospheric pressure plasma jet is excited by pulsed voltages with a kHz-range repetition frequency, plasma bullets are typically generated. One of their most notable properties is that they follow a fixed path. This behavior is generally ascribed to a memory effect, where the remnants of previous bullets provide a guiding channel for the new bullet to follow. In this work the development of the memory effect is investigated during the first several voltage pulses using a high frame-rate camera with image intensifier. Helium, argon and nitrogen are used as feed gas and flow into open air. For helium, all consecutive plasma bullets follow the same trajectory, with the exception of the very first one. In contrast, for argon and nitrogen the length of the trajectory develops during the first ~10 voltage pulses, which is shown to be closely related to transport of remnants in the gas flow.

1. Introduction

Atmospheric pressure plasma jets have received much interest in the past few decades for their numerous potential applications in materials processing and biomedicine [1]. When pulsed voltages in the kHz-range are used to to excite the jet, typically so-called 'plasma bullets' are visible in short exposure ICCD photographs. These plasma bullets are streamer-like discharges with the special property that they are very periodic and all follow the same fixed trajectory. This behavior is usually explained by a memory effect where the presence of discharge remnants from previous plasma bullets provide a guiding channel for the next bullet [1,2]. However, currently not much is known about the precise mechanisms and development of the memory effect during the first cycles of the plasma jet. In this contribution we show how the memory effect develops when helium, argon and nitrogen are used as feed gas and flow into open air. In addition, an experiment to investigate the role of charged species in the discharge remnants is discussed.

2. Development of the memory effect

To investigate the development of the memory effect, the trajectories of the discharges during the first few voltage pulses are recorded. This is done by photographing the optical emission with a high frame-rate camera with image intensifier, which makes it possible to record the trajectories of consecutive individual discharges up to several kHz repetition rates.

When using helium as feed gas, the trajectories of all plasma bullets are the same, with the exception of the very first one. The plasma bullets travel along, and are guided by, the outflowing stream of helium and the remnants of previous discharges only ensure that the jet reignites during the next voltage pulse.

In contrast, when either argon or nitrogen is used as feed gas, a development phase of about 10 cycles is observed. In these first 10 discharges the trajectory of the plasma bullet grows along the axis of the jet until it reaches its final length and becomes repeatable. By numerical simulation of the gas flow, it is found that the length of a trajectory corresponds to the distance particles have travelled in the flow starting from the first discharge. This implies that in this case the guiding mechanism is not just related to the presence of the outflowing feed gas, but rather to the presence of discharge remnants that are transported in the gas flow.

3. The role of charged species

Next we would like to know what species constitute the discharge remnants and what their role is. Previous work by Nijdam *et al* has shown the role free electrons in the guiding of positive streamers [3]. To investigate this for the pulsed plasma jet, another experiment is performed where an external electric field is applied perpendicular to the bullet's propagation direction between two discharges. The first results using nitrogen as feed gas demonstrate that the trajectories can in fact be manipulated this way and hence that charged species play an important role in the memory effect.

References

[1] X Lu, G Naidis, M Laroussi, K. Ostrikov, *Phys. Rep.* **540** (540) 123-166
[2] S Hofmann, A Sobota, P Bruggeman, *IEEE Trans. Plasma Sci.* **40** (2012) 2888-2899
[3] S Nijdam, J Teunissen, E Takahashi, U Ebert, *Plasma Sources Sci. Technol.* **25** (2016) 044001

Departure from Maxwellian electron energy distribution function in microwave argon plasmas at atmospheric pressure

A. Durocher-Jean[1] and L. Stafford[1]

[1]*Département de physique, Université de Montréal, Montréal, Québec, Canada*

Optical emission spectroscopy was used to analyse the EEDF in atmospheric-pressure argon plasmas sustained by surface wave. Using emission lines from Ar >4p levels, an excitation temperature of 0.37eV was obtained from the Boltzmann plot. On the other hand, the electron temperature determined by comparing the emission intensities from Ar 4p-to-4s transitions to those predicted by a collisional-radiative (C-R) model assuming a Maxwellian EEDF yielded 1.55eV. Departure from a Maxwellian EEDF was confirmed by allowing non-Maxwellian distributions in the C-R model and obtaining a much better experimental/theoretical agreement. Moreover, the distribution yielding the best fit was consistent with the excitation temperature at low electron energies but was characterized by a high-energy tail.

1. Introduction

Surface-wave plasmas are very attractive tools to study phenomena in ionized gases because they can be sustained over a wide range of experimental conditions. In many studies reported in literature, the electron population is described by a Maxwellian Electron Energy Distribution Function (EEDF), even under atmospheric-pressure plasma conditions. In this work, optical emission spectroscopy is used to analyse possible departure from Maxwellian EEDFs in argon plasmas produced by surface waves in the microwave regime.

2. Experimental setup and data analysis

The microwave plasma was sustained at 2.45GHz in a fused silica tube (6mm ID, 8mm OD) with a surfaguide wave launcher. All measurements were recorded with an absorbed power of 500W, at 10cm downstream from the launching gap. The Ar mass flow rate was set to 0.5slm and the tube was open to ambient air. Optical emission spectra were recorded over two wavelength ranges. The first one covered the 400-700 nm range and was used to record emission lines from Ar >4p levels. Assuming Boltzmann equilibrium for these states [1], the Ar lines were used to extract an excitation temperature (T_{exc}) from the Boltzmann plot. The second range (700-900 nm) was used to analyse Ar 4p-4s transitions. The Ar lines were then fitted with a collisional-radiative model to extract the mean electron energy $\langle E \rangle$. The electron energy probability function (EEPF) was allowed to be a generalized probability function $\exp[(E/\langle E \rangle)^n]$, where the Maxwellian EEPF corresponds to n=1 and only in such a case is $\langle E \rangle$ the electron temperature T_e.

3. Results

In this study, T_{exc} was 0.37eV whereas the value of T_e obtained assuming a Maxwellian EEPF was 1.55eV. While T_{exc} most likely describes low-energy electrons (up to ~1eV), direct and stepwise excitation reactions considered in the C-R model are sensitive to both low and high-energy electrons, hence the difference. As shown in Fig. 1, departure from a Maxwellian EEDF was confirmed by decreasing the *n* parameter in the generalized EEPF function and obtaining a lower standard deviation (better agreement) between measured and simulated emission spectra. The best fit was obtained for *n*=0.6. In such condition, the EEPF displayed in Fig. 2 presents a similar trend to T_{exc} at low electron energies. However, a high-energy tail is observed, which is consistent with the higher Te value obtained with *n*=1.

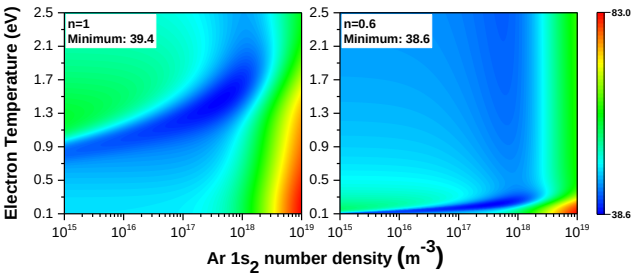

Fig. 1: Percentage standard deviation colormaps for a Maxwellian (left) and *n*=0.6 generalized (right) EEPFs

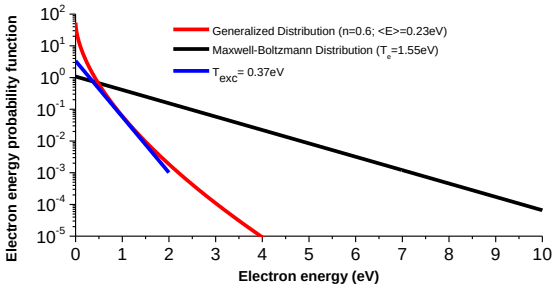

Fig. 2: EEPFs calculated from T_e, T_{exc}, $\langle E \rangle$, and n.

4. References

[1] M. D. Calzada, M. Sáez, and M. C. García, J. Appl. Phys. **88**, 34 (2000).

Topic 6

Tangential and Normal Electric Field Imaging using Mueller Ellipsometry for kHz driven Atmospheric Jet in Controlled Environment

Elmar Slikboer[1, 2], Enric Garcia-Caurel[2], Ana Sobota[3] and Olivier Guaitella[1]

[1] *LPP, CNRS, Ecole Polytechnique, UPMC, Université Paris-Saclay, 91128 Palaiseau, France*
[2] *LPICM, CNRS, Ecole Polytechnique, Université Paris-Saclay, 91128 Palaiseau, France*
[3] *Department of Applied Physics, EPG, Eindhoven University of Technology, The Netherlands*

Imaging Mueller Ellipsometry is applied for the kHz-driven atmospheric pressure plasma jet (APPJ) to measure electric fields in a controlled environment to study the effect of different gas mixtures. The method exploits the electro-optic effect of dielectric BSO and Fe:$LiNbO_3$ crystals to visualize the induced electric field. This field is present due to charges deposited on the target surface by the APPJ. This induces a local change of refractive index according to the Pockels effect. For the first time a Fe:$LiNbO_3$ crystal is examined under exposure of an APPJ, which reveals imaging about the tangential field components.

1. Introduction

The field induced on surfaces as well as the charge transferred to a target are key parameters for the control of any application of atmospheric pressure plasma jets (APPJ). These parameters are in particular strongly dependant on the composition of the surrounding atmosphere in which the APPJ is expanding.

Using the Pockels effect it is possible to measure electric fields induced in dielectric targets. This can be imaged by measuring the retardance light experiences as it travels through the crystal. Electric fields are induced by charges deposited by the APPJ, which is operated at 2 kV with a 30 kHz sine wave. Every positive half period a guided ionization wave is generated and deposits charges at the surface. These are removed with a weak back discharge when the voltage polarity changes [1].

Mueller Ellipsometry is a more general form of Ellipsometry, since it allows depolarization of the light by the sample. As such a complete measurement includes information about the optical properties of the target regarding dichroism, retardation and depolarization. This is important to correctly describe what is happening in the target when it is in contact with the guided ionization waves.

2. Imaging Mueller Ellipsometry and experimental setup

Figure 1 shows the obtained Mueller matrix of BSO after impact of the ionization wave created by the APPJ. Using the differential decomposition method the measured Mueller matrix is analysed to obtain the optical properties of the used crystals. As the light travels at normal incident through the target the induced linear retardance relates to the normal electric field component when the BSO crystal is used. It relates to the tangential component when using Fe:$LiNbO_3$. This is due to the respective crystal structure and orientation, i.e. cubic 23 symmetry for BSO and trigonal 3m for Fe:$LiNbO_3$, while both have a z-cut orientation.

The normal component of the field is strongest at the impact point where the charges are deposited. This is visible in the induced retardance, visible in the matrix elements (3, 4) and (4, 3). The tangential field would show a larger spread within the crystal (figures not included). The images are an average throughout the thickness of the crystal, which is 0.5 mm. The APPJ is targeting the crystal at 45 degrees horizontally and is positioned on the left hand side of the figures. Both the APPJ and target are within an airtight glass cell which allows for measurements in a controlled environment.

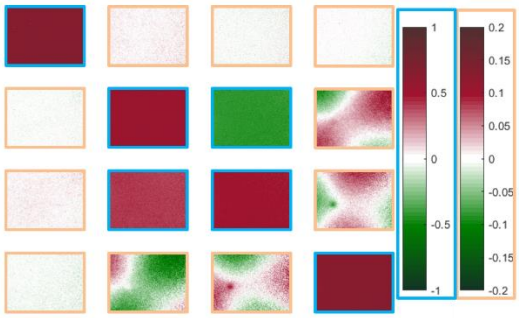

Figure 1: The measured Mueller matrix (rad) of BSO under exposure of the APPJ, after impact of the guided ionization waves. Using 1μs exposure time and 6.7 x 8.9 mm^2 image size.

We have already performed an extensive parametric study with a jet expanding in the room air [2]. This new study investigates the normal and tangential surface field with a similar APPJ in a controlled gas environment.

3. References

[1] E. Slikboer, O Guaitella, A. Sobota, Plasma Sources Sci. Technol. **25.3** (2016) 03LT04

[2] E. Slikboer, E. Garcia-Caurel, O. Guaitella, A. Sobota, Plasma Sources Sci. Technol. **26.3** (2017) 035002

Topic number

Influence of pressure on electrical discharge/arc transition.

R. Landfried, T. Leblanc, E. Odic, Ph. Teste
GeePs | Group of electrical engineering - Paris, UMR CNRS 8507,
CentraleSupélec, Univ. Paris-Sud, Université Paris-Saclay,
Sorbonne Universités, UPMC Univ Paris 06
11 rue Joliot-Curie, Plateau de Moulon 91192 Gif-sur-Yvette CEDEX, France

This paper reports on investigations of transitions between electrical discharges and electric arcs in argon atmosphere for different values of gas pressure. Results show that transitions may occur for same current intensity values whose range was found to be pressure dependent. .

1. Introduction

Electrical discharges and electric arcs have been extensively investigated. , However, few studies have investigated the transitions between discharge and arc [1-3]. In many electrical power systems, electrical discharges can occur. These electrical discharges may lead to electric arcs, resulting in failure and/or destruction of the system. The aim of this work was to study the role of pressure on transition mechanism. In this objective, a specific power supply, which allows generating both electrical discharges and electric arcs with controlled current intensity, was designed and implemented [4].

2. Influence of pressure on the transition

Cylindrical copper or tungsten electrodes were placed in a sealed chamber containing argon gas with pressure ranging from 10^3 to 10^5 Pa. . The electrode gap (denoted *d*) was in the range 3 – 50 mm. For all experiments, electric discharges were first generated by applying high voltage to the argon gas gap.

2.1. Spontaneous transitions

In figure 1 the evolution of the current intensity (in grey) and of the electrode voltage (in black) are plotted.

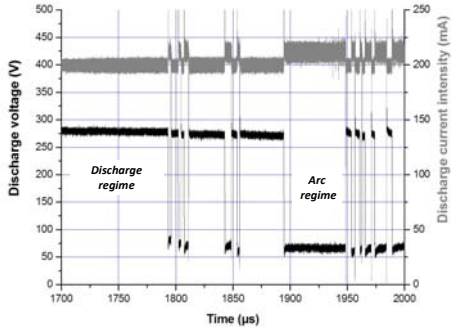

Fig. 1: U(t) and I(t) for $P = 10^4$ and $d = 25$mm.

In this example where $P = 10^4$ Pa and $d = 25$ mm, successive spontaneous discharge-to-arc and arc-to-discharge transitions were observed for approximately constant value of current intensity. These transitions occur in some 100 ns.

2.2. U(I) characteristics

In figure 2, U(I) characteristics are plotted for two different pressure values: 10^4 and 9×10^4 Pa.

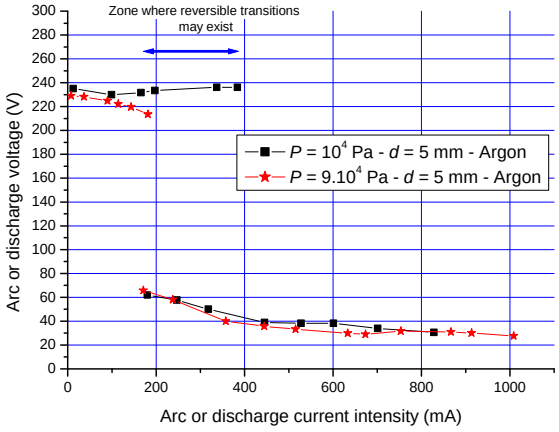

Fig. 2: U(I) characteristics for $P = 10^4$ and 9×10^4 Pa

According to the pressure value, transitions could occur for a precise value of the current intensity or for larger range of current intensity. In this range, discharge and arc may successively exist.

3. References

[1] M. Saiepour, J.E. Harry, Int. J. Electronics, 1991, vol.70, n°2, pp. 459-465.
[2] W.A. Gambling, H. Edels, British Journal of Applied Physics, vol. 5, 1954, pp. 36-39
[3] S.Watanabe, S.Saito, K.Takahashi, T.Onzawa, J. Phys. D: Appl. Phys. 36, 2003, pp. 2521–2525
[4] R. Landfried, PhD thesis, University Paris-Sud 2010

Comparison study of different simulation codes for positive streamers propagating into a region below breakdown

B. Bagheri[1], J. Teunissen[2], U. Ebert[1,3], and more participants of the study

[1]*Centrum Wiskunde & Informatica, PO Box 94079, 1090 GB Amsterdam, The Netherlands*
[2]*Centre for Mathematical Plasma-Astrophysics, KU Leuven, Celestijnenlaan 200B, 3001, Leuven, Belgium*
[3]*Department of Applied Physics, Eindhoven University of Technology, The Netherlands*

For streamer simulations a range of computational models have been developed by various groups for various purposes. These models differ in dimensionality (2D, 3D), model type (particle, fluid or hybrid approach and further differentiation), possible inclusion of electrodes or dielectrics, transport and reaction coefficients, initial conditions and numerical implementation. The aim of the present study is to benchmark the results of different computational models for axisymmetric single positive streamers in air at 1 bar and 300 K. We have invited potential participants to join on March 1, and we will present the current state of the study in July in a poster.

1. Introduction

Streamers are ionized channels with electric field enhancement at their tips that grow rapidly in different gases and liquids. Study of emergence and propagation of streamer discharges have gained a lot of interest from different research groups due to their vast industrial and medical applications. Furthermore, study of streamer discharges is essential since they are responsible for the initial stages of sparks, lightning, and they appear directly as sprite discharges.

Computational models of streamers depend on different factors and parameters, such as:

- the type of the model, e.g. fluid, particle or hybrid models, and the further approximations taken like local field approximation etc.,
- dimensionality (2D, axisymmetric or full 3D),
- mobility and reaction coefficients,
- initial conditions,
- the implementation of photo-ionization,
- electrode shapes and boundary conditions, and
- numerical resolution and accuracy.

We aim to study how simulation results depend on these choices and parameters and approximations involved, and on March 1 (2 days before the deadline of this abstract), we have invited other groups internationally to join the study, after an earlier initiative of Sergey Pancheshnyi in October 2016. We now suggest to compare results for a single axisymmetric positive streamer in air. The results of the comparison study will be presented in a poster.

2. Methodology and Results

Single positive streamer with cylindrical symmetry with size R=1.25 cm, and L=1.25 cm in air at 300K temperature and 1 bar pressure is studied. A homogenous electric field of -1.5 MV/m is imposed by applying a potential difference of 18.75 kV between the two planar electrodes. A needle electrode protruding from the planar anode is mimicked by inserting a package of positive ions on the axis at z=1 cm.

We hope that a number of groups internationally will participate. In Amsterdam, we will use afivo-streamer [1,2] based on the afivo framework [3].

We present the results of the comparison study in a poster.

3. Acknowledgment: B.B. acknowledges funding through the Dutch STW-project 15052, and J.T. through postdoctoral fellowship 12Q6117N of the Belgian-Flemish FWO.

4. References

[1] S. Nijdam, J. Teunissen, E. Takahashi, and U. Ebert, Plasma Sources Sci. Technol. **25** (2016) 044001.

[2] J. Teunissen, https://gitlab.com/MD-CWI-NL/afivo-streamer

[3] J. Teunissen, U. Ebert, *Afivo: a framework for quadtree/octree AMR with shared memory parallelization and geometric multigrid methods,* preprint arxiv.org/abs/1701.04329 submitted to Comp. Phys. Comm., https://gitlab.com/MD-CWI-NL/afivo.

Direct Synthesis of Nanodiamonds by Ar-H_2-CH_4 Microwave Discharges

A. Dias[1], E. Felizardo[1], M. V. Abrashev[2], A. Almeida[3], J. Henriques[1], E. Tatarova[1]

[1] *Instituto de Plasmas e Fusão Nuclear, Instituto Superior Técnico, Universidade de Lisboa, Lisboa, Portugal*
[2]*Faculty of Physics, University of Sofia, 1164 Sofia, Bulgaria*
[3]*Departamento de Engenharia Química, Instituto Superior Técnico, Universidade de Lisboa, Lisboa, Portugal*

A experimental study on microwave plasma based assembly of nanodiamonds at atmospheric pressure conditions is presented. The synthesis method is based on introducing a carbon containing precursor (methane), through a microwave (2.45 GHz) argon plasma environment, where decomposition of methane molecules takes place and carbon atoms and molecules are created and then converted into solid carbon nuclei in the post-discharge zone. The influence of additional hydrogen gas injected into the background gas mixture on the carbon species production and on the structural qualities of fabricated nanodiamonds has been investigated. Optical emission, Fourier transform infrared spectroscopy, Raman spectroscopy, scanning electron microscopy (SEM), and X-ray diffraction techniques (XRD) have been applied to study plasma emissions, the output gas stream composition, and the material and chemical analyses of synthesized nanostructures.

1. Introduction

Nanodiamonds have a 3D structure formed by sp^3 bounded carbon atoms arranged in a tetrahedral symmetry and their dimensions are in the range 2-5 nm. Nanodiamonds have a distinct combination of outstanding unique mechanical, chemical, biological, magneto-optical and electronic properties, which can be improved by adding functional groups. Moreover, they are nontoxic and can be used in biomedical applications, as drug carriers and delivery vehicles. Nanodiamonds are not destroyed by the human immune systems, and can be associated with a multitude of molecules and give targeted drug release. Usually extreme environment are necessary to synthesize nanodiamonds. Nanodiamonds can be found with extremely low concentrations on Earth in crude oil and in certain sediment layers, or in space, in meteorites, interstellar dust or in protoplanetary nebulae. The frequently used method is detonation of high explosive materials.

2. Experimental Setup

Nanodiamonds have been produced by a surface wave induced microwave plasma, using a waveguide surfatron-based setup. The microwave power is provided by a 2.45 GHz generator (Sairem), with maximum power of 2 kW. The generator is connected to a waveguide (WR-340) system, which includes an isolator, directional couplers, a three-stub tuner, a moveable short-circuit and a waveguide surfatron as the field applicator. The discharge ignites in a quartz tube, placed vertically and perpendicularly to the waveguide wider wall. A methane (CH_4) and hydrogen (H_2) gas mixture is introduced into the "hot" microwave argon plasma environment, where decomposition of methane molecules takes place and carbon atoms and molecules are created. Afterwards, carbon atoms and molecules are converted into solid carbon nuclei in the "colder" nucleation zones where nanometer-size particles are generated. The addition of H_2 is important since the surface of sp^3 clusters must be either stabilized through termination with functional groups or reconstructed into sp^2 carbon.

3. Results and Conclusions

XRD, Raman and SEM results showed that atomic hydrogen can kinetically etch the non-diamond sp^2-C and allow diamond-phase sp^3-C to grow. The stability of the nanodiamonds may also depend on the surface terminations, i.e. hydrogen bonds on the nanodiamonds boundaries, therefore, this method can be tuned from non-diamond to diamond phase growth, by controlling the C:H ratio in the gas mixture.

Acknowledgements

This work was funded by Portuguese FCT—Fundação para a Ciência e a Tecnologia, under Project UID/FIS/50010/2013, Project INCENTIVO/FIS/LA0010/2014, and grant SFRH/BD/52413/2013 (PD-F APPLAuSE)

The influence of air impurities on the evolution of plasma species in a capillary helium plasma jet

C. Lazarou[1], C. Anastassiou[1], F. D. Klute[2], J. Franzke[2], G. E. Georghiou[1]

[1] *FOSS Research Centre for Sustainable Energy, Department of Electrical and Computer Engineering, University of Cyprus, Nicosia, 1678, Cyprus*
[2] *ISAS—Leibniz Institut für Analytische Wissenschaften, Bunsen-Kirchhoff-Str. 11, 44139 Dortmund, Germany*

The main aim of this paper is to numerically investigate the evolution of the different species in a capillary helium plasma jet, during the plasma bullet propagation. This study is performed for a wide range of air concentrations in the helium jet core (up to 16000 ppm). The simulation results showed that the helium species are only produced and propagated in the helium jet core (along the axis of symmetry of the tube). On the other hand, the nitrogen and oxygen species (for up to 7000 ppm air in the jet core) were produced and propagated at the side of the jet core. For air concentration levels (in the jet core) higher than 7000 ppm, the production and propagation of the nitrogen and oxygen species converges towards the helium jet core. In order to interpret the results, the mean reaction pathways behind the production of each species are examined. This analysis provides useful insight into the physics behind the evolution and characteristics of the plasma jet.

In recent years, the atmospheric pressure plasma jet (APPJ) has gained much attention due to its low production costs and the wide range of applications. Although significant progress in the understanding of the basic principles of the APPJ has been made, certain areas, such as the evolution and creation of the plasma species, need further research.

With this in mind, a two dimensional axisymmetric model was developed [1], for the study of the helium plasma jet. The configuration and the operational parameters of the helium plasma jet used in the simulation model are the same as for the experimental setup [2]. In Figure 1, the spatial profile of the level of air concentration used as input in the plasma fluid model is shown.

The simulation results showed that the plasma bullet propagated along the axis of symmetry of the tube. The high energetic electrons that promote the reactions pathways for the plasma bullet propagation, has its peak on the plasma bullet head and a crescent like shape centred on the axis of symmetry of the tube. The helium species concentration peaks along the axis of symmetry where the helium ground state atoms are at their maximum.

For levels of air below 7000 ppm in the jet core (~ 0.22 cm from the tube exit) the nitrogen and oxygen ground state molecule concentrations are higher towards the edges of the helium jet whilst their species are generated towards the centre due to the higher electron energy there. As the distance from the tube exit increases, so does the air concentration in the jet core. Once it increases beyond 7000 ppm, the reaction pathways for the production of the nitrogen and oxygen species move towards the axis of symmetry. These results provide good insight into the physics behind the plasma jet evolution and the experimentally observed emitted light.

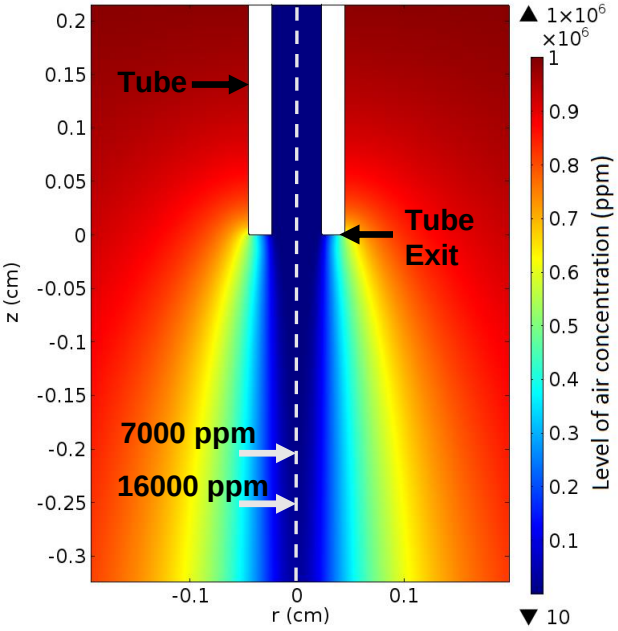

Figure 1: Plasma jet and the distribution of air concentration (ppm) in the domain.

References

[1] C. Lazarou, T. Belmonte, A. S. Chiper and G. E. Georghiou 2016 Plasma Sources Sci. Technol. 25 055023

[2] V. Horvatic, A. Michels, N. Ahlmann, G. Jestel, C. Vadla and J. Franzke 2015 Spectrochim. Acta Part B At. Spectrosc. 113 152–7

Effect of humidity on Partial Discharge Inception Voltage

L. Benmamas, R. Boukadoum, R. Landfried, T. Leblanc, E. Odic, P. Teste

GeePs | Group of electrical engineering - Paris,
UMR CNRS 8507 CentraleSupélec, Univ. Paris-Sud,
Université Paris-Saclay,
Sorbonne Universités, UPMC Univ Paris 06
3 & 11 rue Joliot-Curie, Plateau de Moulon 91192 Gif-sur-Yvette CEDEX, France

The aim of this paper was to investigate the impact of humidity on the Partial Discharge Inception Voltage (PDIV). The effect of humidity was quantified by measuring the PDIV for metallic parallel electrodes under DC voltage and atmospheric pressure. The study was made in absolute humidity in the range [2-80g/m^3], for two temperatures T=25°C and T=50°C. To control environmental conditions a climatic chamber allowing Pressure, Temperature and humidity (P, T, H) variations is used. Considering that the humidity is slightly depending on temperature, the main result of this study shows different PDIV behaviours as a function of humidity for the two considered temperatures.

1. Introduction

The work presented in here is part of a larger study concerning the analysis of breakdown voltage under aeronautical environmental conditions. Many works were interested by the influence of the humidity on PDIV values on enamelled wires [1], [2]. Here we propose to investigate the case of non-insulated electrodes.

1. Experimental set-up

Figure 1 shows the experimental set-up used to perform PDIV measurements. The studied device was two metallic spherical electrodes without any solid insulation. The environmental parameters were controlled using a climatic chamber.

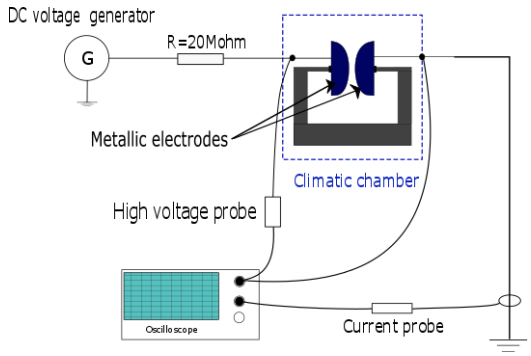

Figure 1: experimental set-up

3. Results and discussion

Figure 2 shows that at T=25°C, the PDIV decreases as the absolute humidity increase until HA=10g/m3, and slightly increases above HA=10g/m3. At higher temperature T=50°C, the behaviour is slightly different: first, PDIV increases with humidity before slightly decreasing above HA=45g/m^3.

In the interval [10g/m^3 - 45g/m^3] the PDIV increases because of water evaporation acting like an electro-negative gas, attaching the electrons responsible of discharges so increasing PDIV. Above this range, the electric field is enhanced locally around water particles created by condensation, so decreasing the PDIV. These observations are in accordance with [1], [2]. These results highlight the importance of correlation between temperature and humidity.

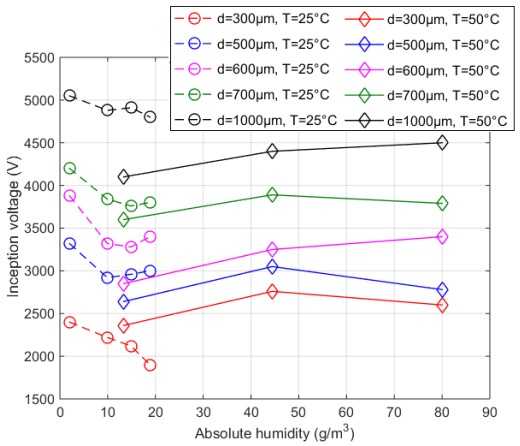

Figure 2: PDIV as a function of absolute humidity for different distances at T=25°C and T=50°C

References

[1] Y. Kikuchi, T. Murata, Y. Uozumi, N. Fukumoto, M. Nagata, Y. Wakimoto, and T. Yoshimitsu, "Effects of ambient humidity and temperature on partial discharge characteristics of conventional and nanocomposite enameled magnet wires," *IEEE Trans. Dielectr. Electr. Insul.*, vol. 15, no. 6, pp. 1617–1625, 2008.

[2] M. Fenger and +G. C. Stone, "Investigations into the Effect of Humiditv on Stator Winding Partial Discharges," vol. 12, no. April, pp. 341–346, 2005.

Nitrogen-containing plasma polymer nanoparticles produced by means of a gas aggregation cluster source

A. Shelemin, A. Choukourov, D. Nikitin, P. Pleskunov, D. Slavinska, H. Biederman

[1]*Charles University in Prague, Faculty of Mathematics and Physics, Department of Macromolecular Physics, V Holesovickach 2, 18000, Prague, Czech Republic*

Nitrogen-containing plasma polymer particles were prepared by means of a gas aggregation cluster source with special attention paid to finding the correlation between the plasma composition and the properties of the particles. It has been shown that the stability and reproducibility of the deposition rate of the particles are significantly dependent on the pressure in an aggregation chamber. On the other hand, the chemical composition of the particles, particularly the nitrogen concentration, can be tuned by the amount of N_2 in the working gas mixture.

1. Introduction

Generation of polymer particles with tuneable size distribution and chemical composition is of high scientific interest. Low-temperature plasma is known to be capable of production particles in the gas phase via plasma polymerization processes. Recent years witnessed the successful application of Gas Aggregation cluster Sources (GAS) for the production of C:H, C:H:N:O, C:F and C:H:Si:O particles. Little is known however about the processes that occur in the plasma during the particle formation. The main aim of this work was to develop a GAS that allows the in-situ diagnostics of the plasma chemistry within the aggregation zone.

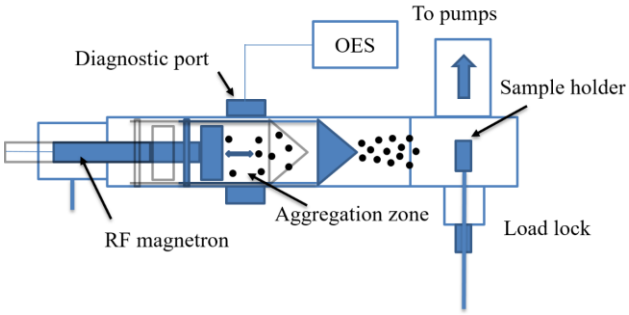

Fig. 1. Scheme of the experiment

2. Experimental

The GAS was based on a 3-inch RF magnetron with a 3-mm thick nylon 6.6 target. The aggregation zone was created by attaching a conical lid with an orifice (∅2 mm) 10 cm opposite to the magnetron. The GAS was constructed to allow moving the entire assembly of the magnetron and the orifice with respect to the static diagnostic ports while maintaining the length of the aggregation zone unchanged (Fig. 1). OES and Langmuir probes were connected to the diagnostic port to monitor the plasma parameters in dependence on the distance from the magnetron. Ar or different Ar/N_2 mixtures were used as working gases. The magnetron power was varied from 20 to 80 W.

3. Results

The deposition parameters were found to produce the particles with the size ranging from 220 nm to 300 nm. The addition of nitrogen into the GAS enhanced the emission from the nitrogen-containing species (Fig. 2) which was accompanied by an increase of the nitrogen content in resultant particles.

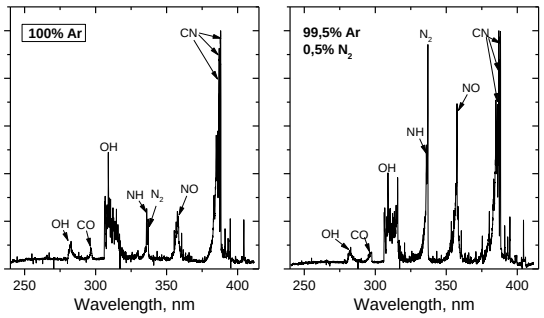

Fig. 2: Optical emission spectra obtained in Ar (left) and with the addition of 0.5 % of N_2 (right).

The ratio between the emission intensity of different species was found to be stable along the axial distance from the magnetron which may point at the longitudinal invariability of the plasma polymerization processes. Langmuir probe measurements showed a decrease of the electron concentration when particles appeared in the gas phase.

Acknowledgements

This work was supported by the grant GACR 13-09853S from the Grant Agency of the Czech Republic.

Quantification of free radicals species generates by He cold atmospheric plasma jet in different liquid media

J.Chauvin[1,2], F.Judée[1], M.Yousfi[1], P.Vicendo[2], N.Merbahi[1]

[1] *Université de Toulouse - LAPLACE, UPS, Toulouse, France*
[2] *Université de Toulouse - IMRCP, CNRS, Toulouse, France*

Short and long live Reactive Oxygen and Nitrogen Species (ROS and RNS) can be generated through the interaction of plasma with liquids. [1] In the present work, free radicals generated by Helium plasma jet in water and biological media (whit and without Fetal Calf Serum (FCS)) were quantified by electron paramagnetic resonance (EPR), fluorometric and colorimetric analysis. Results clearly show the formation of ROS such as hydroxyl radical, superoxide anion radical and singlet oxygen. The major species produced by our Helium plasma jet were identified as nitric oxide, hydrogen peroxide and nitrite-nitrate.

1. Introduction

Plasma Activated Medium (PAM) has shown interest in recent years in cancer treatment and present minimal toxicity for normal tissues [2]. Stored at the right temperature, PAM remains stable several days after their preparation [3].

The observed cytotoxicity effect of PAM is due to the presence of long lifetime ROS and RNS and oxidized biological compounds in PAM.

In the present work the identification of aqueous species formed in PAM and quantitative investigations of ROS, RNS were performed and compared in the case of Milli-Q® water and culture media without and with FCS. EPR, fluorometric and colorimetric analysis were used to identify and quantify free radicals generated by helium plasma jet.

2. Results

Using DMPO as a spin trap for hydroxyl radical, liquids were exposed to plasma for different time (Fig 1).

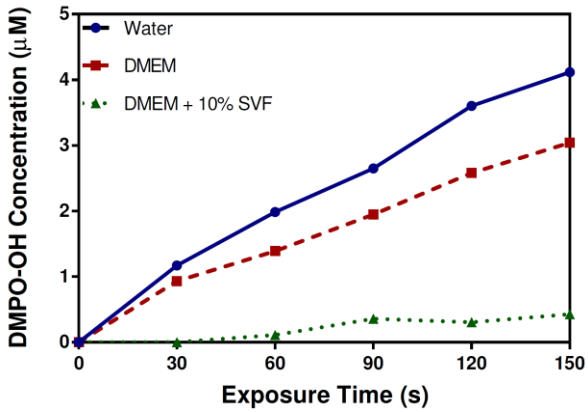

Fig 1. DMPO-OH concentration in water, DMEM+/- 10% FCS as a function of helium plasma jet exposure time.

Results showed that $OH^{\bullet}$ is produced in larger concentration in water than in biological culture media. This can be explained by the oxidizing presence of biomolecules like amino acids, vitamins and proteins.

Hydrogen peroxide (H_2O_2) concentrations in PAM were quantified using a fluorometric Hydrogen Peroxidase Assay kit (Sigma–Aldrich Co., Ltd). In contrast to OH radical H_2O_2 concentration increase linearly but does not depend on the media (Fig 2).

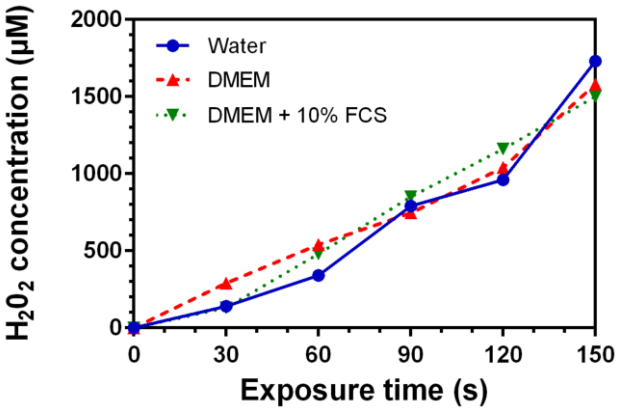

Fig 2. Variation of the concentration of hydrogen peroxide in media as a function of He plasma jet time exposition.

This result indicates that hydrogen peroxide is produced in the plasma jet and transferred in liquids.

3. References

[1] Sun P. *et al*, *Appl Phys Lett*, **98**, (2011) 021501

[2] Judée F. *et al*. *Plasma Med*. **6**, (2016) 15823

[3] Judée, F. *et al. Sci. Rep.* **6**, (2016) 21421

Electron trapping in ultra-cold plasma cloud

R. Ayllon[1], H. Tercas[1], J.T. Mendonca[1]

[1] *Instituto de Plasmas e Fusão Nuclear, Instituto Superior Técnico, Universidade de Lisboa, Lisboa, Portugal*

In the present work, we have dedicated the study of trapping electrons in a cloud of ultra-cold plasma using molecular dynamic simulation. The simple case was studied using only a Coulomb potential as source of interaction. The forces have been calculated using a hierarchical tree code that allows the increase in velocity of computation compared to conventional methods in molecular dynamics. In this case, we have performed the simulations after the ionization of the cloud of cold atoms since we are interested only to the expansion of the particles. During the expansion, we have observed the effect of trapping, and the quasi equilibrium of the particles like the Thomas-Fermi quasi-equilibrium found in the literature.

1. Introduction

Ultra-cold neutral plasmas have become an attractive topic of study in the recent years. They are produced by photo-ionizing laser-cooled cloud of atoms near the ionization threshold [1, 2]. In these systems, the temperature of the electrons can vary in the range of 1K to 1000K, while the ion temperature can be around 100μK to 1K [3].

The evolution of an ultra-cold neutral plasma can be divided into three different stages. The first stage is characterized by the equilibration of the electrons. The second stage is the equilibration of the ions. The last stage is the expansion of the plasma.

During the expansion of the plasma, free electrons scape from the cloud creating an imbalance of charge due to excess of ions that create a small electric field that trap the remaining electrons.

In the present contribution, we tried to show using molecular dynamics simulations, that the effect of electron trapping in an ultra-cold neutral plasma, lead to a model like the known Thomas-Fermi model for heavy atomic systems [4].

2. Numerical Method

In this work, we have used classical molecular dynamics to simulate the dynamics of the ultra-cold plasma after ionization. The Coulomb force in this simulation is calculated using the interaction between the particles using the hierarchical tree method. This method increases the velocity of the simulation and scales as N log(N). Allowing us to increase the number of particles compared to the classical method of pair-wise the interaction.

A reduced ion-electron mass ratio m_i/m_e =100 is applied to reduce the time cost of the simulation, and we have used 50000 electrons and 50000 ions as the number of particle to simulate. We set the initial density with a Gaussian profile, which is common found in experiments. The positions of all particles are initialized randomly. The velocities are defined randomly with Gaussian distribution, in sense the initial temperature of the electrons is $T_e(0)$ = 10K and the initial temperature of the ions is $T_i(0)$ = 0K.

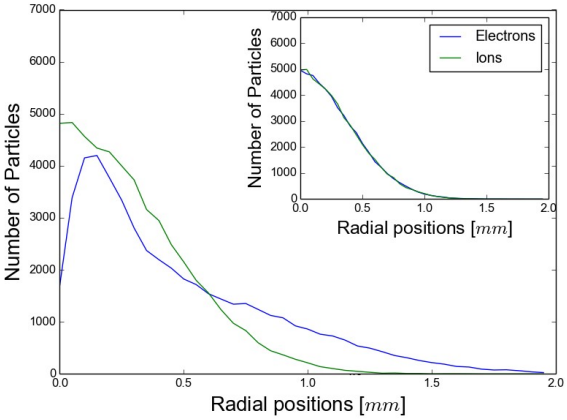

Figure 1. The results of the simulation that computes the number of particles in a radial distribution. Insight figure shows the initial distribution of the particles. The main figure, shows the evolution and the trapping of the electrons after 20 ω^{-1}_{pe}.

3. References

[1] T. C. Killian, S. Kullin, S. D. Bergson, L. A. Orozco, C. Orsel, S. L. Rolston, Phys. Rev. Lett. **83** (1999) 4776

[2] P. M. Robinson, B. L. Tolra, M. W. Noel, T. F. Gallagher, P. Pillet, Phys. Rev. Lett. **85** (2000) 4466

[3] T. C. Killian, T. Pattard, T. Pohl, J. M. Rost, Phys. Rep. **449** (2007) 77

[4] J.T Mendonça, H. Terças, Physics of Ultra-Cold Matter, Springer (2013)

Rotational, vibrational and electronic temperatures of pulsed corona discharge at atmospheric pressure in humid air

H. Guedah[1], A. Abahazem[1], N. Merbahi[2] and M. Yousfi[2]

[1] *Laboratory Materials and Renewable Energies, Physics Department, Cité Dakhla BP 8106, Ibn Zohr University, Agadir, Morocco*
[2] *LAPLACE UMR 5213-CNRS, 118 Route de Narbonne, Bât. 3R2, 31062 Toulouse Cedex 9, Paul Sabatier University, France*

This work is devoted to the studies of pulsed corona discharge in point-to-plane geometry in air humid at atmospheric pressure by optical emission spectroscopy (OES). In the first time the rotational, vibrational and electronic temperatures are studies as a function of several parameters (applied voltage, frequency and rate hygrometry) near the anodic tip. In the second time we fixed applied voltage at 6.4Kv, frequency at 10kHz and rate hygrometry at 100%, then studies the spatial variation along the z axis (from the tip to the cathode plate) of electronic temperature (with a step of 2 mm for point to plane), the objective is to determine the variation of the electronic temperature in the interelectrode space along the discharge. The electronic temperature decrease versus the inter-electrode distance from the tip to the cathode plate. This result is coherent with electron energy in the case of streamer corona discharges in the region close the high voltage tip.

1. Determination of rotational and vibrational temperatures

A free code of LIFbase was used to generate the synthetic spectrum of first negative system N^+_2 and OH [1], which are respectively shows in Figure 1 and Figure 2. The simulated spectra were calculated to minimize the sum of square error between the measured and the calculated spectra by choosing the best fit for the vibrational and rotational temperatures [2]. The vibrational temperature has been determined from N^+_2 (FNS) for (0, 0) and (1, 1) head bands spectra at 391.4 nm and 388.4 nm respectively [3,4]. The rotational temperature has been determined from OH (0, 0) head bands spectra at 309 nm [5].

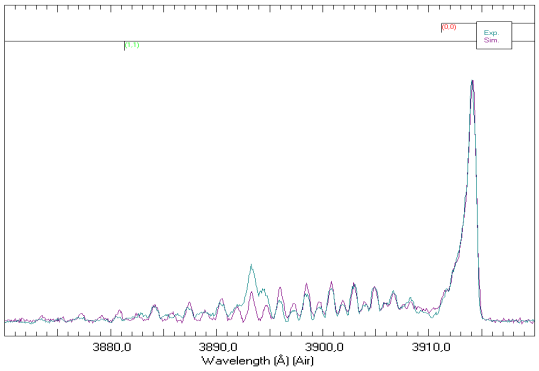

Figure 1. Measured and synthetic spectrum of N^+_2(B-X), vibrational temperature T_{vib}=860K, Va = 6.4kV, f = 10kHz and rate hygrometry of 100%.

2. Effect of operating parameters on the rotational and vibrational temperatures

Based on the above method, the effect of applied voltage, frequency and rate hygrometry on the rotational and vibrational temperatures is studied in this work. As results, the rotational and vibrational temperatures increase versus the applied voltage and rate hygrometry, but the influence of frequency is negligible.

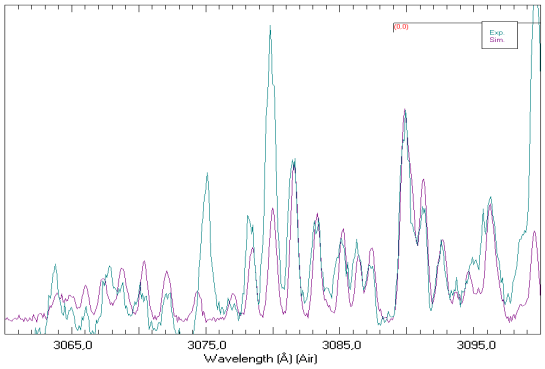

Figure 2. Measured and synthetic spectrum of OH (A-X), rotational temperature T_{rot} = 820K with Va = 6.4kV, f = 10kHz and rate hygrometry of 100%.

3. References

[1] J. Luque and D. R. Crosley, SRI International Report MP, (1999) 99-009.
[2] A. Zerrouki, H. Motomura, Y. Ikeda, M. Jinno and M. Yousfi, Plasma Phys. Control. Fusion 58 (2016) 075006
[3] A. Ricard Reactive Plasmas, (1996) 97–102
[4] N. Britun, M. Gaillard, A. Ricard, Y. M. Kim, K. S. Kim,and J. G. Han, J. Phys. D: Appl. Phys. 40 (2007) 1022–1029.
[5] Y. Nakagawa, R. Ono and T. Oda, J. Appl. Phys. 110 (2011) 073304.

Distributed microwave plasma sources: coupling modes and operation at high pressure for large area deposition

A. Martín Ortega, A. Bès, S. Béchu, A. Lacoste

LPSC, Université Grenoble Alpes, CNRS/IN2P3, 53 rue des Martyrs, 38026 Grenoble Cedex, France

The 2D and 3D distribution of a set of elementary plasma sources enables its use in large area deposition and etching processes. Existing sources, working at 2.45 GHz, provide uniform plasma conditions at low and very low pressures (up to a few Torr). A new challenge is to extend the uniformity of the plasma at higher pressures, where the diffusion is limited by the scaling laws. We will describe the transition between inductive and capacitive coupling modes as a function of frequency (2.45 GHz, 915 MHZ and 352 MHz), gas pressure, source geometry and input power. The understanding of the transition should allow the efficient design of new sources operating at high gas pressure. Interest in this technology will be pointed out through some examples of applications.

1. Introduction

The distribution of individual microwave (MW) plasma sources on a 2D or 3D network allows for the scaling-up of high density plasma processes in the low and very low (few Torr down to mTorr) pressure range [1]. The typical configuration consists on a coaxial applicator which also provides the impedance coupling, ended in a permanent magnet which facilitates the sustainability of the discharge [2]. While this technology has been long studied for low pressures, where fairly uniform and extended plasma can be obtained, its use at higher pressure remains a challenge. Indeed, an increase in pressure will not only reduce the plasma extension according to the scaling laws, but will also change the absorption mode of the electromagnetic wave by the plasma.

Most of the existing MW plasma sources operate with generators of 2.45 GHz of frequency. The use of new sources operating at lower frequencies, such as 915 MHz and 352 MHz, might enable the use of the distributed plasma sources at higher ranges of pressure.

2. Coupling modes

A transition between capacitive and inductive coupling modes can be found when operating the plasma sources at 2.45 GHz as a function of the pressure and absorbed power [2]. This transition occurs at high input power when operating at low (mTorr) gas pressure, with the transition power threshold being greatly reduced at higher pressures. The transition was also found when operating the source at 915 MHz but not at 352 MHz. At lower pressures (mTorr), the transition usually appears together with a change in the spatial distribution of the plasma. At higher pressures (Torr) no sudden change in the spatial distribution for the two different coupling modes is observed.

A possible explanation of the transition based on the comparison between the skin depth and the dimensions of the plasma will be investigated. The larger skin depth of MW at 352 MHz would explain the absence of the inductive coupling mode found at 2.45 GHz. The transition will also be explored at 915 MHz.

3. Plasma extension at high pressure

The extension of the plasma depends on two factors: the plasma diffusion and the power absorption region. While at lower pressures the diffusion is large enough to ensure an extended plasma, at higher pressures the power absorption is localized close to the microwave injection plane, where the critical density is reached.

The decrease of the MW frequency from 2.45 GHz to 915 MHz increases the size of the absorption region by increasing the skin depth. The plasma extension could be further increased by using MW at 352 MHz, but the use of this frequency might be prevented by the absence of the more efficient inductive mode. In addition, the microwaves may propagate along the surface of the applicator and chamber walls, increasing the lateral extension of the plasma.

3. References

[1] A. Lacoste, T. Lagarde, S. Bechu, Y.Arnal and J. Pelletier, P. Sources Sci. and Tech. 11 (2002) 407.

[2] Baele, S. Bechu, A. Bes, J. Pelletier and A. Lacoste: P. Sources Sci. and Tech. 23 (2014) 064006.

Instantaneous charge state of Uranium projectiles in fully ionized plasmas from energy loss experiments

R. Morales, M.D. Barriga-Carrasco, Ignacio Moreno

E.T.S.I. Industriales, Universidad de Castilla-La Mancha, E-13071 Ciudad Real, Spain

The instantaneous charge state of uranium ions traveling through a fully ionized hydrogen plasma has been theoretically studied and compared with an energy loss experiment. For this purpose, two different methods to estimate the instantaneous charge state of the projectile have been employed: (1) rate equations using ionization and recombination cross sections, and (2) equilibrium charge state formulas for plasmas. The equilibrium charge state of projectiles in plasmas is not always reached, and therefore, a non-equilibrium or an instantaneous description of the projectile charge is necessary. The charge state of projectile ions cannot be measured, except after exiting the target, and experimental data remain very scarce. The knowledge of the charge state of heavy ions is of significance on accelerator, fusion plasma physics and high energy density physics applications.

1. Introduction

The inertial confinement fusion driven by heavy ion beams is one of the method to obtain energy using fusion reactions. Understanding the physics of heavy ions traveling through plasmas is an important topic in plasma physics. Heavy ions possess good features to heat small samples of matter reaching the necessary temperature and density for the nuclear fusion takes place.

On the other hand, conventional stripping techniques are limited in their applicability, e.g. short lifetime in foil stripper and lower efficiency in gas stripper. To reach long lifetime and higher efficiency, the use of plasma as a stripping medium has been studied. In stripper devices, one of the most important thing is the prediction of the final charge state distribution of the ion beam and its total energy loss, which the presented work focuses on.

2. Theoretical model

For a projectile traveling through a target, the charge fraction distribution is usually calculated as,

$$\frac{dF_q(t)}{dt} = \sum_{q' \neq q} \alpha(q' \to q) F_{q'}(t) - \sum_{q' \neq q} \alpha(q \to q') F_q(t) \qquad (1)$$

where F_q is the projectile fraction with charge state q and the α are the ionization and recombination rates [1].

On the other hand, the instantaneous charge state can be also estimated by a simple analytic equiation:

$$Q(x) = Q_{eq} - (Q_{eq} - Q_0) \exp\left(-\frac{x}{\lambda_{ion}}\right) \qquad (2)$$

where x is the plasma length, Q_{eq} is the equilibrium charge state and Q_0 is the initial charge state. λ_{ion} is the ionization length estimated from [2].

The energy loss of the projectile is estimated in the RPA approximation as described in [3].

3. Results

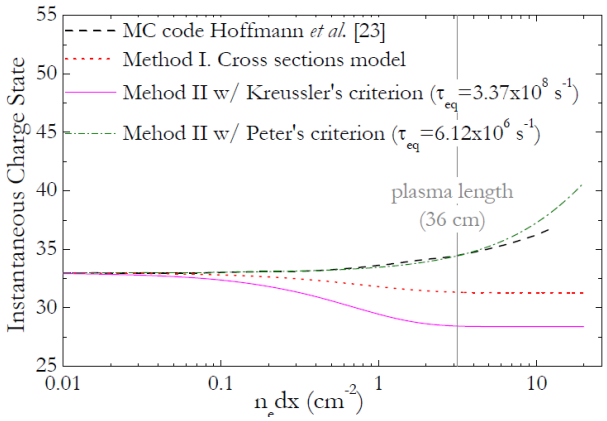

Fig.1: Instantaneous charge state of U ions in a H plasma.

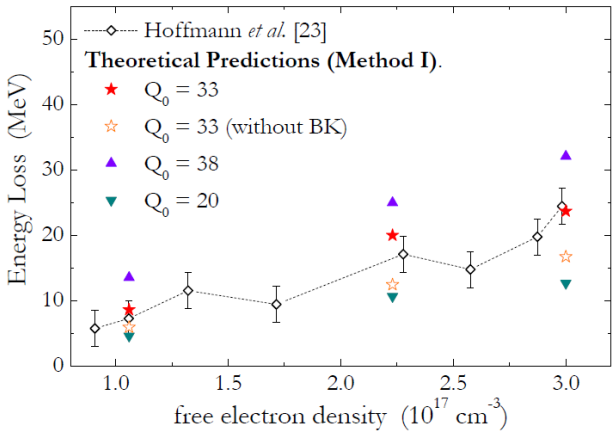

Fig. 2: Energy loss of U ions in a H plasma as a function of plasma density for several initial charge states.

4. References

[1] T. Peter and J. Meyer-ter-Vehn, Phys. Rev. A 43, 2015 (1991).

[2] R. Morales and M.D. Barriga-Carrasco (sent to Phys. Plasmas, accepted).

[3] M.D. Barriga-Carrasco, D. Casas and R. Morales, Phys. Rev. E 93, 033204 (2016).

Experimental study of microwave plasma breakdown in microstrip devices for power limiting applications

A. Simon[1], R. Pascaud[1], T. Callegari[2], L. Liard[2], O. Pascal[2]

[1]*ISAE-SUPAERO, Université de Toulouse, Toulouse, France*
[2]*Université de Toulouse; UPS, INPT, CNRS; LAPLACE (Laboratoire Plasma et Conversion d'Energie); 118 Route de Narbonne, F-31062 Toulouse, France*

This poster presents microstrip devices including self-power-limiting capability thanks to plasma microdischarge. A classic DC microhollow cathode discharge is therefore ignited under the ground plane of the microstrip device. When the microwave power reaches a tunable threshold, the plasma expands to the upper part of the microstrip circuit, which causes a major change in its behaviour. The upper part of the plasma is then controlled both by microwave and DC power. Different microstrip devices are experimentally characterized with their microwave parameters to get insight on the role of the electromagnetic field on the plasma extension. All exhibits the self-power-limiting capability, at different levels depending on the intensity of the microwave electromagnetic field at the plasma location.

1. Plasma as microwave protection element

Plasmas have been used for power protection in high frequency communications for a long time, for example in T/R tubes [1]. The recent explosion of microwave communication devices of smaller power range has triggered a need for protection on microstrip devices.

Plasma presents two main advantages in this purpose: it handles a microwave power higher than any other existing solution (diode, varicap, MEM…) and insertion losses on the device can remain extremely low.

2. Plasma microdischarges in microstrip devices

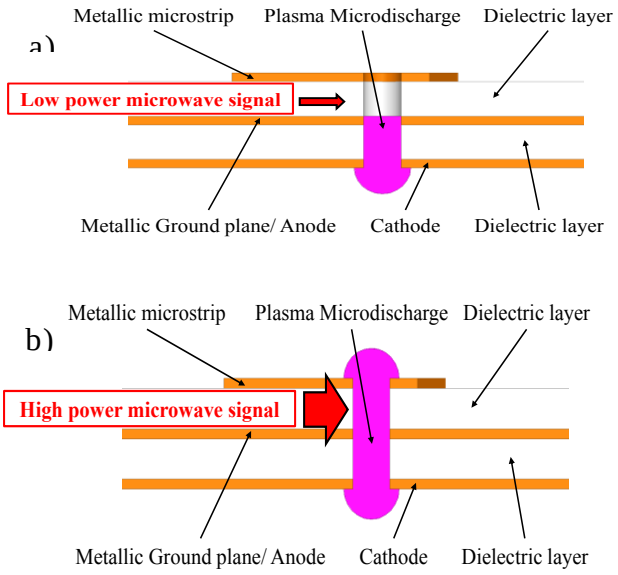

Fig 1: The "off" (a) and "on" (b) state of the microstrip device with self-power-limiting capabilities

The ignition of a Micro Hollow Cathode Discharge (MHCD) with a typical breakdown of 300 V under the ground plane (Figure 1a) allows the generation of plasma above the microstrip line at very low power threshold, typically 1 Watt (Figure 1b) [2].

3. Study of microwave plasma breakdown

In this poster, we present an experimental work that aim at evaluating the characteristics of the plasma generated on the upper part by microwave power.

Each microstrip device is inserted in a vacuum chamber. Pressure in argon varies from 1 to 100 Torr. The plasma is ignited in a cylindrical aperture whose diameter depends on the pressure work. Different microstrip circuits are characterized with S parameters and power balance to understand the role of the electromagnetic field on the plasma formation and stability. Self-power-limiting capability is demonstrated, and the trigger level can be controlled. Depending on the circuit design, plasma effect of the microwave power can be either absorptive or reflective.

4. References

[1] A. Kraszewski, "Microwave Gas Discharge Devices", lliffe Books Ltd. (1967).

[2] R. Pascaud *et al*., Electronics Letters, vol. 51, no. 14, pp. 1090-1092, (2015).

Topic number 10

Influence of target on electric field in kHz-driven atmospheric pressure plasma jet in Helium

A. Sobota[1], V. V. Kovačević[2], G. B. Sretenović[2], I. B. Krstić[2], B. M. Obradović[2], M. M. Kuraica[2], E. Slikboer[3], O. Guaitella[3]

[1]*Eindhoven University of Technology, EPG, Postbus 513, 5600MB Eindhoven, The Netherlands*
[2]*University of Belgrade, Faculty of Physics, PO Box 44, 11001 Belgrade, Serbia*
[3]*LPP, Ecole Polytechnique, Route de Saclay, 91128 Palaiseau, France*
**Contact e-mail:* ana.sobota@tue.nl

The understanding of the dynamic of impingement of atmospheric pressure plasma jet is the key for their use in many applications. The electric field strength has been measured above and onto different surfaces, dielectric, metallic or liquid, by means of Stark polarization spectroscopy. In the case of dielectric surfaces, the electric field strength values are compared with measurements based on Pockels effect obtained with an imaging polarimeter.

1. Introduction

The term "atmospheric pressure plasma jets (APPJ)" represents many diverse plasma sources having usually in common to be operated with a flow of noble gas inside a small diameter tube. They have been the focus of many studies because of their potential interest in biomedical applications and surface treatment technologies. For all these applications, it is always crucial to understand and control the interaction of the APPJ with a target which can be dielectric or conductive, solid or liquid. The surface exposed to an APPJ can be physically and/or chemically modified by the plasma, but the target can also influence the discharge development. A key parameter to study the properties of APPJ in contact with targets is the electric field induced by the plasma above and onto various surfaces.

In this study, electric field in helium plasma jet impacting dielectric, metallic or liquid surfaces is measured by means of Stark polarization spectroscopy as described in [1]. The results on dielectric surfaces are compared with surface electric field strength measurement based on Pockels effect obtained with an imaging polarimeter described in [2]. The influence of gas mixing between helium and surrounding atmosphere is also monitored with Schlieren imaging.

2. Experimental setups

The jet source used for this work has been described in [1,2]. The powered electrode is a needle metal tube (inner diameter of 0.8 mm) centered inside a Pyrex capillary (inner diameter 2.5 mm, outer diameter 4 mm). A metal ring (3 mm long) on the outer side of the capillary is used as the grounded electrode. The gap between the two electrodes was 5 mm, while the distance from the grounded electrode to the end of capillary was 20 mm for the entire study. Helium flow through the capillary is regulated using mass flow controller in range of 700-2000 SCCM. The jet is powered by sine voltage at 30 kHz, 2 kV in amplitude. The jet source was most of the time vertical above a target. The targets used were glass disks, grounded disks, or distilled water reservoir.

3. Results analysis

We had already measured that electric field strength in the plume of this APPJ is increasing with distance from the capillary tip because of gas mixing with air and constriction of the plume [1]. At a given distance from the tip of the capillary, the field strength at the impact on a target is significantly higher than without surfaces. It is shown that enhancement of field due to the surface happens only on a very thin layer above the surface. Very high values of electric field (up to 40 kV/cm) can be obtained on surfaces. The gas flow dynamics above the surface is also strongly modified by the plasma.

3. Acknowledgments

AS would like to thank the European Cooperation in Science and Technology Action COST TD1208 for financial support for a short-term scientific mission

4. References

[1] A. Sobota et al (2016) *Plasma Sources Science and Technology*, **25** (6), 065026.

[2] E. Slikboer et al, contribution to ICPIG 2017

O_2 dissociation in plasma and problem of O_2 cross sections set

J.P. Booth[1], O. Guaitella[1], A. Chatterjee[1], S. Zyryanov[2], D. Lopaev[2], D. Voloshin[2] and T. Rakhimova[2]

[1] *Laboratoire de Physique des Plasmas, CNRS, Ecole Polytechnique, UPMC Univ Paris 06, Univ Paris-Sud*
[2] *Skobeltsyn Institure of Nulcear Physics, Lomonosov Moscow State University, Russian Federation*

DC glow discharges in pure O_2 in a Pyrex tube were studied to determine dissociation rate constant over a wide range of E/N and thereby to probe O_2 dissociation cross section close to threshold. Electric field, E, was found from probe measurements while the gas density, N, from the gas temperature derived from the $O_2(b^1\Sigma_g^+) \rightarrow O_2(X^3\Sigma_g^-)$ emission spectrum. O atom density (as well ratio O/N ratio) was measured by HR TALIF while O/N ratio was also determined by Ar actinometry. Time-resolved actinometry of partially-modulated discharges was used to probe the O loss rate. The O_2 dissociation rate constant was determined as a function of E/N, and compared to calculations from different O_2 cross section sets. This comparison allowed validation of a the self-consistent cross section set for O_2.

1. Introduction

Chemical activity of oxygen plasma is mainly provided by odd oxygen (O atoms and ozone). O_2 dissociation by electron impact is the main channel of O atoms production, therefore the O_2 dissociation cross section, together with electron energy distribution function define the chemical efficiency of oxygen plasmas. Nevertheless, the cross-section for electron impact dissociation of molecular oxygen is the subject of active debate, especially near threshold. The available experimental cross sections near the threshold predict a much lower dissociation rate than that observed. Furthermore, O_2 dissociation is an important electron energy loss channel, influencing electron transport. Cross section sets consistent with observed transport coefficients require an unrealistically high value of the O_2 dissociation cross section. This motivated a study of the dissociation rate constant to validate the near-threshold dissociation cross section and, indirectly, the self-consistent cross sections set for O_2.

2. Experiment

Time-resolved absolute density measurements are needed to probe O atoms kinetics. The measurements were carried out in DC glow discharge in pure O_2, generated in water-cooled Pyrex glass tube of 2 cm diameter and ~50 cm length. The discharge current was controlled by a large (68kΩ) ballast resistor, and could be modulated (5-15%) by shunting a smaller resistor installed between the discharge and ground. The electric field was found from probe measurements, and the gas density was calculated using the gas temperature deduced from the $O_2(b^1\Sigma_g^+) \rightarrow O_2(X^3\Sigma_g^-)$ emission spectrum. The O atom density and O/N ratio was measured by the HR TALIF method while the O/N ratio was also determined from actinometry using Ar atoms. Time-resolved actinometry in partially-modulated discharges was used to probe the loss rate of O atoms.

The O_2 dissociation rate constant as a function of E/N, calculated from the balance between O loss and production rates is shown in figure 1.

This research was conducted in the scope of the KaPPA International Associated Laboratory (LIA), performed within the LABEX Plas@par project, and received financial state aid managed by the Agence Nationale de la Recherche, as part of the programme "Investissements d'avenir" under the reference ANR-11-IDEX-0004-02. It was also supported by the Applied Materials University Research Partnership Program. Russian team was also supported by RFBR grant 16-52-16024.

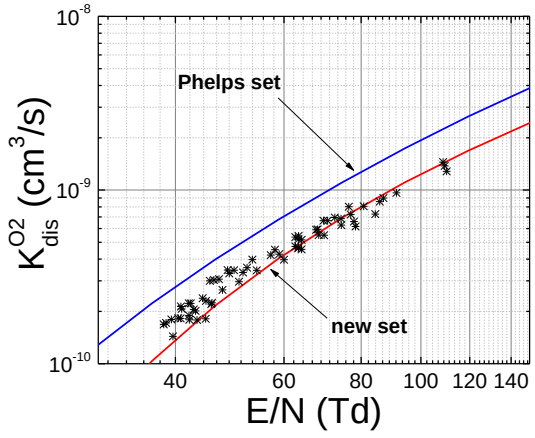

Figure 1. O_2 dissociation rate constant as a function of the reduced electric field E/N.

Micro-glass capillary focusing of plasma ion beams and creation of microstructures

Sanjeev Kumar Maurya and Sudeep Bhattacharjee

Department of Physics, Indian Institute of Technology - Kanpur, Kanpur 208016

Intense microwave plasmas have been used as an ion source for applications in microstructuring. Microstructures having aspect ratio in the range 100 - 1000 have been created using 26 keV Ar, Kr and Ne ion beams with beam size ~ 1.5 µm. To prevent loss of beam current and further focus the beam, micro-glass capillary will be employed after the plasma electrode, from where the beams are extracted. Ion beam current and beam spot size, will be measured as a function of extraction voltage for different capillary outlet diameters. The capillary which provides the smallest beam spot size, will be implemented in the system. Further, different structures will be created using Ar, Kr, and Ne ion beams.

1. Introduction

Ion beam is a necessary tool in science and technology and can be used in many applications such as milling, patterning, high resolution imaging and implantation. Many emerging applications require rapid processing and non-toxic inert gaseous ion beams. In order to serve above applications, there are efforts to develop gaseous plasmas ion beam tools which can be non-toxic and therefore suitable for biomaterials and semiconductors, and provide an option for rapid processing without metallic contamination due to higher currents. To address these requirements, a microwave plasma based multi-element ion beam system has been developed in our laboratory which can deliver ions of a variety of gaseous elements (Ar, Kr, Ne) of beam size ~ 1.5 µm, beam currents in the range ~ 1.5 nA – 10 µA and beam energy up to 30 keV [1].

2. Experimental Setup

The experimental setup consists of three major parts namely, plasma column, beam column and experimental chamber.

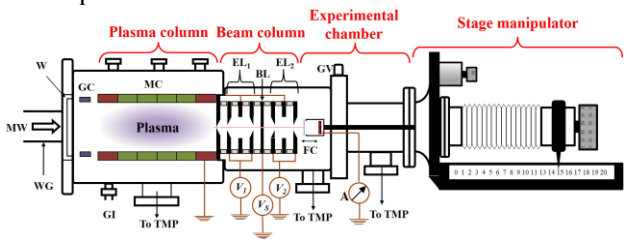

FIG. 1. MW: microwaves, WG: wave guide, W: quartz window, GC: guiding cylinder, GI: gas inlet, MC: multicusp, TMP: turbo molecular pump, EL: Einzel Lens system, BL: beam limiter, FC: Faraday cup, GV: gate valve, V_1, V_S, V_2: high voltages, A: ammeter

In the plasma column, a high density plasma (~10^{11} cm^{-3}) is created with the help of 2.45 GHz microwave and confined in an octupole multicusp. Beam column consists of plasma electrode (PLE), Einzel lens (EL) and beam limiter (BL) which are used to extract and focus the ion beams. EL_1, EL_2 and BL electrodes are biased to negative high voltages V_1 (~ –2 kV), V_2 (= 18–30 kV) and V_S (= 2/3 V_2) respectively to provide the desired acceleration and adequate focusing to the beam. A copper (Cu) thin film (50 nm) biased to V_2 is mounted on the XYZθ stage manipulator for moving the sample in the desired direction with required writing speed. For measuring the ion beam current, a Faraday cup is used after EL_2.

3. Results: Different microstructures (array of spots, lines and a group of letters) have been created on 50 nm Cu thin film using 18 – 30 keV Ar, Kr and Ne ion beams. For Ar ion beams, sputtering yield and milling rate are calculated at normal incident and found to be ~ 8.8 atoms/ion and ~ 0.65 $\mu m^3 s^{-1} nA^{-1}$ respectively which are higher than Ga^+ focused ion beams (30 keV/1pA) for which calculated values are ~ 1.27 atoms/ion and ~ 0.09 $\mu m^3 s^{-1} nA^{-1}$.

Next for further reduction of beam size, micro-glass capillary will be employed after PLE through which ion beam will pass, which will provide self-focusing of the beam without reducing the beam current [2,3]. For this first ion beam current will be measured by varying the extraction voltage (V_1) using only capillary after PLE and then spot size of beam coming out from capillary will be measured. Microstructures will be created employing a capillary in the present ion beam system.

4. References

[1] S. Bhattacharjee and S. Paul Jpn. J. Appl. Phys. **54**, 01AA06 (2015).

[2] S. Paul, A. Jayakiran and S. Bhattacharjee Appl. Phys. Lett. **101**, 223508 (2012).

[3] S. Paul and S. Bhattacharjee J. Phys. D: Appl. Phys. **48**, 025204 (2015).

Spatial and temporal analysis of acetone decomposition and subsequent OH formation in nanosecond diffuse discharge

K. Ouaras, L. Magne, P. Tardiveau, A. Brisset, S. Pasquier, P. Jeanney, B. Bournonville

Laboratoire de Physique des Gaz et des Plasmas, CNRS, Paris-Saclay Université, 91400, Orsay, France

Planar laser induced fluorescence is employed to determine both the acetone (C_3H_6O) and the OH radical distribution during the post-discharge of a high voltage (85 kV), pulsed (10 Hz), nanosecond (10 ns), atmospheric pressure, centimeter gap (1.8 cm), diffuse pin-to-plane discharge operating in air containing different acetone concentrations (2000, 5000 and 10000 ppm). We determine both the spatial (in the whole interelectrode gap) and temporal (in post-discharge (t_{pd})) acetone Destruction and Removal Efficiency fraction DRE and the OH density [OH]. We emphasize both the largest acetone decomposition (~60 %) and the maximal OH density (5.10^{16} cm^{-3}) in the pin region for the highest acetone concentration value (10000 ppm).

1. Introduction

We investigated the spatial and temporal behavior of a pollutant, the acetone using Planar Induced Laser Fluorescence *PLIF* technic. Quantitative values concerning the destruction of the acetone and its conversion into OH are given. These spatial measurements are undertaken in a novel pin-to-plane discharge operated at very high voltage and short pulses. This study is intended to provide useful information about chemical kinetic in atmospheric plasma processes dedicated to environmental remediation.

2. Experimental

The pin-to-plane discharge set-up [1] consists of a pin electrode powered by a nanosecond (10 ns), pulsed (10 Hz) high voltage (85 kV) power supply and a grounded plane electrode which are separated by 18 mm and mounted on a cylindrical stainless steel chamber equipped with optical windows in order to achieve PLIF measurement. The acetone is mixed at 2000, 5000 and 10000 ppm with dry air thanks to a bubbler system and the total gas flow rate is set to 1 L/min. PLIF experiments were performed in temporal post-discharge. The PLIF technic and the absolute calibration for OH density determination have been largely described in the literature [2] and will be not detailed here. Concerning the acetone processing, as the acetone is already introduced in the gas mixture, it consists of taking the LIF image without and with plasma discharge. The subtraction of these two images divided by the LIF image without plasma gives directly the quantitative DRE of acetone,

$$\mathrm{DRE}\ (C_3H_6O) = \frac{[C_3H_6O]_0 - [C_3H_6O]}{[C_3H_6O]_0} \qquad \textbf{(1)}$$

where, $[C_3H_6O]_0$ and $[C_3H_6O]$ are the initial and the final concentration of acetone, respectively.

3. Results: an overview

The **Figure 1** gives an overview of the spatial distribution profile in the interelectrode gap for air plus 10000 ppm of acetone mixture at 85 kV of (a) the acetone DRE and (b) the OH radical density.

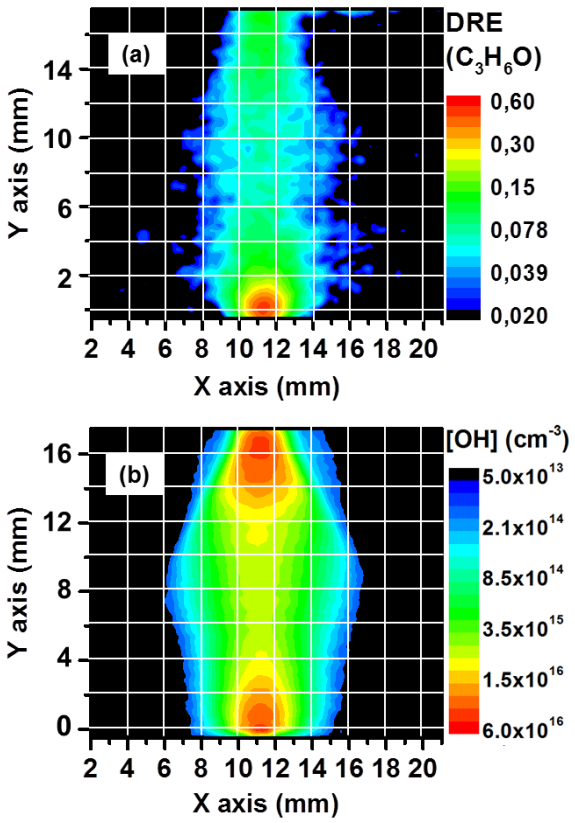

Figure 1. Spatial distribution of (a) DRE of acetone at t_{pd}= 200 µs and (b) OH density at t_{pd}= 0.5 µs.

3. References

[1] P Tardiveau *et al* 2016 *Plasma Sources Sci. Technol.* **25** 054005

[2] T Verreycken *et al* 2013 *J. Phys. D: Appl. Phys.* **46** 464004

The influence of strong magnetic field on the plasma transport*

Chao Dong, Wenlu Zhang, and Ding Li†

Institute of Physics, Chinese Academy of Science, Beijing 100190, China

The full magnetized Fokker-Planck equation is derived through the transform method. The Fokker-Planck coefficients including the magnetic field are calculated by using the binary collision model. The magnetized Landau collision term is obtained. The influence of magnetic field on temperature relaxation has been extensively studied. It is shown that the strong magnetic field may greatly affect the electron anisotropic temperature relaxation, and electron-ion temperature relaxation in the tokamak edge plasma.

1. Introduction

In many celestial and terrestrial environments, the particles' gyro-radii are smaller than the Debye length. For example, in tokamak, the ratio of the thermal gyro-radius to the Debye length for electron could be much smaller than one for the plasma. The magnetic field affects the collision dynamics and associated transport phenomena such as velocity slowing down, temperature relaxation, diffusion, thermal transport etc. It was found that the cross field heat transport can occur even without mass transport when the magnetic field is very strong. [1]

2. Resulting magnetized Fokker-Planck equation

The Fokker-Planck equation in the presence of a uniform magnetic field is derived through the transform method as follows:

$$\frac{\partial f_\alpha(\mathbf{v}_\alpha,\tau)}{\partial\tau}+\Omega_\alpha\mathbf{v}_\alpha\times\hat{\mathbf{e}}_z\cdot\frac{\partial f_\alpha(\mathbf{v}_\alpha,\tau)}{\partial\mathbf{v}_\alpha}$$
$$=-\frac{\partial}{\partial\mathbf{v}_\alpha}\cdot[\langle\Delta\mathbf{V}_\alpha\rangle f_\alpha(\mathbf{v}_\alpha,\tau)]$$
$$+\frac{1}{2}\frac{\partial^2}{\partial\mathbf{v}_\alpha\partial\mathbf{v}_\alpha}:[\langle\Delta\mathbf{V}_\alpha\Delta\mathbf{V}_\alpha\rangle f_\alpha(\mathbf{v}_\alpha,\tau)],$$

where the Fokker-Planck coefficients $\langle\Delta\mathbf{V}_\alpha\rangle$ and $\langle\Delta\mathbf{V}_\alpha\Delta\mathbf{V}_\alpha\rangle$ are calculated based within the binary collision model and the magnetized Landau equation is obtained:

$$\frac{\partial f_\alpha(\mathbf{v}_\alpha,\tau)}{\partial\tau}+\Omega_\alpha\mathbf{v}_\alpha\times\hat{\mathbf{e}}_z\cdot\frac{\partial f_\alpha(\mathbf{v}_\alpha,\tau)}{\partial\mathbf{v}_\alpha}$$
$$=\frac{\partial}{\partial\mathbf{v}_\alpha}\cdot\sum_\beta(2\pi)^3\frac{q_\alpha^2q_\beta^2}{m_\alpha}\int_0^\infty\mathrm{d}t\int\mathrm{d}^3\mathbf{k}\int\mathrm{d}^3\mathbf{v}_\beta\,\tilde{\Phi}_D^2(k)$$
$$\times\exp\{\mathrm{i}\mathbf{k}\cdot[\mathsf{H}_\alpha(t)-\mathsf{H}_\alpha(0)]\cdot\mathbf{v}_\alpha-\mathrm{i}\mathbf{k}\cdot[\mathsf{H}_\beta(t)-\mathsf{H}_\beta(0)]\cdot\mathbf{v}_\beta\}$$
$$\times\mathsf{T}_\alpha^{-1}(t)\cdot\mathbf{k}\mathbf{k}\cdot\left(\frac{1}{m_\alpha}\frac{\partial}{\partial\mathbf{v}_\alpha}-\frac{1}{m_\beta}\frac{\partial}{\partial\mathbf{v}_\beta}\right)[f_\alpha(\mathbf{v}_\alpha,\tau)f_\beta(\mathbf{v}_\beta,\tau)].$$

The above kinetic equation is shown to be identical to the result obtained from the BBGKY approach when the collective effects are neglected and satisfy the conservation of particles, momentum, and energy. [2]

3. Study of plasma transport essential processes

The strong magnetic field may greatly affect the transport essential processes in the plasma. It is shown that the electron-electron (e-e) and ion-ion temperature relaxation rates first increase and then decrease as the magnetic field grows, and the doubly logarithmic term contained in the electron-ion (e-i) temperature relaxation rate. [3] It is found that when the electron thermal gyro-radius is smaller than the Debye length, Debye length is replaced by the electron thermal gyro-radius in the Coulomb logarithm in the electron anisotropic temperature relaxation rate due to e-e collisions and e-i collisions. The e-i temperature relaxation rate contains a doubly logarithmic term arising from the exchange between the electron parallel and the ion perpendicular kinetic energies: [4]

$$\ln\Lambda_B\approx\ln\Lambda+\frac{1}{2}\ln\left(\frac{m_iT_e}{m_eT_i}\right)\ln\left(\frac{\lambda_{De}}{R_{the}}\right),$$
$$for\quad R_{the}<\lambda_{De}<R_{thi}.$$

For $n_e=10^{19}m^{-3}$, $B=3.5\mathrm{T}$, $m_i/m_e=3672$, $T_e=2T_i$, and $\ln\Lambda=15$, we have

$$\ln\Lambda_B/\ln\Lambda=1.37.$$

The other transport processes such as the velocity slowing down, diffusion, thermal conductivity and so on are being studied.

4. References

[1] M. Psimopoulos, D. Li, Royal Soc. Lond. A 437, 55 - 65 (1992).

[2] Chao Dong, Wenlu Zhang, and Ding Li, Phys. Plasmas 23 (8), 082105, 2016.

[3] Dong, Chao; Ren, Haijun; Cai, Huishan; and Li, Ding, Phys. Plasmas, 20 (10), 102518, 2013.

[4] Chao Dong, Haijun Ren, Huishan Cai, and Ding Li, Phys. Plasmas, 20 (3), 032512, 2013.

† Email：dli@iphy.ac.cn

* Supported by National Special Research Program of China For ITER and National Natural Science Foundation of China.

Numerical modelling of stable glow corona discharges by means of stationary solvers of COMSOL Multiphysics

P. G. C. Almeida, N. G. C. Ferreira, and M. S. Benilov

Departamento de Física, FCE, Universidade da Madeira, Largo do Município, 9000 Funchal, Portugal
Instituto de Plasmas e Fusão Nuclear, Instituto Superior Técnico, Universidade de Lisboa, Lisboa, Portugal

The use of stationary solvers for numerical simulations of DC gas discharges carries a number of advantages. This work describes modelling of stable glow corona discharges by means of stationary solvers of COMSOL Multiphysics. As an example, results are shown of calculation of a positive corona in a point-to-plane configuration.

1. Introduction

The physics of glow (stationary) corona discharges has been understood reasonably well and a number of useful theoretical results, including analytical ones, have been obtained under various approximations. It is desirable to have also a fast and robust method of numerical modelling, which could be applied to a wide range of conditions. A standard approach relies on time-dependent solvers; e.g., [1,2]. Advantages offered by stationary solvers in simulations of DC discharges are demonstrated in [3]. In particular, stationary solvers allow computation of discharge modes in the whole range of their existence, thus decoupling physical and numerical stability, and are not subject to the Courant–Friedrichs–Lewy condition and the corresponding limitations on the mesh element size.

2. The approach

As far as COMSOL Multiphysics is concerned, models of DC non-thermal discharges where no insulators are present can be implemented by using the so-called general or coefficient form or by means of using the Transport of diluted species and Electrostatics modules. The only way to accurately implement boundary conditions on the insulator is by means of the Plasma module, which has appropriate internal variables. However, a straightforward application of the Plasma module does not allow working with stationary solvers. The latter can be overcome by building a replica of the Plasma module in the weak form formulation [3]. This approach allows one to introduce also other relevant modifications, in particular, to allow the user to set diffusion coefficients of the ions. However, one loses access to the internal variables of the Plasma module while using this approach.

In this work, the use of stationary solvers with the Plasma module was made possible by, paradoxically, setting equation form as time-dependent and manually controlling which dependent variables are solved for. The above-mentioned modifications were introduced in the Plasma module by editing weak expressions and contributions.

As an example, inception voltages, U_i, and values of the ionization integral, K, computed for the point-to-plane discharge configuration with 1 cm gap [4], are given in Table 1. Also shown are data computed without photoionization, $U_i^{(\gamma)}$ and $K^{(\gamma)}$, and the value of $\ln(1+\gamma^{-1})$.

Table 1: Inception voltages and ionization integral.

γ	U_i (kV)	K	$U_i^{(\gamma)}$ (kV)	$K^{(\gamma)}$	$\ln(1+\gamma^{-1})$
0	12.76	9.58	-	-	-
10^{-4}	12.74	9.54	14.41	12.85	9.23
10^{-3}	12.59	9.25	13.29	10.58	6.91
10^{-2}	11.91	8.01	12.08	8.31	4.62
10^{-1}	10.72	6.03	10.76	6.09	2.40

One can see that $K^{(\gamma)}>\ln(1+\gamma^{-1})$; in other words, the Townsend breakdown condition does not apply. As γ increases, a transition from corona to Townsend discharge occurs as the role of dominating secondary electron production mechanism passes from the secondary electron emission to photoionization.

3. Acknowledgements

The work was supported by FCT of Portugal through the project Pest-OE/UID/FIS/50010/2013.

4. References

[1] P. Dordizadeh et. al., *Plasma Sources Sci. Technol.* **25** (2016) 065009.

[2] L. Liu and M. Becerra, *J. Phys. D: Appl. Phys.* **49** (2016) 225202; **50** (2017) 105204.

[3] P. G. C. Almeida et. al., *Plasma Process Polym*, DOI: 10.1002/ppap.201600122 (2017).

[4] A. A. Kulikovsky, *Phys. Rev. E* **57** (1998) 7066.

$E\times B$-probe modeling for diagnostics of Plasma Propulsion Thruster

Timofey Chernyshev[1], Dariya Krivoruchko[2], Alexander Skrylev[2]

[1] *Joint Institute for High Temperatures of the Russian Academy of Sciences*
[2] *Moscow Institute of Physics and Technology*

Plasma propulsion thrusters (PPT) are actively used in space. However presence of multiply charged ions (MCI) at PPT plume adversely affects main thruster parameters: thrust, mass utilization and lifetime. One of the instruments to measure MCI population is $E\times B$-probe [1]. Analyzing probe spectrum we assess MCI concentration and its velocity (or energy) distribution function (IVDF/IEDF). This diagnostic has been used on different PPT [2]. However for sources with a wide spread of ions velocity (in particular HT), it is a hard to predict probe's parameters needed to resolve peaks for particles with different charges. In this work we present a model of the probe that has been created to predict probe transfer functions and methods for peak separation.

1. Introduction & theory

The interpretation of experimental data made with help of integral methods introduces inaccuracy and does not allow us to recover original IDVF due to asymmetrical broadening of the spectrum that depends on main particle velocity and blending of current peaks related to different ion species. In the work [3] the Fredholm equation for energy spectrum was used for data analysis to recover initial parameters of plasma with needed accuracy. Authors used Gaussian fitting for the raw signal for peak resolution problem. In the present work introduced the methods to determine $E\times B$-probe 's parameters. For this reason we made a program module that allows to calculate needed parameters of the probe and to decode measured spectrum.

Let's define initial Z-charged ion velocity distribution in probe's axis direction as $f(v)$ and filtration speed as $u = E/B$ where E – electric field and B – magnetic field. The probe cuts out a small part of the initial distribution function $f(v) \rightarrow f(v,\ u)$. We can declare the probe's transfer function as $g(v,\ u) = f(v,\ u)/f(v)$. The probe resolution w is determined by the speeds where $g(u,\ v)$ becomes zero. The ion current to the collector surface is defined from Fredholm integral equation as $j = Kf$ with kernel $K = Z \cdot ug(u,\ v)$. The kernel of this equation can be obtained from the probe model. Then IVDF can be reconstructed by solving inverse problem with help of regularization methods.

2. Results & conclusions

The numerical and analytical probe models were created to predict transfer functions, probe resolution and IVDF. These models show that probe's resolution (in velocity units) depend on E^2/B^3 multiplied by geometric constant. In other words common integral interpretation of IVDF is incorrect for high-speed particle fractions. The calculated ions transfer functions dependence on energy shown in fig.1. Modeled broad signal demonstrated in fig.2.

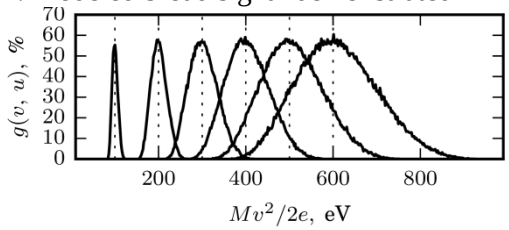

Fig.1. Transfer functions for single charged ions.

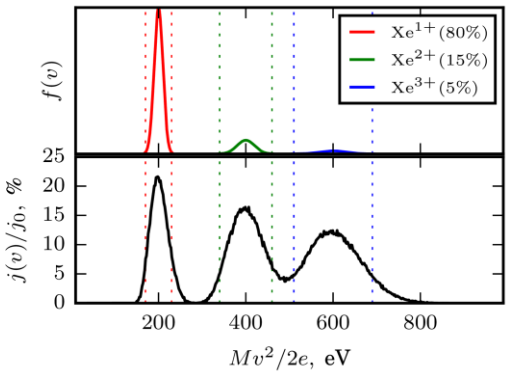

Fig 2. Simulated $E\times B$-signal for defined IEDF.

Also, the probe modification was suggested to better peaks separation. The modeling results are in a good agreement with available experiments data.

3. References

[1] Sang-Wook Kim. Experimental investigations of plasma parameters and species dependent ion energy distribution in the plasma exhaust plume of a hall thruster. PhD thesis. University of Michigan, 2001.

[2] Wensheng Huang et al. Farfield Plume Measurement and Analysis on the NASA-300M and NASA-300MS. Tech. rep. NASA, 2013.

[3] Youbong Lim et al. Observation of a high-energy tail in ion energy distribution in the cylindrical Hall thruster plasma. Physics of Plasmas 21.10 (2014), p. 103502.

Characterization of a ferro-electric packed bed plasma reactor

A.M. Montoro-Damas[2], A. Gómez-Ramírez[1, 2], V. Rico[2], A. R. González-Elípe[1], J. Cotrino[1, 2]

[1] *Departamento de Física Atómica, Molecular y Nuclear, Universidad de Sevilla, Avda. Reina Mercedes, 42022 Sevilla, Spain.*
[2] *Laboratory of Nanotechnology on Surfaces, Instituto de Ciencia de los Materiales de Sevilla (CSIC-Universidad de Sevilla), Sevilla, Spain*

The influence of diverse experimental parameters on characteristics of ferro-electric packed-bed plasma reactor used for hydrogen generation was investigated experimentally. The plasma reactor consisted in two parallel circular metal electrodes (Aluminum), and spherical shaped ferro-electric pellets packed in the discharge area. Barium Titanate ($BaTiO_3$) and (Lead Zirconate Titanate, $Pb[Zr_xTi_{1-x}]O_3$ ($0 \leq x \leq 1$)) PZT was used as ferro-electric materials. Sinusoidal high voltage up to a maximum of 2.5 kV was applied to the upper electrode with a frequency range between 50Hz and 10kHz. The determination of electrical parameters (such as instantaneous power, transferred charge, breakdown voltage, electron density and capacitance properties) was carried out in different reactor configurations.

1. Introduction

The use of atmospheric non-thermal plasmas can be considered as a mature technology in several applications, such as to remove hazardous compounds or to produce valuable chemicals using the energy transfer by energetic electrons. The introduction of ferroelectrics materials into the discharge zone of the non-thermal plasma reactor is a promising way to improve their performance [1, 2]. The plasma parameters of this ferro-electric packed bed reactor are not well understood in spite of the widely applications of this type of reactors. One important property of the ferro-electric packed bed is the locally enhanced electric field inside the dielectric material (pellets and voids), near the contact points between the pellets and pellets/electrodes [3]. The use of this ferroelectric pellets as dielectric material simply reflects that ferroelectrics have spontaneous polarization below the ordering temperature. A small electric field suffices to create large polarization. In a linear response regime that means the susceptibility of the material is very high. By using typical voltage-current characteristic was experimentally monitoring the plasma reactor. These electrical magnitudes present a highly non-linear behavior that conditions the value of the different experimental parameters analyzed.

2. Experimental

Different gas mixtures of CH_4/CO_2, CH_4/O_2, CH_4/H_2O and Air, were introduced in the ferro-electric packed bed plasma reactor. Due to the dielectric (ferroelectric) barriers the reactor has capacitive properties that may be explained with the well know Q-V plot [4]. Analyzing the curvature of the Q-V Lissajous figures, the capacitance of the cell and dielectric barrier can be obtained. The ferroelectric character of the dielectric make that its capacitance be dependent of temperature and applied voltage. From these values an estimation of the breakdown voltage was evaluated and an analysis of the dissipated power from the Q-V Lissajous diagram. The calculation of the electron density relies on the assumption of a collisional regimen, in which the current density depends on the electron density and mobility and the magnitude of the electric field [5]. In order to get an accurate value for the electron density, the fact that the discharge area is not the whole surface of the active electrode has been taken into account.

3. References

[1] F. Holzer, F.D. Kopinke, U. Roland, *Plasma Chem. Plasma Process.* 25, (2005) 595.
[2] H.L. Chen, H.M. Lee, S.H. Chen, M.B. Chang, *Ind. Eng. Chem. Res.* **47** (2008) 2122.
[3] Y. Zhang, H. Wang, W. Jiang, A. Bogaerts, *New J. Phys*. **17** (2015) 083056.
[4] A. V. Pipa, J. Koskulics, R. Brandenburg, and T. Hoder. Rev. Sci. Instrum. 83 (2012) 115112.
[5] K. Takaki , J. Chang, K.G. Kostov, *IEEE Transactions on Dielectrics and Electrical Insulatio*n **11** (2004) 481.

Acknowledgements

We acknowledge financial support from Junta de Andalucía through the project P12–2265MO and from the European Regional Development Funds program (EU-FEDER) and the MINECO (project MAT2013-40852).

Numerical investigation of stability of glow corona discharges and corona-to-streamer transition

N. G. C. Ferreira[1,2], P. G. C. Almeida[1,2], G. V. Naidis[3], and M. S. Benilov[1,2]

[1]*Departamento de Física, Universidade da Madeira, Largo do Município, 9000 Funchal, Portugal*
[2]*Instituto de Plasmas e Fusão Nuclear, Instituto Superior Técnico, Universidade de Lisboa, Lisboa, Portugal*
[3]*Joint Institute for High Temperatures of the Russian Academy of Sciences, Moscow, Russia*

Stability of glow corona discharges against finite perturbations is studied in atmospheric pressure air in a point-to-plane electrode configuration with 1 cm gap. The corona is stable against finite perturbations for applied voltages smaller than 18 kV and unstable for voltages higher than 18 kV. Streamers appear when voltage is higher than 13 kV; sparks may form above 18 kV.

1. Introduction

Positive corona-to-streamer transition is an important research subject; e.g., [1]. A related topic is the stability of positive glow coronas against finite perturbations. Both topics are studied in this work.

2. The model

Species included in the modelling are positive and negative ions and the electrons. The kinetic scheme includes ionization, two and three-body dissociative attachment, electron-ion and ion-ion recombination, as well as photoionization. The equations solved are conservation equations for the charged particles and the Poisson equation. The rate of photoionization was evaluated by means of three-exponential Helmholtz model [2]. Standard boundary conditions have been used.

3. Results and discussion

Stable glow corona discharge was computed by means of a stationary solver for the point-to-plane discharge configuration with 1 cm gap in atmospheric-pressure air [3]. The computed current-voltage characteristic (CVC) is shown in figure 1. Using always the state with current 10^{-7} A and voltage of 12.8 kV as initial condition, the stability of glow corona was studied by increasing the applied voltage and following the evolution of the discharge over time with a time-dependent solver. If the applied voltage is in the range 12.8 up to 13 kV, the discharge evolves into a stable glow corona with no streamer formation. This threshold is marked in figure 1 by line 1. If the applied voltage exceeds 13 kV but is below 18 kV, partial streamers appear, then dissipate and the glow corona reappears. Examples of voltage steps used are: for 13 kV the length of streamer propagation is 2.9 mm; for 14 kV, 4.6 mm; for 15 kV, 6.1 mm; for 16 kV, 8.1 mm. The corona is stable against finite perturbations for applied voltages smaller than 18 kV and unstable for voltages higher than 18 kV; line 2 in figure 1.

If the ballast resistance is low and the applied voltage is maintained equal or higher than 18 kV, then discharge current will increase indefinitely and a spark will be formed. If the ballast resistance is appreciable, the increase in current after gap bridging will provoke a fall in the applied voltage. It may happen that the reduced voltage is insufficient to keep the streamer alive, so the streamer will dissipate rather than become a spark.

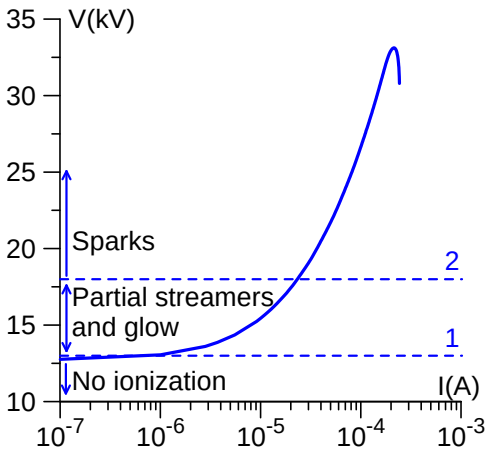

Figure 1: CVC of stable glow corona discharge.

4. Acknowledgements

The work at Universidade da Madeira was supported in part by FCT of Portugal through the project Pest-OE/UID/FIS/50010/2013.

5. References

[1] L. Liu and M. Becerra, *J. Phys. D: Appl. Phys.* **49** (2016) 225202.

[2] A. Bourdon et. al., *Plasma Sources Sci. Technol.* **16** (2007) 656.

[3] A. A. Kulikovsky, Phys. Rev. E **57** (1998) 7066.

Isotope labelling: A new technique to analyse reaction mechanisms in plasma-gas processes

A. Gómez-Ramírez[1, 2], A.M. Montoro-Damas[1], A. R. González-Elípe[2], J. Cotrino[1, 2]

[1] *Departamento de Física Atómica, Molecular y Nuclear, Universidad de Sevilla, Avda. Reina Mercedes, 42022 Sevilla, Spain.*

[2] *Laboratory of Nanotechnology on Surfaces, Instituto de Ciencia de los Materiales de Sevilla (CSIC-Uni. Sevilla), Sevilla, Spain*

This work is concerning the plasma reforming of methane using labelled D_2O molecules as reactant with the aim of identifying some of the key intermediate species intervening in the reaction mechanisms. The study herein reveals important clues about those intermediate plasma processes running in parallel to the main reaction leading to the formation of CO and hydrogen. In concrete, we have found that a considerable exchange of H(D) by D(H) atoms occurs in the exhaust gases (i.e, hydrogen, methane and water) under different operating conditions, proving that much of the plasma energy is used to produce intermediate species which are inefficient for the formation of final products.

Isotope labelling, a classical method in catalysis to ascertain reactions routes [1, 2], has been scarcely applied in plasma processes [3]. In this work we have used deuterated water as labelling compound to analyse the molecular fragmentation during the plasma wet reforming of methane in a parallel plate packed-bed DBD reactor filled with ferroelectric material [4]. Reaction products were monitored by means of a mass spectrometer. Apart from the expected hydrogen (H_2) and carbon monoxide (CO), deuteromethanes and molecular hydrogen isotopes (D_2, HD, CH_3D, CH_2D_2) appear in the reaction products. The existence of isotope labelled molecules (CH_3D, CH_2D_2) is a clear proof of the occurrence of backwards reactions during the wet reforming of methane. These processes imply a waste of energy and, thus, a decrease in the efficiency of the DBD plasma processes, one of the major drawbacks for its industrial implementation. The influence of different parameters, namely, the gas residence time, the current and the addition of oxygen on the H/D distribution and efficiency of the process is analysed.

References

[1] J. Wei, E. Iglesia, Phys. Chem. Chem. Phys. **6 (**2004) 3754.

[2] L.Y.P. Luk, J.J. Ruiz-Pernía, A.S. Adesina, E.J. Loveridge, I. Tuñón, V. Moliner, R.K. Allemann, Angew. Chem., Int. Ed. **54** (2015) 9016.

[3] F. Daou, A. Vincent, J. Amouroux, Plasma Chem. Plasma Process. **23** (2003) 309.

[4] A. M. Montoro-Damas, J. J. Brey, M. A. Rodriguez, A.R. González-Elípe, J. Cotrino, J. Power Sources **296** (2015) 268.

Acknowledgements

We acknowledge financial support from Junta de Andalucía through the project P12–2265MO and from the European Regional Development Funds program (EU-FEDER) and the MINECO (project MAT2013-40852.

The NH_3 plasma transition into "ion-ion" or transient H-E plasma mode

J. Brcka

TEL Technology Center, America, LLC, US-Technology Development Center, Austin, TX 78741, U.S.A.

2D plasma fluid modelling was used to investigate a transient development of the ammonia (NH_3) gas and to determine transient decomposition in high-density plasma produced by a linear inductively coupled plasma (ICP) source. The inclusion of a large number of reactions (103) considering 31 species and including multiple negative ions results in an expulsion of the electrons from the source domain at constant power. Transient development of the discharge demonstrated a lower electron density than in an electropositive (Ar) plasma. Within 60-100 μs the electron density collapses leading to almost electron-free plasma (for t>1ms). The conditions and geometry of the source explored in this study could lead to steady ion-ion plasma formation with H_2 and N_2 being the dominant conversion products.

1. Introduction

Under specific conditions, electronegative gases are able to generate almost electron-free (ion-ion) plasmas [1,2]. In this simulation study, we investigated ammonia (NH_3) gas decomposition by linear inductively coupled plasma (ICP). The aim is to determine the transient behaviour and spatial distribution of all charged species and radical fractions in the NH_3 radical source.

2. Modelling approach

The feasibility study was performed by a computational plasma fluid 2D model that was constructed in 2D space by using a commercial finite-element multiphysics modelling tool. A more detailed description can be found in Refs. [3,4].

3. Results

The model (originally tested in argon) was implemented for the NH_3 gas [3]. Addition of the recent dissociative electron attachment (DEA) cross sections [5] emphasized electronegativity in the plasma. This led to a collapse of the plasma either due to (a) the expulsion of the electrons forming an ion-ion plasma, or (b) decoupling from ICP power by transient H-E transition or (c) insufficiently described N_2 reaction schemes. Further analysis indicated that the initial reaction scheme overestimated the electron generation rate due to assumptions on the ionization from excited states of considered NH_3 and H_2 molecules. That possibly led to more frequent DEA collisions under added new reactions that were leading to NH_2^- and H^- ions. Since, the efficiency of the energy transfer through electrons was reduced - the H-E transition is triggered and plasma collapses into an electrically neutral (ion-ion) plasma formation. Under these conditions the NH_3 converts dominantly into N_2 and H_2 fractions. To maintain again an electron driven plasma - an RF power increase is necessary. The transient concentrations of all species are plotted in Fig. 1.

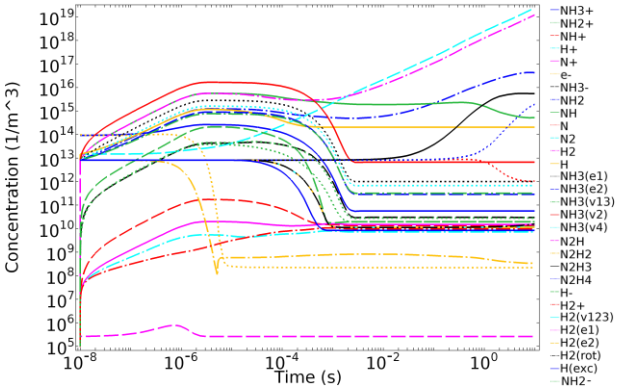

Fig. 1. The transient profiles of charged particles, radicals and neutrals in NH_3 plasma source (90 Pa).

4. Conclusions

The composition and transient reaction pathways in NH_3 plasma are driven by energy transfer efficiency to electrons that are coupled to sustained plasma mode. Recombination processes may lead to conversion into dominant neutral fractions (N_2 and H_2).

3. References

[1] S. Samukawa, K. Sakamoto and K. Ichiki, J. Vac. Sci. Technol. A **20** (2002) 1566.

[2] S. G. Walton and R. F. Fernsler, Plasma Sources Sci. Technol. **18** (2009) 022001.

[3] J. Brcka, 23rd Int. Symp. Plasma Chemistry, Montreal, CA (2017).

[4] J. Brcka, Jap. J. App. Phys. **55**, 07LD08 (2016).

[5] P. Rawat, V. S. Prabhudesai, M. A. Rahman, N. Bhargava Ram and E. Krishnakumar, Int. J. Mass Spectrometry, 277, (2008) 26-102.

The Influence of a Positively Biased Electrode

M. Hopkins[1], B. Scheiner[2], E. Barnat[1], B. Yee[1], S. Baalrud[2]

[1]*Applied Optical and Plasma Sciences, Sandia National Laboratories, New Mexico, USA*
[2]*Physics and Astronomy, University of Iowa, Iowa, USA*

This work reports on our new understanding of the conditions required for an electrode biased above a bulk plasma potential to influence the bulk plasma. One example of a positively biased electrode is a simple Langmuir probe in electron collection mode. Under what conditions does the potential of this electrode influence the bulk plasma? We describe a range of plasma-electrode interfaces (sheath structures), and the relative wall-to-electrode size thresholds that separate them. We include theoretical, experimental, and computational descriptions of sheaths near positively biased electrodes. In particular, we identify the conditions at which the electrode modifies the bulk plasma potential. The modifications to the electron velocity distribution function (EVDF) are investigated, as well as the length scales of that modification (e.g., the electron presheath length scale).

1. Description

As related in [1], based on global current balance arguments, a small positively biased electrode of size A_E in a bulk plasma contained in a grounded vessel of surface area A_W, will have a sheath structure determined by the area ratio A_E/A_W and the mass ratio parameter $\mu = (2.3m_e/m_i)^{1/2}$. In the absence of an electrode, some plasma potential is reached as the loss of electrons and ions to the walls is balanced. Once a positively biased electrode is introduced, however, there is an increased rate of electron loss to it relative to the flux to the grounded wall. This additional electron loss has negligible effect on the bulk plasma if it is sufficiently small. As the electrode area increases, it collects an increasing electron flux, the loss of which results in an increased bulk plasma potential, but still not to the level of the electrode. Continuing to increase the electrode area, and continuing to increase the flux of electrons to the electrode, eventually results in an increased plasma potential that is above the biased electrode. At this point we have an ion sheath at all surfaces, albeit the voltage drop at the electrode is smaller than that at the grounded walls. Simulation [2] and experimental [3] results will be presented.

These transitions occur at approximately $A_E/A_W = \mu$ (electron sheath to an intermediate state), and $A_E/A_W = 1.7\mu$ (intermediate state to ion sheath). The length scale at which the electron sheaths influence the plasma is studied and found to be much longer than previously assumed [4]. The past assumption that the EVDF at the edge of the presheath can be assumed to be half-Maxwellian is found to be incorrect and a new description is provided [5].

Finally, we hope to present some work identifying the role increased electrode potentials have on generating anode spots, and transition/hysteresis effects.

Sandia National Laboratories is a multi-mission laboratory managed and operated by Sandia Corporation, a wholly owned subsidiary of Lockheed Martin Corporation, for the U.S. Department of Energy's National Nuclear Security Administration under contract DE-AC04-94AL85000. This research was supported by the Office of Fusion Energy Science at the U.S. Department of Energy under Contract No. DE-AC04-94SL85000 and the U.S. Department of Energy, Office of Science, Office of Workforce Development for Teachers and Scientists, Office of Science Graduate Student Research (SCGSR) program. The SCGSR program is administered by the Oak Ridge Institute for Science and Education for the DOE under Contract No. DE-AC05-06OR23100.

2. References

[1] S.D. Baalrud, N. Hershkowitz, B. Longmier, Phys. Plasmas **14** (2007), 042109.

[2] M.M. Hopkins, B.T. Yee, S.D. Baalrud, E.V. Barnat, Phys. Plasmas **23** (2016), 063519.

[3] E.V. Barnat, G.R. Laity, S.D. Baalrud, Phys. Plasmas **21** (2014), 103512.

[4] B.T. Yee, B. Scheiner, S.D. Baalrud, E.V. Barnat, M.M. Hopkins, Plasma Sources Sci. Technol. **26** (2017), 025009.

[5] B. Scheiner, S.D. Baalrud, B.T. Yee, M.M. Hopkins, E.V. Barnat, Phys. Plasmas **22** (2015), 123520.

Porous nanostructure thin film titanium dioxide synthesized by atmospheric microwave plasma

M. El Shaer[1], H. H. Afifi[2], M. Mobasher[1], M. Samir[1], M. Habib[1]

[1] *PEARLZ (Plasma & Energy Applications Research Laboratory, Zagazig), Faculty of Engineering, Zagazig University, Zagazig, Egypt*
[2] *National Research Centre, Dokki, Cairo, Egypt*

In certain environmental photocatalysis applications, we use preferably photocatalytic material in form of thin film than in powder. Porous nanostructure thin film structure shows larger treatment area and immobilized nanoparticles. Porous nanostructure TiO_2 is successfully synthesized as thin film by surface wave atmospheric microwave plasma torch in continuous mode at reasonable power. Titanium tetraisopropoxide is used as a precursor and fed into the system using a bubbler under argon flow to deposit TiO_2 thin film on quartz substrate. Raman spectra confirm the formation of anatase phase necessary for photocatalytic activity. UV spectra transmittance percentage decrease, by discharge time increase, indicates appreciable film thickness formation.

1. Introduction

Titanium dioxide (TiO_2) thin film have many applications as photocatalysis and dye-sensitized solar cells, [1]. Porous nanostructure TiO_2 thin film may be very interesting in many environmental applications especially water treatment due to great surface area and immobilized nanoparticles.

A promising technique to synthesize thin layer TiO_2 is atmospheric microwave plasma torch driven by surface-wave.

2. Experimental setup

Plasma is generated by a waveguide atmospheric plasma torch driven by surface-wave as in Fig. 1. The source consists of 2.45 GHz microwave generator for which incident and reflected power are optimized to couple 300 W in plasma.

Titanium Tetraisoproxide (ACROS Organics, +98% purity) is nebulised into a quartz discharge tube 30 cm long and 8 mm inner diameter in which plasma is formed under argon gas flow.

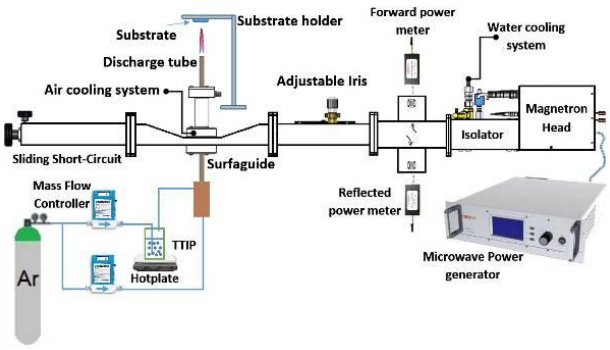

Fig. 1, Microwave plasma torch driven by surface wave

3. Results

For TiO_2 thin film synthesized on a quartz plate, Raman spectrum is shown in Fig. 2.

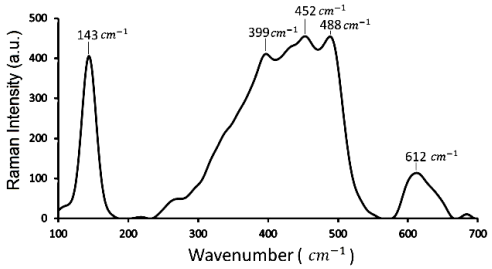

Fig. 2, Raman spectrum of anatase TiO_2 thin film

The bands shown at 143, 397, 452, 488, and 612 cm^{-1} characterize TiO_2 anatase phase formation. UV-VIS spectra for synthesized TiO_2 thin films on quartz substrate are measured taking air as reference at different deposition times. In Fig. 3, transmittance percentage in the UV spectrum in the range 200 to 400 nm, decreases as deposition time increases due to larger film thickness formed on substrate.

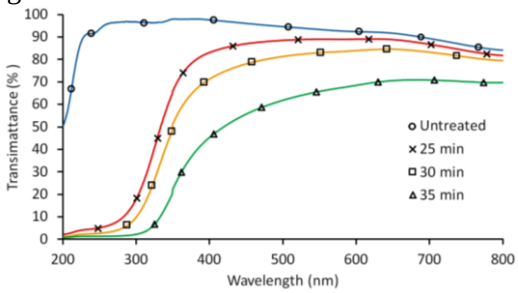

Fig. 3, UV-Vis transmission spectra for TiO_2 thin film

4. Conclusion

Synthesis of thin film porous nanostructure TiO_2 of appreciable thickness is obtained by atmospheric microwave torch at moderate power.

5. References

[1] Y. Gazal, C. Dublanche-Tixier, C. Chazelas, M. Colas, P. Carles, P. Tristant, Thin Solid Films, 600 (2016) 43–52

Topic number

On the electrical properties of the surface DBD and its effect on the resonant power source operation

I. Moralev[1], I. Selivonin[1,2]

[1] *Joint institute for high temperature RAS, Moscow, Russia*

[2] *National research university «MPEI», Moscow, Russia*

The effect of the discharge on the resonant voltage source was studied analytically. The discharge was included into the resonant circuit as a variable capacitor with explicit function $C_p(t)$. This equation was obtained prom charge-voltage cycle The analysis of the resulting linearized equation for voltage perturbation by the discharge was performed by expanding the $C_p(t)$ function into Fourier series and deriving the appropriate coefficients for the harmonics of the perturbation. The aforementioned approach led to the determination of the mean surface charge, voltage decrease, power consumption, voltage nonlinearity, derived as combinations of Fourier coefficients of C(t) function.

Dielectric barrier discharges in surface configuration is widely used in a number of applications, from plasma chemistry to aerodynamics. The key characteristics of the barrier discharge, describing both dissipated power and charge amplitude, is a charge-voltage cycle (CVC). The CVC for surface discharges was studied qualitatively in [1]. The main goal of this work is to built the quantitative physically reasonable model of the system discharge load- power source The work summarizes the measurements of the CVC shape for a wide range of parameters, including operation voltage properties and electrode material and provides a theoretical analysis of the interaction between the discharge load with the resonant output circuit of the power source.

The CVC was measured for a sinuous voltage with various amplitude in the range 0.1-100 kHz, for various electrode materials. It is shown, that for a sufficiently high voltage the shape of the CVC can be described as a piecewise function, including the two "silent "regions and two parabolic regions for forward and backward strokes (fig.1).

The additional capacitance of the discharge can be modeled as $C_p(t)=dQ/dU$ in accordance to [1].For lower voltage, the shape of the CVC in a backward stroke phase was shown to depend on the frequency of the supply voltage and the exposed electrode material.

The effect of the discharge on the resonant voltage source was studied analytically. The discharge was included into the resonant circuit as a variable capacitor with explicit function $C_p(t)$.

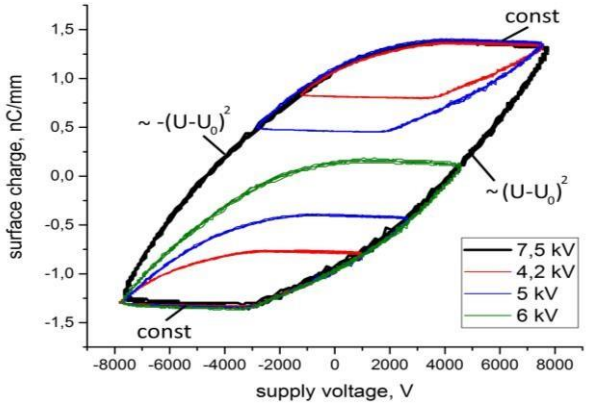

Fig.1 Charge-voltage cycle for different supply voltages

The analysis of the resulting linearized equation (1) for voltage perturbation by the discharge was performed by expanding the $C_p(t)$ function into Fourier series and deriving the appropriate coefficients for the harmonics of the perturbation.
The aforementioned approach led to the determination of the mean surface charge, voltage decrease, power consumption, voltage nonlinearity, derived as combinations of Fourier coefficients of C(t) function.

$$q_p^{"} + q_p\omega_0^2 - \frac{C_p}{C_0}\frac{U_{0a}}{L}sin(\omega t) = 0 \qquad (1)$$

References

[1] J. Kriegseis, S. Grundmann, and C. Tropea, *J. Appl. Phys.*, vol. 110, no. 1, p. 13305, 2011.

Simulations of dust charging and wake formation in magnetized plasmas

W. J. Miloch[1]

[1] *Department of Physics, University of Oslo, Box 1048 Blindern, N-0316 Oslo, Norway*

Dust grains in plasmas acquire electric charge and interact with each other via screened Coulomb (Yukawa) potentials. External magnetic field can influence the charging of dust grains and plasma in their vicinity. This can have implications for the structuring and dynamics of complex (dusty) plasmas. This work presents results from numerical particle-in-cell (PIC) simulations of charging of a single dust grain in magnetized plasmas. Different strengths of magnetic field are considered for both stationary and flowing plasma conditions. Structural properties of the wake, and the wake effects on the interaction between the dust grains are addressed. It is demonstrated that the wake size and the potential structures in the wake, and hence the electric fields, can be significantly affected by the magnetic field.

1. Introduction

Dust grains immersed in plasma are charged by plasma and other currents. Studies of potential and plasma density distributions on and around charged grains in flowing plasmas are essential for the understanding of dynamics of complex (dusty) plasmas [1]. Plasma flows will break the symmetry of charging and lead to formation of wake. This can influence interactions between grains and align them in the direction of the flow [1, 2].

Another reason for the symmetry breaking in dust charging is the magnetic field that restricts the dynamics of plasma. It has been demonstrated in experiments that magnetic field can significantly modify the nonreciprocal dust interactions [3]. The dynamics of systems comprising many grains can significantly differ from the unmagnetized case [4]. However, charging in either weakly or strongly magnetized plasmas is still not well understood.

To understand interactions between many grains in magnetized plasmas, it is crucial to understand the charging of a single grain and wake formation. This work presents first results from particle-in-cell (PIC) simulations of dust charging in magnetized plasmas. The study is carried out with the DiP3D code [2].

2. Results

In the present simulations, the plasma parameters are typical for laboratory dusty plasma experiments, the flow is supersonic, and the magnetic field is considered as a variable parameter. The wake size and strength can be significantly affected by the magnetic field, see Figure 1. Strong magnetic fields diminish ion focusing, and the corresponding potential maxima in the wake become smaller. On the other hand the potential oscillations in the wake get more pronounced, with strong negative minima downstream from the grain. For the considered magnetic fields, the charge on the grains is only little affected and is similar to the unmagnetized case. The changes in the potential distribution and the topology of the wake due to external magnetic fields can have important effects on the interactions between grains and charging of downstream grains.

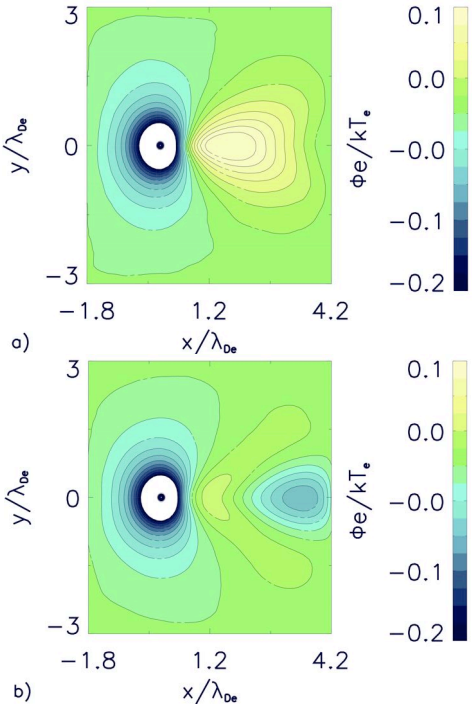

Figure 1: *Potential distribution behind dust grains in supersonic plasma flows (1.2 Mach) for the electron to ion temperature ratio T_e/T_i=100 and magnetic field aligned with the flow of B*=5 Gs *(a), and B*=100 Gs *(b). The flow is in the positive x-direction. In both cases the potential on the grain is* Φ≈-1.1*e/kTe. In the figure only shallow potential variations are shown.*

3. References

[1] P. K. Shukla, A. A. Mamun, *Introduction to Dusty Plasmas* (IOP, Bristol, 2002).

[2] W.J. Miloch, M. Kroll, D. Block *Phys. Plasmas* **17** 103703 (2010).

[3] J. Carstensen, F. Greiner, A. Piel, Phys. Rev. Lett. **109**, 135001 (2012).

[4] T. Ott, H. Löwen, M. Bonitz, Phys. Rev E **89**, 013105 (2014).

Flame initiation in C_2H_2-air mixture in the cathode layer of nanosecond SDBD

E.A. Filimonova, A.N. Bocharov, V.A. Bityurin

Joint Institute for High Temperatures of RAS, Moscow, Russia

In the given work the feasibility of hydrocarbon-air mixture ignition by one nanosecond pulse of the surface dielectric barrier discharge (SDBD) is considered. The goal of work was to define the conditions of a stoichiometric C_2H_2-air mixture ignition and the combustion wave formation before the cathode area is cooled by transferring the heat on the metal electrode and dissipation of it in the unperturbed gas. The range of temperatures (depend on specific deposited energy values) and active species concentrations for the formation of combustion wave have been determined. The important role of gas-dynamics is shown.

1. Introduction and statements

In a number of works the SDBD is suggested to use as an initiator of combustion in an internal combustion engine. The ignition of fuel-air mixture in a single shot regime of SDBD and propagation of combustion wave is demonstrated in experiments [1]. The conclusion about ignition of mixture close to high voltage electrode has been made on the basis of 2D modelling of SDBD and estimations of ignition threshold [1]. However, it's not enough to talk about the formation of combustion wave.

The present work is devoted to the study of inflammability conditions and subsequent formation of combustion wave in C_2H_2-air mixture at P=1 bar and T_0 = 300 K in the near-cathode area of SDBD by one nanosecond pulse. 1D numerical modelling based on the solving of Navie-Stocks equations for the whole mixture, the Poisson equation for the electric field [2] and chemical kinetics [3] was executed. The discharge was considered as a source of active particles and heating of the mixture. The specific power deposited in the cathode layer with the width of Δx=0.01 mm was described as follows:

$$W(t)=E_0\pi/2\tau\cdot\sin(\pi t/2\tau)/\Delta x,$$

where E_0 is an amplitude of deposited energy and τ=40 ns is the pulse duration of discharge. At the end of discharge pulse the concentration of O atoms resulting from dissociation of oxygen by electron impact and quenching of excited N_2 was specified.

2. Results of modelling

The mixture ignition and formation of combustion wave depend on two values: a specific energy deposition per pulse Q and an initial concentration of O atoms. The process of ignition (increasing the gas temperature at t=30-40 μs) and combustion wave formation (widening of temperature profile) is shown in figure. The map of formation/non-formation of combustion wave has been drawn in Q-$[O]_0$ coordinates. Only heating the cathode layer does not bring to inflammation. The presence of O atoms is necessary. To simulate a flame initiation in the discharge systems with a high energy release, the gas-dynamic expansion of hot region and its cooling by heat transfer to the surface of metallic electrode is important to consider. 0-D approach may bring to an inaccurate result.

It was found that combustion is passing through the conversion of fuel to CO and H_2 which burn down later with the production of CO_2 and H_2O. The NO concentration amounts to 0.1-0.2% behind of front of combustion wave.

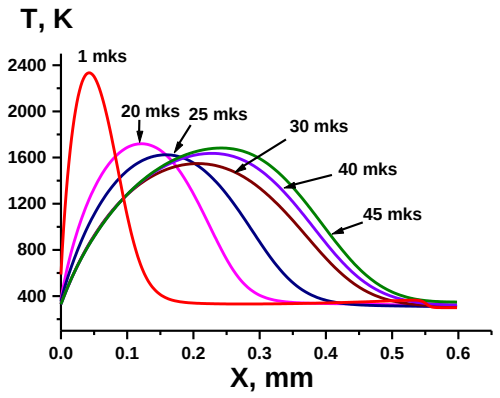

Fig. Formation of combustion wave at Q=5.48 J/cm^3 (1.4 eV/molecule) and $[O]_0$=11.7%.

This work was supported by LIA KaPPA-RFBR Grant No 17-53-16003-a (France- Russia).

3. References

[1] E.M. Anokhin, D.N. Kuzmenko et al. Plasma Sources Sci. Technol. **24** (2015) 045014.

[2] V.A. Bityurin, A.N. Bocharov, Popov N.A. AIAA 2007-0223 Paper (2007).

[3] E.A. Filimonova. J. Phys. D: Appl. Phys. **48** (2015) 015201.

A study of N_2H^+ dominated afterglow plasma using cavity ring-down spectroscopy

P. Dohnal[1], Á. Kálosi[1], Š. Roučka[1], R. Plašil[1], J. Glosík[1]

[1] *Department of Surface and Plasma Science, Faculty of Mathematics and Physics, Charles University in Prague, V Holešovičkách 2, 18000 Prague, Czech Republic*

The first results of experimental study on recombination of N_2H^+ ions with electrons are presented. A stationary afterglow setup equipped with cavity ring-down spectrometer as a main diagnostics tool was used to probe the time evolutions of several rotational states of the vibrational ground state of N_2H^+ ion in discharge and afterglow plasma. A particular attention was given to ascertain that kinetic and rotational temperature of the ions in afterglow is close to the buffer gas temperature. A possibility of helium or H_2 assisted three body recombination channel was taken in to account during the data evaluation. The obtained results will be compared to experimental data from other groups and to the theoretical calculations.

1. Introduction

N_2H^+ was one of the first molecular ions detected in interstellar space [1]. It was observed towards cold dark clouds and protostellar cores and can serve as a probe for determination of physical conditions therein. Especially as a tracer for N_2, that is difficult for direct astronomical observation [2].

The recombination of N_2H^+ molecular ions with electrons was also studied by many groups in different types of experiments [3,4,5]. These results differ by more than order of magnitude.

2. Experiment

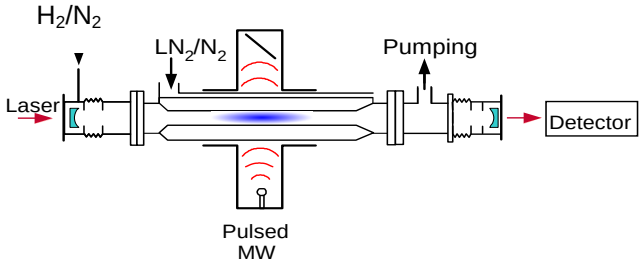

Fig 1. Stationary afterglow with the CRDS absorption spectrometer: SA-CRDS (not to scale). In the middle part of the fused silica discharge tube a discharge is periodically ignited in the microwave resonator (MW, 2.5 GHz, 4–15W). A gas mixture (H_2/N_2 in the figure) is used to form a plasma containing the desired ionic composition. The discharge tube is cooled by liquid nitrogen (LN_2) or by precooled nitrogen vapours.

A stationary afterglow apparatus equipped with cavity ring-down spectrometer (SA-CRDS, for details on the current apparatus and diagnostic technique see reference [6] and Fig. 1) was employed in the experiments. The N_2H^+ ions were produced in a pulsed discharge in a gas mixture of $He/H_2/N_2$ or H_2/N_2. We were able to follow the time evolutions of number densities of different quantum states of studied ions in discharge and afterglow plasma. The kinetic temperature of the ions was determined from the Doppler broadening of the absorption lines while the rotational temperature was calculated from the relative populations of different states of particular ion.

3. Conclusions

Several overtone transitions of N_2H^+ molecular ion in the near infrared spectral region were probed and we have measured the kinetic and rotational temperature of these ions and their evolution in discharge and afterglow plasma. The first results on recombination of N_2H^+ ions with electron will be presented at the conference.

4. Acknowledgement

This work was partly supported by Czech Science Foundation projects GACR 17-08803S and GACR 15-15077S.

5. References

[1] P. Thaddeus et al., Astrophys. J. **201** (1975) L25.

[2] E. Herbst et al., Astrophys. J. **215** (1977) 503-510.

[3] T. Amano et al., J. Chem. Phys. **92** (1990) 6492.

[4] V. Poterya et al., J. Phys. Chem. A **109** (2005) 7181.

[5] E. Vigren et al., Astrophys. J. **757** (2012) 34.

[6] P. Dohnal et al., J. Chem. Phys. **136** (2012) 244304.

Evaluation of plasma parameters during the explosive electron emission pulse of vacuum arc cathode spot cell

M.M. Tsventoukh[1]

[1] *Lebedev Physical Institute of Russian Academy of Sciences, Moscow, Russia*

A simple complete model of the explosive emission pulse of the cathode spot cell has been proposed that involves both – the ignition and the decay of the explosive plasma. The ignition is due to the hydrodynamic tearing of the liquid metal jet, propagating into the plasma generated by the preceding explosive cell. The decay is due to the plasma expansion and the density decrease down to the initiation one. The explosion per se is treated as the transition of the jet material over the critical state.

The average parameters of the plasma have been evaluated. In particular, the plasma basic parameters – the density and temperature are about 10^{20} cm^{-3} and 1 eV respectively.

The ratio of the average pressure to the average current density has been evaluated

$$\langle p\rangle/\langle j\rangle \approx n_0\, T_{cr} / j_{\max},$$

where n_0 is the initial (liquid-metal) density, T_{cr} is the critical temperature, and $j_{\max}$ is the maximal current density during the tearing that is about few GA/cm^2. This ratio gives a specific plasma acceleration force, and the obtained value that is about tens of g cm / C s agrees with the measured recoil force and with the product of measured ion velocity and erosion rate, $v_i \times \gamma_i$.

The average ohmic electric field $\langle E\rangle = \langle j/\sigma\rangle$ has been found to be several tens of kV/cm. This field is responsible for the current transfer through the explosive plasma and, hence, the cathode potential fall formation. For the known cathode potential fall, the corresponding specific plasma size is several micrometers. Such a plasma is formed after the explosion of the entire liquid-metal jet. In addition, the total current flowing through an exploding liquid-metal jet has been estimated to be some amperes.

Finally, a general estimate of the plasma-to-magnetic pressure ratio $\beta = 8\pi p/B^2$, for a current-carrying plasma column has been derived

$$\beta\, \kappa^2\, n\, R^2 = 4 m_e c^2/e^2 = 1.41*10^{13}\ \text{cm}^{-1}$$

(where $\kappa = j\sqrt{\frac{2\pi m_e}{T_e}} / en < 1$ is the current fraction) that indicates that the column compression by a magnetic field ($\beta < 1$) takes place only for large-scale low-density plasmas ($n\, R^2 > 10^{14}$ cm^{-1}), such that occurs far from explosive cells.

Recall that we have considered likely lowest plasma density – near the initiation threshold (10^{18} cm^{-3}) and have derived nearly the maximal current density (exceeding 1 GA/cm^2). One should stress that there is no issues of the space charge emission limitation as the current of this density flows inside a tearing liquid-metal jet.

Work was supported in part by RFBR grants # 15-38-20617-mol_a_ved, 16-08-01306-a and by Dmitry Zimin Dynasty Foundation at 2015 PhD grant.

On steep gradients in plasmas confined at convex-concave magnetic field lines near the minimum in the longitudinal adiabatic invariant

M.M. Tsventoukh[1], A.V. Kaziev[2]

[1] *Lebedev Physical Institute of Russian Academy of Sciences, Moscow, Russia*
[2] *National Research Nuclear University MEPhI, Moscow, Russia*

The formation of large stable plasma gradients, e.g. in form of internal transport barriers, being of a strong both practical and fundamental interest. Normally the larger the gradient the larger the transport, and any deviation due to collective plasma behavior is of great interest.

We have predicted theoretically that there is a strong stabilizing action against convective (flute-interchange) perturbations when plasma is confined by magnetic field of alternating-sign curvature – i.e. with convex–concave field lines [1]. The calculations that have been done for simple combinations of axisymmetric mirrors and cusps according to the kinetic stability criterion, give strongly centrally peaked stable plasma pressure profiles instead of shallow ones.

Connection of the convex and concave field line parts results in a reduction of the space charge that drives the unstable $\boldsymbol{E} \times \boldsymbol{B}$ motion, as there is an opposite direction of the particle drift in a non-uniform field at convex and concave field lines. The pressure peaking arises at the minimum of the second adiabatic invariant $J = \int v_{\parallel}\, \mathrm{d}l$ that takes place at the 'middle' of a tandem mirror–cusp transverse cross-section. Recall that there has been proposition by Arsenin [2-3] that there is a plasma interchange stability due to the alternating-sign curvature.

The simple ideal MHD description gives a strong variation in the stable pressure profile due to the strong variation in the specific volume $\int \mathrm{d}l/B$: the critical profile being $p_{MHD} \propto (\int \mathrm{d}l/B)^{-5/3}$. However, we have found that there is a strong variation in the stable pressure profile at regions of almost equal specific volume – near min $\int \mathrm{d}l/B$, with curvature of alternating sign – with appropriate combination of the convex and concave field line parts.

Instead of the well-known max$J$ principle of the plasma stabilization [4], we have proposed that there is an additional stability of the plasmas nearby the field lines layer of the min$J$. Recall that in tokamak max$J$ region nearly corresponds to the region near the axis within min$q$ [5]. As the minimum in the q nearly corresponds to the minimum in the J, one would expect somewhat reduction in the plasma convective transport near min$q$ according to the mechanism proposed.

We have performed an experimental investigation of the plasma confinement at magnetic confinement device of the alternating-sign curvature [6].

For the experimental research of this effect, a compact magnetic confinement device has been modified by adding of the external current coil to fulfil the field-line curvature requirements. The critical convectively-stable plasma pressure profiles calculation in this experimental geometry and the probe measurements of the spatial plasma distribution in the new magnetic configuration of alternating-sign curvature have been performed.

The experimental results give some support for a conclusion that there is an increase in the ion saturation current at the region near the minimum of the specific volume min $\int \mathrm{d}l/B$. This region corresponds to the average minimum in the second adiabatic invariant, and the kinetic description predicts the stable pressure profile peaking here due to reduction of charge separation by particle drift in alternating-sign curvature.

For further experimental investigations, a stationary microwave device has been used. A mirror geometry has been created by axisymmetric coils, Langmuir and magnetic probes have been used for the measurements.

Work was supported in part by RFBR grants # 15-38-20617-mol_a_ved, 16-08-01306-a and by Dmitry Zimin Dynasty Foundation at 2015 PhD grant.

[1] Tsventoukh 2014 *Nucl. Fusion* **54** 022004
[2] Arsenin V.V. 1983 *JETP Lett* **37** 637
[3] Arsenin V.V. 1986 *JETP Lett* **43** 346
[4] Marshall N. Rosenbluth 1968 *Physics of Fluids* **11** 869
[5] B.B. Kadomtsev 1966 *JETP Lett* **4** (1) 10
[6] Tsventoukh *et al* 2015 *Nucl. Fusion* **55** 062001

Parallel computing of multidimensional hypersonic re-entry flows considering a state-to-state description

M. Castela[1], B. Lopez[1,2], and M. Lino da Silva[1]

[1] *Instituto de Plasmas e Fusão Nuclear, Instituto Superior Técnico, Universidade de Lisboa, Lisboa, Portugal*
[2] *University of Illinois at Urbana-Champaign, Urbana, IL 61801, USA*

The present study aims at assessing and improving the scalability of the recently developed SPARK code. Accurate predictions of hypersonic re-entry flows, surrounding an inter-planetary exploratory spacecraft, are still extremely difficult due to the high coupling between non-equilibrium processes, radiation and the near-flow field during the entry of a spacecraft in a planetary atmosphere. A high-fidelity simulation of these stringent aerothermodynamics conditions is still CPU limited and requires parallel computations. In the framework of the preparatory access to PRACE research infrastructure (Partnership for Advanced Computing in Europe), a 2D-axyssimetric simulation with state-specific chemical description was performed in order to access SPARK scalability tests in extremely demanding computational conditions. Both the numerical simulations and the code scalability tests will be presented.

1. Introduction

Physical-chemical processes occuring in extremely nonequilibrium atmospheric entry flows can only be adequately modelled through a state-to-state description. Yet, coupling of CFD models with state-specific descriptions remains a daunting task.

SPARK aims at improving the prediction capability of numerical simulations of a wide range of applications. For instance, aerothermodynamics properties for hypersonic re-entry flows and thermal heat fluxes have been numerically studied in by [1] using SPARK. Two distinct classes of physical models are implemented in SPARK, enabling the simulation of gas thermodynamics in non-equilibrium conditions considering either multi-temperature models or state-specific models.

2. Numerical setup

The model is implemented in the in-house SPARK solver (Software Package for Aerodynamics, Radiation and Kinetics) [1] dedicated to compressible aerothermodynamics simulations with detailed chemistry, multi-temperature models and state-specific species characterization. SPARK is written in Fortran 03/08 and explores newly supported object-oriented features, enabling the encapsulation of different physical models, numerical methods, mesh-related operations and interface communications by means of derived-types and type-bound procedures.

A 2D-axisymmetric computational domain of a sphere-cone aero-shell geometry is considered. About 10 thousand volume cells are used for the computational domain discretization. A first convergence run is performed using an initial uniform mesh in order to adapt the mesh at the shock boundary layer. It then follows a second convergence run for the final mesh configuration. The mesh is divided into multiple blocks, which allows for multicore parallel computation. Each block having the same computational load, characterized by an evenly distributed number of volume cells. A second-order finite volume scheme is used for spatial discretization. Time integration of convective terms is performed explicitly using a second-order scheme. The system is marched in time towards convergence. A 5-species air mixture (N2, O2, NO, N and O) with a vibrational state-specific description of the molecular species is considered. The chemical model requires handling over 150 internal states and over 15 000 reactions. A very small CFL is required due to the stiffness of the chemical source terms near the shock boundary layer. The code is parallelized using Coarray Fortran feature, based on the Simple Program Multiple Data model, where each replication of the program is called an image.

3. Acknowledgements

IPFN activities received financial support from Fundacão para a Ciencia e Tecnologia through project UID/FIS/50010/2013. We acknowledge PRACE for awarding us access to computing clusters.

3. References

[1] B. Lopez and M. Lino da Silva, 46th AIAA Thermophysics Conference, 13–17 June 2016, Washington, D.C, 2016-4025.

A reinvestigation on the energy levels of CO2 up to the dissociation limit

J. Vargas[1], B. Lopez[1,2], and M. Lino da Silva[1]

[1] *Instituto de Plasmas e Fusão Nuclear, Instituto Superior Técnico, Universidade de Lisboa, Lisboa, Portugal*
[2] *University of Illinois at Urbana-Champaign, Urbana, IL 61801, USA*

The energy levels of the radiative states of CO2 have been extensively studied, and several very accurate databases such as HITRAN/HITEMP or CDSD exist in the literature. However, knowledge on the near-dissociation levels of CO2 is lacking due to the absence of experimental data, or the fact that transitions from these higher-lying levels are hidden by the strongest transitions of lower levels. This study proposes to achieve a better prediction of these states through potential reconstruction methods.

1. Introduction

State-to-state modelling of CO2 vibrational excitation processes is a current "hot-topic" in view of such diverse applications like plasma reforming of CO2 [1] and the modelling of atmospheric entries in Mars and Venus [2]. Typical modelling activities have thus far delved on the legacy from state-to-state modelling of atomic and molecular diatomic plasmas, with preliminary simulations being rather successful in reproducing experimental data. Indeed, the treatment of such a triatomic molecule like CO2 may be simplified with some baseline assumptions like the separability of its three internal modes and the determination of its levels up to dissociation through polynomial models [1]. However, if the accuracy of such approaches is to be increased, improved methods for the calculation of the overall manifold of vibrational levels needs to be achieved, based on potential reconstruction techniques.

2. Potential reconstruction methods

Lower-lying levels of CO2 are accurately described to the 10^{-2} cm^{-1} by such databases like HITRAN [3] or CDSD [4]. From these extensive databases of levels, potential reconstruction methods have been developed by Huang et al. at NASA Ames to determine an accurate potential curve up to 25,000 cm^{-1} [5]. Examples for the assymmetric stretch and bending modes of CO2 are fresented in Fig. 1. This potential curve serves as the baseline for this work. Here we will present an adequate extrapolation of the 3 modes of CO2 up to the dissociation limit by adequate long-range potentials. Near-dissociation levels will then be determined by solving the adequate radial Schrödinger equation on such potentials. The resulting extrapolated levels will follow a smoother and more realistic distribution up to the dissociation limit than the traditional polynomial expansions.

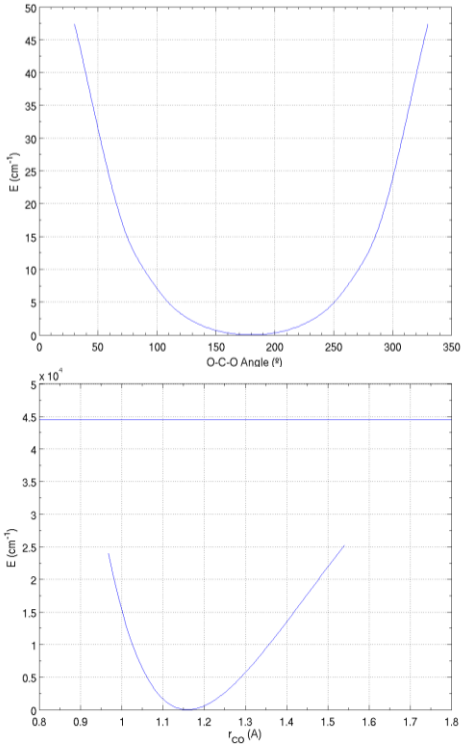

Fig 1: Asymmetric stretch and bending energies of CO2

3. Acknowledgements

IPFN activities received financial support from Fundacão para a Ciencia e Tecnologia through project UID/FIS/50010/2013, and through grant PD/BD/114325/2016 under the APPLAUSE Ph.D programme.

3. References

[1] T. Kozak, Plasma Sources Sci. Tech., 23(4), 2004, pp. 045004.

[2] A. Sahai et al., 2016, AIAA 2016-3695.

[3] L.S. Rothman, R.L. Hawkins, R.B. Wattson, R.R. Gamache, JQSRT, 48(5), 1992, pp. 537-566.

[4] S.A. Tashkun, et al., JQSRT, 112(9), 2011, pp. 1403–1410.

[5] X. Huang et al., J. Chem. Phys., 136(12), 2012, pp. 124311.

Radiation of FM-signal by plasma asymmetrical dipole antenna

S. E. Andreev[1,3], N .N. Bogachev[1,2,3], N. G. Gusein-zade[1,2,3]

[1] *Prokhorov General Physics Institute of the Russian Academy of Sciences, Moscow, Russia*
[2] *Medicobiologic faculyt, Pirogov Russian National Research Medical University (RNRMU), Moscow, Russia*
[3] *Moscow technological university (MIREA), Moscow, Russia*

The actual problem of the development of plasma antennas is a study of the signal radiation. Previously, we had investigated the spectra of the non-modulated signal, which had been radiated by plasma asymmetrical dipole antenna. Amplitudes at multiple frequencies of the input non-modulated signal frequency had been amplified by plasma antenna. In this work, we have experimentally studied the radiation of a frequency modulated signal (FM signal) by plasma asymmetric dipole antenna. We have obtained spectra of the FM signal, which have been radiated by plasma antenna and by same metal antenna. These spectra were compared to each other for analysis of signal nonlinear distortions. Discovered distortions of radiated FM signal from plasma antenna are inappreciable.

Plasma antenna is type of antennas, in which plasma is used as waveguide, radiated or control element [1-7]. Studies of plasma antennas aim to solving problems of modern radio engineering, such as the invention of intelligent antennas with fast reconfigurable antenna characteristics; radar visibility decrease of the antenna devices of military objects and equipment; the security improving of radio systems from the effects of electronic warfare and destruction by atmospheric electrical discharges.

The plasma antenna can be divided into several classes: plasma antenna of discharge tubes; solid-state plasma (silicon) antenna (PSiAn); jet plasma antenna and others. The biggest and most promising class is plasma antennas of the discharge tubes. In this paper we study the plasma asymmetrical dipole antenna (PADA) to the discharge tube [1-7]. One is much the same as a metal asymmetrical dipole antenna (MADA), and consists of a rod (dipole arm), which connect to the central conductor of the coaxial cable, and a conductive disk (screen), which connect to the outer conductor of the coaxial cable. In the case of a plasma antenna metal rod is replaced by a gas discharge tube with plasma. The optimal length of antenna arm is considered quarter wave $l_a=\lambda/4$.

In [7] we had investigated the spectra of the non-modulated signal, which had been radiated by plasma asymmetrical dipole antenna. Amplitudes at multiple frequencies of the input signal frequency had been amplified by plasma antenna.

In this work, we have experimentally studied the radiation of a frequency modulated signal (FM signal) by plasma asymmetric dipole antenna. The experimental setup scheme of FM signal spectra measurements is presented on fig. 1. Modulating signal go from the message source (1) to the broadcast set VX-2100 (2). FM modulated signal from (2) go to the plasma or metal antenna (4) situated on the positioner (3). The plasma or metal antenna radiates signal and the measure antenna (5) receives signal. Amplitude spectrum of FM signal is shown on the screen of spectrum analyzer Agilent PXA N 9030A (6).

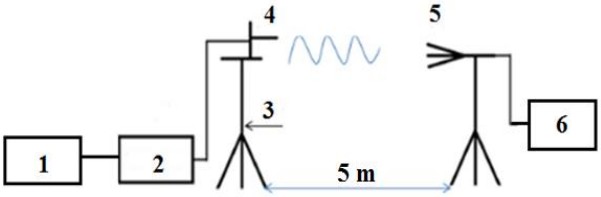

Fig 1. Scheme of the experimental setup.

We have obtained spectra of the FM signal, which have been radiated by plasma antenna and by same metal antenna. These spectra were compared to each other for analysis of signal nonlinear distortions. Discovered distortions of radiated FM signal from plasma antenna are inappreciable.

The studies was supported by Russian Foundation for Basic Research (RFBR), project number is 16-08-00859 a.

[1] G. G. Borg, J. H. Harris, et. al. Applied physics letters **74** (1999) 3272.

[2] J. P. Rayner, A. P. Whichello, A. D. Cheetham, IEEE Trans. on plasma science **32** (2004) 269.

[3] E. N. Istomin, D. M. Karfidov, et. al., Plasma Phys. Rep. **32** (2006) 388.

[4] J. W. Lv. Li Y. Song, Li Z. Chen WSEAS Transactions on Communications **10** (2011) 323.

[5] Z. Kiss'ovski, V. Vachkov IJEAT **5** (2016) 330.

[6] B. A. Belyaev, A. A. Leksikov, et. al., IEEE Trans. on Plasma Science **42** (2014) 1552.

[7] N. N. Bogachev, I. L. Bogdanevich, and N. G. Gusein-zade, 10th EuCAP (2016) doi: 10.1109/EuCAP.2016.7481512

Modes of unipolar and bipolar pulsed discharges in CO_2

V.A. Lisovskiy[1], S.V. Dudin[1], P.A. Ogloblina[2], N.N. Vusyk[1], V.A. Volkov[1], V.D. Yegorenkov[1], A.N. Dakhov[1]

[1] *Kharkov National University, 61022, Kharkov, Svobody Sq. 4, Ukraine*
[2] *Instituto de Plasmas e Fusão Nuclear, Instituto Superior Técnico, Universidade de Lisboa, Lisboa, Portugal*

This paper reports the studies of unipolar and bipolar pulsed discharges in CO_2 in the pressure range from 0.1 to 1 Torr, the frequency range from 20 to 300 kHz and duty cycle values from 12 to 96%. We have demonstrated that with the pressure, frequency, inter-electrode distance and applied voltage fixed one may obtain different discharge structures only by varying the duty cycle values. For example, a unipolar discharge may contain the cathode sheath and the negative glow as well as the above regions and the additional dark Faraday space, the positive column and the anode glow. The unipolar and bipolar pulsed discharges may exist in two modes: one possessing a low discharge current and a diffuse positive column and another one possessing a high current and a contracted stratified positive column.

Pulsed gas discharges are widely applied in lasers, plasma display panels, for plasma nitriding, in light sources etc. Presently a great attention is devoted to the processes taking place in CO_2 plasma because this gas causes the greenhouse effect and because it is prevalent in the atmospheres of some planets and satellites of the Solar system. Therefore we have studied the modes of the unipolar and bipolar pulsed discharges in low pressure carbon dioxide discharge.

Experiments have been performed in the device with flat stainless steel electrodes located inside the discharge tube with the inner diameter of 56 mm, the inter-electrode distance being from 10 to 380 mm. A pulsed unipolar (negative rectangular) or bipolar potential from the generator in the 20–300 kHz frequency range, the duty cycle from 12 до 95 % and applied voltage values up to 1200 V has been fed to the electrodes. The range of the measured discharge current values did not exceed 200 mA. The CO_2 pressure values were from 0.1 Torr to 1 Torr.

We have revealed that an option of varying the frequency and the duty cycle in the pulsed discharge enables one to get not only different current values but to change the discharge structure in the broad range. Thus, keeping the gas pressure, the inter-electrode distance and the voltage applied across them one may get a unipolar discharge consisting of different parts by changing only the duty cycle values. With the duty cycle below 50% one observes the cathode sheath and the negative glow whereas at higher duty cycle values there appear, apart from the above ones, the dark Faraday space, the positive column and the anode glow. Similarly, one may change the bipolar discharge structure substantially varying the duty cycle, the negative glows near the both electrodes may be either symmetric with respect to the discharge center with the duty cycle about 50%, or a brighter negative glow would adhere to one of the electrodes (to which a short pulse of high voltage is fed), and near the other electrode (with a long pulse of low voltage) this glow may be absent.

Note also that the unipolar and bipolar discharges may exist in two modes: one with the low discharge current and a diffuse positive column and another one with a high current and a contracted stratified positive column. In the unipolar discharge the diffuse mode is observed in long inter-electrode gaps and with high values of the duty cycle, i.e. 80% and higher. In the bipolar discharge the diffuse mode takes place at the duty cycle values from 80% to 50% for the frequency of 20 kHz and this range narrows from 80% to 70% for the frequency of 200 kHz. In the high current mode the positive column (if it fits the inter-electrode distance) is usually contracted consisting of a multitude of narrow striations. The presence of such striations usually indicates that the positive column contains a large number of negative ions. In a diffuse positive column with a low discharge current the conversion of CO_2 molecules probably is much less efficient than in a contracted column with a strong current. This is also pointed out by the fact that the reduced electric field in the positive column in the low current mode amounts to about 15 V/(cm Torr), and in the high current mode it grows about twice as large.

ESTHER: A laser-ignited, combustion-driven, two-stage shock-tube for the simulation of hyperbolic planetary entries

M. Lino da Silva[1], B. B. Carvalho[1], R. Rodrigues[1], M. Castela[1], A. Smith[2], A. Chikhaoui[3], and L. Marraffa[4]

[1] *Instituto de Plasmas e Fusão Nuclear, Instituto Superior Técnico, Universidade de Lisboa, Lisboa, Portugal*
[2] *Fluid Gravity Eng., Hampshire, United Kingdom*
[3] *Université Aix-Marseille, Marseille, France*
[4] *ESA / European Space Research and Technology Centre, Aerothermodynamics Section, Noordwijk, The Netherlands*

A new shock-tube facility is being developed by an international consortium led by IST-IPFN, under funding from the European Space Agency. This facility encompasses several key innovations which allows reaching almost unparalleled performance (being capable of shock-speeds above 12km/s) alongside with improved repeatability and cleanliness specifications, made possible by the development of a laser-driven "clean" H2/He/O2 combustion driver, a technology that has been implemented for the first time in a shock-tube facility. A scale test model has been developed to validate this concept, and has allowed reaching successful deflagrations of mixtures up to 100bar filling pressures, for a final combustion pressure in excess of 600bar. Careful tailoring of the gas mixture has allowed avoiding the outset of detonations, providing a very reliable and repeatable proof-of-concept setup for the ESTHER driver section.

1. Outline

An 1064nm Nd:Yag laser has been deployed on the ESTHER test bombe, with the testing of several dilution ratios from He (from 50% to about 80%) and with lean and rich mixtures. The obtained pressure signals (see Fig. 1) have shown that an He dilution around 70% with a lean (O2 rich mixture) allow avoiding the outset of detonation, leading to smooth and repeatable pressure rise signals. The validation of this concept will allow deploying it on the final combustion chamber of the ESTHER facility (see Fig. 2).

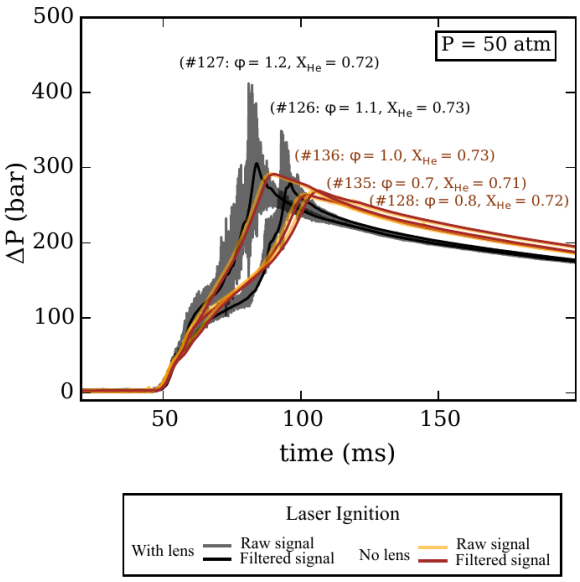

Fig.1: sample pressure signals from laser-ignited shots

2. Acknowledgements

IPFN activities received financial support from European Space Agency through contract 23086 "Kinetic Shock-Tube for Planetary Exploration", and from Fundação para a Ciencia e Tecnologia through project UID/FIS/50010/2013.

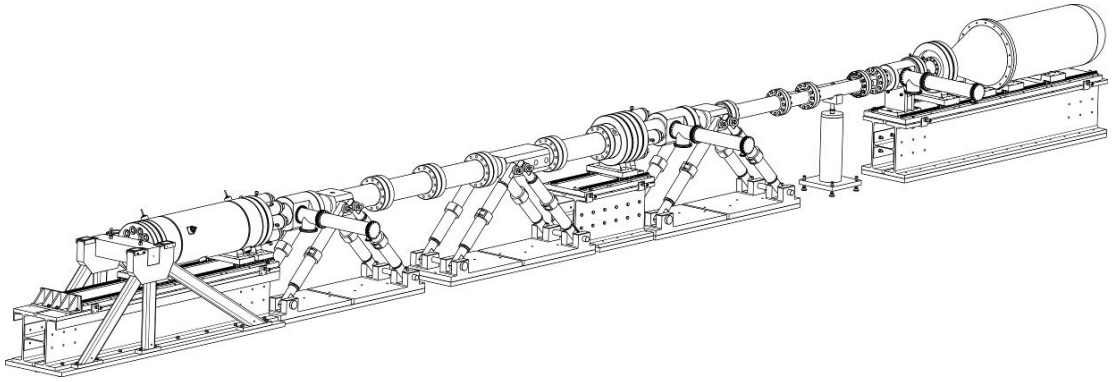

Fig.2: outline view of the ESTHER shock-tube

Mobility of negative ions in H_2O-He mixtures

J. de Urquijo[1], E. Basurto[2], O. González-Magaña[1]

[1] *Instituto de Ciencias Físicas, Universidad Nacional Autónoma de México, P.O. Box 48-3, 62251 Cuernavaca, Mor. México*

[2] *División de Ciencias Básicas e Ingeniería, Universidad Autónoma Metropolitana, Av. San Pablo 180, 02200, Ciudad de México*

We report the measurement of the drift velocity of negative ions in gaseous H_2O-He mixtures over a wide range of total mixture pressure and H_2O concentrations over the range 2-70%. A pulsed Townsend apparatus was used for the measurements. The present mobility data, measured at values of E/N low enough so that the mobility is essentially constant, depend, as expected, on the amount of H_2O in the mixture; additionally, for a fixed H_2O concentration in the mixture, the mobility depends on the total pressure. Because of the relatively high pressures used in this experiment (4-450 Torr), no mass spectrometry of the negative ions was possible. Current work is in progress to identify the ionic species from other means.

1. Introduction

The field of bioplasmas has been growing at a fast rate in view of the many applications in medicine, engineering and basic science. For instance, He-H_2O mixtures are used in atmospheric pressure plasmas to treat wounds in human tissue. While water may be present due to normal ambient humidity, He, a non-reactive rare gas under the present conditions, and with an excellent thermal conductivity, is a preferred carrier gas. Recent studies on the abundance of negative ions in an atmospheric discharge plasma report the formation of OH^- as the dominant species follow by the clusters $OH^-(H_2O)_n$, with n=1-5 [1]. It has been recently found from a study on pure H_2O, performed in a pulsed Townsend apparatus that the same kind of cluster ions are formed (n=1-3) over the pressure range 4-16 Torr [2].

2. Experimental

A pulsed Townsend apparatus was used for these measurements. Details of the experiment and analytical techniques are given in [2]. The measurements were limited to regions of E/N where no ionisation processes take place. Mixture gas pressures between 4-450 Torr were used.

3. Measurements

The variation of the low-field mobility of negative ions in H_2O-He mixtures is shown in Fig. 1 as a function of pressure and H_2O concentration in the mixture. It is interesting to note that apart from the variation of the mobility, K_{00}, with the H_2O content in the mixture, there is also a well-defined dependence with gas pressure. The lines joining the points correspond to a linear dependence between K_{00} and pressure (the pressure scale is logarithmic).

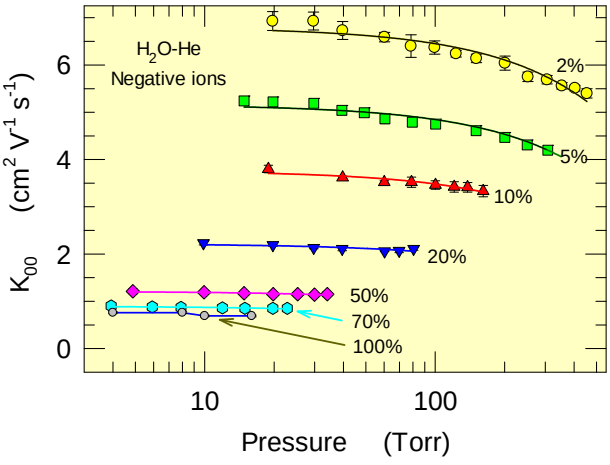

Figure 1. The low-field mobility of negative ions in H_2O-He mixtures. Uncertainties in the mobility values range from 1-3%

Due to the very high pressures used, no mass spectrometric means were used. Current work is underway to determine the ionic species from indirect means [2].

References

[1] P. Bruggeman, F. Iza, D. Lauwers, Y. Aranda, J. Phys. D 43 (2010) 012003

[2] J. de Urquijo, A. Bekstein, G. Ruiz-Vargas and F. J. Gordillo-Vázquez, J. Phys. D 46 (2013) 035201

Acknowledgements

This work has been partially supported by Conacyt, Grant 240073 and PAPIIT-UNAM, IN108417. Thanks are due to A. Bustos and G. Bustos for their technical support.

The use of thermally stimulated luminescence for rapid assessment of plasma treated particulate materials

J. Ráheľ[1], T. Morávek[1], M. Ilčíková[1]

[1] *Masaryk University, Department of Experimental Physics, Kotlářská 2, 611 37 Brno, Czech Republic*

Thermally induced light emission (luminescence) is presented as a particularly suitable tool for monitoring the level of plasma surface activation. The method is relatively fast, exhibits a surprising sensitivity and allows evaluation of even poorly defined surface, which are typical for particulate materials. The examples of three distinct materials are presented – plasma activated PET flakes, cellulose fibres pulp and Al_2O_3 powders.

1. Introduction

The processing of particulate materials (i.e. substances consisting of individual particles) plays a key role in the number of industrial sectors, e.g. ceramic and coatings engineering, pharmaceutical, composites or recycling industries. In many cases, the surface of particulate material needs to be modified to achieve better interaction with given liquid matrix, e.g. solvent or binder. For that, non-thermal plasma treatment (PT) of particles surface may be a suitable choice, chiefly due to its low environmental impact. The vexing problem associated with PT of particulate materials is its problematic transport through the active plasma zone. For instance, fine powders are attached to the electrodes by electrostatic charging, or blown off by the ion wind. These effects cause a poor control on the average PT time of material. Larger particles, such as polymer flakes or wood pulp, suffer from their irregular shape, which increase the risk of insufficient PT at short treatment times. A suitable diagnostic tool allowing rapid assessment of the level of plasma activation is therefore needed for PT optimization.

2. Results

Thermally stimulated luminescence (TSL) experiments were performed on the photon-counting instrument Lumipol 3 (SAS, Bratislava), which detected the spectrally unresolved VIS light emission upon controlled sample heating up to 300°C. The PT was done using the diffuse coplanar dielectric barrier discharge (DCSBD) operated in atm. pressure air.

PET flakes with average size of 2.25×17.7mm were PT for 60 sec to achieve better mechanical properties particleboards made from PET and wood particles [1]. Immediately after the treatment, the PT flakes exhibited 10-fold increase of peak TSL intensity. The cross-check XPS analysis confirmed higher number of oxygen containing surface group. Therefore the chemiluminescence (originating from the recombination of peroxy and hydroperoxy radicals) is most likely detected by TSL.

Cellulose fibre pulp (GREENCEL, Slovakia) was PT to promote its further silanization. TSL measurements showed 2-fold signal increase, while the changes in XPS or FTIR spectra were not that dramatic. Although TSL signal was ambiguous to interpret, it proved again to be a sensitive PT indicator.

Finally the submicron Al_2O_3 powders were PT to enhance their dispersion stability [2]. PT treatment resulted in more than 15-fold rise of TSL signal. Our further analysis indicated that observed TSL signal is that of thermoluminescence – originating from electrons relaxed from the Al_2O_3 trapped states, populated during the previous PT.

3. Acknowledgement

This work was supported by the Czech Science Foundation, Project No. GA17-05620S. This research has been supported by the Project CZ.1.05/2.1.00/03.0086 funded by European Regional Development Fund and Project LO1411 (NPU I) funded by Ministry of Education Youth and Sports of Czech Republic.

4. References

[1] P. Klímek, T. Morávek, J. Ráheľ et al. Composites Part B **90** (2016) 188- 194

[2] Z. Szalay, K. Bodišová et al. Ceramics International **40** (2014) 12737-12743

The collisionless transient pinch

J. E. Allen[1,2,3] and J. Gibson[3]

[1] *University College, Oxford OX1 4BH*
[2] *OCIAM, Mathematical Institute, Oxford, OX2 6GG*
[3] *Blackett Laboratory, Imperial College, London SW7, 2AZ*

The mechanism of the transient pinch at low densities, outlined in an early paper by Rosenbluth, has been studied in detail. The thickness of the surface current layer is found to be the electron inertial length (c/ωpe). The electron and ion trajectories have been calculated, the latter being essentially due to the electrostatic field which transfers the jxB force from the electrons to the positive ions. The collapse velocity is comparable to the Alfvén velocity, but the theory of magnetohydrodynamics (MHD) is not applicable to collision-free plasmas.

References

[1] M. Rosenbluth, Magnetohydrodynamics, ed. R.K.M. Landshoff, (Stanford University Press, 1957) p.57.

Cyclic growth dynamics of nanoparticles in low-pressure rf dusty plasmas

V. Garofano[1], R. Bérard[2,3], L. Stafford[1], C. Joblin[3], and K. Makasheva[2]

[1]*Laboratoire de physique des plasmas, Département de physique, Université de Montréal, Québec, Canada*
[2]*LAPLACE (Laboratoire Plasma et Conversion d'Energie), Université de Toulouse, CNRS, Toulouse, France*
[3]*IRAP-OMP (Institut de Recherche en Astrophysique et Planétologie), Université de Toulouse, CNRS, Toulouse, France*

This work investigates the dust formation dynamics in a low-pressure, axially-asymmetric, rf argon discharge with pulse injection of hexamethyldisiloxane (HMDSO, $Si_2O(CH_3)_6$). Light scattering and optical emission spectroscopy (OES) revealed oscillations over two time scales: a low-frequency cycle ascribed to the precursor injection and a very-low-frequency cycle linked to the dust formation and disappearance. It is found that the amount of injected HMDSO and the rf power significantly modify the period of the formation and disappearance cycle. The impact of these parameters on the low- and high-energy electron populations will be discussed.

When nanoparticles, or dust, grow inside a plasma, they are subjected to numerous forces. The most important ones, that allow or deny confinement of the dust cloud, are the electrostatic and ion drag forces. Their significance comes from the negative charge carried by the dust. However, since dust acts as a sink of the free electrons, it is not obvious that an equilibrium will be reached, in which dust would float indefinitely inside the discharge. In fact, a great number of temporal and spatial instabilities can be observed in low-pressure dusty plasmas.

In our experiment, the plasma is generated between two electrodes separated by 3.5 cm, with the top, smaller, RF driven electrode made of silver and a larger, grounded, bottom electrode. One of the most important specificity in our procedure is the pulsed injection of the precursor, HMDSO ($Si_2O(CH_3)_6$), with a complete cycle of 5 s. It was found that under specific experimental conditions, mainly low rf power (< 50 W) and enough injected precursor, expressed here as flow rate averaged over the injection period (> 0.16 sccm), a dust cloud appears in the plasma. More importantly, the dust cloud presents a formation/loss cyclic behavior with a period of a few hundred seconds (see Fig. 1). Fig. 2 shows the evolution of the period of dust formation/loss cycle with the relevant operating parameters. HMDSO flow rate accelerates this cycle by providing a greater quantity of radicals needed for the dust growth. On the other hand, the rf power increases the period of the cycle, most likely due to an increased fragmentation of the precursor providing more atomic hydrogen, known to act as dust nucleation inhibitor.

In a recent study, we have used optical emission spectroscopy to examine the influence of the dust growth on the low- and high-energy electron populations [1]. It was shown that the electron temperature (T_e) follows the same trend as the dust cyclic formation and loss, while the electron density (n_e) has the opposite behavior. In this study, we will report on the influence of the injected HMDSO amount and the rf power on T_e and n_e.

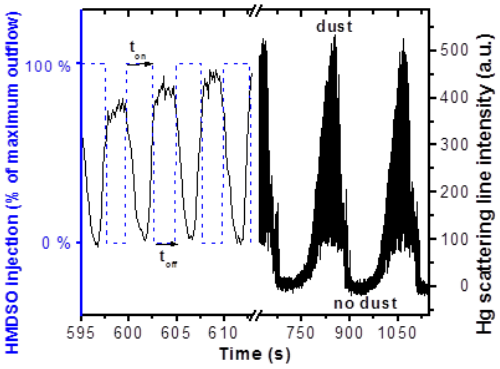

Fig. 1. Time evolution of the injection of the HMDSO precursor (dash-dot) for a duty cycle of 0.56 (t_{on} = 2.8 s) and the intensity of the Hg line at 546 nm (solid line).

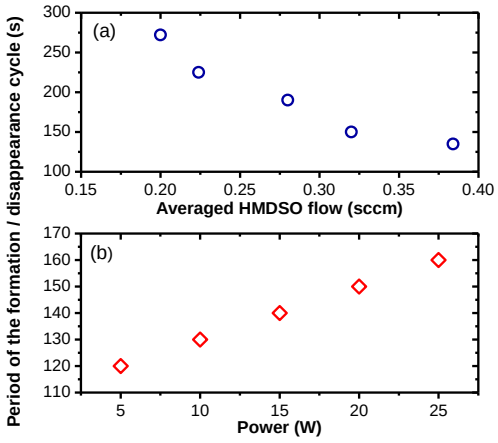

Fig. 2. Evolution of the formation / disappearance period with the averaged HMDSO flow rate (a) and rf power (b).

[1] V. Garofano, L. Stafford, B. Despax, R. Clergereaux, and K. Makasheva, Appl. Phys. Lett. **107**, 183104 (2015).

EHD thruster discharge simulation on N_2-O_2 mixture at low pressure

V.H. Granados[1], P.A. Sá[1], M.J. Pinheiro[2]

[1] *Departamento de Engenharia Física, Faculdade de Engenharia, Universidade do Porto, Porto, Portugal*
[2] *Departamento de Física, Instituto Superior Técnico, Universidade de Lisboa, Lisboa, Portugal*

An axisymmetric 2D self-consistent electrohydrodynamic (EHD) thruster model is presented. In order to emulate air we considered a set of electron-impact reactions along with chemical and surface reactions for a total of 12 species and 26 reactions. The geometry of the thruster consists of a pin anode and a hollow funnel-like cathode to facilitate the flow of neutrals along the cathode interior. The ions tend to neutralize into their ground state upon contact with the electrodes and the simulation border. Additionally, when ions impact the cathode, a secondary electron emission occurs helping sustain the discharge. We found the concentration of each ion along the axis of symmetry to understand their role in the discharge.

1. Introduction and model

DC-discharges are typically studied with simple parallel plate-to-plate geometries which are not beneficial for thrust production. Our model presents a hollow cathode that allows charged particles to move between electrodes while neutrals flow inside the cathode chamber crossing it axially by momentum transfer collisions [1].

We solve the continuity equation for electron density and electron energy density, including source terms governed by the corresponding reaction rates of all the considered reactions.

The total considered species are: e, O, O_2, O_3, N_2^+, N_4^+, O_2^+, O_4^+, $O_2^+N_2$, O^- and O_2^-. For electron-impact reactions we use cross-section data. All reactions may be found on [2]. The pressure is 10 Torr (1333.2 Pa) and the voltage 400 V is applied through a RC circuit with R = 10 MΩ and C = 1 pF.

2. Results and analysis

The discharge was brought to convergence using a time-dependant solver using the finite-element software COMSOL Multiphysics® 5.2a.

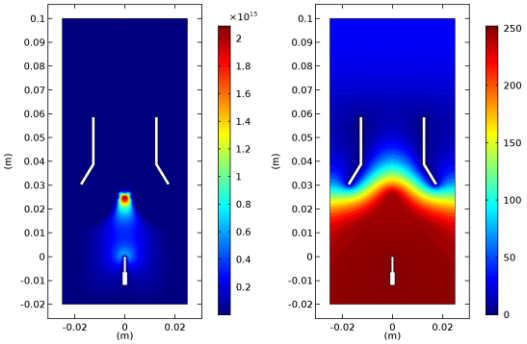

Figure 1: Spatial distribution of (left) electron density in m^{-3} and (right) electric potential in V. Pressure p=10 Torr.

In Figure 1 we can see the spatial distribution of the electron density showing a maximum value of 2.09×10^{15} m^{-3} at the entrance of the cathode chamber, which corresponds to the region where equipotential lines bend the most. The latter is due to the fact that electron cloud moves under the influence of the electric force, which is proportional to the potential gradient pointing to that region.

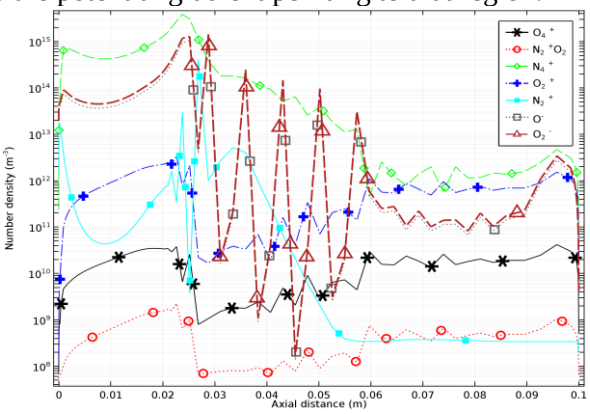

Figure 2: Number densities of all ions along the central axis. Pressure p=10 Torr, potential on anode V=250 V.

Ions number densities along the axial distance from the anode are shown in Figure 2; the N_4^+ specie is the dominant positive ion, followed by O_2^+ and N_2^+ since the momentum transmitted to the neutrals from Lorentzian collisions is proportional to the ions mobility, and considering the higher mobility of N_4^+ in dry air, its contribution is considerable in inducing gas flow velocity. The O_2^+ ion builds up in the region between electrodes reaching a density of 3.4×10^{12} m^{-3} and rapidly decreasing during the potential drop (2-4 cm along the line) and then presenting an increase becoming analogous to the N_4^+ ion outside the chamber.

3. References

[1] V.H. Granados, M.J. Pinheiro, P.A. Sá, Phys. Plasmas **23** (2016) 073514.

[2] L. Xing-Hua, H. Wei, Y. Fan, W. Hong-Yu, L. Rui-Jin, X. Han-Guang. Chin. Phys. B **21** (2012) 075201.

Kinetics of Neon Atmospheric Pressure Plasma Jets

Susumu Kato[1*], Masanori Fujiwara[1], Hiromasa Yamada[1,2], Yutaka Fujiwara[1,2], Satoru Kiyama[1], and Hajime Sakakita[1,2]

[1] *Innovative Plasma Processing Group, Electronics and Photonics Research Institute, National Institute of Advanced Industrial Science and Technology (AIST), 305-8568, Japan*

[2] *Graduate School of Systems and Information Engineering, the University of Tsukuba, 305-8577, Japan*

We propose a simple kinetic model to explain the discharge sustaining mechanism in atmospheric pressure plasma jets (APPJs) by taking into account the metastable kinetics. The discharge in neon APPJs is sustained by the balance between the creation and the loss of the total amount of ions and metastable atoms within the drift current using the simple kinetic model calculation.

1. Introduction

Atmospheric pressure plasma jets (APPJs) have recently attracted much interest not only for many applications [1] but also for plasma physics [2,3]. One of the most interesting phenomena in APPJs is bullet propagation [2]. Another is striation which has been observed between a nozzle exit and a conductive target plate in neon APPJs [3].

It is not clear, however, how the plasma is sustained in neon APPJs. Especially, the role and kinetics of the excited state (metastable) are not clear even though it is believed to be an important role [4]. In this paper, we studied the sustaining mechanism considering the metastable kinetics.

2.Sustaining mechanism and kinetics of discharge

In the experiment there are drift currents around 4 ～ 8 mA at each peak between the nozzle exit and the conductive target plate for applied voltage and frequency of 2.9 k V and 61.7 kHz, respectively [3].

We assumed that the drift current consists of electrons that are supplied from ionization of both metastable and ground state atoms. The plasma is sustained by the balance between the creation of metastable atoms by the electron impact excitation from the ground state and the loss of the total amount of ions and metastable atoms.

A simple kinetic model is proposed to explain the sustaining mechanism. The kinetic model includes only neon and electron reactions, those are

1) $Ne + e \rightarrow Ne^* + e$,
2) $Ne + e \rightarrow Ne^+ + 2e$,
3) $Ne^* + e \rightarrow Ne^+ + 2e$,
4) $Ne_2^+ + e \rightarrow Ne^* + Ne$,
5) $Ne^* + Ne^* \rightarrow Ne^+ + Ne + e$,
6) $Ne^+ + 2Ne \rightarrow Ne_2^+ + Ne$,
7) $Ne^* + 2Ne \rightarrow Ne_2^* + Ne$,
8) $Ne_2^* \rightarrow 2Ne + h\nu$,

where e, Ne^+, Ne^*, Ne_2^+, and Ne_2^* are electron, neon ion, metastable atom, ion diatomic molecule, and excited diatomic molecule, respectively. The rate coefficients related to electrons depend on the electron energy distribution which was decided by the reduced electric field *E/N*, where *N* is the gas density. The rate coefficients and the drift velocity were calculated using the BOLSIG code [5]. In the model, Penning ionization by the mixing of neon gas with surrounding air were ignored.

3. Simulation results

We solved the rate equations for the reduced electric field, which was simplified based on the current waveform [3], assumed to be repetition of rectangular waves of *E/N* = 4.0 Td and their periods with 2.0 and 1.0 μs corresponding to positive and negative current, respectively. Figure shows the time evolution of the electron number density.

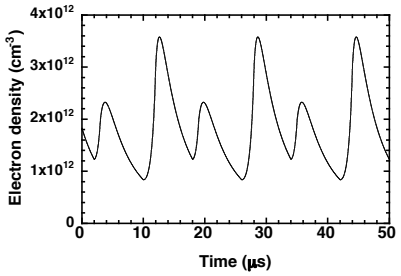

Fig. Time evolution of the electron number density.

Acknowledgements

This work was supported by a JSPS KAKENHI (15H03760) and a Grant-in-Aid for Scientific Research on Priority Area (24108006).

References

[1] D. B. Graves, *J. Phys. D: Appl. Phys.* **45** (2012) 263001; M. G. Kong *et al*., *New J. Phys.* **11** (2009) 115012.

[2] M. Teschke *et al*., IEEE Trans Plasma Sci., **33** (2005) 310; X. Lu *et al*, *Phys. Rep.* **540** (2014) 123.

[3] Y. Fujiwara *et al.*, Jpn. J. Appl. Phys. **55** (2016) 010301.

[4] Q. Li *et al*. J. Appl. Phys. **107** (2010) 043304.

[5] G. J. M. Hagelaar and L. C. Pitchford, *Plasma Sources Sci. Technol.* **14** (2005) 722.

Performance optimisation of a high-pressure argon dielectric barrier discharge excimer lamp: transient behaviour of the VUV output

R. Carman[1], D. Kane[1], N. Goldberg[2], S. Hansen[2] and N. Gore[2]

[1]*Department of Physics and Astronomy, Macquarie University, North Ryde, Sydney, Australia*
[2]*Agilent Technologies Inc., 5301 Stevens Creek Blvd, Santa Clara, CA 95051, USA*

We report an experimental study of the operating characteristics of an air-cooled, high-pressure argon excimer VUV lamp (λ~126nm), driven by a dielectric barrier discharge (DBD), in the regime of high electrical power loadings close to the thermal loading limit. Remarkably, under such conditions, the VUV output is seen to reach a maximum a few seconds after turn-on, and thereafter decrease by ~50% within a few minutes. Although the rate of decrease in the VUV output is shown to be matched in part to the thermally induced rate of gas expansion from the plasma region, we propose this VUV "spiking" behaviour is similar to that reported by Gerasimov (Opt. & Spectros. **83**, 534, 1997) for an interrupted discharge in a liquid N_2 cooled excimer lamp.

1. Introduction

We have investigated the electrical and optical characteristics of a high-pressure argon excimer lamp excited by a dielectric barrier discharge (DBD) when operated with relatively high electrical power loadings. The excimer lamp produces λ=115-140nm (~10eV) photons in the vacuum-ultraviolet (VUV) spectral region which are effective at ionizing many chemical analytes. The availability of intense, narrow-band VUV light sources could potentially make a big impact in the field of mass spectrometry ion sources. The specific aim of this work is to optimise the overall VUV output power and efficiency of an excimer lamp by undertaking a detailed experimental characterisation of its performance over a range of operating parameters for the DBD plasma (namely argon pressure up to ~1bar, short-pulse bipolar and sinusoidal high-voltage waveform excitation, waveform peak voltage, duty-cycle, and repetition frequencies up to 100kHz). A wide range of operating conditions has been tested up to the thermal loading limit of the air-cooled VUV lamp. The optical and electrical diagnostics and techniques employed are broadly similar to those described in [1].

2. Results

The experimental results clearly show an improvement of the overall lamp performance when utilizing short-pulsed high-voltage excitation waveforms compared to conventional sinusoidal ones at comparable electrical input power loadings. Lamp performance, in terms of maximum VUV output optimised at the highest gas pressures and input power loadings investigated (p=800-900mb, ~2W/cm^3). In this regime, however, it was generally observed that the lamp attained maximum VUV output a few seconds after turn-on, after which the output dropped by ~50% over the first few minutes of running, whilst the input power remained unchanged. To investigate the potential to run the lamp with sustained high VUV output, we studied this phenomenon by monitoring the long-term VUV output of the lamp when subjected to several periods of interruption of the electrical power. We observed that the VUV output "spike" decayed exponentially in time in three distinct stages, with two of the deduced time constants matching those for thermally induced expansion of the fill gas from the lamp's plasma region. However, the large ~50% drop in VUV output cannot be attributed solely to a reduction of gas density and/or to the increased average gas temperature in the lamp's plasma region. Similar spiking of the VUV output has been reported previously by Gerasimov et-al [2], in an experimental study of an interrupted discharge in a liquid nitrogen cooled capillary Krypton excimer lamp. They observed a ~50% drop of VUV intensity over several seconds after lamp turn-on, and attributed the initial enhanced VUV output from Xe, Kr and Ar gas fills to enhanced production of the principal VUV emitting species (e.g. $Kr_2^*(1_u,O_u^+)$) via electronic excitation of weakly-bound molecular ground states e.g. $Kr_2(O_g^+)$ formed during the "off" period of a cooled (77K) discharge. We propose that we may be observing the same intrinsic VUV spiking phenomena in an excimer-based VUV lamp, only in our case with gas fills at, or slightly above, room temperature (without liquid nitrogen cooling).

[1] R.J. Carman, D.M. Kane and B.K. Ward, J.Phys.D: Appl.Phys., **43**, (2010) 025205.
[2] G.N. Gerasimov, B.E. Krylov, R. Hallin, A. Arnesen and F. Heijkenskjold, Optics and Spectroscopy, **83**(4), (1997) 534-540.

Topic number: 14

Morphological and spectral features of interstellar carbon dust analogues deposited in high power regime DBD

B. Hodoroaba[1], D. Ciubotaru[1], G.B. Rusu[1], A. Chiper[1], V. Pohoata[1], I. Mihaila[2], I. Topala[1]

[1]*IPARC, Faculty of Physics, Alexandru Ioan Cuza University, Iasi, Romania*
[2]*Integrated Center of Environmental Science Studies in the North-Eastern Development Region (CERNESIM)*

In recent years, particle synthesis using plasma based techniques became an appropriate tool to obtain laboratory analogues of carbon interstellar dust. Thus it is possible to deposit carbon based films or powders on various substrates, with morphological and spectral features similar to the radio telescope observations or dust collectors on-board the space probes. We discuss here the possibility of employing the high power regime DBD in helium-hydrocarbon gas mixtures to synthetize carbon based dust analogues.

1. Introduction

Carbonaceous and silicate dust grains represent around 1 % of the interstellar medium (ISM) total mass. Surface reactions on grains or on ices formed around the grains play important roles in many astrophysical or astrochemical processes. Thus, it is of interest to synthetize nanometer and micrometer sized solid particles, showing morphological and spectral similarities to the ones observed in ISM. Various spectral, morphological or structural criteria can be used to discuss the similarity degree of synthetic products to data from space and Earth based instruments. Plasma particle synthesis represents a good solution to obtain in controlled conditions, showing reproducible chemistry, size distribution and morphological features. We present here results concerning the high power regime DBD deposition of carbon based particles.

2. Experimental

The helium / hydrogen (1%) / hydrocarbon (C_nH_{2n+2}, n= 1 - 4) (10%) containing plasma at atmospheric pressure was generated using a barrier discharge in parallel plate configuration. The discharge was excited using short duration positive voltage pulses, 5.7 kV amplitude, 400 ns pulse width, 100 ns rise time and 1 kHz repetition frequency. The electrode assembly was hosted by a stainless steel chamber, vacuumed prior all experiments. The discharge operation was monitored by electrical, gas temperature, emission spectroscopy measurements and fast imaging. The exit gas from reactor, sampled in vacuumed gas cells with NaCl windows, was analysed by FTIR to identify the molecular composition. The carbonaceous deposits were investigated by electron microscopy (SEM) and various spectroscopic methods (UV-VIS, FTIR, Raman, XPS).

3. Results and discussion

By admixing H_2 and CH_4 to the helium main gas, plasma electrical parameters vary. The amplitudes of both discharge current peaks was around 8 A during the HV pulse rise and fall times. This corresponds to 8 kW power peak and 20 mJ energy per pulse, implying a high power regime as compared with classic DBDs.

The deposits shows spectral features similar to astrophysical products (e.g. the 3.4 μm, 6.8 μm, 7.2 μm bands) and the morphology as revealed by SEM shows the aggregation of sub-micrometric grains to form micrometer sized solid particles.

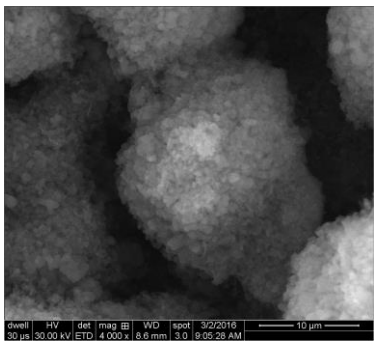

Figure 1. Typical SEM image of a carbon based dust particle obtained in $He/H_2/CH_4$ DBD.

4. Conclusion

The experimental results show the potential of high power regime DBD in deposition of carbon based dust particles and their subsequent classifications as interstellar dust analogues.

5. Acknowledgement

This research was financially supported by Romanian Space Agency (ROSA) under the project STAR CDI ID 486/2017-2019. The POSCCE-O 2.2.1, SMIS-CSNR 13984-901, no. 257/28.09.2010 Project, CERNESIM, is gratefully acknowledged for the infrastructure used in this study.

Formation of Molten Metal Jets and Droplets in the Cathode Spot of Vacuum Arc Discharge

M. Gashkov[1], N. Zubarev[12], G.A. Mesyats[12], I.V. Uimanov[1]

[1] *Institute of Elecrtophysics,Ural Branch of Russian Academy of Science, Yekaterinburg, Russia*
[2] *Lebedev Physical Institute, Russian Acadeny of Science, Moscow, Russia*

The dynamics of molten metal during crater formation in the cathode spot of vacuum arc discharge was theoretically investigated. At the initial stage, a liquid-metal rim is formed around the crater. This process has been numerically simulated in the framework of the two-dimensional axisymmetric heat and mass transfer problem in the approximation of viscous incompressible liquid. At a more developed stage, the motion of liquid metal loses axial symmetry, which corresponds to a tendency toward jet formation. The development of azimuthal instabilities of the rim is analysed in terms of dispersion relations for surface waves. It is shown that maximum increments correspond to instability of the Rayleigh–Plateau type. Estimations of the time of formation of liquid metal jets and their probable number are obtained.

As is known, the cathode spot is a source of liquid metal jets and droplets that play an important role in the self-sustained operation of vacuum arc discharge [1]. They are formed whereas the molten metal is extruded by the pressure of explosive plasma out from craters formed on the cathode. A jet formation mechanism based on the development of azimuthal instability of the Rayleigh–Plateau (RP) type of the boundary of liquid expelled from craters has been proposed in Ref. [2]. However, a qualitative character of models used in [2] does not exclude that the Rayleigh–Taylor (RT) instability also develops, since the characteristic times of RP and RT instabilities are comparable.

The main idea of the present work is to combine numerical and analytical approaches in considering hydrodynamic processes in the cathode spot cell of vacuum arc. In the 2D axisymmetric problem formulation, we have numerically simulated the formation of a liquid metal rim around the crater. At the same time, we analytically studied linear stages of the development of 3D instabilities in the rim with allowance for a change in its geometry.

As can be seen from Fig. 1, the most pronounced growth of perturbations is observed for the azimuthal harmonic with n = 11 and results from development of the RP instability. The harmonic amplitude exhibits for 25 ns an almost fivefold increase, which can provide the formation of jets simultaneously with crater formation. At the same time, the RT instability ensures most rapid growth of the harmonic with n = 5, but it's amplitude exhibits only threefold increase.

The characteristic time of development of the RP instability (i.e., the time for which the surface perturbation amplitude increases by a factor of e ≈ 2.72) amounts to 14 ns, while that for the RT instability is significantly greater and reaches 21 ns.

Thus, the results of our theoretical analysis with allowance for the substantially 3D character of deformations of the liquid rim lead to the conclusion that the RP instability is responsible for the formation of liquid metal jets (see also Ref. [3]).

This work was supported by the RFBR (projects Nos. 16-08-00228 and 17-08-00430) and by the Presidium of the RAS (Program No. 9).

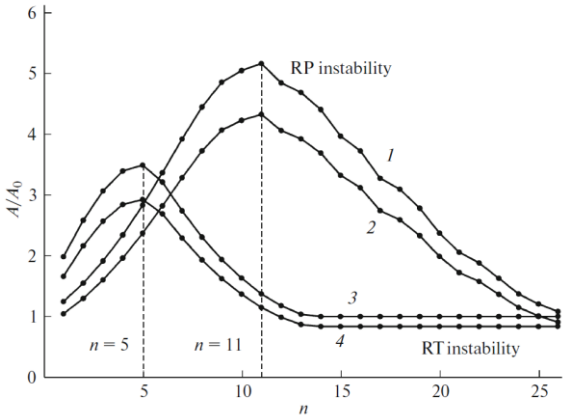

Figure 1. The results of calculations of the growth of amplitudes of azimuthal perturbations on the surface of liquid metal rim for modes with various numbers n during the time interval from t = 10 to 35 ns (A_0 and A being the initial and final values, respectively): (*1*, *2*) upper and lower estimates of the relative amplitude growth due to development of the RP instability; (*3*, *4*) same for development of the RT instability.

[1] G.A. Mesyats. Phys. Usp. **38** (1995) 567.

[2] G.A. Mesyats, N.M. Zubarev. J. Appl. Phys. **117** (2015) 043302.

[3] M.A. Gashkov, N.M. Zubarev, G.A. Mesyats, I.V. Uimanov. Tech. Phys. Lett. **42** (2016) 852.

Study of electric field distribution in helium and hydrogen DBD at lower pressures

S. S. Ivković[1], B. M. Obradović[1], N. Cvetanović[2] and M.M. Kuraica[1]

[1]*University of Belgrade, Faculty of Physics, 11001 Belgrade*
[2]*University of Belgrade, Faculty of Transport and Traffic Engineering, 11000 Belgrade*

The effect of pressure, voltage, electrode gap and surface on the electric field distribution in DBD in helium and hydrogen in the pressure range 5 – 100 mbar was investigated. It was found that the type of the discharge and its characteristic axial electric field distribution strongly depends on the distance between electrodes while influence of the pressure is mostly seen as a change of the field value. It was found that discharge in helium is a subnormal-like for 1 mm gap, and for 5 mm it is a glow-like. The discharge in hydrogen changes from a Townsend-like for 1 mm gap to a glow-like for 5 mm gap.

1. Introduction

Atmospheric dielectric barrier discharges (DBDs) have been widely studied over the last few decades mostly because of their broad application fields [1]. Ease of their implementation was demonstrated in different processes like surface modification, deposition, activation, gas purification, decontamination. Various discharge regimes have been observed and documented using high speed imaging, temporally and spatially resolved optical emission spectroscopy and simulations. In this paper we investigate DBD in helium and hydrogen in the pressure range 5 – 100 mbar. The effect of pressure, voltage, electrode gap and surface on the electrical characteristics of DBDs is investigated. We present the different regimes observed in the DBDs operation, depending on pressure observed trough the electric field distribution in the discharge. Stark polarization spectroscopy of hydrogen Balmer alpha line [2] was used for measurement. Using time-resolved spectroscopy, evolution of the electric field distribution was studied during the discharge development.

2. Experiment

In our experiment the discharge is formed between two parallel electrodes: one metal electrode (40×40 mm^2) is covered with alumina dielectric while the other electrode is made of steel mesh and covered with pyrex glass. The distance between the barriers is set at 1, 2 and 5 mm. The discharge chamber is firstly evacuated down to 10^{-2} mbar, and then the working gas is introduced up to 80 mbar pressure. The amplitude of the sine applied voltage was 1.1 and 1.75 kV at frequency of 19.7 kHz. Voltage is measured using high-voltage probe, and current is monitored using Rogowski coil. For time-space resolved measurement of emission spectra the 1–m spectrometer with ICCD detector was used.

3. Results

It was found that the type of the discharge and its characteristic axial electric field distribution strongly depends on the distance between the electrodes. Influence of the pressure is mainly observed as a change in the electric field strength, while its influence on the shape of the field distribution is minor. According to the measured electric field distributions, the discharge in hydrogen for 1 mm electrode gap is in the Townsend-like mode, for 2 mm it is in subnormal-like and for 5 mm in the glow-like mode. Figure 1 shows that discharge in helium is in subnormal-like mode for 1 mm electrode gap. While measurements for 2 mm and 5 mm gap have shown that discharge is in the glow-like mode.

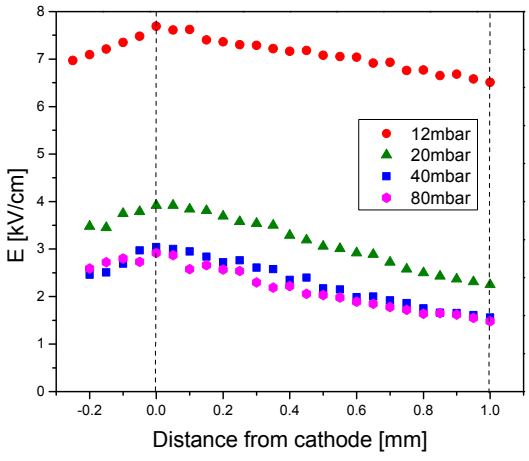

Fig. 1: Electric field distributions for the helium DBD at different pressures. Inter electrode gap is 1 mm.

4. References

[1] U. Kogelschatz Plasma Chem. Plasma Proc. **23** (2003) 1–46.

[2] T. Wujec, H.W. Janus and W. Jelenski, J. Phys. D: Appl. Phys. **36** (2003) 868–877.

Probing internal excitation of trapped $O^+(^4S, ^2D, ^2P)$ ions by reaction with N_2

R. Plašil[1], A. Kovalenko[1], T. D. Tran[1], S. Rednyk[1], Š. Roučka[1], P. Dohnal[1], J. Glosík[1]

[1] *Department of Surface and Plasma Science, Faculty of Mathematics and Physics, Charles University in Prague, Prague, Czech Republic*

When the atomic oxygen cation O^+ takes part as a reactant or a product in experimental studies, electronically exited states may play a significant role. For investigation of ion molecular reactions, a cryo-cooled radiofrequency ion trap is used. Molecular nitrogen was chosen as a monitor gas for probing a presence of long-lived excited $O^+(^2D, ^2P)$ in an ensemble of ions confined in the radiofrequency trap. The fraction of electronically excited ions was determined. The rate coefficient of the reaction of $O^+(^4S)$, the electronic ground state, with nitrogen molecule was measured at low temperatures. The reaction rate coefficient at 61 K was evaluated as $(7.5 \pm 1.5)\times10^{-12}$ cm^3 s^{-1}. It confirms an increase of the coefficient at low temperatures.

Introduction

The atomic oxygen cation O^+ plays a significant role in numerous environments such as planetary ionospheres or technological plasmas. The existence of long-lived $O^+(^2D, ^2P)$ metastable states may be important in many situations. For states $^2D_{3/2}$ and $^2D_{5/2}$ the lifetimes are in the order of hours and for states $^2P_{1/2}$ and $^2P_{3/2}$ in seconds [1]. The excited states carry electronic energy of 3.3 eV and 5.0 eV, respectively. The only exoergic channel for reaction of O^+ in ground state with N_2 is formation of NO^+ (1). The charge transfer (2) is endoergic.

$$O^+(^4S) + N_2 \rightarrow NO^+ + N, \quad \Delta H = -1.13 \text{ eV} \qquad (1)$$

$$O^+(^4S) + N_2 \rightarrow N_2^+ + O, \quad \Delta H = +1.96 \text{ eV} \qquad (2)$$

For the excited states $O^+(^2D, ^2P)$ both reactions are exoergic and for reaction (2) the rate coefficient is close to Langevin rate in the order of 10^{-10} cm^3 s^{-1} [1, 2]. The charge transfer (2) from excited O^+ ion to N_2 is dominant channel.

We used these reactions as a probe for excited states of O^+ ions confined in the radiofrequency trap. In addition we confirmed steep increase of the rate coefficient of the reaction (2) with decreasing temperature [1, 3].

Experiment

A 22-pole radiofrequency ion trap was used for this study. It was placed on a cryo-cooler in an ultra-high vacuum system. The measuring procedure was based on iterative filling of the trap with a well-defined number of primary ions O^+. They react with N_2 and the contents of the trap were analysed after chosen times by means of a quadrupole mass spectrometer with micro-channel plate detector. Additional details may be found in reference [4] and references therein. The O^+ ions were produced in separated ion source by electron impact from N_2O molecule to reduce the ratio of exited states in comparison with a production from O_2.

From the number of N_2^+ we may evaluate a fraction of exited states of O^+ as (5 ± 1)% for electron impact energy E_e = 75 eV and (10 ± 2)% for 145 eV, see Figure 1.

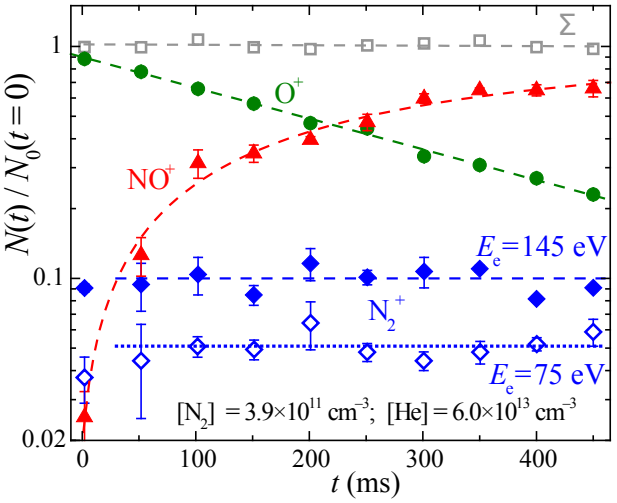

Fig. 1: Evolution of normalized number of ions in rf trap at temperature 61 K. From the increase of NO^+ we may determine the rate coefficient of the reaction (1) $(7.5 \pm 1.5)\times10^{-12}$ cm^3 s^{-1}. The number densities of the N_2 reactant and helium buffer gas are indicated in the figure.

We thank the TU Chemnitz, the DFG, prof. D. Gerlich for lending us the apparatus and Czech Science Foundation grant 17-18067S.

References

[1] J. Glosík *et al.*, J. Phys. B: Atom. Molec. Phys. **11** (1978) 3365.
[2] B.R. Rowe *et al.*, J. Chem. Phys. **73** (1980) 194.
[3] J-L. Le Garrec *et al.*, Chem. Phys. Lett. **372** (2003) 485.
[4] D. Gerlich and G. Borodi, Faraday Discussions **142** (2009) 57.

Investigation of magnetic sheath effect on angle of incident ion at graphite wall

Nam-Kyun Kim[1], Jaemin Song[1], Younggil Jin[1], Ki-Baek Roh[1], and Gon-Ho Kim[1]
[1]*Department of Energy Systems Engineering, Seoul National University, Seoul, Korea*

The ion incident angle on an oblique plasma-facing surface can deviate from the magnetic field line, depending on the characteristics of the plasma sheath which is formed between the plasma and the surface. The characteristics of the sheath in an oblique magnetic field is investigated with respect to the magnetic field strength and the angle. A fluid model predicts that, in a weak magnetic field, the sheath structure consists of a presheath and a sheath. In a strong magnetic field, the sheath structure is composed of a collisional presheath, a magnetic presheath, and a sheath. The characteristics of each region and the ion dynamics inside the regions are also revealed. The observed ion incident angle, which is measured by a noble material probe, verifies the fluid model of the oblique magnetic sheath.

1. Background

In the existence of a strong magnetic field (*B*-field), like in a tokamak, it is easy to consider that the ion incident angle on an oblique surface would be comparable to that of the *B*-field line. However, Ahedo [1] suggested a magnetic sheath model that the electric field (*E*-field) inside the plasma-wall transition region (here, we call it the 'transition region') forces the ions to have the ExB drift motion. Thus, the ion motion becomes 3-D, deviated from the *B*-field line. However, no experimental observation that verifies the model has been carried out. Here, we have verified the Ahedo's model by observing the ion incident angle on an oblique plasma-facing surface in magnetic fields. Some ambiguity of the model has also been corrected.

The governing equation set of the model is,

$$\frac{d^2U}{dx^2}=\frac{e(n_e-n_i)}{\varepsilon_0}\ ,\quad \ln n_e-\frac{eU}{k_BT_e}=const.\ ,\quad n_iV_x=const.$$

$$m_iV_x\frac{d\mathbf{V}}{dx}=e\mathbf{V}\times\mathbf{B}-\left(e\frac{dU}{dx}+\frac{k_BT_i}{n_i}\frac{dn_i}{dx}\right)\hat{\mathbf{x}}-\nu_cm_i\mathbf{V}\ . \qquad (1)$$

Here, the *E*-field is assumed to be aligned along the surface normal (-*x* direction) and the magnetic field is lying on the *xz*-plane as $\mathbf{B}=B(\cos\psi, 0, \sin\psi)$ (Fig. 1).

2. Experiments

A noble 'material probe' has been developed to measure the ion incident angle at the probe surface. When immersing a negatively biased graphite probe to a hydrogen plasma, a bundle of nano-tip is formed on the surface (Fig. 1) along the ion incident direction, due to the physical/chemical etching by energetic incident ions. By analysing the inclined angle on SEM images, the ion angle can be measured.

Experiments were carried out in both the weak and strong *B*-field conditions (an ECR source with < 1 kG and the KSTAR far-SOL with ~ 2 T). The angle between the probe (surface normal direction) and the *B*-field was varied in the range of 0º ~ 85º.

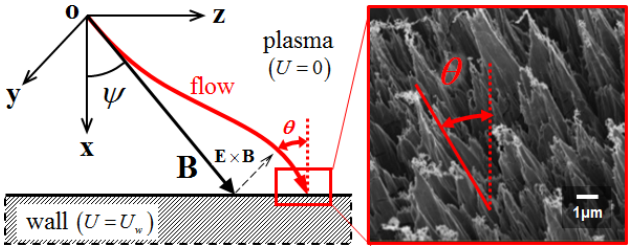

Figure 1. A schematic diagram of the system and the nano-scale tips on the material probe.

3. Results and Discussion

With the parameters of the weak-*B* ECR plasma, the model predicts that the transition region consists of two layers; a presheath and a sheath. In the presheath the ions start to flow along the -*y* direction. The *y*-directional velocity, V_y, is given by,

$$V_y=\frac{\left(V_x^2-C_s^2\right)}{V_{Ti}^2-C_s^2}\frac{1}{B\sin\psi}\frac{dU}{dx}+\frac{V_x}{\sin\psi}\frac{\nu_c}{\omega_{ci}}\ . \qquad (2)$$

Eq. (2) reveals that the E×B drift (1st term on RHS) and the collisional property (2nd term on RHS) both affect the ion motion. In the sheath, the ions are accelerated only in the surface normal direction.

With the parameters of KSTAR far-SOL plasma, it is predicted that the transition region consists of three layers; a collisional presheath, a magnetic presheath, and a sheath. Although there is a weak *E*-field inside the collisional presheath, the strong *B*-field confines the ions thus V_y=0 in the region. The ions start to move along the -*y* direction inside the magnetic presheath, and the velocity,

$$V_y=\left(\frac{V_x^2-C_s^2}{V_{Ti}^2-C_s^2}\right)\frac{1}{B\sin\psi}\frac{dU}{dx}\ , \qquad (3)$$

reveals that only the E×B drift affects the ion motion. The above effects of the sheath make the ion incident angle much narrower than the *B*-field angle. These prediction is greatly supported by our experiments and the details will be discussed in the conference.

[1] E. Ahedo, *Phys. Plasmas* **4**(12), 4419 (1997).

Kinetic damping in the admittance and impedance spectra of the spherical impedance probe

J. Oberrath

Institute of Product and Process Innovation, Leuphana University Lüneburg, Lüneburg, Germany

Active plasma resonance spectroscopy is a widely used diagnostic method, which utilizes the natural ability of plasmas to resonate near the electron plasma frequency. A radio frequent signal is coupled into the plasma via a probe, the spectral response is recorded, and a mathematical model is used to determine plasma parameter like electron density or temperature. By means of functional analytic methods the response function of a probe with arbitrary geometry can be derived in terms of a kinetic description. Based on this general response function the response of a specific probe design can be determined with an expansion in orthogonal basis functions, which will be presented for the spherical impedance probe. The approximated spectra of the admittance and impedance show a broadening, which can only be explained by kinetic effects.

1. Introduction

Active plasma resonance spectroscopy is a plasma diagnostic method which employs the natural ability of plasmas to resonate close to the plasma frequency. Essential for this method is an appropriate model to determine the relation between the resonance frequencies and demanded plasma parameters. Measurements with these probes in plasmas of a few Pa typically show a broadening of the spectrum that cannot be predicted by a fluid model. Thus, a kinetic model is necessary.

2. General Model

A general kinetic model of electrostatic resonance probes valid for all pressures has been presented [1]. This model is used to analyze the dynamic behavior of such probes by means of functional analytic methods. One of the main results is, that the system response function is given in terms of the matrix elements of the resolvent of the dynamic operator evaluated for values on the imaginary axis. The spectrum of this operator is continuous which implies a new phenomenon related to anomalous or non-collisional dissipation. Based on the scalar product, which is motivated by the kinetic free energy, the non-collisional damping can be interpreted: In a periodic state, the probe constantly emits plasma waves which propagate to “infinity”. The free energy simply leaves the “observation range” of the probe which is recorded as damping.

3. Spectra of the spherical Impedance Probe

Based on the general response function the response of a probe in a specific geometry can be derived by means of an expansion in orthogonal basis functions. Truncating this expansion leads to approximated spectra, which show a broadening of the resonances due to kinetic effects.

To demonstrate this broadening in the spectra of an existing probe design, the spherical impedance probe (sIP) is chosen. Based on the approximated response function, the normalized admittance Y and impedance Z of the sIP are computed and compared to the first kinetically determined spectra of Buckley [2]. Their real parts for an elastic collision frequency of 0.15, which is normalized to the plasma frequency, are depicted in Fig. 1 and they are in good agreement with Buckley’s. The half width of the resonance peaks in the admittance and impedance spectrum are about 0.47 and 0.32, respectively. They show clearly a kinetic damping part compared to the collisional damping of 0.15. Differences compared to Buckley’s spectra are probably due to a different collision term in the presented results [1].

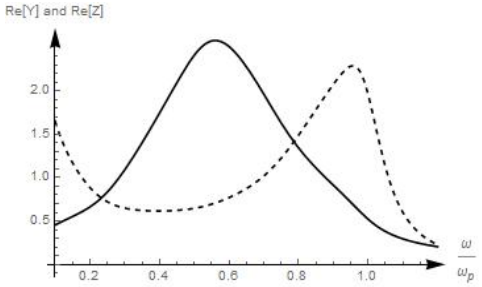

Fig. 1: Real part of the normalized admittance Y (bold) and impedance Z (dashed) of the sIP depended on the normalized frequency.

4. References

[1] J. Oberrath and R.P. Brinkmann, Plasma Sources Sci. Technol. **23**, 045006 (2014).

[2] R. Buckley, J. Plasma. Phys. **1**, 171 (1967).

Memory effect in a dielectric barrier discharge in N_2: phenomena in the gas bulk versus phenomena on the dielectric surfaces

C. Tyl[1], X. Lin[1], N. Naudé[1], S. Dap[1], N. Gherardi[1]

[1] *LAPLACE, Université de Toulouse, CNRS, INPT, UPS, France*

This work is focused on the study of the memory effect in Dielectric Barrier Discharges (DBD) at atmospheric pressure in N_2/NO and N_2/O_2 mixtures leading to a homogeneous Townsend discharge. An experimental approach with electrical measurements on a plane-to-plane DBD configuration is used. The literature suggests that the memory effect is mainly due to the collision of metastable species $N_2(A^3\Sigma_u^+)$ on the dielectric surfaces, but other phenomena in the gas bulk such as associative ionization can also contribute to the stabilization of the discharge. A comparison of the amount of seed electrons generated between two discharges for different gaseous gaps at the same power density gives a first quantification of the two phenomena, as the influence of the metastable species is assumed not to vary with the gaseous gap.

1. Introduction

The DBDs are a robust way to obtain a non-thermal plasma at atmospheric pressure, which has many applications in the surface treatment field. Atmospheric Pressure Townsend Discharges can be obtained in N_2 under specific conditions but it transits to the filamentary mode when the concentration of oxidizing gas exceeds a given threshold, which is not suitable for a homogeneous treatment of the surfaces [1].

The homogeneous regime is connected to a memory effect between two discharges which is highlighted by its electrical characteristics. The discharge current never reaches zero between two discharges. Hence, there is a current jump when the polarity reverses, due to the generation of seed electrons when the electric field is low enough to "trap" them in the gas volume. The origin of those seed electrons is thus the key phenomenon to understand the discharge physics of homogeneous DBDs.

2. Memory effect origin

The phenomena explaining the production of seed electrons under low electric field can be separated into two categories. First, in nitrogen-based mixtures, the collision of long-lived metastable species $N_2(A^3\Sigma_u^+)$ on the dielectric surfaces can enhance the secondary electron emission between two discharges. Secondly, phenomena in the gas bulk have been highlighted by the addition of small quantities of oxidizing gas in nitrogen [1]: despite the metastable species quenching by oxygen, the memory effect increases. The associative ionization of $N(^2P)$ with $O(^3P)$ could then explain the production of seed electrons under low electric field.

3. Experiments and results

The experimental set-up has already been described in a previous publication [2]. Current jump measurements have been made for two different gaseous gaps (1 and 2 mm), in nitrogen with addition of small concentrations of NO (from 0 to 40 ppm), for the same frequency and power density dissipated into the gas.

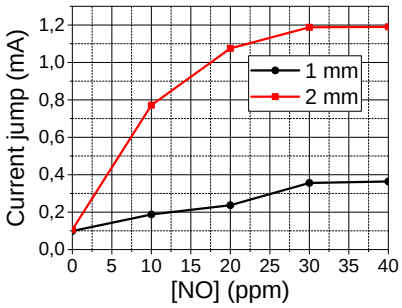

Figure 1: Current jump comparison (gap = 1-2 mm), frequency = 3 kHz, power density = 3.5 W/cm^3

Figure 1 shows that the current jump at 2 mm is twice to four times bigger than at 1 mm when NO is added to N_2. By assuming that the influence of the metastable species on the current jump does not depend on the gaseous gap, as those species do not move with the electric field, this increase would mainly be due to phenomena in the gas bulk. Thus, this comparison is a first approach which can give information on the ratio between the memory effect in the gas bulk and on the dielectric surfaces.

4. References

[1] Naudé N. *et al.*, Proc. Int. Conf. on Phenomena in Ionized Gases (2013)

[2] Massines F. *et al.*, Plasma Phys. Contr. Fusion 47 (2005) B577-B588

Memory effect in Dielectric Barrier Discharge in N_2/O_2 mixture: absolute atom density measurements by Two-photon Absorption Laser-Induced Fluorescence (TALIF) spectroscopy

X.Lin[1], C.Tyl[1], S.Dap[1], N.Naudé[1], N.Gherardi[1]

[1] *LAPLACE, Université de Toulouse, CNRS, INPT, UPS, Franc*

This work is aimed to study the memory effect in Atmospheric Pressure Townsend Discharge in N_2/O_2 mixture. As we found that with the presence of few oxidizing gas, the memory effect is more significant which means more production of seed electrons between two successive discharges. This phenomena may be due to an associative ionization. To verify this hypothesis, the absolute density of $N(^4S)$ and $O(^3P)$ will be determined by two-photon absorption laser-induced fluorescence measurement. Furthermore, with the result of concentration of $N_2(A^3\sum_u^+)$ from the literature, we can estimate the seed electron density, then we make the comparison with the experimental measurements.

Dielectric barrier discharge (DBD) is one kind of nonequilibrium discharge, generally working at atmospheric pressure. For most gases and discharge conditions, the DBD consists in a multitude of microdischarges corresponding to the so called filamentary regime. Under certain conditions, the discharge is homogenous along the electrodes surfaces. For example in helium, one can obtain a glow discharge characterized by a bright zone close to the cathode where the electric field is the higher [1]. In case of nitrogen, another homogeneous regime can be observed which is characterized by a uniform light layer located close to the anode [1]. This regime is called Townsend discharge because it exhibits several typical features similar to the dark Townsend discharge at low pressure.

It has been shown that the occurrence of the homogenous DBD is only possible if a memory effect from one discharge to the following one occurs. This mechanism allows to create seed electrons at low electric field [1]. The bombardment of the cathode dielectric surface by the metastable state $N_2(A^3\sum_u^+)$ resulting in the secondary emission of electrons was identified as a contributor to this memory effect [1]. However and counterintuitively we find that the addition of few oxygen (<100ppm) makes the homogenous discharge more stable, despite the high destruction rate of $N_2(A^3\sum_u^+)$ through quenching by oxygen. Due to this phenomenon we propose an additional memory effect occurring in volume and based on the following reactions [2]:

$N(^2P) + O(^3P) \rightarrow NO^+ + e^-$

where $N(^2P)$ is produced by the reaction:

$N(^4S) + N_2(A^3\sum_u^+) \rightarrow N(^2P) + N_2(X^1\sum_g^+)$.

The aim of the present work is to verify this hypothesis. For this purpose we determine the absolute density of $N(^4S)$ and $O(^3P)$ by using measurements Two-photon Absorption Laser-Induced Fluorescence (TALIF) for N_2/O_2 mixtures. The experimental results of Dilecce *et al.* [3] are used together with optical emission spectroscopy measurements to estimate the concentration of $N_2(A^3\sum_u^+)$ in the discharge. Then a simple 0D model is used to estimate the amount of seed electrons produced in the discharge volume through the aforementioned reaction. It allows to estimate the current jump occurring when the polarity reverses, which can be directly compared to experimental measurements. A relatively good agreement is found between them confirming that this mechanism can be considered as a serious candidate involved in memory effect.

In the future, we plan to measure the $N_2(A^3\sum_u^+)$ metastable density through CRDS measurements in order to improve the accuracy of 0D model. Moreover, it is well known that a large amount of NO(X) can be produced in atmospheric pressure discharges in N_2/O_2 mixture [4]. NO molecules being efficient quencher of $N(^2P)$ and $N_2(A^3\sum_u^+)$, LIF measurements of the NO density will be performed in order to include these reactions in the 0D model.

References

[1] F. Massines *et al*., Eur. Phys. J. Appl. Phys., 47(2): 1-10(2009)

[2] N.A. Popov, Plasma Physics Reports, 35(5), 436-449 (2009)

[3] G. Dilecce *et al.*, Plasma Sources Sci. Technol., 16: 511 (2007)

[4] I.A. Kossyi *et al.*, Plasma Sources Sci. Technol., 1 : 207-220(1992)

Generation of Terahertz Radiation by Beating of Dark Hollow Laser Beams in Magnetized Plasma

Reenu Gill[1], Sheetal Punia[1] and Hitendra. K. Malik[1]

[1] *PWAPA Laboratory, Department of Physics, Indian Institute of Technology Delhi, New Delhi – 110 016, India*

Terahertz radiation (THz) generation has been a fascinating area of research for the last few decades due to its diverse applications in the characterization of electronic materials, chemical/ biological sensing, explosives detections, non destructive testing, astronomy and atmospheric research, short distance wireless communications, etc.There are several ways to generate THz radiation including the schemes of THz generation from semiconductors, nonlinear crystals via electro-optic crystal, photoconductive antennas via time-varying current, air plasmas through ponderomotive force, etc. [1-6].In the present work, we use laser–plasma interaction technique to generate focused and more efficient THz radiation.

In our work we have analytically calculated the electric field of the THz radiation and the efficiency of the scheme when two dark hollow laser beams beat in magnetized plasma. We have considered the electron neutral collisions in plasma. We employ dark hollow beam because it has same power at different beam orders. With the application of magnetic field, we can obtain two or more peaks in the THz field which would be quite useful for medical diagnostics. The effect of collision frequency and order of the dark hollow beams on the nonlinear current and amplitude of the emitted THz radiation are studied. By optimizing the laser parameters and externally applied magnetic field we could obtain the THz radiation with high intensity and amplitude.

References

[1]C. Zhang, Y. Avetisyan, A. Glosser, I. Kawayama, H. Murakami, M. Tonouchi, Optics Express **20**, 8784(2012).

[2] Y. C. Shen, P. C. Upadhyay, H. E. Beere, and E. H. Linfielda, A. G. Davies, I. S. Gregory, C. Baker, W. R.Tribe, and M. J. Evans, Appl. Phys. Lett. **85**, 164 (2004).

[3] H.K. Malik, Phys. Lett. A **379**, 2826(2015).

[4] C. Weiss, R. Wallenstein, and R. Beigang, Appl. Phys. Lett. **77**, 4160 (2000).

[5] D. Singh and H. K. Malik, Plasma Sources Sci. Technol. **24**, 045001 (2015).

[6] M. Singh and R.P. Sharma, EPL **101**, 25001 (2013).

Effect of permanent magnets on plasma confinement and ion beams from a helicon plasma source

Erik Varberg[1] and Åshild Fredriksen[1]

[1] *UiT The Arctic University of Norway, Tromsø*

The experiments in this work was carried out to investigate how permanent magnets (PM) affect the confinement and ion beam properties in an inductively coupled plasma expanding from a helicon source. PMs were added around the exit port of the plasma source, and the effect was investigated experimentally by measuring the ion distribution using a Retarding Field Energy Analyser (RFEA). The plasma parameters obtained with and without the PMs were compared. It was found that the downstream plasma density can in some cases be doubled with PMs mounted. On the other hand, the ion beam velocity was reduced with a factor of typically 0.9. However, because of the increased ion beam density the ion beam flux increased by a factor of up to 1.5.

1. Introduction

In inductively coupled helicon discharges, an ion beam can form at the intersection between the plasma source and the expansion chamber in a diverging magnetic field [1]. The magnetic field in which the plasma expands from the source into the diffusion chamber plays an important role in generating the sharp potential drop, a so-called current-free double layer (CFDL), which again forms the ion beam. For most helicon sources, an axial magnetic field is produced by DC current coils around a cylindrical source. The field lines expand from the source into the source chamber.

In the source of the Njord device [2] a 30 cm long Pyrex glass cylinder with a radius r = 6.9 cm is coupled to the diffusion chamber through a port with radius 10 cm and length 8 cm. Simulations of the expanding magnetic field show that the field lines leaving the edge of the source are crossing the port wall. This field geometry leads to loss of electrons and affects the confinement of the plasma as well as the ion beam generated by the CFDL. In this work, we installed permanent magnets around the circumference of the port and investigated their effect on the plasma confinement and ion beam energy an –flux.

2. Experiment and results

Radio Frequency (RF) power between 100 W and 800 W was fed to a saddle antenna wrapped around the Pyrex tube, underneath a pair of magnetic field coils which generated a maximum axial magnetic field of about 200 G. A stainless steel ring supporting 18 neodymium magnets (Grade N42) was placed around the circumference of the port. Argon gas was fed to the end of the source tube, to provide working pressure between 0.6 μbar and 1.1 μbar for which an ion beam is generated.

A RFEA was used to obtain plasma and beam density, as well as plasma potential and beam energy [3]. Plasma parameters were obtained with and without PMs. Ratios of densities, potentials, as well as beam energy and fluxes could then be derived. It was found that at RF power P > 600 W the downstream plasma density within the beam could be doubled with PMs mounted, while the beam velocity decreased by typically a factor 0.9.

However, the higher ion beam density resulted in a significant increase of the ion beam flux. In Figure 1, the ratio of ion beam fluxes as a function of power is shown.

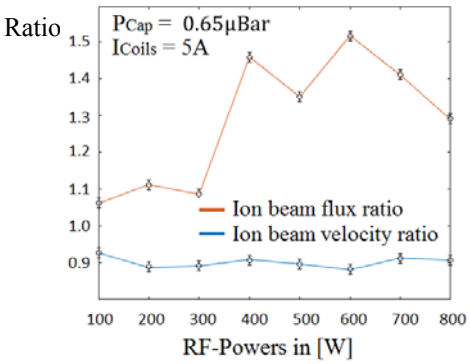

Figure 1. Center ion beam velocity ratio and ion beam flux ratio versus RF-power at pressure P = 0.65mBar and magnetic coil current I_{Coils} = 5 A.

3. References.

[1] C. Charles and R. Boswell, Phys. Plasmas **11** (2004) 1706.

[2] H. Byhring et al., Phys. Plasmas **15** (2008) 102113.

[3] N. Gulbrandsen et al., Phys. Plasmas **22** (2015) 033505.

Studies of laser-induced plasma in argon using emission spectroscopy and laser Thomson scattering: thermodynamic equilibrium and plasma heating by the probe laser beam

T. Pięta[1], M. Sankhe[2], K. Dzierzega[1], S. Pellerin[2], M. Wartel[2], W. Zawadzki[1], and B. Pokrzywka[3]

[1] *M. Smoluchowski Institute of Physics, Jagellonian University, ul. Łojasiewicza 11, 30-348 Kraków, Poland*
[2] *GREMI: Groupe de Recherches sur l'Energétique des Milieux Ionisés, CNRS, Université d'Orléans, France*
[3] *Mt Suhora Observatory, Pedagogical University of Cracow, 30-084 Kraków, Poland*

Scattering of electromagnetic waves by free electron of a plasma, named the Thomson scattering is a powerful and largely used method to measure important plasma parameter – the electron temperature T_e and density n_e. Thomson scattering has played an important role in the studies of nuclear fusion plasmas where it is still the most reliable method for measurements of the electron temperature. However, using high power probe laser beam to generate a scattered signal by free electrons can lead to plasma heating via inverse Bremsstrahlung and thus can modify the plasma parameters. In this work, we have studied the effect of the probe beam laser energy on T_e and n_e in argon plasma and the existence of the local thermodynamic equilibrium (LTE).

1. Experimental setup

The plasma was created with frequency doubled Nd:YAG laser, at 532 nm pulses of 4.5 ns duration and a repetition rate of 10 Hz, by focussing the laser beam in a chamber filled with 1 bar argon. For the Thomson scattering (TS), another Nd:YAG laser at 532 nm, named "the probe laser", with similar duration as the plasma generating one and energy from 1 mJ to 15 mJ, was used. The probe laser beam is directed perpendicularly to the plasma generating one and the emission from laser induced plasma and the scattered light were observed at 90° and imaged onto an entrance slit of a spectrograph (Acton SP-2750i).

The radiation scattered from free charges is mainly due to electrons because their mass is much lower than the mass of ions resulting in their much higher acceleration in an electric field of the laser and consequently large dipole radiation. Applied to laser-induced plasma, TS allows to directly determine parameters of the plasma electrons e.g. T_e and n_e without any assumption about plasma thermodynamic equilibrium.

2. LTE in the argon plasma

Laser-induced plasma (LIP) is usually described statistically assuming the local thermodynamic equilibrium (LTE). At this approach, velocities of plasma components, populations of their energy levels and chemical composition of plasma are described by the Maxwellian velocity distribution function, the Boltzmann distribution function and the Saha-Eggert equation, respectively. Each of these functions is dependent on the distinctive temperature: kinetic, excitation and ionic - which are equal under LTE conditions. Unfortunately, it is very common that the LTE plasma is assumed *a priori*, without any experimental verification. Even if such validation takes place, usually only optical emission methods are applied.

The main goal of this work was to investigate the equilibrium state of laser-induced plasma in argon at different stages of its evolution using optical emission spectroscopy (OES) and laser Thomson scattering (LTS) technique[1]. Spatially resolved electron temperature and electron density were directly derived from TS spectra while excitation temperature was calculated from the spectra of argon atoms and ions employing the Boltzmann plot method.

Our preliminary results show huge discrepancy between intensity ratios of ionic to atomic argon lines computed with measured electron density and temperature and assuming plasma in LTE, and those directly obtained from emission spectra. It implies either incorrect data processing or some principal problems with thermodynamic state in such kind of plasma.

3. TS for the electron parameters measurements

Using high power probe laser beam to generate a scattered signal by free electrons can lead to plasma heating via inverse Bremsstrahlung and modify the plasma parameters Our first results show that in general the electron density seems not to be disturbed or modified by the probe laser. It is not the case for the electron temperature: Te could be considerably increased by the probe laser beam.

[1] K. Dzierżęga, A. Mendys, B. Pokrzywka, *What can we learn about laser-induced plasmas from Thomson scattering experiments*, Spectrochim. Acta Part B 98 (2014), 76

Electric field measurements in DBD plasma jet using intensity ratio of helium lines

M. M. Kuraica[1], G. B. Sretenović[1], V. V. Kovačević[1], I. B. Krstić[1], B. M. Obradović[1], N. Cvetenović[1, 2] and R. Brandenburg[3]

[1] *University of Belgrade, Faculty of Physics, Belgrade, Serbia*
[2] *Faculty of Transport and Traffic Engineering, University of Belgrade, Belgrade, Serbia*
[3] *Leibniz Institute for Plasma Science and Technology (INP Greifswald), Greifswald, Germany*

In this paper a method is proposed and tested for electric field measurements in the streamer head of DBD helium plasma jet. The method uses intensity ratio of two helium singlet lines: He I 2^1P-3^1D at 667.8 nm and He I 2^1P-3^1S at 728.1 nm. The method is based on our earlier work in helium dielectric barrier discharge (DBD). Collisional-radiative model for the involved atomic levels is utilized to obtain the functional dependence of the line ratio on the local electric filed strength. The obtained values of the electric field are compared with the results obtained by Stark polarization spectroscopy.

1. Introduction

One of the most promising and patient friendly plasma devices for biomedical applications is non-thermal atmospheric pressure plasma jet. It can be found in various constructions and under various operation conditions. Non-thermal atmospheric pressure plasma jet requires noble gas as working media and AC or pulsed high voltage supply. It is a source of guided ionization waves, typically one ionization wave – streamer per one voltage half cycle. If discharge gets in contact with target, streamer becomes only one part of the entire discharge which transforms to transient glow discharge. The electric field strength is one the most important parameters of streamer discharges and the knowledge of the electric field in the streamer head can give information about other parameters, such as electron density and production of different active chemical species. The well-established Stark polarization spectroscopy method suffers from a low intensity of used helium lines, thus the new les demanding method would be of great interest [1,2]. Here we present preliminary results of the electric field measurements in the streamer head of DBD helium plasma jet using the intensity ratio of two helium singlet lines: He I 2^1P-3^1D at 667.8 nm and He I 2^1P-3^1S at 728.1 nm [3].

2. Experiment

Investigated DBD plasma jet consisted of quartz capillary of the inner diameter of 1 mm and outer diameter of 2 mm, with two metallic electrodes wrapped around it. The amplitude of applied sinusoidal voltage was 2.5 kV and the frequency was 10 kHz. Five millimetres downstream the exit tube copper grounded electrode was placed. High resolution spectrometer equipped with iCCD camera was used for all measurements.

3. Results

Figure 1 presents comparison of the results obtained by two methods. The preliminary results are promising and further studies should be preceded.

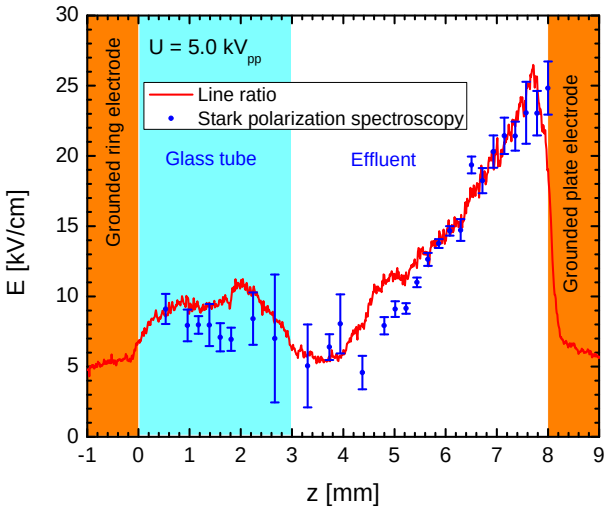

Figure 1: Comparison of the electric field strength inside the capillary of the plasma jet and in the effluent obtained by two independent methods.

4. References

[1] M. M. Kuraica and N. Konjević Appl. Phys. Lett. **70** (1997) 1521–3

[2] G. B. Sretenović, I. B. Krstić, V. V. Kovačević, B. M. Obradović and M. M. Kuraica J. Phys. D. Appl. Phys. **47** (2014)102001

[3] S. S. Ivković, G. B. Sretenović, B. M. Obradović, N. Cvetanović and M. M. Kuraica J. Phys. D. Appl. Phys. **47** (2014) 55204

W-band Extended Interaction Oscillator based on a pseudospark-sourced electron beam

A.W. Cross[1], H. Yin[1], L. Zhang[1], W. He[1], Y. Yin[2], J. Zhao[3] and A.D.R. Phelps[1]

[1] *Department of Physics, SUPA, University of Strathclyde, Glasgow, G4 0NG, United Kingdom*
[2]*University of Electronic Science and Technology of China, Chengdu, 610054, China*
[3]*High Voltage Division, School of Electrical Engineering, Xi'an Jiaotong University, Xi'an, 710049, China*

The pseudospark discharge is a low-pressure gas discharge, capable of generating extremely high currents within short rise times by means of a hollow cathode structure. A high-quality, sub-millimetre diameter electron beam was generated during the discharge process which possesses a high current density and brightness. A pseudospark (PS) sourced electron beam did not require the use of an external guide magnetic field as the beam is self-focused by ion channel focusing. The PS electron beam was used to drive a W-band (75-110 GHz) Extended Interaction Oscillator (EIO). The EIO combines the merit of a short interaction length and is best suited to be driven by a small diameter, high current density electron beam. The pseudospark discharge is therefore an ideal cathode for an EIO. Experimental results presented will show that with a 35 kV discharge voltage, the EIO successfully produced W-band radiation pulses with 200 W peak power and 20 ns duration, agreeing well with the 3D Particle-in-Cell (PIC) simulations using MAGIC.

1. Introduction

A pseudospark (PS) is an axially symmetric, self-sustained, transient, low pressure (typically 50–500 mTorr) gas discharge in a hollow cathode/planar anode configuration, which operates on the low pressure side of the hollow cathode analog to the Paschen curve [1]. The production of higher current-density electron beams, compared to thermionic cathodes, from a pseudospark discharge has been convincingly demonstrated [2]. The current density of a pseudospark-sourced electron beam can achieve ~1kA/cm^2 [3], which enables a wide range of applications in generating millimetre and terahertz radiation.

2. Experimental results

A four-gap pseudospark discharge chamber was used which can hold-off a discharge voltage of up to 40 kV, was connected to a W-band EIO, fig 1.

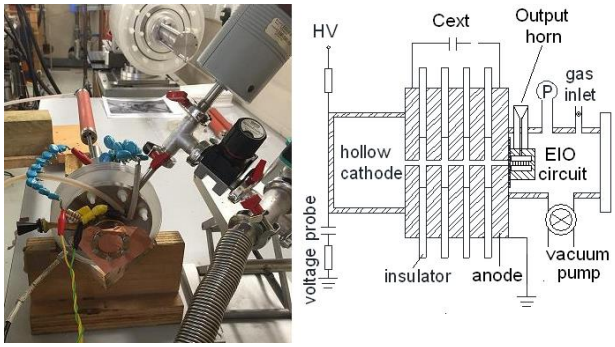

Fig. 1. Experimental setup of the W-band EIO based on a pseudospark-sourced electron beam and the schematic drawing of the experiment.

The discharge voltage was swept from 38 kV to 25kV to achieve the maximum output power. The peak power of the radiation was measured to be 200W. The output frequency was measured to be ~94GHz.

3. Conclusion

The pseudospark-sourced electron beam which is focused by the positive ion channel generated from the pseudospark discharge process was successfully used to drive a W-band EIO circuit to generate coherent radiation. The background unmagnetized plasma can be considered as a dielectric media with a dielectric constant of $\varepsilon_r=1-\omega pe^2/\omega^2$. As the operating frequency is far away from the plasma frequency the plasma would have negligible effect on the output power of the EIO. As the current density of the pseudospark-soured electron is much higher than a thermionic electron beam, it is an excellent electron beam source to drive a pulsed EIO circuit operating at higher frequencies with reasonable high radiation power.

3. References

[1] K. Frank and J. Christiansen, IEEE Trans. Plasma Sci., 17, 748 (1989).
[2] H. Yin, A. W. Cross, at al Phys. Plasmas 16, 063105 (2009).
[3] W. He, L. Zhang D. Bowes, H. Yin, et al Applied Physics Letters, 107, 913, 133501, 2015.

Effect of Plasma Activated Medium on human Head & Neck cancerous Tumor Spheroids.

J.Chauvin[1,2], F.Judée[1], N.Merbahi[1], P.Vicendo[2]

[1] *Université de Toulouse - LAPLACE, UPS, Toulouse, France*

[2] *Université de Toulouse - IMRCP, CNRS, Toulouse, France*

This work investigates the effect of Plasma Activated Medium (PAM) on human head and neck cancerous cells using FaDu multicellular tumour spheroids (MCTS). Results indicate that PAM induces cell detachment as soon as the first day post PAM treatment and in a PAM time-dependant manner. The presence of hydrogen peroxide in PAM has been shown to be responsible for this cell detachment. However, a rapid regrowth of the multicellular tumour spheroids size is observed after PAM treatment probably due to a defense mechanism exhibited by FaDu cells. To counteract this effect, successive treatment were done and growth inhibition obtained.

1. Introduction

Chemotherapy and radiotherapy have a low rate of success against Head and Neck Cancer due to a high level of resistance [1].

For over a decade, cold atmospheric plasma has been studied in the biomedical field. It high reactivity allow the creation of RONS [2] that are cytotoxic on various cancer cell lines [3-4] and may induce cell death via apoptosis [4].

Recently, we reported that PAM induced cell death mainly by the involvement of hydrogen peroxide [3].

This work studies the effect of PAM on FaDu MultiCellular Tumor Spheroids (MCTS) and the involvement of hydrogen peroxide in PAM treatment.

2. Results

The first effect observed is a volume loss at day one post-treatment associated with a cell detachment. This effect may be attributed to H_2O_2. The second effect is a rapid re-growth the following days attributed to the auto-organization of MCTS and FaDu defence mechanism (Fig. 1).

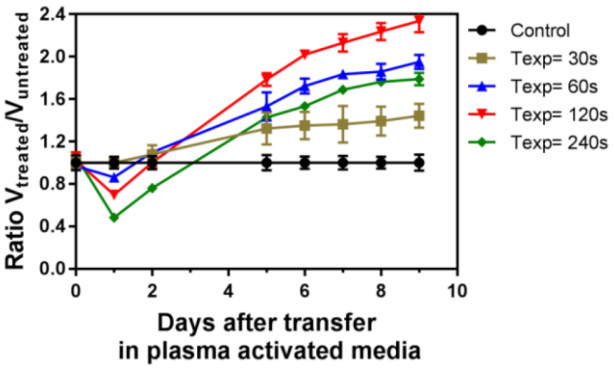

Fig 1. Relative growth of spheroid after PAM treatment for several exposure times.

This increase of spheroids growth may be attributed both to loss of MCTS auto-organization and to FaDu defense mechanisms induced by an external attack.

After 4 successive treatments (Fig. 2), FaDu MCTS were successfully disrupted. However, after each treatment the previously exhibited effects: cell detachment and proliferation were observed until the forth one.

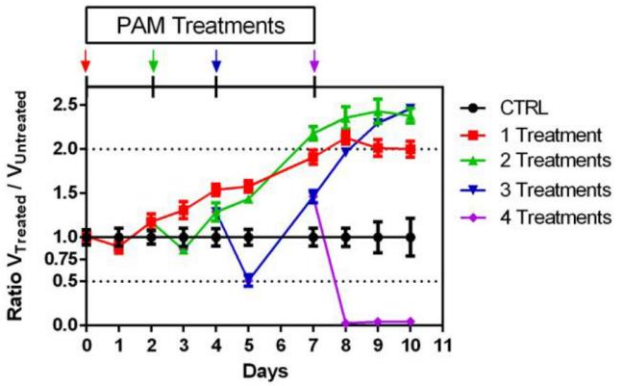

Fig 2. Successive treatment of FaDu spheroids

3. References

[1] Mutschelknaus L, Peters C, Winkler K, Yentrapalli R, Heider T, Atkinson MJ, Exosomes Derived from Squamous Head and Neck Cancer Promote Cell Survival after Ionizing Radiation, *PLoS ONE*, **2016** 11[3]: e0152213

[2] Fridman, A; Plasma Chemistry, *Cambridge: Cambridge University Press*, **2008**, 1017 p

[3] Judée, F.; Fongia, C.; Ducommun, B.; Yousfi, M.; Lobjois, V.; Merbahi, N. Short and Long Time Effects of Low Temperature Plasma Activated Media on 3D Multicellular Tumor Spheroids, *Sci Reports*, **2016**, *6*, 21421.

[4] Utsumi, F.; Kajiyama, H.; Nakamura, K.; Tanaka, H.; Hori, M.; Kikkawa, F. Selective Cytotoxicity of Indirect Nonequilibrium Atmospheric Pressure Plasma against Ovarian Clear-Cell Carcinoma, *Springerplus*, **2014**, 3, 398. DOI: 10.1186/2193-1801-3-398

PTR-TOF analyzis of glow discharge products in Titan related atmosphere

S. Chudjak, F. Krcma, V. Mazankova

Faculty of Chemistry, Brno University of Technology, Brno, Czech Republic

The glow discharge at atmospheric pressure was generated in the nitrogen-methane (1 to 5 %) gaseous mixtures related to the Titan's atmosphere. The discharge itself was monitored by optical emission spectrometry that confirmed presence of active nitrogen species and various radicals formed from methane. Besides them, the CN spectral bands were observed. Intensities of all light emitting species were studied in the dependence on applied power and composition of nitrogen-methane mixture. The stable discharge products were analysed by proton transfer time of flight mass spectrometry of the exhausting gas. Presence of huge number of amino and cyano compounds was confirmed as well as aliphatic and some aromatic hydrocarbons. Their relative concentrations were determined under the same conditions as optical emission spectra were collected.

1. Introduction

The laboratory studies of chemical processes initiated by electrical discharges in extra-terrestrial planetary atmosphere's gaseous mixtures started to be important during last years because of observing many exoplanets and search of potential exo-biology or even exo-life. The most studied exo-atmosphere is Titan's one because it was proposed that current Titan's atmosphere is similar \as Earth atmosphere before life formation.

2. Experimental

The atmospheric pressure DC glow discharge at energy of up to 50 W was created between stainless steel electrodes in pure nitrogen containing 1-5 % of methane. The flow rate of gaseous mixture was fixed at 100 Sccm. Whole system was evacuated before measurement by rotary oil pump to minimize the gaseous mixture contamination by oxygen. The optical emission spectra of discharge were collected using Jobin Yvon TRIAX 550 spectrometer with CCD detector. The exhaust gas was analysed using proton transfer time of flight mass spectrometry allowing simultaneous detection of many stable discharge products without fragmentation.

3. Results

The nitrogen molecular second positive and first negative bands and CN violet CN bands were determined as the most intense in the discharge emission spectra. The hydrogen lines and C_2 Swan molecular bands were determined, too. Using these spectra, the rotational temperature of about 2000 K was calculated. This temperature is nearly independent on the applied power and slightly increases with the increase of the methane content in the gaseous mixture. The vibrational temperature obtained from neutral nitrogen molecule is also not dependent on the applied power but it increases nearly directly proportionally from 300 K (at 1% of methane) to 3600 K (at 5% of methane). In the contrary, vibrational temperatures obtained from nitrogen molecular ion and CN showed the same trend: temperature is decreasing with the increase of nitrogen in the gaseous mixture and they are increasing directly proportionally with applied discharge power. Both of them are significantly higher (up to 5700 K) than was calculated for neutral nitrogen.

An example of PTR-TOF spectrum is given on Fig. 1 there the main determined compounds are marked. Totally, 32 compounds were identified and their relative intensities were studied under the same conditions as were used for the OES measurements.

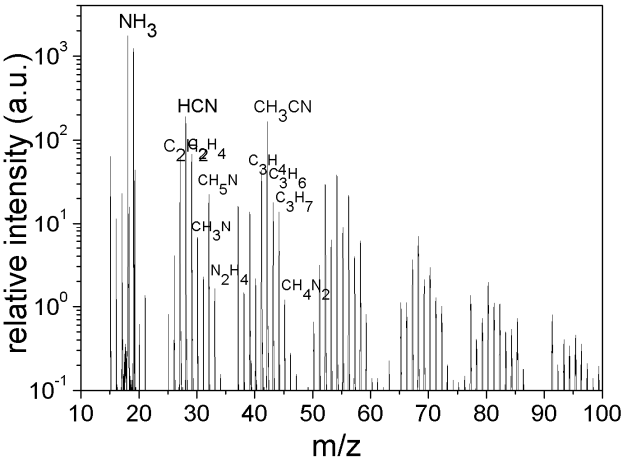

Acknowledgement

This work was supported by the Czech Ministry of Education, Youth and Sports under project LD15011 and in was carried out as a part of broader research done under the frame of COST Action TD1308.

Atmospheric pressure plasma treatment of agricultural seeds with effect on wettability and surface chemical changes

Vlasta Štěpánová[1], Pavel Slavíček[1], Jakub Kelar[1], Jan Prášil[2], Milan Smékal[2], Monika Stupavská[1], Jana Jurmanová[1], Mirko Černák[1]

[1] *Department of Physical Electronics, Faculty of Science, Masaryk University, Czech Republic*
[2] *SEMO a.s, Smržice, Czech Republic*

Diffuse coplanar surface barrier discharge (DCSBD) at atmospheric pressure in ambient air was used for plasma treatment of agricultural seeds. The aim of plasma treatment was improvement of wettability and potential reduction of pathogens. Lettuce seeds were plasma treated for a few seconds and analyzed with SEM, XPS and method for measurement of water uptake. Surface morphology was not affected with plasma treatment. Plasma treatment caused surface chemical changes and improvement of water uptake with only slight decrease of germination in comparison with untreated seeds. Change in percentage of chemical bonds containing carbon and oxygen was observed. Significant increase of O/C ratio after few seconds of plasma treatment was reached.

Improvement of germination, reduction of diseases, changing of water absorption properties are crucial parameters for growth process of agricultural seeds. Different plasma sources are used for plasma treatment of seeds.

Plasma treatment of agricultural seeds e.g. lettuce using Diffuse coplanar surface barrier discharge (DCSBD) operating in ambient air at atmospheric pressure is presented in this contribution.

Diagnostics methods used for evaluation of plasma treated seeds were: scanning electron microscopy (SEM), X-ray photoelectron spectroscopy (XPS) and method for measurement of water uptake (Washburn method).

Germination of plasma treated seeds is depending on the duration of plasma treatment. No structural damages were observed on lettuce seeds plasma treated for 10 s (Figure 1). Improvement of water uptake after the plasma treatment was obvious which is important for planting of seeds. Increase in content of oxygen and decrease in content of carbon was observed after the plasma treatment. O/C ratio significantly increased after plasma treatment which indicates hydrophilization of seeds. Potential effect of plasma treatment on pathogens and microorganisms incidence on seeds will be studied.

The conclusion is that DCSBD plasma treatment in order of few seconds is able to affect the properties of agricultural seeds.

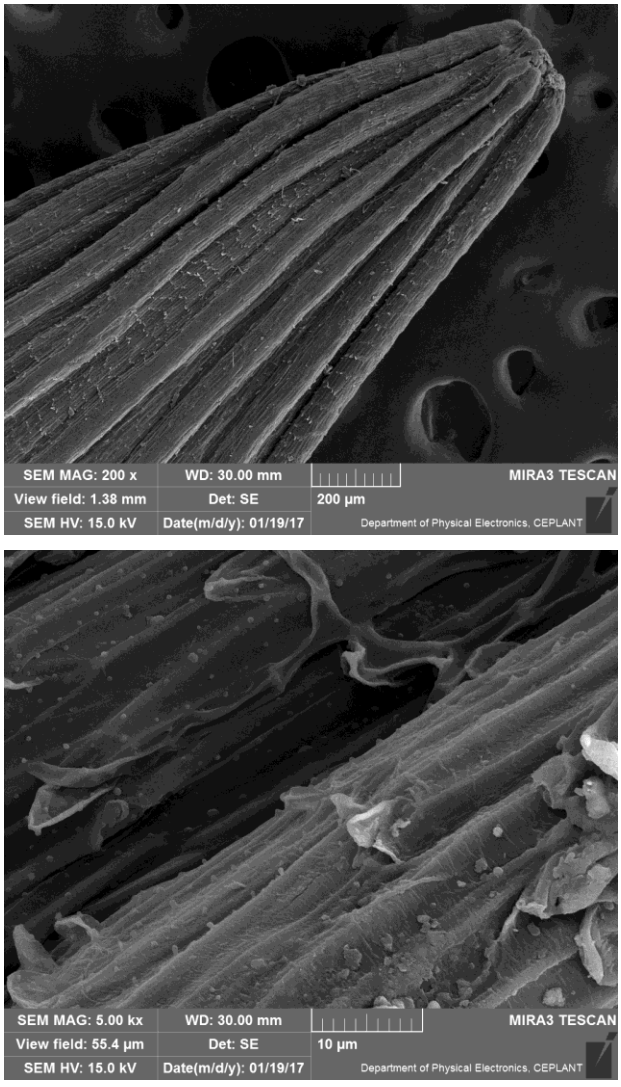

Figure 1. Surface morphology of plasma treated lettuce seeds.

Acknowledgements:
This research has been supported by the project LO1411 (NPU I) funded by Ministry of Education, Youth and Sports of Czech Republic.

Theoretical and experimental study of plasma jet interaction with surface

I. Schweigert[1,2], L. Lin[1], M. Keidar[1]

[1] *George Washington University, Washington D.C. 20052, USA*
[2] *Khristianovich Institute of Theoretical and Applied Mechanics, Novosibirsk 630090, Russia*

Characteristics of streamer propagating over helium jet at atmospheric pressure are studied in 2D simulations and in the experiment. This type of streamer often referred as cold atmospheric plasma jet is widely used for medical applications. We study effect of surface presence and interaction of the streamer with surface with different properties (surface charge, ion-electron emission, biased surface). The enhancement of streamer properties is obtained with biased ring placed some distance from dielectric tube.

Cold atmospheric plasma (CAP) jet becomes attractive research topic due to different applications, in particular for cancer treatments (see for example [1]). The CAP jet forms as a result of ionization along the gas flow passing through high voltage electrodes. Streamer propagates by ionizing neutral particles at front. In Ref. [2], the idea of using a ring with DC voltage was proposed. It was shown that the jet length can be changed by setting up different ring potentials.

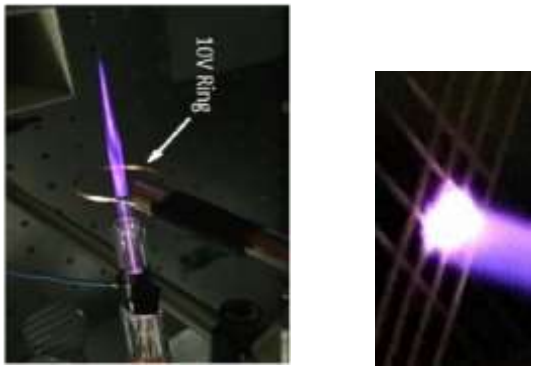

Fig. 1. Experiment: CAP jet with a ring potential and grid.

To study the effect of additional DC voltage from the ring and interaction of jet with a surface we performed experimental and computational analysis of CAP jet shown in Fig.1. The jet is generated by an AC voltage of 4 kV pk-pk at 12.44kHz in a 5LPM helium flow. The ring with applied voltage is place 1 cm apart from the discharge tube. Additionally a grid made from crossed wares covered by dielectric is placed 4 cm apart from discharge tube which models a cell membrane. The photographs of some details of experimental set up is shown in Fig. 1. We have performed 2D simulations of DC discharge in dielectric tube and streamer formation and propagation outside of tube. In our simulation model we use the fluid approach with additional continuity equation for electron energy. The surface charge accumulation and ion-electron emission are taken into account. We assume that streamer propagates over helium at atmospheric gas pressure. In Fig. 2, the ionization rate and electrical field distribution are shown at the time when streamer head is 3 cm apart from the discharge tube exit (at z=2.5 cm) for the case of a 10 V ring potential.

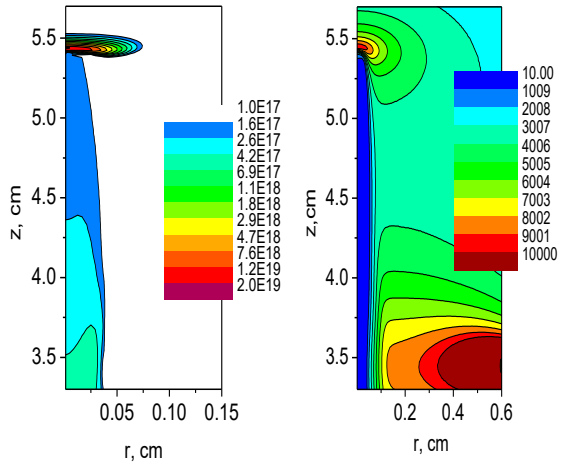

Figure 2. Simulation: Ionization rate, 1/cm^{3}s (left) and electrical field, V/cm (ring) with a ring with 10 V bias.

In simulation the ionization front speed is about 17 km/s. The ionization rate is about 2x10^{19} cm^{-3}s^{-1} and this value is constant during streamer propagation up to 4 cm and then quickly decreases. Note that in simulation the gas flow is assumed to be laminar. Streamer channel radius is 300 microns. The electrical field E in streamer head is about 10 kV/cm. The measured and computed jet characteristics are in good agreement. A variation of ring potential from -1.5 kV to 1.5 kV considerably affect CAP jet properties. The sheath structure and strength of electrical field near grid surface are essentially changed for different surface potentials and emission yield.

[1] M. Keidar at al Br. J. Cancer 105 (2011) 1295.
[2] A. Shashurin, M. N. Shneider, and M. Keidar, Plasma Sources Sci. Technol. 21 (2012) 034006.

Optical Emission Spectroscopy Investigations in a Non-Transferred DC Plasma Torch

Vidhi Goyal, P. Bharathi and G. Ravi

Institute for Plasma Research, Bhat, Gandhinagar-382428, India

We present the nitrogen species evolution and plasma temperature measurements [1] at different operating conditions of a non-transferred dc plasma torch. For estimations of plasma parameters, high resolution optical emission spectroscopy (OES) is performed for wide range of gas flow rates (20 to 60 lpm) in the presence of external magnetic field (100 to 300 G) for various currents (70 to 120 A) at atmospheric pressure with nitrogen as working gas. These OES investigations allow us to study the variation of the dominant species with various operational parameters of the torch. The plasma temperature is estimated from three independent techniques: (i) intensity analysis of molecular bands of first negative systems of N_2^+, (ii) Boltzmann plot of neutral atomic lines and (iii) line broadening analysis of the same neutral nitrogen lines. For the former two techniques, local thermodynamic equilibrium (LTE) is assumed. These estimations yield plasma temperature in the range of 3000 – 8000 K for the range of parameters mentioned above. Additionally, influence of various operating parameters on the plasma temperature is also presented and discussed in this work.

A comprehensive study on the fluctuations of the arc root and column in a non-transferred dc plasma torch requires estimations of plasma parameters for various operational conditions of the torch. Such studies are necessary to understand the complex interaction between different forces that act on the plasma column and lead to the above mentioned fluctuations. In the present work, OES on a dc plasma torch was performed using 0.5 m ARC spectrograph with PI CCD and 1800 l/mm grating. Studies on the behaviour of the species evolution and presence of dominant species are carried out. The plasma temperature is obtained using N_2^+ FNS bands (Fig. 1) and excited emissions from neutral Nitrogen atoms (wavelength range: 740 nm to 1100nm).

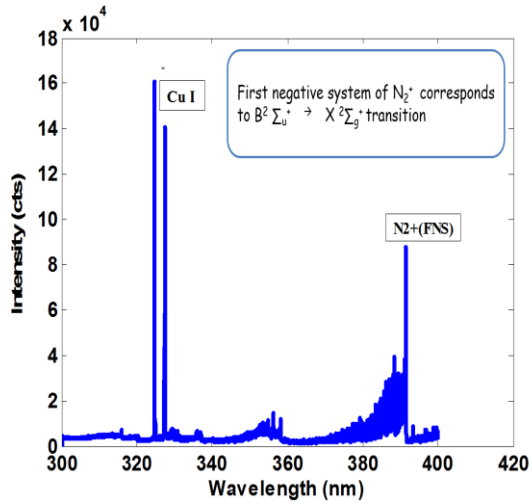

Figure 1 - Experimental data of N_2 FNS band for 20 lpm, 70A discharge current and 100 G external magnetic field.

Study further shows that neutral atomic nitrogen is the dominant species in the discharge. The intensity of dominant specie is maximum at nozzle exit and decreases along the plume. The intensity v/s pressure scaling shows a decrease of intensity indicating a lower temperature at higher gas flow. Few N_2^+ FNS molecular bands (Fig. 2) are also simulated using LIFBASE software to benchmark the experimentally obtained temperature values and show good agreement.

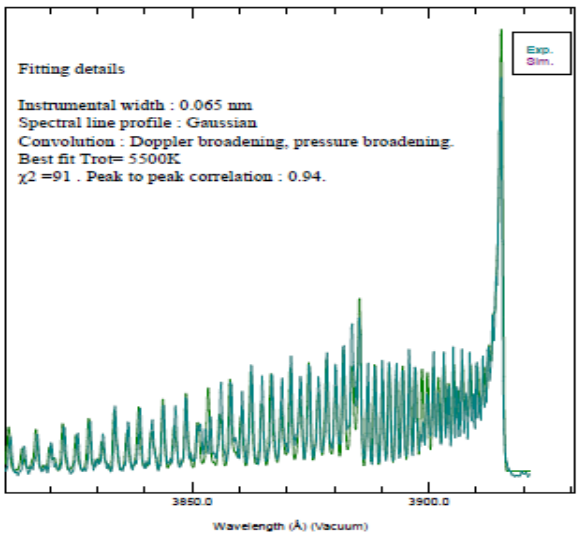

Figure 2 - N_2 FNS band simulation for 20 lpm, 70A discharge current and 100 G external magnetic field.

3. References

[1] Boulos, M. I., Fauchais, P., and Pfender E., Thermal Plasmas: Fundamentals and Applications, Plenum Press, New York, (1994)

Dynamics of a nanosecond diffuse pin-to-plane discharge – Effects of pin material at high overvoltage

P. Tardiveau, A. Brisset, P. Jeanney

Laboratoire de Physique des Gaz et des Plasmas, CNRS, Paris-Saclay Université, 91400, Orsay, France

The dynamics and propagation speed of a pin-to-plane discharge generated in atmospheric air under high nanosecond overvoltage is analyzed and discussed for different pin materials. Pulses of 85kV with 2ns rise time are applied to a conical pin electrode made of different materials: aluminum, titanium, stainless steel, copper, molybdenum and tungsten. Discharge propagation speed is derived from sub-nanosecond time resolved imaging of the discharge front location with an accuracy of 0.3 mm/ns. Results clearly show the slowdown of the discharge with the tungsten electrode and, to a lesser extent, with aluminum. For these two materials, the average speed is decreased respectively by 20 and 10 % compared to the case of copper electrode.

1. Introduction

Pin-to-plane discharges generated under very high overvoltage (> 500%) nanosecond pulses, showing a large and diffuse pattern in atmospheric air, are not extensively studied and fully understood [1]. At such high voltages, the very intense electric field at the pin might induce non local mechanisms and specific behaviour (runaway electrons, X-ray emission). Some previous studies, in similar configurations, seem to show X-rays emission from the electrodes [2], which should depend on their material type since X-rays would arise from high energy electrons impact on the electrodes. Within this scope and considering that possible X-rays could influence the dynamics of discharges by photo-ionization effects, our study focuses on the only effect of the pin electrode material on the propagation speed, all the other experimental parameters remaining unchanged.

2. Experimental

The diffuse discharge starts to develop from a pin electrode with a well calibrated conical shape and a tip radius of about 30 µm. It extends and propagates towards a plane at 25 mm from the pin. A very high electric field (> 5000 Td at the pin, down to 20 Td at the plane) is generated by a +85 kV peak voltage nanosecond pulse (2 ns rise time and 5 ns width) at 5 Hz. Experiments are carried out with synthetic air (1l/min) at atmospheric pressure. Light emission from the discharge (mainly N_2(C-B) spectrum) is recorded with an intensified 4-Picos Stanford Camera (200 ps time gate) through a UV-visible lens (F/2.8). Propagation speed is derived from time resolved sequences of the discharge front location. Taking into account the jitter of the camera (100 ps) and the reproducibility of the discharge for given conditions, uncertainty on measurements is estimated to ± 0.3 mm/ns. **Figure 1** shows the results for six different materials classified, on x-axis, according to the energy of their characteristic X emission line (K_α). Electronic impacts can produce X-rays of respectively 1.5, 8 and 59 keV with aluminum, copper and tungsten.

3. Results

Discharge propagation is clearly slower with tungsten pin (speed 20 % less than with copper) and speed reaches lower maxima for decreasing K_α line energy between copper and aluminum. Pin material can have significant effects on discharge dynamics at very high electric field.

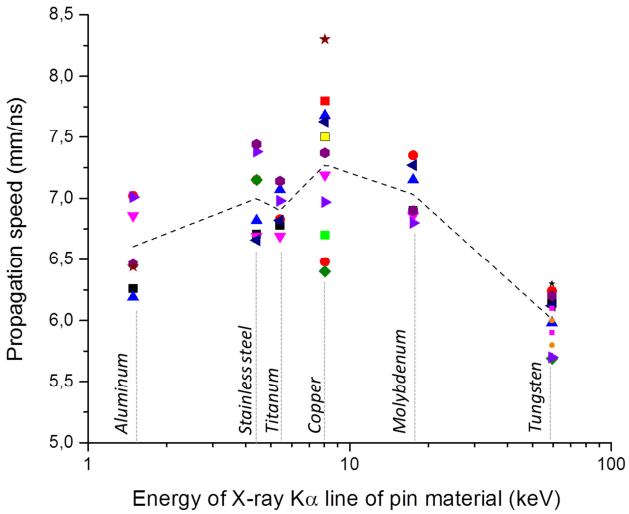

Figure 1. Discharge speed for six different pin anode materials according to the energy of X- ray K_α line

3. References

[1] P Tardiveau *et al* 2016 *Plasma Sources Sci. Technol.* **25** 054005

[2] C V Nguyen *et al* 2010 *J. Phys. D: Appl. Phys.* **43** 025202

Plasma structures induced by external magnetic field

I. Schweigert[1,2], M. Keidar[1]

[1]*George Washington University, Washington D.C. 20052, USA*
[2] *Khristianovich Institute of Theoretical and Applied Mechanics, Novosibirsk, Russia*

The characteristics of 2D periodical structures in propulsion type magnetized plasma are studied in kinetic PIC MCC simulations. With increasing an obliqueness of magnetic field the ridges (maxima) of electron and ion densities form in the plasma volume in cylindrical chamber. These ridges are shifted relative each other that results in the formation of two-dimensional double-layers structure. Depending on Larmor radius and Debye length up to nineteen potential steps appear across the oblique magnetic field.

Recently some methods to control the Hall effect thruster characteristics with applying the oblique magnetic field with respect to the channel walls is widely discussed (see, [1]). Nevertheless with increasing the inclination of the magnetic field, discharge plasma properties can essentially change. For example, a several stationary, magnetized, two-dimensional weak double-layers were observed in a laboratory experiment for this type of plasma by Intrator, Menard, Hershkowitz [2].

In this paper, in kinetic simulations we consider the dc discharge plasma in the external oblique magnetic field at pressure, P=0.0001 Torr. Our purpose is to study the plasma structure modification with changing the electron temperature, magnetic field strength and obliqueness for the conditions similar to the Hall thruster ones. In our simulations, the plasma is embedded in a cylindrical chamber with the radius of 4 cm and the height H=10 cm. All walls are grounded and the cathode is biased with -90 V (grey in Fig. 1). The magnetic field B=25-100 G and magnetic field angle α_B =0-77^o. To describe the plasma in electro-magnetic field at low gas pressure we solve Boltzmann equations for the distribution functions for electrons and ions with particle-in cell Monte Carlo collision method. The Poisson equation was solved to find the electrical potential and electrical field distributions.

The periodical structure with ridges of ion and electron densities was found for larger obliqueness of magnetic field (see Fig.1). With increasing α_B the periodical plasma structure becomes clearly visible. The electron and ion ridges are shifted with respect to each other and double–layer structure appears across B-field and along the potential rise. The double-layers structure forms due to a distortion of local quasineutrality in the presence of oblique magnetic field. The electron is shifted from the ion in the direction normal to B-field and a local charge appears.

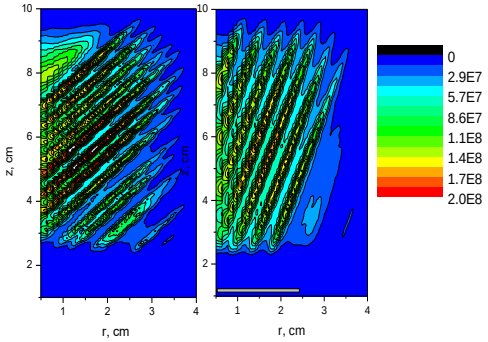

Fig. 1. Distribution of ne, cm-3 for α_B= 55^o (left) and 77 (right), B=50 G, Te=2.5 eV.

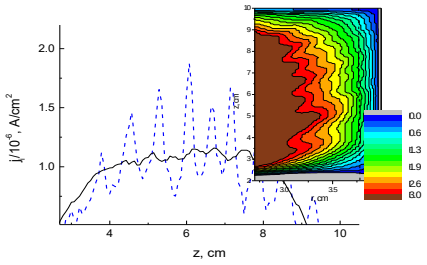

Fig.2. Ion current density over z near side wall for α_B=10^o (solid) and 65 ^{o} (dashed), potential (insert).

The ion current shown in Fig. 2 clearly indicates the periodical plasma structure. This effect can lead to an additional local erosion of wall material.

[1] J.Miedzik, et al, Phys. Plasmas 22, 043511 (2015). K. G. Xu, et al, Phys. Plasmas 19, 103502 (2012).
[2] T. Intrator, J. Menard, and N. Hershkowitz, Physics of Fluids B, 5, 806 (1993).

Role of intracellular RONS in plasma-based cancer treatment

E. Martines[1], P. Brun[2], R. Artico[3], P. Brun[4], R. Cavazzana[1], L. Cordaro[1], G. De Masi[1], D. Fischetto[3], A. Zuin[5], M. Zuin[1]

[1]*Consorzio RFX, Padova, Italy*
[2]*Department of Molecular Medicine, Microbiology Unit, University of Padova, Padova, Italy*
[3]*ENT Department, Civil Hospital, Cittadella (Padova), Italy*
[4]*Department of Molecular Medicine, Histology Unit, University of Padova, Padova, Italy*
[5]*Department of Cardio-Thoracic and Vascular Sciences, University of Padova, Padova, Italy*

We describe an in-vitro study aimed at elucidating the role of Reactive Oxygen and Nitrogen Species (RONS) in promoting a selective killing of cancer cells, and the possibility of emphasizing the selectivity towards cancer cells by combining the plasma treatment with the effect of a molecule known to enhance intracellular ROS production. Lung carcinoma cell lines and cultured primary cells isolated from surgical samples of laryngeal and lung cancers as well as healthy tissue counterparts were treated with an RF plasma source. An increase in the level of endogenous Reactive Oxygen Species (ROS) and of NO was observed, but it was markedly higher in cancer cells than in healthy ones. Incubating the cells with antimycin A (AMA), a molecule known to increase ROS production, the effect could be amplified, An increased expression of hypoxia-inducible factor (HIF)-α amd a higher apoptosis in cancer cells than in healthy ones was observed.

1. Introduction

The mechanism underlying the beneficial effects of a low-power, atmospheric pressure plasmas as a tool for cancer treatment has been traced by several authors to the formation of intracellular Reactive Oxygen and Nitrogen Species (RONS). In this contribution we describe an in-vitro study aimed at elucidating the role of RONS in promoting a selective killing of cancer cells.

2. Experimental procedure

The plasma treatment applied for this study is performed with an indirect plasma source, which uses a RF voltage to ionize a helium flow mixed with ambient air in the region between two brass grids [1]. The helium flow enriched with active chemical species is then sent to the substrate to be treated.

H460, MCF7, A549 lung carcinoma cell lines were grown in DMEM medium + 10% fetal bovine serum (Gibco). Primary cell cultures were established from surgical samples of laryngeal cancer and healthy counterparts. Tissue samples were dissociated with collagenase type IV (Sigma) at 37°C for 15 min. Cells were cultured in DMEM medium + 10% fetal bovine serum, and then exposed to the plasma for 2 min. Reactive oxygen species (ROS) and nitric oxide (NO) were detected 30 min, 4hours, and 24 hours later plasma treatment by flow cytometry. Cell death was assessed 24 hours later plasma treatment using Annexin V-FITC Apoptosis Detection Kit (eBioscience).

3. Results

It has already been reported that this kind of treatment induces an increase in the level of endogenous Reactive Oxygen Species (ROS) in eukaryotic human cells [2]. In the present study, ROS generation was confirmed, but the increase was markedly higher in cancer cells than in healthy ones. The same effect was observed for intracellular nitric oxide (NO). Furthermore, incubating the cells for 15 min. with antimycin A (10ng/mL, AMA), a molecule known to increase ROS production [3], the effect could be amplified, both for ROS and NO. The selective increase in endogenous RONS was associated to increased expression of hypoxia-inducible factor (HIF)-α, an oxygen-sensitive transcriptional activator, and to a higher apoptosis in cancer cells than of their healthy counterparts. Again, these effects were emphasized by incubating with AMA. Overall, these results point to confirm the important role played by RONS in plasma-based cancer treatment, and to the possible combination with chemotherapeutic drugs to better tailor the selective effect induced by the plasma treatment.

5. References

[1] E. Martines, M. Zuin, R. Cavazzana, *et al.*, New J. Phys, **11** (2009) 115014.
[2] Paola Brun, Surajit Pathak, Ignazio Castagliuolo, *et al.*, PLOS ONE **9** (2014) e104397.
[3] W. Y. Hung, K. H. Huang, C. W. Wu, et al., Biochim. Biophys. Acta **1820** (2012) 1102.

A Numerical and Experimental Study of Ion Impingement from RF Discharge on the Mirror Surface in Strong Magnetic Field

A.A. Kobelev[1], A.S. Smirnov[1], N.A. Babinov[2], A.M. Dmitriev[2], E.E. Mukhin[2], and A.G. Razdobarin[2]

[1] *Department of Plasma Physics, Peter The Great St. Petersburg Politechnic University, St. Petersburg, Russia*
[2] *Ioffe Institute, St. Petersburg, Russia*

Optical elements of Thomson scattering diagnostic system in ITER tokamak will require cleaning techniques against the Be-W contaminations. Ion bombardment from radio frequency (rf) discharge is promised to be the most efficient technique for remove of deposited metal films. We present a numerical study of ion transport in collisional rf sheath in presence of strong magnetic field using PIC simulation. Calculated ion flux and energy distribution functions are compared with experimental measurements for different noble gases, discharge frequencies (40 – 100 MHz), inclination angles of magnetic field lines (0 – 90 degrees) and magnetic field strength.

1. Introduction

Thomson scattering of electromagnetic radiation is one the main methods to measure fusion plasma parameters. Based on this phenomenon, optical diagnostic system uses mirrors installed in the vacuum vessel of tokamak reactor. During the ITER tokamak operation, sputtered Be and W elements will be deposited on the mirror surface changing reflectance and measured spectra. Therefore, optical diagnostic system in ITER will require the implementation of mirror cleaning system. Ion bombardment from capacitively coupled plasma (CCP) is considered to be the most promising method to remove contaminations from the mirror surface [1].

Development and optimization of plasma cleaning process requires measuring of ion flux density, ion angular and energy distribution function (IEDF). The study becomes more complicated in presence of strong external magnetic field (~ few T) inclined to the mirror surface.

2. Modeling and experimental results

Self-consistent PIC simulations of ion movement through the collisional oscillating CCP sheath were performed for noble gases (He, Ar and Ne) in presence of strong magnetic field (~ 0.9 T). Both elastic and charge exchange collisions were taken into account. Magnetic field was considered to be spatially uniform. Experimentally measured ion flux density and potential drop across the sheath were used as input parameters for PIC simulation.

Experimental measurements of IEDF were performed using retarding field energy analyzer for different discharge frequencies 40 – 100 MHz at fixed discharge power. Maximal magnetic field strength was 0.9 T.

As the result, we have numerically calculated ion energy and angular distribution functions, plasma sheath thickness and sputtering coefficients for different noble gases, discharge frequency 40 – 100 MHz, inclination angle 0 – 90 degrees and magnetic field strength up to 0.9 T. Simulation results have been compared with experimental measurements of IEDF and .

3. References

[1] A.G. Razdobarin et al, Nucl. Fusion. **55** (2015) 093022 (11pp).

Hydrogen low-pressure pulsed plasma: measurement of H atom decay in the post discharge

X. Yang, D. Kogut, J.M. Layet, G. Cartry

PIIM, Service 241, Aix Marseille Université, Centre de St Jérôme, 13397 Marseille Cedex 20, France

H atom decay in the post discharge of a 10 Pa hydrogen pulsed plasma is measured by two different diagnostics, namely two photon absorption laser induced fluorescence (TALIF) spectroscopy and Pulsed Induced Fluorescence (PIF) which is a simpler method based on optical emission spectroscopy. Both methods are compared and the best one is selected to obtain the atomic hydrogen surface loss coefficient from the measurements.

1. Introduction

Surface loss of atomic or radical species in low-pressure plasmas is a key parameter in modelling low pressure plasmas. It has been shown that the surface loss is strongly dependent on surface state which in turn is dependent on the ion flux to the wall [2], on the ion energy, on the surface temperature, on the species impinging the wall, etc. It is therefore almost impossible to predict theoretically surface loss coefficients. Most of plasma models use published experimental results in similar conditions or fit its value to get a good agreement with experiments. The best practice is to measure the loss coefficient *in-situ*, if possible. This is the aim of the present work. We want to measure hydrogen atom loss coefficient on surfaces using whether two photon absorption laser induced fluorescence (TALIF) spectroscopy, or Pulsed Induced Fluorescence (PIF) which is a simpler method based on optical emission spectroscopy.

2. Experimental set-up and results

2.1. Experimental set-up

A 3 turn loop antenna is installed above a quartz plate on top of a spherical vacuum chamber. Inside the chamber a quartz tube of 160 mm in diameter and 140 mm in height is limiting the plasma extension. A sample holder is placed at the bottom of the tube and holds a quartz sample (or any material under study) of 100 mm in diameter. The plasma geometry is well defined and simplifies both calculation of loss coefficient and plasma modelling. The antenna is powered by a 13.56 MHz Dressler generator through a matchbox. The plasma is operated at 10 Pa of hydrogen or deuterium gas, with injection of 1000 W of RF power. The plasma is pulsed at 1 or 10 Hz with a duty cycle of 10%. The decay of the atomic H density vs. time in the post discharge is measured whether by TALIF or PIF. For TALIF diagnostic, two photon absorption at 205 nm excites ground state hydrogen atoms to the level n = 3. Fluorescence from the level n = 3 to the level n = 2 at 656 nm is measured using a collimating lens, an interference filter and a photomultiplier. For PIF diagnostic, H atoms are re-excited in the time post discharge by a short plasma pulse (probe pulse). The Hα signal at 656 nm at the beginning of the probe pulse is assumed to be proportional to the density of the remaining atoms in the post discharge. For both diagnostics the delay between the main pulse and the laser shot or the probe pulse is varied in order to measure H atoms versus time in the post discharge. The characteristic time of atomic loss in the post discharge is correlated with the surface loss probability.

2.2. Result

Both diagnostics give different results. While H atom density at plasma centre measured by TALIF demonstrates a mono-exponential decay in post discharge, the line integrated H density obtained by PIF demonstrates a bi-exponential decay. In order to understand this difference and to select proper measurement to get the surface loss coefficient we have developed a simple 2D fluid modelling taking into account gas heating and neutral depletion effects. The model allows detailing the difference between a line integrated signal and a measurement at plasma centre. It helps understanding the influence of gas heating on the H atom density variation in post discharge and on the diagnostics.

3. References

[1] Cartry, G., L. Magne, and G. Cernogora Journal of Physics D: Applied Physics 32, nº 15 (1999): L53.

[2] C. M. Samuell and C. S. Corr 2014 Journal of Nuclear Materials 451 pp 211

Effect of secondary electron emission on subnanosecond breakdown in high-voltage pulse discharge

I V Schweigert[1], A L Alexandrov[1],
P Gugin[2], M Lavrukhin[2], P A Bokhan[2], Dm E Zakrevsky[2]

[1] *Khristianovich Institute of Theoretical and Applied Mechanics, Novosibirsk, Russia*
[2]*A V Rzhanov Institute of Semiconductor Physics, Novosibirsk 630090, Russia*

A subnanosecond breakdown in high-voltage pulse discharge is studied in experiment and in kinetic simulations for mid-high pressure in helium. It is shown that the characteristic time of the current growth can be controlled by the secondary electron emission. We test the influence of secondary electron yield on plasma parameters for three types of cathodes made from titanium, silicon carbide and CuAlMg-alloy. By changing the pulse voltage amplitude and gas pressure, the area of existence of subnanosecond breakdown is identified.

Recently serious attention is paid to the study of physical phenomena of subnanosecond current development in discharge plasma in super-high-electric fields at mid- and high-pressures.

In this paper, in the experiment and in PIC MCC simulations we study the breakdown development in the high voltage discharge with 3 types of cathodes made from different materials. All these materials have enhanced secondary electron emission yield. Our purpose is to find a way to decrease the discharge breakdown time by testing different cathode materials and changing the gas pressure and voltage. The breakdown in the high-voltage pulse discharge in helium is studied in the experimental cell with two round cathodes with the total area of 1.6 cm2 placed 6 mm apart. A mesh-anode is placed between the cathodes. The pulse voltage is simultaneously applied to both cathodes and two oppositely directed electron beams are generated due to cathode emission. The voltage amplitude ranges from 4 kV to 12 kV and P=10-35~Torr. The cathodes are symmetrically connected to the external low-inductance circuit and the mesh-anode is grounded. The pulse shape is registered with the low-inductive resistive divider with the rate about 20:1 using oscilloscope Tektronix DPO 70804C with a bandwidth of 8 GHz. The experimental details were described in [1]. In the experiments, the cathodes made from titanium (Ti), silicon carbide (SiC), and CuAlMg alloy were tested. All these materials have large SEE coefficient γ_e, but the dependence of γ_e from the electron energy is different. In our simulations, we solve Boltzmann equations for electrons, ions and fast neutral atoms. Poisson equation describes the electric potential. The details of the model can be found in [2]. The effect of P on breakdown time is shown in Fig.2. The record switching time for SiC and CuAlMg-alloy is τs <0.4ns and for Ti is 4-5 times larger. In conclusion there is a specific range of discharge parameters, 5-10 kV and P=15-35 Torr, within that the record switching time τs <1 ns can be achieved.

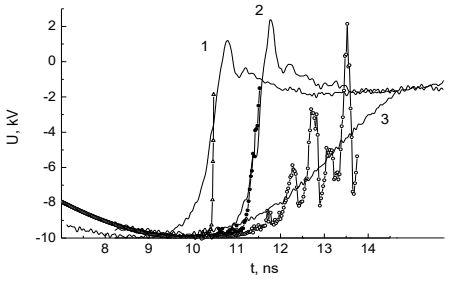

Fig. 1. Voltage measured (solid lines) and calculated (lines with symbols) cathodes from titanium (1), silicon carbide (2) and CuAlMg-alloy (3) for Ua=10 kV and P=25 Torr.

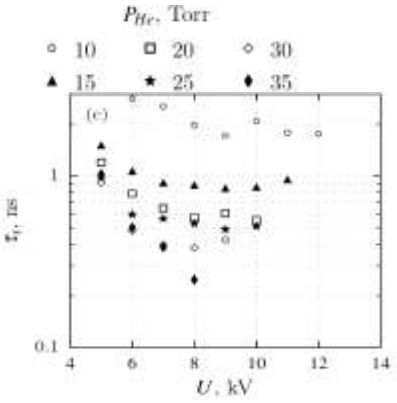

Fig. 2 Breakdown time via U for CuAlMg-alloy cathode for different P.

[1] Bokhan P A et al 2016 In: Generation of runaway electron beams and x-rays in high pressure gases (NY: Nova Science Publishers Inc) 221
[2] I.V. Schweigert, et al PRE, 90, 051101(R) (2014); I.V. Schweigert, et al PSST 24, 044005 (2015)

Bio-relevant NO_x generated by transient spark in atmospheric dry air and air with water electrospray

Z. Machala[1], K. Hensel[1], B. Tarabová[1], M. Janda[1]

[1] *Faculty of Mathematics, Physics and Informatics, Comenius University in Bratislava, Slovakia*

Generation of nitrogen oxides (NO_x) was studied in a DC-driven self-pulsing transient spark (TS) discharge in atmospheric pressure air. The precursors of NO_x production and the TS characteristics were studied by nanosecond time-resolved optical diagnostics. Thanks to the short (~20–50 ns) high current (~1 A) spark pulses, highly reactive non-equilibrium plasma is generated. The NO_x production rate of ~7×10^{16} molecules/J was achieved in dry air, dependent on TS repetition frequency, i.e. power, which is related to the complex frequency-dependent discharge properties and thus NO_2/NO generating mechanisms. With water electrosprayed through the TS, gaseous NO_x formation was lowered but induced chemical changes in water make it of biomedical importance.

1. Introduction

Nitrogen oxides (NO_x) are typical by-products of air plasmas that have important bio-relevant properties, e.g. as antimicrobial (NO_2), physiological (NO), and anesthetics (N_2O) agents. We studied the generation of NO and NO_2 in the transient spark (TS) discharge in atmospheric pressure air, using optical emission spectroscopy combined with the post-discharge gas composition analysis by FTIR.

The TS is a DC-driven repetitive self-pulsing discharge with 20-50 ns short spark current pulses initiated by streamers, with the pulse repetition frequency 1-10 kHz [1]. It has been successfully applied for flue gas cleaning and bio-decontamination of water [2]. The air TS can be combined with the electrospray of water, which induces formation of nitrites, nitrates, hydrogen peroxide and peroxynitrites and demonstrates strong antibacterial properties of such plasma activated water [2].

2. Results

Generation of NO_x in the gas phase was studied in dry air, and in the air humidified by water electrosprayed through the discharge. The dominant stable gas phase products in dry air were nitrogen oxides, while ozone was not detected (<10 ppm detection limit). NO formation steeply increases with the discharge power, as shown in Fig. 1. The sum of NO and NO_2 concentration >400 ppm was achieved with power input below 6 W. The highest NO_x (NO + NO_2) generation rate achieved was around 7×10^{16} molecules/J [3]. Due to their easy dissolution in the water and possibly also due to the discharge cooling by water and thus decreased NO_x formation, the NO_x densities were found lower in air humidified by the water electrospray (Fig. 1).

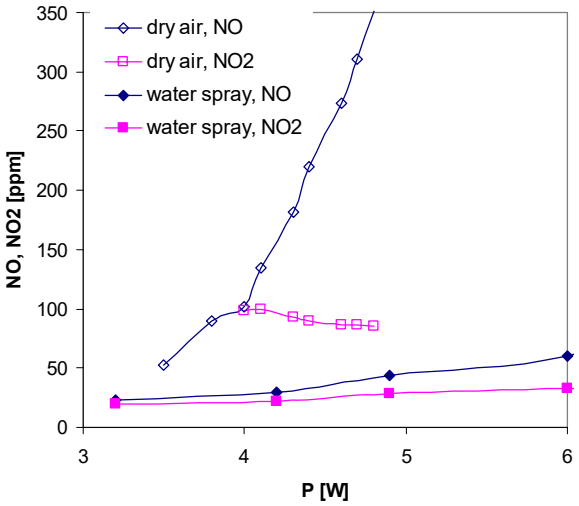

Fig. 1: NO and NO_2 generation in TS in dry air vs. air with water electrospray for increasing dicsharge power.

3. Summary

TS in atmospheric air provided high production rates of NO_x. With sprayed water, gaseous NO_x formation was lowered but induced chemical changes in water make it of biomedical importance.

3. References

[1] M. Janda, V. Martišovitš, L. Dvonč, et al., *Plasma Sources Sci. Technol.*, **23**, 065016 (2014).

[2] Z. Machala, B. Tarabová, K. Hensel, et al., *Plasma Process. Polym.*, **10**, 649 (2013).

[3] M. Janda, V. Martišovitš, K. Hensel, Z. Machala, *Plasma Chem. Plasma Process.* **36**, 767 (2016)

This work was supported by Slovak Research and Development Agency APVV-0134-12 and Slovak grant agency VEGA 1/0918/15.

Method of pulsed DC bias for negative-ion production study on surfaces of insulating materials in low pressure H2 plasmas

R. Moussaoui[1], D. Kogut[1], J.M Layet[1], J. Achard[2], A. Gicquel[2], G. Cartry[1]

[1]*Aix Marseille Université, CNRS, PIIM, UMR 7345, Marseille, France*

2 LSPM, CNRS-UPR 3407 Université Paris 13, 99 Avenue J. B. Clément, F-93430 Villetaneuse

We present a study of negative ion surface production in hydrogen and deuterium low-pressure plasmas. A sample facing a mass spectrometer is negatively DC biased with respect to the plasma potential. Upon the positive ion bombardment some negative ions are formed on the surface and are accelerated towards the mass spectrometer where they are detected according to their energy. In the present contribution, a DC pulsed bias technique is introduced to enable the study of negative ion surface production on insulating samples.

1. Introduction

Negative-ions (NI) production mechanisms in low-pressure plasmas is of interest for many plasma applications such as microelectronics, space propulsion, magnetically confined fusion… In the latter intense hydrogen negative-ion beams are extracted from a low-pressure hydrogen plasma source and accelerated to high energy. They are then neutralized and injected inside the fusion plasma where they deposit their energy and contribute to the plasma heating. Next generation fusion devices requires high intensity (40 A) negative-ion beams which pushes towards the development of efficient negative-ion sources. Volume production of negative-ions by dissociative attachment of electrons on molecules is not efficient enough and these sources rely on surface production. In the present study we investigate surface production of negative ions on diamond materials.

2. Experimental set-up and results

2.1. Experimental set-up

A sample is introduced in a low-pressure (2 Pa) hydrogen plasma and negatively biased (using DC bias) with respect to the plasma potential. The negative-ions formed on the surface upon positive ion bombardment are accelerated by the sheath in front of the sample and then self-extracted towards a mass spectrometer facing the sample at a distance of 4 cm. Negative ions are detected according to their energy and mass, and Negative-Ion Energy Distribution Function (NIEDF) is measured. This experimental method proved to be efficient for the study of negative ions production on different materials. In particular we have shown that boron doped diamond is producing high yield of negative-ions [1] compared to metals such as stainless steel or molybdenum. In order to extent this method to insulating materials that cannot be DC biased we developed a pulsed DC bias method and applied it to the study of non-doped diamond samples.

When an insulating sample is DC biased it acts as a capacitor. The DC bias initially appears on the sample surface. Positive ions are therefore attracted towards the sample and the capacitor is charged by the positive ion saturation current. The rate of change of the surface bias is given by the ratio of the ion saturation current over the sample capacitance ($dV/dt = I_i/C$). For a few µm thick diamond layer the capacitance of a 1 cm^2 sample is on the order of 1 nF. The ion saturation current is below 100 µA/cm2 in our experiment giving a surface bias rate of change on the order of 0.1 V/µs. As the time resolution of the mass spectrometer is 2 µs, measurements can be performed on diamond samples at an almost constant surface bias. We show that with this method it is possible to measure energy distribution functions of negative ions created on insulating materials.

2.2. Result

NIEDF measurements are synchronized with the pulsed DC bias. The surface bias rate of change is determined experimentally based on the energy of the negative ions detected. The sample current is measured by a microamperemeter. A model is developed to better understand the charge of the sample by the positive ions during the pulse ON phase, and the unload of the sample by electrons in the pulse OFF phase. The model is compared to the time resolved measurements of sample bias and current.

The effect of pulse frequency and pulse duty cycle on the negative-ion surface production is studied. It is shown that a low duty cycle (10 %) at a frequency around 1 kHz allows for efficient negative-ion production and detection. Surprisingly, negative-ion surface production on boron-doped diamond is much higher in pulsed mode than in continuous mode. Production on non-doped diamond is as high as the one on boron doped diamond. This effect is attributed to a less defective diamond surface in pulsed mode.

3. References

[1] Kumar et al Journal of Physics D: Applied Physics 44, nº 37 372002

TiC nanopowder plasma-chemical synthesis with titanium tetrachloride raw material in the DC plasma-arc reactor

A.V.Samokhin, D.E.Kirpichev, M.A.Sinaiskiy, N.V.Alexeev

A.A.Baikov Institute of metallurgy and material science, Moscow, Leninskiy av., 49

The possibility of TiC nanopowder plasma-chemical synthesis in the DC plasma-arc reactor is shown. The dependence of the molar ratio C/Ti in the raw material in the range 0.7 – 2.1 and carbon concentration in the TiC product is investigated. Carbon concentration in the TiC nanopowder grows with increase of molar ratio C/Ti in the raw materials. TiC nanopowder with stoichiometric composition was produced at molar ratio C/Ti = 1.4. It was determined that molar ratio C/Ti in raw material more over 1.5 leads to free carbon formation in the TiC nanopowder product. Chlorine concentration decrease in the TiC nanopowder product with molar ratio C/Ti increase in the raw materials is shown.

1. Introduction

Powder materials are claimed of many industry areas. Productions of wear- and corrosion-resistant hard alloys, deposition of coatings are some of them. Nanosized powders allow improve final product properties. Plasma chemical DC-arc processes are allocated with high efficiency; these processes have potential to regulate produced powders characteristics in the wide range. The TiC nanopowder synthesis in the DC plasma-arc reactor is presented.

2. Experimental setup

DC plasma-arc reactor is experimental setup on the base of DC electro-arc thermal plasma generator with power rating 25 kW. The hydrocarbon and chloride mixture are feeded with piston dispenser to vaporizer. Resulting vapour is feeded with transport gas to plasma jet through mixing chamber. Condensed reaction product deposited on the reactor water cooled walls and filter. Contained in exhaust gas chlorine was trapped with alkaline solution scrubber. Experiment parameters of TiC nanopowder production in thermal plasma flow are presented in the table 1.

Table 2. Plasma process parameters ranges

№	Parameter	Range
1	Plasmatron useful power	4.8 – 9.3 kW
2	Plasma forming gas	H_2 + Ar
3	Total plasma forming gases consumption	1.4 – 2.5 n.m^3/h
4	Plasma jet useful enthalpy	1. 6 – 5.9 kWh/n.m^3
5	$TiCl_4$ consumption	0.2 kg/h
6	CH_4 consumption	0.02 – 0.2 n.m^3/h
7	Molar ratio C/Ti	0.7 – 2.2

3. Results and discussion

It is experimentally established that TiC nanopowders are formed at interaction of $TiCl_4$ + CH_4 vapor mixture with hydrogen-argon plasma jet. Produced TiC nanopowder have a single phase and cubic NaCl type crystal latice. It consists of nanosized cubic shape particles with 10-80 nm size and aggregates on its base (fig.1).

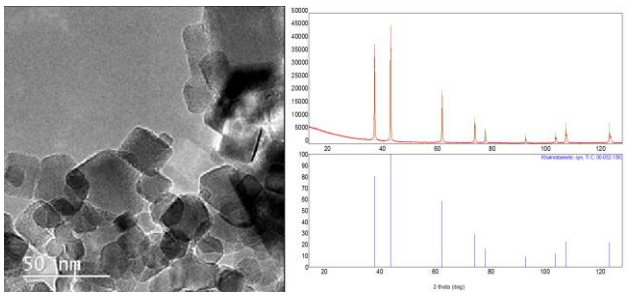

Figure 1. X-ray and SEM results for TiC nanopowders

Output of TiC depended on molar ratio C/Ti. Increase of molar ratio C/Ti from 0.7 to 2.1 leads to increase of TiC output from 60% to 90%. Carbon concentration in the TiC nanopowder increases with molar ratio C/Ti increase. Stoichiometric carbon concentration in the product is reached when C/Ti=1.4. Significant quantity of carbon in the process is in the gaseous phase as a part of methane and its pyrolysis products. Molar ratio C/Ti strong influences on chlorine concentration in the product. Inrease of C/Ti from 0.7 to 0.9 leads to decrease chlorine concentration from 1.6 to 0.4.

This research was conducted with support of the Russian Ministry of Education and Science (Federal Target Program «Research and development on priority directions of scientific-technological complex of Russia for 2014 - 2020 years», project «Development of the principles of the weld metal modification of welded joints of low-carbon, low alloy steels due to the use of nano-sized particles», agreement № 14.578.21.0216, unique code RFMEFI57816X0216).

The temperature of leucoxene melted zone under DC plasma arc anode spot

A.A.Nikolaev, D.E.Kirpichev, A.V.Nikolaev, Yu.V.Tsvetkov

A.A.Baikov Institute of metallurgy and material science, Moscow, Leninskiy av., 49

Leucoxene concentrate is a perspective titanium source. Leucoxene concentrate consists of TiO_2 and SiO_2 with similar mass quantities. Plasma-arc heating of concentrate with carbon allows to separate titanium from silicon. The reaction $SiO_2 + C = SiO + CO$ takes place and volatile SiO evaporates. Experimental results of DC plasma arc melting of leucoxene concentrate in graphite and copper water-cooled crucibles are compared. It was established that melting in the graphite crucible leads the less overheat of leucoxene pool under the anode spot of DC plasma arc then in the copper water-cooled crucible. The calculation method of the temperature field of melting pool is considered.

1. Introduction

Copper water-cooled crucible and graphite crucible were used [1]. The enrichment of TiO_2 was worse in graphite crucible then in cooper water-cooled. The both crucibles had a similar geometry and arc power. The anode spot in graphite crucible was disperse (≈ 10 A/cm^2) and the anode spot in copper crucible was constricted (≈ 100 A/cm^2). Thus the material was not overheated enough in the graphite crucible. The purpose of this work was to calculate the temperature field of the pool surface under the anode spot in both cases.

2. Calculation model

The calculation model is presented on fig.1.

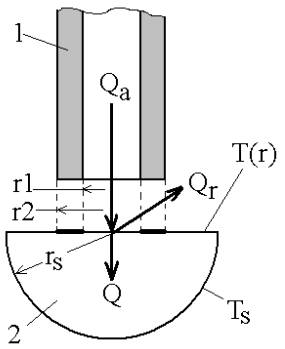

Figure 1. Calculation model scheme. 1 – electrode (graphite hollow cathode); 2 – melted pool (anode); $Q = Q_a - Q_r$ – heat flow into melted pool; Q_a – heat transfer via electrical physical processes in anode spot of DC plasma arc; Q_r – heat radiation of melted surface.

The quantity of Q_a was determined experimentaly on cold anode. It equaled approximately 50 % from arc power [2].

The quantity of Q_r was detemined as:

$$Q_r = 2\pi\varepsilon\sigma\left[\int_0^{r1} r(T(r))^4 dr + \int_{r2}^{rs} r(T(r))^4 dr - 0{,}5T_k^4(r1^2 + rs^2 - r2^2)\right]$$

here r_s – pool radius; r_1, r_2 – inside and outside radiuses of non-radiated area under hot hollow cathode; T_s – periphery temperature of melted pool; T(r) – temperature of the pool surface in dependance of radius.

The temperature field of the pool surface is calculated as:

$$T(r) = 0{,}282\frac{Q}{\lambda r_o}\left[\varphi(r) - \varphi(r_s)\right] + T_s, \qquad (1)$$

here r_o – plasma arc anode spot radius; λ– thermal conductivity of the material; $\varphi(r) = \exp\left(-\frac{r^2}{2r_o^2}\right)\cdot I_o\left(\frac{r^2}{2r_o^2}\right)$, Io – Bessel's function of imaginary argument.

Calculation results are presented in the figure 2.

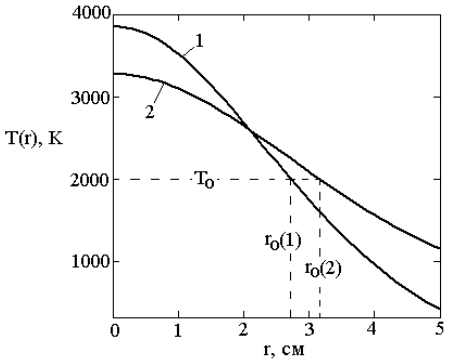

Figure 2. Calculated temperature field of the pool surface. r – radial distance from the center; 1 – copper crucible; 2 – graphite crucible; T_o – anode spot edge isotherm; $r_o(1)$, $r_o(2)$ – anode spot radiuses in cupper and graphite crucibles.

3. Conclusions

The temperature of melted zone under DC plasma arc anode spot is less in hot (graphite) crucible than in cold copper crucible due to less current density.

4. References

[1] A. A. Nikolaev, D. E. Kirpichev, A. V. Samokhin, A. V. Nikolaev. Russian Metallurgy (Metally), Vol. 2016, No. 12, pp. 40–43.

[2] Erohin A.A. Plazmenno-dugovaia plavka metallov i splavov [Plasma-arc melting of metals and alloys]. Moscow, Nauka, 1975, 188 p. (In Russ.).

Model and Simulation of the formation of cathode spot in vacuum arc

Lijun Wang, Xiao Zhang, Shenli Jia

[1] *State Key Laboratory of Electrical Insulation and Power Equipment, Xi'an Jiaotong University, Xi'an, 710049, China*

Abstract: A 2D axisymmetric swirl hydrodynamic model has been developed to describe the formation of cathode spot in vacuum arc. The model includes hydrodynamic equations and thermal conductivity equation which considers surface evaporation and Joule heating. In this model, cathode spot maintains 30μs and during this time, all parameters are fixed. The simulation results show that when the energy flux density coming from the interacting between arc plasma and cathode is 1.5~3*10^{12}W/m^2 and current is 3~6A, the crater diameter is 3~7μm, the crater depth is 1.5~2.5μm and the maximum temperature is 2500~5500K. Besides, in the chromium cathode, the temperature is higher but the molten metal is less because of the lower specific heat and higher melting point.

1. INTRODUCTION

Kesave[1] has shown that vacuum arc in cathode consists of independent cathode spots. During the whole lifetime, cathode spots kept moving. The cellular structure and moving track of a cathode spot have been observed in experiment [2]. Based on these observations, the ecton mechanism was proposed [3]. According to the experimental results, ecton model assumed the size of cathode spot was several microns and the lifetime was several tens of nanoseconds. Old cathode spots extinguished at the edge of contact while new cathode spots appeared in the center of the cathode contact. The beginning of a cathode spot was a micro explosion which resulted in the initial electron emission [4].

Energy flux density coming from interacting between arc plasma and cathode and Joule heat injected energy to cathode contact. Surface evaporation took away a part of energy and the left energy heated cathode material, the temperature could reach several thousand degrees. At such a high temperature, whether copper or chromium, the cathode material was melting. And the pressure caused by cathode plasma extruded the melting material leaving the center of cathode spot, splashing away and becoming droplets, finally, cathode micro jet appeared [5].

To simulate this process, in this paper, A 2D axisymmetric swirl hydrodynamic model has been developed, hydrodynamic equations and thermal conductivity equation are necessary, and the parameters are obtained by fitting the experimental data and predecessors' work[6]. The energy flux density is in magnitude of 10^{12}W/m^2. The current in each cathode spot is limited, however, because the size of cathode spot is only several microns, the current density can reach 10^8A/m^2. Joule heat is produced throughout the contact while the energy flux density only acts on the cathode surface. The cathode plasma pressure is in magnitude of 10^8Pa.

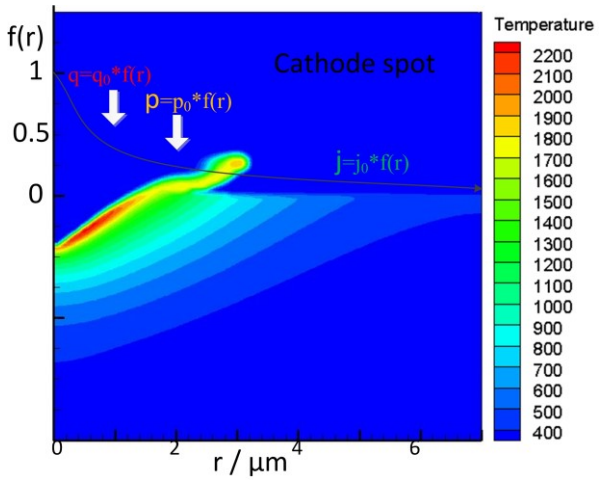

Fig.1 Model of cathode spot

References

[1] I.G. Kesaev. Cathode Processes of Electrical Arc, 1968, Moscow, Russia: Nauka.

[2] J.E. Daalder, Cathode erosion of metal vapor arcs in vacuum, PhD dissertation, Tech. Univ., Eindhoven, 1978.

[3] G.A. Mesyats, Ecton mechanism of the vacuum arc cathode spot, IEEE Transactions on Plasma Sciences, v. 23, N6, pp. 879-883, 1995.

[4] G.A. Mesyats, D.I. Proskurovsky, Pulsed Electrical Discharge in Vacuum. Berlin: Springer, 1989.

[5] G.A. Mesyats and N.M. Zubarev, J. Appl. Phys., 2015, 117, 043302 (1-5).

[6] G.A. Mesyats and N.M. Zubarev, J. Appl. Phys. 2013, 113(20): 203301(1-4).

High-resolution laser-induced fluorescence in the pre-sheath of a positively biased probe

F. Skiff, R. Hood, R. Merlino, and S. Baalrud

Department of Physics and Astronomy, University of Iowa, Iowa City Iowa, USA

We address the general problem of precision measurements of ion distribution functions in the presheath region of a probe. The goal is to obtain sub-millimeter (Debye length) spatial resolution and bandwidth comparable to the ion-plasma frequency. Even with the large scattering cross section of laser-induced fluorescence (LIF) this resolution is not possible directly because of the limited photon count rate. We report measurements of high-resolution ion flow and density profiles and explore the implementation of auto and cross-correlation functions techniques involving both LIF and small electric field probes to measure the fluctuations and ultimately the transport in the presheath region of a positively biased probe in an unmagnetized DC Argon plasma discharge.

1. Introduction

The detailed nature of the plasma sheath continues to be a topic of intense research, being important both for understanding the plasma boundary as well as the currents collected by electric probes. In particular, the importance of instabilities that may occur in the plasma presheath is now recognized. Direct observation of these instabilities is complicated by the fact that they occur in non-uniform regions of the plasma where the relevant spatial and temporal scales are small. The goal of this work is to develop techniques for making in-situ measurements of ion distribution functions with sufficient spatial and temporal resolution to enable measurement of unstable waves and their effects.

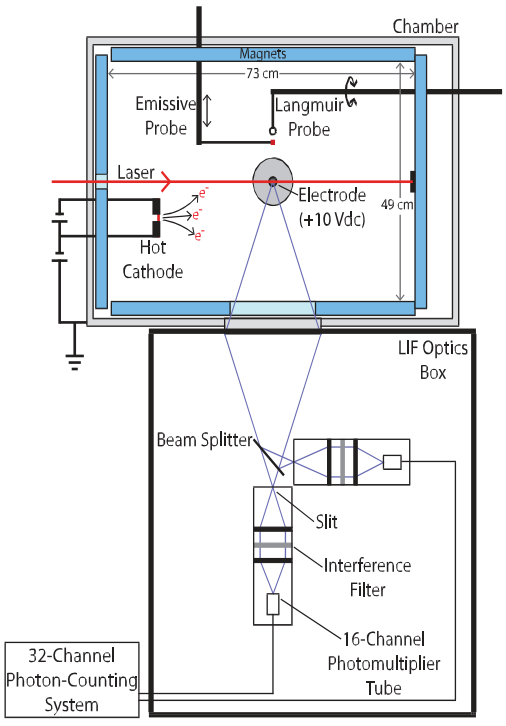

Figure 1 Experiemmental set-up.

2. Experimental set-up

A DC Argon gas discharge in a cylindrical multi-dipole chamber of radius 30 cm and length of 1m is outfitted with a high efficiency imaging light-collection system capable of simultaneously imaging the light from two independent LIF systems onto identical 16 element PMTs connected to a 32 channel photon counting system or to an 120 MHz acquisition system that can time-stamp the arrival of photons in each channel. A schematic of the set-up is shown in figure 1.

By computing auto and cross-correlation functions it is possible to measure power spectra with a photon statistics noise floor that can be improved by obtaining large ensemble averages. Stationary conditions are obtained by feedback control of plasma parameters.

Initial results demonstrating high spatial resolution LIF of the ion distribution functions in the vicinity of a positively biased probe have already been obtained [1]. Preliminary results of high time resolution measurements will be presented and discussed.

3. Acknowlegements

Research supported by the NSF-DOE joint program on plasma science. DOE grant DESC0016473

3.1 References

[1] R. Hood, B. Scheiner, S. D. Baalrud, M. M. Hopkins, E. V. Barnat, B. T. Yee, R. L. Merlino, and F. Skiff, Physics of Plasmas 23, 113503 (2016).

Topic number

Influence of water temperature on stability of three dimensional atmospheric plasma using water-dielectric multi layer electrode

T. Misawa[1]

[1] *Dept. Electrical and Electronic Engineering, Graduate school of Science and Engineering, Saga University*

In this study, the development of discharge method using water dielectric multi layer electrode were carried out in order to improve the stability of three dimensional atmospheric discharge plasma. This electrode is composed of the glass container which include the pure water as an insulator put on the metal electrode. By the interaction between temperature dependency of the dielectric constant of the water and electric discharge, it is possible to easily generate the atmospheric pressure Ar plasma of three dimensional shape. The structure and dynamics of discharge structure of atmospheric plasma was drastically change with the increase of water temperature. This plasma is suitable for plasma treatment of three dimensional shaped objects, fruit and agricultural products.

1. Introduction

The atmospheric discharge technique using the water dielectric multi layer electrode [1] can generate three dimensional shaped atmospheric plasma to which be useful for various application. In this technique, the water temperature has the important role for the phenomena of discharge (Fig.1(a)-(c)). This electrode is composed of metal electrode and glass container which involve the water. The localization of atmospheric discharge arises by un-uniformity of the electric field around the electrode surface. Then, the water around the localized discharge in the container is heated by the strong electric field, and the dielectric constant of same place decreases in comparison with neighbour area. As a result, the localized discharge is moved to the neighbour area, where the dielectric constant is larger than previous discharge place and it is easy to discharge. According to the above effect, it seems to be possible to stably generate the atmospheric plasma in the complicated shaped electrode like the flask shape (Fig.1(d)) [2]. In order to clarify the role of water temperature on atmospheric plasma generated by water dielectric multi layer electrode, the dependence of water temperature on the atmospheric discharge condition using water dielectric multi layer electrode was observed.

2. Experimental setup and discussion

The experiment was carried out using coaxial water dielectric multi layer electrode using strait shaped cooling pipe with constant temperature system. The water temperature was controlled from several to 70 °C. The Ar gas (1 atm in pressure and 3 L/min in flow rate) and ac high voltage (10kHz, 9kVp-p) was applied between inner and outer electrodes. The pattern of the electric discharge along inside surface of inner glass tube was observed by exposure photographing using digital camera. The pattern of discharge changed with increase of water temperature shown in Fig.2. In the case of 1.5 °C, filamentary discharge structure was generated on the inner surface of glass tube (Fig.2(a)). With the increase of water temperature, the uniform atmospheric discharge was generated (Fig.2(b)-(d)). In the case of 70 °C, it was observed that the filamentary discharge structure moves at high speed in the inner glass tube by the high shutter speed observation of 1 [ms], and moving speed was 200-500 [mm/s].

3. References

[1] Tatsuya Misawa, Nobuya Hayashi, Japan patent JP6083093B, PCT/JP2012/079297.

[2] Tatsuya Misawa, et al., Frontier of Applied Plasma Technology, Vol.6, No.1, pp.1-5(2013) (ISSN: 1883-5589).

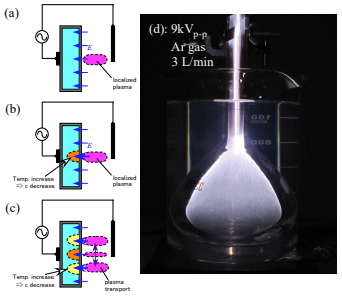

Fig.1 Schematic and typical discharge of water dielectric multi layer electrode

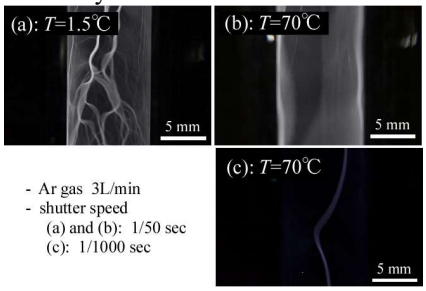

Fig.2 Dependence of water temperature on discharge. (a): T=1.5°C, (b): T=70°C, (c): T=70°C and 1 msec.

Levitation of Dust in a Magnetised RF Plasma

B. J. Harris[1], P. M. Bryant[1]

[1] *Department of Electrical Engineering and Electronics, University of Liverpool*

Dust contamination in plasmas remains a significant problem in fusion machines. Obtaining the plasma parameters, in order to understand dust transport, in a magnetised plasma is a challenging problem. Preliminary results of dust levitation in a magnetised RF plasma show a variation of dust height with increasing magnetic field strength. Emissive probe measurements exhibit a rapid increase in plasma potential followed by a plateau region with increasing magnetic field. Further work, using optical imaging and dust oscillations to provide the plasma parameters and dust charge, will be presented at ICPIG.

1. Introduction

Magnetised dusty plasmas naturally occur in space, fusion and industrial plasmas. Whether in planetary rings, tokamaks, or magnetrons, basic information about dust continues to be elusive. In ITER an estimated 1 ton of dust will be produced per year [1], reducing energy production and initiating disruptive instabilities.

2. Experimental Setup

2.1. Plasma Reactor

Ar plasma is generated at 13.56 MHz in a parallel plate capacitively coupled cell. The Al chamber, 14 cm sq by 7.5 cm deep, is placed inside a uniform magnetic field (to within 0.3 %) by a Helmholtz coil. The 4 cm diameter lower driven electrode is located 4.5 cm from the upper transparent ITO grounded electrode. RF plasma is generated by a Dressler Cesar 136 supply coupled through a matching unit to the powered electrode. Melamine Formaldehyde particles (10 μm diameter) were then levitated, in the plasma, balanced by the sheath electric field and gravity.

2.2. Diagnostics

The dust is illuminated by a laser system that generates a vertically scanning laser sheet. A 300 mW beam, 1 mm diameter at 532 nm, is enlarged to 4 mm by a beam expander. This is transformed into a laser sheet by cylindrical lenses. A system of two rotating mirrors [2] allows vertical adjustment of the laser sheet within the chamber. The light scattered by the dust particles is recorded by a Photron FASTCAM ultima APX camera. An emissive probe, with 50 μm diameter thoriated tungsten wire, was used to measure the plasma potential using the floating potential method in strong emission [3].

3. Results and Conclusions

As shown in Figure 1 at lower pressures (2 Pa) the dust falls with increasing magnetic field. At higher pressures (6 - 10 Pa), the dust falls and then rises with increasing magnetic field. At field strengths greater than 0.04 T, the dust levitation height does not change. This seems to coincide with the plasma potential measurements, which increase up to 0.08 T and then varies weakly with magnetic field. Recently, theoretical studies have shown that a magnetic field changes the dust surface charge [4]. Furthermore, the plasma parameters and electric field are expected to change with increasing magnetic field. This will also alter the dust charge and levitation height. Further experiments using a novel line ratio imaging technique to obtain electron density and temperature maps, at different field strengths, are planned. Also, dust oscillation observations, combined with emissive probe plasma potential measurements, will be used to obtain the dust charge and electric field at different field strengths. These will be presented at ICPIG.

4. References

[1] V.N. Tsytovich *et al*., Physics-Uspekhi **41** (1998) 815.

[2] D. Samsonov *et al*., Rev. Sci. Instrum. **79**, (2008) 035102.

[3] J.P. Sheehan *et al*., Plasma Sources Sci. Technol. **20** (2011) 063001.

[4] D. Lange *et al*., J. Plasma Phys. **82**, (2016) 905820101.

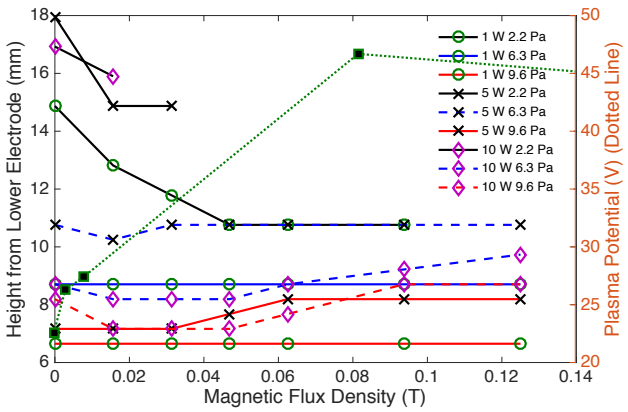

Figure 1 - Change in dust levitation height with magnetic field. The plasma potential measurement at 0.25 T is not shown on the figure.

Synthesis of Metallic Nanoparticles using a Submerged Pulsed Arc

C. L. Rojo Blanco, S. Muhl

Instituto de Investigaciones en Materiales, Universidad Nacional Autonoma de Mexico, CDMX, México,

1. General

We describe the use of a submerged pulsed high-current arc of for the controllable preparation of Fe-Bi nanoparticles using Fe and Bi electrodes. The arc was produced in D.I. water and the nanoparticles were removed from the reaction chamber by the liquid flow. The nanoparticles were separated and collected depending on their characteristics (magnetic, heavy or light). It was found that the heavy and the light nanoparticles were very similar. The structure and the morphology of the nanoparticles were studied using SEM, EDS, XRD and optical absorption. We observed an average particle size between 5 and 20 nm, a high percent of oxygen, a low percent of bismuth in the magnetic nanoparticles and no iron in the heavy and the light nanoparticles. Larger bi-metal spheres of approximately 1.0 micron diameter were observed that had Fe cores covered with Bi. The temporal variation of the arc was studied using a high speed Phantom camera. Both direct observation and shadowgraphy using an expanded 532nm laser were performed. The short time volume and the speed of the bubble explosion increased with the energy applied to the system, and while the volume grew linearly with time, the speed of the expansion was superlinear. Finally, longer times we observed a somewhat complicated the bubble evolution: first the bubble expanded, reached an equilibrium state, it then contracted before again expanding, and then finally it dispersed.

Understanding the nature of near-anode plasma conditions in DC 1 Atm pressure glows and the role that it may play in plasma self-organization

Y. Kovach[1], M.C. Garcia[2], J.E. Foster[1]

[1] *Department of Nuclear Engineering, University of Michigan, Ann Arbor, U.S.A.*
[2] *Department of Applied Physics, Universidad de Cordoba, Cordoba, Spain*

DC atmospheric glows have attracted much interest in recent years. The origin of plasma self-organization on both metal and liquid electrodes is not well understood. These discharges with liquid electrodes can also be used to produce nanoparticles efficiently in solution. In this work, we describe electrical and spectroscopic characteristics of DC atmospheric pressure glows. A spatially resolved spectroscopic survey near the plasma-electrode interface is presented. This detailed information on gas temperature and plasma density yields insight into physical processes taking place there and provides a basis for speculation on the origin of the self-organization. The vapor cloud, which often appears around the main plasma column, is postulated to play a role in mass transport and discharge maintenance. Here, we present spectroscopic measurements of this region and comment on its composition and overall origin. Work supported by DOE DE-SC0001939.

1. Introduction

Self-organization occurs in a variety of biological, physical, chemical, and cognitive systems. In plasma physics, self-organization is observed in phenomena ranging from plasmoid formation in low pressure, RF plasmas to large-scale, and magnetized structures observed on the surface of the sun. Of recent interest is the puzzling formation of self-organization patterns on the surface of liquid anodes in 1 ATM DC glows. Shirai [1] documented an array of such patterns over a broad parameter spaced including the variation of gap spacing, current, and sensitivity to feed gas trace oxygen concentration. While these patterns are of academic interest in regards to understanding collective phenomena, the appearance of the patterns may play an important role in the sub-surface liquid phase chemistry, driving convection and inducing thermal gradients.

In many studies to date, salt water is typically used as the electrolyte in these discharges. In this current work, the effect of a different electrolyte—copper sulfate—was investigated. At similar solution conductivities and applied voltages reported previously with salt water, it was found that the self-organization patterns are markedly different. As can be seen in figure 1 which shows a side-by-side comparison between the salt-water pattern and the copper sulfate pattern. A new, complex, was also observed with $CuSO_4$. What role does the electrolyte play in determining the pattern shape? This observation suggests that electrolyte ion mass or perhaps ionization state of solution ions may play a key role in determining overall pattern shape. This dependence has not previously been explored.

Figure 1 depicts another interesting comparison between the salt-water solution and a copper sulfate solution for a DC glow. The transport of ions and electrons as well as the role of electrolytic species to discharge maintenance is not well understood. What is quite apparent however both cases is the appearance of a prominent halo that surrounds the main plasma column. Spectroscopic analysis of the halo suggests that it consists of sodium in the case of the salt electrolyte and copper in the case of the copper sulfate solution. In this case, clearly the solution ions play a role not only in electrolytic processes in solution but also apparently in the gas phase. How does the introduction of these low ionization potential species into the plasma column affect ionization there? Is penning ionization therefore an important process in discharge maintenance? The relationship between this ionic mass transport into the gas phase requires further elucidation.

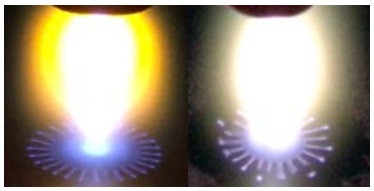

Fig. 1 – Plasma emission clouds image with patterns at 2.2kV, 8mm gap length with 200 sccm He flow. *Note: (L) NaCl solution. (R) $CuSO_4$ solution.*

2. References

[1] N. Shirai, S.Uchida and F. Tochikubo, Plasma Sources Sci. Technol. 23(2014).

Diagnostics of Chemically Active Plasma of RF Capacitive-coupled Discharge in H_2+SiF_4, H_2+GeF_4 and H_2+BF_3 mixtures

R. Kornev[1], P. Sennikov[1], A. Abramov[1], S. Sintsov[2], A. Vodopyanov[2]

[1] *G.G. Devyatykh Institute of Chemistry of High-Purity Substances of RAS, Nizhny Novgorof, Russia*
[2] *Institute of Applied Physics of RAS, Nizhny Novgorod, Russia*

The dependencies of concentration of electrons in chemically active plasma of H_2+A mixtures (where A - SiF_4, GeF_4. BF_3) on H2/A ratios as well as their emission spectra were investigated in RF capacitive-coupled discharge at a pressure of 1 torr. It was found that with the increase in concentration of fluorides in hydrogen mixture the concentration of electrons decreases; mostly it is observed for A=GeF_4 according to its high electron affinity value. SiF, GeF and GeH radicals as well as atomic hydrogen were registered in emission spectra. The line of BF radical is absent.

1. Introduction

Determination of internal parameters of chemically active plasma on the basis of volatile fluorides and, in particular, the concentration of free electrons is an actual task due to sufficiently broad practical application of these substances in plasma chemical technologies. For this purpose it is expedient to use the non-contact methods of MW interferometry and emission spectrosopy. At the same time the plasma should be maintained by the discharge of the same type. In this work this approach was used for investigation of chemically active plasma of H_2+SiF_4, H_2+GeF_4 and H_2+BF_3 mixtures sustained by RF capacitive discharge.

2. Experiment and discussion

Investigations were conducted in RF capacitive-coupled discharge with frequency of 13.56 MHz at a pressure of 1 torr and power of 500 Wt delivered to discharge. H_2/SiF_4 (GeF_4, BF_3) ratio changed from 8 to 36. A generator, tuned to the frequency of 35.7 GHz, was used as the source of probing radiation of MW interferometer. The level of power of reference and probing signals was equal to 65 MWt. The emission spectrum of chemically active plasma was investigated in the range of 350 ÷ 800 nm using HR4000CJ-UV-NIR emission spectrometer.

It was found that under the realized experimental conditions the concentration of free electrons of plasma in pure hydrogen plasma was equal to $n_e = (1.5\pm0.04)\cdot10^{12}$ cm^{-3}. While adding the fluorides to hydrogen plasma its decrease is observed which depends on the ratio of mixture components. The lowest value of n_e takes place for H_2+GeF_4 mixture where it is equal to $(9.8\pm0.04)\cdot10^{11}$ cm^{-3} at the ratio of H_2/GeF_4 = 13.5. With this ratio the values of n_e in H_2+SiF_4 and H_2+BF_3 mixtures negligeably differ from each other and are equal to $(1.1\pm0.04)\cdot10^{12}$ cm^{-3} and $(1.2\pm0.04)\cdot10^{12}$ cm^{-3}, respectively. The emission spectra in the same range of reagent ratios were registered for the studied mixtures. Apart from the lines of atomic hydrogen, the lines assigned to SiF, GeF and GeH radicals were found in the emission spectra of H_2+SiF_4 and H_2+GeF_4 mixtures. At the same time the line of BF radical was not observed in the spectrum of H_2+BF_3 mixture. The process of dissociative attachment of electrons is the main channel of energy transmission from electrons into chemical system [1]. Electron affinity is the main molecular parameter characterizing this process. According to quantum-chemical calculations for GeF_4, the adiabatic electron affinity EA = 1.46 eV [2] and for SiF_4 and BF_3 the value of EA is negative [3, 4] which indicates the absence of "attachement" of electron to these molecules within the framework of the used basis set. Our results conclusively indicate high ability of GeF_4 molecule to attach the electron. This ability is noticeably lower for the molecules of two other fluorides. Should we assume that after the process of electron attachment the dissociation of molecules follows with formation of corresponding radicals, the fact of absence of the line of BF radical in the spectrum of H_2+BF_3 mixture can indicate that the "attachment" of electron to BF_3 is less manifested than in the case with attachement to SiF_4.

3. References

[1] H.Massey. Negative Ions. Cambridge University Press. 1976.

[2] Q.Li, G.Li, W.Xu, Y.Xie, H.F.Schaefer. J.Chem.Phys. **111** (1999) 7945.

[3] R.A.King, V.S.Mastryukov, H.F.Schaefer III. J.Chem.Phys. **105** (1996) 6880.

[4] D.J.Grant, D.A.Dixon, D.Camaioni, R.G.Potter, K.O.Christie. Inorg.Chem. **48** (2009) 8811.

Dielectric Properties of Magnetron Sputtered PTFE Thin Films

V. Satulu, V. Ion, B. Mitu*, G. Dinescu

[1] National Institute for Lasers, Plasma and Radiation Physics,
409 Atomistilor Street, Magurele- Bucharest, 077125, Romania
*mitub@infim.ro

RF magnetron sputtering was involved for synthesis of polytetrafluorethylene thin films. The process was investigated for various RF applied powers and deposition time. The chemical bonds evidence the typical IR absorption bands for PTFE material, with a tendency towards cross linking due to polymerization of volatile fragments sputtered from the polymeric target. The results show the obtainment of smooth films, without cracks, with dielectric constant similar to that of bulk material and very low values of the dielectric losses over a wide frequency range. Such results indicate that the films can be successfully used in electronic devices.

1. Introduction

Fluorinated polymers have found a broad range of applications as thin films, from hydrophobic and super-slippery surfaces to protective coatings or active layer in sensors. In the present contribution, results on magnetron sputtering of polytetrafluorethylene (PTFE) are presented aiming their use for application in electronic devices.

2. Experimental details

Deposition of thin films was performed by RF magnetron sputtering of a PTFE polymeric target at power level in the range 50 – 110 W, on a working pressure of $6x10^{-3}$ mbar, established under an Ar flow of 100 sccm. The magnetron sputtering source is mounted at 45 degrees in respect to the substrate holder plane and positioned at 6 cm distance from it [1]. Deposition uniformity is insured by rotating the substrate holder at a constant speed of 100 rpm.

The deposition rate was obtained by profilometry measurements for samples obtained upon 10 – 30 minutes exposure. The dielectric function of PTFE deposited on Pt/Silicon substrates was determined in two frequency regime: in the low frequency range (1KHz - 5 MHz) by dielectric spectroscopy and in the optical range (UV-VIS-Near IR) by spectroscopic ellipsometry. Surface topography was investigated by means of Atomic Force Microscopy (AFM) on areas of 5x5 μm^2, while the chemical bonds were revealed by Fourier Transformed Infrared Spectroscopy.

3. Results and conclusions

The deposition process is depending on the applied power onto the magnetron sputtering source, with the deposition rate increasing from 1 nm/min at 50W to almost 7 nm/min at 110 W.

The value of dielectric permittivity was calculated in the plane capacitor approximation and was found to be $\varepsilon_r \sim 2.8$, slightly higher than the expected values. A slight decrease of the dielectric constant is encountered on the entire spectral measured range. The electrical losses are small and had values below $7.5*10^{-3}$. In the optical range (300-1700 nm), the refractive index was n~1.44-1.4, with extinction coefficients k below 10^{-4}.

An important characteristic for the utilization of thin films in electronics is a uniform and crack-free surface. The AFM measurements confirm that the obtained deposited films are extremely smooth, regardless the RF power used for deposition, with typical roughness RMS values below 1 nm for film thickness around 200 nm. The investigation of chemical bonding reveal the typical IR absorptions of PTFE, with bands at 978 cm^{-1} associated to CF_3 and those at 1182 cm^{-1} and 1227 cm^{-1} related to CF_2 vibrations. Nevertheless, the band at 1715 cm^{-1} assigned to $C=CF_2$ or $CF=CF_2$ bonds point out toward the crosslinking structure obtained upon target sputtering.

These results are encouraging for utilization of PTFE thin films in various devices, as example as active layers in SAW based sensors.

Acknowledgements

This work has been financed by the Ministry of Research and Innovation in the frame of Nucleus programme - contract 4N/2016.

4. References

[1] V. Satulu, M.D. Ionita, S. Vizireanu, B. Mitu, G. Dinescu, Molecules, 21(12), 2016, 1711.

Visualization of particulates distribution from electrode erosion

Wei Zhong, Yunlong Liu, Ao Xu, Lei Chen

Institute of Electronic Engineering, China Academy of Engineering Physics, Mianyang, China

Particulates generated from electrode erosion in gas spark gap is inevitable and may initiate self-breakdown behavior with high risk. Traditionally, this problem is addressed by empirical method qualitatively. To push this old problem forward, this paper conducts laser confocal microscopy measurement of eroded surface and a statistical method is introduced to obtain visualized distribution of particulates from electrode erosion after different shots. This method allows dense particulates to be classified with their heights in z direction and scattered figures of particulates within certain height range are obtained. Results indicate that the higher-than-10μm particulates start to emerge after 200 discharge shots and particulates number has a waved radial distribution with 0.5mm-wide deposition zone. Based on these quantitative results, the risk of reignition and field-distortion failure that are triggered by particulates can be assessed.

1. Introduction

Particulates is generated from electrode erosion inevitably, when electrode surface is bombarded by ~kA current. These splashing particulates could lead to local field enhancement and degradation of reliability, and even gap failure [1-2], which acts as a key restrictive factor in pulsed power field.

Insepov and Norem [3] indicate that particulates are produced when the plasma pressure splatters liquid droplets away from the molten surface. Traditionally, these eroded features are addressed by empirical methods (SEM etc.) and their horizontal size r could be gained [4]. However, as reported by [5], the field enhancement factor β is function of h/r and information of height h is rarely reported.

This paper performs a statistical analysis of particulates' height and obtains their quantitative distribution from electrode erosion of gas spark gap.

2. Analysis results

Experimental details are described in [6]. Fig. 1(a) gives confocal image of cathode surface after 1000 shots, which is densely covered with particles. Based on statistical analysis, radial distribution of particles number is obtained in Fig. 1(b), which would contribute to tracing where and how the interaction between arc and electrodes occurs.

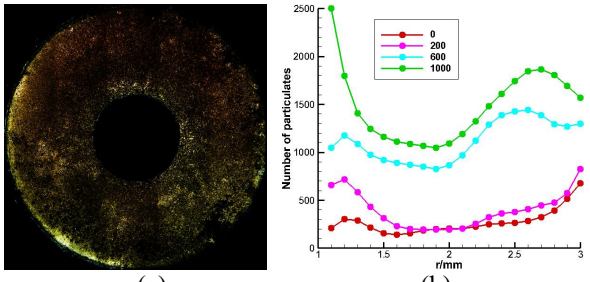

(a) (b)

Fig. 1 (a) electrode surface after 1000 shots; (b) radial distribution of particulates number

Dense particulates on the electrode surface are layered according to their height range with statistical method in [6]. Spatial distribution of particulates are reconstructed and shown in Fig. 2. Particulates are concentrated at the inner edge and 0.5mm-wide deposition zone at r=[2.35, 2.85]mm. These results would throw new light into design of gap reliability.

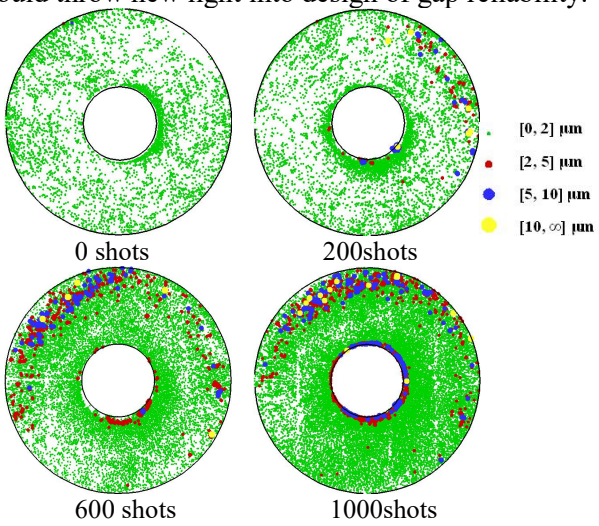

Fig. 2 Reconstructed distribution of particulates

3. References

[1] X. Li, X. Liu, X. Guo, F. Zeng, Q. Zhang. IEEE Trans. Plasma Sci. **42** (2014) 3064.

[2] J.M. Koutsoubis, S.J. MacGregor. J. Phys. D: Appl. Phys. **33** (2000) 1093.

[3] Z. Insepov, J. Norem. J. Vac. Sci. Technol. A. **31** (2013) 11302.

[4] W. Zhong, Y. Liu, A. Xu, S. Shang, D. Jin. 27th Int. Symp. on Dis. and Electri. Insul. in Vac.(2016)

[5] R.G. Forbes, C.J. Edgcombe, U. Valdre. Ultramicroscopy. **95** (2003) 57.

[6] W. Zhong, Y. Liu, L. Wang, D. Jin, X. Tan. J. Phys. D: Appl. Phys. **50** (2017) 015202.

Simulation on the characteristic of plasma evolution in three electrode gas spark gaps

Ao Xu, Lin Yang, Wei Zhong, Yulong Liu, Dazhi Jin, Lei Chen

Institute of Electronic Engineering, China Academy of Engineering Physics, Mianyang, China

The performance of three electrode gas spark gaps is directly effected by the characteristic of plasma evolution while gaps are operating. However, it is difficultly to obtain all the plasma parameters only by experiments. Therefore, it is necessary to study the characteristic of plasma evolution in three electrode gas spark gaps with the help of simulation tools. This paper presents a sequence of images of plasma evolution in three electrode gas spark gap obtained by high speed camera. Then, the simulation results of this experimental geometry are present with the help of a 2D PIC-DSMC code. According to compare results between the experiment and the simulation, it could confirm the validity of the code. Finally, the temporal and spatial density distribution of electrons, ions and neutral particles are cognized, and the temperatures of particles in plasma channel are obtained. It would be helpful to further understand three electrode gas spark gaps.

1. Experiment

Experimental setup is shown in Fig.1, that the electrodes of the three electrode gas spark gap are placed in a vacuum system filled with nitrogen gas at atmospheric pressure. And the camera consists of four intensified charge-coupled device cameras using the same optical axis by means of an internal beam splitter. Then the cathode is grounded, while the anode before switching is at a constant positive voltage of 2kV. The gas spark gap is triggered by applying a 1kV negative (with respect to the cathode) voltage pulse to trigger electrode.

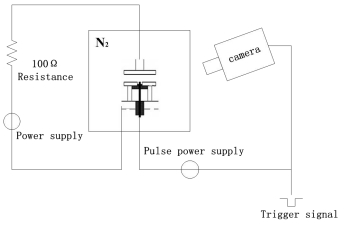

Fig.1 Experimental setup

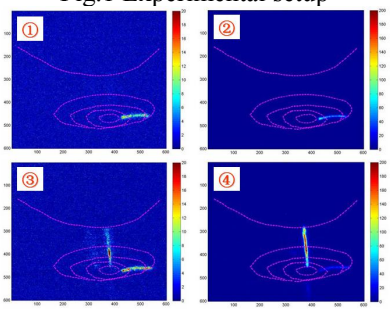

Fig.2 Sequence images of plasma evolution

Fig.2 gives a sequence of images in three electrode gas spark gap, starting abrupt change of trigger pulse. As found in the experiment, the trigger process includes two steps. First, breakdown was initiated between the trigger electrode and the cathode. Second, a streamer was launched from the trigger electrode toward the anode.

2. Simulation

According to the geometry and the voltage of the three electrode gas spark gap in above experiment, a simulation model was established with the help of a 2D axial symmetrical PIC-DSMC code. Then, the mechanisms describing the particles in the gap plasma were as follows: electrons are emitted from trigger electrode according to Fowler-Nodheim filed emission. The electrons move to the gap undergoes various kinds of collisions and produce ions. Moreover, ions and electrons can cause the emission of electrons at all the electrodes.

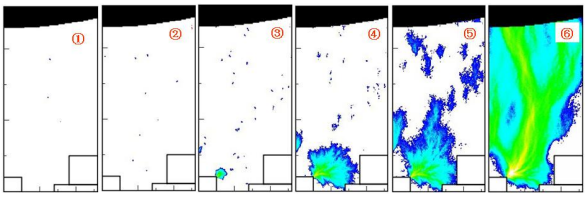

Fig.3 Simulation results of electrons distribution evolution

Fig.3 shows the 2D PIC-DSMC simulation results of the plasma evolution in the three electrode gas spark gap used in above experiment. It is found that the results between the experiment and the simulations are identical. Moreover, detailed change of plasma parameters also can be obtained with the help of PIC-DSMC simulation.

3. Conclusion

With the help of simulation tools, it is possible to obtain the detailed characteristics of plasma evolution in three electrode gas spark gaps. It would be helpful to further improve the performance of these gaps.

Plasma-Laser Assisted Synthesis of Nanoparticles for Antibacterial Coatings

A. Jurov[1,2], N. Krstulović[3], M. Modic[1], N. Hojnik[1,2], A. Nikiforov[4], A. Zille[5], C. Leys[4], U. Cvelbar[1,2]

[1] *Jožef Stefan Institute, Jamova cesta 39, SI-1000 Ljubljana, Slovenia*
[2] *Jožef Stefan International Postgraduate School, Jamova cesta 39, SI-1000 Ljubljana, Slovenia*
[3] *Institute of Physics, Bijenička c. 46, 10000 Zagreb, Croatia*
[4] *Department of Applied Physics, Ghent University, Ghent, Belgium*
[5] *2C2T-Centro de Ciência e Tecnologia Têxtil, Minho University, Guimarães, Portugal*

The "green synthesis" of colloidal nanoparticles and their application for the antibacterial coatings is based on the plasma-laser assisted ablation in liquids. Nanoparticles are synthesized through the process of laser ablation of target in water, which enables additional advantages in comparison with the other standard wet chemical synthesis, such as simplicity and complete utilization of materials. Furthermore, these nanoparticles are used and tested for antibacterial coatings on polymers, where they are grafted or imbedded through atmospheric pressure plasma assisted processes. The advantages of different coatings made from those nanoparticles are presented as well.

1. Motivation

One of the requests in medicine are materials with antibacterial properties, and even though antibacterial coatings are not a novelty, still there is a demand for better effectivity and profitability. The goal of our method is just that, to try the new, simpler, and more affordable approach in the never-ending pursuit for efficiency and inexpensiveness.

2. Experiment

Laser synthesis of nanoparticles in liquids is known as the "green synthesis" technique as it provides not inhalable colloidal nanoparticles of wide variety of metals with no residues or byproducts, and often no further purification is required. Moreover, the laser pulses can additionally generate, de-agglomerate, fragmentate, and re-shape nanoparticles. In addition to those advantages, the laser ablation is a simple and straightforward technique and only a small piece of metal is needed for the process, with no unused remains.

Unlike the methods where nanoparticles are incorporated not only at the surface but in the bulk of polymer material, our method is focused on incorporating nanoparticles only to the surface, keeping the bulk material untouched. This is a cost-efficient route to incorporate nanoparticles into polymers. Within this approach, 3 methods are tested: 1) the polymer surface containing nanoparticles deposited by drop-casting on plasma pre-treated polymer, 2) the polymer surface containing nanoparticles deposited by drop-casting and sequent plasma treatment after water evaporated, and 3) a colloidal Au nanoparticles deposited on polymer surface and plasma treatment with until water evaporates.

Preliminary research was done on various polymers with different colloidal nanoparticles, whereas a special attention was devoted to studies of PVC polymer and Au nanoparticles.

3. Results

The analysis of colloidal nanoparticles exhibits a narrow size distribution which is suitable for antibacterial applications. Moreover, the preliminary results of roughness and contact angle demonstrate appropriate change for nanoparticle impregnation on multiple polymers. Tests done on polymers impregnated with nanoparticles emphasize third method as the best impregnated sample.

4. Conclusion

The presented research shows that chosen methods are a good alternative for the preparation of antibacterial coatings on polymers. Roughness measurements displays interesting results, where a sample made with second method has roughness 20 times higher than untreated polymer, and two times higher than polymer treated only with plasma. Meanwhile, SEM analysis highlights the third method as the best choice for a quick new route to antibacterial coatings.

Ionic composition of the spatial afterglow of an atmospheric pressure He/CO_2 plasma jet by mass spectrometry

A. Hecimovic[1,2], E. Carbone[1], G. Willems[2], K. Sgonina[2], J. Benedikt[2]

[1] *Max-Planck-Institut für Plasmaphysik, Boltzmannstr 2, 85748 Garching, Germany*
[2] *Institute for Experimental physics II, Ruhr-University Bochum, Bochum, Germany*

In this contribution, we report on the first measurements of the dominant positive ions in the effluent of a helium atmospheric pressure plasma jet (APPJ) discharge with CO_2 addition. The plasma is ignited in a He-CO_2 gas mixture with CO_2 flows from 0.1 – 0.5 %. The measurement of the positive ions in the effluent of the jet, at distances from 1 mm to 5 mm is performed using an energy resolved mass spectrometer with 2 pumping stages. It is found that at 1 mm distance the dominant ions in the effluent are $\mathbf{O_2^+}$ ions, and the $C_xO_y^+$ related observed ions are CO_2^+, $C_2O_2^+$, $(CO_2)O_2^+$ and $(CO_2)_2^+$ ions. The key finding is that the most abundant ions are $\mathbf{C_2O_2^+}$, $\mathbf{(CO_2)O_2^+}$. Due to presence of residual water in the system, many clustered ions have been observed as well, such as $(H_2O)_2H^+$, $(H_2O)O_2^+$, $(CO_2)(H_2O)H^+$ and $(CO_2)_2(H_2O)O^+$.

1. Introduction

CO_2 plasma gas conversion carries the promise of both energy storage and the reduction of a greenhouse gas emission produced by industrial processes and power plants. Both for the accurate description of the plasma dynamics via modelling or through plasma diagnostics, it is necessary to have an accurate description of electron kinetics. In that respect, it is necessary to know the ionic composition which will govern recombination rates.

In this contribution, we investigate the positive ions composition in the effluent of an APPJ jet [1] in He+CO_2 gas mixture using energy resolved ion mass spectrometry. The μ-APPJ comprises two RF powered (13.56 MHz) metallic electrodes separated by a 1 mm wide gap. The plasma is ignited between the electrodes in a gas mixture of interest.

Mass spectrometry of atmospheric pressure plasmas has been used for sampling of stable neutral and ion species by using differentially pumped multiple stages [2]. Mass spectrometry has the advantage of measuring the absolute densities of neutral species, but with limitation on measuring them only in the plasma effluent. Using a molecular beam mass spectrometer for neutral species, the neutral species composition of the APPJ in He+CO_2 gas mixture was measured and conversion rates are obtained.

2. Results

The measurement of positive ions in the effluent of the jet, at distances from 1 mm to 5 mm is performed using an energy resolved ion mass spectrometer. The ion signal intensities is optimized for each ion mass and correlated to the area of the energy resolved ionic distribution function.

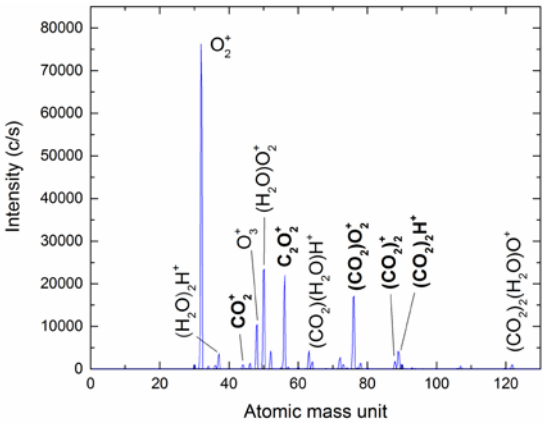

Figure 1. Mass spectrum with 0.1% CO_2/He gas flow ratio and measured at 1 mm from the outlet.

The first observation is that Helium ions are not observed. This is due to their efficient charge transfer reactions will all molecular species present in the discharge and its effluent. It is found that at 1 mm distance the dominant ions in the effluent are O_2^+ ions, and the $C_xO_y^+$ ions. Due to presence residual water in the system, many water based ion clusters have been observed additionally. Increasing the distance and increasing the CO_2 flow result in the reduction of the $C_xO_y^+$ ions (probably due to a decrease of the electron density) and dominance of $C_xH_yO_z^+$ related ion clusters.

3. References

[1] von der Gathen V S, Schaper L, Knake N, Reuter S, Niemi K, Gans T and Winter J 2008 *Journal of Physics D: Applied Physics* **41** 194004

[2] Benedikt J, Hecimovic A, Ellerweg D and von Keudell A 2012 *Journal of Physics D: Applied Physics* **45** 403001.

Synthesis and Characterization of Photocatalytic Titanium Oxide Thin Film Deposited on Glass by Atmospheric Pressure Plasma CVD

Seongchan Kang[1], Rodolphe Mauchauffé[1], Se Youn Moon[1,2*]

[1] *Plasma Experiment and Device Application Lab, Department of Applied Plasma Engineering, Chonbuk National University,*
[2] *Department of Quantum System Engineering, Chonbuk National University,*
567 Baekje-daero, Deokjin-gu, Jeonju, Jeollabuk-do, 561-756, Republic of Korea
**Corresponding author email: symoon@jbnu.ac.kr*

Herein, we report on the deposition and characterization of titanium oxide thin films deposited by atmospheric pressure plasma CVD and on the study of their photocatalytic properties.
This access permits deposition at lower temperatures and easy than normally used in atmospheric pressure based processing. The surface morphology is evidenced by SEM. The transmittance of thin film as well as the material band gap are determined by UV/Vis spectroscopy. The chemical composition is obtained by X-ray Photoelectron Spectroscopy and the crystallinity is assessed by X-ray Diffraction and Raman spectroscopy. Methylene blue degradation in water is performed and monitored by UV/Vis measurement in order to assess the photocatalytic properties of the deposited material.

1. Introduction

Titanium dioxide, TiO_2, has received much attention during the last years due to its photocatalytic properties. Indeed, various applications can be obtained by deposition of TiO_2 thin films such as self-cleaning surfaces and pollutant degradation. Atmospheric pressure plasma deposition appears to be a versatile environmentally friendly process for low-cost and high rate deposition of photoactive mental oxide thin films [1,2]
The majority of works in this area has been conducted using vacuum systems, which leads to many limitations, *e.g.* high running costs, compared to atmospheric pressure processes.
In this work, deposition was performed at atmospheric pressure, facilitating in-line process implementation.

2.Experimental Part

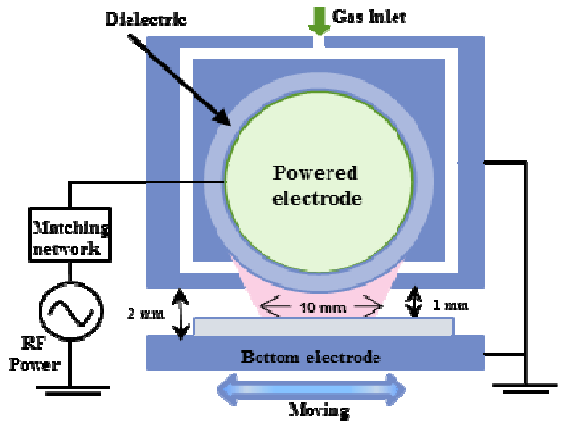

Figure1. Schematic diagram of atmospheric pressure plasma

3. Conclusion

In conclusion, the atmospheric pressure approach reported here appears to be a promising method for the deposition of titanium oxide thin films for photocatalytic applications.

4. References

[1] H Fakhouri, 'Highly efficient photocatalytic TiO2 coatings deposited by open air atmospheric pressure plasma jet with aerosolized TTIP precursor', J. Phys. D: Appl. Phys., 47, 265301, 2014
[2] Q Chen, 'Deposition of photocatalytic anatase titanium dioxide films by atmospheric dielectric barrier discharge', Surf. Coat. Tech., 310, 173–179, 2017

A study on the characteristics of hollow cathode discharge for the development of VUV lamp

Deoggyun Cho[1], Duksun Han[1] and Se Youn Moon[1,2,*]

[1]*Department of Applied Plasma Engineering, Chonbuk National University, Korea*
[2]*Department of Quantum System Engineering, Chonbuk National University, Korea*

The VUV light source can provide a variable for measuring the density of oxygen based on the theory of the absorption spectroscopy. The VUV light source consists of hollow cathode biased by negative voltage and grounded plate to generate high density plasma. Characteristic of hollow cathode is one of the important variables of the VUV light source, which affects the performance of light sources according to the characteristic of the gas-discharge light source. The characteristics of plasma discharge were determined by checking the composition of the molecules and the composition of the particles according to the electrical characteristics and the wavelength of the cases by using optical emission spectroscopy, and the plasma temperature was measured accordingly. In particular, it was confirmed that the possibility of controlling the plasma VUV light in the 130 nm wavelength region was verified, and the possibility of using the plasma discharge as a VUV lamp was verified.

1. Introduction

Ultraviolet(UV) is an electromagnetic radiation with a wavelength from 10nm to 400nm, shorter than that of visible light but longer than X-rays. Long-wavelength ultraviolet radiation can cause chemical reaction and causes many substances to glow or fluoresce. Ionized gas is macroscopically neutral that contains ions, electron, neutral, photon and radicals. The parameters of UV absorption spectroscopy are supported to etch rate, offering potential for control and optimization of semiconductor processing. A hollow cathode lamp is type of lamp used in physics and chemistry as spectral line source and as a frequency tuner for light sources such as lasers. Atomic absorption lines are very narrow. For the Beer-Lambert law to be applicable, the bandwidth of the source should be narrow in comparison with the width of the absorption peak. Otherwise, the signal-to-noise ratio and the slope of the calibration curve would be low; the resulting sensitivity would be poor.

2. Experiment setup

A schematic diagram of UV absorption spectroscopy is presented. It is consists of VUV monochromator, plasma chamber and hollow cathode. The type of the plasma is ICP and the frequency is 13.56MHz. The helium and oxygen gas flow rate is controlled by independent mass flow controller. The monochromator is connected to the ICP chamber with hollow cathode to obtain VUV emission lines.

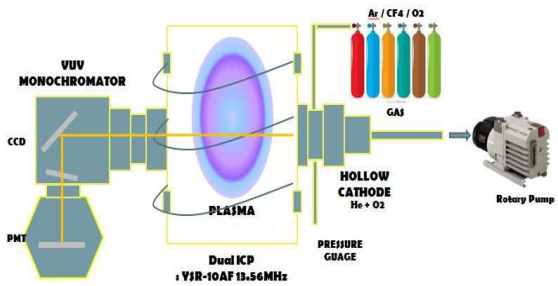

Figure1. Schematic diagram of VUV lamp

3. Result and discussion

We conclude that above currents of mA breaks down and discharge begin to develop from the appearance of the discharges in the hollow cathode and measured current-voltage characteristics. The range of the pressure is showed from 10Torr to 100Torr. The kinds of gas are helium and O2. Spectral measurements have been performed using a 250-900nm Princeton Instruments SCT 320. The difference of the glow mode and hollow mode is the intensity of the wavelength. The 546nm(wavelength) is higher, when the mode is change by hollow mode. The 546nm(wavelength) is helium line. And the wavelength is shifted by gas mixture (helium lonely & helium and O2). In fact we can analyze the condition of plasma by analyzing wavelength. We use boltzmann plot theory for the theoretical verification wavelength. The excitation temperature is very important parameter to analyze the state of plasma. We use NIST atomic spectra database for deduct the excitation temperature in kelvin. The excitation temperature of hollow mode is higher than the excitation temperature of glow mode.

Author Index

D

E

F

G

H

I

J

K

L

M

N

O

P

Q

R

S

T

U

V

W

X

Y

Z